

An Introduction to Acoustics

S.W. Rienstra & A. Hirschberg
Eindhoven University of Technology

23 Dec 2021



This is an extended and revised edition of IWDE 92-06.
Comments and corrections are gratefully accepted.

This file may be used and printed, but for personal or educational purposes only.

© S.W. Rienstra & A. Hirschberg 2004.

Contents

	Page
Preface	
1 Some fluid dynamics	1
1.1 Conservation laws and constitutive equations	1
1.2 Approximations and alternative forms of the conservation laws for ideal fluids	4
2 Wave equation, speed of sound, and acoustic energy	9
2.1 Order of magnitude estimates	9
2.2 Wave equation for a uniform stagnant fluid and compactness	13
2.2.1 Linearization and wave equation	13
2.2.2 Simple solutions	14
2.2.3 Compactness	16
2.3 Speed of sound	17
2.3.1 Ideal gas	17
2.3.2 Water	19
2.3.3 Bubbly liquid at low frequencies	19
2.4 Influence of temperature gradient	20
2.5 Influence of mean flow	22
2.6 Sources of sound	22
2.6.1 Inverse problem and uniqueness of sources	22
2.6.2 Mass and momentum injection	23
2.6.3 Lighthill's analogy	24
2.6.4 Vortex sound	27
2.7 Acoustic energy	29
2.7.1 Introduction	29
2.7.2 Kirchhoff's equation for quiescent fluids	30
2.7.3 Acoustic energy in a non-uniform flow	33
2.7.4 Acoustic energy and vortex sound	35

3	Green's functions, impedance, and evanescent waves	38
3.1	Green's functions	38
3.1.1	Integral representations	38
3.1.2	Remarks on finding Green's functions	41
3.2	Acoustic impedance	41
3.2.1	Impedance and acoustic energy	43
3.2.2	Impedance and reflection coefficient	43
3.2.3	Impedance and causality	44
3.2.4	Impedance and surface waves	47
3.2.5	Acoustic boundary condition in the presence of mean flow	48
3.2.6	Surface waves along an impedance wall with mean flow	50
3.2.7	Instability, ill-posedness, and a regularization	52
3.3	Evanescent waves and related behaviour	54
3.3.1	An important complex square root	54
3.3.2	The Walkman	55
3.3.3	Ill-posed inverse problem	56
3.3.4	Typical plate pitch	56
3.3.5	Snell's law	56
3.3.6	Silent vorticity	59
4	One dimensional acoustics	63
4.1	Plane waves	63
4.2	Basic equations and method of characteristics	65
4.2.1	The wave equation	65
4.2.2	Characteristics	66
4.2.3	Linear behaviour	67
4.2.4	Non-linear simple waves and shock waves	71
4.3	Source terms	73
4.4	Reflection at discontinuities and abrupt changes	77
4.4.1	Jump in characteristic impedance ρc	77
4.4.2	Smooth change in pipe cross section	80
4.4.3	Orifice and high amplitude behaviour	80
4.4.4	Multiple junction	84
4.4.5	Reflection at a small air bubble in a pipe	85
4.5	Attenuation of an acoustic wave by thermal and viscous dissipation	89
4.5.1	Reflection of a plane wave at a rigid wall	89
4.5.2	Viscous laminar boundary layer	93

4.5.3	Damping in ducts with isothermal walls.	94
4.6	One dimensional Green's function	96
4.6.1	Infinite uniform tube	96
4.6.2	Finite uniform tube	97
4.7	Aero-acoustical applications	98
4.7.1	Sound produced by turbulence	98
4.7.2	An isolated bubble in a turbulent pipe flow	101
4.7.3	Reflection of a wave at a temperature inhomogeneity	102
5	Resonators and self-sustained oscillations	108
5.1	Self-sustained oscillations, shear layers and jets	108
5.2	Some resonators	114
5.2.1	Introduction	114
5.2.2	Resonance in duct segment	115
5.2.3	The Helmholtz resonator (quiescent fluid)	122
5.2.4	Non-linear losses in a Helmholtz resonator	124
5.2.5	The Helmholtz resonator in the presence of a mean flow	125
5.3	Green's function of a finite duct	126
5.4	Self-sustained oscillations of a clarinet	129
5.4.1	Introduction	129
5.4.2	Linear stability analysis	129
5.4.3	Rayleigh's Criterion	131
5.4.4	Time domain simulation	131
5.5	Some thermo-acoustics	133
5.5.1	Introduction	133
5.5.2	Modulated heat transfer by acoustic flow and Rijke tube	135
5.6	Flow induced oscillations of a Helmholtz resonator	139
6	Spherical waves	148
6.1	Introduction	148
6.2	Pulsating and translating sphere	148
6.3	Multipole expansion and far field approximation	154
6.4	Method of images and influence of walls on radiation	159
6.5	Lighthill's theory of jet noise	162
6.6	Sound radiation by compact bodies in free space	165
6.6.1	Introduction	165
6.6.2	Tailored Green's function	166
6.6.3	Curle's method	167
6.7	Sound radiation from an open pipe termination	170

7	Duct acoustics	177
7.1	General formulation	177
7.2	Cylindrical ducts	179
7.3	Rectangular ducts	183
7.4	Impedance wall	184
7.4.1	Behaviour of complex modes	184
7.4.2	Attenuation	187
7.5	Annular hard-walled duct modes in uniform mean flow	189
7.6	Behaviour of soft-wall modes and mean flow	193
7.7	Source expansion	195
7.7.1	Modal amplitudes	195
7.7.2	Rotating fan	195
7.7.3	Tyler and Sofrin rule for rotor-stator interaction	196
7.7.4	Point source in a lined flow duct	198
7.7.5	Point source in a duct wall	201
7.7.6	Vibrating duct wall	203
7.8	Reflection and transmission	204
7.8.1	A discontinuity in diameter	204
7.8.2	The iris problem	208
7.8.3	The edge condition	210
7.9	Reflection at an unflanged open end	212
8	Approximation methods	217
8.1	Webster's horn equation	218
8.2	Multiple scales	221
8.3	Helmholtz resonator with non-linear dissipation	225
8.4	Slowly varying ducts	230
8.5	Reflection at an isolated turning point	233
8.6	Ray acoustics in temperature gradient	237
8.7	Refraction in shear flow	242
8.8	Matched asymptotic expansions	243
8.9	Duct junction	250
8.10	Co-rotating line-vortices	255

9	Effects of flow and motion	260
9.1	Uniform mean flow, plane waves and edge diffraction	260
9.1.1	Lorentz or Prandtl-Glauert transformation	260
9.1.2	Plane waves	261
9.1.3	Half-plane diffraction problem	262
9.2	Moving point source and Doppler shift	264
9.3	Rotating monopole and dipole with moving observer	266
9.4	Ffowcs Williams & Hawkings equation for moving bodies	269
	Appendix	274
A	Integral laws and related results	274
A.1	Reynolds' transport theorem	274
A.2	Conservation laws	274
A.3	Normal vectors of level surfaces	276
A.4	Vector identities and theorems	276
B	Orders of magnitude: O and o.	278
C	Fourier transforms and generalized functions	279
C.1	Fourier transforms	279
C.1.1	Causality condition	282
C.1.2	Phase and group velocity	286
C.2	Generalized functions	287
C.2.1	Introduction	287
C.2.2	Formal definition	287
C.2.3	The delta function and other examples	288
C.2.4	Derivatives	289
C.2.5	Fourier transforms	290
C.2.6	Products	291
C.2.7	Higher dimensions and Green's functions	291
C.2.8	Surface distributions	292
C.3	Fourier series	294
C.3.1	The Fast Fourier Transform	297
D	Bessel functions	299
E	Free field Green's functions	307

F	Summary of equations for fluid motion	308
F.1	Conservation laws and constitutive equations	308
F.2	Acoustic approximation	309
F.2.1	Inviscid and isentropic	309
F.2.2	Perturbations of an inviscid non-heat conducting mean flow	311
F.2.3	Myers' Energy Corollary	312
F.2.4	Zero mean flow	312
F.2.5	Time harmonic	312
F.2.6	Irrotational isentropic flow	313
F.2.7	Uniform mean flow	313
F.2.8	Parallel mean flow	315
G	Answers to exercises.	316
	Bibliography	327
	Index	339

Preface

Acoustics was originally the study of small pressure waves in air which can be detected by the human ear: *sound*. The scope of acoustics has been extended to higher and lower frequencies: ultrasound and infrasound. Structural vibrations are now often included in acoustics. Also the perception of sound is an area of acoustical research. In our present introduction we will limit ourselves to the original definition and to the propagation in fluids like air and water. In such a case acoustics is a part of *fluid dynamics*.

A major problem of fluid dynamics is that the equations of motion are non-linear. This implies that an exact general solution of these equations is not available. Acoustics is a first order approximation in which non-linear effects are neglected. In classical acoustics the generation of sound is considered to be a boundary condition problem. The sound generated by a loudspeaker or any unsteady movement of a solid boundary are examples of the sound generation mechanism in classical acoustics. In the present course we will also include some *aero-acoustic* processes of sound generation: heat transfer and turbulence. Turbulence is a chaotic motion dominated by non-linear convective forces. An accurate deterministic description of turbulent flows is not available. The key of the famous Lighthill theory of sound generation by turbulence is the use of an integral equation which is much more suitable to introducing approximations than a differential equation. We therefore discuss in some detail the use of Green's functions to derive integral equations.

Next to Lighthill's approach which leads to order of magnitude estimate of sound production by complex flows we also describe briefly the theory of vortex sound which can be used when a simple deterministic description is available for a flow at low Mach numbers (for velocities small compared to the speed of sound).

In contrast to most textbooks we have put more emphasis on duct acoustics, both in relation to its generation by pipe flows, and with respect to more advanced theory on modal expansions and approximation methods. This particular choice is motivated by industrial applications like aircraft engines and gas transport systems.

This course is inspired by the book of Dowling and Ffowcs Williams: "Sound and Sources of Sound" [55]. We also used the lecture notes of the course on aero- and hydroacoustics given by Crighton, Dowling, Ffowcs Williams, Heckl and Leppington [45].

Among the literature on acoustics the book of Pierce [183] is an excellent introduction available for a low price from the Acoustical Society of America.

In the preparation of the lecture notes we consulted various books which cover different aspects of the problem [16, 18, 20, 40, 51, 73, 90, 96, 102, 116, 126, 153, 168, 176, 179, 227, 241].

1 Some fluid dynamics

1.1 Conservation laws and constitutive equations

In fluid dynamics we consider gas and liquids as a continuum: we assume that we can define a “fluid particle” which is large compared to molecular scales but small compared to the other length scales in our problem. We can describe the fluid motion by using the laws of mass, momentum and energy conservation applied to an elementary fluid particle. The integral form of the equations of conservation are given in Appendix A. Applying these laws to an infinitesimal volume element yields the equations in differential form, which assumes that the fluid properties are continuous and that derivatives exist. In some cases we will therefore use the more general integral laws. A conservation law in differential form may be written as the time derivative of the density of a property plus the divergence of the flux of this property being equal to the source per unit volume of this property in the particle [16, 176, 183, 227, 241].

In differential form¹ we have for the mass conservation:

$$\frac{\partial \rho}{\partial t} + \nabla \cdot (\rho \mathbf{v}) = m, \quad \text{or} \quad \frac{\partial \rho}{\partial t} + \frac{\partial}{\partial x_i} (\rho v_i) = m, \quad (1.1)$$

where ρ is the fluid density and $\mathbf{v} = (v_i)$ is the flow velocity at position $\mathbf{x} = (x_i)$ and time t . In principle we will consider situations where mass is conserved and so in general $m = 0$. The mass source term m can, however, be used as a representation for a complex process which we do not want to describe in detail. For example, the action of a pulsating sphere or of heat injection may be well approximated by such a mass source term.

The momentum conservation law is²:

$$\frac{\partial}{\partial t} (\rho \mathbf{v}) + \nabla \cdot (\mathbf{P} + \rho \mathbf{v} \mathbf{v}) = \mathbf{f} + m \mathbf{v}, \quad \text{or} \quad \frac{\partial}{\partial t} (\rho v_i) + \frac{\partial}{\partial x_j} (P_{ji} + \rho v_j v_i) = f_i + m v_i, \quad (1.2)$$

where $\mathbf{f} = (f_i)$ is an external force density (like the gravitational force), $\mathbf{P} = (P_{ij})$ is minus the fluid stress tensor, and the issuing mass adds momentum by an amount of $m \mathbf{v}$. In some cases one can represent the effect of an object like a propeller by a force density \mathbf{f} acting on the fluid as a source of momentum.

When we apply equation (1.1) we obtain³ for (1.2)

$$\rho \frac{\partial \mathbf{v}}{\partial t} + \nabla \cdot \mathbf{P} + \rho \mathbf{v} \cdot \nabla \mathbf{v} = \mathbf{f}, \quad \text{or} \quad \rho \frac{\partial v_i}{\partial t} + \frac{\partial P_{ji}}{\partial x_j} + \rho v_j \frac{\partial v_i}{\partial x_j} = f_i. \quad (1.3)$$

¹For convenience later we present the basic conservation laws here both in the Gibbs notation and the Cartesian tensor notation. In the latter, the summation over the values 1,2,3 is understood with respect to all suffixes which appear twice in a given term. See also the appendix of [16].

²The dyadic product of two vectors \mathbf{v} and \mathbf{w} is the tensor $\mathbf{vw} = (v_i w_j)$.

³ $(\rho \mathbf{v})_t + \nabla \cdot (\rho \mathbf{v} \mathbf{v}) = \rho_t \mathbf{v} + \rho \mathbf{v}_t + \nabla \cdot (\rho \mathbf{v}) \mathbf{v} + \rho (\mathbf{v} \cdot \nabla) \mathbf{v} = [\rho_t + \nabla \cdot (\rho \mathbf{v})] \mathbf{v} + \rho [\mathbf{v}_t + (\mathbf{v} \cdot \nabla) \mathbf{v}]$.

2 1 Some fluid dynamics

The fluid stress tensor is related to the pressure p and the viscous stress tensor $\boldsymbol{\tau} = (\tau_{ij})$ by the relationship:

$$\mathbf{P} = p\mathbf{I} - \boldsymbol{\tau}, \quad \text{or} \quad P_{ij} = p\delta_{ij} - \tau_{ij} \quad (1.4)$$

where $\mathbf{I} = (\delta_{ij})$ is the unit tensor, and δ_{ij} the Kronecker⁴ delta. In most of the applications which we consider in the sequel, we can neglect the viscous stresses. When this is not the case one usually assumes a relationship between $\boldsymbol{\tau}$ and the deformation rate of the fluid element, expressed in the rate-of-strain tensor $\nabla\mathbf{v} + (\nabla\mathbf{v})^T$. It should be noted that a characteristic of a fluid is that it opposes a rate of deformation, rather than the deformation itself, as in the case of a solid. When this relation is linear the fluid is described as Newtonian and the resulting momentum conservation equation is referred to as the Navier-Stokes equation. Even with such a drastic simplification, for compressible fluids as we consider in acoustics, the equations are quite complicated. A considerable simplification is obtained when we assume Stokes' hypothesis, that the fluid is in local thermodynamic equilibrium, so that the pressure p and the thermodynamic pressure are equivalent. In such a case we have:

$$\boldsymbol{\tau} = \eta(\nabla\mathbf{v} + (\nabla\mathbf{v})^T) - \frac{2}{3}\eta(\nabla\cdot\mathbf{v})\mathbf{I}, \quad \text{or} \quad \tau_{ij} = \eta\left(\frac{\partial v_i}{\partial x_j} + \frac{\partial v_j}{\partial x_i}\right) - \frac{2}{3}\eta\left(\frac{\partial v_k}{\partial x_k}\right)\delta_{ij} \quad (1.5)$$

where η is the dynamic viscosity. Equation (1.5) is what we call a constitutive equation. The viscosity η is determined experimentally and depends in general on the temperature T and the pressure p . At high frequencies the assumption of thermodynamic equilibrium may partially fail resulting in a dissipation related to volume changes $\nabla\cdot\mathbf{v}$ which is described with a volume viscosity parameter not simply related to η [251, 183]. These effects are also significant in the propagation of sound in dusty gases or in air over large distances [241].

In general ($m = 0$) the energy conservation law is given by ([16, 176, 241]):

$$\frac{\partial}{\partial t}\rho\left(e + \frac{1}{2}v^2\right) + \nabla\cdot\left(\rho\mathbf{v}\left(e + \frac{1}{2}v^2\right)\right) = -\nabla\cdot\mathbf{q} - \nabla\cdot(p\mathbf{v}) + \nabla\cdot(\boldsymbol{\tau}\cdot\mathbf{v}) + \mathbf{f}\cdot\mathbf{v} \quad (1.6)$$

or

$$\frac{\partial}{\partial t}\rho\left(e + \frac{1}{2}v^2\right) + \frac{\partial}{\partial x_i}\left(\rho v_i\left(e + \frac{1}{2}v^2\right)\right) = -\frac{\partial q_i}{\partial x_i} - \frac{\partial}{\partial x_i}(p v_i) + \frac{\partial}{\partial x_i}(\tau_{ij} v_j) + f_i v_i$$

where $v = |\mathbf{v}|$, e is the internal energy per unit of mass⁵ and \mathbf{q} is the heat flux due to heat conduction. A commonly used linear constitutive equation for \mathbf{q} is Fourier's law:

$$\mathbf{q} = -K\nabla T, \quad (1.7)$$

where K is the heat conductivity which depends on the pressure p and temperature T . Using the fundamental law of thermodynamics for a reversible process:

$$Tds = de + p d(\rho^{-1}) \quad (1.8)$$

⁴ $\delta_{ij} = 1$ if $i = j$, $\delta_{ij} = 0$ if $i \neq j$.

⁵ We call this *the specific internal energy*, and simply *the energy* when there is no ambiguity.

and the equation for mechanical energy, obtained by taking the inner product of the momentum conservation law (equation 1.2) with \mathbf{v} , we obtain the equation for the entropy⁶

$$\rho T \left(\frac{\partial s}{\partial t} + \mathbf{v} \cdot \nabla s \right) = -\nabla \cdot \mathbf{q} + \boldsymbol{\tau} : \nabla \mathbf{v}, \quad \text{or} \quad \rho T \left(\frac{\partial s}{\partial t} + v_i \frac{\partial s}{\partial x_i} \right) = -\frac{\partial q_i}{\partial x_i} + \tau_{ij} \frac{\partial v_j}{\partial x_i} \quad (1.9)$$

where s is the specific entropy or entropy per unit of mass. When heat conduction $\nabla \cdot \mathbf{q}$ and viscous dissipation $\boldsymbol{\tau} : \nabla \mathbf{v}$ may be neglected, the flow is *isentropic*⁷. This means that the entropy s of a fluid particle remains constant:

$$\frac{\partial s}{\partial t} + \mathbf{v} \cdot \nabla s = 0. \quad (1.10)$$

Except for regions near walls this approximation will appear to be quite reasonable for most of the applications considered. If initially the entropy is equal to a constant value s_0 throughout the fluid, it retains this value, and we have simply a flow of uniform and constant entropy $s = s_0$. Note that some authors define this type of flow isentropic.

Equations (1.1–1.10) still contain more unknowns than equations. As closure condition we introduce an additional constitutive equation, for example $e = e(\rho, s)$, which implies with equation (1.8):

$$p = \rho^2 \left(\frac{\partial e}{\partial \rho} \right)_s \quad (1.11a)$$

$$T = \left(\frac{\partial e}{\partial s} \right)_\rho \quad (1.11b)$$

In many cases we will specify an equation of state $p = p(\rho, s)$ rather than $e = e(\rho, s)$. In differential form this becomes:

$$dp = c^2 d\rho + \left(\frac{\partial p}{\partial s} \right)_\rho ds \quad (1.12)$$

where

$$c^2 = \left(\frac{\partial p}{\partial \rho} \right)_s \quad (1.13)$$

is the square of the isentropic speed of sound c . While equation (1.13) is a definition of the thermodynamic variable $c(\rho, s)$, we will see that c indeed is a measure for the speed of sound. When the same equation of state $c(\rho, s)$ is valid for the entire flow we say that the fluid is *homogeneous*. When the density depends only on the pressure we call the fluid *barotropic*. When the fluid is homogeneous and the entropy uniform ($ds = 0$) we call the flow *homentropic*.

⁶ $\boldsymbol{\tau} : \nabla \mathbf{v} = \nabla \cdot (\boldsymbol{\tau} \cdot \mathbf{v}) - \mathbf{v} \cdot (\nabla \cdot \boldsymbol{\tau})$ since $\boldsymbol{\tau}$ is symmetric. Note the convention $(\nabla \mathbf{v})_{ij} = \frac{\partial}{\partial x_i} v_j$.

⁷When heat transfer is negligible, the flow is *adiabatic*. It is isentropic when it is adiabatic AND reversible.

4 1 Some fluid dynamics

In the following chapters we will use the heat capacity at constant volume C_V which is defined for a reversible process by

$$C_V = \left(\frac{\partial e}{\partial T} \right)_V. \quad (1.14)$$

For an *ideal* gas the energy e is a function of the temperature only

$$e(T) = \int_0^T C_V dT. \quad (1.15)$$

For an ideal gas with constant heat capacities we will often use the simplified relation

$$e = C_V T. \quad (1.16)$$

We call this a *perfect gas*. Expressions for the pressure p and the speed of sound c will be given in section 2.3. A justification for some of the simplifications introduced will be given in chapter 2 where we will consider the order of magnitude of various effects and derive the wave equation. Before going further we consider some useful approximations and some different notations for the basic equations given above.

1.2 Approximations and alternative forms of the conservation laws for ideal fluids

Using the definition of convective (or total) derivative⁸ D/Dt :

$$\frac{D}{Dt} = \frac{\partial}{\partial t} + \mathbf{v} \cdot \nabla \quad (1.17)$$

we can write the mass conservation law (1.1) in the absence of a source ($m = 0$) in the form:

$$\frac{1}{\rho} \frac{D\rho}{Dt} = -\nabla \cdot \mathbf{v} \quad (1.18)$$

which clearly shows that the divergence of the velocity $\nabla \cdot \mathbf{v}$ is a measure for the relative change in density of a fluid particle. Indeed, the divergence corresponds to the dilatation rate⁹ of the fluid particle which vanishes when the density is constant. Hence, if we can neglect density changes, the mass conservation law reduces to:

$$\nabla \cdot \mathbf{v} = 0. \quad (1.19)$$

⁸The total derivative Df/Dt of a function $f = f(x_i, t)$ and velocity field v_i denotes just the ordinary time derivative df/dt of $f(x_i(t), t)$ for a path $x_i = x_i(t)$ defined by $\dot{x}_i = v_i$, *i.e.* moving with a particle along $x_i = x_i(t)$.

⁹Dilatation rate = rate of relative volume change.

This is the continuity equation for *incompressible* fluids. The mass conservation law (1.18) simply expresses the fact that a fluid particle has a constant mass.

We can write the momentum conservation law for a frictionless fluid ($\nabla \cdot \boldsymbol{\tau}$ negligible) as:

$$\rho \frac{D\mathbf{v}}{Dt} = -\nabla p + \mathbf{f}. \quad (1.20)$$

This is Euler's equation, which corresponds to the second law of Newton (force = mass \times acceleration) applied to a specific fluid element with a constant mass. The mass remains constant because we consider a specific material element. In the absence of friction there are no tangential stresses acting on the surface of the fluid particle. The motion is induced by the normal stresses (pressure force) $-\nabla p$ and the bulk forces \mathbf{f} . The corresponding energy equation for a gas is

$$\frac{Ds}{Dt} = 0 \quad (1.10)$$

which states that the entropy of a particle remains constant. This is a consequence of the fact that heat conduction is negligible in a frictionless gas flow. The heat and momentum transfer are governed by the same processes of molecular collisions. The equation of state commonly used in an isentropic flow is

$$\frac{Dp}{Dt} = c^2 \frac{D\rho}{Dt} \quad (1.21)$$

where $c = c(\rho, s)$, a function of ρ and s , is measured or derived theoretically. Note that in this equation

$$c^2 = \left(\frac{\partial p}{\partial \rho} \right)_s \quad (1.13)$$

is not necessarily a constant.

Under reasonably general conditions [2, 152] the velocity \mathbf{v} , like any vector field, can be split into an irrotational part and a solenoidal part:

$$\mathbf{v} = \nabla\varphi + \nabla \times \boldsymbol{\Psi}, \quad \nabla \cdot \boldsymbol{\Psi} = 0, \quad \text{or} \quad v_i = \frac{\partial\varphi}{\partial x_i} + \epsilon_{ijk} \frac{\partial\Psi_k}{\partial x_j}, \quad \frac{\partial\Psi_j}{\partial x_j} = 0, \quad (1.22)$$

where φ is a scalar velocity potential, $\boldsymbol{\Psi} = (\Psi_i)$ a vectorial velocity potential or vector stream function, and ϵ_{ijk} the permutation symbol¹⁰. A flow described by the scalar potential only ($\mathbf{v} = \nabla\varphi$) is called a potential flow. This is an important concept because the acoustic aspects of the flow are linked

¹⁰ $\epsilon_{ijk} = \begin{cases} +1 & \text{if } ijk = 123, 231, \text{ or } 312, \\ -1 & \text{if } ijk = 321, 132, \text{ or } 213, \\ 0 & \text{if any two indices are alike} \end{cases}$ Note that $\mathbf{v} \times \mathbf{w} = (\epsilon_{ijk} v_j w_k)$.

6 1 Some fluid dynamics

to φ . This is seen from the fact that $\nabla \cdot (\nabla \times \Psi) = 0$ so that the compressibility of the flow is described by the scalar potential φ . We have from (1.18):

$$\frac{1}{\rho} \frac{D\rho}{Dt} = -\nabla^2 \varphi. \quad (1.23)$$

From this it is obvious that the flow related to the acoustic field is an irrotational flow. A useful definition of the acoustic field is therefore: the unsteady component of the irrotational flow field $\nabla \varphi$. The vector stream function describes the vorticity $\boldsymbol{\omega} = \nabla \times \mathbf{v}$ in the flow, because $\nabla \times \nabla \varphi = 0$. Hence we have¹¹:

$$\boldsymbol{\omega} = \nabla \times (\nabla \times \Psi) = -\nabla^2 \Psi. \quad (1.24)$$

It can be shown that the vorticity $\boldsymbol{\omega}$ corresponds to twice the angular velocity $\boldsymbol{\Omega}$ of a fluid particle. When $\rho = \rho(p)$ is a function of p only, like in a homentropic flow (uniform constant entropy $ds = 0$), and in the absence of tangential forces due to the viscosity ($\boldsymbol{\tau} = 0$), we can eliminate the pressure and density from Euler's equation by taking the curl of this equation¹², to obtain

$$\frac{\partial}{\partial t} \boldsymbol{\omega} + \mathbf{v} \cdot \nabla \boldsymbol{\omega} = \boldsymbol{\omega} \cdot \nabla \mathbf{v} - \boldsymbol{\omega} \nabla \cdot \mathbf{v} + \nabla \times (\mathbf{f}/\rho). \quad (1.25a)$$

If we apply the mass conservation equation (1.1) we get

$$\rho \left(\frac{\partial}{\partial t} + \mathbf{v} \cdot \nabla \right) \left(\frac{\boldsymbol{\omega}}{\rho} \right) = \boldsymbol{\omega} \cdot \nabla \mathbf{v} - \frac{m\boldsymbol{\omega}}{\rho} + \nabla \times \left(\frac{\mathbf{f}}{\rho} \right). \quad (1.25b)$$

We see that vorticity of the particle is changed either by stretching¹³, by a mass source in the presence of vorticity, or by a non-conservative external force field [240, 113]. In a two-dimensional incompressible flow ($\nabla \cdot \mathbf{v} = 0$), with velocity $\mathbf{v} = (v_x, v_y, 0)$, the vorticity $\boldsymbol{\omega} = (0, 0, \omega_z)$ is not affected by stretching because there is no flow component in the direction of $\boldsymbol{\omega}$. Apart from the source terms $-m\boldsymbol{\omega}/\rho$ and $\nabla \times (\mathbf{f}/\rho)$, the momentum conservation law reduces to a purely kinematic law. Hence we can say that Ψ (and $\boldsymbol{\omega}$) is linked to the kinematic aspects of the flow.

Using the definition of the specific enthalpy i :

$$i = e + \frac{p}{\rho} \quad (1.26)$$

and the fundamental law of thermodynamics (1.8) we find for a homentropic flow (homogeneous fluid with $ds = 0$):

$$di = \frac{dp}{\rho}. \quad (1.27)$$

¹¹ For any vector field \mathbf{A} : $\nabla \times (\nabla \times \mathbf{A}) = \nabla(\nabla \cdot \mathbf{A}) - \nabla^2 \mathbf{A}$.

¹² $\nabla \times (\mathbf{v} \cdot \nabla \mathbf{v}) = \boldsymbol{\omega} \nabla \cdot \mathbf{v} - \boldsymbol{\omega} \cdot \nabla \mathbf{v} + \mathbf{v} \cdot \nabla \boldsymbol{\omega}$, $\nabla \times (\rho^{-1} \nabla p) = -\rho^{-2} (\nabla \rho \times \nabla p) = -\rho^{-1} \rho'(p) (\nabla p \times \nabla p) = 0$.

¹³ The stretching of an incompressible particle of fluid implies by conservation of angular momentum an increase of rotation, because the particle's lateral dimension is reduced. In a viscous flow tangential forces due to the viscous stress do change the fluid particle angular momentum, because they exert a torque on the fluid particle.

Hence we can write Euler's equation (1.20) as:

$$\frac{D\mathbf{v}}{Dt} = -\nabla i + \frac{1}{\rho}\mathbf{f}. \quad (1.28)$$

We define the total specific enthalpy B (Bernoulli constant) of the flow by:

$$B = i + \frac{1}{2}v^2. \quad (1.29)$$

The total enthalpy B corresponds to the enthalpy which is reached in a hypothetical fully reversible process when the fluid particle is decelerated down to a zero velocity (reservoir state). Using the vector identity¹⁴:

$$(\mathbf{v} \cdot \nabla)\mathbf{v} = \frac{1}{2}\nabla v^2 + \boldsymbol{\omega} \times \mathbf{v} \quad (1.30)$$

we can write Euler's equation (1.20) in Crocco's form:

$$\frac{\partial \mathbf{v}}{\partial t} = -\nabla B - \boldsymbol{\omega} \times \mathbf{v} + \frac{1}{\rho}\mathbf{f} \quad (1.31)$$

which will be used when we consider the sound production by vorticity. The acceleration $\boldsymbol{\omega} \times \mathbf{v}$ corresponds to the acceleration of Coriolis experienced by an observer moving with the particle which is rotating at an angular velocity of $\boldsymbol{\Omega} = \frac{1}{2}\boldsymbol{\omega}$.

When the flow is irrotational in the absence of external force ($\mathbf{f} = 0$), with $\mathbf{v} = \nabla\varphi$ and hence $\boldsymbol{\omega} = \nabla \times \nabla\varphi = 0$, we can rewrite (1.28) into:

$$\frac{\partial \nabla\varphi}{\partial t} + \nabla B = 0,$$

which may be integrated to Bernoulli's equation:

$$\frac{\partial \varphi}{\partial t} + B = g(t), \quad (1.32a)$$

or

$$\frac{\partial \varphi}{\partial t} + \frac{1}{2}v^2 + \int \frac{dp}{\rho} = g(t) \quad (1.32b)$$

where $g(t)$ is a function determined by boundary conditions. As only the gradient of φ is important ($\mathbf{v} = \nabla\varphi$) we can, without loss of generality, absorb $g(t)$ into φ and use $g(t) = 0$. In acoustics the Bernoulli equation will appear to be very useful. We will see in section 2.7 that for a homentropic flow we can write the energy conservation law (1.10) in the form:

$$\frac{\partial}{\partial t}(\rho B - p) + \nabla \cdot (\rho \mathbf{v} B) = \mathbf{f} \cdot \mathbf{v}, \quad (1.33a)$$

or

$$\frac{\partial}{\partial t} \left(\rho \left(e + \frac{1}{2}v^2 \right) \right) + \nabla \cdot (\rho \mathbf{v} B) = \mathbf{f} \cdot \mathbf{v}. \quad (1.33b)$$

¹⁴ $[(\mathbf{v} \cdot \nabla)\mathbf{v}]_i = \sum_j v_j \frac{\partial}{\partial x_j} v_i$

8 1 Some fluid dynamics

Exercises

- a) Derive Euler's equation (1.20) from the conservation laws (1.1) and (1.2).
- b) Derive the entropy conservation law (1.10) from the energy conservation law (1.6) and the second law of thermodynamics (1.8).
- c) Derive Bernoulli's equation (1.32b) from Crocco's equation (1.31).
- d) Is the trace $\frac{1}{3}P_{ii}$ of the stress tensor P_{ij} always equal to the thermodynamic pressure $p = (\partial e / \partial \rho^{-1})_s$?
- e) Consider, as a model for a water pistol, a piston pushing with a constant acceleration a water from a tube 1 with surface area A_1 and length ℓ_1 through a tube 2 of surface A_2 and length ℓ_2 . Calculate the force necessary to move the piston if the water compressibility can be neglected and the water forms a free jet at the exit of tube 2. Neglect the non-uniformity of the flow in the transition region between the two tubes. What is the ratio of the pressure drop over the two tubes at $t = 0$?

2 Wave equation, speed of sound, and acoustic energy

2.1 Order of magnitude estimates

Starting from the conservation laws and the constitutive equations given in section 1.2 we will obtain after linearization a wave equation in the next section. This implies that we can justify the approximation introduced in section 1.2, (homotropic flow), and that we can show that in general, sound is a small perturbation of a steady state, so that second order effects can be neglected. We therefore consider here some order of magnitude estimates of the various phenomena involved in sound propagation.

We have defined sound as a pressure perturbation p' which propagates as a wave and which is detectable by the human ear. We limit ourselves to air and water. In dry air at 20°C the speed of sound c is 344 m/s, while in water a typical value of 1500 m/s is found. In section 2.3 we will discuss the dependence of the speed of sound on various parameters (such as temperature, *etc.*). For harmonic pressure fluctuations, the typical range of frequency of the human ear is:

$$20 \text{ Hz} \leq f \leq 20 \text{ kHz.} \quad (2.1)$$

The maximum sensitivity of the ear is around 3 kHz, (which corresponds to a policeman's whistle!). Sound involves a large range of power levels:

- when whispering we produce about 10^{-10} Watts,
- when shouting we produce about 10^{-5} Watts,
- a jet airplane at take off produces about 10^5 Watts.

In view of this large range of power levels and because our ear has roughly a logarithmic sensitivity we commonly use the decibel scale to measure sound levels. The Sound Power Level (PWL) is given in decibel (dB) by:

$$\text{PWL} = 10 \log_{10}(\text{Power}/10^{-12} \text{ W}). \quad (2.2)$$

The Sound Pressure Level (SPL) is given by:

$$\text{SPL} = 20 \log_{10}(p'_{rms}/p_{ref}) \quad (2.3)$$

10 2 Wave equation, speed of sound, and acoustic energy

where p'_{rms} is the root mean square of the acoustic pressure fluctuations p' , and where $p_{ref} = 2 \cdot 10^{-5}$ Pa in air and $p_{ref} = 10^{-6}$ Pa in other media. The sound intensity I is defined as the energy flux (power per surface area) corresponding to sound propagation. The Intensity Level (IL) is given by:

$$IL = 10 \log_{10}(I/10^{-12} \text{ W/m}^2). \quad (2.4)$$

The reference pressure level in air $p_{ref} = 2 \cdot 10^{-5}$ Pa corresponds to the threshold of hearing at 1 kHz for a typical human ear. The reference intensity level $I_{ref} = 10^{-12} \text{ W/m}^2$ is related to this $p'_{ref} = 2 \cdot 10^{-5}$ Pa in air by the relationship valid for progressive plane waves:

$$I = p'^2_{rms} / \rho_0 c_0 \quad (2.5)$$

where $\rho_0 c_0 = 4 \cdot 10^2 \text{ kg/m}^2\text{s}$ for air under atmospheric conditions. Equation (2.5) will be derived later. The threshold of pain¹ (140 dB) corresponds in air to pressure fluctuations of $p'_{rms} = 200$ Pa. The corresponding relative density fluctuations ρ'/ρ_0 are given at atmospheric pressure $p_0 = 10^5$ Pa by:

$$\rho'/\rho_0 = p'/\gamma p_0 \leq 10^{-3} \quad (2.6)$$

where $\gamma = C_P/C_V$ is the ratio of specific heats at constant pressure and volume respectively. In general, by defining the speed of sound following equation 1.13, the relative density fluctuations are given by:

$$\frac{\rho'}{\rho_0} = \frac{1}{\rho_0 c_0^2} p' = \frac{1}{\rho_0} \left(\frac{\partial \rho}{\partial p} \right)_s p'. \quad (2.7)$$

The factor $1/\rho_0 c_0^2$ is the adiabatic bulk compressibility modulus of the medium. Since for water $\rho_0 = 10^3 \text{ kg/m}^3$ and $c_0 = 1.5 \cdot 10^3 \text{ m/s}$ we see that $\rho_0 c_0^2 \simeq 2.2 \cdot 10^9 \text{ Pa}$, so that a compression wave of 10 bar corresponds to relative density fluctuations of order 10^{-3} in water. Linear theory will therefore apply to such compression waves. When large expansion waves are created in water the pressure can decrease below the saturation pressure of the liquid and cavitation bubbles may appear, which results in strongly non-linear behaviour. On the other hand, however, since the formation of bubbles in pure water is a slow process, strong expansion waves (negative pressures of the order of 10^3 bar!) can be sustained in water before cavitation appears.

For acoustic waves in a stagnant medium, a progressive plane wave involves displacement of fluid particles with a velocity u' which is given by (as we will see in equations 2.20a, 2.20b):

$$u' = p'/\rho_0 c_0. \quad (2.8)$$

The factor $\rho_0 c_0$ is called the characteristic impedance of the fluid. By dividing (2.8) by c_0 we see by using (1.13) in the form $p' = c_0^2 \rho'$ that the acoustic Mach number u'/c_0 is a measure for the relative

¹The SPL which we can only endure for a very short period of time without the risk of permanent ear damage.

density variation ρ'/ρ_0 . In the absence of mean flow ($u_0 = 0$) this implies that a convective term such as $\rho(\mathbf{v} \cdot \nabla)\mathbf{v}$ in the momentum conservation (1.20) is of second order and can be neglected in a linear approximation.

The amplitude of the fluid particle displacement δ corresponding to harmonic wave propagation at a circular frequency $\omega = 2\pi f$ is given by:

$$\delta = |u'|/\omega. \tag{2.9}$$

Hence, for $f = 1$ kHz we have in air:

$$\begin{aligned} \text{SPL} = 140 \text{ dB}, & \quad p'_{rms} = 2 \cdot 10^2 \text{ Pa}, & \quad u' = 5 \cdot 10^{-1} \text{ m/s}, & \quad \delta = 8 \cdot 10^{-5} \text{ m}, \\ \text{SPL} = 0 \text{ dB}, & \quad p'_{rms} = 2 \cdot 10^{-5} \text{ Pa}, & \quad u' = 5 \cdot 10^{-8} \text{ m/s}, & \quad \delta = 1 \cdot 10^{-11} \text{ m}. \end{aligned}$$

In order to justify a linearization of the equations of motion, the acoustic displacement δ should be small compared to the characteristic length scale L in the geometry considered. In other words, the acoustical Strouhal number $Str_a = L/\delta$ should be large. In particular, if δ is larger than the radius of curvature R of the wall at edges the flow will separate from the wall resulting into vortex shedding. So a small acoustical Strouhal number R/δ implies that non-linear effects due to vortex shedding are important. This is a strongly non-linear effect which becomes important with decreasing frequency, because δ increases when ω decreases.

We see from the data given above that the particle displacement δ can be significantly smaller than the molecular mean free path $\bar{\ell}$ which in air at atmospheric pressure is about $5 \cdot 10^{-8}$ m. It should be noted that a continuum hypothesis as assumed in chapter 1 does apply to sound even at such low amplitudes because δ is *not* the relevant length scale. The continuum hypothesis is valid if we can define an air particle which is small compared to the dimensions of our *measuring device* (eardrum, diameter $D = 5$ mm) or to the *wave length* λ , but large compared to the mean free path $\bar{\ell} = 5 \cdot 10^{-8}$ m. It is obvious that we can satisfy this condition since for $f = 20$ kHz the wave length:

$$\lambda = c_0/f \tag{2.10}$$

is still large ($\lambda \simeq 1.7$ cm) compared to $\bar{\ell}$. In terms of our ear drum we can say that although a displacement of $\delta = 10^{-11}$ m of an individual molecule cannot be measured, the same displacement averaged over a large amount of molecules at the ear drum can be heard as sound.

It appears that for harmonic signals of frequency $f = 1$ kHz the threshold of hearing $p'_{ref} = 2 \cdot 10^{-5}$ Pa corresponds to the thermal fluctuations p'_{th} of the atmospheric pressure p_0 detected by our ear. This result is obtained by calculating the number of molecules N colliding within half an oscillation period with our eardrum²: $N \sim nD^2c_0/2f$, where n is the air molecular number density³. As $N \simeq 10^{20}$ and $p'_{th} \simeq p_0/\sqrt{N}$ we find that $p'_{th} \simeq 10^{-5}$ Pa.

²The thermal velocity of molecules may be estimated to be equal to c_0 .

³ n is calculated for an ideal gas with molar mass M from: $n = \mathcal{N}_A \rho/M = \mathcal{N}_A p/MRT = p/RT$ (see section 2.3) where \mathcal{N}_A is the Avogadro number

In gases the continuum hypothesis is directly coupled to the assumption that the wave is isentropic and frictionless. Both the kinematic viscosity $\nu = \eta/\rho$ and the heat diffusivity $a = K/\rho C_p$ of a gas are typically of the order of $c\bar{\ell}$, the product of sound speed c and mean free path $\bar{\ell}$. This is related to the fact that c is in a gas a measure for the random (thermal) molecular velocities that we know macroscopically as heat and momentum diffusion. Therefore, in gases the absence of friction goes together with isentropy. Note that this is not the case in liquids. Here, isothermal rather than isentropic wave propagation is common for normal frequencies.

As a result from this relation $\nu \sim c\bar{\ell}$, the ratio between the acoustic wave length λ and the mean free path $\bar{\ell}$, which is an acoustic Knudsen number, can also be interpreted as an acoustic Fourier number:

$$\frac{\lambda}{\bar{\ell}} = \frac{\lambda c}{\nu} = \frac{\lambda^2 f}{\nu}. \quad (2.11)$$

This relates the diffusion length $(\nu/f)^{1/2}$ for viscous effects to the acoustic wave length λ . Moreover, this ratio can also be considered as an unsteady Reynolds number Re_t :

$$Re_t = \frac{\left| \rho \frac{\partial u'}{\partial t} \right|}{\left| \eta \frac{\partial^2 u'}{\partial x^2} \right|} \sim \frac{\lambda^2 f}{\nu}, \quad (2.12)$$

which is for a plane acoustic wave just the ratio between inertial and viscous forces in the momentum conservation law. For air $\nu = 1.5 \cdot 10^{-5} \text{ m}^2/\text{s}$ so that for $f = 1 \text{ kHz}$ we have $Re_t = 4 \cdot 10^7$. We therefore expect viscosity to play a significant rôle only if the sound propagates over distances of 10^7 wave lengths or more ($3 \cdot 10^3 \text{ km}$ for $f = 1 \text{ kHz}$). In practice the kinematic viscosity appears to be a rather unimportant effect in the attenuation of waves in free space. The main dissipation mechanism is the departure from thermodynamic equilibrium, due to the relatively long relaxation times of molecular motion associated to the internal degrees of freedom (rotation, vibration). This effect is related to the so-called bulk or volume viscosity which we quoted in chapter 1.

In general the attenuation of sound waves increases with frequency. This explains why we hear the lower frequencies of an airplane more and more accentuated as it flies from near the observation point (e.g. the airport) away to large distances (10 km).

In the presence of walls the viscous dissipation and thermal conduction will result into a significant attenuation of the waves over quite short distances. The amplitude of a plane wave travelling along a tube of cross-sectional surface area A and perimeter L_p will decrease with the distance x along the tube following an exponential factor $e^{-\alpha x}$, where the damping coefficient α is given at reasonably high frequencies ($A/L_p \gg \sqrt{\nu/\omega}$ but $\omega\sqrt{A}/c_0 < 1$) by [183]:

$$\alpha = \frac{L_p}{2Ac} \sqrt{\pi f \nu} \left(1 + \frac{\gamma - 1}{\sqrt{\nu/a}} \right). \quad (2.13)$$

(This equation will be derived in section 4.5.) For air $\gamma = C_P/C_V = 1.4$ while $v/a = 0.72$. For a musical instrument at 400 Hz, such as the clarinet, $\alpha = 0.05\text{m}^{-1}$ so that a frictionless approximation is not a very accurate but still a fair first approximation. As a general rule, at low amplitudes the viscous dissipation is dominant in woodwind instruments at the fundamental (lowest) playing frequency. At higher frequencies the radiation losses which we will discuss later (chapter 6) become dominant. Similar arguments hold for water, except that because the temperature fluctuations due to compression are negligible, the heat conduction is not significant even in the presence of walls ($\gamma = 1$).

A small ratio ρ'/ρ_0 of acoustic density fluctuations ρ' to the mean density ρ_0 implies that over distances of the order of a few wave lengths non-linear effects are negligible. When dissipation is very small acoustic waves can propagate over such large distances that non-linear effects always become significant (we will discuss this in section 4.2).

2.2 Wave equation for a uniform stagnant fluid and compactness

2.2.1 Linearization and wave equation

In the previous section we have seen that in what we call acoustic phenomena the density fluctuations ρ'/ρ_0 are very small. We also have seen that the fluid velocity fluctuation v' associated with the wave propagation, of the order of $(\rho'/\rho_0)c_0$, are also small. This justifies the use of a linear approximation of the equations describing the fluid motion which we presented in chapter 1.

Even with the additional assumption that the flow is frictionless, the equations one obtains may still be complex if we assume a non-uniform mean flow or a non-uniform density distribution ρ_0 . A derivation of general linearized wave equations is discussed by Pierce [183] and Goldstein [73].

We first limit ourselves to the case of acoustic perturbations ($p', \rho', s', v' \dots$) of a stagnant ($u_0 = 0$) uniform fluid (p_0, ρ_0, s_0, \dots). Such conditions are also described in the literature as a *quiescent* fluid. In a quiescent fluid the equations of motion given in chapter 1 simplify to:

$$\frac{\partial \rho'}{\partial t} + \rho_0 \nabla \cdot v' = 0 \tag{2.14a}$$

$$\rho_0 \frac{\partial v'}{\partial t} + \nabla p' = 0 \tag{2.14b}$$

$$\frac{\partial s'}{\partial t} = 0 \tag{2.14c}$$

where second order terms in the perturbations have been neglected. The constitutive equation (1.13) becomes:

$$p' = c_0^2 \rho'. \tag{2.15}$$

By subtracting the time derivative of the mass conservation law (2.14a) from the divergence of the momentum conservation law (2.14b) we eliminate \mathbf{v}' to obtain:

$$\frac{\partial^2 \rho'}{\partial t^2} - \nabla^2 p' = 0. \quad (2.16)$$

Using the constitutive equation $p' = c_0^2 \rho'$ (2.15) to eliminate either ρ' or p' yields the wave equations:

$$\frac{\partial^2 p'}{\partial t^2} - c_0^2 \nabla^2 p' = 0 \quad (2.17a)$$

or

$$\frac{\partial^2 \rho'}{\partial t^2} - c_0^2 \nabla^2 \rho' = 0. \quad (2.17b)$$

Using the *linearized* Bernoulli equation:

$$\frac{\partial \varphi'}{\partial t} + \frac{p'}{\rho_0} = 0 \quad (2.18)$$

which should be valid because the acoustic field is irrotational⁴, we can derive from (2.17a) a wave equation for $\partial \varphi' / \partial t$. We find therefore that φ' satisfies the same wave equation as the pressure and the density:

$$\frac{\partial^2 \varphi'}{\partial t^2} - c_0^2 \nabla^2 \varphi' = 0. \quad (2.19)$$

Taking the gradient of (2.19) we obtain a wave equation for the velocity $\mathbf{v}' = \nabla \varphi'$. Although a rather abstract quantity, the potential φ' is convenient for many calculations in acoustics. The linearized Bernoulli equation (2.18) is used to translate the results obtained for φ' into less abstract quantities such as the pressure fluctuations p' .

2.2.2 Simple solutions

Two of the most simple and therefore most important solutions to the wave equation are d'Alembert's solution in one and three dimensions. In 1-D we have the general solution

$$p' = f(x - c_0 t) + g(x + c_0 t), \quad (2.20a)$$

$$v' = \frac{1}{\rho_0 c_0} \left(f(x - c_0 t) - g(x + c_0 t) \right), \quad (2.20b)$$

⁴In the case considered this property follows from the fact that $\nabla \times (\rho_0 \frac{\partial}{\partial t} \mathbf{v}' + \nabla p) = \rho_0 \frac{\partial}{\partial t} (\nabla \times \mathbf{v}') = 0$. In general this property is imposed by the definition of the acoustic field.

where f and g are determined by boundary and initial conditions, but otherwise they are arbitrary. The velocity v' is obtained from the pressure p' by using the linearized momentum equation (2.14b). As is seen from the respective arguments $x \pm c_0 t$, the “ f ”-part corresponds to a right-running wave (in positive x -direction) and the “ g ”-part to a left-running wave. This solution is especially useful to describe low frequency sound waves in hard-walled ducts, and free field plane waves. To allow for a general orientation of the coordinate system, a free field plane wave is in general written as

$$p' = f(\mathbf{n} \cdot \mathbf{x} - c_0 t), \quad \mathbf{v}' = \frac{\mathbf{n}}{\rho_0 c_0} f(\mathbf{n} \cdot \mathbf{x} - c_0 t), \quad (2.21)$$

where the direction of propagation is given by the unit vector \mathbf{n} . Rather than only left- and right-running waves as in the 1-D case, in free field any sum (or integral) over directions \mathbf{n} may be taken. A time harmonic plane wave of frequency ω is usually written in complex form⁵ as

$$p' = A e^{i\omega t - i\mathbf{k} \cdot \mathbf{x}}, \quad \mathbf{v}' = \frac{\mathbf{k}}{\rho_0 \omega} A e^{i\omega t - i\mathbf{k} \cdot \mathbf{x}}, \quad c_0^2 |\mathbf{k}|^2 = \omega^2, \quad (2.22)$$

where the wave-number vector, or wave vector, $\mathbf{k} = n\mathbf{k} = n\frac{\omega}{c_0}$, indicates the direction of propagation of the wave (at least, in the present uniform and stagnant medium).

In 3-D we have a general solution for spherically symmetric waves (*i.e.* depending only on radial distance r). They are rather similar to the 1-D solution, because the combination $rp(r, t)$ happens to satisfy the 1-D wave equation (see section 6.2). Since the outward radiated wave energy spreads out over the surface of a sphere, the inherent $1/r$ -decay is necessary from energy conservation arguments.

It should be noted, however, that unlike in the 1-D case, the corresponding radial velocity v'_r is rather more complicated. The velocity should be determined from the pressure by time-integration of the momentum equation (2.14b), written in radial coordinates.

We have for pressure and radial velocity

$$p' = \frac{1}{r} f(r - c_0 t) + \frac{1}{r} g(r + c_0 t), \quad (2.23a)$$

$$v'_r = \frac{1}{\rho_0 c_0} \left(\frac{1}{r} f(r - c_0 t) - \frac{1}{r^2} F(r - c_0 t) \right) - \frac{1}{\rho_0 c_0} \left(\frac{1}{r} g(r + c_0 t) - \frac{1}{r^2} G(r + c_0 t) \right), \quad (2.23b)$$

where $F(z) = \int f(z) dz$ and $G(z) = \int g(z) dz$. Usually we have only outgoing waves, which means for any physical solution that the field vanishes before some time t_0 (causality). Hence, $f(z) = 0$ for $z = r - c_0 t \geq r - c_0 t_0 \geq -c_0 t_0$ because $r \geq 0$, and $g(z) = 0$ for any $z = r + c_0 t \leq r + c_0 t_0$. Since r is not restricted from above, this implies that

$$g(z) \equiv 0 \quad \text{for all } z.$$

⁵The physical quantity considered is described by the real part.

This solution (2.23a,2.23b) is especially useful to describe the field of small symmetric sources (monopoles), modelled in a point. Furthermore, by differentiation⁶ to the source position other solutions of the wave equation can be generated (of dipole-type and higher). For example, since $\frac{\partial}{\partial x}r = \frac{x}{r}$, we have

$$p' = \frac{x}{r^2} \left(f'(r - c_0 t) - \frac{1}{r} f(r - c_0 t) \right), \quad (2.24a)$$

$$v'_r = \frac{1}{\rho_0 c_0} \frac{x}{r^2} \left(f'(r - c_0 t) - \frac{2}{r} f(r - c_0 t) + \frac{2}{r^2} F(r - c_0 t) \right), \quad (2.24b)$$

where f' denotes the derivative of f to its argument.

Since the rôle of r and t is symmetric in f and anti-symmetric in g , we may formulate the causality condition in t also as a boundary condition in r . A causal wave vanishes outside a large sphere, of which the radius grows linearly in time with velocity c_0 . This remains true for any field in free space from a source of finite size, because far away the field simplifies to that of a point source (although not necessarily spherically symmetric).

In the case of the idealization of a time-harmonic field we cannot apply this causality condition directly, but we can use a slightly modified form of the boundary condition in r , called *Sommerfeld's radiation condition*:

$$\lim_{r \rightarrow \infty} r \left(\frac{\partial p'}{\partial t} + c_0 \frac{\partial p'}{\partial r} \right) = 0. \quad (2.25)$$

A more general discussion on causality for a time-harmonic field will be given in section C.1.1. The general solution of sound radiation from spheres may be found in [153, ch7.2].

2.2.3 Compactness

In regions –for example at boundaries– where the acoustic potential φ' varies significantly over distances L which are short compared to the wave length λ , the acoustic flow can locally be approximated as an incompressible potential flow. Such a region is called *compact*, and a source of size, much smaller than λ , is a *compact source*. For a more precise definition we should assume that we can distinguish a typical time scale τ or frequency ω and length scale L in the problem. In dimensionless form the wave equation is then:

$$\sum_{i=1}^3 \frac{\partial^2 \varphi'}{\partial \bar{x}_i^2} = (He)^2 \frac{\partial^2 \varphi'}{\partial \bar{t}^2}, \quad He = \frac{L}{c_0 \tau} = \frac{\omega L}{c_0} = \frac{2\pi L}{\lambda} = kL \quad (2.26)$$

⁶We may freely differentiate the pressure but not the velocity! The unit vectors in spherical coordinates are not position-invariant. However, we conveniently obtain the velocity from $\mathbf{v}' = \frac{i}{k\rho_0 c_0} \nabla p'$. In particular, $v'_r = \frac{i}{k\rho_0 c_0} \frac{\partial p'}{\partial r}$.

where $\bar{t} = t/\tau = \omega t$ and $\bar{x}_i = x_i/L$. The dimensionless number He is called the Helmholtz number. When τ and L are well chosen, $\partial^2\varphi'/\partial\bar{t}^2$ and $\partial^2\varphi'/\partial\bar{x}_i^2$ are of the same order of magnitude, and the character of the wave motion is completely described by He . In a compact region we have:

$$He \ll 1. \quad (2.27)$$

This may occur, as suggested above, near a singularity where spatial gradients become large, or at low frequencies when time derivatives become small. Within the compact region the time derivatives, being multiplied by the small He , may be ignored and the potential satisfies to leading order the Laplace equation:

$$\nabla^2\varphi' = 0 \quad (2.28)$$

which describes an incompressible potential flow ($\nabla \cdot \mathbf{v}' = 0$). This allows us to use incompressible potential flow theory to derive the local behaviour of an acoustic field in a compact region. If the compact region is embedded in a larger acoustic region of simpler nature, it acts on the scale of the larger region as a point source, usually allowing a relatively simple acoustic field. By matching the local incompressible approximation to this “far field” solution (spherical waves, plane waves), the solutions may be determined. The matching procedure is usually carried out almost intuitively in the first order approximation. Higher order approximations are obtained by using the method of Matched Asymptotic Expansions (section 8.8, [45]).

2.3 Speed of sound

2.3.1 Ideal gas

In the previous section we have assumed that the speed of sound $c_0^2 = (\partial p/\partial\rho)_s$ is constant. However, in many interesting cases c_0 is non-uniform in space and this affects the propagation of waves. We therefore give here a short review of the dependence of the speed of sound in gas and water on some parameters like temperature.

Air at atmospheric pressure behaves as an ideal gas. The equation of state for an ideal gas is:

$$p = \rho RT, \quad (2.29)$$

where p is the pressure, ρ is the density and T is the absolute temperature. R is the specific gas constant⁷ which is related to the Boltzmann constant $k_B = 1.38066 \cdot 10^{-23}$ J/K and the Avogadro number $\mathcal{N}_A = 6.022 \cdot 10^{23}$ mol⁻¹ by:

$$R = k_B\mathcal{N}_A/M, \quad (2.30)$$

⁷The universal gas constant is: $\mathcal{R} = k_B\mathcal{N}_A = 8.31431$ J/K mol.

18 2 Wave equation, speed of sound, and acoustic energy

where M is the molar mass of the gas (in kg/mol). For air $R = 286.73$ J/kg K. For an ideal gas we have further the relationship:

$$R = C_P - C_V, \quad (2.31)$$

where C_P and C_V are the specific heats at constant pressure and volume, respectively. For an ideal gas the internal energy e depends only on the temperature [176], with (1.15) leading to $de = C_V dT$, so that by using the second law of thermodynamics, we find for an isentropic process ($ds = 0$):

$$C_V dT = -p d(\rho^{-1}) \quad \text{or} \quad \frac{dT}{T} = \frac{R}{C_V} \frac{d\rho}{\rho}. \quad (2.32)$$

By using (2.29) and (2.31) we find for an isentropic process:

$$\frac{d\rho}{\rho} + \frac{dT}{T} = \frac{dp}{p} = \gamma \frac{d\rho}{\rho}, \quad (2.33)$$

where:

$$\gamma = C_P/C_V \quad (2.34)$$

is the specific-heat ratio. Comparison of (2.33) with the definition of the speed of sound $c^2 = (\partial p/\partial \rho)_s$ yields:

$$c = (\gamma p/\rho)^{1/2} \quad \text{or} \quad c = (\gamma RT)^{1/2}. \quad (2.35)$$

We see from this equation that the speed of sound of an ideal gas of given chemical composition depends only on the temperature. For a mixture of ideal gases with mole fraction X_i of component i the molar mass M is given by:

$$M = \sum_i M_i X_i \quad (2.36)$$

where M_i is the molar mass of component i . The specific-heat ratio γ of the mixture can be calculated by:

$$\gamma = \frac{\sum X_i \gamma_i / (\gamma_i - 1)}{\sum X_i / (\gamma_i - 1)} \quad (2.37)$$

because $\gamma_i / (\gamma_i - 1) = M_i C_{p,i} / \mathcal{R}$ and $\gamma_i = C_{p,i} / C_{v,i}$. For air $\gamma = 1.402$, whilst the speed of sound at $T = 273.15$ K is $c = 331.45$ m/s. Moisture in air will only slightly affect the speed of sound but will drastically affect the damping, due to departure from thermodynamic equilibrium [241].

The temperature dependence of the speed of sound is responsible for spectacular differences in sound propagation in the atmosphere. For example, the vertical temperature stratification of the atmosphere (from colder near the ground to warmer at higher levels) that occurs on a winter day with fresh fallen snow refracts the sound back to the ground level, in a way that we hear traffic over much larger distances than on a hot summer afternoon. These refraction effects will be discussed in section 8.6.

2.3.2 Water

For pure water, the speed of sound in the temperature range 273 K to 293 K and in the pressure range 10^5 to 10^7 Pa can be calculated from the empirical formula [183]:

$$c = c_0 + a(T - T_0) + bp \quad (2.38)$$

where $c_0 = 1447$ m/s, $a = 4.0$ m/sK, $T_0 = 283.16$ K and $b = 1.6 \cdot 10^{-6}$ m/sPa. The presence of salt in sea water does significantly affect the speed of sound.

2.3.3 Bubbly liquid at low frequencies

Also the presence of air bubbles in water can have a dramatic effect on the speed of sound ([118, 45]). The speed of sound is by definition determined by the “mass” density ρ and the isentropic bulk modulus:

$$\mathcal{K}_s = \rho \left(\frac{\partial p}{\partial \rho} \right)_s \quad (2.39)$$

which is a measure for the “stiffness” of the fluid. The speed of sound c , given by:

$$c = (\mathcal{K}_s / \rho)^{\frac{1}{2}} \quad (2.40)$$

increases with increasing stiffness, and decreases with increasing inertia (density ρ). In a one-dimensional model consisting of a discrete mass M connected by a spring of constant \mathcal{K} , we can understand this behaviour intuitively. This mass-spring model was used by Newton to derive equation (2.40), except for the fact that he used the isothermal bulk modulus \mathcal{K}_T rather than \mathcal{K}_s . This resulted in an error of $\gamma^{1/2}$ in the predicted speed of sound in air which was corrected by Laplace [241].

A small fraction of air bubbles present in water considerably reduces the bulk modulus \mathcal{K}_s , while at the same time the density ρ is not strongly affected. As the \mathcal{K}_s of the mixture can approach that for pure air, one observes in such mixtures velocities of sound much lower than in air (or water). The behaviour of air bubbles at high frequencies involves a possible resonance which we will discuss in chapter 4 and chapter 6. We now assume that the bubbles are in mechanical equilibrium with the water, which allows a low frequency approximation. Combining this assumption with (2.40), following Crighton [45], we derive an expression for the soundspeed c of the mixture as a function of the volume fraction β of gas in the water. The density ρ of the mixture is given by:

$$\rho = (1 - \beta)\rho_\ell + \beta\rho_g, \quad (2.41)$$

where ρ_ℓ and ρ_g are the liquid and gas densities. If we consider a small change in pressure dp we obtain:

$$\frac{d\rho}{dp} = (1 - \beta) \frac{d\rho_\ell}{dp} + \beta \frac{d\rho_g}{dp} + (\rho_g - \rho_\ell) \frac{d\beta}{dp} \quad (2.42)$$

where we assume both the gas and the liquid to compress isothermally [45]. If no gas dissolves in the liquid, so that the mass fraction ($\beta\rho_g/\rho$) of gas remains constant, we have:

$$\rho_g \frac{d\beta}{dp} + \beta \frac{d\rho_g}{dp} - \frac{\beta\rho_g}{\rho} \frac{d\rho}{dp} = 0. \quad (2.43)$$

Using the notation $c^2 = dp/d\rho$, $c_g^2 = dp/d\rho_g$ and $c_\ell^2 = dp/d\rho_\ell$, we find by elimination of $d\beta/dp$ from (2.42) and (2.43):

$$\frac{1}{\rho c^2} = \frac{1-\beta}{\rho_\ell c_\ell^2} + \frac{\beta}{\rho_g c_g^2}. \quad (2.44)$$

It is interesting to see that for small values of β the speed of sound c drops drastically from c_ℓ at $\beta = 0$ towards a value lower than c_g . The minimum speed of sound occurs at $\beta = 0.5$, and at 1 bar we find for example in a water/air mixture $c \simeq 24$ m/s! In the case of β not being close to zero or unity, we can use the fact that $\rho_g c_g^2 \ll \rho_\ell c_\ell^2$ and $\rho_g \ll \rho_\ell$, to approximate (2.44) by:

$$\rho c^2 \simeq \frac{\rho_g c_g^2}{\beta}, \quad \text{or} \quad c^2 \simeq \frac{\rho_g c_g^2}{\beta(1-\beta)\rho_\ell}. \quad (2.45)$$

The gas fraction determines the bulk modulus $\rho_g c_g^2/\beta$ of the mixture, while the water determines the density $(1-\beta)\rho_\ell$. Hence, we see that the presence of bubbles around a ship may dramatically affect the sound propagation near the surface. Air bubbles are also introduced in sea water near the surface by surface waves. The dynamics of bubbles involving oscillations (see chapter 4 and chapter 6) appear to induce spectacular dispersion effects [45], which we have ignored here.

2.4 Influence of temperature gradient

In section 2.2 we derived a wave equation (2.17a) for an homogeneous stagnant medium. We have seen in section 2.3 that the speed of sound in the atmosphere is expected to vary considerably as a result of temperature gradients. In many cases, when the acoustic wave length is small compared to the temperature gradient length (distance over which a significant temperature variation occurs) we can still use the wave equation (2.17a). It is however interesting to derive a wave equation in the more general case: for a stagnant ideal gas with an arbitrary temperature distribution.

We start from the linearized equations for the conservation of mass, momentum and energy for a stagnant gas:

$$\frac{\partial \rho'}{\partial t} + \nabla \cdot (\rho_0 \mathbf{v}') = 0 \quad (2.46a)$$

$$\rho_0 \frac{\partial \mathbf{v}'}{\partial t} + \nabla p' = 0 \quad (2.46b)$$

$$\frac{\partial s'}{\partial t} + \mathbf{v}' \cdot \nabla s_0 = 0, \quad (2.46c)$$

where ρ_0 and s_0 vary in space. The constitutive equation for isentropic flow ($Ds/Dt = 0$):

$$\frac{Dp}{Dt} = c^2 \frac{D\rho}{Dt}$$

can be written as⁸:

$$\frac{\partial p'}{\partial t} + \mathbf{v}' \cdot \nabla p_0 = c_0^2 \left(\frac{\partial \rho'}{\partial t} + \mathbf{v}' \cdot \nabla \rho_0 \right). \quad (2.47)$$

Combining (2.47) with the continuity equation (2.46a) we find:

$$\left(\frac{\partial p'}{\partial t} + \mathbf{v}' \cdot \nabla p_0 \right) + \rho_0 c_0^2 \nabla \cdot \mathbf{v}' = 0. \quad (2.48)$$

If we consider temperature gradients over a small height (in a horizontal tube for example) so that the variation in p_0 can be neglected ($\nabla p_0/p_0 \ll \nabla T_0/T_0$), we can approximate (2.48) by:

$$\nabla \cdot \mathbf{v}' = -\frac{1}{\rho_0 c_0^2} \frac{\partial p'}{\partial t}.$$

Taking the divergence of the momentum conservation law (2.46b) yields:

$$\frac{\partial}{\partial t} (\nabla \cdot \mathbf{v}') + \nabla \cdot \left(\frac{1}{\rho_0} \nabla p' \right) = 0.$$

By elimination of $\nabla \cdot \mathbf{v}'$ we obtain:

$$\frac{\partial^2 p'}{\partial t^2} - c_0^2 \rho_0 \nabla \cdot \left(\frac{1}{\rho_0} \nabla p' \right) = 0. \quad (2.49)$$

For an ideal gas $c_0^2 = \gamma p_0 / \rho_0$, and since we assumed p_0 to be uniform, we have that $\rho_0 c_0^2$, given by:

$$\rho_0 c_0^2 = \gamma p_0$$

is a constant so that equation (2.49) can be written in the form:

$$\frac{\partial^2 p'}{\partial t^2} - \nabla \cdot (c_0^2 \nabla p') = 0. \quad (2.50)$$

This is a rather complex wave equation, since c_0 is non-uniform. We will in section 8.6 consider approximate solutions for this equation in the case $(\nabla c_0/\omega) \ll 1$ and for large propagation distances. This approximation is called geometrical or ray acoustics.

It is interesting to note that, unlike in quiescent (*i.e.* uniform and stagnant) fluids, the wave equation (2.50) for the pressure fluctuation p' in a stagnant non-uniform ideal gas is not valid for the density fluctuations. This is because here the density fluctuations ρ' not only relate to pressure fluctuations but also to convective effects (2.47). Which acoustic variable is selected to work with is only indifferent in a quiescent fluid. This will be elaborated further in the discussion on the sources of sound in section 2.6.

⁸Why do we not use (2.15)?

2.5 Influence of mean flow

See also Appendix F. In the presence of a mean flow that satisfies

$$\nabla \cdot \rho_0 \mathbf{v}_0 = 0, \quad \rho_0 \mathbf{v}_0 \cdot \nabla \mathbf{v}_0 = -\nabla p_0, \quad \mathbf{v}_0 \cdot \nabla s_0 = 0, \quad \mathbf{v}_0 \cdot \nabla p_0 = c_0^2 \mathbf{v}_0 \cdot \nabla \rho_0,$$

the linearized conservation laws, and constitutive equation for isentropic flow, become (without sources):

$$\frac{\partial \rho'}{\partial t} + \mathbf{v}_0 \cdot \nabla \rho' + \mathbf{v}' \cdot \nabla \rho_0 + \rho_0 \nabla \cdot \mathbf{v}' + \rho' \nabla \cdot \mathbf{v}_0 = 0 \quad (2.51a)$$

$$\rho_0 \left(\frac{\partial \mathbf{v}'}{\partial t} + \mathbf{v}_0 \cdot \nabla \mathbf{v}' + \mathbf{v}' \cdot \nabla \mathbf{v}_0 \right) + \rho' \mathbf{v}_0 \cdot \nabla \mathbf{v}_0 = -\nabla p' \quad (2.51b)$$

$$\frac{\partial s'}{\partial t} + \mathbf{v}_0 \cdot \nabla s' + \mathbf{v}' \cdot \nabla s_0 = 0. \quad (2.51c)$$

$$\frac{\partial p'}{\partial t} + \mathbf{v}_0 \cdot \nabla p' + \mathbf{v}' \cdot \nabla p_0 = c_0^2 \left(\frac{\partial \rho'}{\partial t} + \mathbf{v}_0 \cdot \nabla \rho' + \mathbf{v}' \cdot \nabla \rho_0 \right) + c_0^2 (\mathbf{v}_0 \cdot \nabla \rho_0) \left(\frac{p'}{p_0} - \frac{\rho'}{\rho_0} \right) \quad (2.51d)$$

A wave equation can only be obtained from these equations if simplifying assumptions are introduced. For a uniform medium with uniform flow velocity $\mathbf{v}_0 \neq 0$ we obtain

$$\left(\frac{\partial}{\partial t} + \mathbf{v}_0 \cdot \nabla \right)^2 p' - c_0^2 \nabla^2 p' = 0 \quad (2.52)$$

where $\frac{\partial}{\partial t} + \mathbf{v}_0 \cdot \nabla$ denotes a time derivative moving with the mean flow.

2.6 Sources of sound

2.6.1 Inverse problem and uniqueness of sources

Until now we have focused our attention on the propagation of sound. As starting point for the derivation of wave equations we have used the linearized equations of motion and we have assumed that the mass source term m and the external force density \mathbf{f} in (1.1) and (1.2) were absent. Without these restrictions we still can (under specific conditions) derive a wave equation. The wave equation will now be non-homogeneous, *i.e.* it will contain a source term q . For example, we may find in the absence of mean flow:

$$\frac{\partial^2 p'}{\partial t^2} - c_0^2 \nabla^2 p' = q. \quad (2.53)$$

Often we will consider situations where the source q is concentrated in a limited region of space embedded in a stagnant uniform fluid. As we will see later the acoustic field p' can formally be determined for a given source distribution q by means of a Green's function. This solution p' is unique. It should be noted that the so-called inverse problem of determining q from the measurement of p' outside the source region does not have a unique solution without at least some additional information on the structure of the source. This statement is easily verified by the construction of another sound field, for example [67]: $p' + F$, for any smooth function F that vanishes outside the source region (*i.e.* $F = 0$ wherever $q = 0$), for example $F \propto q$ itself! This field is outside the source region exactly equal to the original field p' . On the other hand, it is *not* the solution of equation (2.53), because it satisfies a wave equation with another source:

$$\left(\frac{\partial^2}{\partial t^2} - c_0^2 \nabla^2\right)(p' + F) = q + \left(\frac{\partial^2}{\partial t^2} - c_0^2 \nabla^2\right)F. \quad (2.54)$$

In general this source is not equal to q . This proves that the measurement of the acoustic field outside the source region is not sufficient to determine the source uniquely [55].

2.6.2 Mass and momentum injection

As a first example of a non-homogeneous wave equation we consider the effect of the mass source term m on a uniform stagnant fluid. We further assume that a linear approximation is valid. Consider the inhomogeneous equation of mass conservation

$$\frac{\partial}{\partial t}\rho + \nabla \cdot (\rho \mathbf{v}) = m \quad (2.55)$$

and a linearized form of the equation of momentum conservation

$$\frac{\partial}{\partial t}(\rho \mathbf{v}) + \nabla p' = \mathbf{f}. \quad (2.56)$$

The source m consists of mass of density ρ_m of volume fraction $\beta = \beta(\mathbf{x}, t)$ injected at a rate

$$m = \frac{\partial}{\partial t}(\beta \rho_m). \quad (2.57)$$

The source region is where $\beta \neq 0$. Since the injected mass displaces the original mass ρ_f by the same (but negative) amount of volume, the total fluid density is

$$\rho = \beta \rho_m + (1 - \beta) \rho_f \quad (2.58)$$

where the injected matter does not mix with the original fluid. Substitute (2.58) in (2.55) and eliminate $\beta \rho_m$

$$\frac{\partial}{\partial t}\rho_f + \nabla \cdot (\rho \mathbf{v}) = \frac{\partial}{\partial t}(\beta \rho_f). \quad (2.59)$$

Eliminate $\rho \mathbf{v}$ from (2.56) and (2.59)

$$\frac{\partial^2}{\partial t^2} \rho_f - \nabla^2 p' = \frac{\partial^2}{\partial t^2} (\beta \rho_f) - \nabla \cdot \mathbf{f}. \quad (2.60)$$

If we assume, for simplicity, that $p' = c_0^2 \rho'_f$ everywhere, where ρ'_f is the fluctuating part of ρ_f which corresponds to the sound field outside the source region, then

$$\frac{1}{c_0^2} \frac{\partial^2}{\partial t^2} p' - \nabla^2 p' = \frac{\partial^2}{\partial t^2} (\beta \rho_f) - \nabla \cdot \mathbf{f} \quad (2.61)$$

which shows that mass injection is a source of sound, primarily because of the displacement of a volume fraction β of the original fluid ρ_f . Hence injecting mass with a large density ρ_m is not necessarily an effective source of sound.

We see from (2.61) that a *continuous injection of mass* of constant density does not produce sound, because $\partial^2 \beta \rho_f / \partial t^2$ vanishes. In addition, it can be shown in an analogous way that in linear approximation the presence of a *uniform force field* (a uniform gravitational field, for example) does not affect the sound field in a uniform stagnant fluid.

2.6.3 Lighthill's analogy

We now indicate how a wave equation with aerodynamic source terms can be derived. The most famous wave equation of this type is the equation of Lighthill.

The notion of ‘‘analogy’’ refers here to the idea of representing a complex fluid mechanical process that acts as an acoustic source by an acoustically equivalent source term. For example, one may model a clarinet as an idealized resonator formed by a closed pipe, with the effect of the flow through the mouth piece represented by a mass source at one end. In that particular case we express by this analogy the fact that the internal acoustic field of the clarinet is dominated by a standing wave corresponding to a resonance of the (ideal) resonator.

While Lighthill's equation is formally exact (*i.e.* derived *without* approximation from the Navier-Stokes equations), it is only useful when we consider the case of a limited source region embedded in a uniform stagnant fluid. At least we assume that the listener which detects the acoustic field at a point \mathbf{x} at time t is surrounded by a uniform stagnant fluid characterized by a speed of sound c_0 . Hence the acoustic field at the listener should accurately be described by the wave equation:

$$\frac{\partial^2 \rho'}{\partial t^2} - c_0^2 \nabla^2 \rho' = 0 \quad (2.17b)$$

where we have chosen ρ' as the acoustic variable as this will appear to be the most convenient choice for problems like the prediction of sound produced by turbulence. The key idea of the so-called ‘‘aero-acoustic analogy’’ of Lighthill is that we now derive from the exact equations of motion

a non-homogeneous wave equation with the propagation part as given by (2.17b). Hence the uniform stagnant fluid with sound speed c_0 , density ρ_0 and pressure p_0 at the listener's location is assumed to extend into the entire space, and any departure from the "ideal" acoustic behaviour predicted by (2.17b) is equivalent to a source of sound for the observer [122, 123, 186, 84].

By taking the time derivative of the mass conservation law (1.1) and eliminating $\partial m / \partial t$ as in (2.59) we find:

$$\frac{\partial^2}{\partial t \partial x_i}(\rho v_i) = \frac{\partial m}{\partial t} - \frac{\partial^2 \rho}{\partial t^2} = -\frac{\partial^2 \rho_f}{\partial t^2} + \frac{\partial^2 \beta \rho_f}{\partial t^2}. \quad (2.62)$$

By taking the divergence of the momentum conservation law (1.2) we find:

$$\frac{\partial^2}{\partial t \partial x_i}(\rho v_i) = -\frac{\partial^2}{\partial x_i \partial x_j}(P_{ij} + \rho v_i v_j) + \frac{\partial f_i}{\partial x_i}. \quad (2.63)$$

Hence we find from (2.62) and (2.63) the exact relation:

$$\frac{\partial^2 \rho_f}{\partial t^2} = \frac{\partial^2}{\partial x_i \partial x_j}(P_{ij} + \rho v_i v_j) + \frac{\partial^2 \beta \rho_f}{\partial t^2} - \frac{\partial f_i}{\partial x_i}. \quad (2.64)$$

Because $\rho_f = \rho_0 + \rho'$ where only ρ' varies in time we can construct a wave equation for ρ' by subtracting from both sides of (2.63) a term $c_0^2(\partial^2 \rho' / \partial x_i^2)$ where in order to be meaningful c_0 is not the local speed of sound but that at the *listener's location*.

In this way we have obtained the famous equation of Lighthill:

$$\boxed{\frac{\partial^2 \rho'}{\partial t^2} - c_0^2 \frac{\partial^2 \rho'}{\partial x_i^2} = \frac{\partial^2 T_{ij}}{\partial x_i \partial x_j} + \frac{\partial^2 \beta \rho_f}{\partial t^2} - \frac{\partial f_i}{\partial x_i}} \quad (2.65)$$

where Lighthill's stress tensor T_{ij} is defined by:

$$T_{ij} = P_{ij} + \rho v_i v_j - (c_0^2 \rho' + p_0) \delta_{ij}. \quad (2.66)$$

We used

$$c_0^2 \frac{\partial^2 \rho'}{\partial x_i^2} = \frac{\partial^2 (c_0^2 \rho' \delta_{ij})}{\partial x_i \partial x_j} \quad (2.67)$$

which is exact because c_0 is a constant. Making use of definition (1.4) we can also write:

$$\boxed{T_{ij} = \rho v_i v_j - \tau_{ij} + (p' - c_0^2 \rho') \delta_{ij}} \quad (2.68)$$

which is the usual form in the literature⁹. In equation (2.68) we distinguish three basic aero-acoustic processes which result in sources of sound:

⁹The perturbations are defined as the deviation from the uniform reference state (ρ_0, p_0) : $\rho' = \rho - \rho_0$, and $p' = p - p_0$.

- the non-linear convective forces described by the Reynolds stress tensor $\rho v_i v_j$,
- the viscous forces τ_{ij} ,
- the deviation from a uniform sound velocity c_0 or the deviation from an isentropic behaviour $(p' - c_0^2 \rho')$.

As no approximations have been made, equation (2.65) is exact and not easier to solve than the original equations of motion. In fact, we have used four equations: the mass conservation and the three components of the momentum conservation to derive a single equation. We are therefore certainly not closer to a solution unless we introduce some additional simplifying assumptions.

The usefulness of (2.65) is that we can introduce some crude simplifications which yield an order of magnitude estimate for ρ' . Such estimation procedure is based on the physical interpretation of the source term. However, a key step of Lighthill's analysis is to delay this physical interpretation until an integral equation formulation of (2.65) has been obtained. This is an efficient approach because an order of magnitude estimate of $\partial^2 T_{ij} / \partial x_i \partial x_j$ involves the estimation of spatial derivatives which is very difficult, while, as we will see, in an integral formulation we will need only an estimate for an average value of T_{ij} in order to obtain some relevant information on the acoustic field.

This crucial step was not recognized before the original papers of Lighthill [122, 123]. For a given experimental or numerical set of data on the flow field in the source region, the integral formulation of Lighthill's analogy often provides a maximum amount of information about the generated acoustic field.

Unlike in the propagation in a uniform fluid the choice of the acoustic variable appeared already in the presence of a temperature gradient (section 2.4) to affect the character of the wave equation. If we derive a wave equation for p' instead of ρ' , the structure of the source terms will be different. In some cases it appears to be more convenient to use p' instead of ρ' . This is the case when unsteady heat release occurs such as in combustion problems. Starting from equation (2.64) in the form:

$$\frac{\partial^2 p}{\partial x_i^2} = \frac{\partial^2 \rho}{\partial t^2} + \frac{\partial^2}{\partial x_i \partial x_j} (\tau_{ij} - \rho v_i v_j)$$

where we assumed that $m = 0$ and $\mathbf{f} = 0$, we find by subtraction of $c_0^{-2} (\partial^2 / \partial t^2) p'$ on both sides:

$$\frac{1}{c_0^2} \frac{\partial^2 p'}{\partial t^2} - \frac{\partial^2 p'}{\partial x_i^2} = \frac{\partial^2}{\partial x_i \partial x_j} (\rho v_i v_j - \tau_{ij}) + \frac{\partial^2 p_0}{\partial x_i^2} + \frac{\partial^2}{\partial t^2} \left(\frac{p'}{c_0^2} - \rho' \right) \quad (2.69)$$

where the term $\partial^2 p_0 / \partial x_i^2$ vanishes because p_0 is a constant.

Comparing (2.65) with (2.69) shows that the deviation from an isentropic behaviour leads to a source term of the type $(\partial^2 / \partial x_i^2) (p' - c_0^2 \rho')$ when we choose ρ' as the acoustic variable, while we find a term $(\partial^2 / \partial t^2) (p' / c_0^2 - \rho')$ when we choose p' as the acoustic variable. Hence ρ' is more appropriate to describe the sound generation due to non-uniformity as for example the so-called acoustic "Bremsstrahlung" produced by the acceleration of a fluid particle with an entropy different from the

main flow. The sound production by unsteady heat transfer or combustion is easier to describe in terms of p' (Howe [84]).

We see that $(\partial/\partial t)(p'/c_0^2 - \rho')$ acts as a mass source term m , which is intuitively more easily understood (Crighton *et al.* [45]) when using the thermodynamic relation (1.12) applied to a moving particle:

$$\frac{Dp}{Dt} = c^2 \frac{D\rho}{Dt} + \left(\frac{\partial p}{\partial s}\right)_\rho \frac{Ds}{Dt}. \quad (1.12)$$

We find from (1.12) that:

$$\frac{D}{Dt} \left(\frac{p'}{c_0^2} - \rho' \right) = \left(\frac{c^2}{c_0^2} - 1 \right) \frac{D\rho'}{Dt} + \frac{\rho^2}{c_0^2} \left(\frac{\partial T}{\partial \rho} \right)_s \frac{Ds'}{Dt} \quad (2.70)$$

where we made use of the thermodynamic relation:

$$\left(\frac{\partial p}{\partial s}\right)_\rho = \rho^2 \left(\frac{\partial T}{\partial \rho}\right)_s \quad (2.71)$$

derived from the fundamental law of thermodynamics (1.8) in the form:

$$de = T ds - p d(\rho^{-1}). \quad (1.8)$$

As a final result, using the mass conservation law, we find

$$-\frac{\partial^2 \rho_e}{\partial t^2} = \frac{\partial}{\partial t} \left[\left(\frac{c^2}{c_0^2} - 1 + \frac{\rho_e}{\rho} \right) \frac{D\rho'}{Dt} + \frac{\rho^2}{c_0^2} \left(\frac{\partial T}{\partial \rho} \right)_s \frac{Ds'}{Dt} + \nabla \cdot (\mathbf{v}\rho_e) \right] \quad (2.72)$$

where the “excess density” ρ_e is defined as:

$$\rho_e = \rho' - \frac{p'}{c_0^2}.$$

In a free jet the first term in $-\partial^2 \rho_e / \partial t^2$ vanishes for an ideal gas with constant heat capacity (because $c^2/c_0^2 - 1 + \rho_e/\rho = 0$). We see that sound is produced both by spatial density variations $\nabla \cdot (\mathbf{v}\rho_e)$ and as a result of non-isentropic processes $(\rho^2/c_0^2)(\partial T/\partial \rho)_s(Ds'/Dt)$, like combustion.

2.6.4 Vortex sound

While Lighthill’s analogy is very convenient for obtaining order of magnitude estimates of the sound produced by various processes, this formulation is not very convenient when one considers the sound production by a flow which is, on its turn, influenced by the acoustic field. In Lighthill’s procedure

the flow is assumed¹⁰ to be known, with any feedback from the acoustic field to the flow somehow already included. When such a feedback is significant, and in general for homentropic low Mach number flow, the aerodynamic formulation of Powell [186], Howe [84] and Doak [53] based on the concept of vortex sound is most appropriate. This is due to the fact that the vorticity $\boldsymbol{\omega} = \nabla \times \boldsymbol{v}$ is a very convenient quantity to describe a low Mach number flow.

Considering a homentropic non-conductive frictionless fluid, we start our derivation of a wave equation from Euler's equation in Crocco's form:

$$\frac{\partial \boldsymbol{v}}{\partial t} + \nabla B = -\boldsymbol{\omega} \times \boldsymbol{v} \quad (1.31)$$

where $B = i + \frac{1}{2}v^2$, and the continuity equation:

$$\frac{1}{\rho} \frac{D\rho}{Dt} = -\nabla \cdot \boldsymbol{v}. \quad (1.18)$$

Taking the divergence of (1.31) and the time derivative of (1.18) we obtain by subtraction:

$$\frac{\partial}{\partial t} \left(\frac{1}{\rho} \frac{D\rho}{Dt} \right) - \nabla^2 B = \nabla \cdot (\boldsymbol{\omega} \times \boldsymbol{v}). \quad (2.73)$$

As the entropy is constant ($ds = 0$) we have, with (1.12) and (1.27):

$$\frac{\partial}{\partial t} \left(\frac{1}{c^2} \frac{Di}{Dt} \right) - \nabla^2 B = \nabla \cdot (\boldsymbol{\omega} \times \boldsymbol{v}). \quad (2.74)$$

This can be rewritten as

$$\frac{1}{c^2} \frac{D_0^2 B'}{Dt} - \nabla^2 B' = \nabla \cdot (\boldsymbol{\omega} \times \boldsymbol{v}) + \frac{1}{c^2} \frac{D_0^2 B'}{Dt} - \frac{\partial}{\partial t} \left(\frac{1}{c^2} \frac{Di}{Dt} \right) \quad (2.75)$$

where $B' = B - B_0$ and $\frac{D_0}{Dt} = \frac{\partial}{\partial t} + \boldsymbol{U}_0 \cdot \nabla$. For the reference flow \boldsymbol{U}_0 we choose a potential flow with stagnation enthalpy B_0 .

At low Mach number $M = v/c_0$ we have the inhomogeneous wave equation:

$$\frac{1}{c_0^2} \frac{D_0^2 B'}{Dt^2} - \nabla^2 B' = \nabla \cdot (\boldsymbol{\omega} \times \boldsymbol{v}) \quad (2.76)$$

which explicitly stresses the fact that the vorticity $\boldsymbol{\omega}$ is responsible for the generation of sound. (Note: $i' = p'/\rho_0$ and $B' = i' + \boldsymbol{v}_0 \cdot \boldsymbol{v}'$.) Some of the implications of (2.76) will be considered in more detail in the next section. The use of a vortex sound formulation is particularly powerful when a simplified

¹⁰This is not a necessary condition for the use of Lighthill's analogy. It is the commonly used procedure in which we derive information on the acoustic field from data on the flow in the source region.

vortex model is available for the flow considered. Examples of such flows are discussed by Howe [84], Disselhorst & van Wijngaarden [52], Peters & Hirschberg [180], and Howe [89].

In free space for a compact source region Powell [185] has derived this analogy directly from Lighthill's analogy. The result is that the Coriolis force $\mathbf{f}_c = \rho_0(\boldsymbol{\omega} \times \mathbf{v})$ appears to act as an external force on the acoustic field. Considering Crocco's equation (1.31) with this interpretation Howe [85, 88] realized that the natural reference of the analogy is a potential flow rather than the quiescent fluid of Lighthill's analogy. There is then no need to assume free field conditions nor a compact source region. Howe [84] therefore proposes to define the acoustic field as the unsteady scalar potential flow component of the flow:

$$\mathbf{u}_a = \nabla \varphi'$$

where $\varphi' = \varphi - \varphi_0$ and φ_0 is the steady scalar potential.

At high Mach numbers, when the source is not compact, both Lighthill's and Howe's analogy become less convenient. Alternative formulations have been proposed and are still being studied [158].

2.7 Acoustic energy

2.7.1 Introduction

Acoustic energy is a difficult concept because it involves second order terms in the perturbations like the kinetic energy density $\frac{1}{2}\rho_0 v'^2$. Historically an energy conservation law was first derived by Kirchhoff for stagnant uniform fluids. He started from the linearized conservation laws (2.51a–2.51d). Such a procedure is ad-hoc, and the result, an energy expression of the approximation, is not an approximation of the total energy, since a small perturbation expansion of the full non-linear fluid energy conservation law (1.6) will contain zeroth and first order terms and potentially relevant second order terms $O((\rho'/\rho_0)^2)$ which are dropped with the linearization of the mass and momentum equations. However, it appears that for a quiescent fluid these zeroth, first and neglected second order terms are (in a sense) not important and an acoustic energy conservation equation may be derived which is indeed the same as found by Kirchhoff [183].

This approach may be extended to non-uniform flows as long as they are homentropic and irrotational. Things become much less obvious in the presence of a non-uniform mean flow including entropy variations and vorticity. If required, the zeroth, first and neglected second order terms of the expansion may still be ignored, as Myers showed [160], but now at the expense of a resulting energy equation which is not a conservation law any more. The only way to obtain some kind of acoustic energy conservation equation (implying definitions for acoustic energy density and flux) is to redirect certain parts to the “right hand side” to become source or sink terms. In such a case the question of definition,

in particular which part of the field is to be called acoustic, is essential and until now it remains subject of discussion.

As stated before, we will consider as acoustical only that part of the field which is related to density variations and an unsteady (irrotational) potential flow. Pressure fluctuations related to vorticity, which do not propagate, are often referred to in the literature as “pseudo sound”. In contrast to this approach Jenvey [99] calls any pressure fluctuations “acoustic”, which of course results in a different definition of acoustic energy.

The foregoing approach of generalized expressions for acoustic energy for homentropic [160] and more general nonuniform flows [161, 162] by expanding the energy equation for small perturbations is due to Myers. We will start our analysis with Kirchhoff’s equation for an inviscid non-conducting fluid, and extend the results to those obtained by Myers. Finally we will consider a relationship between vorticity and sound generation in a homentropic uniform inviscid non-conducting fluid at low Mach numbers, derived by Howe [85].

2.7.2 Kirchhoff’s equation for quiescent fluids

We start from the linearized mass and momentum conservation laws for a quiescent inviscid and non-conducting fluid:

$$\frac{\partial \rho'}{\partial t} + \rho_0 \nabla \cdot \mathbf{v}' = m', \quad (2.77a)$$

$$\rho_0 \frac{\partial \mathbf{v}'}{\partial t} + \nabla p' = \mathbf{f}', \quad (2.77b)$$

where we assumed that \mathbf{f}' and m' are of acoustic order. Since we assumed the mean flow to be quiescent and uniform there is no mean mass source ($m_0 = 0$) or force ($\mathbf{f}_0 = 0$). From the assumption of homentropy ($ds = 0$) we have¹¹

$$p' = c_0^2 \rho'. \quad (2.15)$$

After multiplying (2.77a) by p'/ρ_0 and (2.77b) by \mathbf{v}' , adding the two equations, and utilizing the foregoing relation (2.15) between density and pressure, we obtain the equation

$$\frac{1}{2\rho_0 c_0^2} \frac{\partial p'^2}{\partial t} + \frac{1}{2}\rho_0 \frac{\partial v'^2}{\partial t} + \nabla \cdot (p' \mathbf{v}') = \frac{p' m'}{\rho_0} + \mathbf{v}' \cdot \mathbf{f}' \quad (2.78)$$

¹¹Note that in order to keep equation (2.15) valid we have implicitly assumed that the injected mass corresponding to m' has the same thermodynamic properties as the original fluid. The flow would otherwise not be homentropic! In this case m'/ρ_0 corresponds to the injected volume fraction β of equation (2.57).

which can be interpreted as a conservation law for the acoustic energy

$$\frac{\partial E}{\partial t} + \nabla \cdot \mathbf{I} = -\mathcal{D} \quad (2.79)$$

if we DEFINE the acoustic energy density E , the energy flux or intensity¹² \mathbf{I} and the dissipation \mathcal{D} as:

$$E = \frac{p'^2}{2\rho_0 c_0^2} + \frac{\rho_0 v'^2}{2}, \quad (2.80a)$$

$$\mathbf{I} = p' \mathbf{v}', \quad (2.80b)$$

$$\mathcal{D} = -\frac{p' m'}{\rho_0} - \mathbf{v}' \cdot \mathbf{f}'. \quad (2.80c)$$

In integral form this conservation law (2.79) can be written for a fixed control volume V enclosed by a surface S with outer normal \mathbf{n} as

$$\frac{d}{dt} \iiint_V E \, d\mathbf{x} + \iint_S \mathbf{I} \cdot \mathbf{n} \, d\sigma = - \iiint_V \mathcal{D} \, d\mathbf{x}, \quad (2.81)$$

where we have used the theorem of Gauss to transform $\iiint_V \nabla \cdot \mathbf{I} \, d\mathbf{x}$ into a surface integral. For a periodic acoustic field the average $\langle E \rangle$ of the acoustic energy over a period is constant. Hence we find

$$\mathcal{P} = \iint_S \langle \mathbf{I} \cdot \mathbf{n} \rangle \, d\sigma = - \iiint_V \langle \mathcal{D} \rangle \, d\mathbf{x}, \quad (2.82)$$

where \mathcal{P} is the acoustic power flow across the volume surface S . The left-hand side of (2.82) simply corresponds with the mechanical work performed by the volume injection (m'/ρ_0) and the external force field \mathbf{f}' on the acoustic field. This formula is useful because we can consider the effect of the movement of solid boundaries like a piston or a propeller represented by source terms m' and \mathbf{f}' . We will at the end of this chapter use formula (2.82) to calculate the acoustic power generated by a compact vorticity field.

We will now derive the acoustic energy equation starting from the original nonlinear energy conservation law (1.6). We consider the perturbation of a uniform quiescent fluid without mass source term ($v_0 = 0$, $m = 0$, $f_0 = 0$, p_0 and ρ_0 constant). We start with equation (1.6) in standard conservation form:

$$\frac{\partial}{\partial t} \left(\rho e + \frac{1}{2} \rho v^2 \right) + \nabla \cdot \left(\mathbf{v} \left(\rho e + \frac{1}{2} \rho v^2 + p \right) \right) = -\nabla \cdot \mathbf{q} + \nabla \cdot (\boldsymbol{\tau} \cdot \mathbf{v}) + \mathbf{f} \cdot \mathbf{v}, \quad (2.83)$$

¹²There is no uniformity in the nomenclature. Some authors define the acoustic intensity as the acoustic energy flux, others as the time-averaged acoustic energy flux.

where we note that the total fluid energy density is

$$E_{tot} = \rho e + \frac{1}{2}\rho v^2, \quad (2.84a)$$

and the total fluid energy flux is

$$\mathbf{I}_{tot} = \mathbf{v}(\rho e + \frac{1}{2}\rho v^2 + p). \quad (2.84b)$$

We have dropped here the mass source term m because, in contrast to the force density \mathbf{f} , it does not correspond to any physical process.

For future reference we state here some related forms, a.o. related to the entropy variation of the fluid. Using the continuity equation we obtain

$$\rho \frac{D}{Dt} \left(e + \frac{v^2}{2} \right) = -\nabla \cdot (p\mathbf{v}) - \nabla \cdot \mathbf{q} + \nabla \cdot (\boldsymbol{\tau} \cdot \mathbf{v}) + \mathbf{f} \cdot \mathbf{v}, \quad (2.85)$$

which by using the fundamental law of thermodynamics (1.8) may yield an equation for the change in entropy s of the fluid:

$$\rho T \frac{Ds}{Dt} - \frac{p}{\rho} \frac{D\rho}{Dt} + \frac{\rho}{2} \frac{Dv^2}{Dt} = -\nabla \cdot (p\mathbf{v}) - \nabla \cdot \mathbf{q} + \nabla \cdot (\boldsymbol{\tau} \cdot \mathbf{v}) + \mathbf{f} \cdot \mathbf{v}. \quad (2.86)$$

By subtraction of the inner product of the momentum conservation equation with the velocity, this may be further recast into

$$\rho T \frac{Ds}{Dt} = -\nabla \cdot \mathbf{q} + \boldsymbol{\tau} : \nabla \mathbf{v}. \quad (2.87)$$

In the absence of friction ($\boldsymbol{\tau} = 0$) and heat conduction ($\mathbf{q} = 0$) we have the following equations for energy and entropy:

$$\rho \frac{D}{Dt} \left(e + \frac{1}{2}v^2 \right) = -\nabla \cdot (p\mathbf{v}) + \mathbf{f} \cdot \mathbf{v} \quad (2.88)$$

$$\frac{Ds}{Dt} = 0. \quad (2.89)$$

We return to the energy equation in standard conservation form, without friction and heat conduction:

$$\frac{\partial}{\partial t} \left(\rho e + \frac{1}{2}\rho v^2 \right) + \nabla \cdot \left(\mathbf{v}(\rho e + \frac{1}{2}\rho v^2 + p) \right) = \mathbf{v} \cdot \mathbf{f}. \quad (2.90)$$

From the fundamental law of thermodynamics (1.8):

$$T ds = de + p d(\rho^{-1}) \quad (1.8)$$

we have for isentropic perturbations: $\left(\frac{\partial e}{\partial \rho}\right)_s = \frac{p}{\rho^2}$, and so

$$\left(\frac{\partial \rho e}{\partial \rho}\right)_s = e + \frac{p}{\rho} = i, \quad \left(\frac{\partial^2 \rho e}{\partial \rho^2}\right)_s = \frac{1}{\rho} \left(\frac{\partial p}{\partial \rho}\right)_s = \frac{c^2}{\rho},$$

where i is the enthalpy (1.26) or heat function. We can now expand the total energy density, energy flux and source for acoustic (*i.e.* isentropic) perturbations up to second order, to find ($v_0 = 0$):

$$\rho e + \frac{1}{2}\rho v^2 = \rho_0 e_0 + i_0 \rho' + \frac{1}{2}\rho_0 c_0^2 \left(\frac{\rho'}{\rho_0}\right)^2 + \frac{1}{2}\rho_0 v'^2, \quad (2.91a)$$

$$\mathbf{v}(\rho e + \frac{1}{2}\rho v^2 + p) = \mathbf{v}'(i_0 \rho_0 + i_0 \rho' + p'), \quad (2.91b)$$

$$\mathbf{v} \cdot \mathbf{f} = \mathbf{v}' \cdot \mathbf{f}'. \quad (2.91c)$$

Noting that the steady state is constant, and using the equation of mass conservation

$$\frac{\partial \rho'}{\partial t} + \nabla \cdot (\rho_0 \mathbf{v}' + \rho' \mathbf{v}') = 0$$

in (2.90), with (2.91a–2.91c) substituted in it, we find that the zeroth and first order terms in ρ'/ρ_0 vanish so that (2.90) becomes within an accuracy of $O((\rho'/\rho_0)^3)$:

$$\frac{\partial}{\partial t} \left(\frac{p'^2}{2\rho_0 c_0^2} + \frac{\rho_0 v'^2}{2} \right) + \nabla \cdot (p' \mathbf{v}') = \mathbf{v}' \cdot \mathbf{f}', \quad (2.92)$$

which demonstrates that Kirchhoff's acoustic energy conservation law (2.79) is not only an energy-like relation of the approximate equations, but indeed also the consistent acoustic approximation of the energy equation of the full fluid mechanical problem.

2.7.3 Acoustic energy in a non-uniform flow

The method of Myers [160] to develop a more general acoustic energy conservation law follows similar lines as the discussion of the previous section. We consider a homentropic flow ($ds = 0$, so that $de = (p/\rho^2)d\rho$) with $v_0 \neq 0$. In this case the total enthalpy $B = e + p/\rho + \frac{1}{2}v^2$ appears to be a convenient variable. In terms of B the energy conservation law (2.90) becomes:

$$\frac{\partial}{\partial t} (\rho B - p) + \nabla \cdot (\rho B \mathbf{v}) = \mathbf{v} \cdot \mathbf{f}. \quad (2.93)$$

The momentum conservation law in Crocco's form (1.31) also involves B :

$$\frac{\partial \mathbf{v}}{\partial t} + \nabla B + \boldsymbol{\omega} \times \mathbf{v} = \mathbf{f}/\rho. \quad (2.94)$$

By subtracting $\rho_0 \mathbf{v}_0$ times the momentum conservation law (2.94) plus B_0 times the continuity equation (1.18) from the energy conservation law (2.93), substituting the steady state momentum conservation law:

$$\nabla B_0 + \boldsymbol{\omega}_0 \times \mathbf{v}_0 = \mathbf{f}_0 / \rho_0, \quad (2.95)$$

subtracting the steady state limit of the resulting equation, and using the vector identity $\mathbf{v} \cdot (\boldsymbol{\omega} \times \mathbf{v}) = 0$, Myers obtained the following energy corollary:

$$\frac{\partial}{\partial t} E_{\text{exact}} + \nabla \cdot \mathbf{I}_{\text{exact}} = -\mathcal{D}_{\text{exact}} \quad (2.96)$$

where E_{exact} , $\mathbf{I}_{\text{exact}}$ and $\mathcal{D}_{\text{exact}}$ are defined by:

$$E_{\text{exact}} = \rho(B - B_0) - (p - p_0) - \rho_0 \mathbf{v}_0 \cdot (\mathbf{v} - \mathbf{v}_0) \quad (2.97a)$$

$$\mathbf{I}_{\text{exact}} = (\rho \mathbf{v} - \rho_0 \mathbf{v}_0)(B - B_0) \quad (2.97b)$$

$$\begin{aligned} \mathcal{D}_{\text{exact}} = & (\rho \mathbf{v} - \rho_0 \mathbf{v}_0) \cdot (\boldsymbol{\omega} \times \mathbf{v} - \boldsymbol{\omega}_0 \times \mathbf{v}_0) - (\mathbf{v} - \mathbf{v}_0) \cdot (\mathbf{f} - \mathbf{f}_0) \\ & - (1 - \rho_0 / \rho) \mathbf{v}_0 \cdot \mathbf{f} - (1 - \rho / \rho_0) \mathbf{v} \cdot \mathbf{f}_0. \end{aligned} \quad (2.97c)$$

These auxiliary quantities E_{exact} , $\mathbf{I}_{\text{exact}}$ and $\mathcal{D}_{\text{exact}}$ have the important property, as Myers showed, that their zeroth and first order terms in the acoustic perturbation expansion in (ρ' / ρ_0) vanish, while the quadratic terms are *only* a function of the mean flow and acoustic (first order) quantities. As a result, the second order approximation of the exact quantities E_{exact} , $\mathbf{I}_{\text{exact}}$ and $\mathcal{D}_{\text{exact}}$ yield (for homentropic flow) a general acoustic energy definition¹³:

$$E = \frac{c_0^2 \rho'^2}{2\rho_0} + \frac{\rho_0 v'^2}{2} + \rho' \mathbf{v}_0 \cdot \mathbf{v}' \quad (2.98a)$$

$$\mathbf{I} = (\rho_0 \mathbf{v}' + \rho' \mathbf{v}_0) \left(\frac{c_0^2 \rho'}{\rho_0} + \mathbf{v}_0 \cdot \mathbf{v}' \right) \quad (2.98b)$$

$$\mathcal{D} = -\rho_0 \mathbf{v}_0 \cdot (\boldsymbol{\omega}' \times \mathbf{v}') - \rho' \mathbf{v}' \cdot (\boldsymbol{\omega}_0 \times \mathbf{v}_0) - (\mathbf{v}' + \rho' \mathbf{v}_0 / \rho_0) \cdot (\mathbf{f}' - \rho' \mathbf{f}_0 / \rho_0). \quad (2.98c)$$

This equation is identical to the acoustic energy conservation law derived by Goldstein [73] starting from the linearized equations of motion (with $\mathbf{f}_0 = 0$). It is important to note that, on the one hand, we have indeed obtained expressions entirely in first order quantities; on the other hand, however, these expressions represent only an acoustic energy conservation law if we adopt the definition that vorticity is non-acoustic and embodies possible acoustic sources or sinks. The present expressions for homentropic flow are further generalized by Myers in recent papers [161] and [162].

¹³Use the vector identity $\mathbf{a} \cdot (\mathbf{b} \times \mathbf{c}) = -\mathbf{c} \cdot (\mathbf{b} \times \mathbf{a})$.

2.7.4 Acoustic energy and vortex sound

Averaging (2.96) over one period for a periodic acoustic field and integrating over space yields, if $\mathbf{f} = 0$:

$$\mathcal{P} = \iint_S \langle \mathbf{I} \cdot \mathbf{n} \rangle d\sigma = - \iiint_V \langle \rho_0 \mathbf{v}_0 \cdot (\boldsymbol{\omega}' \times \mathbf{v}') + \rho' \mathbf{v}' \cdot (\boldsymbol{\omega}_0 \times \mathbf{v}_0) \rangle d\mathbf{x} \quad (2.99)$$

where \mathcal{P} is the acoustic power generated by the flow. It is interesting to compare this expression with the one derived by Howe [85] for a low Mach number compact vorticity distribution $\boldsymbol{\omega}$ in free space in the presence of compact solid surfaces:

$$\mathcal{P} = - \iiint_V \rho_0 \langle (\boldsymbol{\omega} \times \mathbf{v}) \cdot \mathbf{u}_a \rangle d\mathbf{x} \quad (2.100)$$

where \mathbf{u}_a is the acoustic velocity defined as the part of the unsteady velocity field \mathbf{v}' which is the gradient of a potential (irrotational $\nabla \times \mathbf{u}_a = 0$). While (2.99) is not restricted to low Mach numbers it only allows small time dependent perturbations $\boldsymbol{\omega}'$ of the time average vorticity $\boldsymbol{\omega}_0$ and in this sense is more restrictive than Howe's formula. Furthermore, (2.99) is difficult to interpret physically because \mathbf{v}' includes the solenoidal velocity perturbations $\boldsymbol{\omega}' = \nabla \times \mathbf{v}'$.

Howe's equation (2.100) has a simple physical interpretation which in the same way as Lighthill's theory can be called an aero-acoustic analogy (vortex sound). In the absence of vorticity the flow of an inviscid and non-conducting fluid is described by Bernoulli's equation (1.32b):

$$\frac{\partial \varphi}{\partial t} + B = 0. \quad (1.32b)$$

If in the same way as in Lighthill's analogy¹⁴ we extend the potential flow $\mathbf{v} = \nabla \varphi$ in a region where vorticity is present ($\boldsymbol{\omega} \neq 0$) then we can think of the vorticity term ($\boldsymbol{\omega} \times \mathbf{v}$) in Crocco's equation:

$$\frac{\partial \mathbf{v}}{\partial t} + \nabla B = -\boldsymbol{\omega} \times \mathbf{v} \quad (1.28)$$

equivalent to an external force field \mathbf{f} acting on the potential flow (acoustic field). Hence we have:

$$\mathbf{f} = -\rho(\boldsymbol{\omega} \times \mathbf{v}) \quad (2.101)$$

which is the density of the Coriolis force acting on the fluid particle as a result of the fluid rotation. For a compact region at low Mach numbers we can neglect density variation and use the approximation:

$$\mathbf{f} = -\rho_0(\boldsymbol{\omega} \times \mathbf{v}). \quad (2.102)$$

¹⁴In Lighthill's analogy the uniform quiescent fluid at the listener is extended into the source region.

In the absence of mean flow outside the source region we see by application of the integral form of Kirchhoff's energy equation (2.82) that we recover Howe's formula (2.100):

$$\mathcal{P} = \iiint_V \langle \mathbf{f} \cdot \mathbf{u}_a \rangle d\mathbf{x}. \quad (2.103)$$

This could also have been deduced from a comparison of the wave equation (2.76) in which we introduced the approximation $B' = i' = p'/\rho_0$ because $\mathbf{v}_0 = 0$:

$$\frac{1}{c_0^2} \frac{\partial^2 p'}{\partial t^2} - \nabla^2 p' = \rho_0 \nabla \cdot (\boldsymbol{\omega} \times \mathbf{v}) \quad (2.104)$$

and the wave equation (2.61) (without mass injection, $m = 0$):

$$\frac{1}{c_0^2} \frac{\partial^2 p'}{\partial t^2} - \nabla^2 p' = -\nabla \cdot \mathbf{f}. \quad (2.105)$$

This corresponds to Powell's approximation of the vortex sound theory in which we neglect terms of order M both in the wave region and in the source region ($B' = p'/\rho_0$).

In the presence of a uniform flow outside the source region, Goldstein [73] finds the wave equation:

$$\frac{1}{c_0^2} \frac{D_0^2 p'}{Dt^2} - \nabla^2 p' = -\nabla \cdot \mathbf{f} \quad (2.106)$$

where

$$\frac{D_0}{Dt} = \frac{\partial}{\partial t} + \mathbf{v}_0 \cdot \nabla.$$

The energy equation corresponding to (2.106) is for $\mathbf{f}_0 = 0$:

$$\mathcal{P} = \iiint_V \left\langle \left(\mathbf{u}_a + \frac{\rho'}{\rho_0} \mathbf{v}_0 \right) \cdot \mathbf{f} \right\rangle d\mathbf{x} \quad (2.107)$$

which suggests a generalization of Howe's equation with $\mathbf{f} = \rho_0(\boldsymbol{\omega} \times \mathbf{v})$:

$$\mathcal{P} = -\rho_0 \iiint_V \left\langle (\boldsymbol{\omega} \times \mathbf{v}) \cdot \left(\mathbf{u}_a + \frac{\rho'}{\rho_0} \mathbf{v}_0 \right) \right\rangle d\mathbf{x}, \quad (2.108)$$

which corresponds with the use of $B' = p'/\rho_0 + \mathbf{u}_a \cdot \mathbf{v}_0$ as acoustical variable, and $\mathbf{I} = B'(\rho\mathbf{v})'$ as the intensity with $(\rho\mathbf{v})' = \rho_0\mathbf{u}_a + \rho'\mathbf{v}_0$ the fluctuation of mass flux.

This generalization of Howe's equation is indeed derived by Jenvey [99]. Although the above discussion provides an intuitive interpretation of Jenvey's result, it is not obvious that Jenvey's definition of acoustic field agrees with Howe's definition. The range of validity of this energy corollary is therefore not obvious.

In practice Howe's energy corollary is convenient because it is formulated by an integral. Similar to Lighthill's analogy in integral form, it is not sensitive to "random errors" in the model. Integration over the volume and averaging over a period of oscillation smooths out such errors.

Exercises

- a) Calculate the minimum speed of sound of air/water mixtures at a depth of 100 m below sea surface. Assume a temperature $T_0 = 300$ K. Is it true that this speed of sound is independent of the gas as long as $\gamma = C_p/C_v$ is the same?
- b) Derive (2.93) from (2.90).
- c) Is the choice of c_0 in the analogy of Lighthill arbitrary?
- d) Does the acoustic source $\frac{\partial^2}{\partial t^2}(p'/c_0^2 - \rho')$ vanish for isentropic flows?
- e) Is the acoustic variable ρ' the most convenient choice to describe the sound production by unsteady combustion at low Mach numbers?
- f) Is the definition of acoustic intensity $\mathbf{I} = p'\mathbf{v}'$ valid in the presence of a mean flow?
- g) Is it correct that when using B' as acoustic variable instead of p' , one obtains a more accurate prediction of vortex sound in a compact region with locally a high Mach number?
- h) Is the equation $p' = c_0^2 \rho'$ always valid in a stagnant fluid?
- i) Is it correct that the acoustic impedance ρc of an ideal gas depends only on the pressure p ?
- j) Show that the surface of constant phase $\omega t - \mathbf{k} \cdot \mathbf{x} = \text{constant}$, of plane wave solution (2.22), is planar, even if ω is complex.
- k) Show that Kirchhoff's energy definition (2.80) remains valid for the conditions pertaining to (2.49).

3 Green's functions, impedance, and evanescent waves

3.1 Green's functions

3.1.1 Integral representations

Using Green's theorem we can construct an integral equation which combines the effect of sources, propagation, boundary conditions and initial conditions in a simple formula. The Green's function $G(\mathbf{x}, t|\mathbf{y}, \tau)$ is the impulse response of the wave equation:

$$\frac{\partial^2 G}{\partial t^2} - c_0^2 \frac{\partial^2 G}{\partial x_i^2} = \delta(\mathbf{x} - \mathbf{y})\delta(t - \tau). \quad (3.1)$$

Note that the Green's function is a generalized function! (See Appendix C.) The impulse $\delta(\mathbf{x} - \mathbf{y})\delta(t - \tau)$ is released at the source point \mathbf{y} at time τ and G is measured at the observation point \mathbf{x} at time t . The definition of G is further completed by specifying suitable boundary conditions at a surface S with outer normal \mathbf{n} enclosing the volume V in which \mathbf{x} and \mathbf{y} are localized:

$$\mathbf{n} \cdot \nabla G + bG = 0. \quad (3.2)$$

Furthermore, one usually assumes a causality condition for G that there is no field other than due to the δ -source:

$$G(\mathbf{x}, t|\mathbf{y}, \tau) = 0 \quad \text{and} \quad \frac{\partial}{\partial t} G(\mathbf{x}, t|\mathbf{y}, \tau) = 0 \quad (3.3)$$

for $t < \tau$. When the boundary conditions defining the Green's function coincide with those of the physical problem considered the Green's function is called a "tailored" Green's function. The integral equation is in such a case a convolution of the source $q(\mathbf{y}, \tau)$ with the impulse response $G(\mathbf{x}, t|\mathbf{y}, \tau)$. Of course, if the source q is known (and not dependent on the field) this integral equation is at the same time just the solution of the problem. A tailored Green's function is, in general, not easy to find. It will, therefore, appear that sometimes, for certain specific problems, the choice of a Green's function which is not tailored is more convenient.

Before we can discuss this, we have to consider some general properties of Green's functions, such as the important reciprocity relation:

$$G(\mathbf{x}, t|\mathbf{y}, \tau) = G(\mathbf{y}, -\tau|\mathbf{x}, -t). \quad (3.4)$$

For the free field this relation follows immediately from symmetry and causality. In general [152], this property can be derived by starting from the definition of the two Green's functions $G_1 = G(\mathbf{x}, t|\mathbf{y}_1, \tau_1)$ and $G_2 = G(\mathbf{x}, -t|\mathbf{y}_2, -\tau_2)$:

$$\frac{\partial^2 G_1}{\partial t^2} - c_0^2 \frac{\partial^2 G_1}{\partial x_i^2} = \delta(\mathbf{x} - \mathbf{y}_1) \delta(t - \tau_1) \quad (3.5a)$$

and

$$\frac{\partial^2 G_2}{\partial t^2} - c_0^2 \frac{\partial^2 G_2}{\partial x_i^2} = \delta(\mathbf{x} - \mathbf{y}_2) \delta(t - \tau_2). \quad (3.5b)$$

Multiplying (3.5a) by G_2 and subtracting (3.5b) multiplied by G_1 yields after integration over \mathbf{x} and t in V from $t = -\infty$ until a time t' larger than τ_1 and τ_2 :

$$\begin{aligned} \int_{-\infty}^{t'} \iiint_V \left\{ \left[G_2 \frac{\partial^2 G_1}{\partial t^2} - G_1 \frac{\partial^2 G_2}{\partial t^2} \right] - c_0^2 \left[G_2 \frac{\partial^2 G_1}{\partial x_i^2} - G_1 \frac{\partial^2 G_2}{\partial x_i^2} \right] \right\} d\mathbf{x} dt \\ = G(\mathbf{y}_1, -\tau_1|\mathbf{y}_2, -\tau_2) - G(\mathbf{y}_2, \tau_2|\mathbf{y}_1, \tau_1). \end{aligned} \quad (3.6)$$

Partial integration of the left-hand side yields:

$$\iiint_V \left[G_2 \frac{\partial G_1}{\partial t} - G_1 \frac{\partial G_2}{\partial t} \right] d\mathbf{x} \Big|_{t=-\infty}^{t=t'} - c_0^2 \int_{-\infty}^{t'} \iint_S \left[G_2 \frac{\partial G_1}{\partial x_i} - G_1 \frac{\partial G_2}{\partial x_i} \right] n_i d\sigma dt = 0 \quad (3.7)$$

where the first integral vanishes because for $t = -\infty$ both G_1 and G_2 vanish because of the causality condition (3.3). At $t = t'$ the first integral vanishes because $-t'$ is earlier than $-\tau_2$ ($t' > \tau_2$) and therefore both $G_2 = G(\mathbf{x}, -t'|\mathbf{y}_2, -\tau_2) = 0$ and $\partial G_2 / \partial t|_{t=t'} = 0$ because of causality. The second integral vanishes because G_1 and G_2 satisfy the same boundary conditions on boundary S . Replacing \mathbf{y}_1 and τ_1 by \mathbf{y} and τ and \mathbf{y}_2 and τ_2 by \mathbf{x} and t in the right-hand side of (3.6) yields (3.4).

We now will prove that the Green's function $G(\mathbf{x}, t|\mathbf{y}, \tau)$ also satisfies the equation:

$$\frac{\partial^2 G}{\partial \tau^2} - c_0^2 \frac{\partial^2 G}{\partial y_i^2} = \delta(\mathbf{x} - \mathbf{y}) \delta(t - \tau). \quad (3.8)$$

We first note that because of the symmetry of $\delta(t - \tau)$ the time-reversed function $G(\mathbf{x}, -t|\mathbf{y}, -\tau)$ satisfies (3.1):

$$\frac{\partial^2}{\partial t^2} G(\mathbf{x}, -t|\mathbf{y}, -\tau) - c_0^2 \frac{\partial^2}{\partial x_i^2} G(\mathbf{x}, -t|\mathbf{y}, -\tau) = \delta(\mathbf{x} - \mathbf{y}) \delta(t - \tau). \quad (3.9)$$

Using now the reciprocity relation (3.4) and interchanging the notation $\mathbf{x} \leftrightarrow \mathbf{y}$ and $t \leftrightarrow \tau$ we find (3.8).

We have now all that is necessary to obtain a formal solution to the wave equation:

$$\frac{\partial^2 \rho'}{\partial \tau^2} - c_0^2 \frac{\partial^2 \rho'}{\partial y_i^2} = q(\mathbf{y}, \tau). \quad (3.10)$$

After subtracting equation 3.8, multiplied by $\rho'(\mathbf{y}, \tau)$, from equation (3.10), multiplied by $G(\mathbf{x}, t|\mathbf{y}, \tau)$, and then integration to \mathbf{y} over V and to τ between $+t_0$ and t , we obtain:

$$\begin{aligned} \rho'(\mathbf{x}, t) = & \int_{t_0}^{t+} \iiint_V q(\mathbf{y}, \tau) G(\mathbf{x}, t|\mathbf{y}, \tau) \, dy d\tau + \int_{t_0}^{t+} \iiint_V \left[\rho'(\mathbf{y}, \tau) \frac{\partial^2 G}{\partial \tau^2} - G \frac{\partial^2 \rho'(\mathbf{y}, \tau)}{\partial \tau^2} \right] \, dy d\tau \\ & - c_0^2 \int_{t_0}^{t+} \iiint_V \left[\rho'(\mathbf{y}, \tau) \frac{\partial^2 G}{\partial y_i^2} - G \frac{\partial^2 \rho'(\mathbf{y}, \tau)}{\partial y_i^2} \right] \, dy d\tau. \end{aligned} \quad (3.11)$$

Partial integration over the time of the second integral and over the space of the third integral in the right-hand side of (3.11) yields:

$$\begin{aligned} \rho'(\mathbf{x}, t) = & \int_{t_0}^t \iiint_V q(\mathbf{y}, \tau) G(\mathbf{x}, t|\mathbf{y}, \tau) \, dy d\tau - c_0^2 \int_{t_0}^t \iint_S \left[\rho'(\mathbf{y}, \tau) \frac{\partial G}{\partial y_i} - G \frac{\partial \rho'(\mathbf{y}, \tau)}{\partial y_i} \right] n_i \, d\sigma d\tau \\ & - \left[\iiint_V \left[\rho'(\mathbf{y}, \tau) \frac{\partial G}{\partial \tau} - G \frac{\partial \rho'(\mathbf{y}, \tau)}{\partial \tau} \right] \, dy \right]_{\tau=t_0} \end{aligned} \quad (3.12)$$

where the second integral vanishes for a tailored Green's function and the third integral represents the effect of the initial conditions at $\tau = t_0$. For a tailored Green's function, and if $t_0 = -\infty$, we have the superposition principle over elementary sources which we expect intuitively:

$$\rho'(\mathbf{x}, t) = \int_{-\infty}^t \iiint_V q(\mathbf{y}, \tau) G(\mathbf{x}, t|\mathbf{y}, \tau) \, dy d\tau. \quad (3.13)$$

In chapter 4 and 6 we will again reconsider the Green's functions in more detail. For the present time we should remember that (3.12) or (3.13) is only an explicit solution of the wave equation if q is given. When the sound source q depends on the acoustic field ρ' these equations are integral equations rather than an explicit solution.

Even in such a case the integral representation is useful because we have split up the problem into a purely linear problem of finding a Green's function and a second problem of solving an integral equation. Also as stated earlier the integral equation is most convenient for introducing approximations because integration tends to smooth out the errors of the approximations.

The treatment given here is taken from the textbook of Morse and Feshbach [152]. An integral formula for the convective wave equation (2.52) and the corresponding Green's function and integral formulation are found in Goldstein [73].

3.1.2 Remarks on finding Green's functions

In general, a (tailored) Green's function is only marginally easier to find than the full solution of an inhomogeneous linear partial differential equation. Therefore, it is not possible to give a general recipe how to find a Green's function for a given problem. Sometimes an expansion in eigenfunction or modes (like in duct acoustics; see chapter 7) is possible.

It is, however, important to note that very often we can simplify a problem already, for example by integral representations as above, by using free field Green's functions, *i.e.* the Green's function of the problem without the usually complicating boundaries. If the medium is uniform in all directions, the only independent variables are the distance to the source $|\mathbf{x} - \mathbf{y}|$ and time lag $t - \tau$. Furthermore, the delta-function source may be rendered into a more easily treated form by spatial Fourier transformation. Examples are given in Appendix C.2.7 and section 4.6, while a table is given in Appendix E.

3.2 Acoustic impedance

A useful quantity in acoustics is impedance. It is a measure of the amount by which the motion induced by a pressure applied to a surface is impeded. Or in other words: a measure of the lumpiness of the surface. Since frictional forces are, by and large, proportional to velocity, a natural choice for this measure is the ratio between pressure and velocity¹. A quantity, however, that would vary with time, and depend on the initial values of the signal is not very interesting. Therefore, impedance is defined via the Fourier transformed signal as:

$$Z(\mathbf{x}; \omega) = \frac{\hat{p}(\mathbf{x}; \omega)}{\hat{\mathbf{v}}(\mathbf{x}; \omega) \cdot \mathbf{n}_S(\mathbf{x})} \quad (3.14)$$

at a point \mathbf{x} on a surface S with unit normal vector \mathbf{n}_S pointing into² the surface. The impedance is a complex number and a function of ω and position. The real part is called the *resistance*, the imaginary part is called the *reactance*, and its inverse $1/Z$ is called the *admittance*.

In the most general situation the ratio $Z = \hat{p}/(\hat{\mathbf{v}} \cdot \mathbf{n}_S)$ is just a number, with a limited relevance. We cannot consider the impedance Z as a property of the surface S , because Z depends *also* on the acoustic field. However, this is not the case for the class of so-called *locally reacting* linear surfaces. The response of such a surface to an acoustic wave is linear and pointwise, with the result that the impedance is indeed the same for any solution, and therefore a property of the surface alone.

¹In mechanics, impedance denotes originally the ratio between a force amplitude and a velocity amplitude. In some texts, the ratio acoustic pressure/velocity is therefore called "impedance per area" or specific impedance. We reserve the nomenclature "specific impedance" to the (dimensionless) ratio of the impedance and the fluid impedance $\rho_0 c_0$.

²Note that usually the normal vector of a surface is defined out of the surface.

Mathematically it is important to note that an impedance boundary condition is of “mixed type”. Via the general Green's function representation

$$\hat{p} = \iint_S \left(\hat{p} \nabla G + i k \rho_0 c_0 \hat{\nu} G \right) \cdot \mathbf{n}_S \, d\sigma \quad (3.15a)$$

the Helmholtz equation reduces to an integral equation in \hat{p} if surface S has an impedance Z :

$$\hat{p} = \iint_S \left(\nabla G \cdot \mathbf{n}_S + \frac{i k \rho_0 c_0}{Z} G \right) \hat{p} \, d\sigma. \quad (3.15b)$$

Sometimes it is instructive to describe the coupling between two adjacent regions of an acoustic field by means of an equivalent impedance. Suppose we place between these regions (say, region 1 and region 2) a fictitious interface, with an impedance such, that the presence of the surface would generate the same sound field in region 1 as there exists without surface. In that case we could say that the effect of region 2 onto region 1 is described by this impedance.

For example, a free field plane wave $e^{i\omega t - ikx}$, with $k = \omega/c_0$ and satisfying $i\omega\rho_0\mathbf{v} + \nabla p = 0$, would not be reflected by a screen, positioned parallel to the y, z -plane, if this screen has the impedance $Z = \rho_0 c_0$. So for plane waves and in the far field (where the waves become approximately plane) the fluid may be said to have the impedance $\rho_0 c_0$. This inherent impedance of the fluid is used to make Z dimensionless leading to the *specific impedance* $Z/\rho_0 c_0$.

Many other examples are found in 1-dimensional (pipe-) models of acoustic systems where local 3-dimensional behaviour is “packed” in an effective impedance. It may be worthwhile to note that for such models many authors find it convenient to divide Z by the surface S of the pipe cross section. In such a case the impedance is the ratio of the acoustic pressure \hat{p} and the volume flux $(\hat{\mathbf{u}} \cdot \mathbf{n})S$ leaving the control volume. The one-dimensional approach then allows the use of all mathematical tools developed for electrical circuits if we assume \hat{p} to be the equivalent of the electric voltage, $(\hat{\mathbf{u}} \cdot \mathbf{n})S$ the equivalent of the electric current, and a tube to correspond to a transmission line. Further, a compact volume is the equivalent of a capacity, and a compact orifice is a self induction. The pressure difference is in linear approximation due to the inertia of the air in the orifice and hence proportional to the acceleration $(\partial/\partial t)(\hat{\mathbf{u}} \cdot \mathbf{n})$ (section 4.4.3).

3.2.1 Impedance and acoustic energy

For a quiescent fluid the acoustic power flow (2.82) across S for a time-harmonic field $\sim e^{i\omega t}$ is

$$\begin{aligned} \mathcal{P} &= \iint_S \frac{\omega}{2\pi} \int_0^{2\pi/\omega} \operatorname{Re}(\hat{p} e^{i\omega t}) \operatorname{Re}(\hat{\mathbf{v}} \cdot \mathbf{n}_S e^{i\omega t}) dt d\sigma \\ &= \iint_S \frac{1}{4} (\hat{p} \hat{\mathbf{v}}^* + \hat{p}^* \hat{\mathbf{v}}) \cdot \mathbf{n}_S d\sigma \end{aligned} \quad (3.16a)$$

$$= \iint_S \frac{1}{2} \operatorname{Re}(\hat{p}^* \hat{\mathbf{v}} \cdot \mathbf{n}_S) d\sigma, \quad (3.16b)$$

where z^* denotes the complex conjugate of z . If the surface has an impedance Z , the power becomes

$$\mathcal{P} = \iint_S \frac{1}{2} \operatorname{Re}(Z) |\hat{\mathbf{v}} \cdot \mathbf{n}_S|^2 d\sigma. \quad (3.17)$$

Hence, the real part of the impedance (the resistance) is related to the energy flow: if $\operatorname{Re}(Z) > 0$ (for $\omega \in \mathbb{R}$), the surface is *passive* and absorbs energy; if $\operatorname{Re}(Z) < 0$, it is *active* and produces energy.

3.2.2 Impedance and reflection coefficient

If we consider the acoustic field for $x < 0$ in a tube at low frequencies, we can write

$$p(x, t) = \hat{p}(x) e^{i\omega t} = p^+ e^{i\omega t - ikx} + p^- e^{i\omega t + ikx} \quad (3.18)$$

where $k = \omega/c_0$, p^+ is the amplitude of the wave incident at $x = 0$ from $x < 0$ and p^- is the amplitude of the wave reflected at $x = 0$ by an impedance Z . Using the linearized momentum conservation law $\rho_0(\partial v/\partial t) = -\partial p/\partial x$ we find:

$$\hat{v}(x) = \frac{1}{\rho_0 c_0} (p^+ e^{-ikx} - p^- e^{ikx}). \quad (3.19)$$

If we define the reflection coefficient R at $x = 0$ as:

$$R = p^- / p^+ \quad (3.20)$$

we see that because $Z = \hat{p}(0)/\hat{v}(0)$:

$$R = \frac{Z - \rho_0 c_0}{Z + \rho_0 c_0}. \quad (3.21)$$

In two dimensions we have a similar result. Consider a plane wave (amplitude p^+), propagating in the direction $(\cos \vartheta, \sin \vartheta)$ where ϑ is the angle with the positive x -axis (c.f. Fig. 3.6), and approaching from $y < 0$ an impedance wall at $y = 0$. Here it reflects into a wave (amplitude p^-) propagating in the direction $(\cos \vartheta, -\sin \vartheta)$. The pressure field is given by

$$\hat{p}(x, y) = e^{-ikx \cos \vartheta} \left(p^+ e^{-iky \sin \vartheta} + p^- e^{iky \sin \vartheta} \right). \quad (3.22)$$

The y -component of the velocity is

$$\hat{v}(x, y) = \frac{\sin \vartheta}{\rho_0 c_0} e^{-ikx \cos \vartheta} \left(p^+ e^{-iky \sin \vartheta} - p^- e^{iky \sin \vartheta} \right), \quad (3.23)$$

so we have for the impedance

$$Z = \frac{\hat{p}(x, 0)}{\hat{v}(x, 0)} = \frac{\rho_0 c_0}{\sin \vartheta} \frac{p^+ + p^-}{p^+ - p^-} = \frac{\rho_0 c_0}{\sin \vartheta} \frac{1 + R}{1 - R}, \quad (3.24)$$

and for the reflection coefficient

$$R = \frac{Z \sin \vartheta - \rho_0 c_0}{Z \sin \vartheta + \rho_0 c_0}. \quad (3.25)$$

The impedance with no reflection (of a plane surface) is thus $Z = \rho_0 c_0 / \sin \vartheta$.

3.2.3 Impedance and causality

In order to obtain a causal solution of a problem defined by boundary conditions expressed in terms of an impedance Z , the impedance should have a particular form.

Consider an arbitrary plane wave $p_i = f(t - x/c_0)$ incident from $x < 0$, and reflecting into $p_r = g(t + x/c_0)$ by an impedance wall at $x = 0$, with impedance $Z(\omega)$. The total acoustic field is given for $x < 0$ by:

$$p(x, t) = f(t - x/c_0) + g(t + x/c_0), \quad (3.26a)$$

$$v(x, t) = \frac{1}{\rho_0 c_0} \left(f(t - x/c_0) - g(t + x/c_0) \right). \quad (3.26b)$$

The reflected wave g is determined via the impedance condition, and therefore via the Fourier transforms of the p and v . As we have seen above (equation 3.21), we have for the Fourier transforms \hat{f} and \hat{g} :

$$\hat{g}(\omega) = \frac{Z(\omega) - \rho_0 c_0}{Z(\omega) + \rho_0 c_0} \hat{f}(\omega). \quad (3.27)$$

More information can be obtained, however, if we transform the boundary condition back to the time domain

$$p(0, t) = \int_{-\infty}^{\infty} \hat{p}(0, \omega) e^{i\omega t} d\omega \tag{3.28a}$$

$$= \int_{-\infty}^{\infty} Z(\omega) \hat{v}(0, \omega) e^{i\omega t} d\omega \tag{3.28b}$$

leading to the convolution product:

$$p(0, t) = \frac{1}{2\pi} \int_{-\infty}^{\infty} z(t - \tau) v(0, \tau) d\tau \tag{3.29}$$

where

$$z(t) = \int_{-\infty}^{\infty} Z(\omega) e^{i\omega t} d\omega. \tag{3.30}$$

Since $p(0, t)$ should only depend on the values of $v(0, t)$ of the past ($\tau < t$), the Fourier transform $z(t)$ of the impedance $Z(\omega)$ has to satisfy the *causality condition*:

$$z(t) = 0 \quad \text{for} \quad t < 0. \tag{3.31}$$

Of course, the same applies to the admittance $1/Z(\omega)$, when we express $v(0, t)$ in $p(0, t)$. This requires, under conditions as given in theorem (C.1) (p.283),

$$Z(\omega) \text{ and } 1/Z(\omega) \text{ are analytic in } \text{Im}(\omega) < 0. \tag{3.32}$$

Furthermore, since both p and v are real, z has to be real, which implies that Z has to satisfy the *reality condition*:

$$Z^*(\omega) = Z(-\omega) \text{ for } \omega \in \mathbb{R}. \tag{3.33}$$

Indeed, the mass-spring-damper system, given by

$$Z(\omega) = R + i\omega m - iK/\omega, \tag{3.34}$$

satisfies the reality condition if all parameters are real, but is only causal, with zeros and poles in the upper complex half plane, if all parameters are positive or zero.

Equation (3.29) yields an integral equation for g if we use equations (3.26a) and (3.26b) to eliminate p and v :

$$f(t) + g(t) = \frac{1}{2\pi\rho_0c_0} \int_{-\infty}^{\infty} z(t - \tau)(f(\tau) - g(\tau)) d\tau. \tag{3.35}$$

For any incident wave starting at some finite time ($t = 0$) we have $f(t) = 0$ for $t < 0$, so that all in all the infinite integral reduces to an integration over the interval $[0, t]$:

$$f(t) + g(t) = \frac{1}{2\pi\rho_0c_0} \int_0^t z(t-\tau)(f(\tau) - g(\tau)) d\tau. \quad (3.36)$$

For any time t , $g(t)$ is built up from $f(t)$ and the history of f and g along $[0, t]$.

As an example, consider an impedance wall of Helmholtz resonator type which is widely used in turbo fan aircraft engine inlets [201]. Such a wall is described (see next chapter) by:

$$Z(\omega) = \rho_0c_0 \left(R + i\omega m - i \cot\left(\frac{\omega L}{c_0}\right) \right). \quad (3.37)$$

where $R, m, L > 0$. Note that indeed $Z^*(\omega) = Z(-\omega)$. If we write $\frac{\omega L}{c_0} = \xi - i\eta$ and $\frac{c_0 m}{L} = \alpha$, then

$$\operatorname{Re}\left(\frac{Z}{\rho_0c_0}\right) = R + \alpha\eta + \coth(\eta) \frac{1 + \cot(\xi)^2}{\cot(\xi)^2 + \coth(\eta)^2} > 0$$

for $\eta > 0$, so Z is free from zeros in $\operatorname{Im}(\omega) < 0$. From the causality condition it follows that the poles of $\cot\left(\frac{\omega L}{c_0}\right)$ belong to the upper half of the complex ω -plane. Hence, we can Fourier transform Z back to the time domain (C.34) to find:

$$\frac{z(t)}{2\pi\rho_0c_0} = R\delta(t) + m\delta'(t) + \delta(t) + 2 \sum_{n=1}^{\infty} \delta\left(t - \frac{2nL}{c_0}\right) \quad (3.38)$$

where $\delta'(t)$ denotes the derivative of $\delta(t)$. Substitution of (3.38) in (3.36) shows that g can be expressed as a finite sum.

For certain parameter ranges the effect of viscous friction in the resonator neck (*c.f.* 2.13, 4.77) may be included by a term like $\sqrt{i\omega\nu}$; for example [210, 147]

$$Z(\omega) = \rho_0c_0 \left(b\sqrt{i\omega} + R + i\omega m - i \cot\left(\frac{\omega L}{c_0}\right) \right). \quad (3.39)$$

where $b > 0$. Since the complex square root function is subtle, it has to be emphasised that the square root, in the form as used here, should be the *ordinary* (principal value) square root. With a branch cut along the negative real axis for $\sqrt{\cdot}$, the branch cut of $\sqrt{i\omega}$ is then along the positive imaginary ω -axis, yielding a function analytic in $\operatorname{Im}(\omega) < 0$. In particular, $\sqrt{i\omega}$ should *not* be simplified to $\frac{1}{2}\sqrt{2}(1+i)\sqrt{\omega}$, unless the branch cut of $\sqrt{\omega}$ is rotated to the positive imaginary axis, which is of course in actual practice an intricate operation and prone to errors and confusion³.

Moreover, with $(\sqrt{i\omega})^* = \sqrt{-i\omega}$ (for $\omega \in \mathbb{R}$) also the reality condition is satisfied, while Z is still free from zeros in $\operatorname{Im}(\omega) < 0$, since $\operatorname{Re}(\sqrt{i\omega}) \sim \operatorname{Re}(\sqrt{\eta + i\xi}) > 0$ for $\eta > 0$ (see above). Fourier transformed back into time domain we have the causal (generalised) function

$$\int_{-\infty}^{\infty} \sqrt{i\omega} e^{i\omega t} d\omega = 2\sqrt{\pi} \frac{d}{dt} \left(\frac{H(t)}{\sqrt{t}} \right).$$

³In [210] it was too hastily concluded that $\sqrt{\omega}$ is not admissible in a physically possible impedance representation [147]. If $(1+i)\sqrt{\omega}$ is interpreted as $\sqrt{2i\omega}$ with branch cut as described, it is possible.

3.2.4 Impedance and surface waves

Part of sound that is scattered by an impedance wall may be confined to a thin layer near the wall, and behave like a surface wave [26, 258, 54, 167, 9, 192, 50, 236, 253, 207, 5], similar to the type of evanescent waves discussed in section 3.3. Examples of these type of solutions are found as irregular modes in lined ducts (section 7.4), or as sound that propagates with less than the usual $1/r^2$ -decay along an acoustically coated surface.

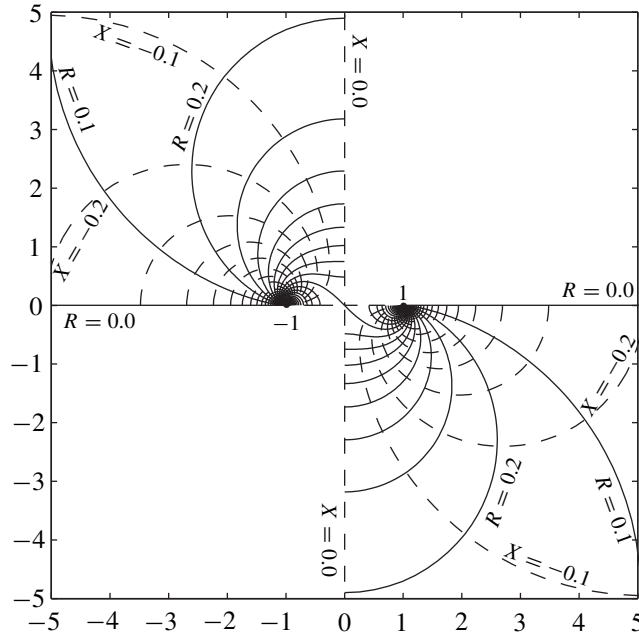


Figure 3.1 Trajectories of α for varying $Z = R + iX$ (no flow).
 Fixed R & $X = 0:-0.1:-\infty$ ———. Fixed X & $R = 0:0.1:\infty$ - - - - - .

Consider in (x, y) -space, $y \geq 0$, a harmonic pressure field $p(x, y) e^{i\omega t}$, satisfying

$$\nabla^2 p + k^2 p = 0, \quad \text{with} \quad ik p(x, 0) = Z \frac{\partial}{\partial y} p(x, 0)$$

where Z denotes the specific impedance (scaled on $\rho_0 c_0$) of the wall $y = 0$, and $k = \omega/c_0$. Suitable solutions are

$$p(x, y) = A e^{-(ik\alpha x \pm ik\gamma y)}, \quad \gamma(\alpha) = \sqrt{1 - \alpha^2}$$

where α is to be determined. The solutions we are interested in remain restricted to the wall, which means that $\pm \text{Im}(\gamma) \leq 0$. The sign of γ depends of course on our definition of the square root. In order to have one and the same expression for all α , *i.e.* $\propto e^{-(ik\alpha x + ik\gamma y)}$, it is therefore most convenient to

select the branch and branch cuts of γ such that $\text{Im}(\gamma) \leq 0$ everywhere (see equation 3.52 and figure 3.5). From the boundary condition it follows that the only solutions that can occur have to satisfy

$$\gamma(\alpha) = -Z^{-1}.$$

It follows that the only impedances that may bear a surface wave have to satisfy

$$\text{Im}(Z) \leq 0.$$

The complex values of scaled wave number α , corresponding to these solutions, are given by

$$\alpha = \pm \sqrt{1 - Z^{-2}}. \quad (3.40)$$

Trajectories of these wave numbers, as function of Z , are plotted in figure 3.1. To include all complex values of Z , we have drawn two fan-shaped families of curves: one for fixed $\text{Re}(Z)$ and one for fixed $\text{Im}(Z)$. Note that un-attenuated waves occur for purely imaginary Z . The thickness of the layer occupied by the wave is of the order $y = O(\lambda |\text{Im}(Z)|)$, where $\lambda = 2\pi/k$, the free field wave length.

3.2.5 Acoustic boundary condition in the presence of mean flow

The boundary condition to describe a vibrating impermeable wall is that the fluid particles follow the wall motion. In linearized form it is applied at the wall's mean or unperturbed position. Without mean flow, the linearized condition simply says that acoustic and wall's normal velocity match.

With mean flow the situation is more subtle. Both the actual normal vector and the mean flow velocity at the actual position differ from the mean values by an amount of acoustic order, which has to be taken into account. This was recognized by several authors for various special cases. Myers gave in [159] the most general formulation, which we will summarize here.

Consider the unsteady surface $S(t)$, which is a perturbation, scaling on a small parameter ε , of the steady surface S_0 . Associate to S_0 an orthogonal curvilinear co-ordinate system (α, β, γ) such that $\alpha = 0$ corresponds to S_0 . The mean flow \mathbf{v}_0 is tangent to the steady surface (section A.3), so

$$\mathbf{v}_0 \cdot \nabla \alpha = 0 \quad \text{at } \alpha = 0.$$

Let $S(t)$ be described, to leading order, by

$$\alpha = \varepsilon g(\beta, \gamma, t) + O(\varepsilon^2).$$

The condition of fluid particles following the surface $S(t)$ becomes

$$\frac{\partial}{\partial t}(\alpha - \varepsilon g) + (\mathbf{v}_0 + \varepsilon \mathbf{v}') \cdot \nabla(\alpha - \varepsilon g) = O(\varepsilon^2) \quad \text{at } \alpha = \varepsilon g,$$

where $\varepsilon \mathbf{v}'$ is the acoustic velocity. The linearization we seek is the acoustic order, *i.e.* $O(\varepsilon)$ when $\varepsilon \rightarrow 0$. This appears to be [159]

$$\mathbf{v}' \cdot \mathbf{n} = \left(\frac{\partial}{\partial t} + \mathbf{v}_0 \cdot \nabla - \mathbf{n} \cdot (\mathbf{n} \cdot \nabla \mathbf{v}_0) \right) \frac{g}{|\nabla \alpha|} \quad \text{at } \alpha = 0, \quad (3.41)$$

where \mathbf{n} is the normal of S_0 , directed away from S_0 into the fluid.

An important application of this result is an impedance wall (section 3.2) with inviscid mean flow. This can be found, for example, in the lined inlet duct of a turbo fan aircraft jet engine. The steady surface S_0 coincides with the impedance wall; the unsteady surface $S(t)$ is the position of a (fictitious) vortex sheet, modelling the boundary layer.

Since a vortex sheet cannot support a pressure difference, the pressure at the wall is the same as near the wall in the flow. If the wall has an impedance $Z \neq 0$ for harmonic perturbations $\sim e^{i\omega t}$ (see 3.14), the velocity and therefore the position g of $S(t)$ is known in terms of the pressure:

$$g = -\frac{1}{i\omega Z} \left(|\nabla \alpha| p \right)_{\alpha=0}.$$

In the mean flow, the impedance wall is now felt as

$$\mathbf{v}' \cdot \mathbf{n}_S = \left(i\omega + \mathbf{v}_0 \cdot \nabla - \mathbf{n}_S \cdot (\mathbf{n}_S \cdot \nabla \mathbf{v}_0) \right) \frac{P}{i\omega Z} \quad \text{at } S_0. \quad (3.42)$$

As is usual, the normal vector \mathbf{n}_S of S_0 is now selected to be directed *into* the wall. If $Z \equiv 0$, the boundary condition is just $p = 0$. For uniform mean flow along a plane wall (3.42) simplifies to

$$\mathbf{v}' \cdot \mathbf{n}_S = \left(i\omega + \mathbf{v}_0 \cdot \nabla \right) \frac{P}{i\omega Z}, \quad (3.43)$$

a result, obtained earlier by Ingard [95]. An application of this generalized boundary condition (3.42) may be found in [202, 205].

Of practical interest are the following observations. As the mean flow field is tangential to the wall, so $\mathbf{v}_0 \cdot \mathbf{n}_S = 0$, the following simplification may be derived

$$-\mathbf{n}_S \cdot (\mathbf{n}_S \cdot \nabla \mathbf{v}_0) = \mathbf{v}_0 \cdot (\mathbf{n}_S \cdot \nabla \mathbf{n}_S),$$

i.e. the expression does not really involve derivatives of \mathbf{v}_0 . (Incidentally, the vector $\mathbf{n}_S \cdot \nabla \mathbf{n}_S$ is tangential to the surface.) Furthermore, since $\nabla \cdot (\rho_0 \mathbf{v}_0) = 0$, we may multiply left and right hand side of (3.42) by ρ_0 and obtain the form

$$\rho_0 \mathbf{v}' \cdot \mathbf{n}_S = \frac{\rho_0 P}{Z} + (\nabla + \mathbf{n}_S \cdot \nabla \mathbf{n}_S) \cdot \left(\frac{\rho_0 \mathbf{v}_0 P}{i\omega Z} \right). \quad (3.44)$$

The last part between brackets may be further simplified to the following two forms (*c.f.* [145, 61])

$$(\nabla + \mathbf{n}_S \cdot \nabla \mathbf{n}_S) \cdot \left(\frac{\rho_0 \mathbf{v}_0 p}{i\omega Z} \right) = \mathbf{n}_S \cdot \nabla \times \left(\mathbf{n}_S \times \frac{\rho_0 \mathbf{v}_0 p}{i\omega Z} \right), \quad (3.45a)$$

$$= \frac{1}{h_\sigma} \frac{\partial}{\partial \tau} \left(h_\sigma \frac{\rho_0 \mathbf{v}_0 p}{i\omega Z} \right), \quad (3.45b)$$

where $v_0 = |\mathbf{v}_0|$ and a local orthogonal coordinate system (τ, σ, ν) is introduced associated to the wall. Coordinate ν is related to the wall normal vector \mathbf{n} , coordinate τ is the arclength along a streamline of \mathbf{v}_0 , and σ is orthogonal to τ in the wall surface. h_σ is a scale factor of σ , defined by $h_\sigma^2 = \left(\frac{\partial}{\partial \sigma} x\right)^2 + \left(\frac{\partial}{\partial \sigma} y\right)^2 + \left(\frac{\partial}{\partial \sigma} z\right)^2$. Note that (3.45b) involves no more than a derivative in streamwise direction.

3.2.6 Surface waves along an impedance wall with mean flow

Consider in (x, y) -space, $y \geq 0$, a uniform mean flow in x -direction with Mach number M , and a harmonic field $\sim e^{i\omega t}$ satisfying (see equation 2.52)

$$\begin{aligned} \left(ik + M \frac{\partial}{\partial x} \right)^2 p - \left(\frac{\partial^2}{\partial x^2} + \frac{\partial^2}{\partial y^2} \right) p &= 0 \\ \left(ik + M \frac{\partial}{\partial x} \right) \mathbf{v} + \nabla p &= 0 \end{aligned}$$

where $k = \omega/c_0$. Pressure p is made dimensionless on $\rho_0 c_0^2$ and velocity \mathbf{v} on c_0 . At $y = 0$ we have an impedance boundary condition given by (see equation 3.42)

$$ikZv = - \left(ik + M \frac{\partial}{\partial x} \right) p$$

where Z denotes the constant specific wall impedance and v the vertical velocity.

Solutions that decay for $y \rightarrow \infty$ are of the type discussed in section 3.3

$$p(x, y) = A e^{-ik\alpha x - ik\Gamma y}.$$

From the equations and boundary condition it follows that

$$(1 - \alpha M)^2 + \Gamma Z = 0, \quad \alpha^2 + \Gamma^2 = (1 - \alpha M)^2.$$

For further analysis it is convenient to introduce the Lorentz or Prandtl-Glauert type transformation (see 7.42 and section 9.1.1),

$$\beta = \sqrt{1 - M^2}, \quad \sigma = M + \beta^2 \alpha, \quad \gamma = \beta \Gamma, \quad \gamma = \sqrt{1 - \sigma^2} \quad (3.46)$$

with the branch and branch cuts of $\gamma(\sigma)$ selected such that $\text{Im}(\gamma) \leq 0$ (see equation 3.52 and figure 3.5).

As a result (see [200, 207]) we have the equation for the reduced axial complex wave number σ as a function of Z

$$(1 - M\sigma)^2 + \beta^3 \gamma(\sigma)Z = 0 \quad (3.47)$$

By squaring we obtain a 4-th order polynomial equation with 4 complex roots. So in our problem we have at most 4 solutions. To investigate the occurrence of these solutions, we analyse in detail the behaviour of possible solutions σ along the branch cuts of γ , because it is there where possible solutions may appear from or disappear to the second Riemann sheet of γ . From a careful analysis (see [200, 207]) it appears that in the Z -plane there are 5 distinct regions with 0, 1, 2, 3, and 4 solutions σ , while in the σ -plane we can identify an egg-shaped area, of radius $\simeq M^{-1}$, inside and outside of which we have 4 regions where solutions σ may occur. See the figures 3.2, 3.3, and figure 3.4.

Inside the egg we have acoustic surface waves (a right-running σ_{SR} and a left-running σ_{SL}). Outside the egg we have hydrodynamic modes (they disappear to infinity with vanishing Mach number) σ_{HS} and σ_{HI} , probably both right-running, such that σ_{HS} is decaying (stable) and σ_{HI} is increasing (unstable). This unstable behaviour depends on the frequency-dependence of Z , and can be proven for an impedance of mass-spring-damper type (3.34) in the incompressible limit [200, 207, 212].

In the limit for hard walls, *i.e.* for $|Z| \rightarrow \infty$ while $\text{Im} Z < 0$, the hydrodynamic surface waves σ_{HI} and σ_{HS} disappear to infinity while the acoustic surface waves σ_{SR} and σ_{SL} approach ± 1 in the

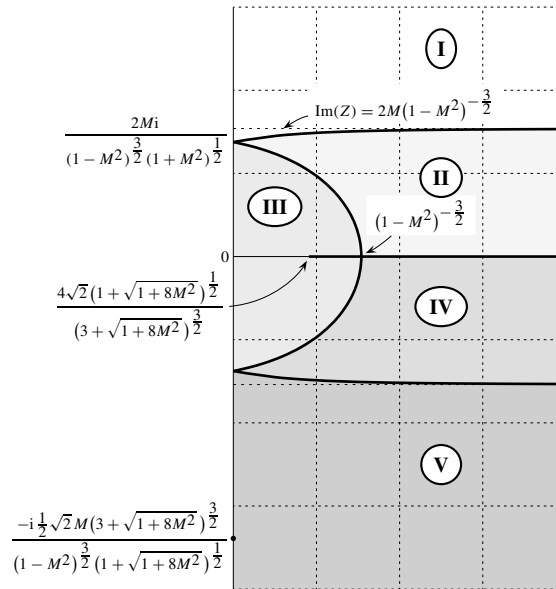


Figure 3.2 Complex impedance Z -plane, with regions of different numbers of surface waves.

No solutions in **I**, $\sigma_{HI} \in \mathbf{II} \dots \mathbf{V}$, $\sigma_{SR} \in \mathbf{III} \dots \mathbf{V}$, $\sigma_{SL} \in \mathbf{IV} \dots \mathbf{V}$, $\sigma_{HS} \in \mathbf{V}$.

Thick lines map to the branch cuts in figure 3.3. In the figure $M = 0.5$ is taken.

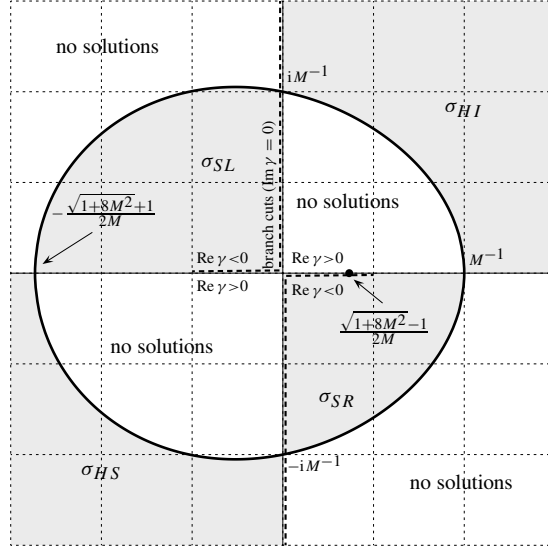


Figure 3.3 Complex reduced wave number σ -plane, with regions of existence of surface waves. Thick lines map to the imaginary Z -axis in figure 3.2 (except for the part in region I where no solutions exist). In the figure, $M = 0.5$ is taken.

following way

$$\sigma_{HI}, \sigma_{HS} \simeq \pm i \frac{\beta^3}{M^2} Z, \quad \sigma_{SR}, \sigma_{SL} \simeq \pm 1 \mp \frac{(1 \mp M)^4}{2Z^2 \beta^6}. \tag{3.48}$$

3.2.7 Instability, ill-posedness, and a regularization

Although the Ingard-Myers limit of a vanishing mean flow boundary layer is very reasonable for a fixed frequency, with all pertaining wavelengths being much longer than the boundary layer thickness, it is totally useless [25, 23] in time domain [210].

The problem is that if we gradually reduce the boundary layer, one of the above hydrodynamic surface waves changes from a convective instability (a positive growth rate for at least part of the wave number spectrum but always with a group velocity directed downstream) to an absolute instability (positive, 0, and negative group velocities yielding unstable behaviour everywhere) [212]. At the same time the growth rate increases until it becomes infinite in the Ingard-Myers limit of a vanishing boundary layer. This implies that in time domain, any perturbation excites in zero time an infinitely large instability. A model or mathematical problem with this property is called *ill-posed*.

The (presumably) convective instability has been observed experimentally [10], but the absolute instability probably only numerically [34]. The reason appears to be [212] that the critical boundary

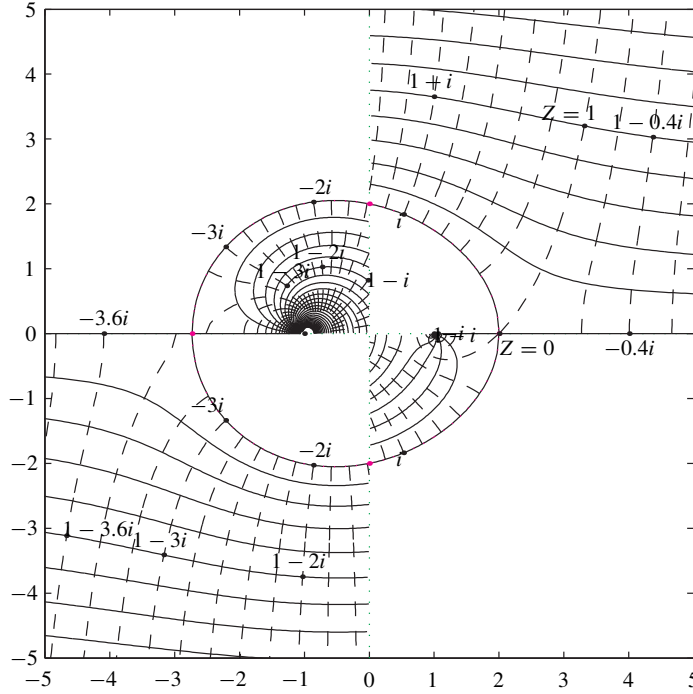


Figure 3.4 Trajectories of σ for varying $Z = R + iX$ and $M = 0.5$.
 Fixed R & $X = -\infty:0.2:\infty$ ———. Fixed X & $R = 0:0.2:\infty$ - - - - - .

layer thickness, where the instability of the system changes from convective to absolute, is in any practical situation so small (several microns) that it has never been realised.

One way to cure this problem of the Ingard-Myers model is to regularise the boundary condition by including the effect of a boundary layer of very thin but non-zero thickness h . For example like in [212] for a flat lined wall of uniform dimensional impedance $Z(\omega)$ and a mean flow $\mathbf{v}_0 = U_\infty \mathbf{e}_x$

$$Z(\omega) = \frac{\left(i\omega + U_\infty \frac{\partial}{\partial x}\right) p' - h\rho_0 i\omega \left(\frac{2}{3}i\omega + \frac{1}{3}U_\infty \frac{\partial}{\partial x}\right) (\mathbf{v}' \cdot \mathbf{n}_S)}{i\omega (\mathbf{v}' \cdot \mathbf{n}_S) + \frac{h}{\rho_0} \frac{\partial^2}{\partial x^2} p' - \frac{1}{3}h i\omega \frac{\partial}{\partial \mathbf{n}_S} (\mathbf{v}' \cdot \mathbf{n}_S)} \quad (3.49)$$

which is to be compared with (3.43). By selecting a boundary layer thicker than the critical thickness (this depends on the assumed liner model), we can guarantee a well-posed model. For a mass-spring-damper liner (3.34) this was found to be

$$h_c \simeq \frac{1}{4} \left(\frac{\rho_0 U_\infty}{R}\right)^2 U_\infty \sqrt{\frac{m}{K}} \quad (3.50)$$

Another form, for circumferential modes in circular ducts, has been proposed by Brambley [24], but without estimate for a sufficient thickness of the boundary layer.

3.3 Evanescent waves and related behaviour

3.3.1 An important complex square root

The wave equation in 2-D has the very important property that a disturbance of (positive) frequency ω and (real) wave number α in (say) x -direction is only radiating sound if frequency and wave number satisfy the inequality

$$|\alpha| < \omega/c_0$$

(a similar inequality holds in 3-D). Outside this regime the generated disturbances are exponentially decaying (evanescent) in y without an associated sound field. This is seen as follows.

Consider in the 2-D half space $y \geq 0$ the harmonic sound field $p(x, y, \omega) e^{i\omega t}$ satisfying the Helmholtz equation

$$\nabla^2 p + k^2 p = 0.$$

where $k = \omega/c_0$. If p , generated by (say) the surface $y = 0$, is given at $y = 0$ as the Fourier integral

$$p(x, 0) = p_0(x) = \int_{-\infty}^{\infty} A(\alpha) e^{-i\alpha x} d\alpha,$$

it is easily verified that the field in $y \geq 0$ may be written as

$$p(x, y) = \int_{-\infty}^{\infty} A(\alpha) e^{-i\alpha x - i\gamma y} d\alpha \quad (3.51)$$

with the important square root (with branch cuts along the imaginary axis, and the real interval $|\alpha| \leq k$; see figure 3.5)

$$\gamma(\alpha) = \sqrt{k^2 - \alpha^2}, \quad \text{Im}(\gamma) \leq 0, \quad \gamma(0) = k. \quad (3.52)$$

The complex square root is here defined such that for any complex α the wave $e^{-i\alpha x - i\gamma y}$ radiates or decays in positive y -direction. This is not necessary (we could always invoke the other solution $\sim e^{+i\gamma y}$), but very convenient if complex α 's are essential in the problem.

If we consider solutions of the Fourier-integral type (3.51), the only α 's to be considered are real. We see that only that part of $p_0(x)$ is radiated into $y > 0$ which corresponds to real positive γ , *i.e.*

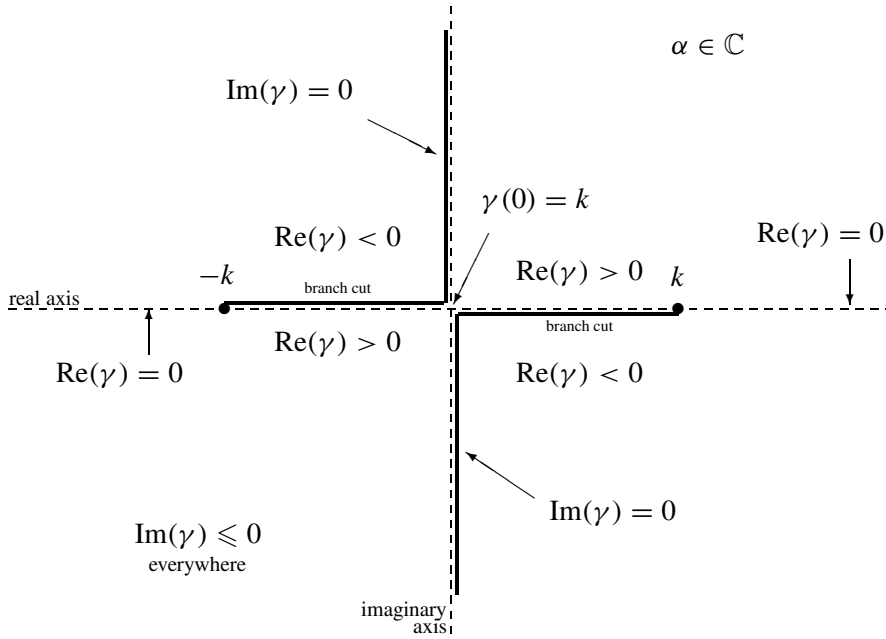


Figure 3.5 Branch cuts and signs of $\gamma = \sqrt{k^2 - \alpha^2}$ in complex α -plane. The definition of $\gamma(\alpha)$ adopted here is the branch of the multi-valued complex square root that corresponds to $\text{Im}(\gamma) \leq 0$ for all α . $\text{Im}(\gamma) = 0$ along the branch cuts. $\gamma(\alpha) \simeq -i \text{sign}(\text{Re } \alpha)$ if $|\alpha| \gg k$. The required definition is most efficiently realised by $\gamma(\alpha) = -i \sqrt[pv]{\alpha^2 - k^2}$, where $\sqrt[pv]{\cdot}$ denotes the principal value (*i.e.* standard) square root.

with $|\alpha| < k$. The rest decays exponentially with y , and is undetectable for $y \rightarrow \infty$. This near field with $|\alpha| > k$ is essentially of hydrodynamic nature, and becomes just an incompressible flow field for $|\alpha| \gg k$. If this is true for all α , including the largest α^{-1} , which scales on the size of the object, it is equivalent to the condition of compactness (2.27), and shows that compact sources are acoustically inefficient.

This distinction between radiating acoustic and non-radiating near field has far reaching implications. We give some examples.

3.3.2 The Walkman

The low frequencies of a small Walkman headphone are not radiated as sound. We do, however, detect the pressure when our ear is in the hydrodynamic near field.

3.3.3 Ill-posed inverse problem

Infinitely many boundary conditions are equivalent in the far field. The above boundary condition $p(x, 0) = p_0(x)$ and any other with the same α -spectrum on $[-k, k]$, for example

$$p(x, 0) = \tilde{p}_0(x) = \int_{-k}^k A(\alpha) e^{-i\alpha x} dx$$

produce the same far field. Therefore, the *inverse* problem of determining p_0 from a measured far field is very difficult (ill-posed). Fine details, with a spatial structure described by $|\alpha| > k$, are essentially not radiating. Indeed, waves are in general more scattered by large than by small objects.

3.3.4 Typical plate pitch

If a metal plate is hit by a hammer, bending waves are excited with time- and space-spectra depending on, say, frequency (ω) and wave number (α) respectively. However, not all frequencies will be radiated as sound. As seen above, for any α only the frequencies larger than αc_0 are radiated. Now, the smallest α occurring is by and large determined by the size of the plate (if we ignore fluid-plate coupling), say $1/L$. Therefore, the smallest frequency that is radiated is given by $\omega_{min} = \alpha_{min} c_0 = c_0/L$.

3.3.5 Snell's law

Also the transmission of sound waves across an interface between two media is most directly described via this notion of sub- and supersonic wave crests. If a plane wave is incident onto the interface, the point of reflection in medium 1 generates a disturbance in medium 2 (Fig. 3.6).

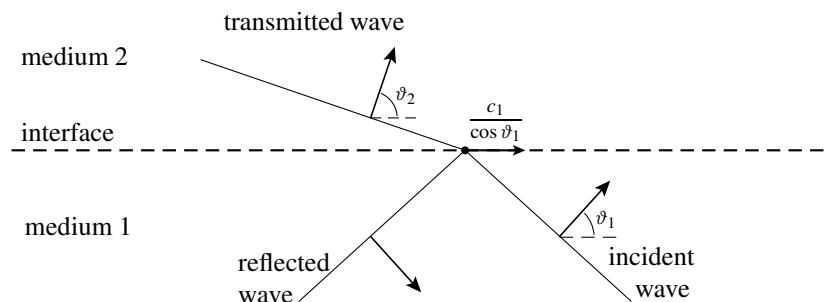


Figure 3.6 Reflection and transmission at a discontinuity.

With soundspeed c_1 in medium 1 and direction⁴ of incidence $(\cos \vartheta_1, \sin \vartheta_1)$ the disturbance velocity, measured along the interface, (the phase speed) is $c_1/\cos \vartheta_1$. Depending on ϑ_1 and the ratio of sound speeds c_1/c_2 this disturbance moves with respect to medium 2 either supersonically, resulting into transmission of the wave, or subsonically, resulting into so-called total reflection (the transmitted wave is exponentially small). In case of transmission the phase speeds of the incident and transmitted wave has to match (the *trace-velocity matching principle*, [183]).

$$\frac{c_1}{\cos \vartheta_1} = \frac{c_2}{\cos \vartheta_2}. \quad (3.53)$$

This is equivalent to Snell's law ([55, 183]), from which we can determine the angle θ_2 of the transmitted wave with the interface.

For the amplitudes (the reflection and transmission coefficients) we have to do a bit more. See for example the next problem.

Snellius along an air-bulk interface

If the interface is between air and a dissipative bulk absorber, covered with a top plate, the idea is the same, but we need a more precise calculation.

Suppose we have in the air $y < 0$

$$\begin{aligned} i\omega\rho_- + \rho_0\nabla\cdot\mathbf{v}_- &= 0, \\ i\omega\rho_0\mathbf{v}_- + \nabla p_- &= 0, \\ p_- &= c_0^2\rho_-, \end{aligned} \quad (3.54)$$

while the bulkabsorber in $y > 0$ is described by the model

$$\begin{aligned} i\omega\Omega\rho_+ + \rho_0\nabla\cdot\mathbf{v}_+ &= 0, \\ (i\omega\rho_e + \sigma)\mathbf{v}_+ + \nabla p_+ &= 0, \\ p_+ &= c_e^2\rho_+. \end{aligned} \quad (3.55)$$

At the interface $y = 0$ we have a pressure jump due to the top plate and continuity of mass

$$\begin{aligned} p_-(x, 0) - p_+(x, 0) &= -\frac{Z}{i\omega\rho_0} \frac{\partial}{\partial y} p_-(x, 0), \\ \frac{\partial}{\partial y} p_-(x, 0) &= \zeta \frac{\partial}{\partial y} p_+(x, 0), \quad \zeta = \frac{\rho_0}{\rho_e - i\sigma/\omega}. \end{aligned} \quad (3.56)$$

⁴Traditionally, the angle used is between the propagation direction and the normal vector of the interface.

Eliminate v to get

$$\begin{aligned} \nabla^2 p + k^2 p &= 0, & k &= \frac{\omega}{c_0}, & y < 0 \\ \nabla^2 p + \mu^2 p &= 0, & \mu &= \frac{\omega}{c_e} \sqrt{\frac{\Omega}{\zeta}}, & y > 0 \end{aligned} \quad (3.57)$$

Assume incident a plane wave of unit amplitude in $y < 0$, propagation in $(\cos \phi, \sin \phi)$ -direction, and a reflected wave, together given by

$$p_-(x, y) = e^{-ikx \cos \phi -iky \sin \phi} + R e^{-ikx \cos \phi +iky \sin \phi} \quad (3.58)$$

Assume the following transmitted wave in $y > 0$, which is caused by the incident wave and therefore has the same x -dependence (the trace-velocity matching principle)

$$p_+(x, y) = f(y) e^{-ikx \cos \phi} \quad (3.59)$$

From the equation for p_+ it follows that $f(y) = T e^{-i\gamma y}$ with $\gamma^2 = \mu^2 - k^2 \cos^2 \phi$. Since the transmitted wave is decaying for $y \rightarrow \infty$, we choose the branch of the square root with $\text{Im}(\gamma) \leq 0$.

$$p_+(x, y) = T e^{-ikx \cos \phi -i\gamma y}, \quad \gamma = \sqrt{\mu^2 - k^2 \cos^2 \phi}, \quad \text{Im} \gamma \leq 0. \quad (3.60)$$

The direction of the transmitted wave is thus

$$\frac{(k \cos \phi, \text{Re} \gamma)}{\sqrt{k^2 \cos^2 \phi + (\text{Re} \gamma)^2}}. \quad (3.61)$$

From the interface conditions we have

$$\begin{aligned} (1 + R) e^{-ikx \cos \phi} - T e^{-ikx \cos \phi} &= (Z/\rho_0 c_0)(1 - R) \sin \phi e^{-ikx \cos \phi} \\ -ik(1 - R) \sin \phi e^{-ikx \cos \phi} &= -i\zeta \gamma T e^{-ikx \cos \phi} \end{aligned}$$

with solution

$$R = \frac{\frac{Z}{\rho_0 c_0} + \frac{k}{\zeta \gamma} - \frac{1}{\sin \phi}}{\frac{Z}{\rho_0 c_0} + \frac{k}{\zeta \gamma} + \frac{1}{\sin \phi}}, \quad T = \frac{2 \frac{k}{\zeta \gamma}}{\frac{Z}{\rho_0 c_0} + \frac{k}{\zeta \gamma} + \frac{1}{\sin \phi}} \quad (3.62)$$

This solution includes the previous problem of a simple change in sound speed c_0 .

3.3.6 Silent vorticity

The field of a moving point source may be entirely acoustical, with essentially no other than convection effects. It is, however, possible, and physically indeed usual, that a fluctuating moving line force generates a surface or sheet of trailing vorticity. This vorticity is generated in addition of the acoustic field and is itself also of acoustic order, but, apart from some coupling effects, silent. Typical examples are (the trailing edge of) a fluctuating wing, a propeller blade, or a flag pole in the wind. The amount of generated vorticity is not a priori known but depends on details of the vortex shedding process (*e.g.* described by the Kutta condition), usually not included in an acoustic model. Indeed, this vorticity solution comes into the problem as an eigensolution as soon as continuity of the potential along mean flow streamlines is released as condition. A potential discontinuity corresponds to a vortex sheet.

Although convected vorticity is silent (it exists without pressure fluctuations) its presence may still be acoustically important. Near a solid surface (typically the surface from which the vorticity is shed) the velocity corresponding to the free vorticity cannot exist, as the field has to satisfy the vanishing normal velocity condition. This induces a fluctuating pressure along the surface which radiates out as sound, apparently from the surface but of course really the vorticity is the source. Examples are the whistling sound produced by a thin pipe or wire in the wind (aeolian sound), and the trailing edge noise – as far as it is due to shed-vorticity – from a blunt-edged airfoil. See for example [197].

We will not consider the generation process here in detail, but only indicate the presence of the eigensolution for a distinct source far upstream.

Consider in a 2D medium a uniform mean flow $(U, 0)$ with velocity perturbations $\nabla\varphi$ and pressure perturbations p small enough for linearization. Bernoulli's equation and the mass conservation equation become then

$$\rho_0 \frac{\partial \varphi}{\partial t} + \rho_0 U \frac{\partial \varphi}{\partial x} + p = 0, \quad (3.63a)$$

$$\frac{\partial p}{\partial t} + U \frac{\partial p}{\partial x} + \rho_0 c_0^2 \nabla^2 \varphi = 0, \quad (3.63b)$$

$$\varphi \rightarrow 0 \quad \text{for} \quad |y| \rightarrow \infty. \quad (3.63c)$$

This may be combined to a wave equation, although the hydrodynamic field is more easily recognized in the present form⁵. Possible eigensolutions (solutions without source) for the free field problem (no

⁵Equations (3.63a,3.63b) may be combined to the convected wave equation

$$c_0^2 \nabla^2 \varphi - (\varphi_{tt} + 2U\varphi_{xt} + U^2\varphi_{xx}) = 0$$

which reduces under the Prandtl-Glauert transformation (see 7.42) $\varphi(x, y, t) = \psi(X, y, T)$ with $X = x/\beta$, $T = \beta t + Mx/c_0\beta$, $M = U/c_0$, $\beta = \sqrt{1 - M^2}$ to the ordinary wave equation for ψ , and a pressure given by $p = -\rho_0(\psi_T + U\psi_X)/\beta$. In this way we may obtain from any no-flow solution ψ a solution to the problem with flow. However, care should be taken. An integrable singularity in $\nabla\psi$, as would occur at a sharp edge, corresponds without flow to a finite pressure. With flow it corresponds to a singular pressure (from the ψ_X -term). If this is physically unacceptable, for example if the edge is a trailing edge and the sound field induces the shedding of vorticity, a Kutta condition of finite pressure is required and the solution is to be modified to include the field of the shed vorticity (a discontinuous φ).

solid objects) are given by

$$p(x, y, t) = 0 \quad (3.64a)$$

$$\varphi(x, y, t) = f(x - Ut, y) \quad (3.64b)$$

$$\nabla^2 f(x, y) = 0. \quad (3.64c)$$

for suitable functions $f(x, y)$. A non-trivial solution f decaying both for $y \rightarrow \infty$ and $y \rightarrow -\infty$ is not possible if f is continuous, but if we allow f to be discontinuous along, say, $y = 0$ (any surface parallel to the mean flow is possible), of course under the additional conditions at $y = 0$ of a continuous pressure p and continuous vertical velocity $\partial\varphi/\partial y$, then we may find with Fourier transformation

$$\varphi(\mathbf{x}, t) = \int_{-\infty}^{\infty} F(\alpha) \text{sign}(y) e^{-\alpha|y| - i\alpha(x - Ut)} d\alpha. \quad (3.65)$$

This discontinuity relates to a concentrated layer of vorticity (vortex sheet), and is a typical (hydrodynamic) phenomenon of acoustics with mean flow. The shedding of vorticity (on the scale of the linear acoustics) would not occur without mean flow.

For a harmonic force (for example, a Von Kármán vortex street modelled by an undulating vortex sheet) with frequency ω we have only one wave number $\alpha = \omega/U$ in the problem:

$$\varphi(\mathbf{x}, t) = F_0 \text{sign}(y) \exp\left(i\omega t - i\frac{\omega}{U}x - \frac{\omega}{U}|y|\right). \quad (3.66)$$

This important parameter ω/U is called the ‘‘hydrodynamic wave number’’. Together with a suitable length scale L it yields the dimensionless number $\omega L/U$ called ‘‘Strouhal number’’.

It may be noted that this hydrodynamic field has an averaged intensity, directed in x -direction, equal to (note that $p \equiv 0$)

$$\langle \mathbf{I} \cdot \mathbf{e}_x \rangle = \frac{1}{2} U \rho_0 \left| \frac{\partial \varphi}{\partial x} \right|^2 = \frac{\omega^2}{U^2} |F_0|^2 e^{-2\frac{\omega}{U}|y|}.$$

The total power output in flow direction is then

$$\int_{-\infty}^{\infty} \langle \mathbf{I} \cdot \mathbf{e}_x \rangle dy = \frac{\omega}{U} |F_0|^2. \quad (3.67)$$

In the case of an acoustic field (for example the field that triggered the vortices associated to the hydrodynamic field) the intensity has a non-zero component in y -direction, and in addition to the purely hydrodynamic power (3.67) some acoustic energy disappears into, or appears from, the vortex sheet $y = 0$. See section 9.1.3 and [120, 197, 88, 199, 75].

Exercises

- a) Consider the sound produced by thunder, modelled as an infinite line source, fired impulsively. Explain the typical long decay after the initial crack.
- b) Consider in (x, y, z) -space the plane $z = 0$, covered uniformly with point sources which are all fired instantaneously at $t = \tau$:
 $\delta(t - \tau)\delta(x - x_0)\delta(y - y_0)\delta(z)$ ($z_0 = 0$). Calculate the sound field at some distance away from the plane.
- c) Consider an infinite equidistant row of harmonically oscillating line sources
 $\sum_n \delta(x - nd)\delta(y) e^{i\omega t}$, placed in the x, z -plane a distance d from each other. Show that constructive interference in the far field will only occur in directions with an angle θ such that
 $kd \cos \theta = 2\pi m; \quad m = 0, 1, 2, \dots$
 where $k = \omega/c_0$.
- d) The same question for a row of alternating line sources.
- e) What is the dimension of $\delta(x)$ if x denotes a physical coordinate with dimension “length”?
- f) Prove the identities (C.36a) and (C.36b).
- g) Consider a finite volume \mathcal{V} with surface \mathcal{S} and outward surface normal \mathbf{n} . On \mathcal{V} is defined a smooth vector field \mathbf{v} . Prove, by using surface distributions, Gauss’ theorem

$$\int_{\mathcal{V}} \nabla \cdot \mathbf{v} \, dx = \int_{\mathcal{S}} \mathbf{v} \cdot \mathbf{n} \, d\sigma.$$
- h) Work out the expression (3.36) for the reflected wave g in the case of formula (3.38) with $m = 0$.
- i) We define an ideal open end as a position at which $\hat{p} = 0$ in a tube. Calculate reflection coefficient R and impedance Z for such an open end.
- j) The same question for an ideal closed end defined by $\hat{v} = 0$.
- k) Given a uniform duct between $x = -\infty$ and $x = 0$, with impedance Z_0 of the plane $x = 0$ seen from the $x < 0$ side. Calculate Z_L , the impedance of the plane $x = -L$, seen from $x < 0$.
- l) Prove causality of the impedance $Z(\omega) = R + i\omega m - iK/\omega$. Find the inverse Fourier transform of both Z and $Y = 1/Z$.
- m) Determine the reflection coefficient R of a harmonic plane wave

$$p(\mathbf{x}) = e^{-i\mathbf{k} \cdot \mathbf{x}} + R e^{-i\bar{\mathbf{k}} \cdot \mathbf{x}}, \quad \mathbf{v}(\mathbf{x}) = \frac{\mathbf{k}}{\rho_0 \Omega} e^{-i\mathbf{k} \cdot \mathbf{x}} + R \frac{\bar{\mathbf{k}}}{\rho_0 \Omega} e^{-i\bar{\mathbf{k}} \cdot \mathbf{x}}$$

with $\mathbf{k} = k(\cos \vartheta, \sin \vartheta)$, $\bar{\mathbf{k}} = k(\cos \vartheta, -\sin \vartheta)$, $k = \|\mathbf{k}\|$, $c_0 k = \Omega$, $\Omega = \omega - u_0 k \cos \vartheta$, incident from $y < 0$ in a mean flow $\mathbf{v}_0 = (u_0, 0)$ against a wall at $y = 0$ with impedance Z . What is the impedance with $R = 0$?

62 3 Green's functions, impedance, and evanescent waves

n) Consider in respectively 1D, 2D and 3D free field, the sound, produced by a point source, given by

$$\frac{1}{c^2} \frac{\partial^2 p}{\partial t^2} - \nabla^2 p = \delta(\mathbf{x}) f(t), \quad f(t < 0) = 0.$$

Show, by using the corresponding Green's functions in Appendix E, that solutions are given by

$$1\text{D} : \quad p(\mathbf{x}, t) = \frac{1}{2}c \int_0^{t - \|\mathbf{x}\|/c} f(\tau) d\tau, \quad \|\mathbf{x}\| = |x|$$

$$2\text{D} : \quad p(\mathbf{x}, t) = \frac{1}{2\pi} \int_0^{\text{arccosh}(ct/\|\mathbf{x}\|)} f\left(t - \frac{\|\mathbf{x}\|}{c} \cosh \theta\right) d\theta, \quad \|\mathbf{x}\| = (x^2 + y^2)^{\frac{1}{2}}$$

$$3\text{D} : \quad p(\mathbf{x}, t) = \frac{1}{4\pi \|\mathbf{x}\|} f\left(t - \frac{\|\mathbf{x}\|}{c}\right), \quad \|\mathbf{x}\| = (x^2 + y^2 + z^2)^{\frac{1}{2}}$$

Apply this to the quasi time harmonic source $f(t) = -H(t) e^{i\omega t}$. Consider the limit for large t and fixed $\|\mathbf{x}\|$, and recover the (outward radiating) Green's functions in frequency domain. Note: the 1D inviscid model has no inherent decay and this case is more subtle. Get rid of the transient part by adopting some artificial viscosity through the slightly complex frequency $\omega - i\varepsilon$ in the limit $\varepsilon \downarrow 0$.

4 One dimensional acoustics

4.1 Plane waves

Plane waves are waves in which the acoustic field only depends on the spatial coordinate (say: x) in the direction of propagation: $p(x, t)$, $\rho(x, t)$, $v(x, t)$, Such waves may emerge, for example, as approximations for spheric waves at large distance from a point source, or as waves propagating at a frequency lower than a critical frequency f_c called the cut-off frequency in a hard-walled pipe. As we will see from the discussion in section 6.4 and section 7.2 the cut-off frequency f_c is of the order of $c_0/2d$ where d is the pipe width (or diameter). The exact value of f_c depends on the shape of the pipe cross section.

If we can neglect friction, then below the cut-off frequency, the (propagating part of the) acoustic field in a pipe consists only of plane waves. The condition for the validity of a frictionless approximation yields a lower bound for the frequency we can consider. At high frequencies, the effect of viscosity is confined to boundary layers of thickness $\delta_A = (2\nu/\omega)^{1/2}$ (where $\nu = \eta/\rho$ is the kinematic viscosity of the fluid) near the walls. In order to make a plane wave approximation reasonable we should have thin viscous boundary layers: $\delta_A/d \ll 1$. Hence the frequency range in which a plane wave approximation is valid in a pipe is given by:

$$\frac{2\nu}{\pi d^2} \ll f < \frac{c_0}{2d}.$$

For air $\nu = 1.5 \times 10^{-5} \text{ m}^2/\text{s}$ while for water a typical value is $\nu = 10^{-6} \text{ m}^2/\text{s}$. Hence we see that a plane wave approximation will in air be valid over the three decades of the audio range for a pipe with a diameter $d = O(10^{-2} \text{ m})$. (Check what happens for larger pipes.) This implies that such an approximation should be interesting when studying pulsations in pipe systems, musical acoustics, speech production, etc.

We therefore focus our attention in this chapter on *the one-dimensional approximation of duct acoustics*. For simplicity we will also assume that any mean flow $u_0 = u_0(x)$ is also one dimensional. We will consider simple models for the boundary conditions. We will assume that the side walls are rigid. This implies that there is no transmission of sound through these walls. This is a drastic assumption which excludes any application of our theory to the prediction of environmental noise induced by pipe flows. In such cases the transmission of the sound from the internal flow to the environment is a crucial factor. A large amplitude in the pipe may be harmless if the acoustic energy stays inside the pipe! Extensive treatment of this transmission problem is given by Norton [168] and Reethof [195].

In general the transmission of sound through elastic structures is described in detail by Cremer and Heckl [39], and Junger and Feit [103]. We further ignore this crucial problem.

In principle the approximation we will use is limited to pipes with uniform cross sections A or, as we will see in section 8.4, to pipes with slowly varying cross sections ($dA/dx \ll \sqrt{A} \ll \lambda$). The most interesting applications of our approximation will concern sound generated in compact regions as a result of sudden changes in cross section or localized fluid injection. As we consider low frequencies ($f < c_0/2d$) a region with a length of the order of the pipe width d will be by definition compact. We will treat these regions separately, taking possible three dimensional effects into account. The (inner-) solution in the compact region is approximated by that of an incompressible flow or a region of uniform pressure¹.

The boundary conditions for this compact region are related to the plane wave regions by means of integral conservation laws (Appendix A). In this way we will consider a large variety of phenomena (temperature discontinuities, jumps in cross sections, multiple junctions, air bubbles, turbulence...). In the present chapter we will assume an infinitely long or semi-infinite pipe. This is a pipe which is so long that as a result of friction the waves travelling towards the pipe end do not induce significant reflections. This will in fact exclude the accumulation of acoustic energy and phenomena like resonance. This effect is discussed in the next chapter.

A consequence of this assumption is that the acoustic field will not have a large amplitude and that we can usually neglect the influence of the acoustic field on a source. The flow is calculated locally with our previously discussed compact region approximation ignoring any acoustical feedback. This excludes fascinating effects such as whistling. These effects will be discussed in chapter 5.

If the end of the pipe is part of the problem, we will include this end by a linear boundary condition of impedance type. The acoustic impedance is a general linear relation in the frequency domain between velocity and pressure, *i.e.* a convolution product in the time domain (section 3.2). Since pressure cannot depend on the future of the velocity (or *vice versa*) the discussion of such a linear boundary condition involves the concept of causality (section 3.2).

We will show how the Green's function formalism can be used to obtain information on aero-acoustic sound generation by turbulence and to estimate the scattering of sound by a temperature non-uniformity. These problems will be reconsidered later for free field conditions in chapter 6. It will then be interesting to see how strong the effect of the confinement is by a comparison of the results obtained in this chapter and chapter 5 with those obtained in chapter 6.

Convective effects on the wave propagation will be discussed in chapter 9. We restrict ourselves now to very low mean flow Mach numbers outside the source regions.

¹For example, the air density fluctuations in an oscillating acoustically compact air bubble in water cannot be neglected, but we can assume that they are uniform within the bubble.

4.2 Basic equations and method of characteristics

4.2.1 The wave equation

We consider a one-dimensional flow in a pipe with uniform cross section. If we neglect friction the conservation laws of mass and momentum are for a one dimensional flow given by:

$$\frac{\partial \rho}{\partial t} + u \frac{\partial \rho}{\partial x} + \rho \frac{\partial u}{\partial x} = \frac{\partial(\rho\beta)}{\partial t} \quad (4.1a)$$

$$\rho \left(\frac{\partial u}{\partial t} + u \frac{\partial u}{\partial x} \right) + \frac{\partial p}{\partial x} = f_x \quad (4.1b)$$

where $\rho\beta$ corresponds to an external mass injection in the flow and f_x is an external force per unit volume.

We assume now that the field consists of a uniform state (ρ_0, p_0, u_0) , plus a perturbation (ρ', p', u') small enough to allow linearization:

$$\rho = \rho_0 + \rho', \quad (4.2a)$$

$$p = p_0 + p', \quad (4.2b)$$

$$u = u_0 + u'. \quad (4.2c)$$

$\partial\beta/\partial t$ and f_x , being the cause of the perturbation, must therefore by definition be small. We substitute (4.2a–4.2c) in (4.1a) and (4.1b). Neglecting second and higher order terms we obtain the linearized equations:

$$\frac{\partial \rho'}{\partial t} + u_0 \frac{\partial \rho'}{\partial x} + \rho_0 \frac{\partial u'}{\partial x} = \rho_0 \frac{\partial \beta}{\partial t} \quad (4.3a)$$

$$\rho_0 \frac{\partial u'}{\partial t} + \rho_0 u_0 \frac{\partial u'}{\partial x} + \frac{\partial p'}{\partial x} = f_x \quad (4.3b)$$

We can eliminate ρ' by using the constitutive equation:

$$p' = c_0^2 \rho' \quad (4.4)$$

which implies that we assume a homentropic flow.

A one-dimensional wave equation is obtained by subtracting the divergence of the momentum conservation law (4.3b) from the convected time derivative $(\partial_t + u_0 \partial_x)$ of mass conservation law (4.3a) (to eliminate u'):

$$\left(\frac{\partial}{\partial t} + u_0 \frac{\partial}{\partial x} \right)^2 p' - c_0^2 \frac{\partial^2 p'}{\partial x^2} = c_0^2 \left(\rho_0 \frac{\partial^2 \beta}{\partial t^2} - \frac{\partial f_x}{\partial x} \right). \quad (4.5)$$

4.2.2 Characteristics

As an alternative we now show the wave equation in characteristic form. This allows a simple geometrical interpretation of the solution of initial condition and boundary condition problems with the help of a so-called (x, t) diagram. In acoustics this procedure is just equivalent with other procedures. However, when considering high amplitude wave propagation (non-linear acoustics or gas dynamics) the method of characteristic will still allow an analytical solution to many interesting problems [241, 116, 176]. Also the characteristics play a crucial rôle in numerical solutions as they determine optimal discretization schemes, and in particular their conditions of stability.

Using the constitutive equation

$$\frac{\partial p}{\partial t} + u \frac{\partial p}{\partial x} = c^2 \left(\frac{\partial \rho}{\partial t} + u \frac{\partial \rho}{\partial x} \right)$$

we can write the mass conservation law (4.1a) as:

$$\frac{1}{\rho c} \left(\frac{\partial p}{\partial t} + u \frac{\partial p}{\partial x} \right) + c \frac{\partial u}{\partial x} = \frac{c}{\rho} \frac{\partial(\rho\beta)}{\partial t}$$

by addition, respectively subtraction, of the momentum conservation law (4.1b) divided by ρ , we find the non-linear wave equation in characteristic form:

$$\left(\frac{\partial}{\partial t} + (u \pm c) \frac{\partial}{\partial x} \right) \left(u \pm \int \frac{dp}{\rho c} \right) = \frac{f_x}{\rho} \pm \frac{c}{\rho} \frac{\partial(\rho\beta)}{\partial t}.$$

In the absence of source terms this simply states that along the characteristics c^\pm the Riemann invariant Γ^\pm is conserved:

$$\Gamma^+ = u' + \int \frac{dp}{\rho c} = \text{constant along } c^+ = \left\{ (x, t) \mid \frac{dx}{dt} = u + c \right\} \quad (4.6a)$$

$$\Gamma^- = u' - \int \frac{dp}{\rho c} = \text{constant along } c^- = \left\{ (x, t) \mid \frac{dx}{dt} = u - c \right\} \quad (4.6b)$$

In the presence of source terms we have:

$$\Gamma^\pm - \Gamma_0^\pm = \int_{c^\pm} \left(\rho_0 c_0^2 \frac{\partial \beta}{\partial t} \pm c_0 f_x \right) dt \quad (4.7)$$

where the integration is along the respective characteristic. For an ideal gas with constant specific heat we find by using the fact that the flow is isentropic:

$$\int \frac{dp}{\rho c} = \frac{2c}{\gamma - 1}.$$

In linear approximation in the absence of sources we have

$$\Gamma^\pm = u' \pm \frac{p'}{\rho_0 c_0} \text{ along the lines defined by } c^\pm : \frac{dx}{dt} = u_0 \pm c_0.$$

4.2.3 Linear behaviour

In the absence of source terms (the homogeneous problem) we can write the linear perturbation p' as the sum of two waves \mathcal{F} and \mathcal{G} travelling in opposite directions (along the c^+ and c^- characteristics):

$$p' = \mathcal{F}(x - (c_0 + u_0)t) + \mathcal{G}(x + (c_0 - u_0)t), \tag{4.8a}$$

$$u' = \frac{1}{\rho_0 c_0} \left(\mathcal{F}(x - (c_0 + u_0)t) - \mathcal{G}(x + (c_0 - u_0)t) \right). \tag{4.8b}$$

This solution can be readily verified by substitution into the homogeneous wave equation. The functions \mathcal{F} and \mathcal{G} are determined by the initial and boundary conditions. As an example we consider two simple problems for the particular case of a quiescent fluid $u_0 = 0$.

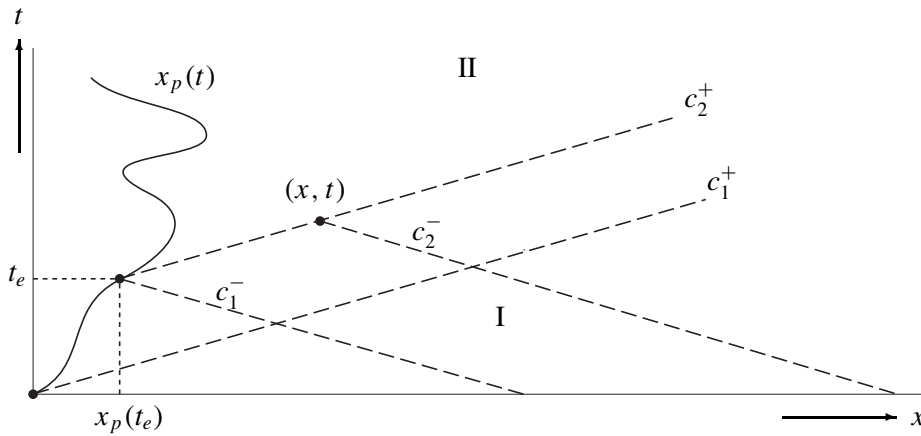


Figure 4.1 Solution by means of characteristics.

Let us first consider a semi-infinite pipe closed by a rigid piston moving with a velocity $u_p(t)$ starting at $t = 0$ and $x = 0$. If $u_p/c_0 \ll 1$ we can use an acoustic approximation to solve the problem. Using the method of characteristics we first observe in a (x, t) diagram (figure 4.1) that there are two regions for $x > 0$:

region I below the line $x = c_0 t$

and

region II above the line $x = c_0 t$.

Region I is a region in which perturbations induced by the movement of the piston cannot be present. The characteristic $c_1^+ : x = c_0 t$ corresponds to the path of the first disturbance generated at $t = 0$

by the starting piston. Hence the fluid in region I is undisturbed and we can write by considering a c^- characteristic (c_1^-) leaving this region:

$$p' - \rho_0 c_0 u' = 0. \quad (4.9)$$

This c_1^- characteristic will meet the piston path $x_p(t) = \int_0^t u_p dt'$ where we have:

$$u' = u_p \quad (4.10a)$$

because we assume the fluid to stick to the piston ($u_p \ll c_0$). Hence from (4.9) and (4.10a) we have the pressure at the piston for any time:

$$p' = \rho_0 c_0 u_p. \quad (4.10b)$$

Now starting from a point $x_p(t)$ on the piston, we can draw a c^+ characteristic (c_2^+) along which we have:

$$p' + \rho_0 c_0 u' = (p' + \rho_0 c_0 u')_p = 2\rho_0 c_0 u_p(t_e) \quad (4.11)$$

where t_e is the retarded or emission time, implicitly given by

$$\boxed{t_e = t - \frac{x - x_p(t_e)}{c_0}.} \quad (4.12)$$

This is the time at which the disturbance travelling along c_2^+ and reaching an observer at (x, t) has been generated by the piston. At any point (x, t) along c_2^+ we can find a c_2^- characteristic originating from the undisturbed region for which (4.9) is valid. Combining (4.9) and (4.11) we see that along c_2^+ we have:

$$u' = u_p(t_e) \quad (4.13a)$$

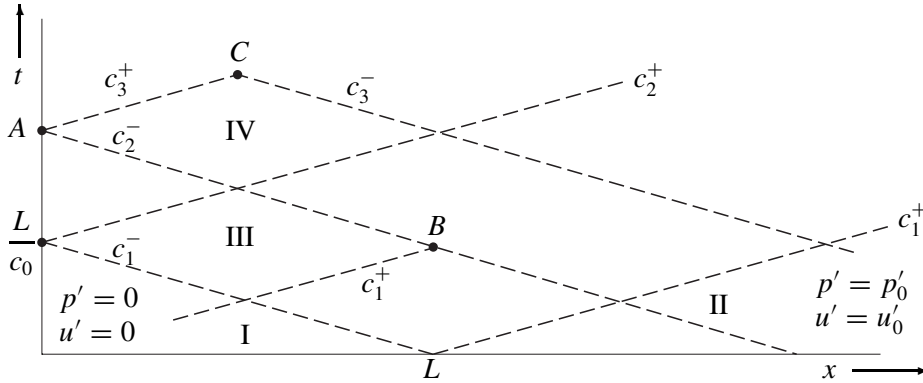
$$p' = \rho_0 c_0 u_p(t_e). \quad (4.13b)$$

We could have obtained this solution directly simply by using (4.8a,4.8b), the general solution of the homogeneous equation. Because the tube is semi-infinite and the piston is the only source of sound, we have only waves travelling in the positive x direction so that (with $u_0 = 0$):

$$p' = \mathcal{F}(x - c_0 t) \quad (4.14a)$$

$$u' = \mathcal{F}(x - c_0 t) / \rho_0 c_0. \quad (4.14b)$$

Using the boundary condition $u' = u_p$ at the piston $x = x_p$ we find the retarded (or emission) time equation (4.12) and so the solution (4.13a,4.13b).


 Figure 4.2 (x, t) diagram for the initial value problem.

We now consider an initial value problem in a semi-infinite pipe. Suppose that the pipe is closed at $x = 0$ by a fixed rigid wall ($u'(x = 0) = 0$) and that in the region $0 < x < L$ the fluid is undisturbed while for $x > L$ there is originally a uniform disturbance (p'_0, u'_0) of the uniform quiescent fluid state valid for $x > 0$ ($p'_0, u'_0 = 0$) (figure 4.2). We can easily delimit the uniform regions I and II in which the initial state will prevail by drawing the c_1^+ and c_1^- characteristics emanating from the point $(x, t) = (L, 0)$.

The state in region IV at the closed pipe end is the next easiest one to determine. We draw the characteristic c_2^- emanating from region II along which we have:

$$c_2^- : p' - \rho_0 c_0 u' = p'_0 - \rho_0 c_0 u'_0. \quad (4.15)$$

At the closed pipe end $u' = 0$ so that for $t > L/c_0$:

$$p'_{IV}(x = 0) = p'_0 - \rho_0 c_0 u'_0 \quad (4.16)$$

In region III we obtain the solution by considering the intersection of the waves c_1^+ and c_1^- emanating from regions I and II respectively:

$$c_1^+ : p' + \rho_0 c_0 u' = 0 \quad (4.17a)$$

$$c_1^- : p' - \rho_0 c_0 u' = p'_0 - \rho_0 c_0 u'_0. \quad (4.17b)$$

Hence:

$$p'_{III} = \frac{1}{2}(p'_0 - \rho_0 c_0 u'_0) \quad (4.18a)$$

$$u'_{III} = -\frac{1}{2}(p'_0 - \rho_0 c_0 u'_0)/\rho_0 c_0. \quad (4.18b)$$

Finally for any point in the region IV above the line $x = c_0(t - L/c_0)$ we have:

$$c_3^+ : p' + \rho_0 c_0 u' = p'_0 - \rho_0 c_0 u'_0 \quad (4.19a)$$

$$c_3^- : p' - \rho_0 c_0 u' = p'_0 - \rho_0 c_0 u'_0 \quad (4.19b)$$

so that we have:

$$u'_{IV} = 0 \quad (4.20a)$$

$$p'_{IV} = p'_0 - \rho_0 c_0 u'_0 \quad (4.20b)$$

as we already found at the closed pipe end ($x = 0$). Of course we could have solved this problem without an (x, t) diagram, but this requires quite an intellectual effort.

From the previous two examples simple rules are obtained to use an (x, t) diagram in combination with the method of characteristics:

- a) Indicate on the x and t axis the initial and boundary conditions.
- b) Draw the characteristics delimiting the undisturbed regions in which the initial conditions prevail.
- c) Consider reflection of these boundary characteristics at boundary conditions. (Contact surface delimiting regions of different uniform state p_0, ρ_0, c_0, \dots will be discussed in section 4.4.) This yields a further subdivision of the (x, t) plane in uniform regions.
- d) Determine the state at the boundaries at the moment the first message from the initial conditions arrives.
- e) Determine the state in regions where two characteristics of opposite families c^+ and c^- emanating from regions where the solution is known meet.

While for initial value problems the method of characteristics is most efficient, we will use Fourier analysis when we consider boundary condition problems. For a steady harmonic perturbation equation (4.8a, 4.8b) becomes:

$$p' = p^+ e^{i\omega t - ikx} + p^- e^{i\omega t + ikx} \quad (4.21a)$$

$$u' = \frac{1}{\rho_0 c_0} (p^+ e^{i\omega t - ikx} - p^- e^{i\omega t + ikx}). \quad (4.21b)$$

where p^\pm are amplitudes which are functions of ω , and k is the wave number ($k = \omega/c_0$).

4.2.4 Non-linear simple waves and shock waves

A general solution of the non-linear one dimensional homentropic flow equations can only be obtained by numerical methods. In the particular case of a wave propagating into a uniform region the solution is considerably simplified by the fact that the characteristics emanating from the uniform region all carry a uniform message. We will show that as a consequence of this the other characteristics in this wave are straight lines in the (x, t) -plane. Such a wave is called a simple wave.

Let us for example consider a wave propagating along c^+ -characteristics which meets c^- -waves emanating from a uniform region. The message carried by the c^- -characteristics is:

$$\Gamma^- = u - \int \frac{dp}{\rho c} = \Gamma_0^- \text{ for all } c^-. \tag{4.22}$$

If we now consider a c^+ -characteristic in the simple wave, we have in addition that Γ^+ is equal to another constant, specific to that particular c^+ :

$$\Gamma^+ = u + \int \frac{dp}{\rho c}. \tag{4.23}$$

Addition and subtraction of (4.22) and (4.23) yields, along the c^+ , the result

$$u = \frac{1}{2}(\Gamma^+ + \Gamma_0^-), \tag{4.24a}$$

$$\int \frac{dp}{\rho c} = \frac{1}{2}(\Gamma^+ - \Gamma_0^-). \tag{4.24b}$$

Hence, the velocity u is constant along the c^+ considered. As in addition to the thermodynamic quantity $\int(dp/\rho c)$ also the entropy s is constant along the c^+ (because the flow is homentropic), we conclude that all thermodynamic variables² are constant along the c^+ . In particular the speed of sound $c = \sqrt{(\partial p/\partial \rho)_s}$ is constant along a c^+ in the simple wave. Therefore, the slope $(u + c)$ of the c^+ characteristic is constant, and the characteristic is a straight line in an (x, t) -diagram.

As an example of an application we consider the simple wave generated for $x > 0$ by a given boundary condition $p(0, t)$ at $x = 0$, assuming a uniform quiescent fluid ($u_0 = 0$) with a speed of sound $c = c_0$ for $t < 0$. The sound speed $c(0, t)$ at $x = 0$ is calculated by using the equation of state

$$\frac{p}{p_0} = \left(\frac{\rho}{\rho_0}\right)^\gamma$$

which implies

$$\frac{c}{c_0} = \left(\frac{p}{p_0}\right)^{\frac{\gamma-1}{2\gamma}}.$$

²For a homogeneous fluid the thermodynamic state is fully determined by two thermodynamic variables.

The message from the c^- -characteristics implies

$$u = \frac{2c_0}{\gamma - 1} \left(\frac{c}{c_0} - 1 \right) = \frac{2c_0}{\gamma - 1} \left(\left(\frac{p}{p_0} \right)^{\frac{\gamma-1}{2\gamma}} - 1 \right).$$

We can now easily construct the simple wave by drawing at each time t the c^+ -characteristic emanating from $x = 0$. We see from these equations that a compression $\frac{\partial}{\partial t} p(0, t) > 0$ implies an increase of both $c(0, t)$ and $u(0, t)$, and of course the opposite for a decompression or expansion. As a result, characteristics at the peak of a compression wave have a higher speed ($u + c$) than those just in front of it. This results into a gradual steepening of the compression wave. This non-linear deformation of the wave will in the end result into a breakdown of the theory because neighbouring c^+ -characteristics in a compression intersect for travelling times larger than t_s or distances larger than x_s given by

$$t_s = - \left[\left(\frac{\partial(u+c)}{\partial x} \right)_{t=0} \right]^{-1}, \quad (4.25a)$$

$$x_s = -t_s^2 \left[\left(\frac{\partial(u+c)}{\partial t} \right)_{x=0} \right]. \quad (4.25b)$$

For weak compressions we find the approximation for an ideal gas with constant γ :

$$x_s \simeq c_0 t_s = \frac{2\gamma p_0 c_0}{\gamma + 1} \left[\left(\frac{\partial p}{\partial t} \right)_{x=0} \right]^{-1}. \quad (4.26)$$

For $t > t_s$ or $x > x_s$ the solution found by integration of the differential equations becomes multiple valued and loses its physical meaning.

The approximation on which the equations are based will already fail before this occurs because the wave steepening involves large gradients so that heat conduction and friction cannot be ignored anymore. This limits the process of wave deformation. For large pressure differences across the wave the final gradients are so large that the wave thickness is only a few times the molecular mean free path, so that a continuum theory fails. The wave structure is in the continuum approximation a discontinuity with jump conditions determined by integral conservation laws. We call this a shock wave. Apart from discontinuous, the solution is also dissipative, as there is production of entropy in the shock wave.

If the wave is initiated by a harmonic perturbation $p'(0, t) = \hat{p} \cos(\omega t)$, the shock formation distance corresponding to the largest value of $\frac{\partial}{\partial t} p'$ is given by

$$\frac{x_s \omega}{c_0} = \frac{2\gamma p_0}{(\gamma + 1) \hat{p}}.$$

In a pipe segment, closed on both sides by a rigid wall, a wave travels easily hundreds of wave lengths before it is attenuated significantly by friction. Therefore, even at apparently modest amplitudes of $\hat{p}/p_0 = O(10^{-2})$ shock waves can appear in a closed tube driven by a piston at its resonance frequency. Recent papers discussing such effects are the review of Crighton ([45]) and the work of

Ockendon *et al.* ([171]). When the pipe segment is open at one end, the wave is inverted each time it reflects at the open end. The non-linear wave distortion due to the wave propagation during half an oscillation period is compensated, at least in first approximation, in the following half period. Under such conditions non-linear effects due to flow separation at the open pipe termination (Disselhorst & Van Wijngaarden [52]) or even turbulence in the acoustical boundary layer ([140], [250], [4], [58]) can appear before non-linear wave distortion becomes dominant.

However, when the pipe is driven by a strongly non-harmonic pressure signal $p'(0, t)$, the wave steepening may lead to a shock wave formation before the open end has been reached. This may, for example, occur in a trombone where the pressure at the exit of the horn shows very sharp peaks, as shown in figure (4.3). The increase of the wave distortion with the amplitude explains in such a musical instrument the increase of brightness (the higher harmonics) of the sound with increasing sound level (Hirschberg [80]). In open-air loudspeaker horns, waves propagate in non-linear way. In mufflers of combustion engines shock waves are also common.

When the non-linear deformation is small, the generation of the first harmonic \hat{p}_1 at $2\omega_0$ by a signal \hat{p} , originally harmonic with frequency ω_0 , is given by [183]:

$$\frac{\hat{p}_1}{\hat{p}} = \frac{x}{2x_s} \tag{4.27}$$

4.3 Source terms

While f_x is a source term in (4.1b) which can be realized by non-uniform gravitational or electromagnetic forces, the source term $\partial^2(\rho\beta)/\partial t^2$ in (4.1a) does not correspond to the creation of mass (because we consider non-relativistic conditions). Hence if we introduce a source term $\partial^2(\rho\beta)/\partial t^2$ this term will be a representation of a complex process which we include in the 1-D inviscid flow model as a source term. For example the effect of fluid injection through a porous side wall in the pipe can be considered by assuming a source term in a uniformly filled pipe with rigid impermeable walls.

In the case of f_x we may also find useful to summarize the effect of a complex flow such as the flow around a ventilation fan by assuming a localized momentum source in a one dimensional model. This is called an actuator disk model. Of course, this kind of representation of a complex process by a simple source is only possible if we can find a model to calculate this source. This is only

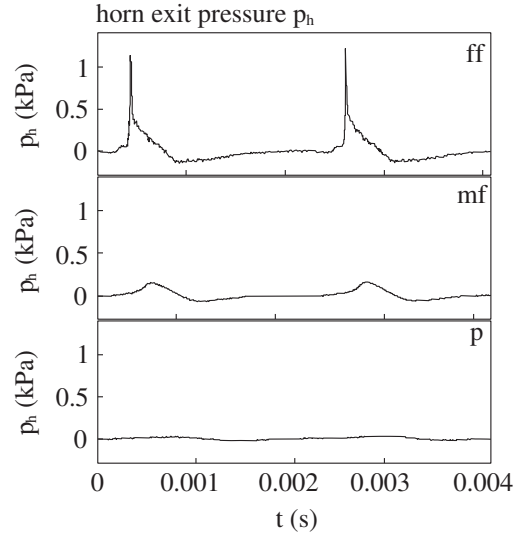


Figure 4.3 The pressure signal measured at the exit of the horn for three playing levels: piano (p), mezzo-forte (mf), and fortissimo (ff).

attractive if a simplified model or an order of magnitude estimate can be used. When the source region is compact we will be able to find such simple relationships between a simplified local flow model and the corresponding 1-D sources by applying integral conservation laws over the source region and neglecting variations in emission time over the source region. The general treatment of the aeroacoustic sources has already been given in section 2.6. We focus here on some additional features which we will use in our applications of the theory.

In a compact region of length L and fixed volume V enclosed by a surface S , we will use the conservation laws for mass and momentum in integral form (App. A):

$$\frac{d}{dt} \iiint_V \rho \, d\mathbf{x} + \iint_S \rho \mathbf{v} \cdot \mathbf{n} \, d\sigma = 0 \quad (4.28a)$$

$$\frac{d}{dt} \iiint_V \rho \mathbf{v} \, d\mathbf{x} + \iint_S (\mathbf{P} + \rho \mathbf{v} \mathbf{v}) \cdot \mathbf{n} \, d\sigma = \iiint_V \mathbf{f} \, d\mathbf{x} \quad (4.28b)$$

where \mathbf{P} is the stress tensor (P_{ij}).

Within the volume V we describe the flow here in full three dimensional detail, so (4.28a) has no source term. However, the source term $\partial^2(\rho\beta)/\partial t^2$ in the one dimensional representation of the mass conservation law is supposed to include the effect of the volume integral $(d/dt) \iiint \rho \, d\mathbf{x}$. In order to understand this we compare the actual source region with a 1-dimensional representation of this source region (figure 4.4). Integration of (4.1a) over the source region yields for a uniform pipe cross

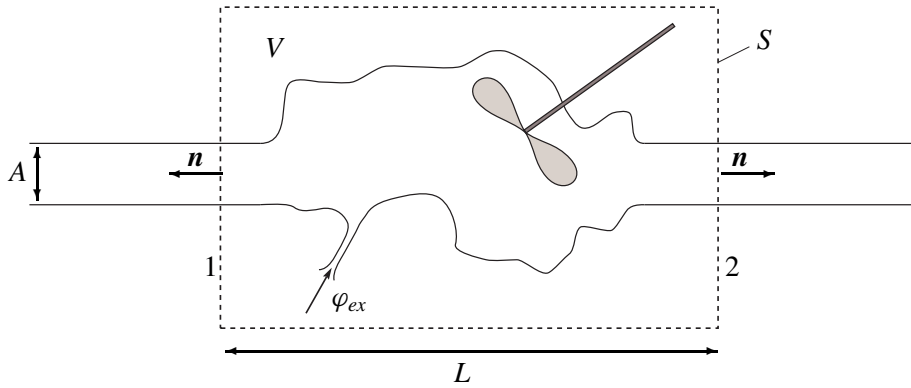


Figure 4.4 One dimensional representation of source region.

section:

$$\int_0^L \frac{\partial \rho}{\partial t} \, dx + (\rho u)_2 - (\rho u)_1 = \int_0^L \frac{\partial(\rho\beta)}{\partial t} \, dx. \quad (4.29)$$

If we assume L to be small compared to the acoustic wave length (compact) and the source term $\partial^2(\rho\beta)/\partial t^2$ to be uniform we can write in linearized form :

$$\frac{\partial\beta}{\partial t} = \Delta u' \delta(x - y) \quad (4.30)$$

for a small source region around $x = y$. The value of $\Delta u' = (u'_2 - u'_1)$ to be used in (4.30) is found by application of (4.28a) to the actual situation. If we assume the flow to be uniform at the planes 1 and 2 of cross-section A , where it enters and leaves the volume V , we obtain:

$$A[(\rho u)_2 - (\rho u)_1] = -\frac{d}{dt} \iiint_V \rho \, d\mathbf{x} + \varphi_{ex} \quad (4.31)$$

where φ_{ex} is the externally injected mass flux into V through the side walls. For identical fluids at both sides and in linearized approximation for a compact source region we have:

$$A\rho_0\Delta u' = -\frac{d}{dt} \iiint_V \rho' \, d\mathbf{x} + \varphi_{ex}. \quad (4.32)$$

Since typical wavelengths are much larger than the compact source region, density and pressure gradients are negligible and we can replace the volume integral by the averaged value. We can write for a homentropic flow

$$\Delta u' = -\frac{V}{A\rho_0 c_0^2} \frac{dp'}{dt} + \frac{\varphi_{ex}}{A\rho_0}.$$

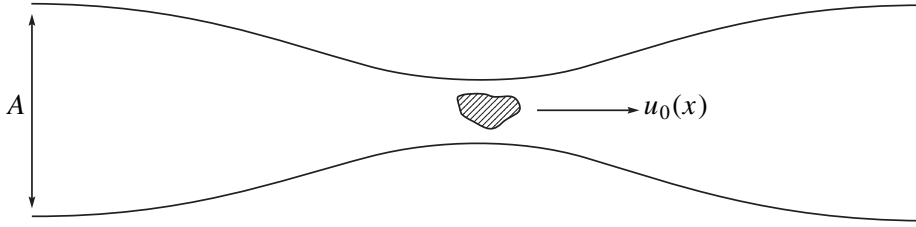
In a similar way, if we can neglect the volume contribution $(d/dt) \iiint_V \rho \mathbf{v} \, d\mathbf{x}$ to the integral conservation law, we obtain in linear approximation (neglecting $\rho_0 u_2'^2$ and $\rho_0 u_1'^2$):

$$f_x = \Delta p' \delta(x - y). \quad (4.33)$$

This source term for the 1-dimensional wave equation can be used as a representation of a complex flow such as that around a ventilation fan.

As an example of a sound source we consider now the effect of the convection of a small fluid particle with a density ρ and speed of sound c (different from ρ_0 and c_0) passing through a sudden change in pipe cross section in which we assume a steady isentropic and subsonic flow $u_0(x)$ (figure 4.5). We will first consider the problem by using the linearized form of the integral conservation laws for small differences in density and speed of sound ($(\rho - \rho_0)/\rho_0 \ll 1$ and $(c - c_0)/c_0 \ll 1$). A more formal discussion of this effect is given by Morfey in [149].

If the volume V_p of the fluid particle is much smaller than the nozzle volume V and if the properties of the fluid particle do not differ much from that of the rest of the fluid, we can assume that the particle

Figure 4.5 Particle convected with the main flow $u_0(x)$ through a nozzle.

is convected with the undisturbed steady flow velocity $u_0(x)$. As the particle is small the pressure over the particle will be uniform and in first approximation equal to the main flow pressure $p_0(x)$. $p_0(x)$ is given by Bernoulli's equation:

$$p_0(x) + \frac{1}{2}\rho_0 u_0^2(x) = \text{constant}. \quad (4.34)$$

The variation in pressure $p_0(x)$ will induce a volume variation of the particle, additional to that of the mean flow, which is related to the variation in the fluid compressibility

$$\mathcal{K} = \frac{1}{\rho} \left(\frac{\partial \rho}{\partial p} \right)_s = \frac{1}{\rho c^2} \quad (4.35)$$

by:

$$A \Delta u' = -(\mathcal{K} - \mathcal{K}_0) V_p \frac{d}{dt} p_0(x_p(t)) \quad (4.36)$$

which implies a source term:

$$\frac{\partial \beta}{\partial t} = -\frac{\mathcal{K} - \mathcal{K}_0}{A} V_p \frac{d}{dt} p_0(x_p(t)) \delta(x - y) \quad (4.37)$$

where:

$$u_p = \dot{x}_p = u_0(x_p). \quad (4.38)$$

because we assume that the particle is convected with the mean flow velocity u_0 . Furthermore the particle will exert an additional force on the fluid due to the density difference $(\rho - \rho_0)$ which implies a force source term:

$$f_x = \Delta p' \delta(x - y) = -\frac{\rho - \rho_0}{A} V_p \frac{D u_p}{D t} \delta(x - y) = -\frac{\rho - \rho_0}{A} V_p u_0 \frac{d u_0}{d x} \delta(x - y). \quad (4.39)$$

This force is due to the difference in inertia between the particle and its environment. Note that for an ideal gas the compressibility \mathcal{K} is given by:

$$\mathcal{K} = \frac{1}{\gamma p}. \tag{4.40}$$

Hence for a small particle in this linear approximation the volume source term (4.37) is due to a difference in γ . This term vanishes if we consider the convection of a hot gas particle (not chemically different from the environment) which we call an entropy spot. In that case sound production will be due to the difference of inertia between the entropy spot and the surrounding fluid. Howe [84] refers to this as acoustical “Bremsstrahlung”.

In a similar way we can describe the effect of a slow variation of the tube cross section area A on sound waves of low frequency (*i.e.* $\frac{d}{dx}A \ll \sqrt{A} \ll \lambda$). With some care we can derive a suitable one-dimensional approximation, called Webster’s horn equation, to describe the wave propagation (see section 8.5). To leading order the momentum conservation law is not affected by the cross section variation. The mass conservation law, however, becomes:

$$\frac{\partial \rho'}{\partial t} + \frac{\rho_0}{A} \frac{\partial Au'}{\partial x} = 0 \tag{4.41}$$

This can be interpreted as the linearized continuity equation (4.3a) with a volume source term

$$\frac{\partial \beta}{\partial t} = \frac{u'}{A} \frac{\partial A}{\partial x} \tag{4.42}$$

4.4 Reflection at discontinuities and abrupt changes

The procedure described in the previous section to incorporate sources in a compact region into a one dimensional model can also be applied to determine jump conditions over rapid changes in a pipe. It should be noted that a mathematically more sound derivation, allowing also higher order corrections, is obtained by using the method of Matched Asymptotic Expansions. This will be worked out in more detail in chapter 8.

4.4.1 Jump in characteristic impedance ρc

We first consider an abrupt change at about $x = y$ in speed of sound c and density ρ between two media, 1 and 2, in a hard-walled pipe with uniform cross section of size L^2 (figure 4.6). If the waves are exactly plane and the interface is exactly straight, the jump conditions across the interface (continuous velocity and pressure) may follow from continuity of streamlines and normal stress. In general, however, it is more subtle. As an illustrative example, we will give the derivation here in detail.

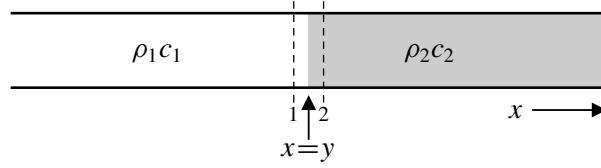


Figure 4.6 Jump in acoustic impedance.

Assume that the typical frequencies ω are low such that the Helmholtz numbers $\varepsilon_1 = \omega L/c_1$ and $\varepsilon_2 = \omega L/c_2$ are small. In that case the acoustic field is 3D only in the immediate neighbourhood of the jump. At about a diameter L away it is practically plane and only dependent on x (see page 182: all modes are evanescent except for the plane wave). Define Ω_1 equal to the volume between the (not necessarily straight and steady) interface $S(t)$ near $x = y$ and the fixed plane $x = y_- = y - L$. Similarly, we define Ω_2 the volume between S and $x = y_+ = y + L$.

Integrate the mass conservation equations in the form of (1.23) over Ω_1 and Ω_2 to obtain

$$\iiint_{\Omega_1} \left[\frac{1}{\rho_1} \frac{d\rho_1}{dt} + \nabla \cdot \mathbf{v}_1 \right] d\mathbf{x} + \iiint_{\Omega_2} \left[\frac{1}{\rho_2} \frac{d\rho_2}{dt} + \nabla \cdot \mathbf{v}_2 \right] d\mathbf{x} = 0$$

After applying Gauss' divergence theorem

$$\begin{aligned} \iiint_{\Omega_1} \frac{1}{\rho_1} \frac{d\rho_1}{dt} d\mathbf{x} - \iint_{x=y_-} u_1 dA + \iint_S (\mathbf{v}_1 \cdot \mathbf{n}_1) dA \\ + \iiint_{\Omega_2} \frac{1}{\rho_2} \frac{d\rho_2}{dt} d\mathbf{x} + \iint_{x=y_+} u_2 dA + \iint_S (\mathbf{v}_2 \cdot \mathbf{n}_2) dA = 0 \end{aligned}$$

and using the fact that at interface S the normal velocity components are continuous and so $(\mathbf{v}_1 \cdot \mathbf{n}_1) = -(\mathbf{v}_2 \cdot \mathbf{n}_2)$, we obtain

$$\iiint_{\Omega_1} \frac{1}{\rho_1} \frac{d\rho_1}{dt} d\mathbf{x} - u_1(y_-)L^2 + \iiint_{\Omega_2} \frac{1}{\rho_2} \frac{d\rho_2}{dt} d\mathbf{x} + u_2(y_+)L^2 = 0$$

After linearisation and estimating the volume integrals $\sim L^3 \rho_t / \rho \sim L^3 \omega \rho' / \rho_0 \sim L^3 \omega v' / c_0 = L^2 \varepsilon v'$, we find that

$$u'_2(y_+) - u'_1(y_-) = O(\varepsilon_1 v'_1, \varepsilon_2 v'_2)$$

In a similar way we integrate the axial momentum equation

$$\iiint_{\Omega_1} \left[\rho_1 \frac{du_1}{dt} + \frac{\partial p_1}{\partial x} \right] d\mathbf{x} + \iiint_{\Omega_2} \left[\rho_2 \frac{du_2}{dt} + \frac{\partial p_2}{\partial x} \right] d\mathbf{x} = 0.$$

After integrating to x

$$\iiint_{\Omega_1} \rho_1 \frac{du_1}{dt} dx - \iint_{x=y_-} p_1 dA + \iint_S p_1 dA + \iiint_{\Omega_2} \rho_2 \frac{du_2}{dt} dx + \iint_{x=y_+} p_2 dA - \iint_S p_2 dA = 0.$$

and using the fact that at S the pressure is continuous, we find

$$\iiint_{\Omega_1} \rho_1 \frac{du_1}{dt} dx - p_1(y_-)L^2 + \iiint_{\Omega_2} \rho_2 \frac{du_2}{dt} dx + p_2(y_+)L^2 = 0.$$

Linearisation and estimating the volume integrals $\sim L^3 \rho u_t \sim L^3 \omega \rho_0 u' \sim L^3 \omega \rho_0 c_0 u' / c_0 \sim L^3 \omega p' / c_0 = L^2 \varepsilon p'$ lead to

$$p'_2(y_+) - p'_1(y_-) = O(\varepsilon_1 p'_1, \varepsilon_2 p'_2)$$

Altogether we have thus approximately the following jump conditions at $x = y$

$$\Delta u' = u'_2 - u'_1 = 0, \tag{4.43a}$$

$$\Delta p' = p'_2 - p'_1 = 0. \tag{4.43b}$$

By using the general solution (4.8a,4.8b) of the homogeneous wave equation, we have at $x = y$ for the jump conditions in the pressure and velocity, respectively:

$$\mathcal{F}_1(y - c_1 t) + \mathcal{G}_1(y + c_1 t) = \mathcal{F}_2(y - c_2 t) + \mathcal{G}_2(y + c_2 t), \tag{4.44a}$$

$$\frac{\mathcal{F}_1(y - c_1 t) - \mathcal{G}_1(y + c_1 t)}{\rho_1 c_1} = \frac{\mathcal{F}_2(y - c_2 t) - \mathcal{G}_2(y + c_2 t)}{\rho_2 c_2}. \tag{4.44b}$$

If, for example, we have a source at $x < y$ generating an incident wave \mathcal{F}_1 , in a tube of infinite length so that $\mathcal{G}_2 = 0$, we obtain

$$\mathcal{G}_1(x + c_1 t) = R \mathcal{F}_1(2y - (x + c_1 t)), \tag{4.45a}$$

$$\mathcal{F}_2(x - c_2 t) = T \mathcal{F}_1\left(\left(1 - \frac{c_1}{c_2}\right)y + \frac{c_1}{c_2}(x - c_2 t)\right), \tag{4.45b}$$

$$\text{where } R = \frac{\rho_2 c_2 - \rho_1 c_1}{\rho_2 c_2 + \rho_1 c_1}, \quad T = \frac{2\rho_2 c_2}{\rho_2 c_2 + \rho_1 c_1}.$$

The factor R between \mathcal{G}_1 and \mathcal{F}_1 is called the reflection coefficient and the factor T between \mathcal{F}_2 and \mathcal{F}_1 the transmission coefficient. We observe that if $\rho_1 c_1 = \rho_2 c_2$ the acoustic wave is not reflected at the contact discontinuity. Inspection of (4.44a,4.44b) for $\rho_1 c_1 = \rho_2 c_2$ also shows that the only solution is $\mathcal{F}_1 = \mathcal{F}_2$ and $\mathcal{G}_1 = \mathcal{G}_2$. This corresponds to results obtained already in section 3.2 when considering harmonic waves.

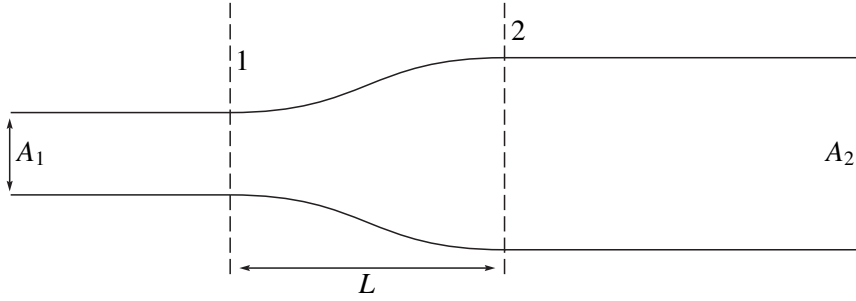


Figure 4.7 Abrupt cross sectional area change.

4.4.2 Smooth change in pipe cross section

We now consider a compact transition in pipe cross sectional area from A_1 to A_2 . If the flow is homentropic and there is no flow separation (vorticity is zero) the pressure difference $\Delta p' = p'_2 - p'_1$ across the discontinuity can be calculated by using the incompressible unsteady Bernoulli equation (1.32b):

$$\Delta p' = \frac{1}{2}\rho_0(u_1'^2 - u_2'^2) - \rho_0 \frac{\partial}{\partial t} \Delta \varphi, \quad (4.46)$$

where $\Delta \varphi = \varphi_2 - \varphi_1$ is the potential difference. In linear approximation:

$$\Delta p' \simeq -\rho_0 \frac{\partial}{\partial t} \Delta \varphi. \quad (4.47)$$

For a compact smooth change in cross section as in figure (4.7) we have continuity of flux $A_1 u_1' = A(x)u'(x)$, while the potential difference can be estimated as $\Delta \varphi = \int_1^2 u' dx \simeq u_1' \int_1^2 (A_1/A(x)) dx \sim u_1' L$. The pressure difference $\Delta p'$ is of the order of $\rho_0 \omega u_1' L$, which is negligible when $L\omega/c_0 \ll 1$. We then have a pressure uniform over the entire region. Note that while this is a very crude approximation, this is a stronger result than just a continuity condition (see section 4.4.4). This condition $\Delta p' = 0$ can be combined with the linearized mass conservation law in the low frequency approximation

$$\rho_0 A_1 u_1' = \rho_0 A_2 u_2' \quad (4.48)$$

to calculate the reflection at a pipe discontinuity.

4.4.3 Orifice and high amplitude behaviour

Instead of a smooth variation of the pipe area A we consider an orifice placed in the pipe with an opening area A_d and a thickness L (figure 4.8). We start with the problem of acoustic wave propagation through a stagnant fluid ($u_0 = 0$). In principle, if we use the approximations (4.47) and (4.48) and if we

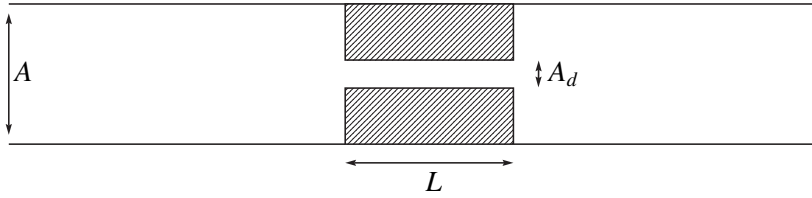


Figure 4.8 Orifice.

neglect the potential jump $\Delta\phi$, we see that the orifice will be completely “transparent” to the acoustic waves. However, if $A_d \ll A$ we find experimentally a significant effect of such an orifice which is due to the inertia of the air in the opening. Assuming a uniform velocity and an incompressible flow without friction we have from (4.47):

$$\Delta p' \simeq -\rho_0 \frac{A}{A_d} L \frac{\partial u'}{\partial t}. \quad (4.49)$$

where u' is the acoustic velocity in the pipe. We could also simply have obtained this result by considering the pressure difference $\Delta p'$ necessary to accelerate the mass of fluid ($\rho_0 A_d L$) in the orifice and noticing that the particle velocity in the orifice is given by:

$$u'_d = \frac{A}{A_d} u'. \quad (4.50)$$

In practice (4.49) yields a lower bound for the pressure drop across the orifice because we neglected the inertia of the air in the region outside the orifice. This effect can be taken into account by introducing an “end correction” δ on both sides:

$$L_{eff} = L + 2\delta \quad (4.51)$$

where δ appears to be of the order of $(A_d/\pi)^{1/2}$. Typically $(8/3\pi)(A_d/\pi)^{1/2}$ for a circular orifice and a larger value for a slit [94]. This explains why a thin orifice ($L \rightarrow 0$) also affects the propagation of acoustic waves in a pipe. For a circular orifice of radius a in a thin plate we have $L_{eff} = \pi a/2$ (see [183]).

If we consider a narrow orifice the local velocity u'_d in the orifice may become quite large. When the acoustic particle displacement u'_d/ω becomes comparable to the radius of curvature of the edges at the entrance and the exit of the orifice non-linear effects and friction will result into acoustically induced vortex shedding [97, 98, 52, 47]. When the fluid particle displacement becomes comparable to the diameter of the orifice $(A_d/\pi)^{1/2} u'_d/\omega = O(1)$ the vortex shedding can be described in terms of the formation of a free jet, by assuming that there is no pressure difference across the boundaries of the jet. The shear layers enclosing the jet are not capable of sustaining a pressure difference. Furthermore, if $A_d/A \ll 1$ we assume that the kinetic energy in the flow $\frac{1}{2}\rho u'_d{}^2$ is lost upon deceleration of the

jet by turbulent mixing with the air in the pipe. This implies that in addition to the linear terms in Bernoulli we should add the non-linear effects:

$$\Delta p' = -\rho_0 \frac{A}{A_d} L \frac{\partial u'}{\partial t} - \frac{1}{2} \rho_0 \left(\frac{A}{A_d} u' \right)^2. \quad (4.52)$$

A typical feature of this effect is that the pressure $\Delta p'$ has now a component $\frac{1}{2} \rho_0 u_d'^2$ which is in phase with the acoustic velocity, and therefore will involve (acoustic) energy losses that were absent in the situations discussed until now. These losses are due to the fact that the kinetic energy in the jet is dissipated by turbulence.

The model proposed here appears quite reasonable but in many cases the surface area of the jet is smaller than A_d which implies additional losses[47]. This effect can be as much as a factor 2. The jet contraction by a factor 2 corresponds to the so called vena contracta at an unflanged pipe entrance. For a thin orifice with sharp edges the jet cross section is a factor $\frac{\pi}{\pi+2}$ narrower than the orifice. When the edges are rounded off the contraction effect disappears rapidly.

It is interesting to consider now how a mean flow affects the acoustic properties of an orifice. We assume that the mean flow velocity u_0 in the pipe is so small compared to the speed of sound c_0 that we can neglect all convective effects on the wave propagation ($u_0/c_0 \ll 1$). As the orifice has a small aperture (A_d/A), the mean flow velocity in the orifice is significant. We assume a stationary frictionless and incompressible flow. The assumption of a frictionless flow fails, however, to describe the flow at the exit of the orifice where as a result of friction the flow separates from the wall and a free jet of surface area A_d is formed.

Assuming further no pressure difference between the jet and its environment we can write for the total pressure difference Δp_0 :

$$\Delta p_0 = -\frac{1}{2} \rho_0 \left(\frac{A}{A_d} u_0 \right)^2. \quad (4.53)$$

For acoustic velocity fluctuations u' we have, neglecting the higher order terms in u' :

$$\Delta p' = -\rho_0 \frac{A}{A_d} L \frac{\partial u'}{\partial t} - \rho_0 \left(\frac{A}{A_d} \right)^2 u_0 u'. \quad (4.54)$$

We see from this equation that even in the linear approximation energy is transferred ($\rho_0 (A/A_d)^2 u_0 \overline{u'^2}$) from the acoustic field to the flow (where it is dissipated by turbulence). This effect is of course a result of the force $\rho_0(\boldsymbol{\omega} \times \boldsymbol{v})$ in Howe's analogy (section 2.6). The vorticity responsible for this is located in the shear layer that confines the free jet. We will describe the formation of a free jet in section 5.1. The consequence of this effect is that an orifice placed in a tube with a mean flow is a very efficient damping mechanism. This device is indeed used downstream of a compressor in order to avoid the low frequency pulsations that may be induced by the compressor into the pipe system. As explained by Bechert [12], for any orifice placed at the end of a pipe one can find a Mach number at

which the reflection coefficient for long acoustic waves vanishes. Such an orifice acts thus as an anechoic termination for low frequencies!

A beautiful property of this damping mechanism is that it is not frequency dependent as long as the frequency is low enough. This is not the case with the effect of friction and heat transfer which are strongly frequency dependent (equation 3.13), in a way that at low frequencies friction is quite inefficient.

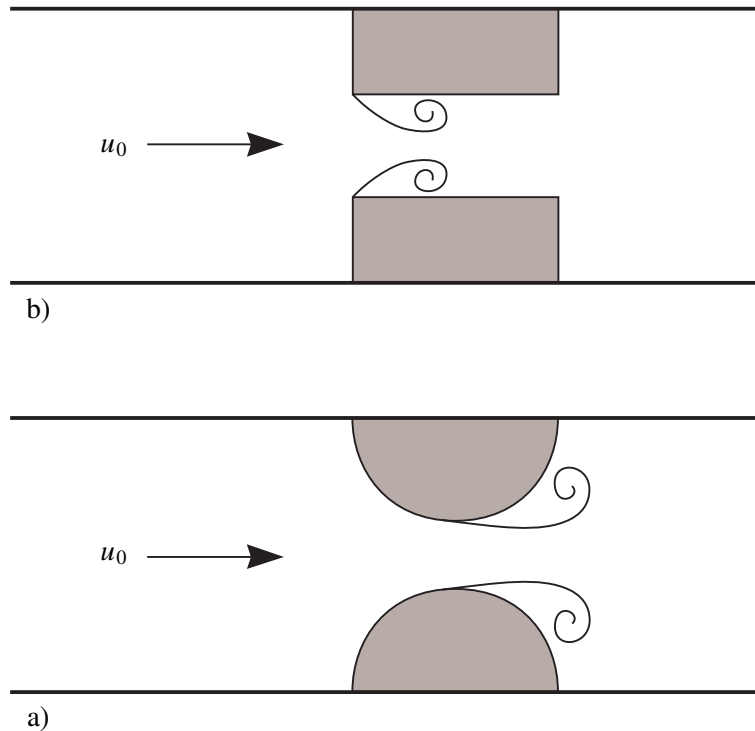


Figure 4.9 Vortex shedding at an orifice.

It is interesting, however, to note that under special flow conditions an orifice can produce sound as a result of vortex shedding. This occurs in particular if the orifice has sharp edges at the entrance where the vortices are shed [8] (figure 4.9a) or when the edges are rounded at the downstream side [261, 79] (figure 4.9b).

The frequency of the sound produced by the vortex shedding is such that the period of oscillation roughly corresponds to the travel time of a vortex through the orifice (a Strouhal number $Sr = fL/(Au_0/A_d) = O(1)$). When this sound source couples with a resonator (see next chapter) large amplitudes may be generated. This is an explanation for human whistling [261, 229]. Flow instabilities of this type also occur around pipe arrays such as used in heat exchangers [20]. Whistling corresponds to self-sustained flow instabilities. In the case of an externally imposed acoustic wave, the

periodic vortex shedding is a non-linear phenomenon which will generate higher harmonics. Hence, suppressing low frequency-pulsations (being mechanically dangerous) with an orifice may be paid by the generation of high frequency noise which is an environmental problem.

A generalization of the procedure which we introduced intuitively for the orifice can be obtained for an arbitrary compact discontinuity in a pipe system. The acoustical effect of this discontinuity can be represented in an acoustical model by a pressure discontinuity $(\Delta p)_{source}$ which is calculated by subtracting from the actual pressure difference Δp the pressure difference $(\Delta p)_{pot}$, corresponding to a potential flow with the same velocity boundary conditions:

$$(\Delta p)_{source} = \Delta p - (\Delta p)_{pot}.$$

The actual pressure difference Δp can be measured or calculated as a function of the main flow velocity u_0 and the acoustical velocity fluctuation u' . The potential flow difference $(\Delta p)_{pot}$ is calculated. This procedure is in particular powerful when we can use a quasi-stationary flow model. We then use the incompressible continuity equation and Bernoulli: $Su = \text{constant}$ and $p + \frac{1}{2}\rho_0 u^2 = \text{constant}$, to calculate $(\Delta p)_{pot}$, while Δp is measured in the form $\Delta p = C_D \frac{1}{2}\rho u^2$ as a function of various parameters. When convective effects are taken into account in the wave propagation, it appears to be important to define the aeroacoustic source in terms of a discontinuity $(\Delta B)_{source}$ in the total enthalpy rather than in the pressure.

4.4.4 Multiple junction

In the previous sections we used the equation of Bernoulli to derive pressure jump conditions for a discontinuous change in pipe diameter. We could also have obtained a similar expression by considering the law of energy conservation. The use of Bernoulli is a stronger procedure. To illustrate this statement we consider the reflection of waves at a multiple junction. As an example consider a *T* shaped junction between three pipes of cross-sectional surface A_1 , A_2 and A_3 , respectively (figure 4.10).

We define along each pipe a x -coordinate with a positive direction outwards from the junction. The conservation of mass for a compact junction yields:

$$A_1 u'_1 + A_2 u'_2 + A_3 u'_3 = 0 \quad (4.55)$$

while from the equation of Bernoulli we find:

$$p'_1 = p'_2 = p'_3 \quad (4.56)$$

Note that closed side branches are very popular as reflectors to prevent the propagation of compressor induced pulsations. It is interesting to note that flow may also drastically affect the acoustic properties of a multiple junction and make the use of this device quite dangerous. In particular if we consider

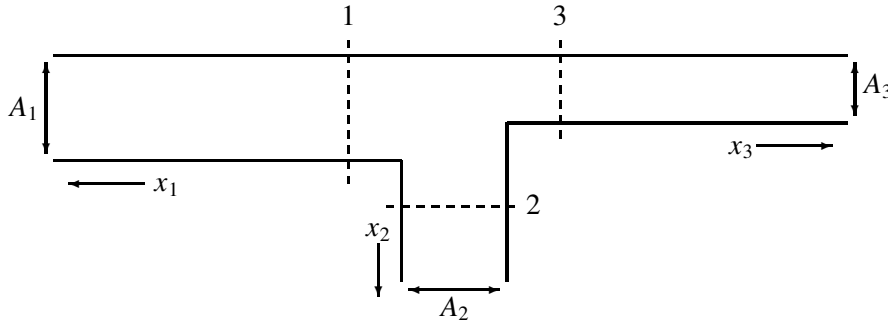


Figure 4.10 Multiple junction.

junctions with closed side branches, the shear layer separating the main flow from the stagnant fluid in the pipe is unstable. Coupling of this instability with a resonant acoustic field may result into pulsation levels of the order of $p' \simeq O(\rho c_0 u_0)$ ([28, 111, 264]). Again, the amplitude of these pulsations depends crucially on the shape of the edges of the junction, in the same way as the shape of the edges was crucial in the orifice problem. More about this will be explained in the next chapter.

For a T-shaped junction of a main pipe with a closed side branch or a grazing flow along an orifice in the wall the quasi-steady theory for a main flow u_0 indicates that the shear layer can be represented by an acoustical pressure discontinuity: $(\Delta p)_{source} = -K\rho_0 u_0 u'$, where K is unity for a uniform main flow. For an orifice small compared to the boundary layer thickness of the main flow K is of the order of 0.7 because of the velocity defect in the boundary layer relative to the main flow velocity u_0 . This effect is discussed by Ronneberger [218], Tijdeman [243] and Cummings [48].

4.4.5 Reflection at a small air bubble in a pipe

Air bubbles in the water circuit of the central heating of a house are responsible for a very characteristic, high-frequency sound. As a first step to the understanding of this effect we now consider the reflection of a harmonic wave on a small air bubble of radius a (Volume $V_p = (4\pi/3)a^3$) placed in a pipe filled with water at a static pressure p_0 . If the bubble is small compared to the characteristic acoustic wave length we can assume that the pressure p'_b in the bubble will be uniform. We neglect surface tension effects and assume that the bubble pressure p'_b is equal to the surrounding water pressure.

In the low frequency limit, when the inertial forces in the flow around the bubble can be neglected, the pressure induced by a passing acoustic plane wave in the water around the bubble will be practically uniform: $\Delta p' = 0$. The bubble will react quasi-statically to the imposed acoustic pressure variation p' . Since the air-filled bubble is much more compressible than water, the presence of the bubble results

into a volume source term, giving rise to a jump in acoustic velocity across a control volume including the bubble:

$$\Delta u' \simeq -\frac{V_p}{A\gamma p_0} \frac{dp'}{dt} \quad (4.57)$$

where we neglected the water compressibility compared to the air compressibility ($\mathcal{K}_{air} = 1/\gamma p_0$) and we assume an adiabatic compression (taking $\gamma = 1$ would imply an isothermal compression as we expect for very low frequencies). The reflection coefficient for a wave \mathcal{F}_1 incident to the bubble can now be calculated from the jump conditions for $\Delta p'$ and $\Delta u'$. Assuming $\mathcal{G}_2 = 0$ we find from the continuity of pressure:

$$\mathcal{F}_1 + \mathcal{G}_1 - \mathcal{F}_2 = 0 \quad (4.58)$$

and from (4.57):

$$\mathcal{F}_1 - \mathcal{G}_1 - \mathcal{F}_2 = \frac{\rho_w c_w V_p}{A\gamma p_0} \frac{d}{dt} (\mathcal{F}_1 + \mathcal{G}_1). \quad (4.59)$$

By subtraction of (4.58) from (4.59) we can eliminate \mathcal{F}_2 and find:

$$\mathcal{G}_1 = -\frac{\rho_w c_w V_p}{2A\gamma p_0} \frac{d}{dt} (\mathcal{F}_1 + \mathcal{G}_1) \quad (4.60)$$

The inertia of the water around the bubble will dramatically influence the interaction between the bubble and acoustic waves at higher frequencies. If we assume that the acoustic wave lengths in both air and water are very large compared to the bubble radius we still can assume a uniform pressure in the bubble. This implies also that the bubble will remain spherical. The oscillations of the bubble radius:

$$a = a_0 + \hat{a} e^{i\omega t} \quad (4.61)$$

around the equilibrium value a_0 will induce a radial flow of the water around the bubble if we assume that the bubble is small compared to the pipe diameter. In the low frequency approximation considered here, this flow is incompressible. Hence we have for the radial velocity v_r :

$$v_r = \left(\frac{a}{r}\right)^2 \left(\frac{\partial a}{\partial t}\right) \simeq i\omega \left(\frac{a_0}{r}\right)^2 \hat{a} e^{i\omega t} \quad (4.62)$$

where we have assumed $\hat{a}/a_0 \ll 1$. The pressure variation in the bubble:

$$p_b = p_0 + \hat{p}_b e^{i\omega t} \quad (4.63)$$

can be related to the incompressible far field (still near the bubble compared to the pipe radius) by applying the linearized Bernoulli equation:

$$p + \rho_w \frac{\partial \varphi}{\partial t} = p_b + \rho_0 \frac{\partial \varphi_b}{\partial t}. \quad (4.64)$$

Using (4.62) we can calculate $(\varphi - \varphi_b)$:

$$\varphi - \varphi_b = \int_a^\infty v_r dr \simeq i\omega a_0 \hat{a} e^{i\omega t} \quad (4.65)$$

so that:

$$p - p_b = \rho_w \omega^2 a_0 \hat{a} e^{i\omega t}. \quad (4.66)$$

Assuming the air in the bubble to be an ideal gas with $p_b \sim \rho_b'$ and neglecting the dissolution of air in water so that $a^3 \rho_b = \text{constant}$, we find:

$$\frac{1}{\rho_b} \frac{\partial \rho_b}{\partial t} = \frac{1}{\gamma p_b} \frac{\partial p_b}{\partial t} = -\frac{3}{a} \frac{\partial a}{\partial t} \quad (4.67)$$

or in linear approximation:

$$\frac{\hat{p}_b}{p_0} = -3\gamma \frac{\hat{a}}{a_0}. \quad (4.68)$$

Combining (4.66) with (4.68) and assuming that $p = p_0 + \hat{p}' e^{i\omega t}$ we have:

$$\hat{p}' = \rho_w a_0 \hat{a} (\omega^2 - \omega_0^2) \quad (4.69)$$

where the resonance frequency ω_0 (Minnaert frequency) is defined by:

$$\omega_0^2 = \frac{3\gamma p_0}{a_0^2 \rho_w}. \quad (4.70)$$

The reflection coefficient $R = \mathcal{G}_1 / \mathcal{F}_1$ can now be calculated in a similar way as from (4.58) and (4.59) with the modified source term $\Delta u' = 4\pi i \omega a_0^2 \hat{a} A^{-1} e^{i\omega t}$. Since $\Delta p' = 0$, we have:

$$\mathcal{F}_1 + \mathcal{G}_1 - \mathcal{F}_2 = 0 \quad (4.71a)$$

and

$$\mathcal{F}_1 - \mathcal{G}_1 - \mathcal{F}_2 = \rho_w c_w \frac{4\pi i \omega a_0 (\mathcal{F}_1 + \mathcal{G}_1)}{A \rho_w (\omega^2 - \omega_0^2)} \quad (4.71b)$$

or

$$R = \frac{\mathcal{G}_1}{\mathcal{F}_1} = -\left(1 + \frac{A(\omega^2 - \omega_0^2)}{2\pi i \omega c_w a_0}\right)^{-1}. \quad (4.72)$$

We see that at resonance $\omega = \omega_0$ the wave is fully reflected by the bubble, and the reflection coefficient is $R = -1$. We have of course obtained such a dramatic result because we have neglected all the dissipation mechanisms which can limit the amplitude of the bubble oscillation. The compressibility

of the water flow around the bubble yields already such a mechanism which limits the amplitude of the oscillation at the resonance frequency ω_0 . This is, however, only one of the many amplitude-limiting mechanisms.

For small bubbles, when the diffusion length for heat transfer into the bubble is comparable to the bubble radius, heat transfer is a significant energy loss [188]. This occurs for: $a = O((K_{air}/\omega\rho_{air}C_P)^{1/2})$. For larger bubbles heat transfer is negligible. For smaller bubbles the compression occurs isothermally and one should put $\gamma = 1$ in the theory. However, the change of γ from 1.4 to 1 does not introduce damping. It is only in the intermediate range that the heat flux results in a significant rate of volume change in phase with the acoustic pressure. (As it is the work $W = \int p'dV = \int_0^T p'(dV/dt)dt$ which determines the losses, a volume V proportional to p' implies for a periodic oscillation $W \sim \int_0^T p'(dp'/dt)dt = 0$.)

Another limitation of the amplitude of the oscillation is the highly non-linear behaviour of the pressure for oscillation amplitudes \hat{a} comparable to a_0 . If $a \rightarrow 0$ the pressure in the bubble increases dramatically ($p_b \sim a^{-3\gamma}$). Linear theory fails and the bubble may start showing chaotic behaviour (referred to as acoustical chaos) [118].

As an isolated air bubble already has a strong effect on the acoustics of a water filled tube, a large amount of bubbles will have a dramatic effect. In section 2.3 we already considered the low frequency limit for the speed of sound in a bubbly liquid. We have seen that a small volume fraction of bubbles can considerably reduce the speed of sound. This is due to the large compressibility of the air in the bubbles. As ω reaches ω_0 this effect will become dramatic resulting in a full reflection of the waves (speed of sound zero) [45, 103]. In the frequency range $\omega_0 < \omega < \omega_0 c_w / c_{air}$ no wave propagation is possible in an ideal bubbly liquid. Above the anti-resonance frequency $\omega_0 c_w / c_{air}$ the bubble movement is in opposition to the applied pressure fluctuations. The radius increases when the pressure increases. This is just opposite to the low frequency behaviour (figure 4.11). As a result the bubbly mixture will be stiffer than water, and $c > c_w$! Sound speeds of up to 2500 m/s were indeed observed in bubbly water with $\beta = 2 \times 10^{-4}$!

Another fascinating effect of bubble resonance is its role in the very specific, universal, sound that rain is known to generate when it hits a water surface [189]. First it should be noted that bubble oscillation is such an efficient source of sound that any rain impact sound is dominated by it. Now, in spite of the wide range of velocities and sizes of rain drops that occurs, the universality of the sound of rain is due to the fact that only bubbles are formed of just one³ particular size. This is a result of the following coincidence. On the one hand, not any combination of drop size and drop velocity occurs: rain drops fall at terminal velocity (balance of air drag and drop weight) which is an increasing function of the droplet radius. On the other hand, not any combination of drop size and drop velocity generates bubbles upon impact on water. At each drop size there is one drop velocity where bubbles are formed. This bubble formation velocity is a decreasing function of the droplet radius. Combining

³*i.e.* a narrow range

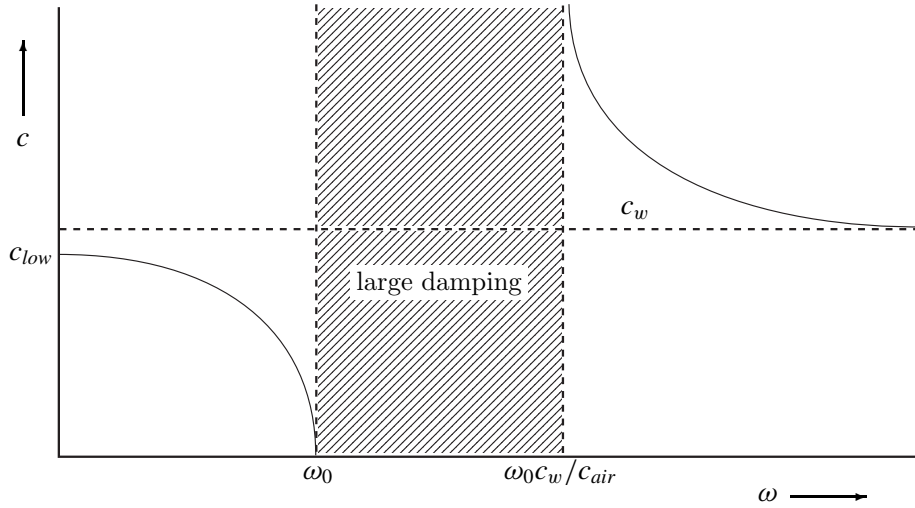


Figure 4.11 Idealized frequency dependence of the speed of sound in a bubbly liquid. The low-frequency limit c_{low} , slightly lower than c_w , is given in equation (2.44) or (2.45).

these increasing and decreasing functions, we see that they intersect just at one combination of radius and velocity, with just one bubble size.

4.5 Attenuation of an acoustic wave by thermal and viscous dissipation

4.5.1 Reflection of a plane wave at a rigid wall

Consider a pipe $-\infty < x \leq 0$, closed at $x = 0$ by a rigid wall. Inside the pipe a plane wave $p^+(x, t) = \mathcal{F}(t - x/c_0)$ travels in positive direction and reflects into a left-running wave $p^-(x, t)$. Without visco-thermal losses, the boundary condition of vanishing velocity becomes

$$u(0, t) = \frac{p^+(0, t) - p^-(0, t)}{\rho_0 c_0} = 0.$$

This implies a reflected wave $p^-(x, t) = \mathcal{F}(t + x/c_0)$, equal in amplitude and shape to the incident wave, and therefore a reflection coefficient of unity

$$R = \frac{p^-(0, t)}{p^+(0, t)} = 1.$$

In reality unsteady heat transfer at the wall will act as a sink of sound, slightly reducing the reflection coefficient. This heat transfer is a result from the difference between the wall temperature T_w , which remains practically constant, and the bulk temperature T of the gas, which varies with the adiabatic pressure fluctuations $p' = p^+ + p^-$. We will limit our analysis to small temperature differences ($T - T_w$) and small departures from the quiescent reference state. This allows a linearized theory, so that we can consider the reflection of a harmonic wave, denoted in complex form as

$$p(x, t) = \hat{p}(x) e^{-i\omega t}$$

with amplitude \hat{p} outside the neighbourhood of the wall being given by $\hat{p}(x) = \hat{p}^+ e^{-ikx} + \hat{p}^- e^{ikx}$. (Likewise, in the following the hatted quantities with “^” will denote their corresponding, x -dependent, complex amplitudes.)

We *define* (see also section 8.8) the thermal boundary layer thickness δ_T as the width of the region near the wall in which the rate of increase of internal energy is just balancing the net rate of heat conduction (in this region the wave equation is not valid):

$$\left(\rho_0 C_p \frac{\partial}{\partial t} T \sim \omega \rho_0 C_p T' \right) \simeq \left(K_0 \frac{\partial^2}{\partial x^2} T \sim K_0 \frac{T'}{\delta_T^2} \right).$$

Hence, the characteristic length scale for the thermal boundary layer is

$$\delta_T = \sqrt{\frac{2K_0}{\omega \rho_0 C_p}}. \quad (4.73)$$

We will now calculate the temperature profile within the thermal boundary layer. This will allow us to calculate the deviation $\hat{\rho}_e = \hat{\rho} - \hat{p}/c_0^2$ between the density fluctuations in the boundary layer and the density fluctuations \hat{p}/c_0^2 corresponding to adiabatic compression of an ideal acoustic flow as found outside the boundary layer. This excess density $\hat{\rho}_e$ has to be supplied by a fluid flow towards the wall at the edge of the boundary layer. This velocity \hat{u}_∞ can be interpreted by an observer, outside the boundary layer, as due to a displacement \hat{d}_T of the rigid wall in a hypothetical fluid without heat conduction. The work performed by this “virtual” wall displacement on the acoustic field corresponds to the sound dissipation by the thermal conduction in the boundary layer.

This approximation is based on the key assumption that the acoustic wave length is much larger than the thickness δ_T of the thermal boundary layer: $\omega \delta_T / c_0 \ll 1$. In such a case we can assume at the edge of the boundary layer a uniform adiabatic flow, $(d\hat{u}/dx)_\infty = 0$, of a uniform fluid $(\hat{p}_\infty, \hat{\rho}_\infty)$. The non-uniformity associated with the acoustic wave propagation is negligible on the length scale we consider. The boundary layer flow is described by the one-dimensional conservation laws (1.1,1.2,1.6,1.7) in

linearized form:

$$i\omega\hat{\rho} = -\rho_0\frac{d\hat{u}}{dx}, \quad (4.74a)$$

$$i\omega\rho_0\hat{u} = -\frac{d\hat{p}}{dx} + \frac{4}{3}\eta_0\frac{d^2\hat{u}}{dx^2}, \quad (4.74b)$$

$$i\omega C_V\rho_0\hat{T} = -p_0\frac{d\hat{u}}{dx} + K_0\frac{d^2\hat{T}}{dx^2}. \quad (4.74c)$$

Since in a liquid acoustic wave propagation is isothermal we can limit our analysis to a gas. We assume an ideal gas with:

$$\frac{\hat{p}}{p_0} = \frac{\hat{\rho}}{\rho_0} + \frac{\hat{T}}{T_0}.$$

The boundary conditions are given by:

$$\begin{aligned} \hat{T}(0) = \hat{T}_w, \quad \hat{u}(0) = 0, \quad \frac{\hat{T}_\infty}{T_0} = \frac{\gamma - 1}{\gamma} \frac{\hat{p}_\infty}{p_0}, \\ \hat{p}(x) \rightarrow \hat{p}_\infty = \hat{p}^+ + \hat{p}^- \quad (x/\delta_T \rightarrow -\infty), \end{aligned}$$

where we have introduced, for generality, the fluctuation of the wall temperature \hat{T}_w . After the study of the reflection of a wave at an isothermal wall ($\hat{T}_w = 0$) we can use the same theory to calculate the sound generated by fluctuations of the wall temperature ($\hat{T}_w \neq 0$).

After eliminating \hat{u} from the energy equation by using the mass conservation law, and eliminating $\hat{\rho}$ by means of an ideal gas law, we obtain

$$i\omega\left(\frac{\hat{T}}{T_0} - \frac{\gamma - 1}{\gamma} \frac{\hat{p}}{p_0}\right) = a_0\frac{d^2}{dx^2}\left(\frac{\hat{T}}{T_0}\right)$$

where $a_0 = K_0/\rho_0 C_p$ is the heat diffusivity coefficient. In terms of the excess density, with

$$\frac{\hat{\rho}_e}{\rho_0} = \frac{1}{\rho_0}\left(\hat{\rho} - \frac{\hat{p}}{c_0^2}\right) = \frac{\hat{\rho}}{\rho_0} - \frac{\hat{p}}{\gamma p_0} = \frac{\gamma - 1}{\gamma} \frac{\hat{p}}{p_0} - \frac{\hat{T}}{T_0},$$

this equation becomes

$$i\omega\frac{\hat{\rho}_e}{\rho_0} = a_0\frac{d^2}{dx^2}\left(\frac{\hat{\rho}_e}{\rho_0}\right) - a_0\frac{\gamma - 1}{\gamma} \frac{d^2}{dx^2}\left(\frac{\hat{p}}{p_0}\right).$$

Combining the momentum and mass conservation laws we have

$$\omega^2\hat{\rho} = -\frac{d^2\hat{p}}{dx^2} + \frac{4}{3}\eta_0\frac{d^3\hat{u}}{dx^3}.$$

Assuming that viscosity is not dominant – which we can check from the solution to be obtained – we see that

$$\frac{d^2}{dx^2} \left(\frac{\hat{p}}{\rho_0} \right) \simeq -\frac{\omega^2 \hat{p}}{p_0} = -\frac{\omega^2 \gamma}{c_0^2} \frac{\hat{p}}{\rho_0}.$$

The relative pressure variation across the boundary layer (4.73) is of the order of

$$\frac{\hat{p} - \hat{p}_\infty}{p_0} \sim \frac{\omega^2 \delta_T^2}{c_0^2} \left(\frac{\hat{p}}{\rho_0} \right)$$

while $\hat{\rho}_e/\rho_0$ is of the same order of magnitude as \hat{p}/ρ_0 , because $\gamma - 1 = O(1)$. This implies that if we neglect terms of the order of $\omega^2 \delta_T^2/c_0^2$, we have

$$i\omega \frac{\hat{\rho}_e}{\rho_0} = a_0 \frac{d^2}{dx^2} \left(\frac{\hat{\rho}_e}{\rho_0} \right).$$

This equation has the solution

$$\frac{\hat{\rho}_e}{\rho_0} = \left[\frac{\hat{\rho}_e}{\rho_0} \right]_w \exp\left((1+i)x/\delta_T\right) \quad (4.75)$$

$$\text{where } \left[\frac{\hat{\rho}_e}{\rho_0} \right]_w = \frac{\gamma - 1}{\gamma} \frac{\hat{p}_\infty}{p_0} - \frac{\hat{T}_w}{T_0}.$$

Using the equation of mass conservation, the velocity $\hat{u}(-\delta_T)$ at the edge of the boundary layer is given by the integral of the density across the boundary layer as follows. (Note that we have chosen the positive x -direction towards the wall.)

$$\hat{u}(0) - \hat{u}(-\delta_T) = -i\omega \int_{-\delta_T}^0 \frac{\hat{\rho}}{\rho_0} dx.$$

The difference between this velocity and the velocity $i\omega(\hat{\rho}_\infty/\rho_0)\delta_T$ that would occur in the absence of heat conduction, can be interpreted as a fictitious wall velocity \hat{u}_T given by

$$\hat{u}_T = i\omega \hat{d}_T = i\omega \int_{-\delta_T}^0 \frac{\hat{\rho} - \hat{\rho}_\infty}{\rho_0} dx = i\omega \int_{-\infty}^0 \frac{\hat{\rho}_e}{\rho_0} dx,$$

where \hat{d}_T is the fictitious wall displacement amplitude. Substitution of solution (4.75) yields

$$\hat{d}_T = \frac{1}{2}(1-i)\delta_T \left[\frac{\hat{\rho}_e}{\rho_0} \right]_w, \quad (4.76a)$$

$$= \frac{1}{2}(1-i)\delta_T \frac{\gamma - 1}{\gamma} \frac{\hat{p}_\infty}{p_0} \quad \text{if } T_w = 0 \text{ (an isothermal wall)}. \quad (4.76b)$$

For an isothermal wall ($\hat{T}_w = 0$) these wall effects, leading to the effective velocity \hat{u}_T , have the same effect to the incident acoustic wave as an impedance of the wall. This equivalent impedance Z_T , defined as the ratio of the acoustic pressure fluctuations \hat{p}_∞ at the wall and the flow velocity \hat{u}_T directed towards the wall (c.f. Eq. 3.14), is then given by

$$Z_T = \frac{\hat{p}_\infty}{\hat{u}_T} = \frac{\hat{p}_\infty}{i\omega\hat{d}_T} = \rho_0 c_0 \frac{(1-i)c_0}{(\gamma-1)\omega\delta_T}$$

The corresponding time averaged acoustic intensity is found to be

$$\langle I_T \rangle = \langle p'u' \rangle = \frac{1}{2} \operatorname{Re}(1/Z_T) |\hat{p}_\infty|^2 = \frac{1}{4} (\gamma-1) \frac{\omega\delta_T}{\rho_0 c_0^2} |\hat{p}_\infty|^2$$

which indicates an energy flux from the acoustic field towards the wall and therefore an absorption of energy.

4.5.2 Viscous laminar boundary layer

The viscous attenuation of a plane acoustic wave propagating along a pipe can often be described in a similar way as the thermal attenuation by means of a displacement thickness \hat{d}_V of the wall. We consider first the simple case of a laminar boundary layer in the case of wave propagation in a stagnant and uniform fluid. The wave propagates in the x -direction and induces an acoustic velocity parallel to the wall which has an amplitude \hat{u}_∞ in the bulk of the flow. The no-slip condition at the wall, $\hat{u}_w = 0$, induces a viscous boundary layer of thickness

$$\delta_V = \sqrt{2\nu_0/\omega} = \delta_T \sqrt{Pr}. \quad (4.77)$$

where $Pr = \nu_0 \rho_0 C_p / K_0$ is Prandtl's number. This viscous boundary layer is usually referred to as the Stokes layer. Neglecting terms of the order of $(\omega\delta_V/c_0)^2$ and using Euler's equation we can write the x -momentum conservation law in the boundary layer as

$$i\omega\rho_0\hat{u} = -\frac{dp}{dx} + \eta_0 \frac{d^2\hat{u}}{dy^2} = i\omega\rho_0\hat{u}_\infty + \eta_0 \frac{d^2\hat{u}}{dy^2},$$

where y is the direction normal to and towards the wall (so $y \leq 0$). The y -momentum conservation law reduces to the pressure being uniform across the viscous boundary layer. The boundary conditions are

$$\hat{u}(0) = \hat{u}_w = 0, \quad \hat{u}(y) \rightarrow \hat{u}_\infty \text{ if } y/\delta_V \rightarrow -\infty.$$

The solution is then

$$\hat{u} = \hat{u}_\infty \left[1 - \exp\left(\frac{(1+i)y}{\delta_V}\right) \right]. \quad (4.78)$$

The displacement thickness d_V is defined as the fictitious wall position for which the acoustical mass flux of a uniform flow with the velocity \hat{u}_∞ is equal to the actual mass flow. This implies:

$$\hat{d}_V = - \int_{-\infty}^0 \left(1 - \frac{\hat{u}}{\hat{u}_\infty}\right) dy = -\frac{1}{2}(1 - i)\delta_V. \quad (4.79)$$

4.5.3 Damping in ducts with isothermal walls.

In section 4.5.1 we have considered the attenuation of an acoustic wave that reflects normally to a wall. This attenuation was due to the heat conduction in the thermal boundary layer. In the previous section 4.5.2 we have described the laminar viscous boundary layer associated to a plane wave propagating along a duct (parallel to the wall). In a gas such a propagation will also induce a thermal boundary layer, determined by the pressure fluctuations p'_∞ in the bulk of the flow. The expression for the displacement thickness \hat{d}_T derived in section 4.5.1 can be applied.

Using the concept of displacement thickness we will calculate the attenuation of a plane wave travelling in x -direction along a pipe of cross-sectional area A and cross-sectional perimeter L_p . We assume that the boundary layers are thin compared to the pipe diameter.

The bulk of the flow is described by the following plane wave, satisfying Euler's equation in linear approximation:

$$p'_\infty = \hat{p}_\infty e^{i\omega t - ikx}, \quad i\omega\rho_0 u'_\infty = ikp'_\infty,$$

where k is a complex wave number (the imaginary part will describe the attenuation). Incorporating the displacement thickness to the mass conservation law integrated over the pipe cross section yields (Lighthill [126])

$$\frac{\partial}{\partial t} [\rho_\infty (A + L_p \hat{d}_T)] = \frac{\partial}{\partial x} [\rho_\infty u_\infty (A + L_p \hat{d}_V)]$$

In linear approximation for a harmonic wave this becomes

$$i\omega \left(\frac{\hat{p}_\infty}{c_0^2} A + \rho_0 L_p \hat{d}_T \right) = ik\rho_0 \hat{u}_\infty (A + L_p \hat{d}_V)$$

where we made use of the isentropic relationship $\hat{p}_\infty = c_0^2 \hat{\rho}_\infty$. After substitution of the expressions for the displacement thickness \hat{d}_T (4.76b) and \hat{d}_V (4.79)

$$\hat{d}_T = \frac{1}{2}(1 - i)\delta_T \frac{\gamma - 1}{\gamma} \frac{\hat{p}_\infty}{p_0}, \quad \text{and} \quad \hat{d}_V = -\frac{1}{2}(1 - i)\delta_V,$$

and elimination of \hat{u}_∞ by means of the Euler's equation, we find a homogeneous linear equation for \hat{p}_∞ , which yields the dispersion relation

$$\frac{k^2}{k_0^2} = \frac{A + \frac{1}{2}(1-i)(\gamma-1)L_p\delta_T}{A - \frac{1}{2}(1-i)L_p\delta_V},$$

where $k_0 = \omega/c_0$. Expanding this expression for small δ_T and δ_V (using the fact that $\delta_V/\delta_T = \sqrt{Pr} = O(1)$) and retaining the first order term, we obtain the result of Kirchhoff

$$k - k_0 = \frac{1}{4}(1-i)\frac{L_p}{A}\delta_V k_0 \left(1 + (\gamma-1)\frac{\delta_T}{\delta_V}\right), \quad (4.80)$$

which corresponds to equation (2.13). More accurate expressions at low frequencies, when the acoustical boundary layers are not thin, are discussed by Tijdeman [242] and Kergomard [107]. At high frequencies the viscosity becomes significant also in the bulk of the flow (Pierce [183]).

At high amplitudes ($\hat{u}_\infty\delta_V/\nu \geq 400$) the acoustical boundary layer becomes turbulent (Merkli [140], Eckmann [58], Akhavan [4], Verzicco [250]). In such a case the damping becomes essentially non-linear. Akhavan [4] presents results indicating that a quasi-stationary turbulent flow model provides a fair first guess of the wall shear stress.

For an isothermal (liquid) flow the quasi-steady approximation yields

$$k^2 - k_0^2 = -\frac{1}{4}ik_0\frac{L_p}{A}c_f\hat{u}_\infty$$

where the friction coefficient c_f is defined (and determined) by

$$c_f = -\frac{4A}{L_p\frac{1}{2}\rho_0 U_0^2} \frac{dp_0}{dx}$$

which relates the mean pressure pressure gradient (dp_0/dx) to the stagnation pressure $\frac{1}{2}\rho_0 U_0^2$ of a mean flow through the pipe. Note that since $(k - k_0)$ depends on the amplitude \hat{u}_∞ of the acoustical velocity this model implies a non-linear damping. The transition from laminar to turbulent damping can therefore be a mechanism for saturation of self-sustained oscillations (see chapter 5).

For smooth pipes, Prandtl proposed a correlation formula for c_f as a function of the Reynolds number of the flow. The influence of wall roughness is described in the Moody diagram. Such data are discussed by Schlichting [227]. In the case of a turbulent gas flow the thermal dissipation is rather complex. This makes a low frequency limit difficult to establish. In the presence of a mean flow various approximations describing the interaction between the acoustic waves and the turbulent main flow have been discussed by Ronneberger [219] and Peters [181]. The formula of Kirchhoff derived above appears to be valid at low Mach numbers ($U_0/c_0 \ll 1$) as long as the Stokes viscous boundary layer

thickness δ_V remains less than the laminar sublayer $\delta_L \simeq 15\nu/\sqrt{\tau_w\rho_0}$ of the turbulent main flow (where the wall shear stress $\tau_w = c_f \frac{1}{8}\rho_0 U_0^2$).

When $\delta_L \ll \delta_V$, we can use a quasi-stationary approximation. The transition from the high frequency limit to the quasi-stationary limit is discussed in detail by Ronneberger [219] and Peters [180]. These references also provide information about the Mach number dependence of the wave number.

4.6 One dimensional Green's function

4.6.1 Infinite uniform tube

We consider a one dimensional approximation for the propagation of waves in a pipe. This approximation will be valid only if the frequencies generated by the sources of sound in the pipe are lower than the cut-off frequency. As the acoustic field observed at position x far from a source placed at y is induced by a plane wave, the observer position in the cross section of the pipe is indifferent. Applying the reciprocity principle (section 3.1) we see that in the low frequency approximation the signal observed at x should also be indifferent for the position of the source in the cross section of the tube at y . Hence as the source position within a cross section is indifferent we can consider the source to be smeared out over this cross section resulting in a 1-dimensional source. We therefore look for the corresponding one-dimensional Green's function $g(x, t|y, \tau)$ defined by:

$$\frac{\partial^2 g}{\partial t^2} - c_0^2 \frac{\partial^2 g}{\partial x^2} = \delta(t - \tau)\delta(x - y). \quad (4.81)$$

Comparison of this wave equation with the wave equation (4.5) in the presence of source term $\rho_0 \partial\beta/\partial t$ and forces f_x :

$$\frac{\partial^2 p'}{\partial t^2} - c_0^2 \frac{\partial^2 p'}{\partial x^2} = c_0^2 \left(\rho_0 \frac{\partial^2 \beta}{\partial t^2} - \frac{\partial f_x}{\partial x} \right) \quad (4.5)$$

indicates that we can assume that (4.81) is a particular case of (4.5) for $f_x = 0$ and:

$$\frac{\partial \beta}{\partial t} = \frac{1}{\rho_0 c_0^2} H(t - \tau)\delta(x - y). \quad (4.82)$$

For an infinitely long tube the solution is:

$$g(x, t|y, \tau) = \begin{cases} \frac{1}{2c_0} H\left(t - \tau + \frac{x - y}{c_0}\right) & \text{for } x < y, \\ \frac{1}{2c_0} H\left(t - \tau - \frac{x - y}{c_0}\right) & \text{for } x > y. \end{cases} \quad (4.83)$$

This result is obtained intuitively by using (4.30) which implies that g is the pressure wave generated by a piston moving with a velocity $u' = (2\rho_0c_0^2)^{-1}H(t - \tau)$ for $x = y + \varepsilon$ and a second piston with a velocity $u' = -(2\rho_0c_0^2)^{-1}H(t - \tau)$ for $x = y - \varepsilon$. Equations (4.83) are then obtained by using the method of characteristics (section 4.2).

Of course, the above result (4.83) is more efficiently written as:

$$g(x, t|y, \tau) = \frac{1}{2c_0}H\left(t - \tau - \frac{|x - y|}{c_0}\right). \tag{4.84}$$

The combination $t - |x - y|/c_0$ is the time at which the signal observed at (x, t) has been emitted by the source at y . This time is called the retarded or emission time t_e :

$$t_e = t - \frac{|x - y|}{c_0}. \tag{4.85}$$

4.6.2 Finite uniform tube

We can also fairly easily construct a Green's function for a semi-infinite pipe ($x < L$) terminated at $x = L$ by an ideal open end at which by definition $g(L, t|y, \tau) = 0$. By constructing the wave reflecting at this ideal open end with the method of characteristics we find:

$$g(x, t|y, \tau) = \frac{1}{2c_0} \left\{ H\left(t - \tau + \frac{x - y}{c_0}\right) + H\left(t - \tau - \frac{x - y}{c_0}\right) - H\left(t - \tau + \frac{x + y - 2L}{c_0}\right) \right\} \tag{4.86}$$

which we can also write for $x < L$ as:

$$g(x, t|y, \tau) = \frac{1}{2c_0} \left\{ H\left(t - \tau - \frac{|x - y|}{c_0}\right) - H\left(t - \tau - \frac{|x + y - 2L|}{c_0}\right) \right\}. \tag{4.87}$$

This solution could also have been obtained by assuming the pipe to be part of an infinitely long pipe, in which at the point $x = 2L - y$ a second point source is placed with opposite sign of and synchronous with the original point source at $x = y$. This second source, called *image source*, is constructed such that it generates the field due to reflection by the boundary at $x = L$ in the original problem, and therefore brings into effect the boundary condition at $x = L$. This *method of images* can be generalized to the case of a finite pipe segment ($0 < x < L$). In such a case we will have to consider the contribution of an infinite number of images corresponding to the reflections of the original waves at the boundaries. For example, the field in a finite pipe with hard walled ends is equivalent with the

field in an infinite pipe with equal sources in $x = -y, \pm 2L \pm y, \pm 4L \pm y, \dots$. This comes down to a right-hand-side of equation 4.81 of

$$\sum_{n=-\infty}^{\infty} \delta(t - \tau) \left(\delta(x - y - 2nL) + \delta(x + y - 2nL) \right)$$

and a solution

$$g(x, t|y, \tau) = \frac{1}{2c_0} \sum_{n=-\infty}^{\infty} \left\{ H\left(t - \tau - \frac{|x - y - 2nL|}{c_0}\right) + H\left(t - \tau - \frac{|x + y - 2nL|}{c_0}\right) \right\}. \quad (4.88)$$

The Green's function is clearly more complex now. Furthermore, the addition of mass by the source in the finite volume results into a (roughly) linear growth of g in t . (Verify this for $x = y = \frac{1}{2}L$ and $\tau = 0$.) This is of particular interest in the time-harmonic case. When the end conditions are such that multiple reflections are physically relevant they imply that constructive and destructive interferences will select waves corresponding to standing wave patterns or resonances of the tube. This problem will be discussed further in the next chapter.

4.7 Aero-acoustical applications

4.7.1 Sound produced by turbulence

We consider a turbulent jet in an infinitely extended pipe (figure 4.12). We suppose that the jet diameter

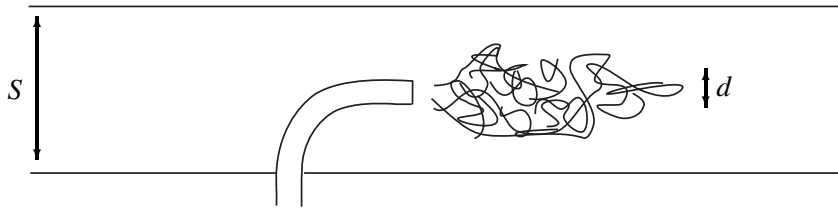


Figure 4.12 Turbulent jet in a pipe.

d and the jet velocity u_0 are such that the characteristic frequency u_0/d of the sound produced in the pipe is low enough to use a one dimensional approximation. We will use the integral formulation of Lighthill to obtain an order of magnitude estimate for the sound pressure level produced by this flow, assuming that the mean flow in the pipe is negligible. We also assume that the jet temperature and density is the same as that of the environment (homogeneous fluid and homentropic flow). If Reynolds

number $Re = u_0 d / \nu \gg 1$ and Mach number $M = u_0 / c_0 \ll 1$ we can use Lighthill's analogy in the form⁴:

$$\frac{\partial^2 \rho'}{\partial t^2} - c_0^2 \frac{\partial^2 \rho'}{\partial x_i^2} = \frac{\partial^2 (\rho_0 v_i v_j)}{\partial x_i \partial x_j}. \quad (4.89)$$

As we use a tailored Green's function (we neglect the effect of the flow injection device) the density ρ' can be estimated by:

$$\rho'(x, t) = \int_{t_0}^t \iiint_V \frac{\partial^2 (\rho_0 v_i v_j)}{\partial y_i \partial y_j} G(\mathbf{x}, t | \mathbf{y}, \tau) \, dy d\tau. \quad (4.90)$$

Using the approximate Green's function derived in the previous section (Eq. 4.84) we have:

$$\rho'(x, t) = \int_{t_0}^t \iiint_V \frac{\partial^2 (\rho_0 v_i v_j)}{\partial y_i \partial y_j} g(x, t | y, \tau) S^{-1} \, dy d\tau. \quad (4.91)$$

After two partial integrations, assuming the source to be limited in space, we obtain:

$$\rho'(x, t) = \int_{t_0}^t \iiint_V \frac{\partial^2}{\partial y^2} g(x, t | y, \tau) S^{-1} \rho_0 u^2 \, dy d\tau. \quad (4.92)$$

We moved the differentiation from the unknown source term towards the known, and explicitly available, Green's function (4.84). We now note that:

$$\frac{\partial g}{\partial y} = -\frac{1}{2c_0^2} \delta\left(t - \tau - \frac{|x - y|}{c_0}\right) \frac{\partial |x - y|}{\partial y}, \quad (4.93)$$

so that from:

$$\frac{\partial |x - y|}{\partial y} = -\text{sign}(x - y) = -\frac{\partial |x - y|}{\partial x} \quad (4.94)$$

we have the following important symmetry in the Green's function of an infinite pipe:

$$\frac{\partial g}{\partial y} = -\frac{\partial g}{\partial x}. \quad (4.95)$$

⁴While the assumption that friction is a negligible source of sound was already formulated by Lighthill, a reasonable confirmation of its validity was only provided thirty years later by the work of Morfey [150] and Obermeier [170]. The exact range of validity is still subject of research.

We substitute this result in (4.92). Since the integration is to the source position g , we can now remove one of the differentiations to x from the integral, resulting in the expression:

$$\rho'(x, t) = \frac{\partial}{\partial x} \int_{t_0}^t \iiint_V \frac{\rho_0 u^2}{2Sc_0^2} \delta(t_e - \tau) \text{sign}(x - y) \, \mathbf{y} d\tau. \quad (4.96)$$

with $t_e = t - |x - y|/c_0$. The time integration can now be carried out:

$$\rho'(x, t) = \frac{\partial}{\partial x} \iiint_V \frac{1}{2Sc_0^2} [\rho_0 u^2]_{\tau=t_e} \text{sign}(x - y) \, \mathbf{y} \quad (4.97)$$

where we used the property (C.26) of the δ -function. At sufficiently large distances the only length scale in the solution is the characteristic wave length $c_0 d/u_0$ corresponding to the characteristic frequency⁵ u_0/d of the turbulence in the jet. Hence we can estimate:

$$\frac{\partial}{\partial x} \simeq \frac{1}{c_0} \frac{\partial}{\partial t} \sim \frac{u_0}{c_0 d} = \frac{M_0}{d}. \quad (4.98)$$

Because the sound production by turbulence decreases very fast with decreasing mean flow velocity, the volume of the free jet contributing to the sound production is limited to a region of the order of d^3 . In this region the turbulent velocity fluctuations are of the order of u_0 . Hence we find at large distances:

$$\rho' \sim \frac{M_0}{d} \frac{\rho_0 u_0^2}{2Sc_0^2} d^3 \quad (4.99)$$

implying:

$$\overline{\rho'^2} \sim \left(\frac{1}{2} \rho_0 M_0^3 d^2 / S \right)^2. \quad (4.100)$$

This is the result obtained by Ffowcs Williams [66]. This Mach number dependence has indeed been observed in a pipe downstream of an orifice for sufficiently high Mach numbers. At low Mach numbers the sound production is dominated by the dipole contribution of $O(M^4)$ due to the interaction of the flow with the orifice [141].

A discussion of the sound production by confined circular jets is provided by Reethof [195] for arbitrary jet Mach numbers. Reethof finds for subsonic jets ($M_0 < 1$) a ratio of the radiated power to the flow power $\eta_{ac} = 3 \times 10^{-4} M_0^3$. For supersonic jets ($M_0 > 1$) typical values are $\eta_{ac} = 1.6 \times 10^{-3} (M_0^2 - 1)^{1/2}$. In that case the Mach number is taken from $M_0^2 = \frac{2}{\gamma-1} [(p_1/p_2)^{(\gamma-1)/\gamma} - 1]$, where p_1/p_2 is the ratio of the pressure across the orifice.

The dependence of the sound production on the jet geometry is discussed by Verge [249] and Hirschberg [81]. For planar jets issued from a slit of height h the typical frequencies are of the order of $0.03u_0/h$ (Bjørnø [17], Sato [226]). This implies that correlations developed for subsonic circular jets are useless for planar jets.

⁵We assume a jet with circular cross section.

4.7.2 An isolated bubble in a turbulent pipe flow

Consider an isolated bubble of radius a_0 small compared to the pipe diameter D . Assume a turbulent pipe flow. The sound produced by the turbulence will, locally, be enhanced by the presence of the bubble. If we assume that the frequencies in the turbulence, typically $O(u_0/D)$, are much smaller than the bubble resonance frequency ω_0 , we can calculate the sound produced by the interaction of the bubble with the turbulence.

The Green's function is calculated by using the reciprocity principle. We consider the acoustic response of the bubble for a plane wave emitted from the observer position x towards the bubble. For the sake of simplicity we consider this incident wave to be harmonic $p_{in} = \hat{p}_{in} e^{i\omega t - ikx}$. The bubble pressure response \hat{p}_b is, as is shown in 5.4.5 (use (4.72) with $\hat{p}_{in} = \mathcal{F}_1$ and $\hat{p}' = \mathcal{F}_2$), given by:

$$\hat{p}_b = - \frac{\left(\frac{\omega_0}{\omega}\right)^2}{1 - \left(\frac{\omega_0}{\omega}\right)^2 - \frac{2\pi i a_0 c_w}{S\omega}} \hat{p}_{in}. \quad (4.101)$$

Using Bernoulli and the continuity equation we can calculate the pressure distribution around the bubble:

$$\hat{p} - \hat{p}_b = -\rho_w i\omega(\varphi - \varphi_b) \quad (4.102)$$

where:

$$\varphi - \varphi_b = \int_{a_0}^r \frac{i\omega \hat{a} a_0^2}{r^2} dr = i\omega \hat{a} a_0 \left(1 - \frac{a_0}{r}\right). \quad (4.103)$$

Furthermore, we have:

$$\frac{\hat{a}}{a_0} = -\frac{\hat{p}_b}{3\gamma p_0}, \quad (4.104)$$

so that $\hat{p}(r)$ is given by:

$$\hat{p} = \hat{p}_b \left(1 - \left(\frac{\omega}{\omega_0}\right)^2 \left(1 - \frac{a_0}{r}\right)\right) = \frac{1 - \left(\frac{\omega_0}{\omega}\right)^2 - \frac{a_0}{r}}{1 - \left(\frac{\omega_0}{\omega}\right)^2 - \frac{2\pi i a_0 c_w}{S\omega}} \hat{p}_{in}. \quad (4.105)$$

Taking for \hat{p}_{in} the Fourier transform of $(2c_0 S)^{-1} H(t - \tau - |x - y|/c_0)$ we obtain as \hat{p} the Fourier transform $\hat{G}(x|y)$ of the Green's function $G(x, t|y, \tau)$:

$$\hat{G}(x|y) = \frac{e^{-i\omega\tau - ik|x-y|}}{2i\omega c_w S} \cdot \frac{1 - \left(\frac{\omega_0}{\omega}\right)^2 - \frac{a_0}{r}}{1 - \left(\frac{\omega_0}{\omega}\right)^2 - \frac{2\pi i a_0 c_w}{S\omega}}. \quad (4.106)$$

Using Lighthill's analogy we now can compare the response of the pipe to turbulence, with and without bubble. We obtain by partial integration:

$$\rho' = \int_{t_0}^t \iiint_V \rho_0 v_i v_j \frac{\partial^2 G}{\partial y_i \partial y_j} dy d\tau. \quad (4.107)$$

If we consider a small turbulent spot in the direct neighbourhood of the bubble the ratio of the responses is given by:

$$\frac{\frac{\partial^2 G_b}{\partial r^2}}{\frac{\partial^2 G_0}{\partial y^2}} = \frac{\frac{\partial^2 G_b}{\partial r^2}}{\frac{\partial^2 G_0}{\partial x^2}} = \frac{\frac{c_w^2 a_0}{\omega^2 r^3}}{1 - \left(\frac{\omega_0}{\omega}\right)^2 - \frac{2\pi i a_0 c_w}{S\omega}}. \quad (4.108)$$

At the resonance frequency ω_0 this yields a factor $(a_0 S / 4\pi r^3)(\rho_w c_w^2 / 3\gamma p_0)^{\frac{1}{2}}$ while for low frequencies we find $(a_0 / r)^3 (\rho_w c_w^2 / 3\gamma p_0)$. If $r = O(a_0)$ we see that the sound produced by turbulence in the neighbourhood of the bubble will be dramatically enhanced.

The major contribution of the bubble turbulence interaction will be at low frequencies. An important reason for this is that for typical conditions in water flow, the length scale of vortices corresponding to pressure fluctuations at the bubble resonance frequency $\omega_0 / 2\pi$ is much smaller than the bubble radius [46]. In such a case these pressure fluctuations are averaged out at the bubble surface and do not have any significant contribution to the spherical oscillations of the bubble. An example of sound production by bubbles in a pipe flow is the typical sound of a central heating system when air is present in the pipes. Also the romantic sound of water streams and fountains is dominated by bubbles. In those cases, however, we have a three-dimensional environment.

4.7.3 Reflection of a wave at a temperature inhomogeneity

As a last example of the use of the integral equation based on the Green's function formalism we consider the interaction of a wave with a limited region in which the gas temperature $T(x)$ is non-uniform ($0 < x < L$). We assume the pipe to be horizontal and that gravity is negligible. Hence, at rest the pressure is uniform. The gas density is given by:

$$\rho / \rho_0 = T / T_0 \quad (4.109)$$

and the speed of sound c is given by:

$$c / c_0 = (T / T_0)^{\frac{1}{2}} \quad (4.110)$$

where ρ_0 , T_0 and c_0 are the properties of the uniform region. We now further assume that $|T - T_0|/T_0 \ll 1$ so that we can use a linear approximation in which we assume that the scattered sound wave p'' is weak compared to the amplitude p'_i of the incident wave. In such a case we can write $p' = p'_{in} + p''$, so that the linearized 1-D wave equation (2.50):

$$\frac{\partial^2 p'}{\partial t^2} - \frac{\partial}{\partial x} \left(c^2 \frac{\partial p'}{\partial x} \right) = 0$$

can be approximated by:

$$\frac{\partial^2 p''}{\partial t^2} - c_0^2 \frac{\partial^2 p''}{\partial x^2} = \frac{\partial}{\partial x} \left((c^2 - c_0^2) \frac{\partial p'_{in}}{\partial x} \right). \quad (4.111)$$

The source term has been linearized by assuming that the pressure fluctuations are equal to the (undisturbed) incident wave amplitude. It is the source term considered by Powell [186] for the description of sound scattering at entropy spots.

Using the integral formulation (3.13) and the one dimensional Green's function g we find:

$$p'' = \int_{-\infty}^{\infty} \int_0^L \frac{\partial}{\partial y} (c^2 - c_0^2) \frac{\partial p'_{in}}{\partial y} g \, dy d\tau. \quad (4.112)$$

Partial integration yields

$$p'' = - \int_{-\infty}^{\infty} \int_0^L (c^2 - c_0^2) \frac{\partial p'_{in}}{\partial y} \frac{\partial g}{\partial y} \, dy d\tau. \quad (4.113)$$

From equation (4.84) we have

$$\frac{\partial g}{\partial y} = \frac{1}{2c_0^2} \text{sign}(x - y) \delta(t_e - \tau) \quad (4.114)$$

(with $t_e = t - |x - y|/c_0$) and hence

$$\begin{aligned} p'' &= -\frac{1}{2c_0^2} \int_0^L \text{sign}(x - y) (c^2 - c_0^2) \int_{-\infty}^{\infty} \delta(t_e - \tau) \frac{\partial p'_{in}}{\partial y} \, d\tau \, dy \\ &= -\frac{1}{2c_0^2} \int_0^L \text{sign}(x - y) (c^2 - c_0^2) \frac{\partial}{\partial y} p'_{in}(y, t_e) \, dy. \end{aligned} \quad (4.115)$$

If we take for example

$$p'_{in} = \hat{p}_{in} H(x - c_0 t) \quad (4.116)$$

and use the relation $c^2/c_0^2 = T/T_0$, then we have for (say) $x < 0$

$$\begin{aligned}
 p'' &= \frac{1}{4} \hat{p}_{in} \int_0^L \frac{T - T_0}{T_0} \delta\left(y - \frac{x + c_0 t}{2}\right) dy \\
 &= \begin{cases} \frac{1}{4} \hat{p}_{in} \frac{T(\frac{1}{2}(x + c_0 t)) - 1}{T_0} & \text{if } 0 < x + c_0 t < 2L \\ 0 & \text{otherwise.} \end{cases}
 \end{aligned}
 \tag{4.117}$$

Exercises

- a) Show that for an acoustic wave travelling in the negative x direction we have:

$$u' = -p' / \rho_0 c_0.$$

- b) Consider a rigid piston at ($x = 0$) separating the fluid I for $x < 0$ from the fluid II at $x > 0$ in an infinitely long pipe of 10^{-2} m^2 cross section. Assume that the piston oscillates with a frequency ω and an amplitude a . Calculate the force necessary to move the piston as a function of time ($\rho_{0,I} = 1.2 \text{ kg/m}^3$, $c_{0,I} = 344 \text{ m/s}$, $\rho_{0,II} = 1.8 \text{ kg/m}^3$ and $c_{0,II} = 279 \text{ m/s}$, $\omega = 10^3 \text{ rad/s}$, $a = 10^{-3} \text{ m}$). Use linear theory and verify if it is indeed valid.

- c) *Water hammer effect:*

Consider a steady flow of water in a rigid horizontal pipe which we stop suddenly by closing a valve. Calculate the pressure on both sides of the valve for flow velocities of 0.01 m/s and 1 m/s. What is the force on the valve for a pipe cross section surface of 10^{-2} m^2 .

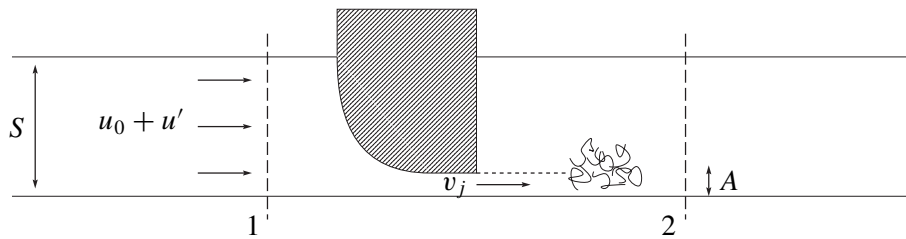


Figure 4.13 Exercise d)

- d) The same problem as c) but with a slowly closing valve in an infinitely long pipe (figure 4.13). Assume the area of the valve opening to be a given function of time:

$$A = A(t).$$

Suppose further that the flow separates at the exit of the valve forming a free jet into the pipe downstream of the valve. If $A \ll S$ we can neglect the recovery of dynamic pressure ($\frac{1}{2} \rho v_j^2$) upon declaration of the fluid by turbulent mixing of the jet with the fluid in the pipe. Hence the pressure drop Δp across the valve is $\Delta p = \frac{1}{2} \rho v_j^2$ if we neglect inertial effects in the valve (we assume $\sqrt{A}(\partial v_j / \partial t) \ll v_j^2$).

- e) Show that, in the absence of aero-acoustic sources, the conservation of acoustic energy implies a continuity of pressure ($\Delta p' = 0$) across a compact discontinuity in a pipe, like a sudden change in diameter.
- f) Calculate the reflection coefficient R and the transmission coefficient T for a contact surface between water and air. Consider both the cases of a wave incident from the air and water sides in the direction normal to the surface.
- g) Same question as f) for a discontinuity in temperature of 30 K in air at atmospheric pressure (corresponding to the temperature difference from inside our mouth to outside in the winter).
- h) Calculate the reflected and transmitted acoustic intensities I for questions f) and g).
- i) Consider a semi-infinite tube closed at $x = 0$ by a harmonically moving piston ($u_p = \hat{u}_p e^{i\omega t}$). The tube is filled with air. At a distance L from the piston there is a temperature jump of 30 K . Calculate the amplitude of the waves in steady state conditions.
- j) Calculate the reflection coefficient R and the transmission coefficient T for a low frequency wave \mathcal{F}_1 incident from the left to a stepwise area change from A_1 to A_2 in an infinitely long pipe. Assume linear behaviour and no mean flow.
- k) Same exercise as j) for a combined stepwise change in cross section and specific acoustic impedance jump $\Delta\rho c$ of the fluid.
- l) A closed pipe end can be considered as a change of area such, that $A_2/A_1 \rightarrow 0$, while an open end can be approximated by a change with $A_2/A_1 \rightarrow \infty$. Calculate in both cases the reflection coefficient R , using the result of exercise j).
- m) Calculate the reflection coefficient for a harmonic wave at an orifice, assuming linear behaviour and no mean flow.
- n) What are the conditions for which we can neglect friction in the orifice?
- o) Consider an orifice of $d = 1\text{ mm}$ diameter, without sharp edges, in a pipe, of diameter $D = 1\text{ cm}$, filled with air at room conditions. At which amplitude (in dB) one would expect non-linear losses due to acoustical flow separation for a harmonic wave (with a frequency of 10 Hz , 100 Hz and 1000 Hz) if there is no mean flow. Such orifices are used in hearing-aid devices for protection.
- p) When flow separation occurs as a result of mean flow, the end correction δ is affected. At low frequencies by about a factor 3 compared to high frequencies or the linear behaviour without flow separation. Explain qualitatively this effect. (Why can we expect a decrease of δ ?)
- q) Consider a wave $\mathcal{G}_1(t + x_1/c_0)$ incident on a junction of three semi-infinite tubes (with cross sections A_1, A_2 , and A_3). Assuming no other incident wave ($\mathcal{G}_2 = \mathcal{G}_3 = 0$) calculate the reflection and transmission coefficients.
- r) Consider a pipe of cross sectional area A_1 ($A_1 = A_3$) with a closed side branch of section A_2 and of length L (figure 4.14). Calculate the reflection and transmission coefficients $R = \mathcal{F}_1/\mathcal{G}_1$ and $T = \mathcal{F}_3/\mathcal{G}_1$ for an incident harmonic wave
- $$\mathcal{G}_1 = e^{i\omega t + ikx_1}$$
- if we assume that $\mathcal{G}_3 = 0$. The wave number k is defined as $k = \omega/c_0$. What are the conditions for which $R = 0$? What are the conditions for which $R = 1$? What are the conditions for which $R = -1$?

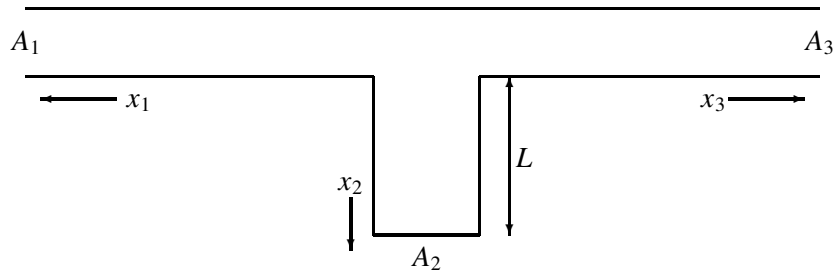


Figure 4.14 Tube with closed side branch.

- s) Calculate the low frequency limit of the reflection coefficient $R = \mathcal{F}_1/\mathcal{G}_1$ for an air bubble of 1 mm in a pipe of 1 cm diameter for a harmonic wave of frequency ω . Assume $p_0 = 1$ bar.
 - t) Calculate the pressure p_b in an air bubble of mean radius a_0 in water for an incident wave $p_{in} = \hat{p}_{in} e^{i\omega t - ikx}$ in a pipe of cross section $A_p \gg a_0^2$.
 - u) In the model described above (section 4.4.5) the pressure in the bubble is assumed to be uniform. Is this a reasonable approximation for an air bubble of 1 mm radius in water up to the resonance frequency ω_0 for $p_0 = 1$ bar?
 - v) In the above model the acoustic pressure imposed on the bubble by the incident acoustic field is assumed to be uniform across the pipe diameter. Is this a reasonable approximation for a bubble with a radius $a_0 = 1$ mm placed in a pipe of diameter $D = 1$ cm filled with water at ambient pressure? Assume a frequency $\omega = \omega_0$.
 - w) In the above model we assumed the bubble to be small compared to the pipe diameter, and far from the walls. Estimate ω_0 for a bubble placed at the wall.
 - x) Is the model valid for a bubble which is large compared to the pipe diameter? Why?
 - y) Determine the physical dimensions of the Green's function by substitution in the wave equation (4.81).
 - z) Verify (4.84) by Fourier transformation of (4.81) and then using section C.1.
- A) Construct the Fourier transformed Green's function for a semi-infinite ($x < L$) tube terminated at $x = L$ by an impedance Z_L .
 - B) Construct the Fourier transformed Green's function for a source placed left from a small bubble placed in an infinite tube.
 - C) Show that for low frequencies $G(\mathbf{x}, t|\mathbf{y}, \tau) = g(x, t|\mathbf{y}, \tau)/S$ for $|x - y| \gg \sqrt{S}$ in a tube of uniform cross section S .
 - D) Explain (4.95) in terms of the effect of displacement of the source or observer on the Green's function for an infinite tube.
 - E) Calculate using (4.99) the sound pressure level in a tube of 10 cm diameter due to the inflow of a air jet of 1 cm diameter with a velocity of 10 m/s. Assume atmospheric conditions and room temperature. Are the assumptions valid in this case? Are the assumptions valid if $u_0 = 10^2$ m/s ?

- F) Same question as E) for a jet placed at the end of a semi-infinite pipe closed by a rigid wall, as indicated in figure 4.15.

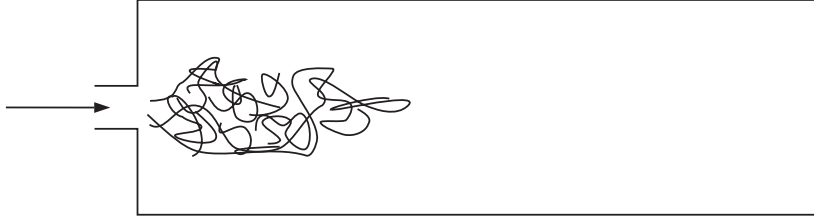


Figure 4.15 Exercise F)

- G) Calculate the amplification factor for turbulence noise at resonance $(S/a_0^2)(\rho_w c_w^2/3\gamma p_0)^{\frac{1}{2}}$, and at low frequencies $\rho_w c_w^2/3\gamma p_0$ for an air bubble of diameter $2a_0 = 1$ mm in a pipe of $D = 1$ cm diameter filled with water at atmospheric pressure.
- H) In principle the turbulent pressure fluctuations in a pipe have a broad spectrum with a maximum around a characteristic frequency u_0/D . Consider a flow velocity of 1 m/s. Do you expect the characteristic frequency of turbulence to be large or small compared to the resonance frequency $\omega_0/2\pi$ of an air bubble with $2a_0 = 1$ mm as in question G)?
- I) For a small bubble the surface tension σ contributes significantly to the internal pressure p_b of the bubble. For a spherical bubble we have:

$$p_b = p_{water}(a) + \frac{2\sigma}{a}.$$

In equilibrium $p_{water}(a) = p_0$. If we consider the oscillation of such a bubble we find a resonance frequency:

$$\omega_0 = \left(\frac{3\gamma p_0}{\rho_w a_0^2} + \frac{4\sigma}{\rho_w a_0^3} \right)^{\frac{1}{2}}.$$

Derive this formula. Given the surface tension σ of water is 7×10^{-2} N/m, calculate the bubble radius for which the surface tension becomes important.

- J) The sound in bubbly liquid is often due to the oscillations of bubbles caused by a rapid local acceleration or to oscillations induced by the coalescence or collapse of bubbles. This yields the typical “bubbling” noise of a fountain or brook. As an example consider the difference in volume ΔV between the sum of the volumes of two bubbles of equal radii $a_0 = 10^{-4}$ m and a single bubble containing the same gas (after coalescence). This difference in volume is due to surface tension effects (see previous question). Assume that the new bubble is released with a radius a corresponding to the original volume of the two smaller bubbles. The bubble will oscillate around its new equilibrium radius. The movement will be damped out by radiation. Calculate the amplitude of the acoustic pressure waves generated in a pipe of 1 cm diameter filled with water as a function of time.

5 Resonators and self-sustained oscillations

5.1 Self-sustained oscillations, shear layers and jets

When using Lighthill's analogy to estimate the intensity of the sound produced by a turbulent flow in section 4.7.1 we have assumed that the sound source is independent of the acoustic field. This assumption was not justified but it seems reasonable if the acoustic velocities in the flow are "small enough". In fact this hypothesis breaks down in a large number of very interesting cases. In many of these cases the acoustic feedback (influence of the sound field on the sound source) results in the occurrence of a sharply defined harmonic oscillation, due to the instability of the flow. Whistling, jet-screach and reheat-buzz are examples of such oscillations. In general the maintenance of such oscillations implies the existence of a feedback loop as shown in figure 5.1.

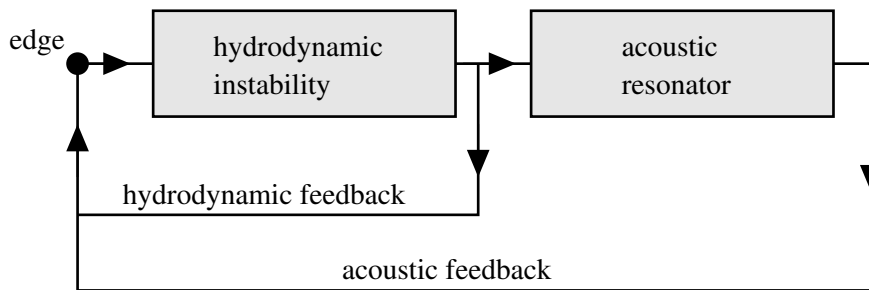


Figure 5.1 Flow-acoustic oscillator.

In most cases the acoustic field interacts with an intrinsically unstable hydrodynamic flow (jet, shear layer) at a sharp edge where the flow separates from the wall. This separation point appears to be a localized region where the acoustic flow and the hydrodynamic flow are strongly coupled. We will now consider this interaction in some detail.

In principle, if the flow were frictionless and is described accurately by a potential flow, the velocity at an edge would be infinitely large. This can be understood by considering the flow in a pipe at a bend (figure 5.2).

The fluid particles passing the bend feel a centrifugal force $\rho u_y^2/r$ per unit volume. If the flow is stationary it is obvious that there should be a centripetal force compensating the centrifugal force. In a frictionless flow the only force available is the pressure gradient $-\partial p/\partial r$. Hence, we see that the

pressure at the outer wall in the bend should be larger than at the inner wall. Using the equation of Bernoulli for a stationary incompressible flow ($p + \frac{1}{2}\rho v^2 = \text{constant}$) we conclude that the velocity is larger at the inner wall than at the outer wall! (See figure 5.3.)

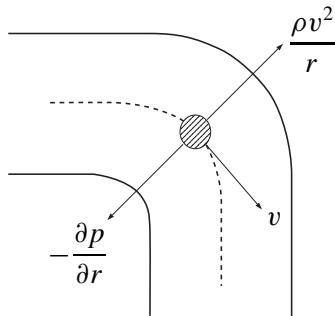


Figure 5.2 Flow in a bend.

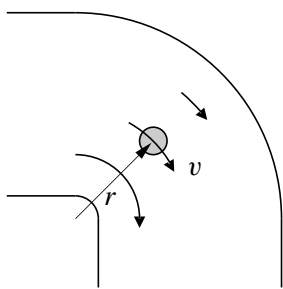


Figure 5.3 Frictionless flow in a bend.

We could also have found this result kinematically by noticing that if a particle in an *irrotational* flow follows a curved path there should be a gradient $\partial v/\partial r$ which “compensates” the rotation which the particle undergoes by following a curved path.

The fact that the pressure is larger at the outer wall can also be understood as a consequence of the inertia of the flow which is trying to follow a straight path and “hits” the wall. The pressure built up at the wall yields the force necessary to bend the streamlines.

A particle in the flow close to the inner wall is just like a ball rolling into a well (figure 5.4). The Bernoulli equation, which represents in this case the law of conservation of mechanical energy, tells that the pressure decrease implies a decrease of potential energy p which is compensated by an increase of kinetic energy $\frac{1}{2}\rho v^2$. When leaving the well (bend) the kinetic energy is again converted into pressure as the particle climbs again (the adverse pressure gradient).

A frictionless flow is only possible far from the wall. Even at high Reynolds numbers there is always a thin region at the wall where friction forces are of the same order of magnitude as the inertial forces. We call this thin region of thickness δ a viscous boundary layer.

It can be shown that because the flow is quasi-parallel the pressure in the boundary layer is uniform and equal to the local pressure of the frictionless flow just outside the boundary layer. More accurately: this implies that the normal pressure gradient $\mathbf{n} \cdot \nabla p$ at the wall is negligible in the boundary layer. In the boundary layer the friction decelerates the flow to satisfy the

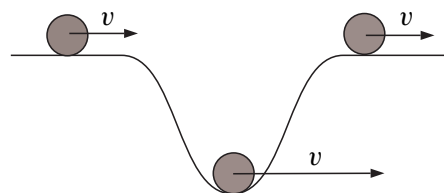


Figure 5.4 Ball passing along a well.

“no-slip boundary condition” at the wall: $\mathbf{v} = 0$ (for a fixed wall; figure 5.5). As is clear from figure 5.5 the flow in the boundary layer is not irrotational. The boundary layer is a region of concentrated vorticity.

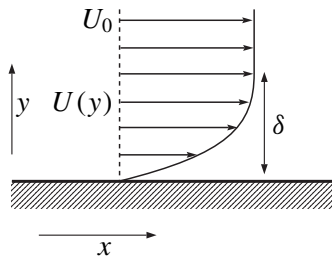


Figure 5.5 Boundary layer velocity profile.

If we consider now a sharp bend the velocities following potential flow theory should now become infinitely large at the inner edge (figure 5.6). (This can be verified by integration of the radial momentum conservation law.) The assumptions used to derive the flow pattern break down: the viscous term $\eta \nabla^2 \mathbf{v}$ which we have neglected in the equation of motion becomes dominant near the edge. This results into a flow separation. The flow separation can be understood qualitatively when we think of the ball in figure 5.4 in the case of a very deep well and in presence of friction. In such a case the ball never succeeds in climbing up the strong pressure gradient just behind the edge.

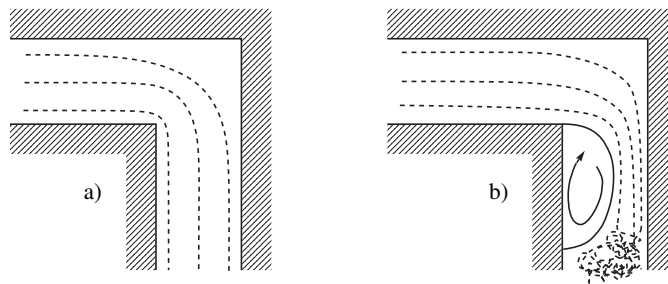


Figure 5.6 Sharp bend. a) potential flow; b) actual flow.

The separation of the boundary layer at the edge implies an injection of vorticity in the main stream. This vorticity is concentrated in the shear layer separating the mean flow from a dead water region (figure 5.6) just behind the bend. Taking the circulation along a path enclosing part of such a shear layer clearly shows that the circulation per unit length ($d\Gamma/d\ell$) in the shear layer is just equal to the velocity jump across the layer: $d\Gamma/d\ell = \Delta v$ (figure 5.7).

This complex process of separation can be described within the frame of a frictionless theory by stating that the velocity at a sharp edge should remain finite. This so-called “Kutta condition” implies that a thin shear layer should be shed at the edge. The shear layer contains a distribution of vorticity such that the velocity induced at the edge by the vorticity just compensates the singularity of the potential flow (which would exist in absence of shear layer).

It can be shown that this condition also implies that the shear layer is shed tangentially to the wall at the side of the edge where the flow velocity is the largest. The validity of a Kutta condition for an unsteady flow has been the subject of quite a long controversy. At this moment for a sharp edge

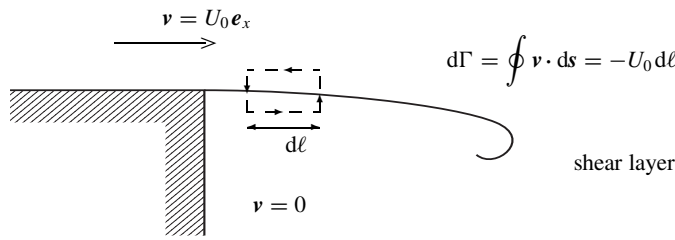


Figure 5.7 Circulation in the shear layer

this is an accepted principle. Hence if next to a stationary flow we impose an unsteady potential flow (acoustic perturbation) the amount of vorticity shed at the edge will be modulated because we modify the singular potential flow at the edge.

We see therefore that within a potential flow theory the sharp edges play a crucial rôle because they are locations at which a potential flow can generate vorticity.¹ It is not surprising therefore that in nature the feedback from the acoustic field on a flow will often be concentrated at an edge.

Self-sustained oscillations imply an amplification of the acoustic perturbations of the main flow by flow instability (this is the energy supply in the feedback loop). The instability of a thin shear layer can be understood by considering as a model an infinitely long row of line vortices in a 2-D flow (figure 5.8).

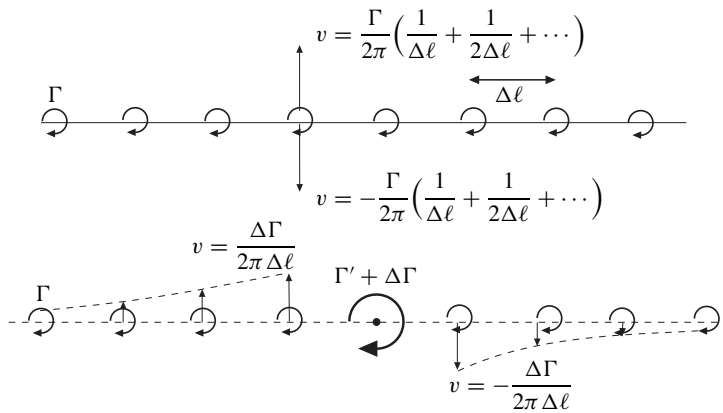


Figure 5.8 Instability of a vortex row induced by a non-uniformity of $d\Gamma/d\ell$.

¹In a two dimensional frictionless incompressible flow $D\omega/Dt = 0$ so that there is no interaction between the vortical and potential flow which can change ω within the flow.

The velocity induced by a line vortex of strength Γ is calculated using Biot-Savart's law:

$$u_{\vartheta} = \frac{\Gamma}{2\pi r}, \quad (5.1)$$

where r is the distance between the point at which we consider the velocity and the vortex. As we see in figure 5.8a a row of vortices is (meta)stable because the velocity induced on a given vortex by the vortices left of the point are just compensated by the velocities induced by the vortices at the right (by symmetry). This is, however, a metastable situation as any perturbation will induce a growing flow instability. For example a lateral displacement of one of the vortices out of the row is sufficient. Hence we understand (figure 5.8b) that a modulation of the vorticity by acoustic perturbations can induce a roll up of the shear layer into a vortex structure as shown in figure 5.9.

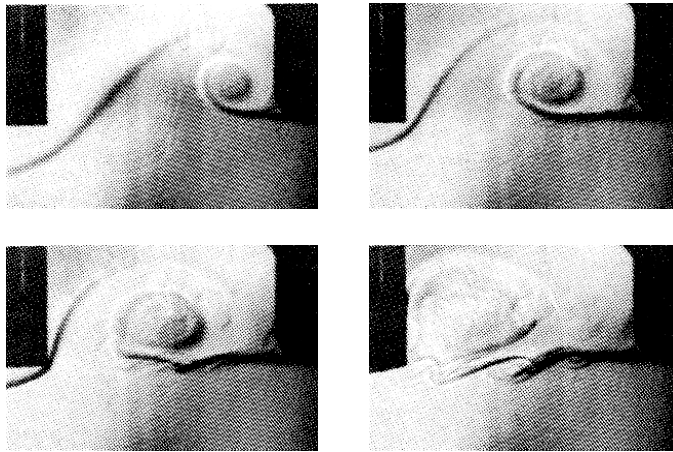


Figure 5.9 Shear layer instability.

The most unstable type of flows is the flow between two shear layers of opposite vorticity: jets and wakes (figure 5.10). A wake appears to be so unstable that when friction forces are sufficiently small (above a certain Reynolds number) it is absolutely unstable [91]. Hence, any perturbation will result in a break up of the wake structure shown in figure 5.10. A typical result of this is the occurrence of vortices, periodically shed from a cylinder for $Re > 50$, which is known as the Von Kármán vortex street [20]. This periodic vortex shedding is responsible for the typical whistle of an empty luggage grid on a car. A jet left alone (free jet) will also exhibit some specific oscillations at moderate Reynolds numbers ($Re = O(10^3)$) [18]. Turbulence will, however, kill any clear structure at higher Reynolds numbers. A jet needs a little help to start whistling. However, there are many ways to persuade him to whistle!

Extensive reviews of these jet oscillations are given by Blake and Powell [19], Rockwell [215, 217], and Verge [246]. We consider here only two examples:

- the edge tone;
- the jet screech.

In the first case the jet oscillations are controlled by placing a sharp edge in the jet. The interaction of the jet with the edge induces a complex time dependent flow. At low Mach numbers the flow can be described locally as an incompressible flow (compact) and a description of the jet oscillation can be obtained without considering sound propagation or radiation [43]. As the phase condition in the feedback loop is determined by the travel time of perturbations along the jet, the oscillation frequency will be roughly proportional to the main flow velocity V_0 in the jet. Self-sustained oscillations occur for those frequencies for which the phase of the signal changes by a multiple of 2π as the signal travels around the feedback loop. We assume an instantaneous feedback from the jet-edge interaction towards the separation point from which the shear layers bounding the jet emerge. The phase shift is therefore determined by the jet.

As a rough first order estimate the perturbations travel in the shear layer with a compromise between the velocities at both sides of the shear layer (about $\frac{1}{2}V_0$). A more accurate estimate can be obtained by considering the propagation of infinitesimal perturbations on an infinite jet as proposed by Rayleigh [18, 194]. In spite of the apparent simplicity of the geometry an exact analytical theory of edge tone instabilities is not available yet.

Like in the case of many other familiar phenomena there does not exist any simple “exact” theory for jet oscillations. Actually, the crudest models such as proposed by Holger [82] are not less realistic than apparently more accurate models.

The most reasonable linear theory until now is the one proposed by Crighton [43]. A major problem of such a linear theory is that it only predicts the conditions under which the system is stable or unstable. It is not able to predict the amplitude of self-sustained oscillations. At the end of this chapter we will discuss the model of Nelson [166] for a shear-layer which is very similar to the model of Holger [82] for an oscillating free jet. Both models do predict an amplitude for sound production by the oscillating flow.

Placing such an edge tone configuration near an acoustic resonator will dramatically influence its behaviour. A resonator is a limited region of space in which acoustic energy can accumulate, just like mechanical energy can accumulate in the oscillations of a mass-spring system. The sound radiated by

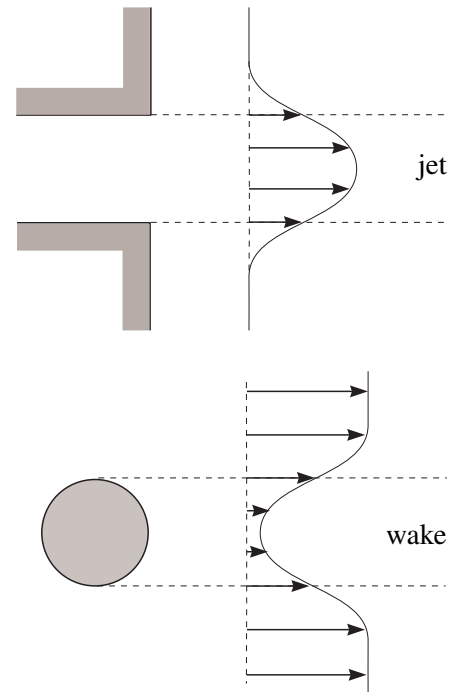


Figure 5.10 Jet and wake.

the edge-jet interaction results now in a second feedback path through the oscillations of the resonator. In such a case the resonator often imposes its resonance frequency to the system. The phase change that a signal undergoes as it travels around the feedback loop is now not only determined by the jet but also by the delay in the acoustic response of the participating resonator. The oscillation condition is still that the total phase change should be a multiple of 2π . When the frequency is close to the resonance frequency of the resonator, a small variation in frequency results into a large phase shift and this easily compensates the change in travel time along the jet. An example of such a system is the flute or the recorder.

In many textbooks the flute oscillation is described as an acoustically driven edge-tone system. It is rather tragicomic that one describes a system which we would like to understand in terms of the behaviour of a system which we hardly understand. As stated by Coltman [35] this is “a rather circular procedure in view of the fact that there are many gaps in the theoretical basis for both”. Simplified models of the recorder are proposed by Fabre [62] and Verge [248, 246, 247, 249]. It indeed appears that a recorder is not simply an “edge tone” coupled to a resonator.

We do not always need an edge for jet oscillations. In the jet screech we have a supersonic jet which has a cell structure due to the formation of shocks and expansions when the jet pressure at the exit is not equal to that of the environment (figure 5.11). The interaction of acoustic perturbations with the edges at the pipe exit results into the formation of periodically shed vortices. The vortex interaction with a shock wave appears to generate strong acoustic pulses. In particular the interaction with the third cell appears to result into a localized periodic source of sound. The acoustic wave travels back towards the pipe exit via the quiescent environment of the jet. This feedback loop can be blocked by placing a wall of absorbing material around the jet [184, 217]. This reduces the jet oscillations, demonstrating that the feedback loop described is the one which controls the jet oscillations. A review of some related supersonic flow oscillations is given by Jungowski [104].

Many of the features observed in a jet oscillation can also be observed in a shear layer separating a uniform main flow from a dead water region in a cavity [216] (closed side branch in a pipe system or open roof of a car). We will discuss these types of oscillations after we have discussed the acoustics of some elementary type of acoustic resonators.

5.2 Some resonators

5.2.1 Introduction

Before considering other types of acoustically controlled flow instabilities we will focus our attention on the acoustic resonator. This is an essential step because in many applications the identification of the resonator is sufficient to find a cure to self-sustained oscillations. Furthermore resonators are also used to impede the propagation of sound or to enhance absorption. An example of this behaviour is the reflection of acoustic waves by an air bubble in a pipe filled with water (section 4.4.5). We start

our discussion with explaining the occurrence of resonance in a duct segment. We then will discuss the behaviour of the Helmholtz resonator.

5.2.2 Resonance in duct segment

We will first discuss the behaviour of a pipe segment excited by an oscillating piston. The most efficient way to do this is to consider this behaviour in linear approximation for a harmonically oscillating

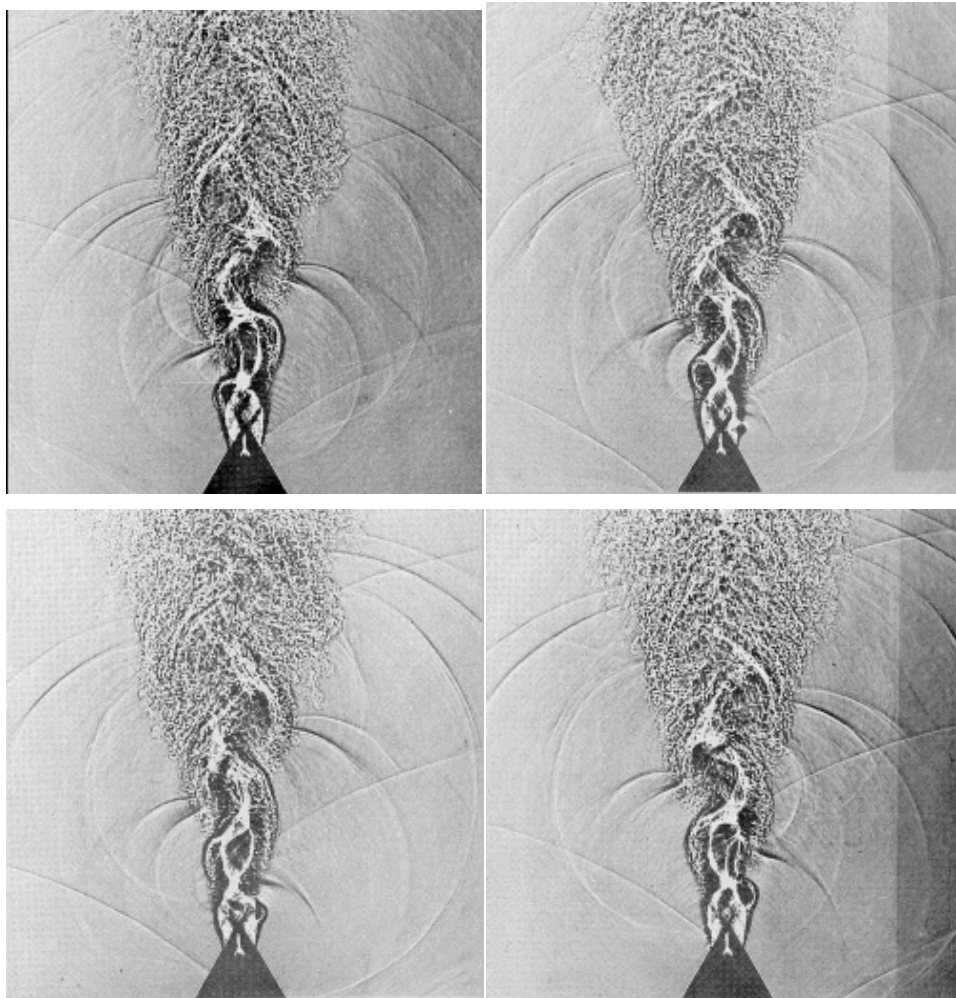


Figure 5.11 Under-expanded supersonic jet with typical cell structure. We observe acoustic waves generated by the interaction of a vortex with the shock. The vortex is shed periodically at the nozzle lip. Acoustical feedback has been reinforced in this experiment of Poldervaart and Wijnands (TUE) by placing reflectors around the jet nozzle.

piston. We will see at the end of this section that at critical frequencies the theory does not provide a solution if we neglect friction. In the time domain we can understand this so-called resonance behaviour more easily. For this reason we will start our discussion by considering the problem in the time domain.

Consider a pipe segment $0 < x < L$ closed at $x = L$ by a rigid wall ($\hat{u} \cdot \mathbf{n} = 0$) and at $x = 0$ by an oscillating piston with a velocity $u_p(t)$:

$$u_p = \hat{u}_p E(t) \quad \text{at} \quad x = 0 \tag{5.2}$$

where, in order to simplify the notation, we introduced in this subsection the auxiliary function

$$E(t) = H(t) e^{i\omega t} . \tag{5.3}$$

We assume that $\hat{u}_p/c_0 \ll 1$ so that an acoustic approximation is valid. We consider only plane waves ($\omega A^{1/2}/c_0 \ll 1$) and we neglect friction and heat transfer ($(\nu/\omega A)^{1/2} \ll 1$). The piston starts oscillating at $t = 0$ and we assume that initially the fluid in the pipe is quiescent and uniform ($u_0 = 0$). In such a case at least for short times the linear (acoustic) approximation is valid. We can now calculate the acoustic field by using the method of characteristics as described in section 4.2. We will describe the calculation in detail. However, a reader only interested in the final result can jump to the final result, equation (5.12).

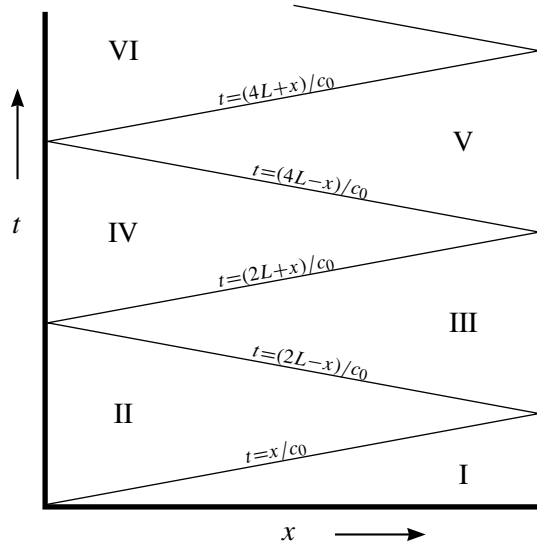


Figure 5.12 Wave pattern induced by a moving piston at $x = 0$, starting at $t = 0$.

In region I we have a quiescent fluid:

$$p_I = 0 \quad \text{and} \quad u_I = 0. \tag{5.4}$$

In region II we have the c^+ waves generated at the piston:

$$p_{\text{II}} = p_{\text{II}}^+ \left(t - \frac{x}{c_0} \right). \quad (5.5)$$

Using the boundary condition $u_{\text{II}} = u_p$ for $x = 0$ we find:

$$p_{\text{II}}^+(t) = \rho_0 c_0 u_p(t) = \rho_0 c_0 \hat{u}_p E(t). \quad (5.6)$$

In region III we have a superposition of the c^+ waves emanating from region II and the c^- waves generated at the wall $x = L$:

$$p_{\text{III}} = p_{\text{II}}^+ \left(t - \frac{x}{c_0} \right) + p_{\text{III}}^- \left(t + \frac{x - L}{c_0} \right). \quad (5.7)$$

p_{III}^- can be determined by application of the boundary condition $u_{\text{III}} = 0$ at $x = L$:

$$\hat{u}_p E \left(t - \frac{L}{c_0} \right) - \frac{1}{\rho_0 c_0} p_{\text{III}}^-(t) = 0. \quad (5.8)$$

Hence we have:

$$p_{\text{III}} = \rho_0 c_0 \hat{u}_p \left\{ E \left(t - \frac{x}{c_0} \right) + E \left(t + \frac{x - 2L}{c_0} \right) \right\}. \quad (5.9)$$

In region IV we have a superposition of the c^- waves from region III and the c^+ waves generated at the piston $x = 0$:

$$p_{\text{IV}} = p_{\text{III}}^- \left(t + \frac{x - L}{c_0} \right) + p_{\text{IV}}^+ \left(t - \frac{x}{c_0} \right). \quad (5.10)$$

p_{IV}^+ is determined by applying the boundary condition $u_{\text{IV}} = u_p$ at $x = 0$:

$$\hat{u}_p E \left(t - \frac{2L}{c_0} \right) - \frac{1}{\rho_0 c_0} p_{\text{IV}}^+(t) = \hat{u}_p E(t) \quad (5.11)$$

and so we find:

$$p_{\text{IV}} = \rho_0 c_0 \hat{u}_p \left\{ E \left(t - \frac{x}{c_0} \right) + E \left(t + \frac{x - 2L}{c_0} \right) + E \left(t - \frac{x + 2L}{c_0} \right) \right\}. \quad (5.12)$$

In region V we have the c^+ waves from region IV superimposed on the c^- waves generated at the wall $x = L$:

$$p_{\text{V}} = p_{\text{IV}}^+ \left(t - \frac{x}{c_0} \right) + p_{\text{V}}^- \left(t + \frac{x - L}{c_0} \right). \quad (5.13)$$

As before, p_v^- is determined by applying the boundary condition $u_v = 0$ at $x = L$. We find:

$$p_v = \rho_0 c_0 \hat{u}_p \left\{ E\left(t - \frac{x}{c_0}\right) + E\left(t + \frac{x - 2L}{c_0}\right) + E\left(t - \frac{x + 2L}{c_0}\right) + E\left(t + \frac{x - 4L}{c_0}\right) \right\}. \quad (5.14)$$

If we now limit ourselves to the position $x = 0$ we see that after each period of time $2L/c_0$ a new wave is added to the original waves reflected at the wall and piston. These original waves have now an additional phase of $2kL$, where $k = \omega/c_0$.

Substituting $x = 0$ in (5.13) and generalizing the structure of the formula we find for $2NL/c_0 < t < 2(N+1)L/c_0$:

$$p_{2N} = 2\rho_0 c_0 \hat{u}_p e^{i\omega t} \left\{ \sum_{n=0}^N e^{-2iknL} H\left(t - \frac{2nL}{c_0}\right) - \frac{1}{2} \right\}. \quad (5.15)$$

This structure could also have been obtained by using the method of images described in section 4.6.2. We consider the piston as a volume source placed at $x = 0^+$. Placing image sources in an infinitely extended tube at $x = \pm 2nL/c_0$ and summing up all the waves generated yields:

$$p = \rho_0 c_0 \hat{u}_p E\left(t - \frac{|x|}{c_0}\right) + \rho_0 c_0 \hat{u}_p \sum_{n=1}^{\infty} \left\{ E\left(t - \frac{|x - 2nL|}{c_0}\right) + E\left(t - \frac{|x + 2nL|}{c_0}\right) \right\}. \quad (5.16)$$

Note that this series contains always only a finite number of non-zero terms, because for large n the argument of the Heaviside function in E becomes negative. So we have (for $t > 0$)

$$\frac{p}{\rho_0 c_0 \hat{u}_p} e^{-i\omega t} = e^{-ikx} \sum_{n=0}^{N_1} e^{-2iknL} + e^{ikx} \sum_{n=1}^{N_2} e^{-2iknL},$$

$$N_1 = \left\lfloor \frac{c_0 t - x}{2L} \right\rfloor, \quad N_2 = \left\lfloor \frac{c_0 t + x}{2L} \right\rfloor,$$

where $\lfloor q \rfloor$ denotes the integer part of q . It may be verified that after substitution of $x = 0$ in (5.16) we find (5.15), with $N = \lfloor c_0 t / 2L \rfloor$. The geometric series may be summed², so we obtain:

$$\frac{p}{\rho_0 c_0 \hat{u}_p} e^{-i\omega t} = \begin{cases} e^{-ikx} \frac{1 - e^{-2ik(N_1+1)L}}{1 - e^{-2ikL}} + e^{ikx-2ikL} \frac{1 - e^{-2ikN_2L}}{1 - e^{-2ikL}} & \text{if } kL \neq \pi\ell, \\ e^{-ikx} (N_1 + 1) + e^{ikx} N_2 & \text{if } kL = \pi\ell, \end{cases} \quad (5.17)$$

where $\ell = 1, 2, 3, \dots$. For $kL \neq \pi\ell$, and allowing for a small amount of damping by giving ω a small negative imaginary part, p converges towards a finite value. We call this the steady state limit. If

²Note that: $\sum_{n=0}^N a^n = \begin{cases} \frac{1 - a^{N+1}}{1 - a} & \text{if } a \neq 1, \\ N + 1 & \text{if } a = 1, \end{cases} \quad \sum_{n=1}^N a^n = \begin{cases} a \frac{1 - a^N}{1 - a} & \text{if } a \neq 1, \\ N & \text{if } a = 1. \end{cases}$

$kL = \pi \ell$ for any $\ell = 1, 2, 3 \dots$, the pressure increases without limit, at least as long as linear theory is valid. We call this a resonance of the tube, with the resonance frequencies given by $\frac{1}{2}\ell c_0/L$. The resulting equations are

$$\frac{p}{\rho_0 c_0 \hat{u}_p} e^{-i\omega t} \rightarrow \begin{cases} -i \frac{\cos(kx - kL)}{\sin kL} & \text{if } kL \neq \pi \ell, \\ \cos(kx) \frac{c_0 t}{L} & \text{if } kL = \pi \ell. \end{cases} \quad (5.18)$$

When resonance occurs the linearized wave equation is only valid during the initial phase of the build up and if there are no losses at the walls. As a result of the temperature dependence of the speed of sound the compression waves tend to steepen up and shock waves are formed. Shock waves are very thin regions with large velocity and temperature gradients in which viscous force and heat transfer induce a significant dissipation [7, 33]. This extreme behaviour will, however, only occur in closed tubes at high pressures or at high amplitude (section 4.2).

In an open tube at high amplitudes vortex shedding at the pipe end will limit the amplitude [49]. If we assume an acoustic particle displacement at the open pipe end which is large compared to the tube diameter d we can use a quasi-stationary model to describe (locally) the flow. This is a model similar to the one discussed for an orifice in section 4.4.3.

Let's assume that the tube is terminated by a horn as shown in figure 5.13. In such a case flow sep-

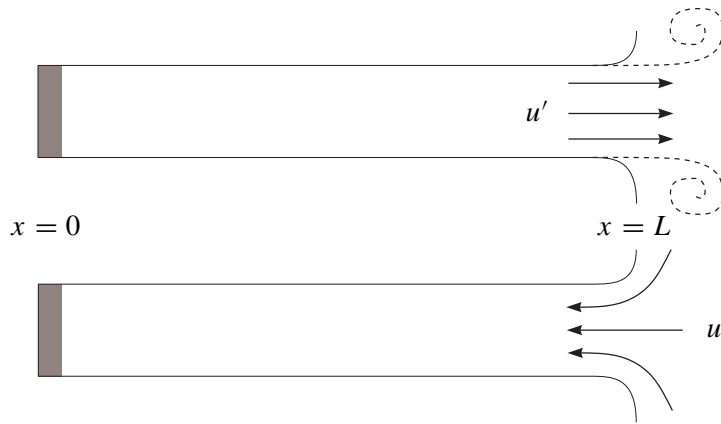


Figure 5.13 Flow at an open pipe termination at high acoustic amplitudes.

aration will occur only while the acoustic flow is outgoing (figure 5.13a). Assuming a dominant fundamental harmonic $\hat{u} \sin \omega t$, the power W_e corresponding to the energy losses due to the formation of the jet can be calculated from:

$$W_e = \frac{S}{T} \int_0^T u' \Delta p dt \quad (5.19)$$

where $\Delta p = -\frac{1}{2}\rho_0 u'^2$ for $0 < t < \frac{1}{2}T$ and $u' > 0$ because a free jet is formed which cannot sustain a pressure difference³. In terms of the Vortex Sound theory of Howe we would say that when the jet is formed during the outflow there is a deviation from potential flow resulting into $p' = p'_{ex}$, while potential flow theory would predict $p' = p'_{ex} - \frac{1}{2}\rho_0 u'^2$. This is due to the vorticity in the jet which results into a source of sound, that we can represent by a pressure source $\Delta p = -\frac{1}{2}\rho_0 u'^2$.

For $\frac{1}{2}T < t < T$ and $u' < 0$ we have:

$$\Delta p = 0 \quad (5.20)$$

because we have a potential inflow into the pipe. Hence:

$$W_e \simeq -\frac{\frac{1}{2}\rho_0 \hat{u}^3 S}{T} \int_0^{\frac{1}{2}T} \sin^3 \omega t \, dt = -\frac{1}{3\pi} \rho_0 \hat{u}^3 S. \quad (5.21)$$

The amplitude of the acoustic field in the tube can now be estimated by assuming that the losses W_e at the open end balance the acoustic power W_p delivered by the piston:

$$W_p = \frac{S}{T} \int_0^T u_p p'(x=0) \, dt. \quad (5.22)$$

Assuming that friction losses at the pipe wall are negligible we have:

$$W_p \simeq \frac{1}{2} S u_p \rho_0 c_0 \hat{u}, \quad (5.23)$$

where \hat{u} is measured at the open pipe exit. Hence we find from $W_e + W_p = 0$:

$$\frac{\hat{u}}{c_0} = \sqrt{\frac{3\pi}{2} \frac{u_p}{c_0}}. \quad (5.24)$$

The model proposed here is valid when the Strouhal number based on the diameter and the acoustical velocity is smaller than 1, *i.e.* $\omega d < \hat{u}$.

The non-linear behaviour of resonators, occurring for example with flow separation, makes such devices efficient sound absorbers. Sound is “caught” by the resonator and dissipated by vortex shedding.

In many cases the most significant losses are friction losses at the wall. We will discuss the influence of radiation from an open pipe end in section 6.7. When a plane wave approximation is valid a harmonic acoustic field in a pipe with uniform cross section can in the absence of mean flow still be described by:

$$p' = p^+ e^{i\omega t - ikx} + p^- e^{i\omega t + ikx}. \quad (5.25)$$

³We assume that due to turbulence all the kinetic energy in the jet is dissipated further downstream. We assume also that flow separation occurs at the junction between the pipe and the horn. This is quite pessimistic, since the separation is expected to be delayed considerably by the gentle divergence of the horn.

The wave number k , however, is now complex and is in first order approximation given by:

$$k = k_0 + (1 - i)\alpha \quad (5.26)$$

where $k_0 = \omega/c_0$ and α is the damping coefficient given by equation (2.13), derived in section 4.5. (In a liquid one should assume $\gamma \simeq 1$.)

Damping also affects the impedance Z_c of an infinite tube. To leading order approximation one finds [126]:

$$Z_c = \frac{p'}{u'} = \pm Z_0 \frac{k_0}{k} \quad (5.27)$$

where the sign indicates the direction of the wave propagation ($+x$ or $-x$) and $Z_0 = \rho_0 c_0$. We further see that wave speed c is affected:

$$c = c_0 \frac{\text{Re}(k)}{k_0} \quad (5.28)$$

While friction is relatively easily taken into account for harmonic waves, in the time domain friction involves a convolution integral which makes the solution of problems more difficult to analyse [33]. We will now further limit our discussion to the case of harmonic waves. Hence we seek only for a steady state solution and we assume that linear acoustics is valid.

As an example we consider a piston with a velocity $u_p = \hat{u}_p e^{i\omega t}$ at $x = 0$ exciting a tube of cross section S closed at $x = L$ by a rigid wall. We neglect the radiation losses at $x = L$ (which we will discuss further in section 6.7). The boundary conditions at $x = 0$ and $x = L$ can be written in terms of equation (5.25) as:

$$\hat{u}_p = \frac{p^+ - p^-}{Z_c} \quad (5.29)$$

and

$$0 = p^+ e^{-ikL} - p^- e^{ikL} \quad (5.30)$$

so that we find:

$$p^+ = \frac{Z_c \hat{u}_p}{1 - e^{-2ikL}}. \quad (5.31)$$

In contrast to our earlier example p^+ does not become infinitely large with resonance because k is complex. The impedance Z_p seen by the piston at $x = 0$ is given by:

$$Z_p = \frac{p^+ + p^-}{\hat{u}_p} = -i Z_c \cotg(kL). \quad (5.32)$$

Upon resonance, $\text{Re}(k) = n\pi/L$ with $n = 1, 2, 3, \dots$, we find for the case $\alpha L \ll 1$:

$$Z_p \simeq \frac{Z_c}{\alpha L}. \quad (5.33)$$

When the damping (αL) predicted by laminar boundary layer theory is small the oscillation amplitudes may become so large that the acoustical boundary layers become turbulent. This implies a non-linear energy dissipation as discussed in section 4.5.3.

5.2.3 The Helmholtz resonator (quiescent fluid)

The resonance conditions for a duct segment (5.25) imply that the tube length should be of the order of magnitude of the acoustic wave length ($kL = O(1)$). In many technical applications this would imply that resonators used to absorb sound should be large (and expensive). A solution to this problem is to use a non-uniform pipe in the shape of a bottle. When the bottle is small compared to the acoustic wave length (for low frequencies), the body of the bottle acts as an acoustic spring while the neck of the bottle is an acoustic mass (figure 5.14).

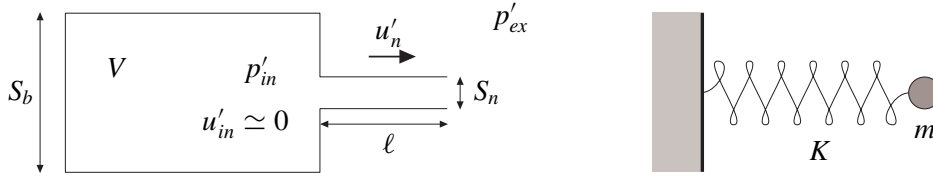


Figure 5.14 Helmholtz resonator as mass-spring system.

If the cross-sectional area S_b of the bottle is large compared to the cross sectional area S_n of the neck, the acoustic velocities in the bottle will be small compared to those in the neck. Hence we may in first order approximation assume that the pressure and density perturbations p'_{in} and ρ'_{in} in the bottle are uniform. Furthermore, as we have assumed the bottle neck (length ℓ) to be acoustically compact, *i.e.* short compared to the wave length, $k\ell \ll 1$, we can neglect compressibility and integrate the line integral of the momentum equation along a streamline from a point inside to a point outside as follows. Use identity (1.30) and the fact that $\boldsymbol{\omega} \times \mathbf{v}$ is orthogonal to a streamline to obtain

$$\rho_0 \int_{in}^{ex} \frac{\partial \mathbf{v}'}{\partial t} \cdot \mathbf{ds} + \frac{1}{2} \rho_0 (u'_{ex}{}^2 - u'_{in}{}^2) + (p'_{ex} - p'_{in}) = \int_{in}^{ex} \mu \nabla^2 \mathbf{v}' \cdot \mathbf{ds} \quad (5.34)$$

Assuming that the streamline does not change in time (for example the center streamline) we have

$$\int_{in}^{ex} \frac{\partial \mathbf{v}'}{\partial t} \cdot \mathbf{ds} = \frac{d}{dt} \int_{in}^{ex} \mathbf{v}' \cdot \mathbf{ds} \quad (5.35)$$

The velocity line integral evidently scales on a typical length times a typical velocity. If friction effects are minor and the velocity is reasonably uniform, we can use the neck velocity u'_n with a corresponding

length being the neck length ℓ , added by a small end correction δ (4.51) to take into account the inertia of the acoustic flow at both ends just outside the neck (inside and outside the resonator); see section 5.2.3.1. Then we have:

$$\int_{in}^{ex} \mathbf{v}' \cdot \mathbf{ds} = (\ell + 2\delta)u'_n. \quad (5.36)$$

The stress term line integral is far more difficult to assess. Apart from u'_n itself, it will depend on flow profile, Reynolds number, wall heat exchange, turbulence, separation from sharp edges, and maybe more. Following Melling [138], we will take these effects together in a resistance factor R , which will a priori be assumed to be relatively small, to have resonance and a small decay per period in the first place.

$$\int_{in}^{ex} \mu \nabla^2 \mathbf{v}' \cdot \mathbf{ds} \simeq -Ru'_n \quad (5.37)$$

Due to separation from the outer exit, we have with outflow $u_{in} \simeq 0$ with $u_{ex} = u'_n$ jetting out, while similarly during inflow, $u_{ex} \simeq 0$ with $u_{in} = u'_n$ jetting into the cavity. The pressure in the jets, however, has to remain equal to the surrounding pressure (p'_{ex} and p'_{in} respectively) because the boundary of the jet cannot support a pressure difference. Therefore, we have altogether

$$\rho_0(\ell + 2\delta) \frac{d}{dt} u'_n + \frac{1}{2} \rho_0 u'_n |u'_n| + Ru'_n = p'_{in} - p'_{ex} \quad (5.38)$$

In order to have a second equation between p'_n and u'_n we apply the integral mass conservation law on the volume V of the bottle. The change of mass must be equal to the flux through the bottle neck, which is in linearised form for the density perturbation ρ'_{in} :

$$V \frac{d\rho'_{in}}{dt} = -\rho u'_n S_n \simeq -\rho_0 u'_n S_n. \quad (5.39)$$

Assuming an adiabatic compression of the fluid in the bottle we can eliminate ρ'_{in} by using the constitutive equation:

$$p'_{in} = c_0^2 \rho'_{in}. \quad (5.40)$$

Elimination of ρ'_{in} and u'_n from (5.38) by using (5.39) and (5.40) yields:

$$\frac{(\ell + 2\delta)V}{c_0^2 S_n} \frac{d^2 p'_{in}}{dt^2} + \frac{V^2}{2\rho_0 c_0^4 S_n^2} \frac{dp'_{in}}{dt} \left| \frac{dp'_{in}}{dt} \right| + \frac{RV}{\rho_0 c_0^2 S_n} \frac{dp'_{in}}{dt} + p'_{in} = p'_{ex}. \quad (5.41)$$

When the damping is small, there exist solutions without external forcing p'_{ex} , *i.e.* resonance solutions.

$$\frac{(\ell + 2\delta)V}{c_0^2 S_n} \frac{d^2 p'_{in}}{dt^2} + p'_{in} = 0.$$

Hence we see that the Helmholtz resonator reacts as a mass-spring system with a resonance frequency ω_0 given by:

$$\omega_0^2 = \frac{S_n c_0^2}{(\ell + 2\delta)V}. \quad (5.42)$$

When the amplitude is small, the damping will in general be linear. For larger amplitudes the damping will be nonlinear, which among other things generates other harmonics than the frequency of the driving force; see section 5.2.4. A spectacular effect of additional damping occurs when the flow in the neck is superimposed on a mean flow, forcing vortex shedding from the exit even without nonlinear terms; see section 5.2.5.

5.2.3.1 Intermezzo: End correction

If, as is the case in many technical applications, an orifice is used instead of bottle neck ($\ell = 0$), the use of a reasonable estimate for δ is important. For an orifice with a circular aperture we have in the limit of small k

$$\delta = 0.85 \left(\frac{S_n}{\pi} \right)^{\frac{1}{2}}. \quad (5.43)$$

For an unflanged thin-walled open-pipe end we can use for small k the approximation:

$$\delta = 0.61 \left(\frac{S_n}{\pi} \right)^{\frac{1}{2}}. \quad (5.44)$$

See also section 6.7. Values of δ for various other geometries are given by Ingard [94].

5.2.4 Non-linear losses in a Helmholtz resonator

The theory described in the previous section assumes that there is no-flow separation. Flow separation will certainly occur when the acoustic particle displacement has an amplitude comparable to the diameter of the neck. The Strouhal number $Sr = \omega(S_n/\pi)^{1/2}/u'_n$ yields a measure for this effect. When $Sr \ll 1$ flow separation will only occur locally at sharp edges of the neck (or orifice). When $Sr = O(1)$ flow separation will occur even if these edges are rounded off. In principle the effect of flow separation can under these circumstances be described by assuming the formation of a quasi-stationary jet as for the pipe end (section 5.2.2). A multiple-scales solution for this problem may be found in section 8.3.

In the case of an orifice with sharp edges, one should take into account the fact that the jet diameter tends to be smaller than the orifice diameter by a factor β called the vena contracta factor. For a thin orifice $\beta \simeq 0.6$ [47]. Using a quasi-stationary Bernoulli equation this implies an enhancement of the pressure loss Δp by a factor β^{-2} . Furthermore losses occur for an orifice in both flow directions, while in a pipe with horn we assumed losses to occur only upon outgoing acoustic flow.

5.2.5 The Helmholtz resonator in the presence of a mean flow

We consider a Helmholtz resonator of volume V , neck length ℓ and neck surface S_n in which we inject a continuous volume flow $Q_0 = u_0 S_n$ (figure 5.15). Neglecting the viscous dissipation, but otherwise

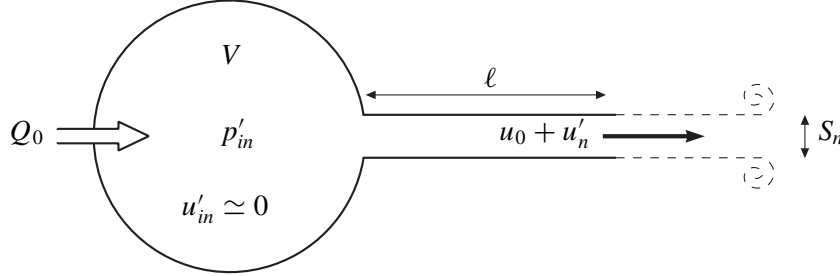


Figure 5.15 Helmholtz resonator with a mean flow.

using the same equation as before we now find

$$\rho_0(\ell + 2\delta) \frac{du'_n}{dt} + \frac{1}{2} \rho_0 (u_0 + u'_n)^2 + p'_{ex} = p_0 + p'_{in} \quad (5.45)$$

where we used the fact that $u'_{ex} = u'_n$ because the total flow is always an outflow. Further, we assumed that the pressure in the jet is uniform and equal to p'_{ex} , the fluctuations due to an external acoustic source. (This is a reasonable assumption for $u_0/c \ll 1$ and $\omega(S_n/\pi)^{1/2}/u_0 \ll 1$). Separating the zero and first order terms in the acoustic perturbations and neglecting second order terms we find

$$p_0 = \frac{1}{2} \rho_0 u_0^2 \quad (5.46)$$

and

$$\rho_0(\ell + 2\delta) \frac{du'_n}{dt} + \rho_0 u_0 u'_n + p'_{ex} = p'_{in}. \quad (5.47)$$

Using the linearized mass conservation law we have neglecting terms of order $(u_0/c_0)^2$:

$$V \frac{d\rho'_{in}}{dt} = -(\rho_0 u'_n + \rho'_{ex} u_0) S_n. \quad (5.48)$$

Eliminating ρ'_{in} by using the constitutive equation $p'_{in} = c_0^2 \rho'_{in}$ and eliminating p'_{in} from (5.47) and (5.48) we find:

$$\frac{d^2 u'_n}{dt^2} + \frac{u_0}{\ell + 2\delta} \frac{du'_n}{dt} + \omega_0^2 u_n = -\frac{\omega_0^2 M_0}{\rho_0 c_0} p'_{ex} - \frac{1}{\rho_0(\ell + 2\delta)} \frac{dp'_{ex}}{dt}.$$

ω_0 is defined by equation (5.42) and $M_0 = u_0/c_0$. For a harmonic excitation $p'_{ex} = \hat{p}_{ex} e^{i\omega t}$ we find:

$$\frac{\rho_0 c_0 \hat{u}_n}{\hat{p}_{ex}} = - \frac{M_0 + i\omega_1 \omega / \omega_0^2}{1 - (\omega / \omega_0)^2 + iM_0 \omega_1 \omega / \omega_0^2} \tag{5.49}$$

where $\omega_1 = c_0 / (\ell + 2\delta)$. We see that the mean flow induces a damping factor which we might a priori not have expected because we did not assume friction losses nor heat transfer.

The key assumption which has introduced damping is that we have assumed that the pressure perturbation at the pipe exit is equal to the environment pressure perturbation p_{ex} . This is true, because the flow leaves the exit as a jet⁴, which implies separation of the flow at the pipe exit and a Kutta condition to be added to an inviscid model (section 5.1)! This implies that a varying exit velocity u_n modulates the vorticity shed at the edges of the pipe exit, which is, on its turn, a loss of kinetic energy for the acoustic field. This confirms that the Kutta condition is indeed a quite significant assumption [42].

5.3 Green’s function of a finite duct

Formally, the Green’s function of a finite duct can be obtained if we neglect friction and losses at the pipe terminations by using the method of images (section 4.6.2 and section 5.2.2). For a pipe segment $0 < x < L$ closed by rigid walls a source at $x = y$ in the pipe segment is represented by a row of sources (in an infinitely long pipe) at positions given by (figure 5.16)

$$x_n = \pm(2n + 1)L \pm y; \quad n = 0, 1, 2, 3, \dots \tag{5.50}$$

The Green’s function is the sum of all the contributions of these sources:

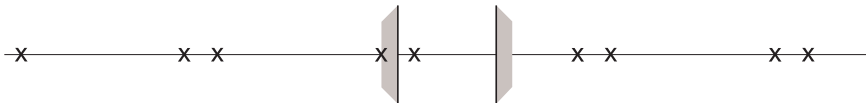


Figure 5.16 Images of source at $x = y$.

⁴A very interesting proof of the fact that a quasi-stationary subsonic free jet cannot sustain any pressure difference with the environment is provided by Shapiro [230].

$$\begin{aligned}
 g(x, t|y, \tau) = \frac{1}{2c_0} \sum_{n=0}^{\infty} \left\{ H \left(t - \tau + \frac{x + (2n+1)L - y}{c_0} \right) \right. \\
 + H \left(t - \tau + \frac{x + (2n+1)L + y}{c_0} \right) \\
 + H \left(t - \tau - \frac{x - (2n+1)L - y}{c_0} \right) \\
 \left. + H \left(t - \tau - \frac{x - (2n+1)L + y}{c_0} \right) \right\}. \tag{5.51}
 \end{aligned}$$

It is clear that such a formal solution has no simple physical interpretation.

Another representation for the 1-D Green's function on $[0, L]$ that might be useful in some applications is found by a series expansion of the Fourier transform \hat{g} of g :

$$\hat{g} = \sum_{n=0}^{\infty} A_n f_n(x) \tag{5.52}$$

in a suitable basis $\{f_n\}$. In this case we will *not* start from elementary solutions of the wave equation. The functions f_n we will consider will (only) satisfy the boundary conditions at $x = 0$ and $x = L$, so that their sum will automatically satisfy these conditions *if* this sum converges uniformly. Hence we will construct now a *tailored* Green's function (section 3.1). Furthermore, it is evidently necessary that the basis $\{f_n\}$ is complete, and convenient that it is orthogonal to some suitable inner product. Let's now for simplicity assume that the pipe segment is limited by a rigid wall at $x = 0$ and an impedance Z_L at $x = L$. Consider:

$$f_n = \sin(K_n x) \tag{5.53}$$

with K_n determined by the equation

$$\frac{\tan(Y)}{Y} = i \frac{Z_L}{kL} \tag{5.54}$$

with $K_n L = Y$. Note that for $n \rightarrow \infty$ ($Z_L \neq 0$)

$$K_n L \simeq (n + \frac{1}{2})\pi + \frac{ikL}{(n + \frac{1}{2})\pi Z_L} + \dots \tag{5.55}$$

so that for large n , f_n approaches the Fourier-sine series basis. The number of solutions between 0 and $(n + \frac{1}{2})\pi$ (for $n \rightarrow \infty$) is not always exactly n . Depending on Z_L/kL it may differ by 1. For example, if $Z_L/kL = iC$ and C is real, there is no purely imaginary solution $Y = i\sigma$ with $\tanh(\sigma)/\sigma = -C$ if $C > 0$ or $C < -1$, and exactly one solution if $-1 < C < 0$, which disappears to infinity if $C \rightarrow 0$. Finally, we note that $\{f_n\}$ is orthogonal to the L_2 inner product:

$$(f_n, f_m) = \int_0^L f_n(x) f_m(x) dx. \tag{5.56}$$

(Note: *not* .. $f_m^*(x)$..), which is easily seen by direct integration:

If $n \neq m$:

$$\int_0^L \sin(K_n x) \sin(K_m x) dx = \frac{\sin(K_n L - K_m L)}{2(K_n - K_m)} - \frac{\sin(K_n L + K_m L)}{2(K_n + K_m)} = 0 \quad (5.57)$$

after application of (5.54).

If $n = m$:

$$\int_0^L \sin^2(K_n x) dx = \frac{1}{2}L - \frac{\sin(2K_n L)}{4K_n} = \Lambda_n. \quad (5.58)$$

We now seek an expression for the Green's function, defined by:

$$\frac{d^2 \hat{g}}{dx^2} + k^2 \hat{g} = -\frac{\delta(x-y)}{c_0^2} \quad (5.59)$$

in the form (5.52). Substitution of the series, multiplication left- and right-hand side by f_m , and integrating over $[0, L]$ yields (because of orthogonality):

$$(k^2 - K_m^2) \Lambda_m A_m = -f_m(y)/c_0^2. \quad (5.60)$$

Hence we have:

$$\hat{g}(x, y) = \frac{1}{c_0^2} \sum_{n=0}^{\infty} \frac{f_n(x) f_n(y)}{(K_n^2 - k^2) \Lambda_n}. \quad (5.61)$$

We see explicitly that:

- i) the Green's function is indeed symmetric in x and y (source and observation points) as stated earlier in section 3.1 (reciprocity), and
- ii) any source with a frequency $\omega = K_n c_0$ (so that $K_n = k$) yields an infinite field, in other words: resonance. Note that in general K_n is complex, so that such a source strength increases exponentially in time.

When the frequency ω of the source is close to a resonance frequency this resonance will dominate the response of the pipe segment and we can use a single mode approximation of the Green's function. This is the approximation which we will use when discussing the thermo-acoustic oscillations in a pipe segment (Rijke tube, section 5.5).

5.4 Self-sustained oscillations of a clarinet

5.4.1 Introduction

The coupling of acoustic oscillations to mechanical vibrations is a technically important problem [255]. In some case such a coupling can cause the failure of a security valve. Instead of looking at a technical application we are going to consider a musical instrument. The model used is very crude and only aims at illustrating the principles of two methods of analysis:

- the stability analysis;
- the temporal simulation.

In the first case we consider a linear model and deduce the minimal blowing pressure necessary to obtain self-sustained oscillations. In the second case we consider a simplified non-linear model developed by McIntyre *et al.* [135] which can be used for time domain simulation. The aim of the simplification is to allow for a real time simulation of a clarinet! We will restrict our discussion to the principle of the solution of the problem. The results of the calculations can be found in the literature.

5.4.2 Linear stability analysis

A simplified model of a reed instrument like a clarinet is a cylindrical pipe fed by a pressure reservoir P_0 (the mouth) through a valve (reed). The reed has a mass m_r and is maintained at a rest position h_r by a spring of constant K_r . The aperture h of the valve is assumed to be controlled by the pressure difference $\Delta p = P_0 - p'$ between the mouth pressure P_0 and the acoustic pressure p' in the pipe just behind the reed (figure 5.17). The equation of motion of the reed is:

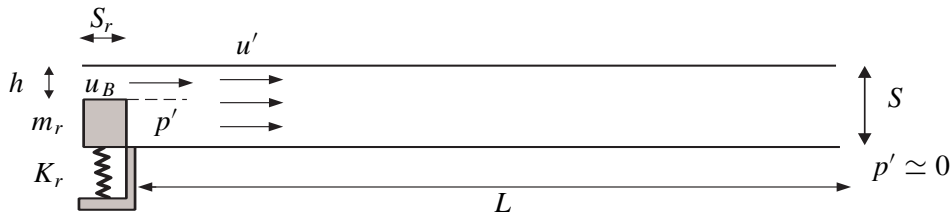


Figure 5.17 Simplified clarinet.

$$m_r \frac{d^2 h}{dt^2} + \gamma_r \frac{dh}{dt} + K_r (h - h_r) = -S_r (P_0 - p') = -S_r \Delta p. \quad (5.62)$$

γ_r is the damping coefficient of the reed, S_r is the surface of the reed and h is the aperture of the reed channel through which the air flows from the mouth to the pipe. We assume that the flow in the reed

channel is quasi-stationary and that at the end of the reed channel a free jet is formed. Neglecting pressure recovery by mixing of the jet with the air in the pipe we assume the pressure p' to be uniform in the jet and equal to the pressure at the pipe inlet.

The flow volume Q_r of air into the pipe is given in this approximation (if we neglect friction) by the equation of Bernoulli:

$$Q_r = u_B h w = h w (2|\Delta p|/\rho)^{\frac{1}{2}} \text{sign}(\Delta p) \quad (5.63)$$

where w is the width of the reed channel and u_B the (Bernoulli) velocity of the air in the jet. The acoustic velocity u' at the entrance of the pipe ($x = 0$) is given by:

$$u' = \frac{Q_r}{S} \quad (5.64)$$

where S is the pipe cross sectional area. If we consider a small perturbation of the rest position ($p' \ll P_0$) we can linearize the equations and consider the behaviour of a harmonic perturbation $p' = \hat{p} e^{i\omega t}$.

The steady state values of h and Q_r are given by:

$$h_0 = h_r - \frac{S_r P_0}{K}, \quad Q_0 = u_0 h_0 w, \quad u_0 = (2P_0/\rho_0)^{\frac{1}{2}}.$$

The linear perturbations are governed by the equations:

$$(-\omega^2 m_r + i\omega \gamma_r + K_r) \hat{h} = S_r \hat{p} \quad (5.65a)$$

$$\hat{u}_B = -\frac{u_0 \hat{p}}{2P_0} \quad (5.65b)$$

$$\hat{Q}_r = w(\hat{h} u_0 + h_0 \hat{u}_B). \quad (5.65c)$$

We further assume that the acoustical behaviour of the pipe is described by an impedance $Z_p(\omega)$ so that:

$$\hat{p} = Z_p \hat{Q}_r / S. \quad (5.65d)$$

Since the system of equations 5.65a–5.65d is homogeneous, it can only be satisfied if the determinant vanishes. This condition yields an equation from which we can calculate ω for a given P_0 :

$$\frac{-\omega^2 m_r + i\omega \gamma_r + K_r}{S_r u_0} = \left(\frac{S}{Z_p w} + \frac{h_0 u_0}{2P_0} \right)^{-1}. \quad (5.66)$$

If $\text{Im}(\omega) > 0$ the perturbations are damped, and if $\text{Im}(\omega) < 0$ the perturbations grow in time. It is clear that the steady state amplitude in a clarinet can only be reached by non-linear saturation of the system because linear theory predicts a monotonically growing or decaying amplitude. When $\text{Im}(\omega) = 0$

the perturbations are neutral, they do not change in amplitude. If we assume $\text{Im}(\omega) = 0$ equation (5.66) becomes an equation for $\text{Re}(\omega)$ and P_0 . This allows to determine the threshold of pressure above which oscillations occur and the frequency of the most unstable mode which starts oscillating. A discussion of the solution of this clarinet model, including non-linear effects, is given by Gazengel [71] and Kergomard in [79].

It is interesting to note that in some cases the inertia of the flow in the reed which we neglected is the main driving force for instability. This is for example the case in harmonium reeds [235] and for valves in water like river gates [110]. A discussion of the flow through double reeds and the vocal folds is given by Hirschberg [79].

5.4.3 Rayleigh's Criterion

An interesting analysis of the problem of clarinet oscillation is already obtained by considering the very simple quasi-stationary reed model:

$$h = h_r - \frac{S_r \Delta p}{K} \quad \text{and} \quad Q_r = hw \sqrt{\frac{2|\Delta p|}{\rho_0}} \text{sign}(\Delta p).$$

When $\Delta p = 0$ there is obviously no flow because $u = \sqrt{2|\Delta p|/\rho_0} \text{sign}(\Delta p)$ vanishes. When $\Delta p > h_r K/S_r = \Delta p_{max}$ the reed closes and $h = 0$. Between these two zero's of Q_r it is obvious that $Q_r > 0$ and should be a maximum at a pressure difference which we call critical $\Delta p_{crit} \simeq \frac{1}{3} \Delta p_{max}$. The acoustical power

$$W = \frac{1}{T} \oint p' dV = \frac{1}{T} \int_0^T p' \frac{dV}{dt} dt = \frac{1}{T} \int_0^T p' Q'_r dt$$

produced by the fluctuating volume flow $Q'_r = \frac{dV}{dt}$ should at least be positive. We consider here an oscillation period T in order to sustain oscillations. Fluctuations $Q'_r = (dQ_r/dp')p'$ in Q_r induced by pressure fluctuations in the pipe are negative for $\Delta p < \Delta p_{crit}$ and positive for $\Delta p > \Delta p_{crit}$. This explains the presence of a blowing pressure threshold below which the clarinet does not play. The criterion $\oint p' Q'_r dt > 0$ is called the Rayleigh criterion for acoustical instability. We will use it again in the analysis of thermo-acoustical oscillations.

5.4.4 Time domain simulation

Early attempts to describe the non-linearity of a clarinet were based on a modal expansion of the acoustic field in the pipe. This implies that the Green's function was approximated by taking the contribution of a few (one to three) modes⁵ into account (equation (5.61)). The typical procedure is

⁵Standing waves in the pipe closed at the reed end.

further to assume a weak non-linearity which implies that a perturbation method like the method of averaging can be used to calculate the time dependence of the modes [70]. A full solution is obtained by the method of harmonic balance discussed by Gilbert [72].

As stated by McIntyre [135] the non-linearity in a clarinet is not weak. In fact the most spectacular non-linearity is due to the limited movement of the reed upon closing. The collision of the reed against the wall of the mouthpiece can result in a chaotic behaviour [71]. The key feature of a clarinet mouthpiece is that this abrupt non-linearity is replaced by a softer non-linearity because upon touching the wall the reed gradually closes as it is bent on the curved wall of the mouthpiece (called the lay) and its stiffness increases because the oscillating part is becoming shorter.

However, the high resonance frequency of the reed $\omega_r^2 = K_r/m_r$ suggests that a quasi-stationary model of the reed could be a fair first approximation. Hence McIntyre [135] proposes to use the steady approximation of (5.62):

$$K_r(h - h_r) = -S_r(P_0 - p') = -S_r\Delta p \quad (5.67)$$

combined with (5.63), (5.64) and (5.65d). The numerical procedure is further based on the knowledge that the acoustic pressure p' at the reed is composed of an outgoing wave p^+ and an incoming wave p^- (result of the reflection of earlier p^+ wave at the pipe end):

$$p' = p^+ + p^-. \quad (5.68)$$

The pipe has a characteristic impedance $Z_c (= \rho_0 c_0$ when friction is neglected) so that:

$$u' = \frac{p^+ - p^-}{Z_c}. \quad (5.69)$$

If we now define the reflection function $r(t)$ as the acoustic wave p^- induced by a pressure impulse $p^+ = \delta(t)$, we find:

$$p^- = r * p^+ \quad (5.70)$$

where $*$ indicates a convolution (equation C.10). Elimination of p^+ and p^- from (5.68)–(5.70) yields:

$$p' = Z_c u' + r * (Z_c u' + p') \quad (5.71)$$

where u' is calculated at each time step by using (5.63), (5.66), and (5.67):

$$u' = \frac{w}{S} \left(h_r - \frac{S_r \Delta p}{K_r} \right) \left(\frac{2|\Delta p|}{\rho_0} \right)^{\frac{1}{2}} \text{sign}(\Delta p). \quad (5.72)$$

The solution is obtained by integrating (5.71) step by step, using the previous value of p' to calculate u' in the convolution of the right-hand side (5.71).

The interesting point in McIntyre’s approach is that he uses a reflection function $r(t)$ (which is the Fourier transform of $R(\omega) = (Z_p - \rho c)/(Z_p + \rho c)$) rather than z_p , the Fourier transform of Z_p . Using z_p would have given the integral equation:

$$p' = z_p * u' \tag{5.73}$$

which can be combined with (5.72) to find a solution. It appears, however, that (5.73) is a numerically slowly converging integral because z_p has an oscillatory character corresponding to the response p' of a close tube to an impulse $u' = \delta(t)$ (tube closed at pipe inlet).

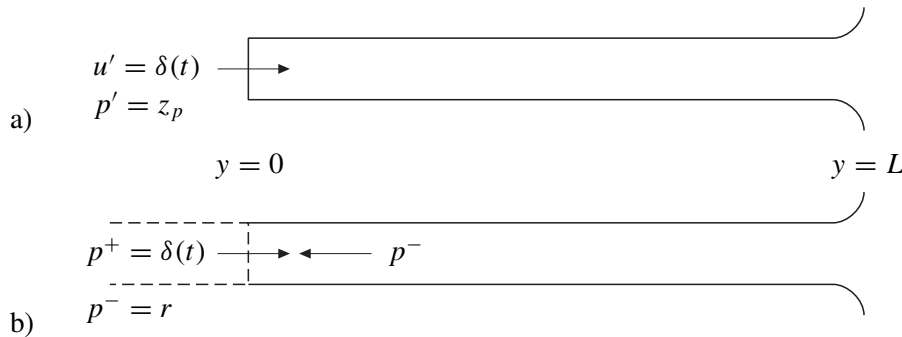


Figure 5.18 Difference between z_p and r .

The reflection function r is in fact calculated in a semi-infinite tube and therefore has not such an oscillatory character (figure 5.18). So it appears that a Green’s function which is not tailored may be more appropriate than a tailored one.

5.5 Some thermo-acoustics

5.5.1 Introduction

We have focused our attention until now on wave propagation and interaction of acoustic fields with isentropic flows. In section 2.6 we have seen that variations s' in entropy should act as a volume sound source (if we use p' as acoustic variable). We will now discuss such effects as an interesting example of self-sustained oscillations in resonators. At low Mach numbers in gases, entropy variations due to dissipation are negligible (order $0.2 M^2$). Entropy fluctuations occur mainly as a result of combustion (or vapour condensation) in the bulk of the flow or as a result of heat conduction at the wall. Mixing of hot and cold gases results into fluctuations of the entropy caused by the unsteady heat conduction (equation 2.87). For ideal gases one can, however, show that this sound source has a vanishing monopole strength (Morfey [149], Obermeier [169]). Convection of entropy spots during

the mixing of a hot jet with the environment dominates the low Mach number behaviour (Crighton [45], Morfey [149]). This sound source has the character of a dipole.

Combustion instability is often triggered by the strong dependence of combustion processes on temperature. The reaction rates depend exponentially on T . Hence temperature fluctuations associated with pressure fluctuations will induce variation in combustion rate. This implies a source of sound which, if it is in phase with the acoustic field, can lead to instability. Even in free space this implies a strong increase in sound production. We experience this effect when we ignite the flame of a gas burner. Placed in a closed tube a flame can couple with standing waves. This type of instability is known in aircraft engine as a re-heat buzz (Keller [106], Bloxsidge *et al.* [21]). The “singing flame” has already been discussed extensively by Rayleigh [194]. More recent information on the interaction of combustion with acoustic is found in Crighton *et al.* [45], Candel & Poinot [30], McIntosh [134], and Putnam [190].

We will now focus our attention on the effect of unsteady heat transfer at walls. This type of interaction has already attracted the attention of Rayleigh [194] in the form of the Rijke tube oscillation. This experiment was carried out first by De Rijke around 1848 [214]. He found that placing an electrically heated gauze in the lower part of a vertical tube open at both ends would induce strong acoustical oscillations. De Rijke considered the use of such a device as an organ pipe. The subject has been studied as a model for combustion instability by many scientists, among which Merk [139], Kwon and Lee [114], Bayly [11], Heckl [77], Gervais [182], and Raun [193].

Closely related phenomena of acoustical oscillations induced by a temperature gradient in a tube is used by scientists to detect the level of liquid Helium in a reservoir. This phenomenon has been extensively studied by Rott [155, 220, 221, 222, 223, 265], in a very systematic series of papers. The fascinating aspect of this phenomenon is that it can be inverted, acoustic waves interacting with a wall induce a transfer of heat which can be used to design an acoustically driven cooling machine. Such engines have been studied by Wheatley [259], Radebaugh [191] and Swift [238]; see also [177]. The ultimate engine consists of two thermo-acoustic couples (elements with a temperature gradient): one at the hot side which induces a strong acoustic field and a second at the cold side which is driven by the first (figure 5.19) [239]. This is a cooling machine without moving parts!

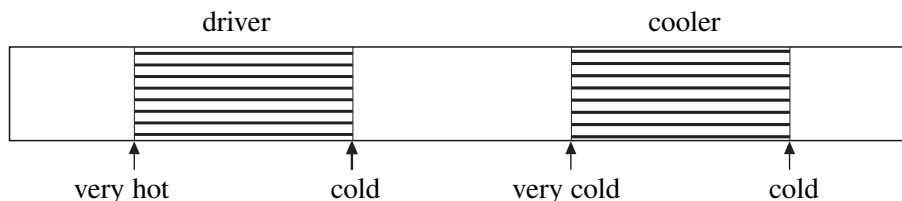


Figure 5.19 Heat driven acoustical cooling engine.

We will limit our discussion to a simple analysis of the Rijke tube oscillation.

5.5.2 Modulated heat transfer by acoustic flow and Rijke tube

We consider a thin strip of metal of temperature T_w and width w aligned along the mean flow direction in a uniform flow u_∞ . Along the strip viscous and thermal boundary layers $\delta_V(x)$ and $\delta_T(x)$ will develop. We assume that δ_V/w and δ_T/w are small and that $\omega w/u_\infty \ll 1$, while $\delta_V/\delta_T = O(1)$. For small fluctuations u' of u_∞ around an average value u_0 the fluctuations in the heat transfer coefficient can be calculated as described by Schlichting [227] for any mean flow of the type $u_0 \sim x^n$ (wedge flow). We now limit ourselves to the flat plate ($n = 0$) and we use a low frequency limit from which the memory effect will become more obvious than from Schlichting's solution. We further approximate the velocity and temperature profiles in the boundary layers by:

$$u(y) = \frac{u_\infty}{\delta_V} y \quad (5.74)$$

$$\frac{T(y) - T_w}{T_\infty - T_w} = \frac{y}{\delta_T}. \quad (5.75)$$

Such an approximation is only valid for low frequencies and small perturbation amplitudes, corresponding to $\omega w/u_\infty \ll 1$ and $u'/u_0 \ll 1$. Outside the boundary layers the flow is uniform. In this approximation the viscous stress τ_w at the wall is given by:

$$\tau_w = \eta \frac{u_\infty}{\delta_V} \quad (5.76)$$

and the heat transfer q at the wall by:

$$q = -K \left(\frac{\partial T}{\partial y} \right)_{y=0} = -K \frac{T_\infty - T_w}{\delta_T}. \quad (5.77)$$

Using an integral formulation of the conservation law in boundary layer approximation we find [227]:

$$\left[\frac{\partial}{\partial t} + \frac{1}{3} u_\infty \frac{\partial}{\partial x} \right] \delta_V^2 = 4\nu - \frac{2\delta_V^2}{u_\infty} \frac{\partial u_\infty}{\partial t} \quad (5.78a)$$

$$\left[\frac{\partial}{\partial t} + \frac{2}{3} u_\infty \left(\frac{\delta_T}{\delta_V} \right) \frac{\partial}{\partial x} \right] \delta_T^2 = 4a + \frac{1}{3} u_\infty \left(\frac{\delta_T}{\delta_V} \right)^3 \frac{\partial}{\partial x} \delta_V^2 \quad \text{for } \delta_T < \delta_V \quad (5.78b)$$

$$\left[\frac{\partial}{\partial t} + u_\infty \left(1 - \left(\frac{\delta_T}{\delta_V} \right)^2 \right) \frac{\partial}{\partial x} \right] \delta_T^2 = 4a - u_\infty \left(\frac{2}{3} - \frac{\delta_T}{\delta_V} \right) \frac{\partial}{\partial x} \delta_V^2 \quad \text{for } \delta_T > \delta_V \quad (5.78c)$$

where a is the thermal diffusivity of the gas:

$$a = \frac{K}{\rho C_P}. \quad (5.79)$$

Note that we have used the assumption $(T_w - T_\infty)/T_\infty \ll 1$ in order to keep the equations simple. This is certainly a very crude approximation in a Rijke tube. The boundary conditions are:

$$\delta_V(0) = \delta_T(0) = 0 \quad \text{at } x = 0. \quad (5.80)$$

In air we have $Pr < 1$ and hence in general $\delta_V < \delta_T$. We will, however, use further the assumption $Pr = 1$ because we do not expect an essentially different physical behaviour.

The stationary solution of (5.78a) is:

$$\delta_V = \left(\frac{12\nu x}{u_0} \right)^{\frac{1}{2}} \quad (5.81)$$

while δ_T can be calculated from (5.78b):

$$\delta_T = \delta_V. \quad (5.82)$$

Using the notation $\delta_0 = \delta_T = \delta_V$ for the stationary solution we find in linear approximation:

$$\left[\frac{\partial}{\partial t} + \frac{1}{3}u_0 \frac{\partial}{\partial x} \right] \delta'_V = -\frac{\delta_0}{u_0} \frac{\partial u'}{\partial t} - \frac{1}{3}u_0 \left(\frac{\delta'_V}{\delta_0} + \frac{u'}{u_0} \right) \frac{\partial \delta_0}{\partial x} \quad (5.83a)$$

$$\left[\frac{\partial}{\partial t} + \frac{2}{3}u_0 \frac{\partial}{\partial x} \right] \delta'_T = +\frac{1}{3}u_0 \frac{\partial \delta'_V}{\partial x} + \frac{1}{3}u_0 \left(\frac{\delta'_V - \delta'_T}{\delta_0} - \frac{u'}{u_0} \right) \frac{\partial \delta_0}{\partial x}, \quad (5.83b)$$

where $u_\infty = u_0 + u'$. These equations can be solved by integration along the characteristics: ($x = \frac{1}{3}u_0 t$) for (5.83a) and ($x = \frac{2}{3}u_0 t$) for (5.83b). We see that the perturbations in δ'_T move along the strip with a phase velocity $\frac{2}{3}u_0$ which implies a “memory” of the heat transfer q for perturbations u' of the mean flow. This memory is crucial for the understanding of the Rijke tube instability.

The Rijke tube is an open pipe of length $2L$ (figure 5.20). In the pipe we place a row of hot strips (or a hot gauze). When the tube is vertical a flow u_0 will be induced by free convection (the tube is a chimney). When the tube is horizontal we impose u_0 by blowing.

It appears that the tube starts oscillating at its fundamental frequency $f_0 = c/4L$ when the heating element is placed at $x = -\frac{1}{2}L$, at a quarter of the tube length in the upstream direction (at the lower part of the tube for a vertical tube). We will now explain this. Note that some excitation of higher modes can be obtained but these are weak because of increased radiation losses at high frequencies. Hence we will assume that only the fundamental mode can be excited. This corresponds to a single mode expansion of the Green's function (5.61). As proposed by Rayleigh [194] we start our analysis by placing the warming element at the center of the tube ($x = 0$).

As shown in figure 5.21 the acoustic velocity u' at $x = 0$ will vanish for the fundamental mode. The variation of heat transfer q is only due to the temperature fluctuations $T' = (\gamma - 1)\gamma^{-1}p'$ of the gas

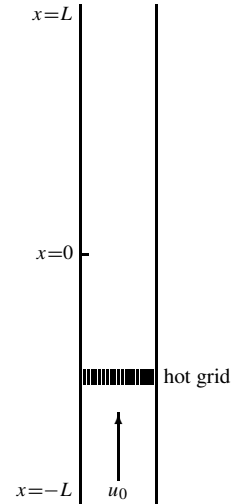


Figure 5.20 Rijke tube.

in the main flow. If we neglect the “memory” effect of the heat capacity of the boundary layers the heat flux \mathbf{q} decreases when p' increases because $T_w - T$ is reduced.

The acoustic effect of the unsteady heat transfer \mathbf{q} is given in a quantitative way by the linearized equation 2.69 in which (2.70) has been substituted:

$$\frac{1}{c_0^2} \frac{\partial^2 p'}{\partial t^2} - \nabla^2 p' \simeq \frac{\rho_0}{c_0^2 T_0} \left(\frac{\partial T}{\partial \rho} \right)_s \frac{\partial}{\partial t} \nabla \cdot \mathbf{q} \tag{5.84}$$

which corresponds to a volume source term $\partial^2(\beta \rho_f)/\partial t^2$ in (2.65) or in linearized form $\partial(m/\rho_0)/\partial t$. As derived in section 2.7 the power W produced by the source is (2.82):

$$W = \iiint_V \left\langle p' \frac{m}{\rho_0} \right\rangle dV. \tag{5.85}$$

This equation can also be derived from the equation for the work A performed by volume variation dV :

$$A = \oint p dV \tag{5.86}$$

which can be written as:

$$A = \int_0^T p \left(\frac{dV}{dt} \right) dt \tag{5.87}$$

where $dV/dt = \int m/\rho_0 dV$ and $T = 2\pi/\omega$ is the oscillation period. The rate of volume injection dV/dt corresponds to the volume integral $\int_V \nabla \cdot \mathbf{q} dx = \int_S \mathbf{q} \cdot \mathbf{n} d\sigma$ which is the integral of the heat

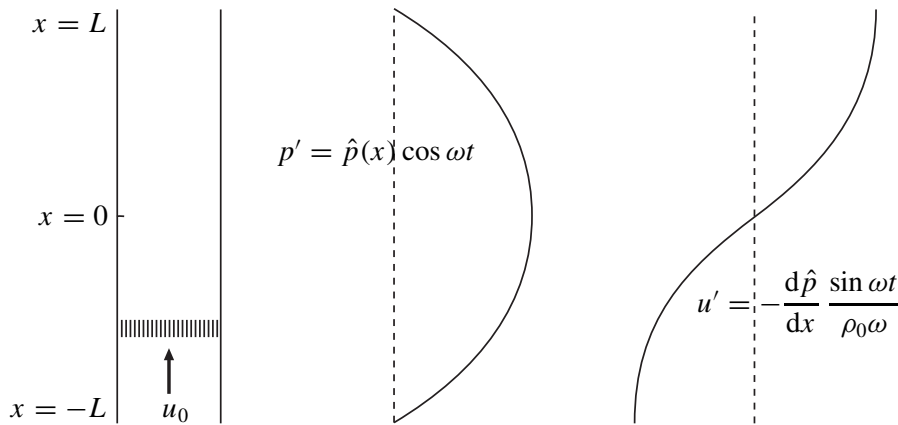


Figure 5.21 Pressure p' and acoustic velocity u' distribution for the fundamental mode.

transfer from the heating element. Furthermore, as the transfer of heat from the wall to the gas implies an expansion of the gas we can also understand (5.84) in terms of (5.87).

We now easily understand that as q is opposite in phase with p' the presence of a hot element at $x = 0$ will damp oscillations of the fundamental mode of the pipe. Hence we understand that the Rijke tube oscillation is due to modulation of q by the acoustic velocity fluctuations u' . An optimal amplitude of q is obtained just at the end of the pipe at $x = -L$ where u' has the largest amplitude. However, at this place p' is close to zero so that we see from (5.85) that the source is ineffective at this position. We therefore see that the position $x = -\frac{1}{2}L$ is a compromise between an optimum for p' and an optimum for q . We still have to understand why it should be $x = -\frac{1}{2}L$ and not $x = \frac{1}{2}L$. The key of this is that for $x < 0$ the pressure p' increases when the acoustic velocity u' enters the pipe ($u' > 0$) upwards while for $x > 0$ the velocity is downwards at that time. If the heat transfer would react instantaneously on u' then q would vary as $\sin(\omega t)$ while p' varies as $\cos(\omega t)$. As a consequence W integrated over a period of oscillation would vanish. Hence the occurrence of oscillations is due to a delay τ in the reaction of q on u' . As the delay τ is due to the “memory” of the boundary layer we expect that $\tau > 0$, since the boundary layer integrates, and cannot anticipate on perturbations of u' .

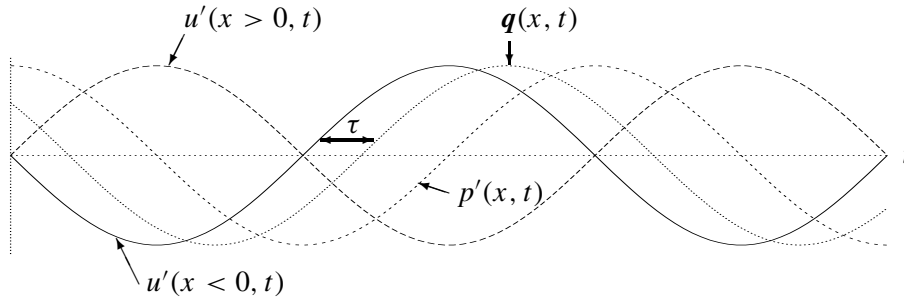


Figure 5.22 Sketch of time dependence of p' and u' in the upper ($x > 0$) and lower ($x < 0$) part of the tube. A memory effect of $\frac{1}{2}\pi$ will shift the phase of the heat transfer q from that of u' (the quasi-steady approximation) toward that of p' . It is the part of q which is in phase with p' that produces the sound in a Rijke tube.

As we see from the diagram of figure 5.22 for $\omega\tau = \frac{1}{2}\pi$, the delayed heat flux q is in phase with p' if $x < 0$. Pulsations induced by a hot grid placed at $x > 0$ would involve a larger delay: $\omega\tau = \frac{3}{2}\pi$. As we will explain such a condition implies a very low flow velocity and hence much weaker oscillations. In practice this oscillation mode at low velocities is not observed. The time delay τ is determined by the time that a perturbation in δ'_T remains along the strip. When we blow very hard the residence time τ of a perturbation δ'_T in the boundary layer on the strip will be very short because we expect from (5.83b) that:

$$\tau = O\left(\frac{3w}{2u_0}\right) \quad (5.88)$$

where w denotes the length of the heated strip in flow direction. When we do not blow hard enough the boundary layers δ_0 will be very thick. The hot gas remains around the warming element blocking

the heat transfer. Also when $\pi \leq \omega\tau \leq 2\pi$ we expect that the oscillations will be damped out. Hence, an optimum of pulsations may be expected for $\omega\tau = \frac{1}{2}\pi$:

$$\frac{w\omega}{u_0} = \frac{\pi}{3}. \tag{5.89}$$

This behaviour is indeed verified by experiments. Of course in order to obtain a stable oscillation the temperature T_w should reach a critical limit. For a horizontal tube at a fixed u_0 , imposed by blowing through the pipe, this is less critical⁶ than in a vertical pipe where the temperature element also drives the main flow u_0 . In experiments with a horizontal pipe it is quite easily observed that blowing too hard reduces τ such, that pulsations disappear.

While we have seen that certain conditions are favourable for an oscillation we did not yet discuss the non-linear effects leading to saturation. The most obvious effect is that when the acoustic particle displacement becomes comparable to the width of the strip:

$$\frac{u'}{\omega w} = O(1), \tag{5.90}$$

back flow will occur from the wake towards the strip. The strip is then surrounded by pre-heated gas and this blocks the heat transfer. Note that at very large amplitudes ($u'/\omega w > 1$) there is a wake upstream of the strip during part of the oscillation period. We now understand, by combination of (5.89) and (5.90), why in the experiment one finds typical amplitudes of the order of $u' = O(u_0)$. The proposed saturation model has first been used by Heckl [77]. It is interesting to note that Rayleigh [194] describes this non-linear effect of saturation as a “driving” mechanism.

A comprehensive theory of the Rijke tube oscillation, including non-linear effects and the influence of large temperature differences, has not yet been presented. We see that such a theory is not necessary to predict the order of magnitude of the oscillation amplitude. On the contrary, it is sufficient to isolate the essential limiting non-linearity.

5.6 Flow induced oscillations of a Helmholtz resonator

In view of the large amount of applications in which they occur, flow induced pulsations of a Helmholtz resonator or wall cavity have received considerable attention in the literature [13, 29, 49, 216, 56, 76, 86, 87, 92, 137, 165, 166, 218]. In principle the flow instability has already been described qualitatively in section 5.1. We will now more specifically consider a grazing uniform flow.

⁶Since the design of a vertical Rijke tube driven by natural convection is not easy we provide here the dimensions of a simple tube. For a glass pipe of $2L=30$ cm length and an inner diameter of $d=2.5$ cm, one should use a metal gaze made of wires of 0.2 mm to 0.5 mm diameter, the wires being separated by a distance in the order of 1 mm. This gaze can be cut in a square of 2.5×2.5 cm². The bended corners can be used to fix the gaze at its position ($x = -\frac{1}{2}L$). A small candle is a very suitable heat source. The pipe will produce its sound after the candle is drawn back.

We will now discuss models which can be used to predict the order of magnitude of the pulsations. The configuration which we consider is shown in figure 5.23. Self-sustained oscillations with a frequency ω close to the resonance frequency ω_0 of the resonator occur when the phase condition for a perturbation in the feedback loop (shear layer/resonator) is satisfied and the gain is sufficiently large. When $\omega = \omega_0$ we find a maximum of the pulsation amplitude and the phase condition is entirely determined by the shear layer. In principle we should add to the convection time of the perturbation along the shear layer a phase shift at the “receptivity” point upstream and another at the “excitation” point downstream. These corrections are either due to “end corrections” or to the transition from a pressure perturbation p' in the resonator to a velocity or displacement perturbation of the shear layer. We now ignore these effects for the sake of simplicity and because we do not have available any theory that predicts these corrections.

In both configurations of figure 5.23 in first order approximation perturbations of the shear layer (at the opening of the resonator) propagate with a velocity u_c of the order of $\frac{1}{2}u_0$. It appears from experiment that when the travel time of a perturbation across the opening width w roughly matches the oscillation period $2\pi/\omega_0$ of the resonator (or a multiple of $2\pi/\omega_0$) pulsations occur. Typically one finds a velocity $u_c \simeq 0.4u_0$. Hence the phase condition for instability is [79]:

$$\frac{\omega_0 w}{0.4u_0} = 2\pi n; \quad n = 1, 2, 3, \dots \quad (5.91)$$

More complex phase condition depending on the geometry and the Mach number has been reported by [18, 216, 218]. The first hydrodynamic mode ($n = 1$) is usually the strongest because it corresponds

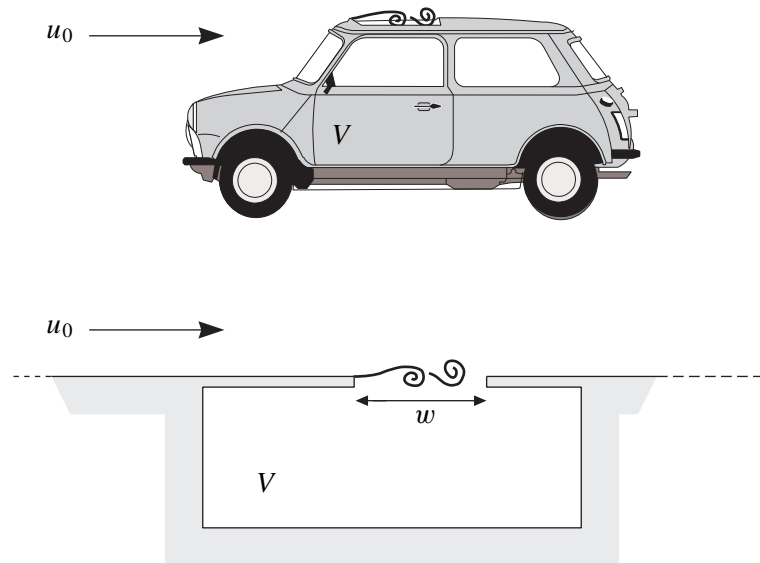


Figure 5.23 Helmholtz resonator in a wall with grazing flow.

with the highest velocity at which pulsations occur. Furthermore when the hydrodynamic wave length (w/n) becomes comparable to the gradient length δ in the grazing velocity profile (boundary layer thickness at the wall) the flow becomes stable and the perturbations are damped. Typically for:

$$\frac{\delta\omega_0}{0.4u_0} > 2 \quad (5.92)$$

the flow is linearly stable. A currently used cure for pulsations is to place a device called ‘‘spoiler’’ which increases δ just upstream of the cavity [28, 216]. Equation (5.92) can be used to choose a reasonable spoiler height. However, we found in some experiments that this is no guarantee for stability [28]. Equation (5.92) imposes an upper bound to the hydrodynamic mode instability. In most experiments mode numbers higher than $n = 5$ are not observed. A remarkable exception is the oscillation found inside solid propellant rockets for which $6 \leq n \leq 12$ [252].

It is often assumed that the perturbations along the shear layer grow according to a linear theory. It appears that a linear theory is only valid for low pulsation amplitudes, in the range of $u'/u_0 \leq 10^{-3}$. In the experiments one observes in most cases for a grazing uniform flow a spectacular non-linear behaviour of the shear layer [28]. The vorticity of the shear layer is concentrated into discrete vortices. At moderate acoustic amplitude $u'/u_0 = O(10^{-1})$ one can assume that the acoustic field only triggers the flow instability but does not modify drastically the amount of vorticity Γ shed at the upstream edge of the slot. This leads to the model of Nelson [28, 79, 165, 166] in which one assumes a vortex of strength Γ given by:

$$\frac{d\Gamma}{dt} = \frac{d\Gamma}{dx} \cdot \frac{dx}{dt} = u_0 \cdot \frac{1}{2}u_0 \quad (5.93)$$

travelling at a velocity $u_c = 0.4u_0$ across the slot (see figure 5.7). A new vortex is generated following Nelson’s experimental observations at the moment that the acoustic velocity u' is zero and is increasing (directed into the resonator, p' in the resonator is at a minimum).

Using Howe’s analogy as described in section 2.6 and 2.7 one can calculate the acoustic pulsation amplitude. As the source strength $\nabla \cdot (\omega \times \mathbf{x})$ is independent of u' we find a finite amplitude by balancing the friction, radiation and heat transfer losses with the power generated by the vortices. As friction and radiation losses scale on u'^2 , we would expect from this theory to find pressure amplitudes scaling with the dynamical pressure of the flow $p' = O(\frac{1}{2}\rho_0 u_0^2)$. This occurs indeed when the edges of the slot are sharp. Typically, the acoustic power W generated by vortices due to instability of the grazing flow along an orifice of area ($w \times B$) is given by

$$W = O(5 \cdot 10^{-2}) \frac{1}{2} \rho_0 u_0^2 w B u'$$

where u' is the amplitude of the acoustic velocity fluctuations through the orifice.

The amplitude of the pulsations depends critically on the shape of the edge at which vortex shedding occurs. This effect can be understood as follows. Upon formation of a new vortex the acoustic field u'

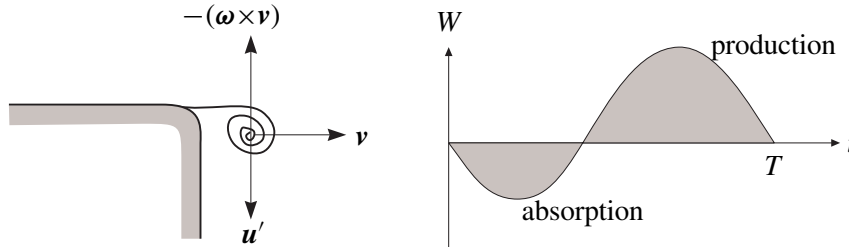


Figure 5.24 Absorption of acoustic energy by vortex shedding.

is directed towards the interior of the resonator. Using Howe’s formula:

$$W = -\rho_0 \iiint_V \langle (\boldsymbol{\omega} \times \mathbf{v}) \cdot \mathbf{u}' \rangle dV, \tag{2.100}$$

we see that the vortex is initially absorbing energy from the acoustic field (figure 5.24) because $-(\boldsymbol{\omega} \times \mathbf{v})$ is opposite to \mathbf{u}' . At a sharp edge \mathbf{u}' is large because the potential (acoustic) flow is singular. When an edge is rounded off \mathbf{u}' is not singular (figure 5.25) and the initial absorption will be modest.

The net sign of W over a period $T = 2\pi/\omega_0$ of oscillation depends of course also on the amount of energy produced by the vortex in the second half of the acoustic period when the acoustic velocity \mathbf{u}' is directed outwards from the resonator [28, 111]. Of course, when u_0 is so large that the travel time ($w/0.4u_0$) of the vortex across the slot is shorter than half a period ($w/0.4u_0 < \frac{1}{2}T$), then only absorption occurs. Self-sustained oscillations are impossible in this case. This effect can easily be experienced by whistling with our lips. If we increase the blowing velocity the sound disappears.

The main amplitude limitation mechanism at high amplitudes, $u'/u_0 > 0.2$, is the shedding of vorticity by the acoustic flow. At the upstream edge this implies an increase of the shed vorticity Γ with u' and a dependence of the initial damping on u'^3 . Howe [88] observes that at high amplitudes the vortex sound absorption scales on u'^3 whereas the sound production scales on $u'u_0^2$. Hence, when those effects balance each other, the amplitude u' scales on u_0 . This behaviour is indeed observed

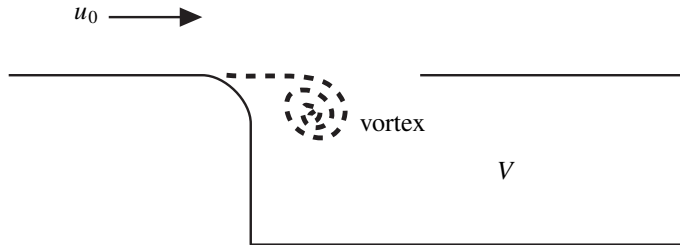


Figure 5.25 Rounded upstream edge.

[28, 111]. A typical amplitude observed in Helmholtz resonators is $u'/u_0 = O(10^{-1})$. This amplitude is also typical of a recorder flute or a whistle [79, 247].

In [111] it is observed that at very high amplitudes ($u'/u_0 = O(1)$) in a resonator formed by side branches along a pipe, non-linear wave propagation resulting into the generation of non-resonant cavity modes was a major amplitude limiting mechanism. Another possible mechanism at high amplitudes is the transition of acoustical flow from laminar into turbulent (section 4.5.3).

The discussion given here provides some qualitative indications for various basic phenomena of cavity oscillation. Models as the one of Nelson [165, 166] provide insight but are not able to predict accurately the amplitude of the oscillations. In many engineering applications insight is sufficient for taking remedial measures. However, when a prediction of the amplitude is required a more detailed flow model is needed. Such models are not yet available.

Exercises

- a) Calculate the impedance seen by a piston placed at the end $x = 0$ of a tube closed at $x = L$ by an impedance $Z(L)$. Neglect friction in the tube. For $Z(L) = \infty$ (closed wall) calculate the power generated by the piston. Calculate the amplitude of the acoustic field for $Z(L) \neq \infty$.
- b) When the impedance $Z(L)$ at a pipe end is small, $|Z(L)| \ll \rho_0 c_0$, one can consider the pipe being terminated at virtual position $x = L + \delta$ by a purely resistive impedance $Z(L)' = \text{Re } Z(L)$. δ is called the end correction of the pipe. Derive a relationship between δ and $Z(L)$.

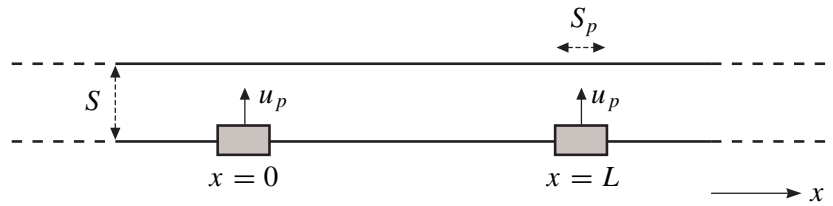


Figure 5.26 Two pistons along a pipe.

- c) Consider two identical pistons of surface S_p placed at a distance L from each other along an infinitely extended pipe (figure 5.26) of cross sectional surface S . Assume that the two pistons move harmonically with the same velocity $\hat{u}_p e^{i\omega t}$. Show that under specific conditions the acoustic field vanishes for $x > L$ and $x < 0$. How large is the amplitude of the acoustic field under these circumstances for $0 < x < L$?
- d) Consider a piston placed at the end of a closed side branch of cross sectional surface S_1 along a main pipe with a cross sectional surface S_2 (figure 5.27). The side branch has a length L . The edges of the junction at the main pipe are rounded off. Calculate the amplitude \hat{p} of the acoustic field at the piston following linear theory for $\omega S^{1/2}/c < 1$ as a function of S_1/S_2 and L . Estimate the largest amplitudes that may be reached before linear theory fails.

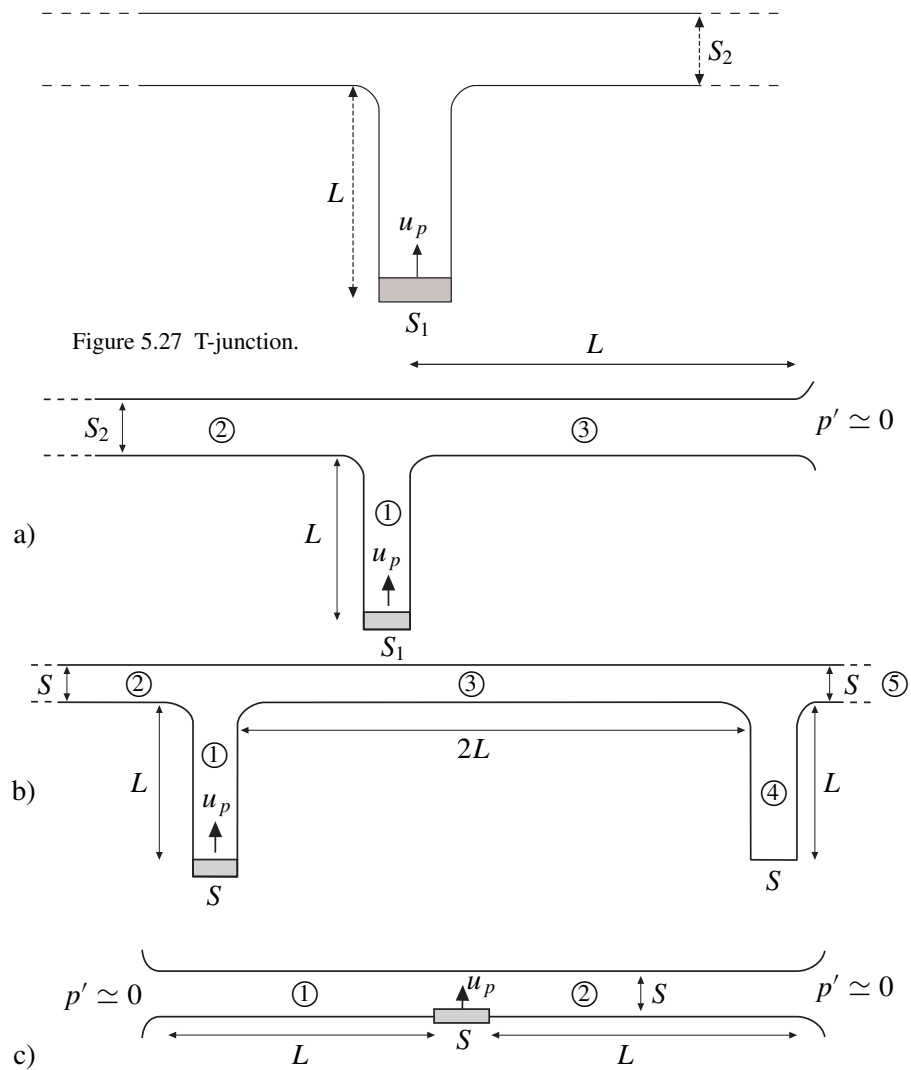


Figure 5.28 Coupled T-junctions.

- e) What is the impedance Z_p of the piston for the configurations of figure 5.28a, b and c. Assume that radiation losses at the open ends are negligible. Neglect friction in the pipe. Are these configurations at certain critical frequencies equivalent to closed resonators?
- f) Consider a clarinet as a cylindrical pipe segment of 2 cm diameter and 1 m long driven by a piston with a velocity $u_p = \hat{u}_p e^{i\omega t}$. Assume that $\hat{u}_p = 1$ m/s which is a typical order of magnitude. Assume that the pipe is driven at the first (lowest) resonance frequency. Calculate the pressure at the piston assuming an ideal open end behaviour without radiation losses or flow separation. Calculate the amplitude of the fluid particle displacement at the pipe end. Calculate the same quantities if a quasi-stationary model is

used at the pipe end to describe flow separation of the outgoing acoustic flow while friction is neglected. Is a quasi-stationary model reasonable?

- g) A pipe segment with a different cross sectional area S_2 than the cross section S_1 of the rest of the pipe can be used as a filter to prevent the propagation of waves generated by a piston. Two solutions can be considered $S_2 > S_1$ and $S_1 < S_2$ (figure 5.29a and b). Assuming an ideal open end at $x = L_1 + L_2 + L_3$, provide a set of equations from which we can calculate the amplitude of the acoustic velocity \hat{u}_{end} at the pipe end for a given velocity \hat{u}_p of the piston.

h) *Introduction:*

A possible 3-D model for a kettle drum consists of a cavity in free space, with acoustic perturbations $p = \hat{p} e^{i\omega t}$ in- and outside the cavity:

$$\nabla^2 \hat{p} + k^2 \hat{p} = 0, \quad i\omega\rho_0 \hat{\mathbf{u}} + \nabla \hat{p} = 0$$

for $k = \omega/c_0$. The cavity is hard-walled on all sides ($\hat{\mathbf{u}} \cdot \mathbf{n} = 0$) except one, which is closed by an elastic membrane (tension T , mass density σ). The membrane displacement $\eta = \hat{\eta} e^{i\omega t}$ is driven by (and drives...) the pressure difference across the membrane:

$$T \nabla^2 \hat{\eta} + \omega^2 \sigma \hat{\eta} = p_{upper} - p_{lower}$$

The normal velocity $\hat{\mathbf{u}} \cdot \mathbf{n}$ at both sides of the membrane is equal to $\partial \eta / \partial t = i\omega \hat{\eta} e^{i\omega t}$, as the air follows the membrane.

A basic musical question is: what is the spectrum of this system, *i.e.* for which (discrete) set $\{\omega_n\}$ does there exist a solution without forcing? Note that since the waves radiate away into free space any solution will decrease and die out (called “radiation damping”), and (in general) the possible ω_n 's will be *complex*, with $\text{Im}(\omega_n) > 0$.

Problem:

A 1-D variant of the kettle drum problem is a semi-infinite pipe ($0 \leq x < \infty$) of typical radius a , closed

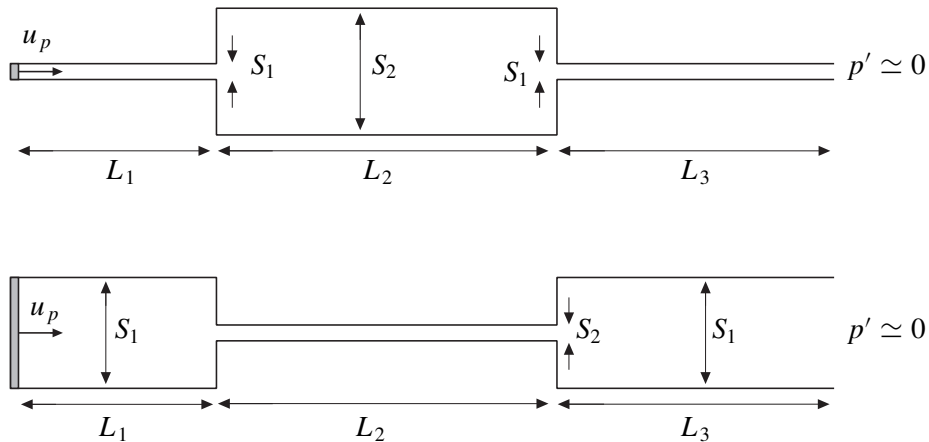


Figure 5.29 Resonators in a pipe.

at $x = 0$, and a piston-like element at $x = L$ (modelling the membrane) driven by the pressure difference across $x = L$, and kept in position by a spring.

$$\begin{aligned} \hat{p}_{xx} + k^2 \hat{p} &= 0 && \text{for } x \in (0, L) \cup (L, \infty) \\ -8Ta^{-2} \hat{\eta} + \omega^2 \sigma \hat{\eta} &= \hat{p}(L+) - \hat{p}(L-) && \text{at } x = L \\ \hat{p}_x &= 0 && \text{at } x = 0 \\ \hat{p}_x &= \omega^2 \rho_0 \hat{\eta} && \text{at } x = L \\ \text{outgoing waves} &&& \text{for } x \rightarrow \infty. \end{aligned}$$

Determine the equation for ω , solve this for some simple cases, and try to indicate the general solution graphically in the complex ω -plane for dimensionless groups of parameters. Are there solutions with $\text{Im}(\omega) = 0$? How are these to be interpreted physically?

- i) Consider the Helmholtz resonator as an acoustic mass-spring system. What are the acoustic mass m and the spring constant K of this mass-spring system.
- j) Assuming that $p'_{ex} = 0$, how would the Helmholtz resonator react to a periodic volume injection $Q = \hat{Q} e^{i\omega t}$ into the bottle (e.g. a piston moving in the bottom wall).

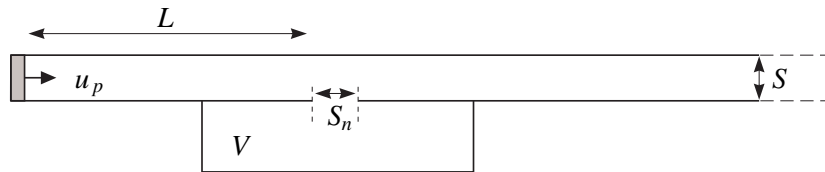


Figure 5.30 Helmholtz resonator driven by a piston.

- k) Consider a Helmholtz resonator in a semi-infinite pipe driven by a piston at $x = 0$ (figure 5.30). Calculate the transmitted acoustic field following linear theory. What is the condition for which there is no transmission.

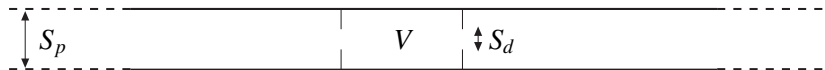


Figure 5.31 Two orifices

- l) Consider the volume V between two orifices of equal aperture surface $S_d \ll S_p$ in a pipe of surface S_p (figure 5.31). Calculate the transmission coefficient and reflection coefficient following linear theory for an acoustic wave $p^+ e^{i\omega t - ikx}$ incident from the left.
- m) Consider a volume V filled with air connected by a short pipe of length ℓ to a pipe filled with water (figure 5.32). Calculate the reflection and transmission coefficient following linear theory for a wave $p^+ e^{i\omega t - ikx}$ incident from the left.

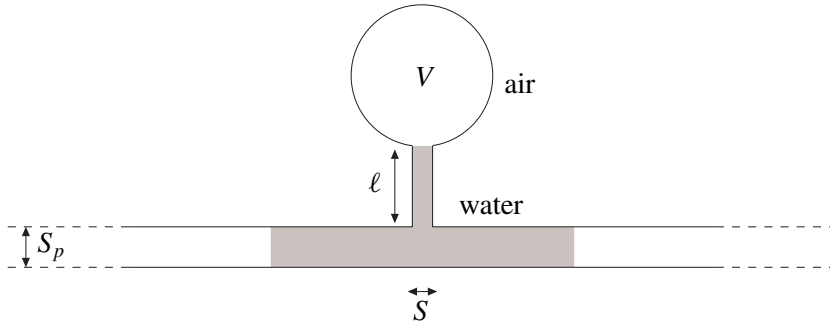


Figure 5.32 Exercise m

- n) Assuming $\rho_0 \omega \ell \hat{u} \gg \frac{1}{2} \rho_0 \hat{u}^2$, estimate the maximum acoustic velocity \hat{u} which can be reached for given volume injection $\hat{Q} e^{i\omega t}$ in a Helmholtz resonator if friction and heat transfer are neglected. Compare this with the maximum pressure which can be reached in a $\frac{1}{4}\lambda$ pipe resonator (with one open end).
- o) Calculate the value of $\hat{p}_{in}/\hat{p}_{ex}$ at resonance for a Helmholtz resonator in the presence of mean flow of velocity u_0 through the neck.
- p) Using the integral formulation (3.12) on $[0, L]$ using the Green's function g_a corresponding to the geometry of figure 5.18a (with $(\partial g_a/\partial y)_{y=0} = 0$ and $(g_a)_{y=L}$ corresponding to the impedance of the pipe seen from the position $y = 0$) we find:

$$p' = -\rho_0 c_0^2 \int_{-\infty}^t \left[\left(\frac{\partial g_a}{\partial \tau} \right) u'(y, \tau) \right]_{y=0} d\tau.$$

Derive this equation starting from (3.12). This equation is equivalent to (5.73).

- q) Calculate the expected acoustic *optimal* amplitude in a vertical Rijke tube of 1 m length and 5 cm diameter in which a gauze with a strip of width $w = 1$ mm has been placed at $x = -0.25$ m. Do you expect that at this amplitude vortex shedding at the pipe end will be a significant acoustic energy loss mechanism?
- r) Consider a Helmholtz resonator with a volume V and a slot aperture $w \times B$ placed in a wall with a grazing flow (figure 5.23). Given that the maximum power is given by

$$W = 0.05 \frac{1}{2} \rho_0 u_0^2 \hat{u} w B$$

estimate the amplitude of the acoustic pressure \hat{p} in the resonator for air if:

$$V = 3 \text{ m}^3, \quad w = 0.3 \text{ m}, \quad B = 0.5 \text{ m}.$$

(A car with open roof!). Assume that the effective neck length is $\ell \simeq w$.

- s) Give an order of magnitude of the acoustical pressure fluctuations in a clarinet.

6 Spherical waves

6.1 Introduction

In the previous chapter we have considered the low frequency approximation of the acoustics of pipes and resonators. Radiation of sound from such systems was assumed to be a small effect for the internal acoustic field, and therefore could be neglected in our analysis. However, if sound would not escape we would not hear it. Hence, for the calculation of environmental noise the radiation is crucial. Furthermore, as sound often is transferred through walls, the vibration of elastic structures is an essential part of the radiation path. To keep things manageable we will assume that the vibrating objects are small compared to the wave length (compact bodies) and that we radiate sound into an unbounded homogeneous quiescent fluid (free space).

Starting from an exact solution of the acoustic field induced by the pulsation and translation of a sphere (section 6.2) we will derive an expression for the free field Green's function G_0 (6.36,6.37). Taylor's series expansion of G_0 will be used to introduce the concepts of monopole, dipole, quadrupole, etc, and multipole expansion (section 6.3). The method of images will appear to be a very powerful tool to get insight into the effect of boundaries on radiation (section 6.4). After a summary of the classical application of Lighthill's analogy to free jets (section 6.5) we will consider the radiation of a compact body by using Curle's formalism (section 6.6). This will be used to get insight into the sound generated by a ventilator. Finally the radiation from an open pipe termination will be discussed (section 6.7).

Note. Two-dimensional acoustic waves have a complex structure as may be seen from the Green's functions given in Appendix E (see the discussion by Dowling *et al.* [55]).

6.2 Pulsating and translating sphere

The wave equation in 3-D allows quite complex solutions. However, for the particular case of a spherically symmetric acoustic field the wave equation reduces to:

$$\frac{1}{c_0^2} \frac{\partial^2 p'}{\partial t^2} - \frac{1}{r^2} \frac{\partial}{\partial r} \left(r^2 \frac{\partial p'}{\partial r} \right) = 0 \quad (6.1)$$

where r is the distance between the observation point and the origin. The key for solving (6.1) is that we can formulate a 1-D wave equation for (rp') :

$$\frac{1}{c_0^2} \frac{\partial^2(rp')}{\partial t^2} - \frac{\partial^2(rp')}{\partial r^2} = 0. \quad (6.2)$$

This result can easily be understood because acoustic energy scales with p'^2 (equation 2.80a). Hence, as the surface of a spherical wave increases with r^2 the amplitude $p'(r)$ should decrease as r^{-1} to keep energy constant as the wave propagates.

Compared to 1-D waves the relationship between pressure p' and acoustic velocity v' now shows a drastically new behaviour which depends on the ratio of r and the acoustic wave length. In three dimensions we have a region with $kr \ll 1$ called “near field” in which we find a behaviour of v' which is close to that of an incompressible flow, while for $kr \gg 1$ we find a “far field” region in which the waves behave locally as plane waves. The radius of curvature of the wave front is large compared to the wave length.

These features may be derived from the radial component of the (linearized) momentum conservation law:

$$\rho_0 \frac{\partial v'}{\partial t} = -\frac{\partial p'}{\partial r} \quad (6.3a)$$

and the linearized mass conservation law:

$$\frac{\partial(\rho' r^2)}{\partial t} = -\rho_0 \frac{\partial(v' r^2)}{\partial r}. \quad (6.3b)$$

The mass in a volume shell $4\pi r^2 dr$ changes as a result of the difference between $4\pi r^2 v'$ and $4\pi(r + dr)^2 v'(r + dr)$ in flux. We eliminate ρ' by using the constitutive equation $p' = c_0^2 \rho'$, and eliminate v' by subtracting the time derivative of r^2 times the momentum equation (6.3a) from the spatial derivative of the mass equation (6.3b). This yields the wave equation (6.1).

The general, formal solution of (6.2) is:

$$rp' = \mathcal{F}\left(t - \frac{r}{c_0}\right) + \mathcal{G}\left(t + \frac{r}{c_0}\right), \quad (6.4)$$

combining an outgoing wave \mathcal{F} and an incoming wave \mathcal{G} . Far away there is no incoming wave, so we *define* the “free field” as the region for which $\mathcal{G} = 0$. This result of a vanishing incoming wave in free space may also be formulated as a boundary condition at $r \rightarrow \infty$ (2.23a, 2.23b, 2.25).

As already stated, the acoustic velocity v' has a rather complex behaviour, in contrast with the 1-D situation. This behaviour is found by substitution of (6.4) into the momentum conservation law (6.3a):

$$\rho_0 \frac{\partial v'}{\partial t} = -\frac{\partial p'}{\partial r} = \frac{1}{r^2} \mathcal{F}\left(t - \frac{r}{c_0}\right) + \frac{1}{c_0 r} \mathcal{F}'\left(t - \frac{r}{c_0}\right). \quad (6.5)$$

We now observe that the first term of (6.5) corresponds, for r/c_0 much smaller than the typical inherent time scale, to an incompressible flow behaviour ($r^2 v' = \text{constant}$) while the second term corresponds to wave-like phenomena. Only the second term does contribute to the acoustic energy flux $\langle I \rangle = \langle p' v' \rangle$. This may be verified by substitution of a harmonic solution into (6.5):

$$p' = \hat{p} e^{i\omega t} = \frac{A}{4\pi r} e^{i\omega t - ikr} \quad (6.6)$$

we find

$$\hat{v} = \frac{\hat{p}}{i\omega\rho_0 r} + \frac{\hat{p}}{\rho_0 c_0} = \frac{\hat{p}}{\rho_0 c_0} \left(-\frac{i}{kr} + 1 \right). \quad (6.7)$$

The first term in \hat{v} is $\frac{1}{2}\pi$ out of phase with \hat{p} and therefore does not contribute to $\langle I \rangle = \langle p' v' \rangle$. Hence:

$$\langle p' v' \rangle = \frac{1}{4} (\hat{v} \hat{p}^* + \hat{v}^* \hat{p}) = \frac{\hat{p} \hat{p}^*}{2\rho_0 c_0}. \quad (6.8)$$

A very systematic discussion of this fundamental solution is given by Lighthill [126].

Using (6.5) we can now determine the acoustic field generated by a pulsating sphere of radius $a(t)$. If $(\partial a / \partial t) / c_0 \ll 1$, we can use linear acoustics, while the movement of the sphere boundary yields the equation derived from (6.5):

$$\rho_0 \frac{\partial^2 a}{\partial t^2} = \frac{1}{a^2} \mathcal{F} \left(t - \frac{a}{c_0} \right) + \frac{1}{c_0 a} \mathcal{F}' \left(t - \frac{a}{c_0} \right). \quad (6.9)$$

For a compact sphere the first term is dominating ($a(\partial^2 a / \partial t^2) / c_0^2 \ll 1$). We find exactly the result which we could anticipate from (2.61), the second derivative to time of the volume of the sphere is the source of sound.

A steady expansion of the sphere ($\partial a / \partial t = \text{constant}$) does not (in this approximation) generate sound. The second term of (6.9) is dominating for large sphere radii ($a(\partial^2 a / \partial t^2) / c_0^2 \gg 1$). In such a case the action of the wall movement is that of a piston which generates plane waves. For harmonic oscillations of the sphere ($a = a_0 + \hat{a} e^{i\omega t}$), the amplitude A of the radiated field is found from (6.6) by substitution of $\hat{v} = i\omega \hat{a}$ in (6.7) at $r = a_0$.

$$\hat{p}(a_0) = \frac{A}{4\pi a_0} e^{-ika_0} = -\frac{\omega^2 \rho_0 a_0 \hat{a}}{1 + ika_0}.$$

Hence

$$\hat{p}(r) = -\rho_0 c_0^2 k \hat{a} \frac{k^2 a_0^2}{1 + ika_0} \frac{e^{-ik(r-a_0)}}{kr}. \quad (6.10)$$

We can also determine the acoustic impedance Z

$$Z(\omega) = \frac{\hat{p}(a_0)}{\hat{v}(a_0)} = \frac{\hat{p}(a_0)}{i\omega\hat{a}} \quad (6.11)$$

Using (6.7) we find:

$$\frac{Z}{\rho_0 c_0} = \frac{ika_0}{1 + ika_0} = \frac{ika_0 + (ka_0)^2}{1 + (ka_0)^2}. \quad (6.12)$$

We see that the real part of the radiation impedance of a compact sphere ($ka_0 \ll 1$) is very small:

$$\operatorname{Re}\left(\frac{Z}{\rho_0 c_0}\right) \simeq (ka_0)^2 \quad (6.13)$$

Hence (see (3.17)) a compact vibrating object in free space will be a very ineffective source of sound. This effect becomes even more dramatic when we consider the radiation of a compact vibrating object of constant volume. The most simple example of this behaviour is a translating sphere of constant radius a_0 . This is what we call a dipole radiation source, in contrast to the monopole source corresponding to a compact pulsating sphere.

The solution of the problem is easily obtained since we can generate from the spherically symmetric solution (6.4) non-spherically symmetric solutions by taking a spatial derivative (see equation 2.24b). If φ is a (spherically symmetric) solution of the wave equation:

$$\frac{1}{c_0^2} \frac{\partial^2 \varphi}{\partial t^2} - \nabla^2 \varphi = 0 \quad (6.14)$$

then any derivative of φ , such as $(\partial\varphi/\partial x_i)$ or $(\partial\varphi/\partial t)$, is also a solution:

$$\frac{1}{c_0^2} \frac{\partial^2}{\partial t^2} \left(\frac{\partial\varphi}{\partial x_i} \right) - \nabla^2 \left(\frac{\partial\varphi}{\partial x_i} \right) = 0, \quad (6.15)$$

in particular, any derivative of Eq. (6.6) is a solution. So if we try to find the field of a translating sphere with velocity v_0 (in x -direction), where at its surface the radial flow velocity is given by:

$$v'(a_0, \vartheta) = \left. \frac{\mathbf{v}_0 \cdot \mathbf{r}}{a_0} \right|_{|r|=a_0} = v_0 \cos \vartheta. \quad (6.16)$$

we can use the derivative in the x -direction. For a harmonic oscillation $v_0 = \hat{v}_0 e^{i\omega t}$ with $(\hat{v}_0/\omega a_0) \ll 1$ the pressure field p' is given by:

$$\hat{p} = A \frac{\partial}{\partial x} \left(\frac{e^{-ikr}}{r} \right) = A \cos \vartheta \frac{\partial}{\partial r} \left(\frac{e^{-ikr}}{r} \right) \quad (6.17)$$

because $\frac{\partial r}{\partial x} = \cos \vartheta$. This pressure is related to the acoustic velocity v' by the momentum conservation law (6.3a):

$$i\omega\rho_0\hat{v} = -A \cos \vartheta \frac{\partial^2}{\partial r^2} \left(\frac{e^{-ikr}}{r} \right). \quad (6.18)$$

Using the boundary condition (6.16) for $r = a_0$ we can now calculate the amplitude A for given \hat{v}_0 :

$$i\omega\rho_0\hat{v}_0 = -A \frac{2 + 2ika_0 - (ka_0)^2}{a_0^3} e^{-ika_0} \quad (6.19)$$

so that the pressure field (6.17) can be written as:

$$\hat{p} = \frac{-i\omega\rho_0\hat{v}_0 a_0^3 \cos \vartheta}{2 + 2ika_0 - (ka_0)^2} \frac{\partial}{\partial r} \left(\frac{e^{-ik(r-a_0)}}{r} \right). \quad (6.20)$$

In the limit of $(ka_0) \ll 1$ we see that:

$$\hat{p} \simeq -\frac{1}{2}(ka_0)^2 \rho_0 c_0 \hat{v}_0 \frac{a_0 \cos \vartheta}{r} \left(1 - \frac{i}{kr} \right) e^{-ikr}. \quad (6.21)$$

Again we observe a near field behaviour with a pressure decreasing as r^{-2} and for which \hat{p} is $\frac{1}{2}\pi$ out of phase with \hat{v}_0 . This pressure field simply corresponds to the inertia of the incompressible flow induced by the movement of the fluid from the front towards the back of the moving sphere. From (6.21) for $r = a_0$ with $(ka_0) \ll 1$ we see that:

$$\hat{p}(a_0) = \frac{1}{4}\rho_0 c_0 \hat{v}_0 \cos \vartheta (2ika_0 + i(ka_0)^3 + (ka_0)^4 + \dots). \quad (6.22)$$

Hence, as the drag on the sphere, which is in phase with \hat{v}_0 , scales as $a_0^2 \text{Re}[\hat{p}(a_0)]$, we see that the acoustic power generated by the sphere scales as $\rho_0 c_0 \hat{v}_0^2 a_0^2 (ka_0)^4$. This is a factor $(ka_0)^2$ weaker than the already weak radiation power of a compact pulsating sphere. So we now understand the need of a body in string instruments or of a sound board in a piano. While the string is a compact oscillating cylinder (row of oscillating spheres), which does not produce any significant sound directly, it induces vibrations of a plate which has dimensions comparable with the acoustic wave length and hence is radiating with an acoustic impedance $\rho_0 c_0$ which is a factor $(ka_0)^4$ more efficient than direct radiation by the string.

Note. In order to provide a stable sound one should avoid in string instruments elastic resonances of the body which are close to that of the string. If this is not the case the two oscillators start a complex interaction, which is called for a violin a “wolf tone”, because it has a chaotic behaviour [135].

Having discussed aspects of bubble acoustics in a pipe in section 4.4.5, we will now consider some specific free field effects. Consider the oscillation of a compact air bubble in water as a response to an incident plane wave $p_{in} = \hat{p}_{in} e^{i\omega t - ikx}$ in free space (deep under water). We can locally assume

the pressure p_b in the bubble to be uniform and we assume a spherical oscillation of the bubble of equilibrium radius a_0 :

$$a = a_0 + \hat{a} e^{i\omega t}. \quad (6.23)$$

The pressure in the bubble is given by:

$$p'_b = p'_{in} + p'_r(a_0) \quad (6.24)$$

where $p'_r(a_0)$ is the acoustic pressure due to the spherical waves generated by the bubble oscillation. We have neglected surface tension. Furthermore, we assume an ideal gas behaviour in the bubble:

$$\frac{p'_b}{p_0} = -3\gamma \frac{a'}{a_0} \quad (6.25)$$

where $\gamma = 1$ for isothermal compression and $\gamma = C_p/C_v$ for isentropic compression. $\hat{p}_r(a)$ is related to \hat{a} by the impedance condition:

$$\hat{p}_r(a) = i\omega \hat{a} Z \quad (6.26)$$

and $Z(\omega)$ is given by equation (6.12). Hence combining (6.24) with (6.25) and (6.26) we find:

$$-\frac{3\gamma p_0}{a_0} \hat{a} = \hat{p}_{in} + i\omega \hat{a} Z \quad (6.27)$$

or:

$$\hat{p}_r(a_0) = i\omega \hat{a} Z = -\frac{\hat{p}_{in}}{1 - i \frac{3\gamma p_0}{\omega a_0 Z}} \quad (6.28)$$

and

$$\hat{p}_r = \hat{p}_r(a_0) \frac{a_0}{r} e^{-ik(r-a_0)}. \quad (6.29)$$

Using (6.12) we can write (6.28) as:

$$\hat{p}_r(a_0) = -\frac{\hat{p}_{in}}{1 - \left(\frac{\omega_0}{\omega}\right)^2 (1 + ika_0)} \quad (6.30)$$

where ω_0 is the Minnaert frequency defined by:

$$\omega_0^2 = \frac{3\gamma p_0}{\rho_0 a_0^2}. \quad (6.31)$$

It is interesting to note that at resonance ($\omega = \omega_0$) under typical conditions a bubble is compact because:

$$(k_0 a_0)^2 = \left(\frac{\omega_0 a_0}{c_0}\right)^2 = \frac{3\gamma p_0}{\rho_0 c_0^2} \quad (6.32)$$

is small as long as $p_0 \ll \rho_0 c_0^2$.

For water $\rho_0 c_0^2 = 2 \times 10^4$ bar, hence up to $p_0 = 100$ bar one can still assume bubble oscillations at resonance to be compact. Equation (6.30) has many interesting further applications [55, 118]. For example, sonar detection of fishes by using a sweeping incident sound frequency yields information about the size of fishes because the resonance frequency ω_0 of the swim bladder yields information on the size a_0 of the fish. Furthermore, at resonance sound is scattered quite efficiently:

$$\hat{p}_r = -i \frac{\hat{p}_{in}}{k_0 r} e^{-ik(r-a_0)}. \quad (6.33)$$

Hence the fish scatters sound with an effective cross section of the order of the acoustic wave length at ω_0 (an effective increase of the cross section by a factor $(k_0 a_0)^{-1}$). As we know a_0 from ω_0 the intensity of the scattered field yields information on the amount of fish. Another fascinating effect of bubble resonance is the very specific sound of rain impact on water [189].

6.3 Multipole expansion and far field approximation

The free field Green's function G_0 defined by equation (3.1)

$$\frac{\partial^2 G_0}{\partial t^2} - c_0^2 \sum \frac{\partial^2 G_0}{\partial x_i^2} = \delta(\mathbf{x} - \mathbf{y}) \delta(t - \tau) \quad (3.1)$$

and the Sommerfeld radiation condition (2.25), may be found in Appendix E, but can be derived as follows. We start with considering the Fourier transform \hat{G}_0 of G_0 , with

$$G_0 = \int_{-\infty}^{\infty} \hat{G}_0 e^{i\omega t} d\omega$$

and satisfying

$$\sum \frac{\partial^2 \hat{G}_0}{\partial x_i^2} + k^2 \hat{G}_0 = -\frac{1}{2\pi c_0^2} \delta(\mathbf{x} - \mathbf{y}) e^{-i\omega\tau}, \quad (6.34)$$

where $k = \omega/c_0$. From symmetry arguments, \hat{G}_0 can only be a function of distance $r = |\mathbf{x} - \mathbf{y}|$, so the solution of (6.34) has the form (see equation (6.6))

$$\hat{G}_0 = \frac{A}{4\pi r} e^{-ikr} \quad (6.35)$$

where A is to be determined. Integration of (6.34) over a small sphere B_ε around \mathbf{y} , given by, say, $r = \varepsilon$, yields by application of Gauss' theorem

$$\begin{aligned} \iiint_{B_\varepsilon} \sum \frac{\partial^2 \hat{G}_0}{\partial x_i^2} + k^2 \hat{G}_0 \, d\mathbf{x} &= \iiint_{B_\varepsilon} -\frac{1}{2\pi c_0^2} \delta(\mathbf{x} - \mathbf{y}) e^{-i\omega\tau} \, d\mathbf{x} = \\ \iint_{\partial B_\varepsilon} \sum \frac{\partial \hat{G}_0}{\partial x_i} n_i \, d\sigma + \iiint_{B_\varepsilon} k^2 \hat{G}_0 \, d\mathbf{x} &= 4\pi \varepsilon^2 \frac{\partial \hat{G}_0}{\partial r} + O(\varepsilon^2) = -A + O(\varepsilon) = -\frac{1}{2\pi c_0^2} e^{-i\omega\tau} \end{aligned}$$

where n_i denotes the outward normal of B_ε , and we used the fact that ε is small. If we let $\varepsilon \rightarrow 0$ we find that $A = (2\pi c_0^2)^{-1} e^{-i\omega\tau}$. So we have:

$$\hat{G}_0 = \frac{e^{-i\omega\tau - ikr}}{8\pi^2 c_0^2 r} = \frac{e^{-i\omega(\tau + r/c_0)}}{8\pi^2 c_0^2 r} \quad (6.36)$$

(note the factor $-1/2\pi$ difference with the Green's function of a regular Helmholtz equation) and, using equation (C.33),

$$G_0 = \frac{\delta(t - \tau - r/c_0)}{4\pi r c_0^2}. \quad (6.37)$$

In order to derive the general multipole expansion we will first consider the field at a single frequency. By using the free-field Green's function (Appendix E) we find the acoustic field for a given time-harmonic source distribution $\hat{q}(\mathbf{x}) e^{i\omega t}$ in a finite volume V to be given by

$$\hat{\rho}' = \frac{\hat{p}'}{c_0^2} = \iiint_V \hat{q}(\mathbf{y}) \hat{G}_0(\mathbf{x}|\mathbf{y}) \, d\mathbf{y} = \iiint_V \hat{q}(\mathbf{y}) \frac{e^{-ikr}}{4\pi c_0^2 r} \, d\mathbf{y}. \quad (6.38)$$

Suppose the origin is chosen inside V . We are interested in the far field, *i.e.* $|\mathbf{x}|$ is large, and a compact source, *i.e.* kL is small where L is the typical diameter of V . This double limit can be taken in several ways. As we are interested in the radiation properties of the source, which corresponds with $k|\mathbf{x}| \geq O(1)$, we will keep $k\mathbf{x}$ fixed. In that case the limit of small k is the same as small \mathbf{y} , and we can expand in a Taylor series around $\mathbf{y} = \mathbf{0}$

$$\begin{aligned} r &= (|\mathbf{x}|^2 - 2(\mathbf{x} \cdot \mathbf{y}) + |\mathbf{y}|^2)^{1/2} = |\mathbf{x}| \left(1 - \frac{\mathbf{x} \cdot \mathbf{y}}{|\mathbf{x}|^2} + \frac{|\mathbf{y}|^2}{2|\mathbf{x}|^2} - \frac{(\mathbf{x} \cdot \mathbf{y})^2}{2|\mathbf{x}|^4} + \dots \right) \\ &= |\mathbf{x}| \left(1 - \frac{|\mathbf{y}|}{|\mathbf{x}|} \cos \theta + \frac{1}{2} \frac{|\mathbf{y}|^2}{|\mathbf{x}|^2} \sin^2 \theta + \dots \right) \end{aligned}$$

(where θ is the angle between \mathbf{x} and \mathbf{y}) and

$$\begin{aligned} \frac{e^{-ikr}}{r} &= \frac{e^{-ik|\mathbf{x}|}}{|\mathbf{x}|} \left(1 + (1 + ik|\mathbf{x}|) \frac{1}{|\mathbf{x}|^2} \sum_{j=1}^3 x_j y_j + \dots \right) \\ &= \sum_{l,m,n=0}^{\infty} \frac{y_1^l y_2^m y_3^n}{l! m! n!} \left[\frac{\partial^{l+m+n}}{\partial y_1^l \partial y_2^m \partial y_3^n} \frac{e^{-ikr}}{r} \right]_{y_1=y_2=y_3=0}. \end{aligned} \quad (6.39)$$

As r is a symmetric function in \mathbf{x} and \mathbf{y} , this is equivalent to

$$\frac{e^{-ikr}}{r} = \sum_{l,m,n=0}^{\infty} \frac{(-1)^{l+m+n}}{l! m! n!} y_1^l y_2^m y_3^n \frac{\partial^{l+m+n}}{\partial x_1^l \partial x_2^m \partial x_3^n} \frac{e^{-ik|\mathbf{x}|}}{|\mathbf{x}|}. \quad (6.40)$$

The acoustic field is then given by

$$\hat{\rho}' = \frac{1}{4\pi c_0^2} \sum_{l,m,n=0}^{\infty} \frac{(-1)^{l+m+n}}{l! m! n!} \iiint_V y_1^l y_2^m y_3^n \hat{q}(\mathbf{y}) \, d\mathbf{y} \frac{\partial^{l+m+n}}{\partial x_1^l \partial x_2^m \partial x_3^n} \frac{e^{-ik|\mathbf{x}|}}{|\mathbf{x}|}. \quad (6.41)$$

As each term in the expansion is by itself a solution of the reduced wave equation, this series yields a representation in which the source is replaced by a sum of elementary sources (monopole, dipoles, quadrupoles, in other words, multipoles) placed at the origin ($\mathbf{y} = 0$). Expression (6.41) is the multipole expansion of a field from a finite source in Fourier domain. From this result we can obtain the corresponding expansion in time domain as follows.

With Green's function (6.37) we have the acoustic field from a source $q(\mathbf{x}, t)$

$$\rho' = \int_{-\infty}^{\infty} \iiint_V q(\mathbf{y}, \tau) \frac{\delta(t - \tau - r/c_0)}{4\pi r c_0^2} \, d\mathbf{y} d\tau = \iiint_V \frac{q(\mathbf{y}, t - r/c_0)}{4\pi r c_0^2} \, d\mathbf{y} \quad (6.42)$$

If the dominating frequencies in the spectrum of $q(\mathbf{x}, t)$ are low, such that $\omega L/c_0$ is small, we obtain by Fourier synthesis of (6.41) the multipole expansion in time domain (see Goldstein [73])

$$\begin{aligned} \rho' &= \frac{1}{4\pi c_0^2} \sum_{l,m,n=0}^{\infty} \frac{(-1)^{l+m+n}}{l! m! n!} \frac{\partial^{l+m+n}}{\partial x_1^l \partial x_2^m \partial x_3^n} \left[\frac{1}{|\mathbf{x}|} \iiint_V y_1^l y_2^m y_3^n q(\mathbf{y}, t - |\mathbf{x}|/c_0) \, d\mathbf{y} \right] \\ &= \sum_{l,m,n=0}^{\infty} \frac{\partial^{l+m+n}}{\partial x_1^l \partial x_2^m \partial x_3^n} \left[\frac{(-1)^{l+m+n}}{4\pi |\mathbf{x}| c_0^2} \mu_{lmn}(t - |\mathbf{x}|/c_0) \right] \end{aligned} \quad (6.43)$$

where $\mu_{lmn}(t)$ is defined by:

$$\mu_{lmn}(t) = \iiint_V \frac{y_1^l y_2^m y_3^n}{l! m! n!} q(\mathbf{y}, t) \, d\mathbf{y}. \quad (6.44)$$

The (lmn) -th term of the expansion (6.43) is called a multipole of order 2^{l+m+n} . Since each term is a function of $|\mathbf{x}|$ only, the partial derivatives to x_i can be rewritten into expressions containing derivatives to $|\mathbf{x}|$. In general, these expressions are rather complicated, so we will not try to give the general formulas here. It is, however, instructive to consider the lowest orders in more detail as follows.

The first term corresponds to the monopole:

$$\rho'_0 = \frac{\mu_0(t - |\mathbf{x}|/c_0)}{4\pi c_0^2 |\mathbf{x}|} \tag{6.45}$$

where we wrote for brevity $\mu_0 = \mu_{000}$. We have concentrated the source at the origin and

$$\mu_0(t) = \iiint_V q(\mathbf{y}, t) \, d\mathbf{y}. \tag{6.46}$$

The next term is the dipole term:

$$\rho'_1 = - \sum_{i=1}^3 \frac{x_i}{|\mathbf{x}|} \frac{\partial}{\partial |\mathbf{x}|} \left(\frac{\mu_{1,i}(t - |\mathbf{x}|/c_0)}{4\pi c_0^2 |\mathbf{x}|} \right) \tag{6.47}$$

where we wrote for brevity: $\mu_{1,1} = \mu_{100}$, $\mu_{1,2} = \mu_{010}$ and $\mu_{1,3} = \mu_{001}$. If q is a point source this dipole term is easily visualized as shown in figure 6.1.

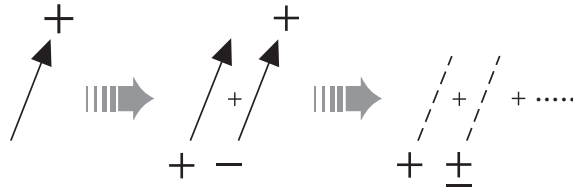


Figure 6.1 First step in the multipole expansion of a point source.

The dipole of strength $\mu_{1,i}$, which we should place at the origin ($\mathbf{y} = 0$):

$$\mu_{1,i}(t) = \iiint_V y_i q(\mathbf{y}, t) \, d\mathbf{y}, \tag{6.48}$$

is obtained by bringing the (point) source q towards the origin while increasing its strength and that of the opposite (point) source $-q$ at the origin in such a way that we keep $|\mathbf{y}|q$ constant.

A dipole field is not isotropic because in a direction normal to the vector \mathbf{y} the two sources forming the dipole just compensate each other, while in the other directions due to a difference in emission

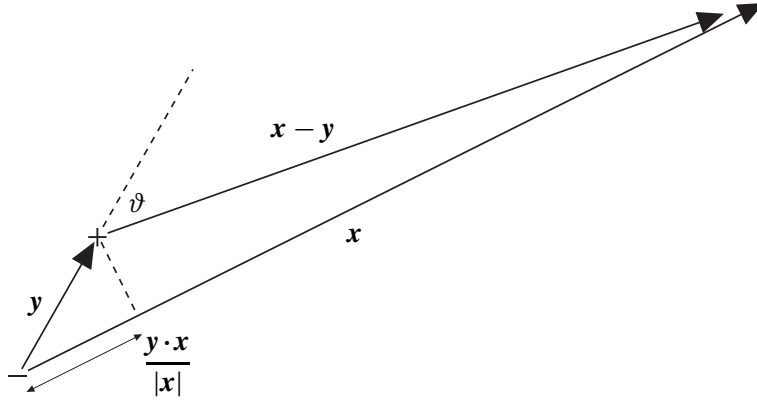


Figure 6.2 Retarded or emission time difference is $(\mathbf{y} \cdot \mathbf{x}/|\mathbf{x}|)/c_0 = (|\mathbf{y}| \cos \vartheta)/c_0$.

time there is a net acoustic field. This effect of the difference in retarded time (figure 6.2) between the sources in the dipole simplifies in the far field as follows. Writing (6.47) as:

$$\rho'_1 = - \sum_{i=1}^3 \frac{x_i}{|\mathbf{x}|} \iiint_V \frac{y_i}{4\pi c_0^2} \left\{ -\frac{1}{c_0 |\mathbf{x}|} \frac{\partial}{\partial t} q(\mathbf{y}, t - |\mathbf{x}|/c_0) - \frac{1}{|\mathbf{x}|^2} q(\mathbf{y}, t - |\mathbf{x}|/c_0) \right\} d\mathbf{y} \quad (6.49)$$

we see that for large distances ($k|\mathbf{x}| \gg 1$) the acoustic field due to the dipole contribution is given by:

$$\rho'_1 \simeq \sum_{i=1}^3 \frac{x_i}{4\pi c_0^3 |\mathbf{x}|^2} \frac{\partial}{\partial t} \iiint_V y_i q(\mathbf{y}, t - |\mathbf{x}|/c_0) d\mathbf{y} = \sum_{i=1}^3 \frac{x_i}{4\pi c_0^3 |\mathbf{x}|^2} \left[\frac{d}{dt_e} \mu_{1,i}(t_e) \right]_{t_e = t - |\mathbf{x}|/c_0} \quad (6.50)$$

where $\mu_{1,i}(t)$ is the dipole strength. If the source has a particular form, for example it represents a force density f_i like in (2.65):

$$q(\mathbf{y}, \tau) = - \sum_{i=1}^3 \frac{\partial f_i}{\partial y_i}, \quad (6.51)$$

we observe that the surface integral of the monopole term vanishes because we assumed a finite source region, outside which $\mathbf{f} = \mathbf{0}$. We see that the force field f_i is equivalent to an acoustic dipole of strength:

$$\mu_{1,i} = \iiint_V f_i d\mathbf{y} \quad (6.52)$$

which corresponds simply to the total force \mathbf{F} on V . In a similar way it is clear that the Lighthill stress tensor T_{ij} induces a quadrupole field because from (2.65) we have:

$$q = \sum_{i,j=1}^3 \frac{\partial^2 T_{ij}}{\partial y_i \partial y_j}.$$

By partial integration it follows that the strength of the quadrupole is:

$$\mu_{2,ij} = \iiint_V T_{ij} \, d\mathbf{x}, \quad (6.53)$$

where we wrote for brevity $\mu_{2,11} = \mu_{200}$, $\mu_{2,12} = \mu_{110}$, $\mu_{2,13} = \mu_{101}$, etc. . In the far field approximation, where the retarded (or emission) time effect can be estimated by replacing $(\partial/\partial|\mathbf{x}|)$ by $-c_0^{-1}(\partial/\partial t)$, we find for a quadrupole field

$$\rho' \simeq \sum_{i,j=1}^3 \frac{x_i x_j}{4\pi c_0^2 |\mathbf{x}|^3} \frac{1}{c_0^2} \left[\frac{d^2}{dt_e^2} \mu_{2,ij}(t_e) \right]_{t_e=t-|\mathbf{x}|/c_0}. \quad (6.54)$$

6.4 Method of images and influence of walls on radiation

Using G_0 we can build the Green's function in presence of walls by using the method of images as discussed in section 4.6. The method of images is simple for a plane rigid wall and for a free surface. In the first case the boundary condition $\mathbf{v}' \cdot \mathbf{n} = 0$ is obtained by placing an image of equal strength q at the image point of the source position (figure 6.3). For a free surface, defined by the condition $p' = 0$ (air/water interface seen from the water side), we place an opposite source $-q$ at the image point.

For a rigid wall at $x_1 = 0$ we simply have the Green's function:

$$G(\mathbf{x}, t|\mathbf{y}, \tau) = \frac{\delta(t - \tau - r/c_0)}{4\pi c_0^2 r} + \frac{\delta(t - \tau - r^*/c_0)}{4\pi c_0^2 r^*} \quad (6.55)$$

where

$$r = \sqrt{(x_1 - y_1)^2 + (x_2 - y_2)^2 + (x_3 - y_3)^2},$$

$$r^* = \sqrt{(x_1 + y_1)^2 + (x_2 - y_2)^2 + (x_3 - y_3)^2}.$$

We easily see from figure 6.3 that a source placed close to a rigid wall will radiate as a source of double strength ($|y_1|k \ll 1$) while a source close to a free surface will radiate as a dipole.

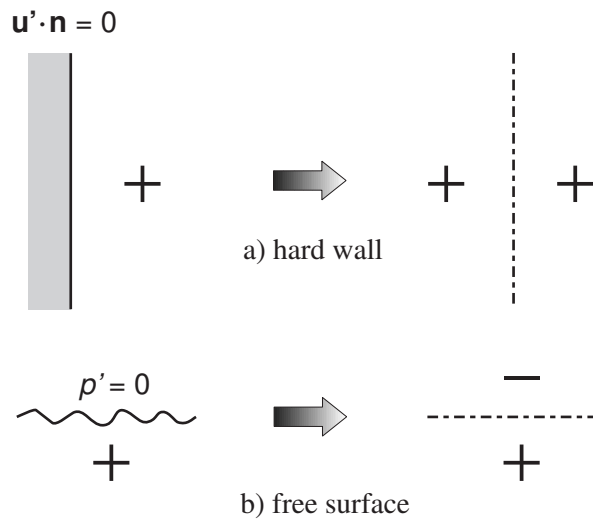


Figure 6.3 Images of sources in plane surfaces

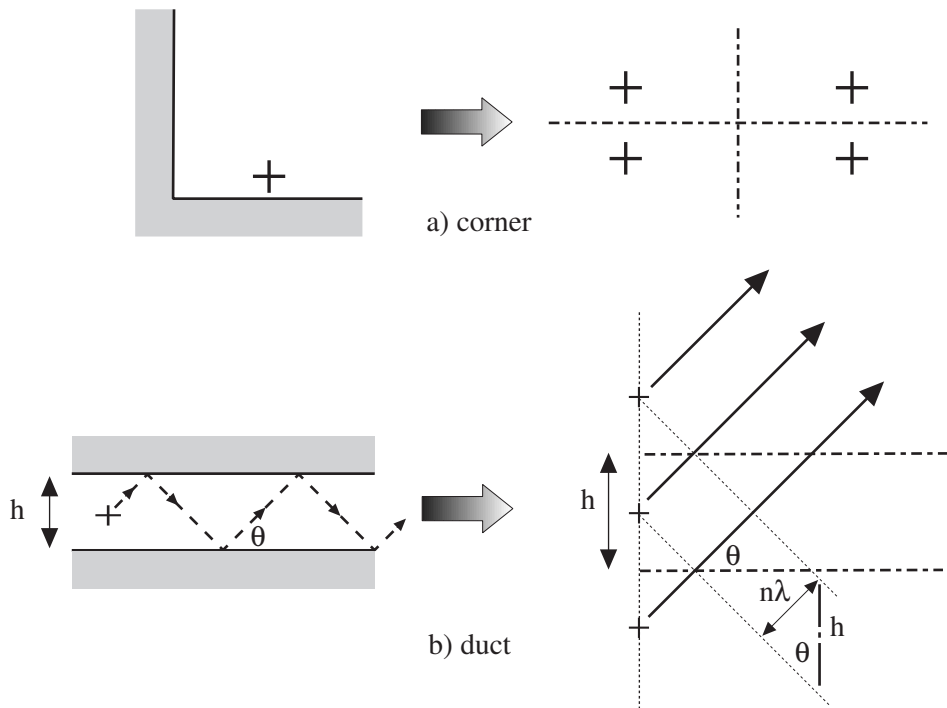


Figure 6.4 Application of the method of images.

When more than a wall is present the method of images can be used by successive reflections against the walls. This is illustrated in figure 6.4. When a harmonic source is placed half way between two rigid walls separated by a distance h (at $y = \frac{1}{2}h$) the radiated field is equivalent to that of an infinite array of sources placed at a distance h from each other (figure 6.4b). We immediately see from this that there are directions ϑ in which the sources in the array interfere positively. The interference condition is simply:

$$h \sin \vartheta = n\lambda; \quad n = 0, 1, 2, \dots \tag{6.56}$$

where λ is the acoustic wave length. For this symmetrically placed source only symmetric modes can occur. When the source is placed at one of the walls ($y = 0$ or h) we find the interference condition given by

$$h \sin \vartheta = \frac{1}{2}n\lambda; \quad n = 0, 1, 2, \dots \tag{6.57}$$

since the source and its images form an array of sources placed at a distance $2h$ from each other.

The condition $n = 0$ corresponds to plane waves in a tube. The conditions $n > 0$ correspond to higher order mode propagation in the “duct” formed by the two walls. This can also be seen for a duct of square cross section for which the image source array becomes two-dimensional. We clearly see from this construction that higher order modes will not propagate at low frequencies because when ($h < \frac{1}{2}\lambda$), there are no other solutions than $\vartheta = 0$ to equation (6.57). This justifies the plane wave approximation used in chapter 4 (see further chapter 7). We see also that at low frequencies (for plane waves) the radial position of a source does not affect the radiation efficiency. For a higher mode, on the other hand, the sound field is not uniform in the duct cross section and the source radiation impedance is position dependent. The first non-planar mode has a pressure node on the duct axis and cannot be excited by a volume source placed on the axis ($\oint p' Q dt = 0$). This explains the difference between condition (6.56) and (6.57) for the excitation of a higher mode. A more comprehensive treatment of pipe modes is given in chapter 7.

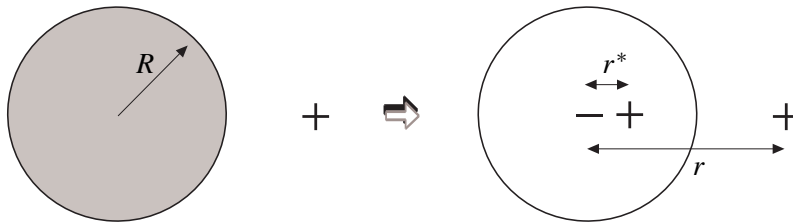


Figure 6.5 Image of a line source in a compact cylinder.

The method of images can also be used for a line source close to a compact cylinder of radius R or a point source near a compact sphere of radius a [142]. For a line source near a cylinder we should place an identical line source at the inverse point r^* defined by:

$$r^* = r (R/|r|)^2 \tag{6.58}$$

and an opposite line source (*i.e.* a sink) at $\mathbf{r} = 0$ on the cylinder axis (figure 6.5). For a sphere we should place a source q^* at \mathbf{r}^* defined by:

$$q^* = q a/|\mathbf{r}| \quad (6.59)$$

and

$$\mathbf{r}^* = \mathbf{r} (a/|\mathbf{r}|)^2 \quad (6.60)$$

while in order to keep the mass balance we place a line of uniformly spaced sinks of total strength q^* stretching from \mathbf{r}^* to the center of the sphere ($\mathbf{r} = 0$) [142].

6.5 Lighthill's theory of jet noise

Consider a free turbulent jet formed at the exit of a circular pipe of diameter D . The mean flow velocity in the pipe is u_0 . We assume that $u_0 \ll c_0$ and that the entropy is uniform (air jet in air with uniform temperature). The key idea of Lighthill was that the sound produced by the turbulence was originated from a volume of order D^3 and that the influence of the pipe walls on the sound radiation could be neglected.

In such a case combining (2.65) with (3.13) and using the free space Green's function G_0 given by (6.37) we find:

$$\rho'(\mathbf{x}, t) = \int_{-\infty}^t \iiint_V \frac{\partial^2 T_{ij}}{\partial y_i \partial y_j} G_0(\mathbf{x}, t|\mathbf{y}, \tau) \, dy d\tau. \quad (6.61)$$

Partial integration (twice) yields:

$$\rho'(\mathbf{x}, t) = \int_{-\infty}^t \iiint_V \frac{\partial^2 G_0}{\partial y_i \partial y_j} T_{ij}(\mathbf{y}, \tau) \, dy d\tau. \quad (6.62)$$

Because G_0 is only a function of $r = |\mathbf{x} - \mathbf{y}|$ we have:

$$\frac{\partial G_0}{\partial y_i} = \frac{\partial G_0}{\partial r} \frac{\partial r}{\partial y_i} = -\left(\frac{x_i - y_i}{r}\right) \frac{\partial G_0}{\partial r} = -\frac{\partial G_0}{\partial x_i}. \quad (6.63)$$

Approaching the source towards the observation point has the same effect as approaching the observation point towards the source. Hence we can write (6.62) as:

$$\rho'(\mathbf{x}, t) = \frac{\partial^2}{\partial x_i \partial x_j} \int_{-\infty}^t \iiint_V G_0(\mathbf{x}, t|\mathbf{y}, \tau) T_{ij}(\mathbf{y}, \tau) \, dy d\tau. \quad (6.64)$$

The integration variable y_i does not interfere with x_i . Using now (6.37) we can carry out the time integration:

$$\rho'(\mathbf{x}, t) = \frac{\partial^2}{\partial x_i \partial x_j} \iiint_V \frac{T_{ij}(\mathbf{y}, t - r/c_0)}{4\pi c_0^2 r} d\mathbf{y}. \quad (6.65)$$

In the far field the only length scale is the wave length, hence we have replaced the problem of the estimate of a space derivative ($\partial/\partial y_i$) at the source by the problem of the estimate of the characteristic frequency of the produced sound. In the far field approximation we have:

$$\rho'(\mathbf{x}, t) \simeq \frac{x_i x_j}{4\pi c_0^2 |\mathbf{x}|^2} \frac{\partial^2}{c_0^2 \partial t^2} \iiint_V \frac{T_{ij}(\mathbf{y}, t - |\mathbf{x}|/c_0)}{|\mathbf{x}|} d\mathbf{y}. \quad (6.66)$$

For high Reynolds number we can neglect the effect of viscosity (if it were not small turbulence would not occur!). If we assume a homentropic compact flow we have (2.68):

$$T_{ij} \simeq \rho_0 v_i v_j. \quad (6.67)$$

The first estimates of Lighthill for a circular¹ free jet are:

- the characteristic time scale for large eddy's in the flow is (D/u_0) .
- the Reynolds stress scales as ρu_0^2 .
- the relevant volume V is of order D^3 .

Hence we should replace $(\partial/\partial t)$ by u_0/D in (6.66) and we find:

$$\rho'(\mathbf{x}, t) \sim \frac{1}{4\pi c_0^4} \left(\frac{u_0}{D}\right)^2 \frac{\rho_0 u_0^2 D^3}{|\mathbf{x}|} \quad (6.68)$$

or in terms of intensity $\overline{\rho'^2}$ and Mach number $M_0 = u_0/c_0$:

$$\overline{\rho'^2} \sim \left(\frac{\rho_0 D}{4\pi |\mathbf{x}|}\right)^2 M_0^8. \quad (6.69)$$

This is the celebrated 8-th power law of Lighthill which ".. represents a triumph of theory over experiment; before the publication of U^8 , most reports of measured jet noise data gave a U^4 variation, which was then quickly recognized, post U^8 , as associated with noise sources *within* the engine itself, rather than with the jet exhaust turbulent mixing downstream of the engine. In fact, variation of intensity with U^8 is now generally accepted as *defining* jet mixing noise .." (Crighton, l.c.); see figure 6.6. Equation (6.69) tells us that turbulence in free space is a very ineffective source of sound. When a more detailed description of the flow is used to estimate T_{ij} one can also find the directivity pattern

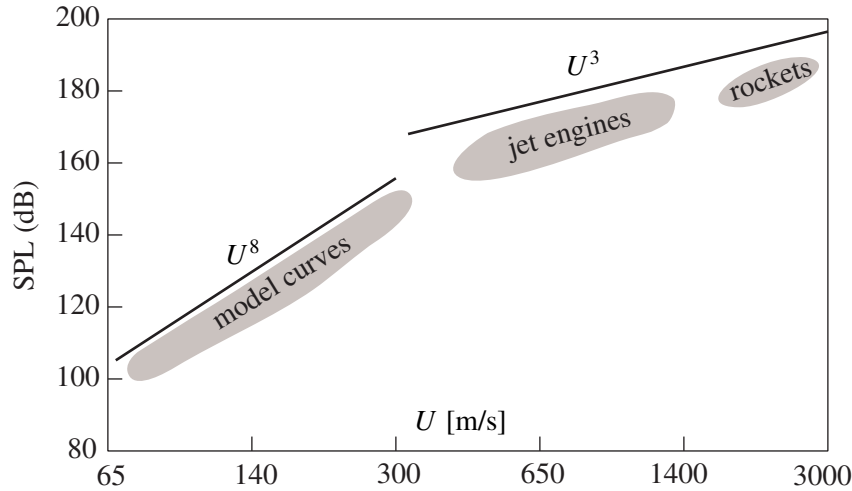


Figure 6.6 Sound power generated by a jet.

of the radiation field [73, 18, 196]. This directivity pattern results from Doppler effects and refraction of the sound waves by the shear layer surrounding the jet.

As the Mach number approaches unity the character of the sound production changes drastically because the flow is not compact any more ($D/\lambda \sim M_0$) and because at higher Mach numbers shock waves appear if the jet is not properly expanded. These shocks generate noise by interaction with turbulence (random vorticity) and vortices (coherent structures) [69].

Moreover, it is obvious that the generated power cannot grow indefinitely with a power M^8 . There is a natural maximum corresponding to the kinetic energy flux in the jet $\frac{1}{2}\rho u_0^3 \cdot \frac{\pi}{4}D^2$. This natural upper bound prevails above $M > 1$ and the sound intensity scales above $M > 1$ as M_0^3 . The typical fraction of flow power transferred to the acoustic field at high Mach number by a properly expanded supersonic jet is 10^{-4} ($M > 1$). Following Goldstein [73] the acoustic power W generated by a subsonic homentropic jet is given by

$$\frac{W}{\frac{1}{8}\rho_0 u_0^3 \pi D^2} = 8 \times 10^{-5} M_0^5. \quad (6.70)$$

Hence at Mach $M_0 = 0.1$ we can estimate that only a fraction 10^{-9} of the hydrodynamic power is transferred to the acoustic field. This is the key of the problem of calculating the acoustic field from a numerical calculation of the flow pattern at low Mach numbers. In order to achieve this we have to calculate the flow field within an accuracy which is far above the typical score (5%) of turbulence modelling nowadays. However, the simple scaling law of Lighthill already tells us that in order to

¹See Bjørnø [17] for planar jets.

reduce turbulence noise we should reduce the Mach number. A very useful result as we will see from exercise k) below.

Lighthill's analogy in the form of equation (6.66) is often used to obtain acoustical information from numerical calculations of turbulent flow. Such calculations can be based on an incompressible model which by itself does not include any acoustic component.

When the jet has a different entropy than the environment (hot jet or different fluid) the sound production at low Mach numbers is dominated by either Morfey's dipole source term $(\partial/\partial y_i)((c^2 - c_0^2)/c_0^2)(\partial p'/\partial y_i)$ or by a volume source term due to diffusion and heat transfer (entropy fluctuations). When a hot gas with constant caloric properties is mixed with the cold environment the monopole sound source is negligible compared to the dipole due to convective effects ([149]). One finds then a sound power which at low Mach numbers scales at M_0^6 . Upon increasing the Mach number the turbulent Reynolds stress can become dominant and a transition to the cold jet behaviour (M_0^8) can be observed in some cases.

In hot jets with combustion, vapour condensation or strongly temperature dependent caloric gas properties the monopole source dominates ([45]), and a typical M_0^4 scaling law is found for $\bar{\rho}^2$.

The influence of the viscosity on the sound generation by a free jet has been studied by Morfey [150], Obermeier [170] and Iafrati [93].

6.6 Sound radiation by compact bodies in free space

6.6.1 Introduction

In principle, when a compact body is present in a flow we have two possible methods to calculate the sound radiation when using Lighthill's theory (section 2.6). In the first case we use a *tailored* Green's function which is often easy to calculate in the far field approximation by using the reciprocity principle (3.4). In the second case we can use the *free field* Green's function G_0 which implies that we should take surface contributions in equation (3.12) into account. This second method is called Curle's method [73, 18]. The advantage of the method of Curle is that we still can use the symmetry properties of G_0 like:

$$\frac{\partial G_0}{\partial y_i} = -\frac{\partial G_0}{\partial x_i}. \quad (6.71)$$

Furthermore, we will see that the surface terms have for compact rigid bodies quite simple physical meaning. We will see that the pulsation of the volume of the body is a volume source while the force on the body is an aero-acoustic dipole. In this way we can in fact say that if we know the aerodynamic (lift and drag) force on a small propeller we can represent the system by the reaction force acting on the fluid as an aero-acoustic source, ignoring further the presence of the body in the calculation of the radiation.

6.6.2 Tailored Green's function

The method of tailored Green's function has of course the nice feature of a simple integral equation (3.13). We will, however, in general not have a simple symmetry relation allowing to move the space derivative outside the integral. The construction of the tailored Green's function in the far field approximation is in fact equivalent to considering the acoustic response of the body to a plane incident wave. In applications like the effect of a bubble on turbulence noise we already did this for a bubble in a duct (section 4.7).

The method of images discussed in section 6.4 is an efficient procedure to construct a Green's function for simple geometries. This is obvious when we consider a plane rigid wall. Using the reciprocity principle we send a plane wave p'_{in} and look at the resulting acoustic field in the source point y . The acoustic field in y is built out of the incident wave p'_{in} and the wave reflected at the surface p'_r . In the method of images we simply assume that p'_r comes from an image source, as shown in figure 6.7.

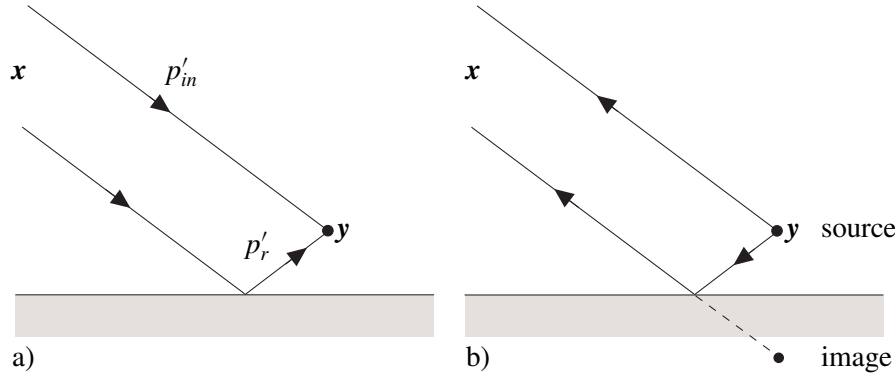


Figure 6.7 a) Acoustic response to a plane wave. b) Sound emitted by the source in the same observers direction.

When calculating the Green's function we should take in free space as amplitude of the incident wave p'_{in} the amplitude calculated from (6.37). For compact bodies or sources close to a surface we can neglect the variation in travel time of p'_{in} over the source region and we find:

$$p'_{in} = \frac{\delta(-t + \tau - |\mathbf{x}|/c_0)}{4\pi |\mathbf{x}|c_0^2} \quad (6.72)$$

where the signs of t and τ have been changed because of reciprocity relation (3.4). When considering harmonic waves we have from (6.36) that:

$$\hat{p}_{in} = \frac{e^{-ikr}}{8\pi^2 c_0^2 r} \quad (6.73)$$

where in the far field approximation $r \simeq |\mathbf{x}|$. The Green's function is found by adding the system response p'_r (or \hat{p}_r) to the incident wave p'_{in} . Once a tailored Green's function has been obtained we

find by using (3.13):

$$\rho'(\mathbf{x}, t) = \int_{-\infty}^t \iiint_V q(\mathbf{y}, \tau) G(\mathbf{x}, t | \mathbf{y}, \tau) \, d\mathbf{y} d\tau. \quad (3.13)$$

By partial integration and assuming that the sources are the volume sources $\partial^2 T_{ij} / \partial x_i \partial x_j$ as defined in (2.65) which are limited to a small region of space we find:

$$\rho'(\mathbf{x}, t) = \int_{-\infty}^t \iiint_V \frac{\partial^2 G}{\partial y_i \partial y_j} T_{ij} \, d\mathbf{y} d\tau. \quad (6.74)$$

Comparison of the space derivative of the tailored Green's function with that of the free space Green's function G_0 yields an amplification factor A of the radiated field:

$$A = \left| \frac{\partial^2 G}{\partial y_i \partial y_j} \right| / \left| \frac{1}{c_0^2} \frac{\partial^2 G_0}{\partial t^2} \right| \quad (6.75)$$

where we made use of the approximation $\partial^2 G_0 / \partial x_i \partial x_j \simeq (\partial^2 G_0 / \partial t^2) / c_0^2$ in the far field, and assumed that the flow is not influenced by the foreign body ($T_{ij} = \text{constant}$).

Using this procedure one can show [18, 55, 73] that turbulence near the edge of a semi-infinite plane produces a sound field for which $\overline{\rho'^2}$ scales as M_0^5 which implies for $M_0 \ll 1$ a dramatic increase (by a factor M_0^{-3}) compared to free field conditions. This contribution to trailing edge noise is very important in aircraft noise and wind turbine noise.

6.6.3 Curle's method

When we place a cylinder of diameter d in a turbulent jet with a main flow velocity u_0 , the cylinder will not only enhance the radiation by the already present turbulence. A cylinder will affect the flow. Behind the cylinder at high Reynolds numbers we have an unstable wake. Above a Reynolds number of $Re = u_0 d / \nu = 40$ the wake structure is dominated by periodic vortex shedding if $40 \leq Re \leq 3 \times 10^5$ and for $Re \geq 3.5 \times 10^6$ [18, 20, 78]. The frequency f_V of the vortex shedding is roughly given by:

$$\frac{f_V d}{u_0} = 0.2. \quad (6.76)$$

Hence the sound produced by vortex shedding has in contrast with turbulence a well-defined frequency. The periodic shedding of vorticity causes an oscillating lift force on the cylinder, with an amplitude L per unit length given by

$$L = -\rho_0 \Gamma u_0, \quad (6.77)$$

where Γ is the circulation of the flow around the cylinder. By definition the lift force is perpendicular to the mean flow direction (\mathbf{u}_0). In dimensionless form the lift is expressed as a lift coefficient C_L :

$$C_L = \frac{L}{\frac{1}{2}\rho u_0^2 d}. \quad (6.78)$$

The lift coefficient of a cylinder is in a laminar flow of order unity. However, C_L is strongly affected by small disturbances and the lift force is not always coherent along the cylinder. This results in a C_L for a rigid stationary cylinder ranging

$$\begin{aligned} &\text{from } (C_L)_{rms} \simeq 0.1 && \text{for } Re \leq 2 \times 10^5 \\ &\text{to } (C_L)_{rms} \simeq 0.3 && \text{for } Re \geq 5 \times 10^5, \\ &\text{while } (C_L)_{peak} \simeq 1.0 && \text{for } Re \leq 2 \times 10^5 \\ &\text{and } (C_L)_{peak} \simeq (C_L)_{rms} && \text{for } Re \geq 2 \times 10^5. \end{aligned}$$

The drag force has a fluctuating component corresponding to $(C_D)_{rms} \simeq 0.03$. Elastic suspension of a cylinder enhance considerably the coherence of vortex shedding resulting into a typical value of $C_L \simeq 1$. The calculation of the sound production by vortex shedding when using a tailored Green's function is possible but is not the easiest procedure. We will now see that Curle's method relates directly the data on the lift and drag to the sound production.

Consider a body which, for generality, is allowed to pulsate, and is enclosed by a control surface S (figure 6.8). We want to calculate the field ρ' in the fluid and hence we define the control volume V at the fluid side of S . The outer normal \mathbf{n} on S is directed towards the body enclosed by S . (Note that we use here the convention opposite from Dowling *et al.* [55]!) Using equation (3.12) combined with Lighthill's analogy (2.65), ignoring external mass sources and force fields and taking $t_0 = -\infty$ yields

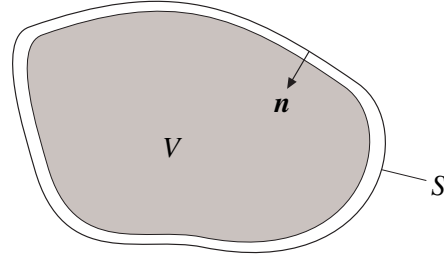


Figure 6.8 Control volume V and surface S and outer normal \mathbf{n} .

$$\rho' = \int_{-\infty}^t \iiint_V \frac{\partial^2 T_{ij}}{\partial y_i \partial y_j} G_0(\mathbf{x}, t|\mathbf{y}, \tau) \, dy d\tau - c_0^2 \int_{-\infty}^t \iint_S \left[\rho' \frac{\partial G_0}{\partial y_i} - G_0 \frac{\partial \rho'}{\partial y_i} \right] n_i \, d\sigma d\tau. \quad (6.79)$$

Applying partial integration twice yields:

$$\begin{aligned} \rho' = \int_{-\infty}^t \iiint_V T_{ij} \frac{\partial^2 G_0}{\partial y_i \partial y_j} \, dy d\tau + \int_{-\infty}^t \iint_S \left\{ \left[G_0 \frac{\partial T_{ij}}{\partial y_i} n_j - T_{ij} \frac{\partial G_0}{\partial y_j} n_i \right] \right. \\ \left. + c_0^2 \left[G_0 \frac{\partial \rho'}{\partial y_i} n_i - \rho' \frac{\partial G_0}{\partial y_i} n_i \right] \right\} d\sigma d\tau. \quad (6.80) \end{aligned}$$

Using the definition (2.66) of T_{ij} and its symmetry ($T_{ij} = T_{ji}$):

$$T_{ij} = P_{ij} + \rho v_i v_j - c_0^2 \rho' \delta_{ij} \quad (2.66)$$

we find:

$$\begin{aligned} \rho' = & \int_{-\infty}^t \iiint_V T_{ij} \frac{\partial^2 G_0}{\partial y_i \partial y_j} dy d\tau + \int_{-\infty}^t \iint_S G_0 \left(\frac{\partial P_{ij} + \rho v_i v_j}{\partial y_j} \right) n_i d\sigma d\tau \\ & - \int_{-\infty}^t \iint_S (P_{ij} + \rho v_i v_j) \frac{\partial G_0}{\partial y_j} n_i d\sigma d\tau. \end{aligned} \quad (6.81)$$

Using the momentum conservation law (1.2) in the absence of external forces ($f_i = 0$):

$$\frac{\partial}{\partial \tau} (\rho v_i) + \frac{\partial}{\partial y_j} (P_{ij} + \rho v_i v_j) = 0$$

and the symmetry of G_0 (6.70), we obtain:

$$\begin{aligned} \rho' = & \int_{-\infty}^t \iiint_V T_{ij} \frac{\partial^2 G_0}{\partial x_i \partial x_j} dy d\tau - \int_{-\infty}^t \iint_S G_0 \frac{\partial (\rho v_i)}{\partial \tau} n_i d\sigma d\tau \\ & + \int_{-\infty}^t \iint_S (P_{ij} + \rho v_i v_j) \frac{\partial G_0}{\partial x_j} n_i d\sigma d\tau. \end{aligned} \quad (6.82)$$

The spatial partial derivatives ($\partial/\partial x_j$) do not refer to \mathbf{y} and can be taken outside the integral. In the far field they can be approximated by the time derivatives $-(x_j/|\mathbf{x}|)c_0^{-1}(\partial/\partial t)$. Furthermore, in the second integral in (6.82) we can make use of the general symmetry in the time coordinate of any Green's function:

$$\frac{\partial G}{\partial t} = -\frac{\partial G}{\partial \tau}. \quad (6.83)$$

(The effect of listening later is the same as shooting earlier!) In order to use (6.83) we therefore first move the time derivative ($\partial/\partial \tau$) from ρv_i towards G_0 by partial integration. We finally obtain:

$$\begin{aligned} \rho' \simeq & \frac{x_i x_j}{|\mathbf{x}|^2 c_0^2} \frac{\partial^2}{\partial t^2} \int_{-\infty}^t \iiint_V T_{ij} G_0 dy d\tau - \frac{\partial}{\partial t} \int_{-\infty}^t \iint_S \rho v_i G_0 n_i d\sigma d\tau \\ & - \frac{x_j}{c_0 |\mathbf{x}|} \frac{\partial}{\partial t} \int_{-\infty}^t \iint_S (P_{ij} + \rho v_i v_j) G_0 n_i d\sigma d\tau. \end{aligned} \quad (6.84)$$

Using the δ -function in G_0 of equation (6.37), we can carry out the time integrals and we have Curle's theorem

$$\begin{aligned} \rho' \simeq & \frac{x_i x_j}{4\pi |\mathbf{x}|^2 c_0^4} \frac{\partial^2}{\partial t^2} \iiint_V \left[\frac{T_{ij}}{r} \right]_{t=t_e} \mathrm{d}\mathbf{y} - \frac{1}{4\pi c_0^2} \frac{\partial}{\partial t} \iint_S \left[\frac{\rho v_i n_i}{r} \right]_{t=t_e} \mathrm{d}\sigma \\ & - \frac{x_j}{4\pi |\mathbf{x}| c_0^3} \frac{\partial}{\partial t} \iint_S \left[(P_{ij} + \rho v_i v_j) \frac{n_i}{r} \right]_{t=t_e} \mathrm{d}\sigma \end{aligned} \quad (6.85)$$

where $r = |\mathbf{x} - \mathbf{y}|$ and the retarded time t_e is

$$t_e = t - r/c_0 \simeq t - |\mathbf{x}|/c_0. \quad (6.86)$$

The first term in (6.85) is simply the turbulence noise as it would occur in absence of a foreign body (except for the fact that the control volume V excludes the body).

The second term is the result of movement of the body. For a rigid body at a fixed position we have $v_i n_i = \mathbf{v} \cdot \mathbf{n} = 0$. This term is important when the body is pulsating. For a compact body we have then a simple volume source term. This term can be used to describe the flow out of a pipe. Note that ρ is the fluid density just outside the control surface so that we consider the displacement of fluid around the body, rather than a mass injection.

The last integral in (6.85) is the momentum flux through the surface and the pressure and viscous forces. For a fixed rigid body $\rho v_i v_j = 0$ because $\mathbf{v} = 0$ at a surface ("no slip" condition in viscous flow). In the case of a compact, fixed, and rigid body, we can neglect the emission time variation along the body, and we have $r \simeq |\mathbf{x}|$. The instantaneous force F_i of the fluid *on the body* (lift and drag) is then

$$F_i(t_e) \simeq \iint_S [P_{ij}]_{t=t_e} n_j \mathrm{d}\sigma. \quad (6.87)$$

Hence, for a fixed rigid compact body we have:

$$\rho'(\mathbf{x}, t) = \frac{x_i x_j}{4\pi |\mathbf{x}|^3 c_0^4} \frac{\partial^2}{\partial t^2} \iiint_V T_{ij}(\mathbf{y}, t - |\mathbf{x}|/c_0) \mathrm{d}\mathbf{y} - \frac{x_j}{4\pi |\mathbf{x}|^2 c_0^3} \frac{\partial}{\partial t} F_j(t - |\mathbf{x}|/c_0). \quad (6.88)$$

6.7 Sound radiation from an open pipe termination

Horns and tubes are used as an impedance matching between a volume source and free space. We use such a device to speak! Without vocal tract the volume source due to the vocal fold oscillation would be a very inefficient source of sound. We consider now the radiation of sound from such a tube.

We know the behaviour of sound waves in a duct at low frequencies (chapter 4). We know how sound propagates from a point source in free space. We are now able to find the radiation behaviour of a pipe end by matching the two solutions in a suitable way. If the frequency is low enough compared to the pipe diameter, the flow near the pipe end is incompressible in a region large enough to allow the pipe opening to be considered as a monopole sound source. The strength of this monopole is determined by the pipe end velocity v' . For convenience, we assume that the pipe end is acoustically described for the field inside the pipe by an impedance Z_p . The pressure p' in the pipe consists of a right-running incident wave and a left-running reflected wave:

$$p' = p^+ + p^-. \quad (6.89)$$

The acoustic velocity in the pipe is related to the acoustic pressure in the pipe by:

$$v' = \hat{v} e^{i\omega t} = \frac{p^+ - p^-}{\rho_0 c_0}. \quad (6.90)$$

Assuming a redistribution of the acoustic mass flow $v'S$ through the pipe end with cross section S into the surface of a compact sphere of radius r and surface $4\pi r^2$ (conservation of mass), we can calculate the radiated power for a harmonic field in- and outside the pipe, by using (6.13):

$$IS = \langle p'v' \rangle S = \frac{1}{2} \hat{v} \hat{v}^* \operatorname{Re}(Z_p) S = \frac{1}{2} \left(\frac{S}{4\pi r^2} \hat{v} \right) \left(\frac{S}{4\pi r^2} \hat{v}^* \right) (k^2 r^2 \rho_0 c_0) (4\pi r^2). \quad (6.91)$$

From this conservation of energy relation we find for the real part of the radiation impedance Z_p of an unflanged pipe:

$$\operatorname{Re}(Z_p) = \frac{1}{4\pi} k^2 S \rho_0 c_0 \quad (6.92)$$

which is for a pipe of radius a :

$$\operatorname{Re}(Z_p) = \frac{1}{4} (ka)^2 \rho_0 c_0. \quad (6.93)$$

This result is the low frequency limit of the well-known theory of Levine and Schwinger [121].

The imaginary part $\operatorname{Im}(Z_p)$ takes into account the inertia of the air flow in the compact region just outside the pipe. It appears that $\operatorname{Im}(Z_p)$ is equal to $k\delta$, where δ is the so-called “end correction”. This seen as follows. Just outside the pipe end, in the near field of the monopole, the pressure is a factor $\rho_0 c_0 k r$ lower than the acoustic velocity, which is much smaller than the $\rho_0 c_0$ of inside the pipe (see equation 6.7). Therefore, the outside field forces the inside pressure to vanish at about the pipe end. Although the exact position of this fictitious point $x = \delta$ (the “end correction”), where the wave in the pipe is assumed to satisfy the condition $p = 0$, depends on geometrical details, it is a property of the pipe end and therefore $\delta = O(a)$. This implies that the end correction amounts to leading order in ka

to nothing but a phase shift of the reflected wave and so to a purely imaginary impedance Z_p . Up to order $(ka)^2$ this impedance can now be expressed as:

$$Z_p = (ik\delta + \frac{1}{4}(ka)^2)\rho_0c_0 \quad (6.94)$$

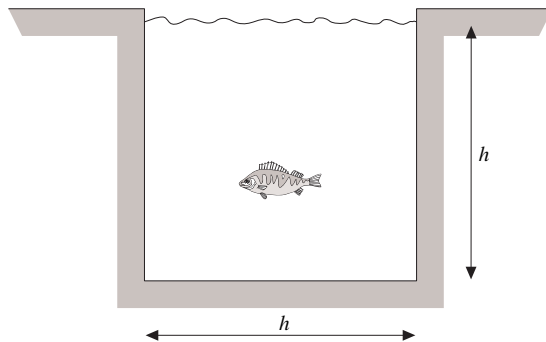
where it appears that²:

$$0.61a \leq \delta \leq 0.85a \quad (6.95)$$

for circular pipes [181]. The lower limit corresponds to an unflanged pipe while the upper limit corresponds to a pipe end with an infinite baffle (flanged). See also section 7.9.

Exercises

- Note that the acoustic field generated by a compact translating sphere is a dipole (equation 6.21) we find the typical $\cos \vartheta = x_i y_i / |\mathbf{x}||\mathbf{y}|$ directivity. What are the source and the sink forming the dipole? (Explain qualitatively.)
- A vortex ring with time dependent vorticity is a dipole. (Explain qualitatively.)
- An electrical dipole radiates perpendicularly to the axis of the dipole. What is the reason for this difference in directivity of electrical and acoustic dipoles?
- Why is the boundary condition $p' = 0$ reasonable for acoustic waves reflecting at a water/air interface (on the water side)?
- We have seen (section 6.2) that a translating sphere induces a dipole field. Moving parts of a rigid machine also act as dipoles if they are compact. Explain why a body translating in an oscillatory manner close to the floor produces more sound when it moves horizontally than vertically.
- The acoustic pressure p' generated by a monopole close to a wall increases by a factor 2 in comparison with free field conditions. Hence the radiated I intensity increases by a factor 4. How much does the power generated by the source increase?
- The cut-off frequency f_c above which the first higher mode propagates in a duct with square cross section appears to be given by $\frac{1}{2}\lambda = \frac{1}{2}c_0f_c = h$. figure 6.4 suggests that this would be $c_0f_c = h$ for a source placed in the middle of the duct. Explain the difference.
- In a water channel with open surface sound does not propagate below a certain cut-off frequency f_c . Explain this and calculate f_c for a square channel cross section $h = 3$ m.



$$2 - \frac{1}{\pi} \int_0^\infty \log(2I_1(x)K_1(x)) \frac{dx}{x^2} = 0.612701035 \dots, \quad 2 \int_0^\infty J_1(x)^2 \frac{dx}{x^2} = \frac{8}{3\pi} = 0.848826363 \dots$$

- i) Consider a sphere oscillating (translating periodically) in an infinite duct with hard walls and square cross section. Discuss the radiation as function of the oscillation frequency and the direction of oscillation (along the duct axis or normal to the axis). Relate the dipole strength δQ to the amplitude of the acoustic waves for $f < f_c$ in a pipe of cross sectional area S .
- j) Explain by using the method of images why a line quadrupole placed near a cylinder, parallel to the axis of the cylinder (figure 6.9), will radiate as a line dipole. (This explains that turbulence near such a cylinder will radiate quite effectively [136]!)

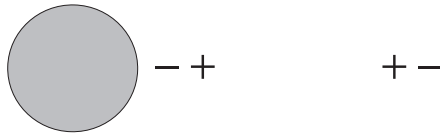


Figure 6.9 A line quadrupole near a cylinder.

- k) Consider two jet engines developing the same thrust with diameters D_1 and $D_2 = 2D_1$, respectively. Assuming a low Mach number estimate the ratio of the sound power generated by both engines.
- l) Which scaling rule do you expect for the Mach number dependence of the sound produced by a hot steam in cold air?
- m) Which scaling rule do you expect for the Mach number dependence of the sound produced by a bubbly liquid jet in water?
- n) Typical entropy fluctuations due to friction at the pipe wall from which the jet is leaving correspond to temperature fluctuations $T'/T_0 \simeq 0.2M^2$. At which Mach number do you expect such effect to become a significant source of sound?
- o) A subsonic jet with $M \ll 1$ is compact if we consider the sound produced by turbulence. Why?
- p) Estimate the amplification of turbulence noise due to the presence of a cylinder of diameter d near a free jet of diameter D at a main speed u_0 if we assume that the cylinder does not affect the flow.
- q) Same question for a small air bubble of diameter $2a$ near a free jet of diameter D and speed u_0 . Assume a low frequency response of the bubble.

- r) Consider a small ventilator rotating at a radial frequency ω in a uniform flow u_0 . The fan feels at a certain distance r from the axis of the ventilator an effective wind velocity v_{eff} which is a combination of the axial velocity u_0 and the tangential velocity ωr (where we neglect the air rotation induced by the fan) (figure 6.10). Assume that $u_0 = 0.1 \omega R$. If we concentrate on the tip of the fan ($r = R$) we have a lift

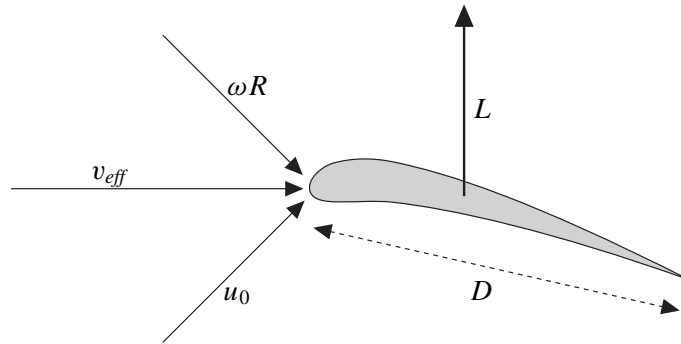


Figure 6.10 The forces on a fan blade (Exercise r)

force L , per unit length, which is normal to v_{eff} . The magnitude of L is given by:

$$L = \frac{1}{2} \rho v_{eff}^2 D C_L$$

where D is the width of the profile of the blade. Typically C_L is $O(1)$ for a well-designed ventilator. Consider first a ventilator with a single blade. Discuss the contribution of the tangential and axial components of the lift for L on the noise. What is the effect of having a second blade on the ventilator? (See figure 6.11.) A well-designed ventilator has many blades. How does this affect sound production?

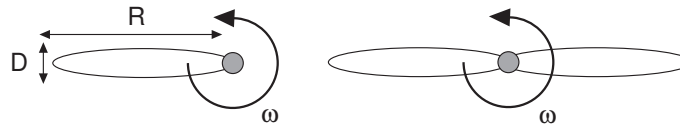


Figure 6.11 Single and dual bladed ventilator (Exercise r)

- s) How does the presence of duct walls influence the low-frequency sound production of an axial ventilator placed in the duct.
- t) Consider an airplane with a rotor placed just behind the wing (figure 6.12). Discuss the sound production (frequency, directivity ...).

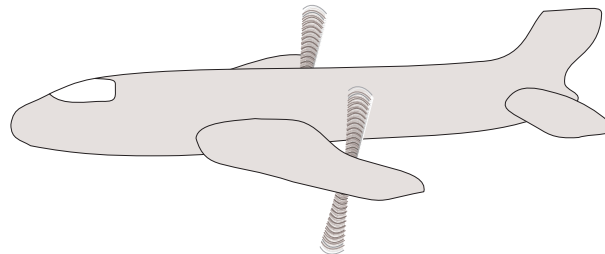


Figure 6.12 Propeller in pusher position (Exercise t)

- u) Can we consider an aircraft propeller as a compact body?
- v) What is the Mach number dependence of the sound produced by a small (compact) body placed in a turbulent flow?
- w) Estimate the low frequency impedance Z_p of a flanged pipe termination.
- x) Assuming a low frequency, calculate the power radiated in free space by a piston placed at the end of a circular pipe of radius a and length L (figure 6.13). What is the ratio between this power at resonance $k_0L = (n + \frac{1}{2})\pi$, and the power which would be radiated by the piston without a pipe.

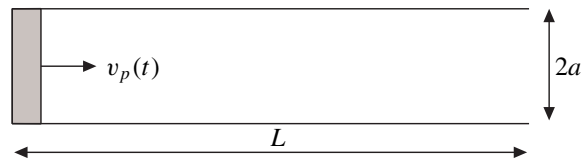


Figure 6.13 Piston in cylindrical pipe (Exercise x)

- y) Consider a conical pipe driven by a piston of surface S_1 and with an outlet surface S_2 (figure 6.14). Determine the sound field inside the pipe. **Hint.** Use spherical waves centred at the cone top!

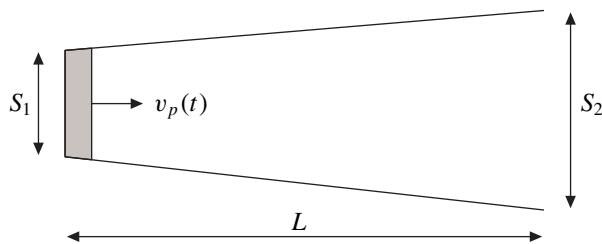


Figure 6.14 Piston in conical pipe (Exercise y)

- z) A small transistor radio is not able to produce low frequencies (why?). We hear low frequencies because our ear is artificially guessing these low frequencies when we supply a collection of higher harmonics (figure 6.15). On the other hand, when using a Walkman we are actually provided with real, low frequencies. Why is this possible even though the loudspeaker is a miniature device?

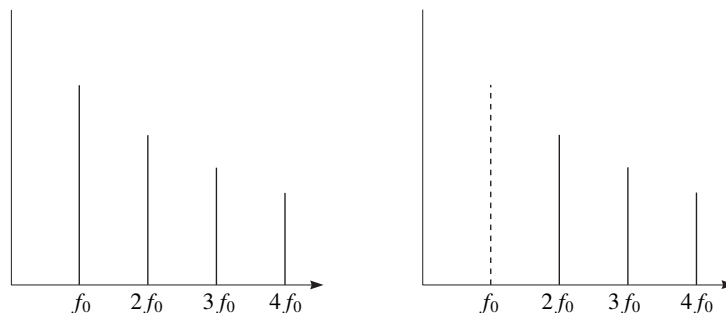


Figure 6.15 We hear the missing fundamental! (Exercise z)

- A) Calculate the friction and radiation losses in a clarinet. Assume a tube radius of 1 cm and a length of 1 m. Carry out the calculation for the first three modes of the instrument. What is the difference between the radiation losses of a clarinet and of a flute with the same pipe dimensions.
- B) How far can we be heard when we scream in quiescent air if we produce 10^{-5} W acoustic power?
- C) Calculate the ratio between the acoustic impedance experienced by an air bubble of radius $a_0 = 1$ mm in water at atmospheric pressure:
- in free space;
 - in an infinite duct of cross sectional area $S = 10^{-4}$ m².
- D) Consider two twin pipes of length L and radius a , placed along each other in such a way that corresponding ends of either pipe just touch each other. Assume that the pipes are acoustically excited and oscillate in opposite phase. How does the radiation losses of the system scale with L and a .

7 Duct acoustics

In a duct of constant cross section the reduced wave (or Helmholtz) equation may be solved by means of a series expansion in a particular family of solutions, called modes. They are related to the eigensolutions of the two-dimensional Laplace operator acting on a cross section. Therefore, the terminology of modes contains many references to the corresponding eigenvalues.

Modes are interesting mathematically because they form, in general, a complete basis by which any solution can be represented. Physically, modes are interesting because they are solutions in their own right, not just mathematical building blocks, and by their simple structure the usually complicated behaviour of the total field is more easily understood.

7.1 General formulation

The time-harmonic sound field in a duct of constant cross section with linear boundary conditions that are independent of the axial coordinate may be described by an infinite sum of special solutions, called modes, that retain their shape when travelling down the duct. They consist of an exponential term multiplied by the eigenfunctions of the Laplace operator corresponding to a duct cross section.

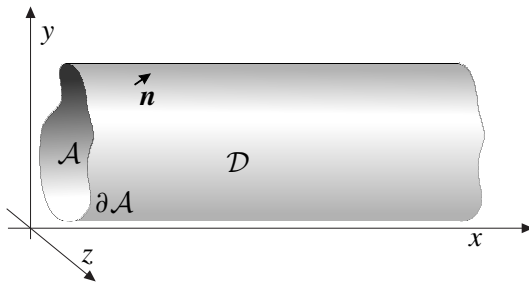


Figure 7.1 A duct \mathcal{D} of cross section \mathcal{A} .

Consider the two-dimensional area \mathcal{A} with a smooth boundary $\partial\mathcal{A}$ and an externally directed unit normal \mathbf{n} . For physical relevance \mathcal{A} should be simply connected, otherwise we would have several independent ducts. When we consider, for definiteness, this area be part of the y, z -plane, it describes the duct \mathcal{D} (see Fig. 7.1) given by

$$\mathcal{D} = \{(x, y, z) | (y, z) \in \mathcal{A}\} \quad (7.1)$$

with axial cross sections being copies of \mathcal{A} and where the normal vectors \mathbf{n} are the same for all x . All lengths are made dimensionless on a suitable radius or diameter $R = O(\sqrt{\mathcal{A}})$, velocities on the uniform sound speed c_0 , time on R/c_0 , density on the uniform mean density ρ_0 , pressure on $\rho_0 c_0^2$, intensity on $\rho_0 c_0^3$, and power on $\rho_0 c_0^3 R^2$. We assume only time harmonic perturbations of dimensional frequency $\tilde{\omega}$. The dimensionless frequency $\omega = \tilde{\omega}R/c_0$ is then equivalent to the Helmholtz number, an important dimensionless number in duct acoustics.

In the usual complex notation (with $+i\omega t$ -sign convention), the acoustic field

$$p(\mathbf{x}, t) \equiv p(\mathbf{x}, \omega) e^{i\omega t}, \quad \mathbf{v}(\mathbf{x}, t) \equiv \mathbf{v}(\mathbf{x}, \omega) e^{i\omega t} \quad (7.2)$$

satisfies in the duct ($\mathbf{x} \in \mathcal{D}$) the equations

$$\nabla^2 p + \omega^2 p = 0, \quad (7.3a)$$

$$i\omega \mathbf{v} + \nabla p = 0. \quad (7.3b)$$

Solutions of a more general time-dependence may be constructed via Fourier synthesis in ω (equation C.2). At the duct wall we assume the boundary condition

$$\mathcal{B}(p) = 0 \text{ for } \mathbf{x} \in \partial\mathcal{D} \quad (7.4)$$

where \mathcal{B} is typically of the form (*c.f.* for example Eqs. (3.14) or (3.42))

$$\mathcal{B}(p) = a(y, z)(\mathbf{n} \cdot \nabla p) + b(y, z)p + c(y, z)\frac{\partial}{\partial x}p. \quad (7.5)$$

Self-similar solutions (called *modes*) of the form $p(x, y, z) = \phi(x)\psi(y, z)$ exist for $\phi(x) = e^{-ikx}$ with particular values of k and associated functions ψ . This leads to general solutions given by

$$p(x, y, z) = \sum_{n=0}^{\infty} C_n \psi_n(y, z) e^{-ik_n x} \quad (7.6)$$

where ψ_n are the eigenfunctions of the Laplace operator reduced to \mathcal{A} , *i.e.* solutions of

$$\begin{aligned} -\left(\frac{\partial^2}{\partial y^2} + \frac{\partial^2}{\partial z^2}\right)\psi &= \alpha^2 \psi \text{ for } (y, z) \in \mathcal{A}, \\ \text{with } \tilde{\mathcal{B}}(\psi; \alpha) &= 0 \text{ for } (y, z) \in \partial\mathcal{A}, \end{aligned} \quad (7.7)$$

where α^2 is the corresponding eigenvalue and the eigenmode boundary condition operator $\tilde{\mathcal{B}}$ is

$$\tilde{\mathcal{B}}(\psi; \alpha) = a(y, z)(\mathbf{n} \cdot \nabla \psi) + b(y, z)\psi - ik(\alpha)c(y, z)\psi. \quad (7.8)$$

The axial wave number k is given by one of the square roots $k = \pm\sqrt{\omega^2 - \alpha^2}$ (+ for right and - for left running). Each term in the series expansion, *i.e.* $\psi_n(y, z) e^{-ik_n x}$, is called a *duct mode*. If the

duct cross section is circular or rectangular and the boundary condition is uniform everywhere, the solutions of the eigenvalue problem are relatively simple and may be found by separation of variables. These eigensolutions consist of combinations of exponentials and Bessel functions in the circular case or combinations of trigonometric functions in the rectangular case. Some other geometries, like ellipses, do also allow explicit solutions, but only in special cases such as with hard walls. For other geometries one has to fall back on numerical methods for the eigenvalue problem. As a final remark, we note that the above solution only needs a minor adaptation to cope with a uniform mean flow inside the duct.

By application of Green's theorem it can easily be shown that the set of eigenfunctions $\{\psi_n\}$ is *bi-orthogonal* to their complex conjugates $\{\psi_n^*\}$. In other words, the innerproduct

$$(\psi_n, \psi_m^*) = \iint_{\mathcal{A}} \psi_n \psi_m^* d\sigma \quad \begin{cases} = 0 & \text{if } n \neq m, \\ \neq 0 & \text{if } n = m. \end{cases} \quad (7.9)$$

(Some care is required when, due to a symmetric geometry, each α_n is linked to more than one ψ_n .) This implies that for real ψ_n and real α_n , which is for example the case for hard-walled ducts where $Z = \infty$, the set of eigenfunctions is bi-orthogonal to itself: in other words is *orthogonal*. This orthogonality can be used to obtain the amplitudes of the expansion. It is then natural to normalise ψ_n such that $(\psi_n, \psi_n^*) = 1$. See section 7.7.

In the following sections, we will present the modes with their properties and applications for cylindrical ducts with both hard walls and soft walls of impedance type, as well as for rectangular ducts.

7.2 Cylindrical ducts

Consider a duct of (dimensionless) radius 1 with polar coordinates (r, θ, x) . In these coordinates we have

$$\nabla = \mathbf{e}_x \frac{\partial}{\partial x} + \mathbf{e}_r \frac{\partial}{\partial r} + \mathbf{e}_\theta \frac{1}{r} \frac{\partial}{\partial \theta}, \quad (7.10a)$$

$$\nabla^2 = \frac{\partial^2}{\partial x^2} + \frac{\partial^2}{\partial r^2} + \frac{1}{r} \frac{\partial}{\partial r} + \frac{1}{r^2} \frac{\partial^2}{\partial \theta^2}, \quad (7.10b)$$

and so the reduced wave equation (7.3a) becomes

$$\frac{\partial^2 p}{\partial x^2} + \frac{\partial^2 p}{\partial r^2} + \frac{1}{r} \frac{\partial p}{\partial r} + \frac{1}{r^2} \frac{\partial^2 p}{\partial \theta^2} + \omega^2 p = 0. \quad (7.11)$$

We begin with a hard-walled hollow duct, which has the wall boundary condition

$$\frac{\partial p}{\partial r} = 0 \quad \text{at } r = 1. \quad (7.12)$$

Solutions of modal type may be found by separation of variables, *i.e.* by assuming the form $p = F(x)\psi(y, z) = F(x)G(r)H(\vartheta)$

$$\left(\frac{d^2 H}{d\vartheta^2}\right)/H = -m^2 \quad (7.13a)$$

$$\left(\frac{d^2 G}{dr^2} + \frac{1}{r} \frac{dG}{dr}\right)/G = \frac{m^2}{r^2} - \alpha^2 \quad (7.13b)$$

$$\left(\frac{d^2 F}{dx^2}\right)/F = \alpha^2 - \omega^2 \quad (7.13c)$$

so that

(a) $H(\vartheta) = e^{-im\vartheta}$, $m = 0, \pm 1, \pm 2, \dots$.

Here, use is made of the condition of continuity from $\vartheta = 0$ to $\vartheta = 2\pi$.

(b) $G(r) = J_m(\alpha_{m\mu}r)$, $\mu = 1, 2, \dots$, where:

J_m denotes the ordinary Bessel function of the first kind (Appendix D);

$\alpha_{m\mu} = j'_{m\mu}$ is the μ -th nonnegative non-trivial zero of J'_m , to satisfy the boundary condition $G'(1) = 0$.

(c) $F(x) = e^{\mp ik_{m\mu}x}$, with:

$$k_{m\mu} = \sqrt{\omega^2 - \alpha_{m\mu}^2} \quad \text{such that } \operatorname{Re}(k_{m\mu}) \geq 0, \operatorname{Im}(k_{m\mu}) \leq 0.$$

Although technically speaking $\{\alpha_{m,\mu}^2\}$ are the eigenvalues of (minus) the cross-sectional Laplace operator, it is common practice to refer to $\alpha_{m\mu}$ as the radial eigenvalue or radial modal wave number, to m as the circumferential eigenvalue or circumferential wave number, and to $k_{m\mu}$ as the axial eigenvalue or axial wave number. The associated solutions are called duct modes, and they form a complete set of building blocks suitable for constructing any sound field in a duct. At the same time, they are particular shape-preserving solutions with easily interpretable properties.

Note that all $\alpha_{m\mu}$ and m are real, while only a finite number of $k_{m\mu}$ are real; see figure 7.2). The branch we selected here of the complex square root $k_{m\mu}$ is such that $e^{-ik_{m\mu}x}$ describes a right-running wave and $e^{ik_{m\mu}x}$ a left-running wave. This will be further clarified later.

These modes (normalized for later use)

$$p_{m\mu}(x, r, \vartheta) = U_{m\mu}(r) e^{-im\vartheta \mp ik_{m\mu}x}, \quad (7.14)$$

$$U_{m\mu}(r) = N_{m\mu} J_m(\alpha_{m\mu}r), \quad N_{m\mu} = \left\{ \frac{1}{2} (1 - m^2/\alpha_{m\mu}^2) J_m(\alpha_{m\mu})^2 \right\}^{-1/2},$$

form (for fixed x) a complete set (in L_2 -norm over (r, ϑ)), so by superposition we can write any

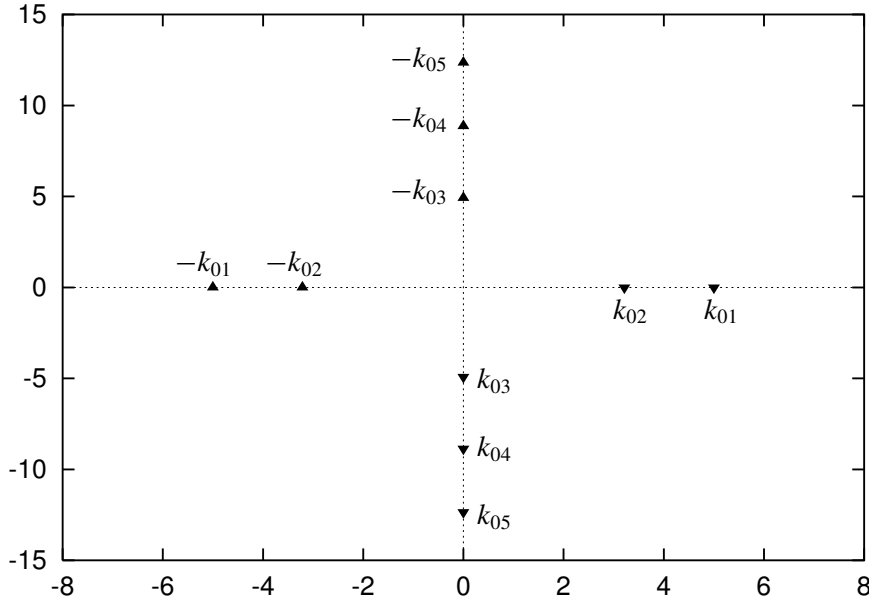


Figure 7.2 Complex axial wave numbers $\pm k_{m\mu}$ ($m = 0$, $\omega = 5$). They are found along the branch cuts of the square root of figure 3.5, where $\sqrt{\omega^2 - k_{m\mu}^2} = j_{m\mu}$ is real positive.

solution as the following modal expansion:

$$p(x, r, \vartheta) = \sum_{m=-\infty}^{\infty} \sum_{\mu=1}^{\infty} (A_{m\mu} e^{-ik_{m\mu}x} + B_{m\mu} e^{ik_{m\mu}x}) U_{m\mu}(r) e^{-im\vartheta}. \quad (7.15)$$

The normalization factor $N_{m\mu}$ is chosen such that a modal amplitude $A_{m\mu}$ scales with the energy content of the corresponding mode (see below).

A surface of constant phase, *i.e.* $m\vartheta + \text{Re}(k_{m\mu})x = \text{constant}$, is a helicoid of pitch $2\pi m / \text{Re}(k_{m\mu})$; see figure 7.3.

An important special case is the plane wave $m = 0$, $\mu = 1$, with

$$j'_{01} = 0, \quad \alpha_{01} = 0, \quad k_{01} = \omega, \quad N_{01} = \sqrt{2}, \quad p_{01} = \sqrt{2} e^{-i\omega x}.$$

In fact, this is the only non-trivial eigenvalue equal to zero. All others are greater, the smallest being given by

$$j'_{11} = 1.84118 \dots$$

Since the zeros of J'_m form an ever increasing sequence both in m and in μ (with $j'_{m\mu} \simeq (\mu + \frac{1}{2}m - \frac{1}{4})\pi$ for $\mu \rightarrow \infty$) (see Appendix D), there are for any ω always a (finite) $\mu = \mu_0$ and $m = m_0$ beyond which $\alpha_{m\mu}^2 > \omega^2$, so that $k_{m\mu}$ is purely imaginary, and the mode decays exponentially in x .

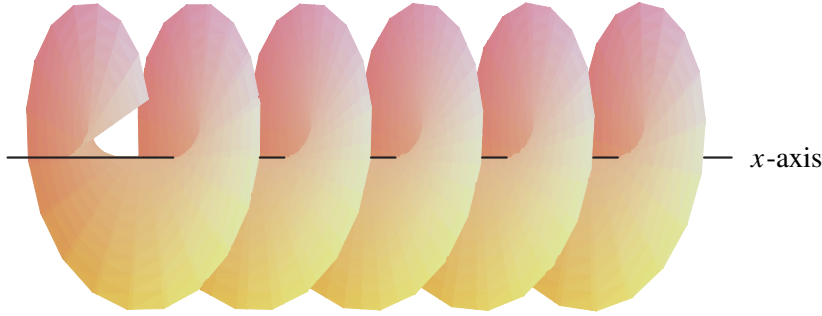


Figure 7.3 Surface of constant phase $m\vartheta + \text{Re}(k_{m\mu})x$.

So we see that there are always a *finite* number of modes with *real* $k_{m\mu}$ (see figure 7.2). Since they are the only modes that propagate (see below), they are called *cut-on*. The remaining infinite number of modes, with *imaginary* $k_{m\mu}$, are evanescent and therefore called *cut-off*. This cut-on and cut-off modes are essentially similar to the radiating and evanescent waves discussed in section 3.3.

For low frequency, *i.e.* for

$$\omega < j'_{11} = 1.84118 \dots$$

all modes are cut-off except for the plane wave. In this case a plane wave approximation (*i.e.* considering only the first mode) is applicable if we are far enough away from any sources, changes in boundary condition, or other scattering objects, for the generated evanescent modes to become negligible.

From the orthogonality relation¹ of equation 7.9 (note that we have here a hard-walled duct)

$$\int_0^1 \int_0^{2\pi} U_{m\mu}(r) e^{-im\vartheta} \left(U_{n\nu}(r) e^{-in\vartheta} \right)^* r d\vartheta dr = 2\pi \delta_{mn} \delta_{\mu\nu} \quad (7.16)$$

we find by integration of the time-averaged axial intensity

$$\langle \mathbf{I} \cdot \mathbf{e}_x \rangle = \frac{1}{4} (p u^* + p^* u) = \frac{1}{2} \text{Re}(p u^*)$$

over a duct cross section $x = \text{constant}$ the transmitted acoustic power

$$\mathcal{P} = \frac{\pi}{\omega} \sum_{m=-\infty}^{\infty} \sum_{\mu=1}^{\infty} \left[\text{Re}(k_{m\mu}) (|A_{m\mu}|^2 - |B_{m\mu}|^2) + 2 \text{Im}(k_{m\mu}) \text{Im}(A_{m\mu}^* B_{m\mu}) \right]. \quad (7.17)$$

The summation over $\text{Re}(k_{m\mu})$ contains only a *finite* number of non-zero terms: the cut-on modes. By taking either $A_{m\mu}$ or $B_{m\mu}$ equal to zero, it is clear that a cut-on $\exp(-ik_{m\mu}x)$ -mode propagates

¹ $\delta_{ij} = 1$ if $i = j$, $\delta_{ij} = 0$ if $i \neq j$

in *positive* direction, and a cut-on $\exp(ik_{m\mu}x)$ -mode in *negative* direction (for the present $+i\omega t$ -sign convention). Indeed, with $\text{Im}(k_{m\mu}) \leq 0$, the respective cut-off modes decay in the propagation direction, and we can say that a mode propagates or decays exponentially depending on the frequency being lower or higher than the cut-off or resonance frequency

$$f_c = \frac{j'_{m\mu} c_0}{2\pi a}. \quad (7.18)$$

As is clear from the second part of expression (7.17), cut-off modes may transport energy by interaction between right- and left-running ($A_{m\mu}$ and $B_{m\mu}$) modes. It should be noted, however, that (depending on the choice of the origin $x = 0$) usually either the right- or left-running cut-off modes $A_{m\mu}$ or $B_{m\mu}$ are exponentially small, and the product $A_{m\mu}^* B_{m\mu}$ is therefore quickly negligible.

The axial *phase velocity* (C.19) of a cut-on mode is equal to

$$v_{ph} = \frac{\omega}{k_{m\mu}} \quad (7.19)$$

The axial *group velocity* (C.21) of a cut-on mode is given by

$$v_g = \left(\frac{dk_{m\mu}}{d\omega} \right)^{-1} = \frac{k_{m\mu}}{\omega}. \quad (7.20)$$

Note that

$$v_g v_{ph} = 1, \quad \text{with } v_g < 1 < v_{ph}. \quad (7.21)$$

The axial group velocity is lower than the soundspeed because the modal wave fronts do not propagate parallel to the x -axis, but rather follow a longer path, spiralling around the x -axis, with a right-hand rotation for $m > 0$ and a left-hand rotation for $m < 0$.

7.3 Rectangular ducts

In a completely analogous way as in the foregoing section 7.2, the general modal solution, similar to (7.15), of sound propagation in a rectangular hard walled duct, can be found as follows.

Separation of variables $p(x, y, z) = F(x)G(y)H(z)$ applied to $\nabla^2 p + \omega^2 p = 0$ in the duct $0 \leq y \leq a$, $0 \leq z \leq b$, results into $G_{yy} = -\alpha^2 G$, $H_{zz} = -\beta^2 H$ and $F_{xx} = -(\omega^2 - \alpha^2 - \beta^2)F$, where α and β are eigenvalues to be determined from the hard-wall boundary conditions. We obtain

$$\begin{aligned} G(y) &= \cos(\alpha_n y), & \alpha_n &= n\pi/a, & n &= 0, 1, 2, \dots \\ H(z) &= \cos(\beta_m z), & \beta_m &= m\pi/b, & m &= 0, 1, 2, \dots \\ F(x) &= e^{\mp ik_{nm}x}, & k_{nm} &= (\omega^2 - \alpha_n^2 - \beta_m^2)^{1/2}, \end{aligned}$$

where $\text{Re}(k_{nm}) \geq 0$ and $\text{Im}(k_{nm}) \leq 0$. So the general, normalised, solution is

$$p(x, y, z) = \sum_{n=0}^{\infty} \sum_{m=0}^{\infty} \frac{\cos(\alpha_n y)}{\sqrt{[\frac{1}{2}]_{n \neq 0}} a} \frac{\cos(\beta_m z)}{\sqrt{[\frac{1}{2}]_{m \neq 0}} b} (A_{nm} e^{-ik_{nm}x} + B_{nm} e^{ik_{nm}x}). \quad (7.22)$$

Note that the normalisations for the $n = 0$, respectively $m = 0$ modes miss the factor $\frac{1}{2}$.

If it is useful to distinguish between even and odd modes (in y or z), we can find these by noting that the geometrically even modes correspond with the even indices and the geometrically odd modes with the odd indices. With the new index $\nu = 1, \dots$, we find for $\cos(\alpha_n y)$

$$\begin{aligned} \text{even: } n = 2(\nu - 1), \quad \cos(\alpha_n y) &= -(-1)^\nu \cos\left((\nu - 1)\frac{2\pi}{a}(y - \frac{1}{2}a)\right), \\ \text{odd: } n = 2\nu - 1, \quad \cos(\alpha_n y) &= (-1)^\nu \sin\left((\nu - \frac{1}{2})\frac{2\pi}{a}(y - \frac{1}{2}a)\right). \end{aligned}$$

The same follows for $\cos(\beta_m z)$.

7.4 Impedance wall

7.4.1 Behaviour of complex modes

When the duct is lined with sound absorbing material of a type that allows little or no sound propagation in the material parallel to the wall, the material is called *locally reacting* and may be described by a wall impedance $Z(\omega)$ (scaled on $\rho_0 c_0$). This gives in the acoustic problem the following boundary condition in the frequency domain:

$$i\omega p \Big|_{r=1} = -Z(\omega) \frac{\partial p}{\partial r} \Big|_{r=1}, \quad (7.23)$$

the impedance being defined as $p/(\mathbf{v} \cdot \mathbf{n})$ with \mathbf{n} a normal pointing *into* the surface. A typical practical example is: the inlet of an aircraft turbojet engine. The previous concept of a modal expansion, with modes again retaining their shape travelling down the duct, is also here applicable. The general solution has a form similar to (7.14) and (7.15), the hard walled case. Only the eigenvalues $\alpha_{m\mu}$ are now defined by

$$\frac{J_m(\alpha_{m\mu})}{\alpha_{m\mu} J'_m(\alpha_{m\mu})} = \frac{iZ}{\omega}, \quad (7.24)$$

related to $k_{m\mu}$ by the same square root as before:

$$k_{m\mu} = \sqrt{\omega^2 - \alpha_{m\mu}^2},$$

but another normalization may be more convenient. A normalization that preserves the relation

$$\int_0^1 U_{m\mu}(r)U_{m\mu}^*(r)r \, d\vartheta \, dr = 1$$

(note that now the modes are *not* orthogonal) is

$$N_{m\mu} = \left\{ \frac{|\alpha_{m\mu} J'_m(\alpha_{m\mu})|^2 \operatorname{Re}(Z)}{\operatorname{Im}(\alpha_{m\mu}^2) \omega} \right\}^{-1/2}. \quad (7.25)$$

Qualitatively, the behaviour of these modes in the complex $k_{m\mu}$ -plane is as follows.

If $\operatorname{Im}(Z) > 0$, all modes may be found not too far from their hard wall values on the real interval $(-\omega, \omega)$ or the imaginary axis (that is, with $\alpha_{m\mu} = j'_{m\mu}$, and $\operatorname{Im}(k_{m\mu}) \leq 0$.) More precisely, if we vary Z from $|Z| = \infty$ to $Z = 0$, $\alpha_{m\mu}$ varies from its $|Z| = \infty$ -value $j'_{m\mu}$ to its $Z = 0$ -value $j_{m\mu}$. ($j_{m\mu}$ is the μ -th zero of J_m .) These $j_{m\mu}$ and $j'_{m\mu}$ are real and interlaced according to the inequalities $j'_{m\mu} < j_{m\mu} < j_{m,\mu+1} < \text{etc.}$, so the corresponding $k_{m\mu}$ are also interlaced and shift into a direction of increasing mode number μ .

However, if $\operatorname{Im}(Z) < 0$ (for $+i\omega t$ -sign convention), a couple of two modes wander into their quarter of the complex plane in a more irregular way, and in general quite far away from the others. In figure 7.5 this behaviour is depicted by the trajectories of the modes as the impedance varies along lines of constant real part (figure 7.4). Compare this figure with figure 3.1 of the related 2-D problem, which may be considered as the high-frequency approximation of the duct problem. (Note the notation! α in the 2-D problem corresponds to $k_{m\mu}$ here.) For small enough $\operatorname{Re}(Z)$ (smaller than, say, 2) we see

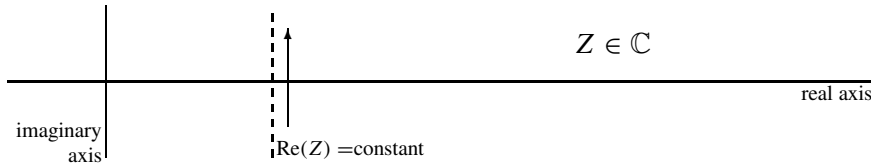


Figure 7.4 Complex impedance plane.

the first ($\mu=1$) mode being launched into the complex $k_{m\mu}$ -plane when $\operatorname{Im}(Z)$ is negative, and then returning as a (for example) $\mu=4$ or 2 mode when $\operatorname{Im}(Z)$ is positive. We will call these irregular modes *surface waves*: their maximum is at the wall surface, and away from the wall they decay exponentially ([200]). This is most purely the case for an imaginary impedance $Z = iX$. See figure 7.6.

A solution $\alpha_{m\mu} = iQ_{m\mu}$, $Q_{m\mu}$ real, may be found² satisfying

$$\frac{I_m(Q_{m\mu})}{Q_{m\mu} I'_m(Q_{m\mu})} = -\frac{X}{\omega} \quad \text{if} \quad -\frac{\omega}{m} < X < 0, \quad (7.26)$$

²The function $h(z) = z I'_m(z) / I_m(z)$ increases monotonically in z , with $h(0) = m$, and $h(z) \sim z$ as $z \rightarrow \infty$.

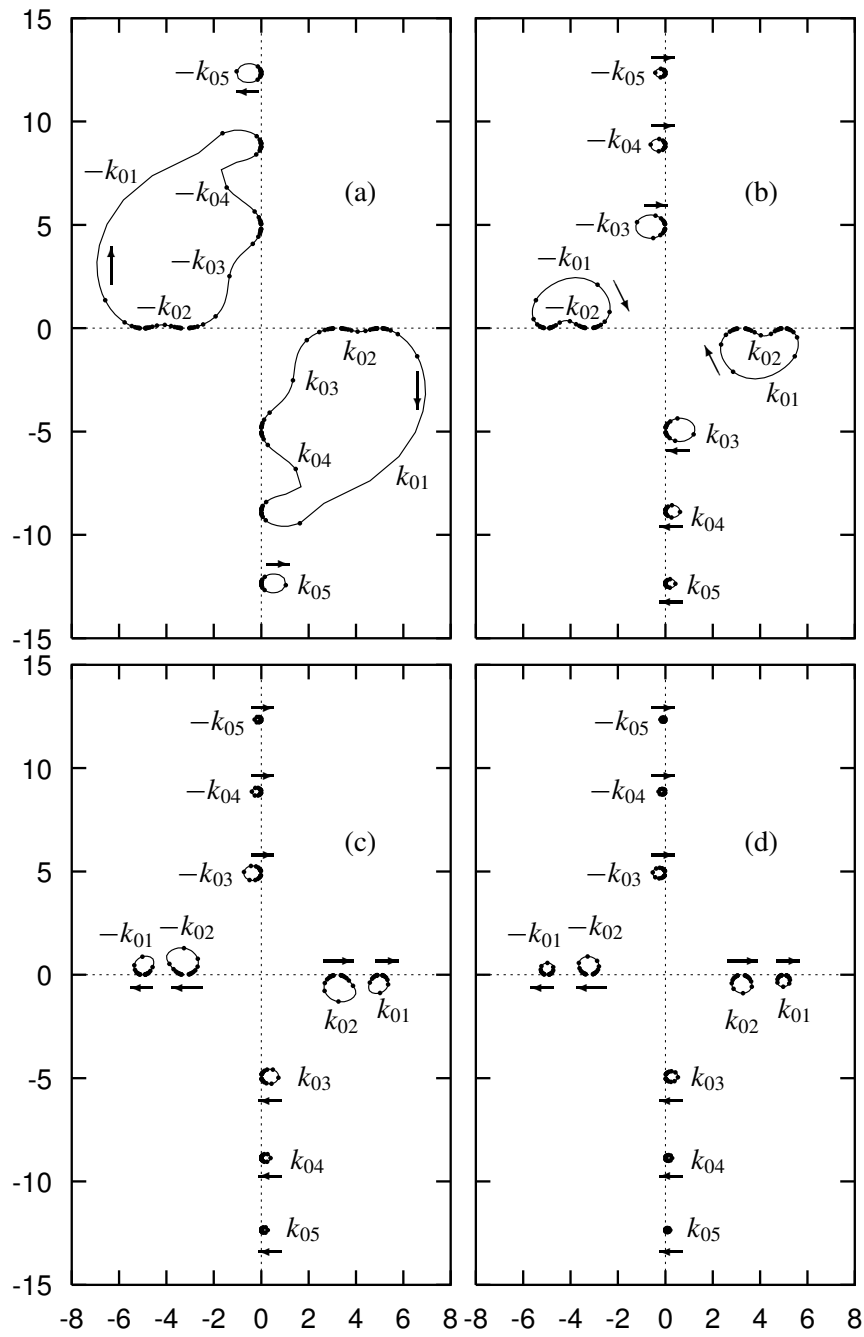


Figure 7.5 Trajectories of $k_{m\mu}$ ($m = 0, \omega = 5$) for $\text{Im}(Z)$ varying from $-\infty$ to ∞ and fixed $\text{Re}(Z) =$ (a) 0.5, (b) 1.0, (c) 1.5, (d) 2.0.

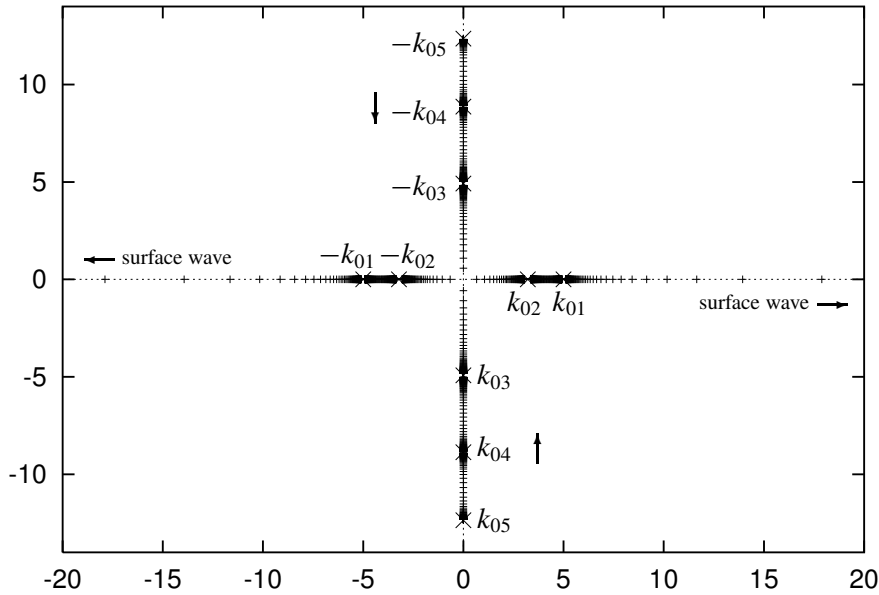


Figure 7.6 Trajectories of $k_{m\mu}$ ($m = 0, \omega = 5$) for $\text{Im}(Z)$ varying from $-\infty$ to ∞ and fixed $\text{Re}(Z) = 0.0$

such that $Q_{m\mu} = 0$ at $X = -\omega/m$, and $Q_{m\mu} \rightarrow \infty$ if $X \uparrow 0$.

The modal shape in r , described by $J_m(\alpha_{m\mu}r) = i^m I_m(Q_{m\mu}r)$, is exponentially restricted to the immediate neighbourhood of $r = 1$ and indeed shows the surface wave character, since the modified Bessel function $I_m(x)$ has exponential behaviour for $x \rightarrow \infty$. It is interesting to note that the corresponding axial wave number $k_{m\mu} = (\omega^2 + Q_{m\mu}^2)^{1/2}$ is now *larger* than ω . Hence, the modal phase velocity is smaller than the sound speed, which is indeed to be expected for a *non-radiating* surface wave. The group velocity (7.20) depends on $Z(\omega)$.

7.4.2 Attenuation

Usually, lining is applied to reduce the sound level by dissipation. It is a simple exercise to verify that the time-averaged intensity at the wall directed into the wall (*i.e.* the dissipated power density) of a mode is

$$\langle \mathbf{I} \cdot \mathbf{e}_r \rangle \propto \text{Im}(\alpha_{m\mu}^2). \tag{7.27}$$

A natural practical question is then: which impedance Z gives the greatest reduction. This question has, however, many answers. In general, the optimum will depend on the source of the sound. If more than one frequency contributes, we have to include the way $Z = Z(\omega)$ depends on ω . Also

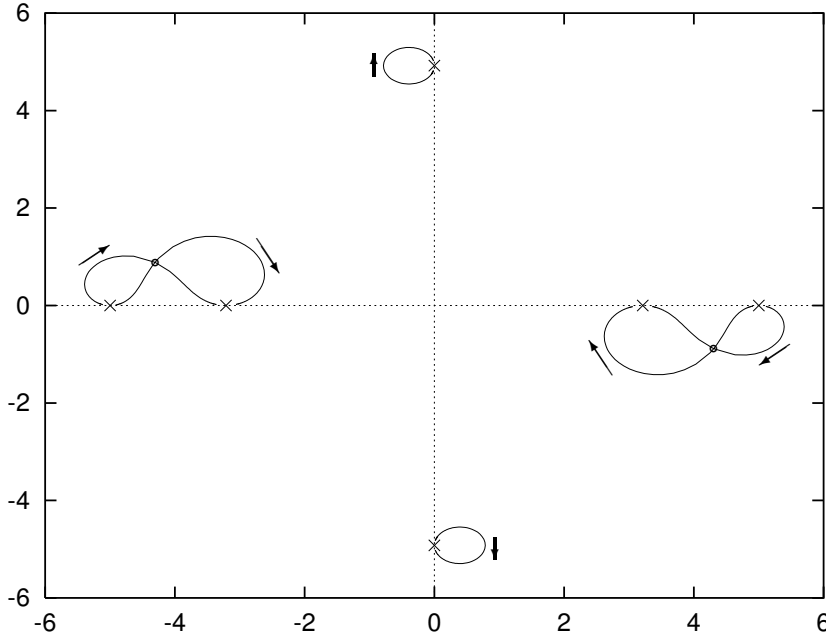


Figure 7.7 Trajectories of $k_{m\mu}$ ($m = 0$, $\omega = 5$) passing Cremer's optimum. At $Z = (1.4165, -0.6082)$ the first two modes coalesce as $k_{01}=k_{02}=(4.3057, -0.8857)$. $\text{Im}(Z)$ varies from $-\infty$ to ∞ and $\text{Re}(Z)$ is fixed at 1.4165 .

the geometry may play a rôle. Although it is strictly speaking not dissipation, the net reduction may benefit from reflections at discontinuities in the duct (hard/soft walls, varying cross section).

A simple approach would be to look at the reduction per mode, and to maximize the decay rate of the least attenuated mode, *i.e.* the one with the *smallest* $|\text{Im}(k_{m\mu})|$. A further simplification is based on the observation that the decay rate $\text{Im}(k_{m\mu})$ of a mode increases with increasing order, so that a (relatively) large decay rate is obtained if the first and second mode (of the most relevant m) *coalesce* (Cremer's optimum). This is obtained if also the derivative to $\alpha_{m\mu}$ of (7.24) vanishes, yielding the additional condition

$$J'_m(\alpha_{m\mu})^2 + \left(1 - \frac{m^2}{\alpha_{m\mu}^2}\right) J_m(\alpha_{m\mu})^2 = 0 \quad (7.28)$$

(see also exercise 7d). An example is given in figure 7.7. Note that no mode is lost, as the two corresponding modes degenerate into

$$J_m(\alpha_{m\mu}r) N_{m\mu} e^{-ik_{m\mu}x - im\vartheta} , \quad (7.29a)$$

$$\left(\alpha_{m\mu}x J_m(\alpha_{m\mu}r) - ik_{m\mu}r J'_m(\alpha_{m\mu}r)\right) N_{m\mu} e^{-ik_{m\mu}x - im\vartheta} . \quad (7.29b)$$

7.5 Annular hard-walled duct modes in uniform mean flow

With uniform mean flow (see equation 2.52), the modal theory still applies. In view of applications, we consider an annular duct of (scaled) inner radius h .

Consider the following linearized equations for small perturbations

$$\left(i\omega + M \frac{\partial}{\partial x}\right)p + \nabla \cdot \mathbf{v} = 0, \quad (7.30a)$$

$$\left(i\omega + M \frac{\partial}{\partial x}\right)\mathbf{v} + \nabla p = 0, \quad (7.30b)$$

with hard-wall boundary conditions. Eliminate \mathbf{v} to obtain the convected wave equation

$$\left(i\omega + M \frac{\partial}{\partial x}\right)^2 p - \nabla^2 p = 0, \quad (7.31)$$

Note, however, the possibility of convective incompressible pressureless disturbances of the form

$$\mathbf{v} = \mathbf{F}(r, \theta) e^{-i\frac{\omega}{M}x}, \text{ such that } \nabla \cdot \mathbf{v} = 0 \text{ and } p \equiv 0.$$

Fully written out, equation (7.31) becomes

$$\left(i\omega + M \frac{\partial}{\partial x}\right)^2 p - \left(\frac{\partial^2}{\partial x^2} + \frac{\partial^2}{\partial r^2} + \frac{1}{r} \frac{\partial}{\partial r} + \frac{1}{r^2} \frac{\partial^2}{\partial \vartheta^2}\right)p = 0. \quad (7.32)$$

The eigenvalue problem can now be solved, and we may expand the general solution in Fourier-Bessel modes

$$p(x, r, \theta) = \sum_{m=-\infty}^{\infty} \sum_{\mu=1}^{\infty} \left(A_{m\mu} e^{-ik_{m\mu}^+ x} + B_{m\mu} e^{-ik_{m\mu}^- x}\right) U_{m\mu}(r) e^{-im\theta} \quad (7.33)$$

where the radial modes and radial and axial wave numbers satisfy

$$U_{m\mu}'' + \frac{1}{r} U_{m\mu}' + \left(\alpha_{m\mu}^2 - \frac{m^2}{r^2}\right) U_{m\mu} = 0 \quad (7.34a)$$

$$\alpha_{m\mu}^2 = (\omega - M k_{m\mu})^2 - k_{m\mu}^2 \quad (7.34b)$$

$$k_{m\mu}^{\pm} = \frac{-\omega M \pm \sqrt{\omega^2 - (1 - M^2)\alpha_{m\mu}^2}}{1 - M^2} \quad (7.34c)$$

and solution

$$U_{m\mu}(r) = N_{m\mu} \left(\cos(\tau_{m\mu}) J_m(\alpha_{m\mu} r) - \sin(\tau_{m\mu}) Y_m(\alpha_{m\mu} r)\right). \quad (7.35)$$

The corresponding phase and group velocities for cut-on modes are found to be

$$v_{ph}^{\pm} = \frac{\omega}{k_{m\mu}^{\pm}} = \frac{\omega^2 M \pm \omega \sqrt{\omega^2 - (1 - M^2)\alpha_{m\mu}^2}}{\omega^2 - \alpha_{m\mu}^2}, \quad (7.36a)$$

$$v_g^{\pm} = \left(\frac{dk_{m\mu}^{\pm}}{d\omega} \right)^{-1} = \frac{k_{m\mu}^{\pm}}{\omega - M k_{m\mu}^{\pm}} + M = \pm \frac{(1 - M^2) \sqrt{\omega^2 - (1 - M^2)\alpha_{m\mu}^2}}{\omega \mp M \sqrt{\omega^2 - (1 - M^2)\alpha_{m\mu}^2}}. \quad (7.36b)$$

while $(v_g^{\pm} - M)(v_{ph}^{\pm} - M) = 1$. Due to the mean flow, the axial modal wave numbers are shifted to the left ($M > 0$), or right ($M < 0$), by a fixed amount of $-\omega M/(1 - M^2)$, while the (dimensionless) cut-off frequency is lowered from $\omega = \alpha_{m\mu}$ for no flow to $\omega = \alpha_{m\mu} \sqrt{1 - M^2}$ with flow. So with flow more modes are possibly cut-on than without. Note that (for $M > 0$) the rightrunning modes that become cut-on in this way (and only these) have a negative real part of their axial wave number. Indeed, rightrunning modes with a frequency along the interval

$$\alpha_{m\mu} \sqrt{1 - M^2} < \omega < \alpha_{m\mu}$$

have phase velocities that are *opposite* to their group velocities, the speed of information. The same applies for left-running modes if $M < 0$. Since $v_g^+ > 0$ and $v_g^- < 0$, this shows that it is not the sign of $k_{m\mu}$ but of its radical that corresponds with the direction of propagation [148]; *c.f.* equation (7.42).

Eigenvalues $\alpha_{m\mu}$ are determined via boundary condition $U'_{m\mu}(1) = U'_{m\mu}(h) = 0$

$$J'_m(\alpha) Y'_m(\alpha h) - J'_m(\alpha h) Y'_m(\alpha) = 0 \quad (7.37)$$

The normalization is such that $\int_h^1 U^2(r) r dr = 1$ (*c.f.* [199]), so

$$N_{m\mu} = \frac{\frac{1}{2} \sqrt{2} \pi \alpha_{m\mu}}{\left\{ \frac{1 - m^2/\alpha_{m\mu}^2}{J'_m(\alpha_{m\mu})^2 + Y'_m(\alpha_{m\mu})^2} - \frac{1 - m^2/\alpha_{m\mu}^2 h^2}{J'_m(\alpha_{m\mu} h)^2 + Y'_m(\alpha_{m\mu} h)^2} \right\}^{\frac{1}{2}}} \quad (7.38)$$

and

$$\tau_{m\mu} = \arctan \left\{ \frac{J'_m(\alpha_{m\mu})}{Y'_m(\alpha_{m\mu})} \right\}. \quad (7.39)$$

This implies the following choice of signs

$$\cos \tau_{m\mu} = \text{sign}(Y'_m(\alpha_{m\mu})) \frac{Y'_m(\alpha_{m\mu})}{\sqrt{J'_m(\alpha_{m\mu})^2 + Y'_m(\alpha_{m\mu})^2}}, \quad (7.40a)$$

$$\sin \tau_{m\mu} = \text{sign}(Y'_m(\alpha_{m\mu})) \frac{J'_m(\alpha_{m\mu})}{\sqrt{J'_m(\alpha_{m\mu})^2 + Y'_m(\alpha_{m\mu})^2}}, \quad (7.40b)$$

with the advantage that it reduces to the expected limit $N_{m\mu} J_m(\alpha_{m\mu} r)$ for $h \rightarrow 0$. Other choices, for example without the factor $\text{sign}(Y'_m)$, are also possible.

The modes are physically interesting because their shape remains the same. Mathematically, they are interesting because they form a complete and orthonormal L_2 -basis for the solutions of the convected wave equation (except for the pressureless convected perturbations):

$$\int_0^{2\pi} \int_h^1 U_{m\mu}(r) U_{n\nu}(r) e^{im\theta} e^{-in\theta} r \, dr d\theta = 2\pi \delta_{mn} \delta_{\mu\nu} \quad (7.41)$$

It is convenient to introduce the *Lorentz* or *Prandtl-Glauert* type transformation (see 3.46 and section 9.1.1)

$$\begin{aligned} \beta &= \sqrt{1 - M^2}, \quad x = \beta X, \quad \omega = \beta \Omega, \quad \alpha_{m\mu} = \Omega \gamma_{m\mu} \\ k_{m\mu}^\pm &= \frac{\pm \Omega \sigma_{m\mu} - \Omega M}{\beta}, \quad \sigma_{m\mu} = \sqrt{1 - \gamma_{m\mu}^2}, \end{aligned} \quad (7.42)$$

where $\sigma_{m\mu}$ is positive real or negative imaginary, then we have for pressure p and axial acoustic velocity v

$$p = \sum_{m=-\infty}^{\infty} \sum_{\mu=1}^{\infty} \left(A_{m\mu} e^{-i\Omega \sigma_{m\mu} X} + B_{m\mu} e^{i\Omega \sigma_{m\mu} X} \right) e^{i\Omega M X} U_{m\mu}(r) e^{-im\theta} \quad (7.43a)$$

$$v = \sum_{m=-\infty}^{\infty} \sum_{\mu=1}^{\infty} \left(\frac{\sigma_{m\mu} - M}{1 - M \sigma_{m\mu}} A_{m\mu} e^{-i\Omega \sigma_{m\mu} X} - \frac{\sigma_{m\mu} + M}{1 + M \sigma_{m\mu}} B_{m\mu} e^{i\Omega \sigma_{m\mu} X} \right) e^{i\Omega M X} U_{m\mu}(r) e^{-im\theta} \quad (7.43b)$$

This includes the important case of the plane wave $m = 0, \mu = 1$, with $\alpha_{01} = 0, k_{01}^\pm = \pm \omega / (1 \pm M)$ and $U_{01} = (2/(1 - h^2))^{1/2}$, such that

$$p(x, r, \theta) = \left[A_{01} e^{-\frac{i\omega x}{1+M}} + B_{01} e^{\frac{i\omega x}{1-M}} \right] \left(\frac{2}{1 - h^2} \right)^{1/2}, \quad (7.44a)$$

$$v(x, r, \theta) = \left[A_{01} e^{-\frac{i\omega x}{1+M}} - B_{01} e^{\frac{i\omega x}{1-M}} \right] \left(\frac{2}{1 - h^2} \right)^{1/2}. \quad (7.44b)$$

If we have at position $x = 0$ a given pressure and axial velocity profiles $P(0, r, \theta)$ and $V(0, r, \theta)$, we can expand these profiles in the following Fourier-Bessel series

$$P(0, r, \theta) = \sum_{m=-\infty}^{\infty} \sum_{\mu=1}^{\infty} P_{m\mu} U_{m\mu}(r) e^{-im\theta}, \quad (7.45a)$$

$$V(0, r, \theta) = \sum_{m=-\infty}^{\infty} \sum_{\mu=1}^{\infty} V_{m\mu} U_{m\mu}(r) e^{-im\theta}, \quad (7.45b)$$

where

$$P_{m\mu} = \frac{1}{2\pi} \int_0^{2\pi} \int_h^1 P(0, r, \theta) U_{m\mu}(r) e^{im\theta} r \, dr d\theta, \quad (7.46a)$$

$$V_{m\mu} = \frac{1}{2\pi} \int_0^{2\pi} \int_h^1 V(0, r, \theta) U_{m\mu}(r) e^{im\theta} r \, dr d\theta. \quad (7.46b)$$

If these pressure and velocity profiles satisfy the above propagation model of sound in uniform mean flow, the corresponding amplitudes $A_{m\mu}$ and $B_{m\mu}$ are found from identifying

$$P_{m\mu} = A_{m\mu} + B_{m\mu}, \quad (7.47a)$$

$$V_{m\mu} = \frac{\sigma_{m\mu} - M}{1 - M\sigma_{m\mu}} A_{m\mu} - \frac{\sigma_{m\mu} + M}{1 + M\sigma_{m\mu}} B_{m\mu}, \quad (7.47b)$$

leading to

$$A_{m\mu} = \frac{(1 - M\sigma_{m\mu})(\sigma_{m\mu} + M)P_{m\mu} + (1 - M^2\sigma_{m\mu}^2)V_{m\mu}}{2\sigma_{m\mu}(1 - M^2)}, \quad (7.48a)$$

$$B_{m\mu} = \frac{(1 + M\sigma_{m\mu})(\sigma_{m\mu} - M)P_{m\mu} - (1 - M^2\sigma_{m\mu}^2)V_{m\mu}}{2\sigma_{m\mu}(1 - M^2)}. \quad (7.48b)$$

From the axial intensity in hard-walled flow duct

$$\langle \mathbf{I}_x \rangle = \frac{1}{2} \operatorname{Re}[(p + Mu)(u^* + Mp^*)] \quad (7.49)$$

we obtain the axial power:

$$\begin{aligned} \mathcal{P} = \pi\beta^4 \sum_{m=-\infty}^{\infty} \left[\sum_{\mu=1}^{\mu_0} \sigma_{m\mu} \left[\frac{|A_{m\mu}|^2}{(1 - M\sigma_{m\mu})^2} - \frac{|B_{m\mu}|^2}{(1 + M\sigma_{m\mu})^2} \right] + \dots \right. \\ \left. \sum_{\mu=\mu_0+1}^{\infty} \frac{2|\sigma_{m\mu}|}{(1 + M^2|\sigma_{m\mu}|^2)^2} \cdot \left[\operatorname{Im}(A_{m\mu} B_{m\mu}^*) (1 - M^2|\sigma_{m\mu}|^2) - \operatorname{Re}(A_{m\mu} B_{m\mu}^*) 2M|\sigma_{m\mu}| \right] \right] \quad (7.50) \end{aligned}$$

where μ_0 is the number of cut-on modes. Note the coupling between left- and right-running cut-off modes.

7.6 Behaviour of soft-wall modes and mean flow

Consider a cylindrical duct with soft wall of specific impedance Z and uniform mean flow of Mach number M . For this configuration the acoustic field allows again modes, similar to the no-flow situation, although their behaviour with respect to possible surface waves is more complicated [207].

We start with modes of the same form as for the hard wall case (equations 7.33 with 7.42, and 7.43a) for pressure p and radial velocity v (we drop the exponentials with $i\omega t$ and $im\theta$)

$$p = e^{-i\Omega\sigma X + i\Omega M X} J_m(\Omega\gamma r), \quad v = \frac{i\beta\gamma}{1 - M\sigma} e^{-i\Omega\sigma X + i\Omega M X} J'_m(\Omega\gamma r),$$

where $\gamma^2 + \sigma^2 = 1$ and the sign of σ depends (in general) on the direction of propagation³. From the boundary condition (see equation 3.42)

$$i\omega Z v = \left(i\omega + M \frac{\partial}{\partial x}\right) p$$

we find the equation for reduced axial wave number σ for any given Z , m , and ω

$$(1 - M\sigma)^2 J_m(\Omega\gamma) - i\beta^3 Z \gamma J'_m(\Omega\gamma) = 0. \quad (7.51)$$

A graphical description of their behaviour as a function of $\text{Im } Z$ (from $+\infty$ down to $-\infty$) and fixed $\text{Re } Z$ is given in the series of figures (7.8). For large enough frequency, ω , the behaviour of the modes can be classified as follows. When σ is near a hard-wall value, the mode described is really of acoustic nature, extending radially through the whole duct. However, when σ is far enough away from a hard-wall value, the imaginary part of $\Omega\gamma$ becomes significant. The complex Bessel function $J_m(\Omega\gamma r)$ becomes exponentially decaying away from the wall, and the mode is radially restricted to the duct wall region. In other words, it has become a surface wave, of two-dimensional nature, approximately described by the theory of section 3.2.6 (eqn. 3.47).

The “egg” (figure 3.3), indicating the location of possible surface waves in the 2D limit, is drawn in the figures by a dotted line. The 2D surface wave solutions are indicated by black lines. The behaviour of the modes is to a certain extent similar to the no-flow situation (section 7.4.1, figures 7.5), although the effect of the mean flow is that we have now 4 rather than 2 possible surface waves.

For large $\text{Re } Z$, the modes remain near their hard-wall values. For lower values of $\text{Re } Z$ the behaviour becomes more irregular. The modes change position with a neighbour, and some become temporarily a surface wave. The two hydrodynamic modes disappear to infinity for $\text{Im } Z \rightarrow -\infty$ like is described in equation (3.48).

³Note that if $\sigma = 1/M$, i.e. if $\gamma = \pm i\beta/M$, we have to rescale the modal amplitude such that $p = 0$. In this case the mode is a pressureless vorticity mode, comparable with (3.66).

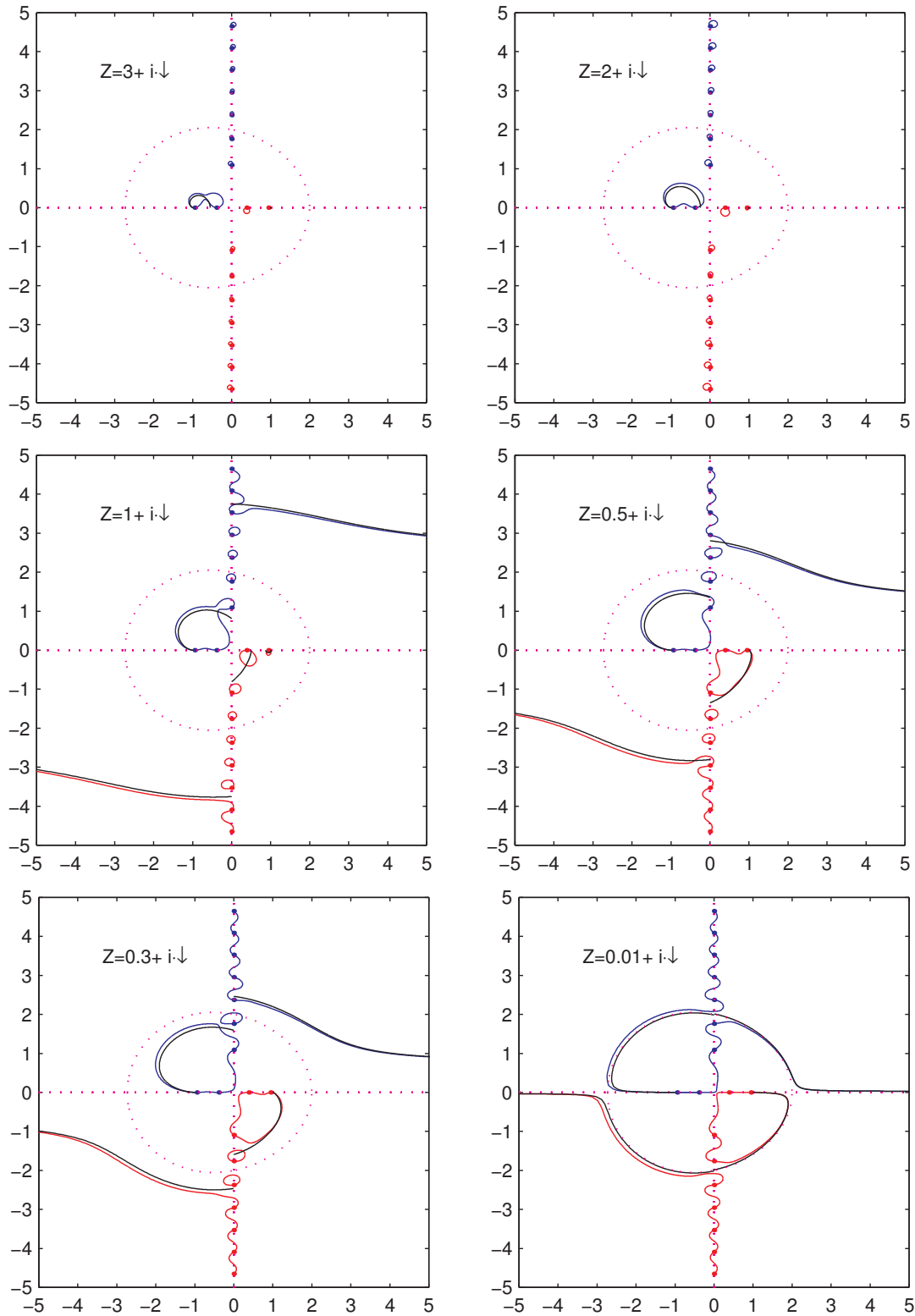


Figure 7.8 Trajectories of reduced wave number $\sigma_{m\mu}$ ($m = 1, \omega = 5$) where $M = 0.5$, for $\text{Im}(Z)$ varying from $-\infty$ to ∞ and fixed $\text{Re}(Z)$. The 2D surface wave solutions of eqn. (3.47) are included as black lines.

7.7 Source expansion

7.7.1 Modal amplitudes

A source at $x = 0$, defined by

$$p(x, r, \vartheta) \Big|_{x=0} = p_0(r, \vartheta)$$

produces in a hard walled duct a sound field (7.15) with modal amplitudes given by (in $x > 0$)

$$A_{m\mu} = \frac{1}{2\pi} \int_0^{2\pi} \int_0^1 p_0(r, \vartheta) U_{m\mu}(r) e^{im\vartheta} r \, dr d\vartheta \quad (7.52a)$$

$$B_{m\mu} = 0 \quad (7.52b)$$

(use (7.16)), and the same in $x < 0$ but with A and B interchanged. Note that, similar to the evanescent waves of section 3.3, details of the source (averaged out for the lower modes in the process of integration), only contribute to higher order modes and do not generate sound if these modes are cut-off.

7.7.2 Rotating fan

Of practical interest, especially in aircraft noise reduction [244], is the following model of a propeller or fan with B identical blades, equally spaced $\Delta\vartheta = 2\pi/B$ radians apart, rotating with angular speed Ω . If at some time $t = 0$ at a fixed position x the field due to one blade is given by the shape function $q(\vartheta, r)$, then from periodicity the total field is described by

$$\begin{aligned} p(r, \vartheta, 0) &= q(\vartheta, r) + q(\vartheta - \Delta\vartheta, r) + \cdots + q(\vartheta - (B-1)\Delta\vartheta, r) \\ &= \sum_{k=0}^{B-1} q\left(\vartheta - \frac{2\pi k}{B}, r\right). \end{aligned}$$

This function, periodic in ϑ with period $2\pi/B$, may be expanded in a Fourier series:

$$p(\vartheta, r, 0) = \sum_{n=-\infty}^{\infty} q_n(r) e^{-inB\vartheta}.$$

Since the field is associated to the rotor, it is a function of $\vartheta - \Omega t$. So at a time t

$$p(\vartheta, r, t) = \sum_{k=0}^{B-1} q\left(\vartheta - \Omega t - \frac{2\pi k}{B}, r\right) = \sum_{n=-\infty}^{\infty} q_n(r) e^{inB\Omega t - inB\vartheta} \quad (7.53)$$

(with $q_{-n} = q_n^*$ because p is real). Evidently, the field is built up from harmonics of the blade passing frequency $B\Omega$. Note that each frequency $\omega = nB\Omega$ is now linked to a circumferential periodicity $m = nB$, and we jump with steps B through the modal m -spectrum. Since the plane wave ($m = 0$) is generated with frequency $\omega = 0$ it is acoustically not interesting, and we may ignore this component. An interesting consequence for a rotor in a duct is the observation that it is not obvious if there is (propagating) sound generated at all: the frequency must be higher than the cut-off frequency. For any harmonic ($n > 0$) we have:

$$f_m = \frac{m\Omega}{2\pi} > \frac{j'_{m1}c_0}{2\pi a} \quad (7.54)$$

which is for the tip Mach number M_{tip} the condition

$$M_{tip} = \frac{a\Omega}{c_0} > \frac{j'_{m1}}{m}. \quad (7.55)$$

Since the first zero of J'_m is always (slightly) larger than m (Appendix D), it implies that the tip must rotate *supersonically* ($M_{tip} > 1$) for the fan to produce sound.

Of course, in practice a ducted fan with subsonically rotating blades will not be entirely silent. For example, ingested turbulence and the turbulent wake of the blades are not periodic and will therefore not follow this cut-off reduction mechanism. On the other hand, if the perturbations resulting from blade thickness and lift forces alone are dominating as in aircraft engines, the present result is significant, and indeed the inlet fan noise level of many aircraft turbo fan engines is greatly enhanced at take off by the inlet fan rotating supersonically (together with other effects leading to the so-called *buzzsaw noise* ([233])).

7.7.3 Tyler and Sofrin rule for rotor-stator interaction

The most important noise source of an aircraft turbo fan engine at inlet side is the noise due to interaction between inlet rotor and neighbouring stator.

Behind the inlet rotor, or fan, a stator is positioned (figure 7.9) to compensate for the rotation, or swirl, in the flow due to the rotor. The viscous and inviscid wakes from the rotor blades hit the stator vanes which results into the generation of sound ([228]). A very simple but at the same time very important and widely used device to reduce this sound is the “Tyler and Sofrin selection rule” ([233, 244]). It is based on elegant manipulation of Fourier series, and amounts to nothing more than a clever choice of the rotor blade and stator vane numbers, to link the first (few) harmonics of the sound to duct modes that are cut-off and therefore do not propagate.

Consider the same rotor as above, with B identical blades, equally spaced $\Delta\vartheta = 2\pi/B$ radians apart, rotating with angular speed Ω , and a stator with V identical vanes, equally spaced $\Delta\vartheta = 2\pi/V$ radians apart. First, we observe that the field generated by rotor-stator interaction must have the time

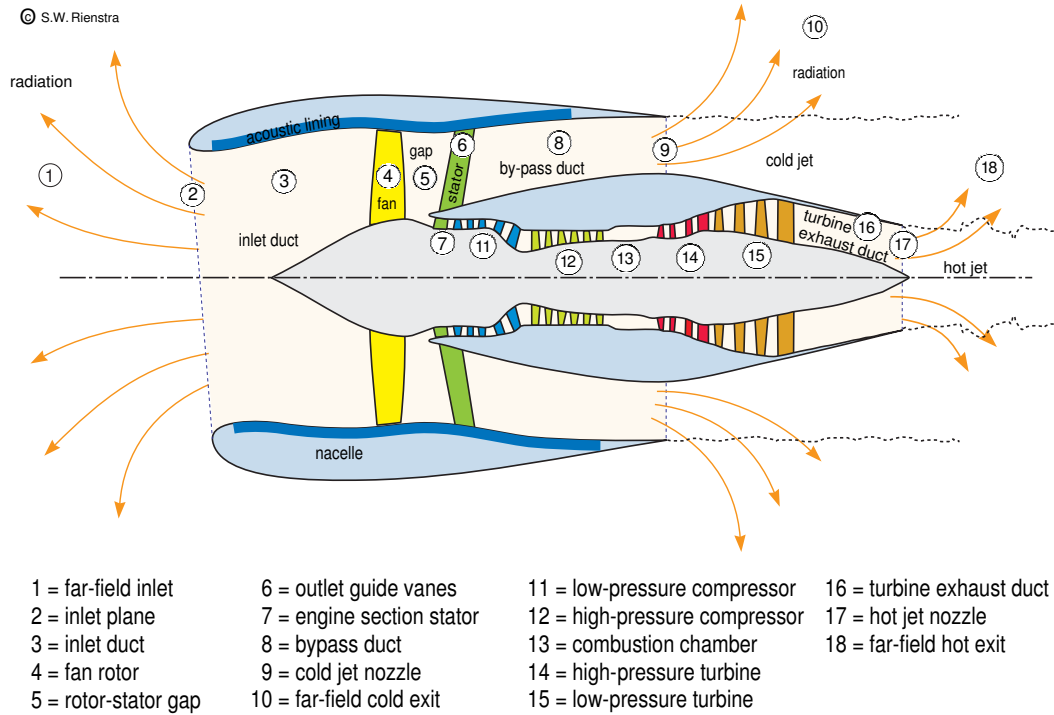


Figure 7.9 Sketch of high by-pass turbo fan engine. Note the fan (or inlet rotor), which produces with the stator (or outlet guide vanes) the important *rotor-stator interaction* noise. This is to be attenuated by the acoustically lined walls of the inlet and bypass duct.

dependence of the rotor, and is therefore built up from harmonics of the blade passing frequency $B\Omega$. Furthermore, it is periodic in ϑ , so it may be written as

$$p(r, \vartheta, t) = \sum_{n=-\infty}^{\infty} Q_n(r, \vartheta) e^{inB\Omega t} = \sum_{n=-\infty}^{\infty} \sum_{m=-\infty}^{\infty} Q_{nm}(r) e^{inB\Omega t - im\vartheta} .$$

However, we can do better than that, because most of the m -components are just zero. The field is periodic in ϑ with the stator periodicity $2\pi/V$ in such a way that when we travel with the rotor over an angle $\Delta\vartheta = 2\pi/V$ in a time step $\Delta t = \Delta\vartheta/\Omega$ the field must be the same:

$$p(r, \vartheta, t) = \sum_{n=-\infty}^{\infty} \sum_{m=-\infty}^{\infty} Q_{nm}(r) e^{inB\Omega(t-\Delta t) - im(\vartheta-\Delta\vartheta)} .$$

This yields for any m the restriction: $-inB\Omega\Delta t + im\Delta\vartheta = 2\pi ik$, or

$$m = kV + nB \tag{7.56}$$

where k is any integer, and n the harmonic of interest. By selecting B and V such that the lowest $|m|$ possible is high enough for the harmonic of interest to be cut-off, this component is effectively absent for a long enough inlet duct. In practice, only the first harmonic is reduced in this way. A recent development is that the second harmonic, which is usually cut-on, is reduced by selecting the mode number m to be of opposite sign of n , which means: counter rotating with respect to the rotor. In this case the rotor itself acts as a shield obstructing the spiralling modes to leave the duct ([228]).

In detail: for a cut-off n -th harmonic (we only have to consider positive n) we need

$$\frac{nB\Omega}{2\pi} < \frac{j'_{m1}c_0}{2\pi a} \quad \text{or} \quad nBM_{tip} < j'_{m1}.$$

Since typically M_{tip} is slightly smaller than 1 and j'_{m1} is slightly larger than $|m|$ we get the analogue of evanescent wave condition $k < |\alpha|$ (section 3.3)

$$nB \leq |m| = |kV + nB|.$$

The only values of kV for which this inequality is not satisfied automatically is in the interval $-2nB < kV < 0$. If we make the step size V big enough so that we avoid this interval for $k = -1$, we avoid it for any k . So we have finally the condition: $V \geq 2nB$.

Consider, as a realistic example, the following configuration of a rotor with $B = 22$ blades and a stator with $V = 55$ vanes. The generated m -modes are for the first two harmonics:

$$\begin{aligned} \text{for } n = 1: \quad m &= \dots, -33, 22, 77, \dots, \\ \text{for } n = 2: \quad m &= \dots, -11, 44, 99, \dots, \end{aligned}$$

which indeed corresponds to only cut-off modes of the first harmonic ($m = 22$ and larger) and a counter rotating cut-on second harmonic ($m = -11$).

7.7.4 Point source in a lined flow duct

Consider a cylindrical duct of non-dimensional radius 1, a mean flow of subsonic Mach number M , and harmonic pressure and velocity perturbations p of non-dimensional angular frequency ω . The pressure is excited by a point source at \mathbf{x}_0 , and satisfies the equation

$$\nabla^2 p - \left(i\omega + M \frac{\partial}{\partial x} \right)^2 p = \delta(\mathbf{x} - \mathbf{x}_0), \quad (7.57)$$

so $p(\mathbf{x}; \mathbf{x}_0)$ represents the Green's function of the system. Note that we use the $e^{i\omega t}$ - convention. The impedance boundary condition at $r = 1$ (3.42), becomes in terms of the pressure

$$\left(i\omega + M \frac{\partial}{\partial x} \right)^2 p + i\omega Z \frac{\partial p}{\partial r} = 0 \quad \text{at } r = 1. \quad (7.58)$$

For a hollow duct finiteness of p is assumed at $r = 0$. Finally, we adopt radiation conditions that says that we only accept solutions that radiate away from the source position \mathbf{x}_0 .

We represent the delta-function by a generalized Fourier series in ϑ and Fourier integral in x

$$\delta(\mathbf{x} - \mathbf{x}_0) = \frac{\delta(r - r_0)}{r_0} \frac{1}{2\pi} \int_{-\infty}^{\infty} e^{-i\kappa(x-x_0)} d\kappa \frac{1}{2\pi} \sum_{m=-\infty}^{\infty} e^{-im(\vartheta-\vartheta_0)}. \quad (7.59)$$

where $0 < r_0 < 1$, and write accordingly

$$p(x, r, \vartheta) = \sum_{m=-\infty}^{\infty} e^{-im(\vartheta-\vartheta_0)} p_m(x, r) = \sum_{m=-\infty}^{\infty} e^{-im(\vartheta-\vartheta_0)} \int_{-\infty}^{\infty} \hat{p}_m(r, \kappa) e^{-i\kappa(x-x_0)} d\kappa. \quad (7.60)$$

Substitution of (7.59) and (7.60) in (7.57) yields for \hat{p}_m

$$\frac{\partial^2 \hat{p}_m}{\partial r^2} + \frac{1}{r} \frac{\partial \hat{p}_m}{\partial r} + \left(\alpha^2 - \frac{m^2}{r^2} \right) \hat{p}_m = \frac{\delta(r - r_0)}{4\pi^2 r_0},$$

with

$$\alpha^2 = \Omega^2 - \kappa^2, \quad \Omega = \omega - \kappa M.$$

This has solution

$$\hat{p}_m(r, \kappa) = A(\kappa) J_m(\alpha r) + \frac{1}{8\pi} H(r - r_0) (J_m(\alpha r_0) Y_m(\alpha r) - Y_m(\alpha r_0) J_m(\alpha r))$$

where use is made of the Wronskian

$$J_m(x) Y'_m(x) - Y_m(x) J'_m(x) = \frac{2}{\pi x}. \quad (7.61)$$

A prime denotes a derivative to the argument, x . $A(\kappa)$ is to be determined from the boundary conditions at $r = 1$, which is (assuming uniform convergence) per mode

$$i\Omega^2 \hat{p}_m + \omega Z \hat{p}'_m = 0 \quad \text{at } r = 1.$$

A prime denotes a derivative to r . This yields

$$A = \frac{1}{8\pi} \left[Y_m(\alpha r_0) - \frac{i\Omega^2 Y_m(\alpha) + \omega \alpha Z Y'_m(\alpha)}{i\Omega^2 J_m(\alpha) + \omega \alpha Z J'_m(\alpha)} J_m(\alpha r_0) \right],$$

and thus

$$\hat{p}_m(r, \kappa) = J_m(\alpha r_0) \frac{i\Omega^2 G_m(r_>, \alpha) + \omega Z H_m(r_>, \alpha)}{8\pi E_m(\kappa)},$$

where $r_> = \max(r, r_0)$, $r_< = \min(r, r_0)$ and

$$\begin{aligned} E_m(\kappa) &= i\Omega^2 J_m(\alpha) + \omega\alpha Z J'_m(\alpha) \\ G_m(r, \alpha) &= J_m(\alpha) Y_m(\alpha r) - Y_m(\alpha) J_m(\alpha r) \\ H_m(r, \alpha) &= \alpha J'_m(\alpha) Y_m(\alpha r) - \alpha Y'_m(\alpha) J_m(\alpha r) \end{aligned}$$

By substituting the defining series we find that G_m and H_m are analytic functions of α^2 , while both E_m and $J_m(\alpha r_<)$ can be written as α^m times an analytic function of α^2 . As a result, $\hat{p}_m(r, \kappa)$ is a meromorphic⁴ function of κ . It has isolated poles $\kappa = \kappa_{m\mu}^\pm$, given by

$$E_m(\kappa_{m\mu}^\pm) = 0,$$

which is equivalent to (7.51). The final solution is found by Fourier back-transformation: close the integration contour around the lower half plane for $x > x_0$ to enclose the complex modal wave numbers of the right-running modes, and the upper half plane for $x < x_0$ to enclose the complex modal wave numbers of the left-running modes. In figure 7.10 a typical location of the integration contour with no-flow modes is shown. See also figures 7.5, 7.6 and 7.8.

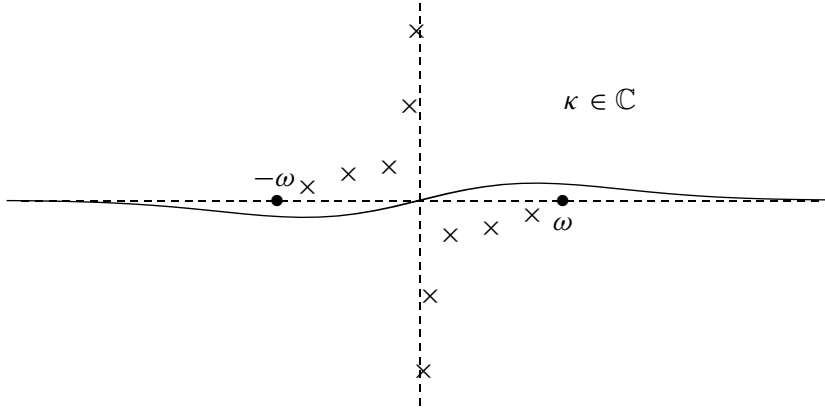


Figure 7.10 Contour of integration in the κ -plane.

We define

$$Q_{m\mu} = \pm \left[(\kappa_{m\mu} + \Omega_{m\mu} M) \left(1 - \frac{m^2}{\alpha_{m\mu}^2} - \frac{\Omega_{m\mu}^4}{(\omega \alpha_{m\mu} Z)^2} \right) - \frac{2i M \Omega_{m\mu}}{\omega Z} \right],$$

where $+/-$ relates to right/left-running modes. With the result

$$\left. \frac{dE_m}{d\kappa} \right|_{\kappa=\kappa_{m\mu}} = \pm \omega Z Q_{m\mu} J_m(\alpha_{m\mu})$$

⁴A meromorphic function is analytic on the complex plane except for isolated poles.

the integral is evaluated as a sum over the residues in the poles at $\kappa = \kappa_{m\mu}^+$ for $x > x_0$ and at $\kappa_{m\mu}^-$ for $x < x_0$. From eigenvalue equation $E_m(\kappa_{m\mu}^\pm) = 0$ and the Wronskian (7.61) we obtain

$$i\Omega_{m\mu}^2 G_m(r_>, \alpha_{m\mu}) + \omega Z H_m(r_>, \alpha_{m\mu}) = -\frac{2\omega Z}{\pi J_m(\alpha_{m\mu})} J_m(\alpha_{m\mu} r_>).$$

where $\alpha_{m\mu} = \alpha(\kappa_{m\mu})$. We can skip the distinction between $r_>$ and $r_<$ and achieve the soft wall modal expansion

$$p_m(x, r) = -\frac{1}{2\pi i} \sum_{\mu=1}^{\infty} \frac{J_m(\alpha_{m\mu} r) J_m(\alpha_{m\mu} r_0)}{Q_{m\mu} J_m^2(\alpha_{m\mu})} e^{-i\kappa_{m\mu}(x-x_0)} \quad (7.62)$$

where for $x > x_0$ the sum pertains to the right-running waves, corresponding to the modal wave numbers $\kappa_{m\mu}^+$ found in the lower complex half plane, and for $x < x_0$ the left-running waves, corresponding to $\kappa_{m\mu}^-$ found in the upper complex half plane (see [207]).

Only if a mode from the upper half plane is to be interpreted as a right-running instability (their existence is still an unresolved problem), its contribution is to be excluded from the set of modes for $x < x_0$ and included in the modes for $x > x_0$. The form of the solution remains exactly the same, as we do no more than deforming the integration contour into the upper half plane.

It may be noted that expression (7.62) is continuous in (x, r) , except at (x_0, r_0) where the series slowly diverges like a harmonic series. As may be expected from the symmetry of the configuration, the clockwise and anti-clockwise rotating circumferential modes are equal, *i.e.* $p_m(x, r) = p_{-m}(x, r)$.

Furthermore, the solution is continuous in r_0 , while $p_m \rightarrow 0$ if $r_0 \rightarrow 0$ for all $m \neq 0$. As a result, we find for $r_0 = 0$ the expected cylindrically symmetric $p(x, r, \theta) = p_0(x, r)$.

Solution (7.62) is very general. It includes both the no-flow solution (take $M = 0$) and the hard walled duct (take $Z = \infty$). Without mean flow the problem becomes symmetric in x and it may be notationally convenient to write $\alpha_{m\mu}^\pm = \alpha_{m\mu}$, $\kappa_{m\mu}^+ = \kappa_{m\mu}$ and $\kappa_{m\mu}^- = -\kappa_{m\mu}$.

Finding all the eigenvalues $\kappa_{m\mu}^\pm$ is evidently crucial for the evaluation of the series (7.62), in particular when surface waves (Section 3.2.6) occur. An example of $p_m(x, r)$ is plotted in figure 7.11.

7.7.5 Point source in a duct wall

A problem, closely related to the previous one, is the field from a source $\mathbf{v} \cdot \mathbf{e}_r = -\delta(x-x_0)$ in the duct wall $r = 1$. Consider for simplicity a hard-walled duct without mean flow. We have for the pressure

$$\frac{1}{i\omega} \frac{\partial p}{\partial r} \Big|_{r=1} = \frac{1}{2\pi} \int_{-\infty}^{\infty} e^{-i\kappa(x-x_0)} d\kappa \frac{1}{2\pi} \sum_{m=-\infty}^{\infty} e^{-im(\vartheta-\vartheta_0)}. \quad (7.63)$$

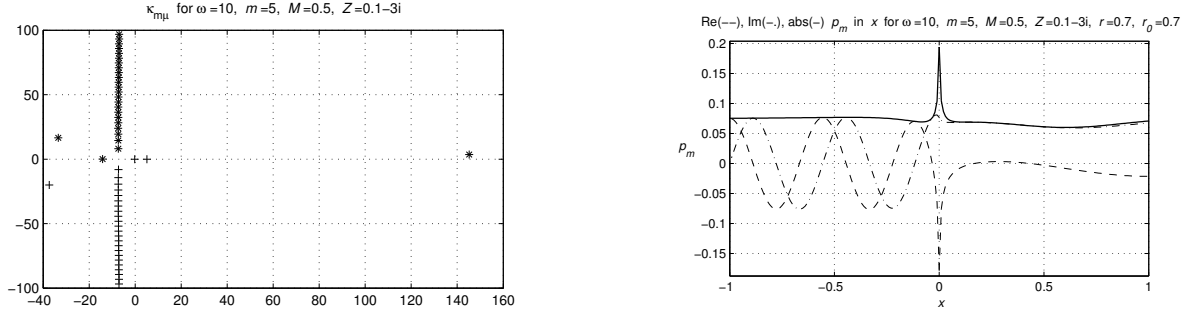


Figure 7.11 Eigenvalues $\kappa_{m\mu}^{\pm}$ and $\text{Re}(p_m)$, $\text{Im}(p_m)$ and $|p_m|$ is plotted of the $m = 5$ -th component of the point source field in a lined flow duct with $\omega = 10$, $Z = 0.1 - 3i$, $x_0 = 0$, $r_0 = 0.7$, $M = 0.5$ at $r = 0.7$ and $\theta = \theta_0$. Note the presence of 3 surface waves.

We solve equation (7.3a) again via Fourier transformation in x , and Fourier series expansion in ϑ . We obtain

$$p(x, r, \vartheta) = \sum_{m=-\infty}^{\infty} e^{-im(\vartheta-\vartheta_0)} \int_{-\infty}^{\infty} A_m(\kappa) J_m(\alpha(\kappa)r) e^{-i\kappa(x-x_0)} d\kappa \tag{7.64}$$

where $\alpha(\kappa)^2 = \omega^2 - \kappa^2$. From the Fourier transformed boundary condition (7.63) it follows that $\alpha A_m J'_m(\alpha) = -\omega/4\pi^2 i$, so

$$p(x, r, \vartheta) = -\frac{\omega}{4\pi^2 i} \sum_{m=-\infty}^{\infty} e^{-im(\vartheta-\vartheta_0)} \int_{-\infty}^{\infty} \frac{J_m(\alpha r)}{\alpha J'_m(\alpha)} e^{-i\kappa(x-x_0)} d\kappa.$$

The poles of the *meromorphic* integrand are found at $\kappa = \pm\kappa_{m\mu}$ (we use the symmetry in x), and since the waves must be outgoing the integration contour in the κ -plane must be located as in figure 7.10. Closing the contour via $\text{Im}(\kappa) \rightarrow -\infty$ for $x > 0$ and via $\text{Im}(\kappa) \rightarrow +\infty$ yields the solution, in the form of a series over the residue-contributions⁵ in $\kappa = \pm\kappa_{m\mu}$. This yields the modal expansion

$$p(x, r, \vartheta) = \frac{\omega}{2\pi} \sum_{m=-\infty}^{\infty} \sum_{\mu=1}^{\infty} \frac{J_m(\alpha_{m\mu}r) e^{-i\kappa_{m\mu}|x-x_0|-im(\vartheta-\vartheta_0)}}{(1 - m^2/\alpha_{m\mu}^2) J_m(\alpha_{m\mu}) \kappa_{m\mu}}. \tag{7.65}$$

The contribution of the $m = 0, \mu = 1$ plane-wave mode is

$$\frac{1}{2\pi} e^{-i\omega|x|}.$$

⁵Near $\kappa = \kappa_{m\mu}$ is $J'_m(\alpha(\kappa)) \simeq -(\kappa - \kappa_{m\mu})\kappa_{m\mu}\alpha_{m\mu}^{-1} J''_m(\alpha_{m\mu})$.

7.7.6 Vibrating duct wall

When, instead of a point, a finite part of the wall vibrates (*e.g.* [112]) as

$$r = 1 - \eta(x, \vartheta) e^{i\omega t} \quad \text{for} \quad -L \leq x \leq L \quad (7.66)$$

then the solution may be found as follows. We write as a Fourier sum

$$\eta(x, \vartheta) = \sum_{m=-\infty}^{\infty} e^{-im\vartheta} \eta_m(x) = \sum_{m=-\infty}^{\infty} e^{-im\vartheta} \int_{-\infty}^{\infty} \hat{\eta}_m(\kappa) e^{-i\kappa x} d\kappa.$$

Similar to above we find the solution $p(x, r, \vartheta)$ as a formal Fourier integral, which can be rewritten, by using result (7.65) and the Convolution Theorem (C.10) (p.281), as

$$p(x, r, \vartheta) = i\omega^2 \sum_{m=-\infty}^{\infty} \sum_{\mu=1}^{\infty} \frac{1}{\kappa_{m\mu}} \frac{\alpha_{m\mu}^2}{\alpha_{m\mu}^2 - m^2} \frac{J_m(\alpha_{m\mu} r)}{J_m(\alpha_{m\mu})} e^{-im\vartheta} \int_{-L}^L \eta_m(x') e^{-i\kappa_{m\mu}|x-x'|} dx' \quad (7.67)$$

with the plane-wave contribution

$$i\omega \int_{-L}^L \eta_0(x') e^{-i\omega|x-x'|} dx'.$$

A naive interpretation of this formula might suggest the contradictory result that the field, built up from hard-wall modes with vanishing r -derivative at the wall, does not satisfy the boundary condition of the moving wall. This is not the case, however, because the infinite series is not uniformly converging (at least, its radial derivative). Pointwise, the value at the wall is not equal to the limit to the wall, while it is only the limit which is physically relevant.

Although in the source region no simple modes can be recognized, outside this region, *i.e.* for $|x| > L$, the remaining integral is just the Fourier transform times exponential, $\hat{\eta}_m(\pm\kappa_{m\mu}) \exp(-\kappa_{m\mu}|x|)$, and the solution is again just a modal sum of right- or left-running modes.

7.8 Reflection and transmission

7.8.1 A discontinuity in diameter

One single modal representation is only possible in segments of a duct with constant properties (diameter, wall impedance). When two segments of different properties are connected to each other we can use a modal representation in each segment, but since the modes are different we have to reformulate the expansion of the incident field into an expansion of the transmitted field in the neighbouring segment, using conditions of continuity of pressure and velocity. This is called [146]: *mode matching*. Furthermore, these continuity conditions cannot be satisfied with a transmission field only, and a part of the incident field is reflected. Each mode is scattered into a modal spectrum of transmitted and reflected modes.

Consider a duct with a discontinuity in diameter at $x = 0$ (figure 7.12): a radius⁶ a along $x < 0$ and a radius b along $x > 0$. It is no restriction to assume for definiteness $a > b$. Because of circumferential symmetry there is no scattering into other m -modes, and we consider only a single m -mode of frequency ω . At the walls we have the boundary condition of vanishing normal velocity. At the interface $x = 0, 0 \leq r \leq b$ we have continuity of pressure and continuity of axial velocity.

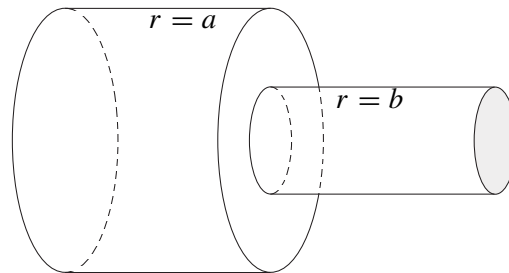


Figure 7.12 Duct with discontinuous diameter.

At the edges we have the so-called *edge condition* [144]: the energy integral of the field in a neighbourhood of an edge must be finite (no source hidden in the edge). This condition is necessary in a geometry with edges because the boundary conditions lose their meaning at an edge.

⁶In the present dimensionless formulation, where a and b are scaled on a reference duct radius, usually $a = 1$ or $b = 1$.

The incident fields $p_{in}^{(1)}$ ($x < 0$, right-running) and $p_{in}^{(2)}$ ($x > 0$, left-running), given by (see 7.14)

$$\begin{aligned} p_{in}^{(1)} &= \sum_{\nu=1}^{\infty} A_{m\nu}^{(1)} U_{m\nu}(r) e^{-ik_{m\nu}x - im\vartheta}, & U_{m\nu}(r) &= \frac{J_m(\alpha_{m\nu}r)}{\sqrt{\frac{1}{2}(a^2 - m^2/\alpha_{m\nu}^2)J_m(\alpha_{m\nu}a)^2}}, \\ p_{in}^{(2)} &= \sum_{\nu=1}^{\infty} A_{m\nu}^{(2)} V_{m\nu}(r) e^{ik_{m\nu}x - im\vartheta}, & V_{m\nu}(r) &= \frac{J_m(\beta_{m\nu}r)}{\sqrt{\frac{1}{2}(b^2 - m^2/\beta_{m\nu}^2)J_m(\beta_{m\nu}b)^2}}, \end{aligned} \quad (7.68a)$$

where $U_{01} = (\frac{1}{2}a^2)^{-\frac{1}{2}}$ and $V_{01} = (\frac{1}{2}b^2)^{-\frac{1}{2}}$, are scattered at $x = 0$ into $p_{sc}^{(1)}$ ($x < 0$, left-running) and $p_{sc}^{(2)}$ ($x > 0$, right-running), given by

$$\begin{aligned} p_{sc}^{(1)} &= \sum_{\nu=1}^{\infty} B_{m\nu}^{(1)} U_{m\nu}(r) e^{ik_{m\nu}x - im\vartheta}, \\ p_{sc}^{(2)} &= \sum_{\nu=1}^{\infty} B_{m\nu}^{(2)} V_{m\nu}(r) e^{-ik_{m\nu}x - im\vartheta}. \end{aligned} \quad (7.68b)$$

Suitable conditions of convergence of the infinite series are assumed, while

$$\begin{aligned} \alpha_{m\nu} &= j'_{m\nu}/a, & k_{m\nu} &= \sqrt{\omega^2 - \alpha_{m\nu}^2}, & \operatorname{Re}(k_{m\nu}) &\geq 0, & \operatorname{Im}(k_{m\nu}) &\leq 0, \\ \beta_{m\nu} &= j'_{m\nu}/b, & \ell_{m\nu} &= \sqrt{\omega^2 - \beta_{m\nu}^2}, & \operatorname{Re}(\ell_{m\nu}) &\geq 0, & \operatorname{Im}(\ell_{m\nu}) &\leq 0. \end{aligned} \quad (7.68c)$$

The total field is evidently $p_{in}^{(1)} + p_{sc}^{(1)}$ in $x < 0$ and $p_{in}^{(2)} + p_{sc}^{(2)}$ in $x > 0$. Since we will work with a finite number of modes, we will assume right from the start P modes in $x < 0$ and Q modes in $x > 0$.

Continuity of pressure at $x = 0$ requires that

$$\sum_{\nu=1}^P U_{m\nu}(A_{m\nu}^{(1)} + B_{m\nu}^{(1)}) = \sum_{\nu=1}^Q V_{m\nu}(B_{m\nu}^{(2)} + A_{m\nu}^{(2)}), \quad 0 \leq r \leq b \quad (7.69)$$

Multiply both sides by $V_{m\mu}(r)r$ for $\mu = 1 \dots Q$ and integrate from $r = 0$ to $r = b$. Since $\{V_{m\mu}\}$ is an orthonormal set, the integrals on the right-hand-side vanish if $\nu \neq \mu$ and are equal to unity if $\nu = \mu$. On the left-hand-side we obtain series with terms containing

$$M_{m\mu\nu} = \int_0^b V_{m\mu}(r)U_{m\nu}(r)r \, dr = -\frac{b}{\alpha_{m\nu}^2 - \beta_{m\mu}^2} V_{m\mu}(b)U'_{m\nu}(b), \quad (7.70)$$

where the integral is evaluated by using equations (D.58) and (D.59). If $\alpha_{m\nu} = \beta_{m\mu}$ (in particular the plane wave $\alpha_{01} = \beta_{01} = 0$)

$$M_{m\mu\nu} = \sqrt{\frac{(\alpha_{m\nu}^2 b^2 - m^2)J_m(\alpha_{m\nu}b)^2}{(\alpha_{m\nu}^2 a^2 - m^2)J_m(\alpha_{m\nu}a)^2}}, \quad M_{011} = \frac{b}{a}.$$

If we introduce the amplitude vectors $\mathbf{a} = (A_{m1}, \dots)^\top$, $\mathbf{b} = (B_{m1}, \dots)^\top$ (of length P in $x < 0$ or Q in $x > 0$) and the $Q \times P$ matrix $\mathcal{M}_{QP} = \{M_{m\mu\nu}\}$, we have eventually the matrix equation

$$\mathcal{M}_{QP}(\mathbf{a}_P^{(1)} + \mathbf{b}_P^{(1)}) = \mathbf{b}_Q^{(2)} + \mathbf{a}_Q^{(2)}. \quad (7.71)$$

In a similar way we find from continuity of pressure gradient (*i.e.* axial velocity),

$$\begin{aligned} \sum_{v=1}^P U_{mv} k_{mv} (A_{mv}^{(1)} - B_{mv}^{(1)}) &= 0, & b \leq r \leq a \\ \sum_{v=1}^P U_{mv} k_{mv} (A_{mv}^{(1)} - B_{mv}^{(1)}) &= \sum_{v=1}^Q V_{mv} \ell_{mv} (B_{mv}^{(2)} - A_{mv}^{(2)}), & 0 \leq r \leq b \end{aligned} \quad (7.72)$$

via multiplication both sides by $U_{m\mu}(r)r$ and integration from $r = 0$ to $r = a$, the following matrix equation

$$\mathbf{k}_{PP}(\mathbf{a}_P^{(1)} - \mathbf{b}_P^{(1)}) = \mathcal{M}_{PQ}^\top \boldsymbol{\ell}_{QQ}(\mathbf{b}_Q^{(2)} - \mathbf{a}_Q^{(2)}), \quad (7.73)$$

with again the matrix \mathcal{M} , and diagonal matrices \mathbf{k} and $\boldsymbol{\ell}$ derived from k_{mv} and ℓ_{mv} . Together with (7.71), this results eventually into the desired amplitudes of the scattered field

$$\begin{aligned} \mathbf{b}_P^{(1)} &= (\mathcal{I}_{PP} + \mathcal{N}_{PQ} \mathcal{M}_{QP})^{-1} (\mathcal{I}_{PP} - \mathcal{N}_{PQ} \mathcal{M}_{QP}) \mathbf{a}_P^{(1)} + 2(\mathcal{I}_{PP} + \mathcal{N}_{PQ} \mathcal{M}_{QP})^{-1} \mathcal{N}_{PQ} \mathbf{a}_Q^{(2)}, \\ \mathbf{b}_Q^{(2)} &= 2(\mathcal{I}_{QQ} + \mathcal{M}_{QP} \mathcal{N}_{PQ})^{-1} \mathcal{M}_{QP} \mathbf{a}_P^{(1)} - (\mathcal{I}_{QQ} + \mathcal{M}_{QP} \mathcal{N}_{PQ})^{-1} (\mathcal{I}_{QQ} - \mathcal{M}_{QP} \mathcal{N}_{PQ}) \mathbf{a}_Q^{(2)}, \end{aligned} \quad (7.74)$$

where \mathcal{I} is the unit matrix and an auxiliary matrix \mathcal{N} is introduced given by

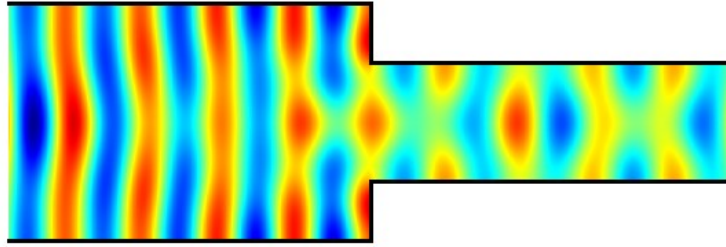
$$\mathcal{N}_{PQ} = \mathbf{k}_{PP}^{-1} \mathcal{M}_{PQ}^\top \boldsymbol{\ell}_{QQ}.$$

A convenient representation is the scattering matrix

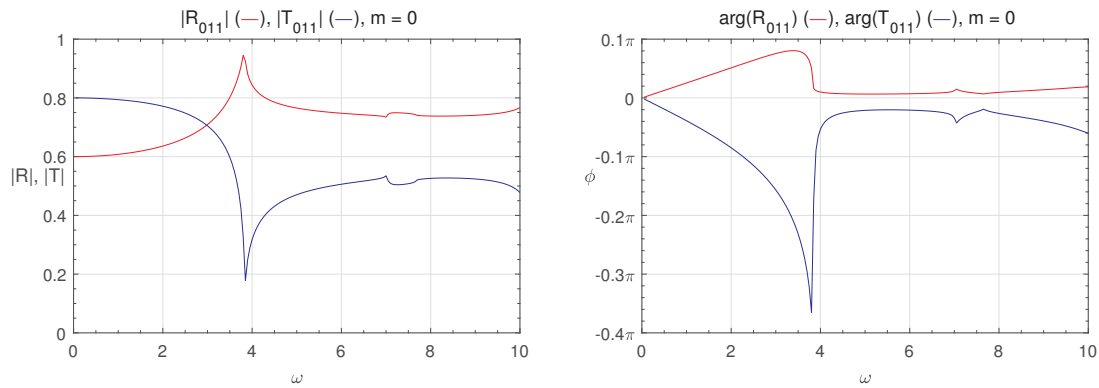
$$\begin{bmatrix} \mathbf{b}_P^{(1)} \\ \mathbf{b}_Q^{(2)} \end{bmatrix} = \mathcal{S} \begin{bmatrix} \mathbf{a}_P^{(1)} \\ \mathbf{a}_Q^{(2)} \end{bmatrix} = \begin{bmatrix} \mathcal{S}_{11} & \mathcal{S}_{12} \\ \mathcal{S}_{21} & \mathcal{S}_{22} \end{bmatrix} \begin{bmatrix} \mathbf{a}_P^{(1)} \\ \mathbf{a}_Q^{(2)} \end{bmatrix}, \quad (7.75)$$

where

$$\begin{aligned} \mathcal{S}_{11} &= (\mathcal{I}_{PP} + \mathcal{N}_{PQ} \mathcal{M}_{QP})^{-1} (\mathcal{I}_{PP} - \mathcal{N}_{PQ} \mathcal{M}_{QP}), \\ \mathcal{S}_{12} &= 2(\mathcal{I}_{PP} + \mathcal{N}_{PQ} \mathcal{M}_{QP})^{-1} \mathcal{N}_{PQ}, \\ \mathcal{S}_{21} &= 2(\mathcal{I}_{QQ} + \mathcal{M}_{QP} \mathcal{N}_{PQ})^{-1} \mathcal{M}_{QP}, \\ \mathcal{S}_{22} &= -(\mathcal{I}_{QQ} + \mathcal{M}_{QP} \mathcal{N}_{PQ})^{-1} (\mathcal{I}_{QQ} - \mathcal{M}_{QP} \mathcal{N}_{PQ}). \end{aligned}$$



(a) Pressure field snapshot.

(b) Reflection \mathcal{R}_{011} and transmission \mathcal{T}_{011} matrices (modulus and phase) for varying frequency $0 < \omega < 10$.Figure 7.13 Incident plane wave ($\omega = 10$, $m = 0$, $\mu = 1$) in duct of radius $a = 1$, scattering at discontinuous diameter change to $b = 0.5$. The chosen modal series truncation is $P = 500$ and $Q = 250$.

Since $\mathbf{b}^{(1)} = \mathcal{S}_{11}\mathbf{a}^{(1)}$ and $\mathbf{b}^{(2)} = \mathcal{S}_{21}\mathbf{a}^{(1)}$ if $\mathbf{a}^{(2)} = 0$, \mathcal{S}_{11} is the reflection matrix⁷ \mathcal{R}_{PP} , and \mathcal{S}_{21} is the transmission matrix \mathcal{T}_{PQ} of a wave only incident from the left. The matrices \mathcal{R} and \mathcal{T} are introduced to acknowledge the fact that each incident mode reflects and transmits into a modal spectrum. When acting on the incident field amplitude vector $\mathbf{a}^{(1)}$, they produce the reflection and transmission field amplitude vectors $\mathbf{b}^{(1)}$ and $\mathbf{b}^{(2)}$, respectively. Therefore, they are called “reflection matrix” and “transmission matrix”. The same can be said of \mathcal{S}_{12} and \mathcal{S}_{22} for a wave incident only from the right. A suitable choice of P and Q [132, 144, 117, 131, 262, 203] allows for a certain balance between the accuracy in $x < 0$ and in $x > 0$, in such a way that the respective highest radial modal wave numbers α_{mP} and β_{mQ} are comparable in size. This means that $P/a \simeq Q/b$, or $P/Q \simeq a/b$.

It should be noted that we should take P/Q not too different from a/b , as this ratio appears to play a role in the way the series solution satisfies the edge condition [144]. This is particularly true for the following iris problem.

⁷... or its transpose, depending on the index notation convention.

7.8.2 The iris problem

When an abrupt contraction of the duct diameter is immediately followed by an expansion to the previous diameter (an infinitely thin orifice plate), we call this an iris. In this case one might be tempted to solve the problem directly by matching the modal expansions at either side of the iris plate. This solution will, however, not converge to the correct (*i.e.* physical) solution.

The above method of section 7.8, however, is well applicable to this problem too, if we consider the iris as a duct (albeit of zero length) connecting the two main ducts at either side of the iris. Each transition – from the duct at the left (1) to the iris (2), and from the iris to duct at the right (3) – is to be treated as above. Since the matrices of each transition are similar, the final system of matrix equations may be further simplified [203].

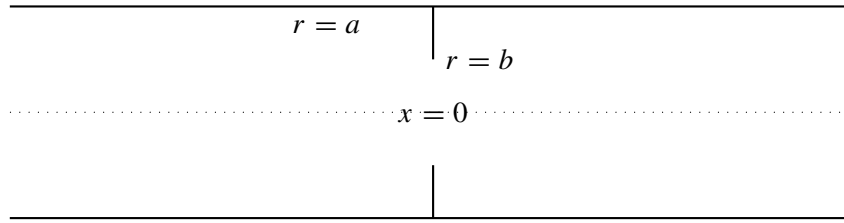


Figure 7.14 Duct of radius a with iris of radius b

Consider semi-infinite ducts of radius a in $x < 0$ (region 1) and $x > 0$ (region 3), separated by an iris of radius $b < a$ at $x = 0$ (region 2). Assume right-running (in 1) and left-running (in 3) incident modes of frequency ω and circumferential order m with amplitudes $\mathbf{a}_P^{(1)} = (A_{m1}^{(1)}, \dots, A_{mP}^{(1)})^\top$ and $\mathbf{a}_P^{(3)} = (A_{m1}^{(3)}, \dots, A_{mP}^{(3)})^\top$, resulting in reflected and transmitted modes with amplitude vectors $\mathbf{b}_P^{(1)} = (B_{m1}^{(1)}, \dots, B_{mP}^{(1)})^\top$ and $\mathbf{b}_P^{(3)} = (B_{m1}^{(3)}, \dots, B_{mP}^{(3)})^\top$. At interface $x = 0$ (including the hard-walled iris) we have continuity of axial velocity

$$\sum_{v=1}^P U_{mv} k_{mv} (A_{mv}^{(1)} - B_{mv}^{(1)}) = \sum_{v=1}^P U_{mv} k_{mv} (B_{mv}^{(3)} - A_{mv}^{(3)}).$$

Multiply both sides by $U_{m\mu}(r)r$ and integrate from $r = 0$ to $r = a$, use orthogonality of the basis functions, and obtain

$$k_{m\mu} (A_{m\mu}^{(1)} - B_{m\mu}^{(1)}) = k_{m\mu} (B_{m\mu}^{(3)} - A_{m\mu}^{(3)}),$$

or in vectorial form

$$\mathbf{a}_P^{(1)} + \mathbf{a}_P^{(3)} = \mathbf{b}_P^{(1)} + \mathbf{b}_P^{(3)}. \quad (7.76)$$

Continuity of pressure in the iris requires

$$\sum_{v=1}^P U_{mv} (A_{mv}^{(1)} + B_{mv}^{(1)}) = \sum_{v=1}^P U_{mv} (B_{mv}^{(3)} + A_{mv}^{(3)})$$

Multiply both sides by $V_{m\mu}(r)r$ and integrate from $r = 0$ to $r = b$, use orthogonality of the basis functions and relation (7.76), to obtain the matrix equations (with the same matrix \mathcal{M} as in (7.70))

$$\mathcal{M}_{QP}\mathbf{a}_P^{(1)} = \mathcal{M}_{QP}\mathbf{b}_P^{(3)}, \quad \mathcal{M}_{QP}\mathbf{a}_P^{(3)} = \mathcal{M}_{QP}\mathbf{b}_P^{(1)}. \quad (7.77)$$

If $Q \geq P$, we would (in general) obtain the evidently incorrect answer that $\mathbf{b}^{(3)} = \mathbf{a}^{(1)}$ and $\mathbf{b}^{(1)} = \mathbf{a}^{(3)}$, as this would imply that the iris has no effect. It is therefore important that $Q < P$. In order to reveal the effect of the iris we expand the axial velocity in the modes $A_{mv}^{(2)}, B_{mv}^{(2)}$ of the iris (assume the iris is a duct of length 0 and radius b) and get

$$\sum_{v=1}^Q V_{mv} \ell_{mv} C_{mv}^{(2)} = \sum_{v=1}^P U_{mv} k_{mv} (A_{mv}^{(1)} - B_{mv}^{(1)}),$$

where $C_{mv}^{(2)} = A_{mv}^{(2)} - B_{mv}^{(2)}$, or in vector form $\mathbf{c}^{(2)} = \mathbf{a}^{(2)} - \mathbf{b}^{(2)}$. This gives us the additional identity

$$\mathcal{M}_{PQ}^\top \boldsymbol{\ell}_{QQ} \mathbf{c}^{(2)} = \mathbf{k}_{PP} (\mathbf{a}_P^{(1)} - \mathbf{b}_P^{(1)}). \quad (7.78)$$

With the same auxiliary matrix \mathcal{N} as above

$$\mathcal{N}_{PQ} = \mathbf{k}_{PP}^{-1} \mathcal{M}_{PQ}^\top \boldsymbol{\ell}_{QQ}$$

we have

$$\mathcal{M}_{QP} \mathcal{N}_{PQ} \mathbf{c}^{(2)} = \mathcal{M}_{QP} \mathbf{a}_P^{(1)} - \mathcal{M}_{QP} \mathbf{a}_P^{(3)}.$$

from which we can derive a non-trivial iris expansion, given by vector $\mathbf{c}^{(2)}$. Eventually we have

$$\begin{aligned} \mathbf{b}_P^{(1)} &= (\mathcal{I}_{PP} - \mathcal{N}_{PQ} (\mathcal{M}_{QP} \mathcal{N}_{PQ})^{-1} \mathcal{M}_{QP}) \mathbf{a}_P^{(1)} + \mathcal{N}_{PQ} (\mathcal{M}_{QP} \mathcal{N})^{-1} \mathcal{M}_{QP} \mathbf{a}_P^{(3)}, \\ \mathbf{b}_P^{(3)} &= \mathcal{N}_{PQ} (\mathcal{M}_{QP} \mathcal{N}_{PQ})^{-1} \mathcal{M}_{QP} \mathbf{a}_P^{(1)} + (\mathcal{I}_{PP} - \mathcal{N}_{PQ} (\mathcal{M}_{QP} \mathcal{N}_{PQ})^{-1} \mathcal{M}_{QP}) \mathbf{a}_P^{(3)}. \end{aligned} \quad (7.79)$$

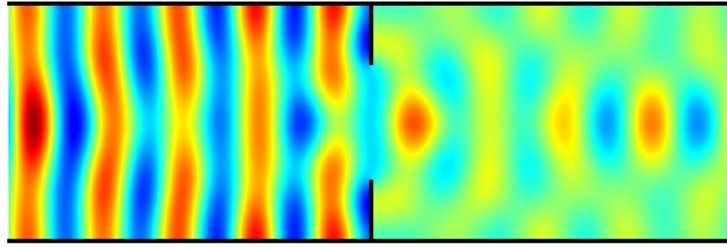
A convenient representation is the scattering matrix

$$\begin{bmatrix} \mathbf{b}_P^{(1)} \\ \mathbf{b}_P^{(3)} \end{bmatrix} = \mathcal{S} \begin{bmatrix} \mathbf{a}_P^{(1)} \\ \mathbf{a}_P^{(3)} \end{bmatrix} = \begin{bmatrix} \mathcal{S}_{11} & \mathcal{S}_{12} \\ \mathcal{S}_{21} & \mathcal{S}_{22} \end{bmatrix} \begin{bmatrix} \mathbf{a}_P^{(1)} \\ \mathbf{a}_P^{(3)} \end{bmatrix} \quad (7.80a)$$

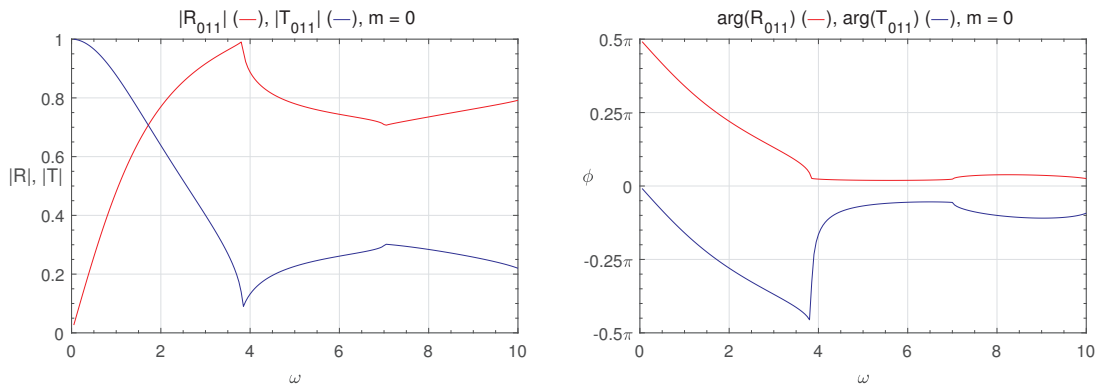
where

$$\mathcal{S}_{12} = \mathcal{S}_{21} = \mathcal{N}_{PQ} (\mathcal{M}_{QP} \mathcal{N}_{PQ})^{-1} \mathcal{M}_{QP}, \quad \mathcal{S}_{11} = \mathcal{S}_{22} = \mathcal{I}_{PP} - \mathcal{S}_{12} \quad (7.80b)$$

Since $\mathbf{b}_P^{(1)} = \mathcal{S}_{11} \mathbf{a}_P^{(1)}$ and $\mathbf{b}_P^{(3)} = \mathcal{S}_{21} \mathbf{a}_P^{(1)}$ if $\mathbf{a}_P^{(2)} = 0$, \mathcal{S}_{11} the reflection matrix \mathcal{R} , and \mathcal{S}_{21} the transmission matrix \mathcal{T} of single mode, incident from side (1).



(a) Pressure field snapshot.



(b) Reflection \mathcal{R}_{011} and transmission \mathcal{T}_{011} matrices (modulus and phase) for varying frequency $0 < \omega < 10$.

Figure 7.15 Incident plane wave ($\omega = 10$, $m = 0$, $\mu = 1$) in duct of radius $a = 1$, scattering at iris of diameter $b = 0.5$. The chosen modal series truncation is $P = 500$ and $Q = 250$.

7.8.3 The edge condition

An aspect that is not an issue for smoothly curved scattering surfaces, is the possible singularity at sharp edges, and the associated non-uniqueness of the solution. The hard-wall boundary condition, like any condition that involves a normal derivative $\mathbf{v} \cdot \mathbf{n}$, is not valid at a sharp edge because the normal vector \mathbf{n} is not defined there. As a result, the solution may be mathematically non-unique by virtue of a spurious line source that “hides” itself at the edge creating an additional field that satisfies all the equations and boundary conditions, but is nevertheless physically not acceptable. This problem finds its origin in the otherwise very reasonable modelling assumptions of an infinitely sharp edge and a vanishingly small viscosity [6]. It can be cured by replacing the missing boundary condition by the so-called edge condition [22], [100, p. 566–569]. This edge condition says that no acoustic energy should radiate from any small neighbourhood of the edge.

Its role remains in the usual engineering practice somewhat in the background, possibly because it

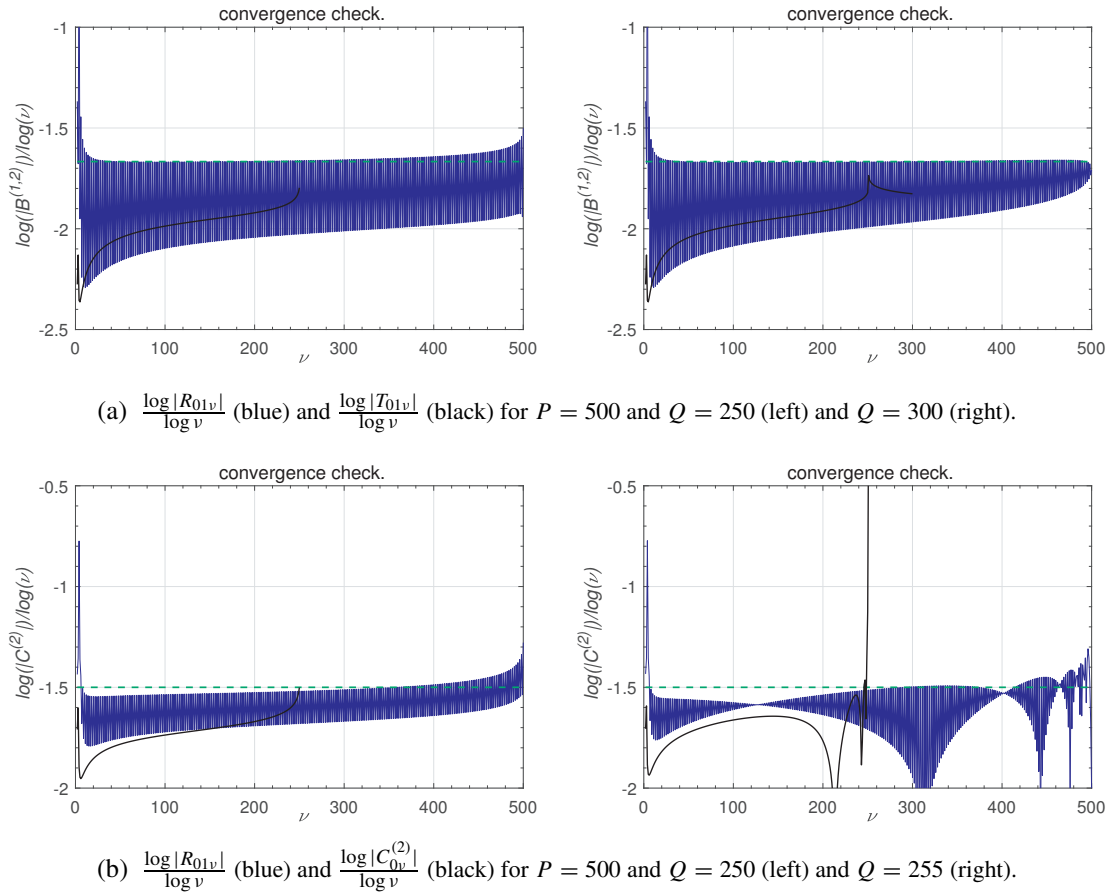


Figure 7.16 Convergence check of incident plane wave ($\omega = 10$, $m = 0$, $\mu = 1$) in duct of radius $a = 1$, scattering at a duct junction (a) or an iris (b) of diameter $b = 0.5$. The default modal series truncation is $P = 500$ and $Q = 250$.

is somehow satisfied “automatically” by the numerical process. It is therefore a puzzling question in what way we implicitly enforced the edge condition, whether the found solution satisfies the edge condition in the first place, and how any of the other (non-physical) solutions could have been found if we had wished so.

Mitra *et al.* [144, 143] came with a very interesting explanation in the context of modal series expansions, in which this condition is related to the convergence rate of the series. The edge condition obeying singularity of pressure or velocity potential, written in (locally defined) distance ϱ to the edge, near a hard walled edge of outer angle α , is $p = O(\varrho^{\pi/\alpha})$. In a Fourier-type series representation this corresponds with

$$p \sim \varrho^{\pi/\alpha} \sim \sum_{n=1}^{\infty} \frac{\sin n\varrho}{n^{1+\pi/\alpha}}, \quad v \sim \varrho^{\pi/\alpha-1} \sim \sum_{n=1}^{\infty} \frac{\sin n\varrho}{n^{\pi/\alpha}}.$$

Note that the series for p will be uniformly convergent, in contrast to (for $\alpha < \pi$) the only pointwise converging series for v . Apart from a possible additional constant, it makes no difference for the behaviour near $q = 0$ if the series is in $\sin nq$ or $\cos nq$.

In the present problems of the duct junction ($\alpha = \frac{3}{2}\pi$) and iris ($\alpha = 2\pi$) we may expect edge behaviour $O(q^{2/3})$ and $O(q^{1/2})$ in p and thus modal amplitudes convergence rates of $O(v^{-5/3})$ and $O(v^{-3/2})$. In numerical practice, it is common to check afterwards if the edge condition has been satisfied. Consider for example the duct junction (figure 7.13) and iris (figure 7.15) examples. For large enough index v , the convergence rate λ of an amplitude $A_v \sim Cv^\lambda$ is approached by $\log |A_v| / \log v = \lambda + O(1/\log v)$. This has been plotted in figures 7.16a (duct junction) and 7.16b (iris). We see that for $P = 500$ and $Q = 250$ (following the ratio $a/b = 2$) the estimated rate (green dashed line) of $\lambda = -\frac{5}{3}$ and $\lambda = -\frac{3}{2}$ is reasonably well approached, and we are confident that the anticipated edge singularities are indeed achieved. For higher values of Q this is only partly the case. Taking into account that the error term of $O(1/\log v)$ is only slowly decreasing, the modes of the reflected field seem to obey the edge condition, but the modes of the transmitted field (a) and especially inside the iris (b) very abruptly change to λ 's that are probably (a) or certainly (b) incorrect.

It is clear that the questions around the edge condition in mode matching have not been fully answered yet. For a part this may be caused by the fact that the spurious solutions (with a false δ -function source at the edge rim) cannot be described by the present Fourier-type modal functions, at least not in regular sense. Perhaps some progress can be made by including generalised series (see section C.3) like for the comparable, but otherwise unrelated problem of the Kutta condition at the trailing edge of a flat plate in mean flow [204].

7.9 Reflection at an unflanged open end

The reflection and diffraction at and radiation from an open pipe end of a modal sound wave depends on the various problem parameters like Helmholtz number ω , mode numbers m, μ and pipe wall thickness. A canonical problem amenable to analysis is that of a hard-walled, cylindrical, semi-infinite pipe of vanishing wall thickness. The exact solution (by means of the Wiener-Hopf technique) was first found by Levine and Schwinger (for $m = 0$) in their celebrated paper [121]. Generalizations for higher modes may be found in [257] and with uniform [199] or jet mean flow [156, 157].

Inside the pipe we have the incident mode with reflected field, given by $p(x, r, \vartheta) = p_{m\mu}(x, r) e^{-im\vartheta}$ where

$$p_{m\mu}(x, r) = U_{m\mu}(r) e^{-ik_{m\mu}x} + \sum_{\nu=1}^{\infty} R_{m\mu\nu} U_{m\nu}(r) e^{ik_{m\nu}x}. \quad (7.81)$$

Outside the pipe we have in the far field

$$p_{m\mu}(x, r) \simeq D_{m\mu}(\xi) \frac{e^{-i\omega\varrho}}{\omega\varrho} \quad (\omega\varrho \rightarrow \infty), \quad (7.82)$$

where $x = \varrho \cos \xi$, $r = \varrho \sin \xi$, and $D_{m\mu}(\xi)$ is called the directivity function, and $|D_{m\mu}(\xi)|$ is the radiation pattern. (Note that the limits $\varrho \rightarrow \infty$ and $\xi \downarrow 0$ or $\xi \uparrow \pi$ may be non-uniform.)

The reflection matrix⁸ $\mathcal{R}_m = \{R_{m\mu\nu}\}$ and the directivity function are both described by complex integrals, which have to be evaluated numerically. Some important properties are:

- At resonance $\omega = \alpha_{m\mu}$ we have total reflection in itself, $R_{m\mu\mu} = -1$, and no reflection in any other mode, $R_{m\mu\nu} = 0$.
- Near resonance $\omega \sim \alpha_{m\mu}$ the modulus $|R_{m\mu\nu}(\omega)|$ behaves linearly from the left, and like a square root from the right side; the behaviour of the phase $\arg(R_{m\mu\nu}(\omega))$ is similar but reversed: linearly from the right and like a square root from the left.
- A reciprocity relation between the μ , ν and the ν , μ -coefficients⁹:

$$k_{m\nu} R_{m\mu\nu} = k_{m\mu} R_{m\nu\mu}.$$

- In the forward arc, $0 < \xi < \frac{1}{2}\pi$, $D_{m\mu}(\xi)$ consists of lobes (maxima interlaced by zeros), while $D_{01}(0) = \frac{1}{2}\sqrt{2}i\omega^2$ and $D_{m\mu}(0) = 0$.
- In the rearward arc, $\frac{1}{2}\pi \leq \xi < \pi$, $D_{m\mu}(\xi)$ is free of zeros, and tends to zero for $\xi \rightarrow \pi$ if $m \geq 1$ and to a finite value if $m = 0$.
- If $k_{m\nu}$ is real and $\nu \neq \mu$, the zeros of $D_{m\mu}(\xi)$ are found at $\xi = \arcsin(\alpha_{m\nu}/\omega)$.
- If the mode is cut on, the main lobe is located at $\xi_{m\mu} = \arcsin(\alpha_{m\mu}/\omega)$.

- If $\omega \rightarrow 0$, the radiation pattern of the plane wave $m\mu = 01$ becomes spherically shaped and small like $O(\omega^2)$, while the reflection coefficient becomes $R_{011} \simeq -\exp(-i2\delta\omega)$, where $\delta = 0.6127$. The dimensional distance δa is called the end correction, since $x = \delta a$ is a fictitious point just outside the pipe, at which the wave appears to reflect with $p = 0$. See also (6.95,5.44).

Based on the method presented in [199], plots of $R_{m\mu\nu}$ and $|D_{m\mu}(\xi)|$ may be generated, as given in figures 7.17 and 7.18.

Of the reflection coefficient we have plotted modulus $|R_{m\mu\nu}(\omega)|$ and phase $\varphi_{m\mu\nu} = \arg(R_{m\mu\nu})$ as a

⁸The matrix appears (in transposed form) if the amplitudes are written as vectors:

$$p_m = \sum_{\mu=1}^{\infty} A_{m\mu} U_{m\mu} e^{-ik_{m\mu}x} + \sum_{\nu=1}^{\infty} B_{m\nu} U_{m\nu} e^{ik_{m\nu}x}, \quad \text{with } B_{m\nu} = \sum_{\mu=1}^{\infty} R_{m\mu\nu} A_{m\mu}, \quad \text{i.e., } \mathbf{B}_m = \mathcal{R}_m^T \mathbf{A}_m.$$

⁹For no flow. With (uniform) flow it depends on the Kutta condition [199].

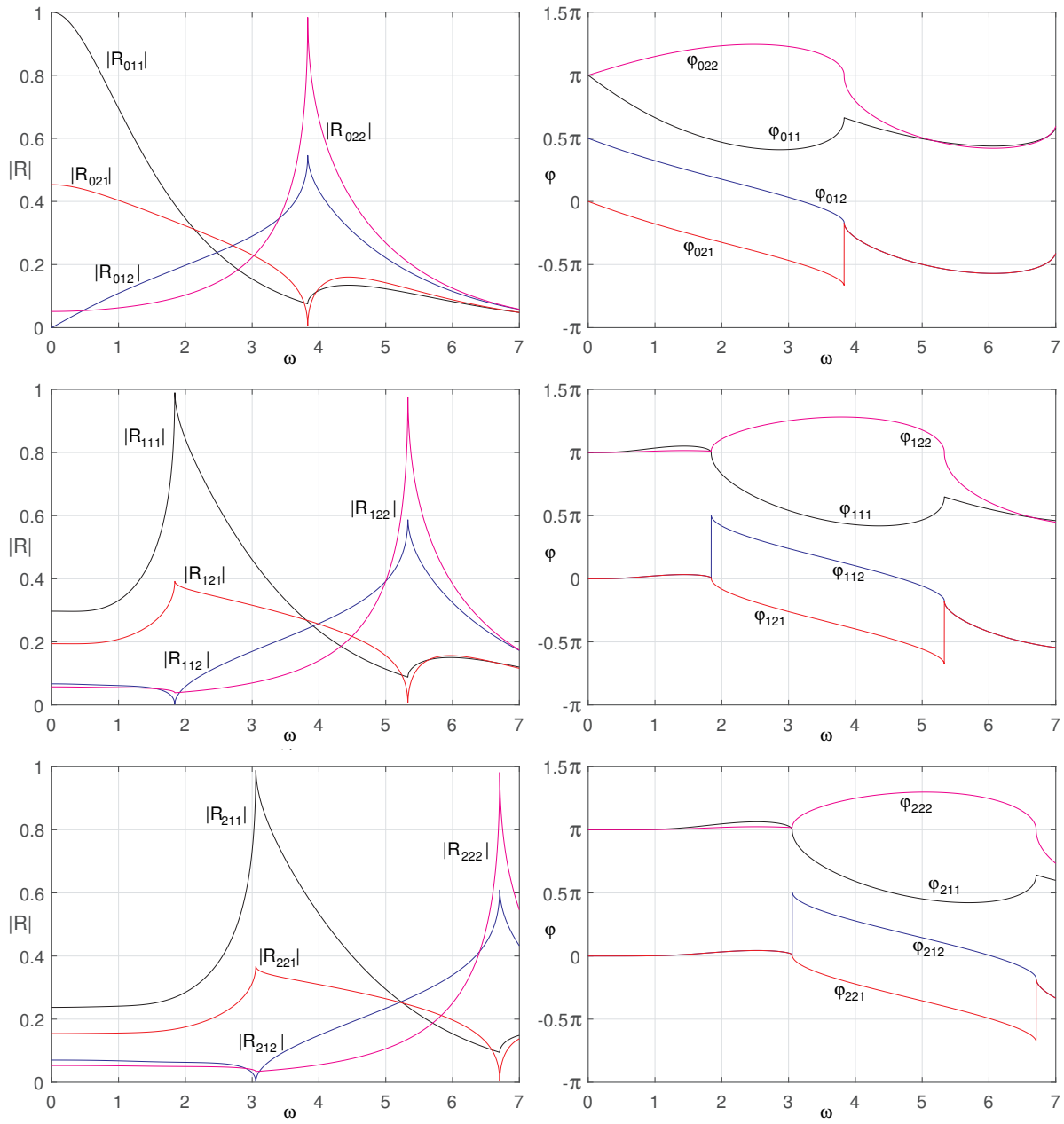


Figure 7.17 Modulus and phase of reflection coefficients $R_{m\mu\nu}$ as a function of $\omega = 0 \dots 7$ for $m = 0, 1, 2$ of incident mode $\mu = 1, 2$ reflecting in mode $\nu = 1, 2$.

function of $\omega = 0 \dots 7$, for $m = 0, 1, 2$ and $\mu, \nu = 1, 2$. Note that the resonance (cut-off) frequencies are $\omega = 3.8317$ and 7.0156 for $m = 0$, $\omega = 1.8412$ and 5.3314 for $m = 1$, and $\omega = 3.0542$ and 6.7061 for $m = 2$.

The radiation pattern is plotted, on dB-scale, of the first radial mode ($\mu = 1$) for $m = 0$ and $m = 1$, and $\omega = 2, 4, 6$. For $m = 0$ the main lobe is at $\xi_{01} = 0$, while the zeros are found for $\omega = 4$ at $\xi = 73.3^\circ$, and for $\omega = 6$ at $\xi = 39.7^\circ$. For $m = 1$ we have the main lobe at $\xi_{11} = 67.0^\circ, 27.4^\circ, 17.9^\circ$ for $\omega = 2, 4, 6$. The zero is found at $\xi = 62.7^\circ$ for $\omega = 6$.

Furthermore, the trend is clear that for higher frequencies the refraction effects become smaller, and the sound radiates more and more like rays [32]. It is instructive to compare the wave front velocity of a mode (the sound speed, dimensionless 1) and the axial phase velocity v_{ph} (7.19). As the mode spirals through the duct, the wave front makes an angle $\xi_{m\mu}$ with the x -axis such that $\cos(\xi_{m\mu}) = 1/v_{ph} = k_{m\mu}/\omega$. Indeed,

$$\xi_{m\mu} = \arccos(k_{m\mu}/\omega) = \arcsin(\alpha_{m\mu}/\omega)$$

is the angle at which the mode radiates out of the open end, *i.e.* the angle of the main lobe.

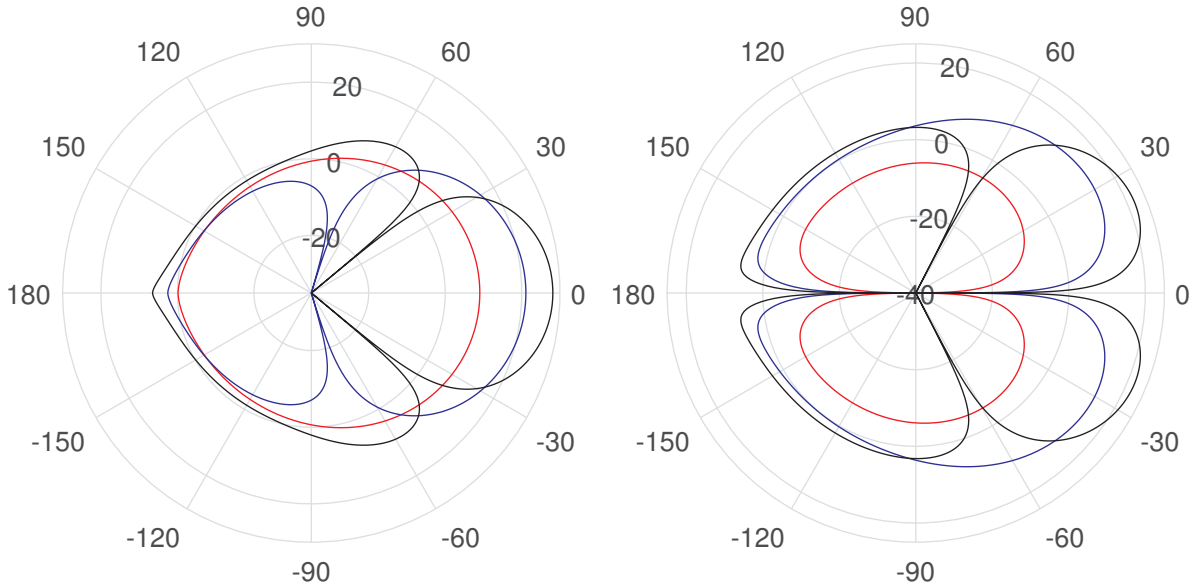


Figure 7.18 Radiation pattern $20 \log_{10} |D_{m\mu}|$ for $\mu = 1$ and $\omega = 2, 4, 6$, and $m = 0$ (left) and $m = 1$ (right).

Exercises

- a) Consider a hard-walled duct of radius $a = 0.1$ m with an acoustic medium with $c_0 = 340$ m/s. A harmonic source with frequency $f = 500$ Hz is positioned at $x = 0$ half-way the radius. A microphone is to be placed an axial distance $x = D$ away from the source, such that the plane wave is detected at least 20 dB louder than the other modes.
- What is the cut-off frequency ?
 - Assuming that all excited modes have about the same initial amplitude, ignoring details like r -variation of higher-order modes: what is the necessary distance D ?
 - What is D for frequency f tending to zero ?

- b) Investigate the behaviour of $k_{m\mu}$ (equation 7.26) for $\omega \rightarrow \infty$. Find analytical approximate expressions of the surface waves.

- c) Find in a similar way as for equation (7.65), by Fourier transformation to x , the field of a harmonic point source *inside* a hard-walled infinite duct. Verify this by an alternative approach based on representation (D.57).

- d) Consider a cylindrical duct of radius R , with an acoustic medium of density ρ_0 and soundspeed c_0 , and lined with sound absorbing material of uniform impedance Z . Inside the duct we have a sound field of angular frequency ω and circumferential periodicity m . For definiteness the sound field may be described in complex form as a linear combination of the modes $J_m(\alpha_{m\mu}r) e^{i\omega t - im\theta \mp ik_{m\mu}x}$, $\mu = 1 \dots$

We define the optimal impedance Z_{opt} as the impedance that maximises the modal attenuation, *i.e.* $|\text{Im}(k_{m\mu})|$, of the least attenuated mode (Cremer's optimum). You may assume that this optimum is found at one of the values of Z where two modes coincide (see also figure 7.7).

- Derive the eigenvalue equation $F(\alpha, Z) = 0$ for radial wave number $\alpha_{m\mu}$. This is a dimensional version of equation (7.24). Note that coinciding solutions are found where $F(\alpha, Z)$ and $\frac{\partial}{\partial \alpha} F(\alpha, Z)$ vanish simultaneously.

- Show that Z_{opt} takes the form

$$Z_{\text{opt}} = \rho_0 c_0 \left(\frac{\omega R}{c_0} \right) K_m,$$

where K_m is a fixed number to be determined numerically.

- Find numerically K_m for $m = 0, 1, 2$.

8 Approximation methods

Mathematical modelling is the art of sorting out the whole spectrum of effects that play a role in a problem, and then making a selection by including what is relevant and excluding what is too small. This selection is what we call a “model” or “theory”. Models and theories, applicable in a certain situation, are not “isolated islands of knowledge” provided with a logical flag, labelling it “valid” or “invalid”. A model is never unique, because it depends on the type, quality and accuracy of answers we are aiming for, and of course the means (time, money, numerical power, mathematical skills) that we have available.

Normally, when the problem is rich enough, this spectrum of effects does not simply consist of two classes “important” and “unimportant”, but is a smoothly distributed hierarchy varying from “essential” effects via “relevant” and “rather relevant” to “unimportant” and “absolutely irrelevant” effects. As a result, in practically any model we select there will be effects that are small but not small enough to be excluded. We can ignore this fact, and just assume that all effects that constitute our model are equally important. This is the usual approach when the problem is simple enough for analysis or a brute force numerical simulation.

There are situations, however, where it could be wise to utilise the smallness of these small but important effects in such a way that we simplify the problem without reducing the quality of the model. Usually, an otherwise intractable problem becomes solvable and we gain great insight in the problem.

Perturbation methods do this in a systematic manner by using the sharp fillet knife of mathematics in general, and asymptotic analysis in particular. From this perspective, perturbation methods are ways of modelling with other means and are therefore much more important for the understanding and analysis of practical problems than they’re usually credited with. David Crighton [44] called “*Asymptotics - an indispensable complement to thought, computation and experiment in applied mathematical modelling*”.

Examples are numerous: simplified geometries reducing the spatial dimension, small amplitudes allowing linearization, low velocities and long time scales allowing incompressible description, small relative viscosity allowing inviscid models, zero or infinite lengths rather than finite lengths, etc.

The question is: how can we use this gradual transition between models of different level. Of course, when a certain aspect or effect, previously absent from our model, is included in our model, the change is abrupt and usually the corresponding equations are more complex and more difficult to solve. This is, however, only true if we are merely interested in exact or numerically “exact” solutions. But an exact solution of an approximate model is not better than an approximate solution of an exact model.

So there is absolutely no reason to demand the solution to be more exact than the corresponding model. If we accept approximate solutions, based on the inherent small or large modelling parameters, we do have the possibilities to gradually increase the complexity of a model, and study small but significant effects in the most efficient way.

The methods utilizing systematically this approach are called “perturbations methods”. Usually, a distinction is made between regular and singular perturbations. A (loose definition of a) regular perturbation is where the solution of the approximate problem is everywhere close to the solution of the unperturbed problem.

In acoustics we have as typical examples of modelling hierarchies: wave propagation in a uniform medium or with simple boundaries being considerably simpler than in a non-uniform medium or with complicated boundaries. For a uniform medium and simple boundary conditions, many exact analytical results are available. For an arbitrary non-uniform medium or complex boundary conditions, we usually have to resort to numerical methods. Analytical approximations and perturbation methods come into play for cases in between where the problem differs only a little from one which allows full analytical treatment.

We will consider here three methods relevant in acoustical problems. The first is the problem of Webster’s horn, an example of a regular perturbation method [133] known as method of slow variation, since the typical axial length scale is much greater than the transverse length scale. The others are examples of singular perturbation methods. The method of multiple scales (related to the WKB method) describes problems in which in the problem several length scales act in the same direction, for example a wave propagating through a slowly varying environment. The method of matched asymptotic expansions is used to analyse problems in which several approximations, valid in spatially distinct regions, are necessary.

In order to quantify the used small effect in the model, we will always introduce a small positive dimensionless parameter ε . Its physical meaning depends on the problem. It will usually stem from a characteristic amplitude, wave number, or medium gradient.

8.1 Webster’s horn equation

Consider the following problem of low frequency sound waves propagating in a slowly varying duct or horn [119, 209]. The typical length scale of duct variation is assumed to be much larger than a diameter, and of the same order of magnitude as the sound wave length. We introduce the ratio between a typical diameter and this length scale as the small parameter ε , and write for the duct surface and wave number k

$$r = R(X, \theta), \quad X = \varepsilon x, \quad k = \varepsilon \kappa. \quad (8.1)$$

By writing R as a function of slow variable X , rather than x , we have made our formal assumption of slow variation explicit in a convenient and simple way, since

$$\frac{\partial R}{\partial x} = \varepsilon \frac{\partial R}{\partial X} = O(\varepsilon).$$

The crucial step will now be the assumption that the propagating sound wave is *only* affected by the geometric variation induced by R . Any initial or entrance effects are absent or have disappeared. As a result the acoustic field p is a function of X , rather than x , and its axial gradient scales on ε , as $\frac{\partial p}{\partial x} = O(\varepsilon)$.

It is convenient to introduce the following function S and its gradients

$$S = r - R(X, \theta), \quad (8.2)$$

$$\nabla S = \varepsilon S_X \mathbf{e}_x + S_r \mathbf{e}_r + \frac{S_\theta}{r} \mathbf{e}_\theta = -\varepsilon R_X \mathbf{e}_x + \mathbf{e}_r - \frac{R_\theta}{r} \mathbf{e}_\theta, \quad (8.3)$$

$$\nabla_\perp S = S_r \mathbf{e}_r + \frac{S_\theta}{r} \mathbf{e}_\theta = \mathbf{e}_r - \frac{R_\theta}{r} \mathbf{e}_\theta. \quad (8.4)$$

At the duct surface $S = 0$ the gradient ∇S is a vector normal to the surface (see section A.3), while the transverse gradient $\nabla_\perp S$, directed in the plane of a cross section $X = \text{const.}$, is normal to the duct circumference $S(X = c, r, \theta) = 0$.

Inside the duct we have the reduced wave equation (Helmholtz equation)

$$\varepsilon^2 p_{XX} + \nabla_\perp^2 p + \varepsilon^2 \kappa^2 p = 0, \quad (8.5)$$

at the solid wall the boundary condition of vanishing normal velocity

$$\nabla p \cdot \nabla S = \varepsilon^2 p_X S_X + \nabla_\perp p \cdot \nabla_\perp S = 0 \quad \text{at} \quad S = 0. \quad (8.6)$$

This problem is too difficult in general, so we try to utilize in a systematic manner the small parameter ε . Since the perturbation terms are $O(\varepsilon^2)$, we assume the asymptotic expansion

$$p(X, r, \theta; \varepsilon) = p_0(X, r, \theta) + \varepsilon^2 p_1(X, r, \theta) + O(\varepsilon^4).$$

After substitution in equation (8.5) and boundary condition (8.6), further expansion in powers of ε^2 and equating like powers of ε , we obtain to leading order a Laplace equation in (r, θ)

$$\nabla_\perp^2 p_0 = 0 \quad \text{with} \quad \nabla_\perp p_0 \cdot \nabla_\perp S = 0 \quad \text{at} \quad S = 0.$$

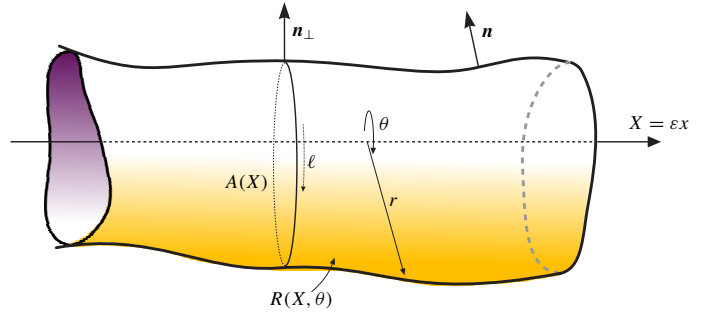


Figure 8.1 Geometry of Webster horn.

An obvious solution is $p_0 \equiv 0$. Since the solution of the Laplace equation with boundary conditions in the normal derivative are unique up to a constant (here: a function of X), we have

$$p_0 = p_0(X).$$

To obtain an equation for p_0 in X we continue with the $O(\varepsilon^2)$ -equation and corresponding boundary condition

$$\nabla_{\perp}^2 p_1 + p_{0XX} + \kappa^2 p_0 = 0, \quad \nabla_{\perp} p_1 \cdot \nabla_{\perp} S = - p_{0X} S_X. \quad (8.7)$$

The boundary condition can be rewritten as

$$\nabla_{\perp} p_1 \cdot \mathbf{n}_{\perp} = \frac{p_{0X} R_X}{|\nabla_{\perp} S|} = \frac{p_{0X} R R_X}{\sqrt{R^2 + R_{\theta}^2}}$$

where $\mathbf{n}_{\perp} = \nabla_{\perp} S / |\nabla_{\perp} S|$ is the transverse unit normal vector. By integrating equation (8.7) over a cross section \mathcal{A} of area $A(X)$, using Gauss' theorem, and noting that $A = \int_0^{2\pi} \frac{1}{2} R^2 d\theta$, and that a circumferential line element is given by $d\ell = (R^2 + R_{\theta}^2)^{1/2} d\theta$, we obtain

$$\begin{aligned} \iint_{\mathcal{A}} \nabla_{\perp}^2 p_1 + p_{0XX} + \kappa^2 p_0 d\sigma &= \int_{\partial\mathcal{A}} \nabla_{\perp} p_1 \cdot \mathbf{n}_{\perp} d\ell + A(p_{0XX} + \kappa^2 p_0) = \\ & p_{0X} \int_0^{2\pi} R R_X d\theta + A(p_{0XX} + \kappa^2 p_0) = A_X p_{0X} + A(p_{0XX} + \kappa^2 p_0) = 0. \end{aligned}$$

Finally, we have obtained for the leading order field p_0 the Webster horn equation [14, 59, 151, 183, 224, 225, 256], which is, for convenience written in the original variables x and k , given by

$$\frac{1}{A} \frac{d}{dx} \left(A \frac{d}{dx} p_0 \right) + k^2 p_0 = 0. \quad (8.8)$$

By introducing $A = D^2$ and $\phi = D p_0$, the equation may be transformed into

$$\phi'' + \left(k^2 - \frac{D''}{D} \right) \phi = 0. \quad (8.9)$$

This can be solved analytically for certain families of cross sectional shapes A . For example, the term D''/D becomes a constant if

$$D = a e^{mx} + b e^{-mx},$$

(parameterized by a , b , and m), and the equation (8.8) simplifies to

$$\phi'' + (k^2 - m^2) \phi = 0$$

which can be solved by elementary methods. In the special case $m \rightarrow 0$ such that $a = \frac{1}{2}(A_0 + A_1/m)$ and $b = \frac{1}{2}(A_0 - A_1/m)$, the shape reduces to the conical horn $A = (A_0 + A_1x)^2$. For $b = 0$ we have the exponential horn, and if $b = a$ the catenoidal horn.

The parameter m is clearly most important since it determines whether the wave is propagating ($m < k$) or cut-off ($m > k$).

8.2 Multiple scales

Introduction

By means of the method of multiple scales we will consider problems typically of waves propagating in a slowly varying but otherwise infinite medium (ray acoustics), or waves propagating in a slowly varying duct.

In both cases there is a small parameter in the problem which is the corner stone of the approximation. This small parameter is the ratio between a typical wave length and the length scale over which the medium or duct varies considerably (say, order 1).

Intuitively, it is clear that over a short distance (a few wave lengths) the wave only sees a constant medium or geometry, and will propagate approximately as in the constant case, but over larger distances it will somehow have to change its shape in accordance with its new environment.

A technique, utilizing this difference between small scale and large scale behaviour is the method of multiple scales ([163, 15]). As with most approximation methods, this method has grown out of practice, and works well for certain types of problems. Typically, the multiple scale method is applicable to problems with on the one hand a certain global quantity (energy, power) which is conserved or almost conserved and controls the amplitude, and on the other hand two rapidly interacting quantities (kinetic and potential energy) controlling the phase.

An illustrative example

We will illustrate the method by considering a damped harmonic oscillator

$$\frac{d^2y}{dt^2} + 2\varepsilon \frac{dy}{dt} + y = 0 \quad (t \geq 0), \quad y(0) = 0, \quad \frac{dy(0)}{dt} = 1 \quad (8.10)$$

with $0 < \varepsilon \ll 1$. The exact solution is readily found to be

$$y(t) = \sin(\sqrt{1 - \varepsilon^2} t) e^{-\varepsilon t} / \sqrt{1 - \varepsilon^2} \quad (8.11)$$

A naive approximation for small ε and fixed t would give

$$y(t) = \sin t - \varepsilon t \sin t + O(\varepsilon^2) \quad (8.12)$$

which appears to be not a good approximation for large t for the following reasons:

- 1) if $t = O(\varepsilon^{-1})$ the second term is of equal importance as the first term and nothing is left over of the slow exponential decay;
- 2) if $t = O(\varepsilon^{-2})$ the phase has an error of $O(1)$ giving an approximation of which even the sign may be in error.

In the following we shall demonstrate that this type of error occurs also if we construct a straightforward approximate solution directly from equation (8.10). However, knowing the character of the error, we may then try to avoid them. Suppose we can expand

$$y(t; \varepsilon) = y_0(t) + \varepsilon y_1(t) + \varepsilon^2 y_2(t) + \dots \tag{8.13}$$

Substitute in (8.10) and collect equal powers of ε :

$$\begin{aligned} O(\varepsilon^0) : \quad & \frac{d^2 y_0}{dt^2} + y_0 = 0 \quad \text{with } y_0(0) = 0, \quad \frac{dy_0(0)}{dt} = 1, \\ O(\varepsilon^1) : \quad & \frac{d^2 y_1}{dt^2} + y_1 = -2 \frac{dy_0}{dt} \quad \text{with } y_1(0) = 0, \quad \frac{dy_1(0)}{dt} = 0, \end{aligned}$$

then

$$y_0(t) = \sin t, \quad y_1(t) = -t \sin t, \quad \text{etc.}$$

Indeed, the straightforward, Poincaré type, expansion (8.13) that is generated breaks down for large t , when $\varepsilon t \geq O(1)$. As is seen from the structure of the equations for y_n , the quantity y_n is excited (by the “source”-terms $-2dy_{n-1}/dt$) in its eigenfrequency, resulting in resonance. The algebraically growing terms of the type $t^n \sin t$ and $t^n \cos t$ that are generated are called in this context: *secular*¹ terms.

Apart from being of limited validity, the expansion reveals nothing of the real structure of the solution: a slowly decaying amplitude and a frequency slightly different from 1. For certain classes of problems it is therefore advantageous to incorporate this structure explicitly in the approximation.

Introduce the slow time scale

$$T = \varepsilon t \tag{8.14}$$

and identify the solution y with a suitably chosen other function Y that depends on both variables t and T :

$$y(t; \varepsilon) = Y(t, T; \varepsilon). \tag{8.15}$$

¹From astronomical applications where these terms occurred for the first time in this type of perturbation series: secular \approx occurring once in a century; saeculum = generation, about 100 years.

The underlying idea is the following. There are, of course, infinitely many functions $Y(t, T; \varepsilon)$ that are equal to $y(t, \varepsilon)$ along the line $T = \varepsilon t$ in (t, T) -space. So we have now some freedom to prescribe additional conditions. With the unwelcome appearance of secular terms in mind it is natural to think of conditions, chosen such that no secular terms occur when we construct an approximation.

Since the time derivatives of y turn into partial derivatives of Y

$$\frac{dy}{dt} = \frac{\partial Y}{\partial t} + \varepsilon \frac{\partial Y}{\partial T}, \quad (8.16)$$

equation (8.10) becomes for Y

$$\frac{\partial^2 Y}{\partial t^2} + Y + 2\varepsilon \left(\frac{\partial Y}{\partial t} + \frac{\partial^2 Y}{\partial t \partial T} \right) + \varepsilon^2 \left(\frac{\partial^2 Y}{\partial T^2} + 2 \frac{\partial Y}{\partial T} \right) = 0. \quad (8.17)$$

Assume the expansion

$$Y(t, T; \varepsilon) = Y_0(t, T) + \varepsilon Y_1(t, T) + \varepsilon^2 Y_2(t, T) + \dots \quad (8.18)$$

and substitute this into equation (8.17) to obtain to leading orders

$$\begin{aligned} \frac{\partial^2 Y_0}{\partial t^2} + Y_0 &= 0, \\ \frac{\partial^2 Y_1}{\partial t^2} + Y_1 &= -2 \frac{\partial Y_0}{\partial t} - 2 \frac{\partial^2 Y_0}{\partial t \partial T}, \end{aligned}$$

with initial conditions

$$\begin{aligned} Y_0(0, 0) &= 0, & \frac{\partial}{\partial t} Y_0(0, 0) &= 1, \\ Y_1(0, 0) &= 0, & \frac{\partial}{\partial t} Y_1(0, 0) &= -\frac{\partial}{\partial T} Y_0(0, 0). \end{aligned}$$

The solution for Y_0 is easily found to be

$$Y_0(t, T) = A_0(T) \sin t \quad \text{with} \quad A_0(0) = 1, \quad (8.19)$$

which gives a right-hand side for the Y_1 -equation of

$$-2 \left(A_0 + \frac{\partial A_0}{\partial T} \right) \cos t.$$

No secular terms occur (no resonance between Y_1 and Y_0) if this term vanishes:

$$A_0 + \frac{\partial A_0}{\partial T} = 0 \quad \longrightarrow \quad A_0 = e^{-T}. \quad (8.20)$$

Note (this is typical), that we determine Y_0 fully only on the level of Y_1 , however, without having to solve Y_1 itself.

The present approach is by and large the multiple scale technique in its simplest form. Variations on this theme are sometimes necessary. For example, we have not completely got rid of secular terms. On a longer time scale ($t = O(\varepsilon^{-2})$) we have in Y_2 again resonance because of the “source”: $e^{-T} \sin t$, yielding terms $O(\varepsilon^2 t)$. We see that a second time scale $T_2 = \varepsilon^2 t$ is necessary.

Sometimes, the occurrence of higher order time scales is really an artefact of the fast variable being slowly varying due to external effects, like a slowly varying problem parameter. In this case the fast variable is to be strained locally by a suitable strain function in the following way

$$\tilde{t} = \frac{1}{\varepsilon} \int^{\varepsilon t} \omega(\tau; \varepsilon) d\tau. \quad (8.21)$$

(The need for the $1/\varepsilon$ -factor is immediately clear if we observe that $\tilde{t} = \varepsilon^{-1} \omega \varepsilon t = \omega t$ for a constant $\omega = O(1)$.) For linear wave-type problems we may anticipate the structure of the solution and assume the WKB hypothesis (see [15, 83])

$$y(t; \varepsilon) = A(T; \varepsilon) e^{i\varepsilon^{-1} \int_0^T \omega(\tau; \varepsilon) d\tau}. \quad (8.22)$$

We have

$$\begin{aligned} \frac{\partial y}{\partial t} &= \left(i\omega A + \varepsilon \frac{\partial A}{\partial T} \right) e^{i\varepsilon^{-1} \int_0^T \omega d\tau} \\ \frac{\partial^2 y}{\partial t^2} &= \left(-\omega^2 A + 2i\varepsilon \omega \frac{\partial A}{\partial T} + i\varepsilon \frac{\partial \omega}{\partial T} A + \varepsilon^2 \frac{\partial^2 A}{\partial T^2} \right) e^{i\varepsilon^{-1} \int_0^T \omega d\tau} \end{aligned}$$

so that substitution in (8.10) and suppressing the exponential factor yields

$$(1 - \omega^2)A + i\varepsilon \left(2\omega \frac{\partial A}{\partial T} + \frac{\partial \omega}{\partial T} A + 2\omega A \right) + \varepsilon^2 \left(\frac{\partial^2 A}{\partial T^2} + 2 \frac{\partial A}{\partial T} \right) = 0.$$

Note that the secular terms are now not explicitly suppressed. The necessary additional condition is here that the solution of the present type *exists* (assumption 8.22), and that each higher order correction is no more secular than its predecessor. With some luck and ingenuity this is just sufficient to determine A and ω . In general, this is indeed not completely straightforward. So much freedom may be left that ambiguities can result.

Finally, the solution is found as the following expansion

$$\begin{aligned} A(T; \varepsilon) &= A_0(T) + \varepsilon A_1(T) + \varepsilon^2 A_2(T) + \dots \\ \omega(T; \varepsilon) &= \omega_0(T) + \varepsilon^2 \omega_2(T) + \dots \end{aligned} \quad (8.23)$$

Note that ω_1 may be set to zero since the factor $\exp(i \int_0^T \omega_1(\tau) d\tau)$ may be incorporated in A . Substitute and collect equal powers of ε :

$$\begin{aligned} O(\varepsilon^0) : \quad & (1 - \omega_0^2)A_0 = 0 && \rightarrow \omega_0 = 1, \\ O(\varepsilon^1) : \quad & \frac{\partial A_0}{\partial T} + A_0 = 0 && \rightarrow A_0 = e^{-T}, \\ O(\varepsilon^2) : \quad & 2i \left(\frac{\partial A_1}{\partial T} + A_1 \right) = (1 + 2\omega_2) e^{-T} && \rightarrow \omega_2 = -\frac{1}{2}, A_1 = 0. \end{aligned}$$

The solution that emerges is indeed consistent with the exact solution.

8.3 Helmholtz resonator with non-linear dissipation

An interesting application of the multiple scale technique is the Helmholtz resonator, derived in equation (5.41). In this way we will be able to investigate the small non-linear terms that will be seen to represent a small damping. See also [231].

We start with equation (5.41)

$$\frac{\ell V}{c_0^2 S_n} \frac{d^2 p'_{in}}{dt^2} + \frac{V^2}{2\rho_0 c_0^4 S_n^2} \frac{dp'_{in}}{dt} \left| \frac{dp'_{in}}{dt} \right| + \frac{RV}{\rho_0 c_0^2 S_n} \frac{dp'_{in}}{dt} + p'_{in} = p'_{ex}. \quad (5.41)$$

where we wrote for simplicity $\ell := \ell + 2\delta$.

For a proper analysis it is most clarifying to rewrite the equation into non-dimensional variables. For this we need an inherent timescale and pressure. For vanishing amplitudes and negligible dissipation the equation describes a harmonic oscillator, so the reciprocal of its angular frequency $\omega_0 = (c_0^2 S_n / \ell V)^{1/2}$ is the obvious timescale of the problem. By dividing the nonlinear damping term by the acceleration term we find the pressure level $2\rho_0 c_0^2 \ell S_n / V$ at which the nonlinear damping would be just as large as the other terms. So for a pressure that is a small fraction ε of this level we have a problem with only little nonlinear damping. In addition we assume that the linear damping is small and (to make the problem interesting) of the same order of magnitude as the nonlinear damping. Anticipating the fact that we will consider (in the forced problem) the external pressure exciting near resonance, the driving amplitude p'_{ex} will be an order smaller than p'_{in} .

In order to make all this explicit we introduce a small parameter ε (selected, as we just explained, via the external forcing amplitude), and make dimensionless

$$\begin{aligned} \tau = \omega_0 t, \quad \omega_0 &= \left(\frac{c_0^2 S_n}{\ell V} \right)^{\frac{1}{2}}, \quad R = \varepsilon \rho_0 c_0 \left(\frac{\ell S_n}{V} \right)^{\frac{1}{2}} r, \\ p'_{in} &= 2\varepsilon \rho_0 c_0^2 \frac{\ell S_n}{V} y, \quad p'_{ex} = 2\varepsilon^2 \rho_0 c_0^2 \frac{\ell S_n}{V} F, \quad \text{where } 0 < \varepsilon \ll 1, \end{aligned} \quad (8.24)$$

to obtain

$$\frac{d^2y}{d\tau^2} + \varepsilon \frac{dy}{d\tau} \left| \frac{dy}{d\tau} \right| + \varepsilon r \frac{dy}{d\tau} + y = \varepsilon F. \quad (8.25)$$

The initial value problem

We will start with the response to a stepwise change of external pressure, so we assume $F = 0$, and prescribe a $y = 1$ at $t = 0$. This yields the problem

$$\frac{d^2y}{d\tau^2} + \varepsilon \frac{dy}{d\tau} \left| \frac{dy}{d\tau} \right| + \varepsilon r \frac{dy}{d\tau} + y = 0, \quad \text{with } y(0) = 1, \quad \frac{dy(0)}{d\tau} = 0. \quad (8.26)$$

By comparing the acceleration y'' with the damping $\varepsilon(y'|y'| + ry')$ it may be inferred that on a timescale $\varepsilon\tau$ the influence of the damping is $O(1)$. So we conjecture a slow timescale $\varepsilon\tau$, and split up the time dependence in two by introducing the slow timescale T and the dependent variable Y

$$T = \varepsilon\tau, \quad y(\tau; \varepsilon) = Y(t, T; \varepsilon), \quad \frac{dy}{d\tau} = \frac{\partial Y}{\partial \tau} + \varepsilon \frac{\partial Y}{\partial T},$$

and obtain for equation (8.26)

$$\begin{aligned} \frac{\partial^2 Y}{\partial \tau^2} + Y + \varepsilon \left(2 \frac{\partial^2 Y}{\partial \tau \partial T} + \frac{\partial Y}{\partial \tau} \left| \frac{\partial Y}{\partial \tau} \right| + r \frac{\partial Y}{\partial \tau} \right) + O(\varepsilon^2) = 0 \\ Y(0, 0; \varepsilon) = 1, \quad \left(\frac{\partial}{\partial \tau} + \varepsilon \frac{\partial}{\partial T} \right) Y(0, 0; \varepsilon) = 0. \end{aligned} \quad (8.27)$$

The error of $O(\varepsilon^2)$ results from the approximation $\frac{\partial}{\partial \tau} Y + \varepsilon \frac{\partial}{\partial T} Y \simeq \frac{\partial}{\partial \tau} Y$, and is of course only valid outside a small neighbourhood of the points where $\frac{\partial}{\partial \tau} Y = 0$. We assume the regular expansion

$$Y(t, T; \varepsilon) = Y_0(t, T) + \varepsilon Y_1(t, T) + O(\varepsilon^2)$$

and find for the leading order

$$\frac{\partial^2 Y_0}{\partial \tau^2} + Y_0 = 0, \quad \text{with } Y_0(0, 0) = 1, \quad \frac{\partial}{\partial \tau} Y_0(0, 0) = 0 \quad (8.28)$$

with solution

$$Y_0 = A_0(T) \cos(\tau - \Theta_0(T)), \quad \text{where } A_0(0) = 1, \quad \Theta_0(0) = 0.$$

For the first order we have the equation

$$\begin{aligned} \frac{\partial^2 Y_1}{\partial \tau^2} + Y_1 = -2 \frac{\partial^2 Y_0}{\partial \tau \partial T} - \frac{\partial Y_0}{\partial \tau} \left| \frac{\partial Y_0}{\partial \tau} \right| - r \frac{\partial Y_0}{\partial \tau} = 2 \frac{dA_0}{dT} \sin(\tau - \Theta_0) \\ - 2A_0 \frac{d\Theta_0}{dT} \cos(\tau - \Theta_0) + A_0^2 \sin(\tau - \Theta_0) |\sin(\tau - \Theta_0)| + r A_0 \sin(\tau - \Theta_0) \end{aligned} \quad (8.29)$$

with corresponding initial conditions (they are unimportant for the leading order result). The secular terms are suppressed if the first harmonics (cos and sin) of the right-hand side cancel. For this we use the Fourier series expansion (section C.3, eq. C.45e)

$$\sin \tau | \sin \tau | = -\frac{8}{\pi} \sum_{n=0}^{\infty} \frac{\sin(2n+1)\tau}{(2n-1)(2n+1)(2n+3)} \quad (8.30)$$

and we obtain the equations

$$2\frac{dA_0}{dT} + \frac{8}{3\pi}A_0^2 + rA_0 = 0 \quad \text{and} \quad \frac{d\Theta_0}{dT} = 0 \quad (8.31)$$

with solution $\Theta_0 = 0$ and

$$A_0(T) = \frac{\frac{1}{2}r}{\left(\frac{4}{3\pi} + \frac{1}{2}r\right) e^{\frac{1}{2}rT} - \frac{4}{3\pi}} \quad (8.32)$$

With little linear dissipation (r small) this reduces to an algebraic decay, *viz.* $A_0(T) = (1 + \frac{4}{3\pi}T)^{-1}$, and with little nonlinear dissipation (r large) to the exponential decay $A_0(T) = e^{-\frac{1}{2}rT}$. All together we have

$$p_{in} \simeq 2\varepsilon\rho_0c_0^2 \frac{\ell S_n}{V} \frac{\frac{1}{2}r \cos \tau}{\left(\frac{4}{3\pi} + \frac{1}{2}r\right) e^{\frac{1}{2}r\tau} - \frac{4}{3\pi}}, \quad \text{with} \quad \tau = \left(\frac{c_0^2 S_n}{\ell V}\right)^{\frac{1}{2}} t. \quad (8.33)$$

Comparison with a numerically obtained “exact” solution shows that this approximation happens to be quite good.

The response to harmonic forcing

Suppose we excite the Helmholtz resonator harmonically by an external forcing $p'_{ex} = C \cos(\omega t)$ of frequency ω . In the scaled variables τ and F this becomes

$$\varepsilon F = \varepsilon F_0 \cos(\Omega\tau), \quad \text{with} \quad \omega = \Omega\omega_0.$$

So we have the forced oscillator

$$\frac{d^2y}{d\tau^2} + \varepsilon \frac{dy}{d\tau} \left| \frac{dy}{d\tau} \right| + \varepsilon r \frac{dy}{d\tau} + y = \varepsilon F_0 \cos(\Omega\tau) \quad (8.34)$$

where we don't care about initial conditions, because we are only interested in the stationary state.

When we stay away from resonance conditions, in other words when $1 - \Omega^2$ is not small, the solution is relatively simple. The internal pressure follows the external excitation both in amplitude and in

time dependence. The nonlinear terms hardly play a role, because the driving amplitude is small. So to leading order in ε we have the solution

$$y(\tau) = \varepsilon F_0 \frac{(1 - \Omega^2) \cos \Omega\tau + \varepsilon r \Omega \sin \Omega\tau}{(1 - \Omega^2)^2 + \varepsilon^2 r^2 \Omega^2} = A \cos(\Omega\tau - \theta),$$

$$A = \frac{\varepsilon F_0}{\sqrt{(1 - \Omega^2)^2 + \varepsilon^2 r^2 \Omega^2}}, \quad \tan \theta = \frac{\varepsilon r \Omega}{1 - \Omega^2}. \quad (8.35)$$

We see that near resonance this solution is not valid anymore. When $1 - \Omega^2 = O(\varepsilon)$, amplitude A rises to levels of $O(1)$, and the assumption that the nonlinear damping is negligible is not correct. At the same time, it should be noticed that this corresponds with the most important situations (with the most achieved damping). So it is worthwhile to analyse this problem in more detail. As the physics of the problem essentially change when $\Omega^2 = 1 + O(\varepsilon)$, we assume

$$\Omega = 1 + \varepsilon \Delta. \quad (8.36)$$

To facilitate the analysis we remove the ε -dependence from the driving force, so we make again a slight shift in the time coordinate and introduce

$$\tilde{\tau} = \Omega\tau \quad (8.37)$$

to obtain

$$\Omega^2 \frac{d^2 y}{d\tilde{\tau}^2} + \varepsilon \Omega^2 \frac{dy}{d\tilde{\tau}} \left| \frac{dy}{d\tilde{\tau}} \right| + \varepsilon \Omega r \frac{dy}{d\tilde{\tau}} + y = \varepsilon F_0 \cos(\tilde{\tau}) \quad (8.38)$$

To leading order this becomes

$$(1 + 2\varepsilon \Delta) \frac{d^2 y}{d\tilde{\tau}^2} + \varepsilon \frac{dy}{d\tilde{\tau}} \left| \frac{dy}{d\tilde{\tau}} \right| + \varepsilon r \frac{dy}{d\tilde{\tau}} + y = \varepsilon F_0 \cos(\tilde{\tau}) \quad (8.39)$$

When we substitute the assumed expansion $y(\tilde{\tau}; \varepsilon) = y_0(\tilde{\tau}) + \varepsilon y_1(\tilde{\tau}) + \dots$, and collect like powers of ε , we find for y_0

$$\frac{d^2 y_0}{d\tilde{\tau}^2} + y_0 = 0 \quad (8.40)$$

with general solution

$$y_0(\tilde{\tau}) = A_0 \cos(\tilde{\tau} - \theta_0). \quad (8.41)$$

Although y_0 is the result of driving force F , we don't have any information yet so we can't determine the integration constants A_0 and θ_0 at this level. Therefore we continue with the next order y_1 .

$$\frac{d^2 y_1}{d\tilde{\tau}^2} + y_1 = F_0 \cos(\tilde{\tau}) - 2\Delta \frac{d^2 y_0}{d\tilde{\tau}^2} - \frac{dy_0}{d\tilde{\tau}} \left| \frac{dy_0}{d\tilde{\tau}} \right| - r \frac{dy_0}{d\tilde{\tau}}$$

$$= F_0 \cos(\tilde{\tau}) + 2\Delta A_0 \cos(\tilde{\tau} - \theta_0) + A_0 |A_0| \sin(\tilde{\tau} - \theta_0) |\sin(\tilde{\tau} - \theta_0)| + r A_0 \sin(\tilde{\tau} - \theta_0). \quad (8.42)$$

From the argument that we are only interested in the stationary state it follows that no resonant excitation is allowed in the right-hand-side of the equation for y_1 . This is effectively very similar to the condition of absent secular terms of the previous initial value problem. So we can use the same techniques to suppress the cos- and sin-terms, and use equation (8.30) to obtain

$$F_0 \cos \theta_0 = -2\Delta A_0, \quad F_0 \sin \theta_0 = \left(\frac{8}{3\pi}|A_0| + r\right) A_0 \tag{8.43}$$

with solution

$$\left[\left(\frac{8}{3\pi}|A_0| + r\right)^2 + 4\Delta^2\right]A_0^2 = F_0^2, \quad \tan \theta_0 = -\frac{\frac{8}{3\pi}|A_0| + r}{2\Delta}. \tag{8.44}$$

This equation has several solutions, and it may not be immediately clear which is the correct one. To solve $A_0 = A_0(\Delta)$ is difficult, but it is easy to write Δ^2 as a function of A_0 :

$$\Delta^2 = \frac{1}{4} \left[\frac{F_0^2}{A_0^2} - \left(\frac{8}{3\pi}|A_0| + r\right)^2 \right].$$

Since $\Delta^2 \geq 0$ we see immediately that two solutions exist only for a finite interval in A_0 , these two are \pm symmetric (we only need to consider one), while $\Delta \rightarrow \pm\infty$ only when $A_0 \rightarrow 0$. In particular,

$$A_0 \simeq \frac{F_0}{2|\Delta|}, \quad \tan \theta_0 \simeq -\frac{r}{2\Delta} \quad \text{or} \quad \theta_0 \simeq -\frac{r}{2\Delta} + n\pi,$$

which is in exact agreement with the asymptotic behaviour for $\Omega = 1 + \varepsilon\Delta$, Δ large, of (8.35). In fact, by tracing the solution parametrically as a function of Δ , we can see that if we start with $\theta_0 = 0$ for $\Delta \rightarrow -\infty$, we end with $\theta_0 = \pi$ for $\Delta \rightarrow \infty$. See figure 8.2 for an example.

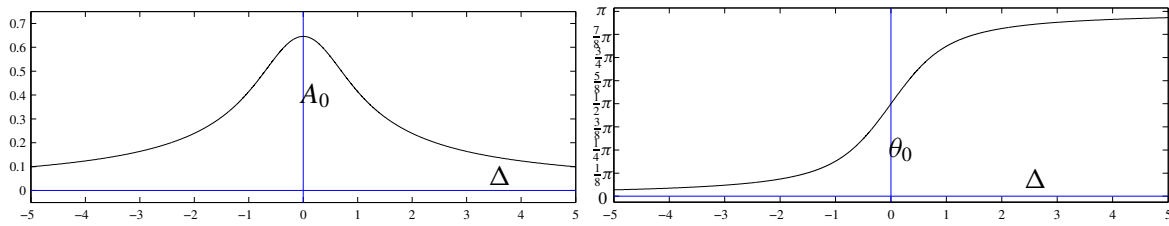


Figure 8.2 Solutions of amplitude A_0 and phase θ_0 as a function of Δ , for $r = 1$ and $F_0 = 1$. See (8.44)

8.4 Slowly varying ducts

Consider a hard-walled circular cylindrical duct with a slowly varying diameter (*c.f.* [205, 202, 213, 164, 37, 208, 174]), described in polar coordinates (x, r, θ) as

$$r = a(\varepsilon x) \quad (8.45)$$

with ε a dimensionless small parameter. In this duct we have an acoustic medium with constant mean

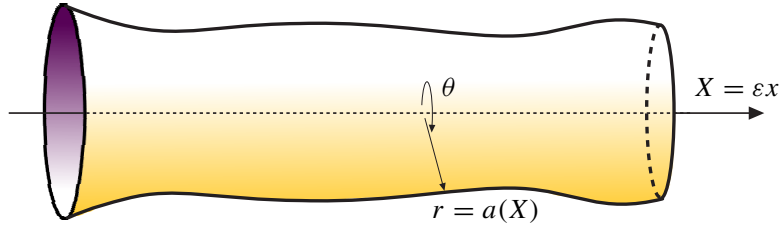


Figure 8.3 Sketch of geometry of slowly varying circular duct.

pressure and a slowly varying sound speed $c_0 = c_0(\varepsilon x)$ (for simplicity no variation in r and θ is assumed). Sound waves of circular frequency ω are described by a variant of the Helmholtz equation

$$\nabla \cdot \left(\frac{1}{k^2} \nabla p \right) + p = 0 \quad (8.46)$$

where $k = k(\varepsilon x) = \omega/c_0(\varepsilon x)$, with boundary condition a vanishing normal velocity component at the wall, so

$$\mathbf{n} \cdot \nabla p = 0 \quad \text{at } r = a(\varepsilon x). \quad (8.47)$$

Since (section A.3)

$$\mathbf{n} \propto \nabla (r - a(\varepsilon x)) = \mathbf{e}_r - \varepsilon a'(\varepsilon x) \mathbf{e}_x,$$

(where $a'(z) = da(z)/dz$) this is

$$\frac{\partial p}{\partial r} - \varepsilon a'(\varepsilon x) \frac{\partial p}{\partial x} = 0 \quad \text{at } r = a(\varepsilon x). \quad (8.48)$$

We know that for constant a and constant k the general solution can be built up from modes of the following type (chapter 7)

$$\begin{aligned} p &= A J_m(\alpha_{m\mu} r) e^{-im\theta - ik_{m\mu} x}, \\ \alpha_{m\mu} &= j'_{m\mu}/a, \\ k_{m\mu}^2 &= k^2 - \alpha_{m\mu}^2, \quad \text{Re}(k_{m\mu}) \geq 0, \quad \text{Im}(k_{m\mu}) \leq 0, \end{aligned} \quad (8.49)$$

and we assume for the present problem, following the previous section, that there are solutions close to these modes. We introduce the slow variable

$$X = \varepsilon x$$

so that $k = k(X)$, and we seek a solution of slowly varying modal type:

$$p = A(X, r; \varepsilon) e^{-im\theta} e^{-i\varepsilon^{-1} \int_0^X \gamma(\xi; \varepsilon) d\xi} \quad (8.50)$$

Since

$$\begin{aligned} \nabla \cdot \left(\frac{1}{k^2} \nabla p \right) &= \frac{\partial}{\partial x} \left(\frac{1}{k^2} \frac{\partial p}{\partial x} \right) + \frac{1}{k^2} \left(\frac{\partial^2 p}{\partial r^2} + \frac{1}{r} \frac{\partial p}{\partial r} + \frac{1}{r^2} \frac{\partial^2 p}{\partial \theta^2} \right) \\ \frac{\partial p}{\partial x} &= \left(-i\gamma A + \varepsilon \frac{\partial A}{\partial X} \right) \exp(\dots) \\ \frac{\partial^2 p}{\partial x^2} &= \left(-\gamma^2 A - 2i\varepsilon\gamma \frac{\partial A}{\partial X} - i\varepsilon \frac{\partial \gamma}{\partial X} A + \varepsilon^2 \frac{\partial^2 A}{\partial X^2} \right) \exp(\dots) \end{aligned}$$

we have for (8.46) after multiplication with k^2 :

$$\begin{aligned} \left[-\gamma^2 A - 2i\varepsilon\gamma \frac{\partial A}{\partial X} - i\varepsilon \frac{\partial \gamma}{\partial X} A + \varepsilon^2 \frac{\partial^2 A}{\partial X^2} - 2\varepsilon \frac{1}{k} \frac{\partial k}{\partial X} \left(-i\gamma A + \varepsilon \frac{\partial A}{\partial X} \right) \right. \\ \left. + \frac{\partial^2 A}{\partial r^2} + \frac{1}{r} \frac{\partial A}{\partial r} - \frac{m^2}{r^2} A + k^2 A \right] \exp(\dots) = 0. \end{aligned}$$

After suppressing the exponential factor, this is up to order $O(\varepsilon)$

$$\begin{aligned} \mathcal{L}(A) &= i\varepsilon \frac{k^2}{A} \frac{\partial}{\partial X} \left(\frac{\gamma A^2}{k^2} \right), \\ \frac{\partial A}{\partial r} + i\varepsilon \frac{\partial a}{\partial X} \gamma A &= 0 \quad \text{at } r = a(X), \end{aligned} \quad (8.51)$$

where we introduced for short the Bessel-type operator (see Appendix D)

$$\mathcal{L}(A) = \frac{\partial^2 A}{\partial r^2} + \frac{1}{r} \frac{\partial A}{\partial r} + \left(k^2 - \gamma^2 - \frac{m^2}{r^2} \right) A$$

and rewrote the right-hand side in a form convenient later. Expand

$$A(X, r; \varepsilon) = A_0(X, r) + \varepsilon A_1(X, r) + O(\varepsilon^2)$$

$$\gamma(X; \varepsilon) = \gamma_0(X) + O(\varepsilon^2)$$

substitute in (8.51), and collect like powers of ε .

$$\begin{aligned} O(1) : \quad \mathcal{L}(A_0) &= 0 \\ \frac{\partial A_0}{\partial r} &= 0 \quad \text{at } r = a(X), \end{aligned} \tag{8.52}$$

$$\begin{aligned} O(\varepsilon) : \quad \mathcal{L}(A_1) &= i \frac{k^2}{A_0} \frac{\partial}{\partial X} \left(\frac{\gamma_0 A_0^2}{k^2} \right) \\ \frac{\partial A_1}{\partial r} &= -i \frac{\partial a}{\partial X} \gamma_0 A_0 \quad \text{at } r = a(X). \end{aligned} \tag{8.53}$$

Since variable X plays no other rôle in (8.52) than that of a parameter, we have for A_0 the “almost-mode”

$$\begin{aligned} A_0(X, r) &= P_0(X) J_m(\alpha(X)r), \\ \alpha(X) &= j'_{m\mu}/a(X), \\ \gamma_0^2(X) &= k^2(X) - \alpha^2(X), \quad \operatorname{Re}(\gamma_0) \geq 0, \operatorname{Im}(\gamma_0) \leq 0, \end{aligned} \tag{8.54}$$

The amplitude P_0 is still undetermined, and follows from a solvability condition for A_1 . As before, amplitude P_0 is determined at the level of A_1 , without A_1 necessarily being known.

Multiply left- and right-hand side of (8.53) with $r A_0/k^2$ and integrate to r from 0 to $a(X)$. For the left-hand side we utilize the self-adjointness of $r\mathcal{L}$.

$$\begin{aligned} \int_0^a \frac{r A_0}{k^2} \mathcal{L}(A_1) dr &= \frac{1}{k^2} \int_0^a r A_0 \mathcal{L}(A_1) - r A_1 \mathcal{L}(A_0) dr = \frac{1}{k^2} \left[r A_0 \frac{\partial A_1}{\partial r} - r A_1 \frac{\partial A_0}{\partial r} \right]_0^a \\ &= -i \frac{\gamma_0 a}{k^2} \frac{\partial a}{\partial X} A_0^2. \end{aligned}$$

For the right-hand side we apply the Leibniz integral rule

$$i \int_0^a \frac{\partial}{\partial X} \left(\frac{\gamma_0 A_0^2}{k^2} \right) r dr = i \frac{d}{dX} \int_0^a \frac{r \gamma_0 A_0^2}{k^2} dr - i \frac{\gamma_0 a}{k^2} \frac{\partial a}{\partial X} A_0^2.$$

As a result

$$\int_0^a \frac{r \gamma_0 A_0^2}{k^2} dr = \left[\frac{\gamma_0}{2k^2} P_0^2 \left(r^2 - \frac{m^2}{\alpha^2} \right) J_m(\alpha r)^2 \right]_0^a = \frac{\gamma_0 P_0^2}{2k^2} a^2 \left(1 - \frac{m^2}{j_{m\mu}^2} \right) J_m(j'_{m\mu})^2 = \text{constant}$$

or:

$$P_0(X) = \text{const.} \frac{k(X)}{a(X) \sqrt{\gamma_0(X)}} = \text{const.} \frac{k(X) \alpha(X)}{\sqrt{\gamma_0(X)}} \tag{8.55}$$

It is not accidental that the above integral $\int_0^a (r \gamma_0 A_0^2 / k^2) dr$ is constant. The transmitted power of p is to leading order

$$\begin{aligned} \mathcal{P} &= \int_0^{2\pi} \int_0^a \frac{1}{2} \operatorname{Re}(pu^*) r dr d\theta = \frac{\pi}{\omega \rho_0} \int_0^a \operatorname{Im}\left(p \frac{\partial}{\partial x} p^*\right) r dr \\ &= \frac{\pi}{\omega \rho_0} \operatorname{Re}(\gamma_0) e^{2\varepsilon^{-1} \int_0^X \operatorname{Im}(\gamma_0) d\xi} \int_0^a |A_0|^2 r dr. \end{aligned} \tag{8.56}$$

This is for propagating modes (γ_0 real) constant:

$$\mathcal{P} = \frac{\pi}{\omega \rho_0} \gamma_0 |P_0|^2 \frac{1}{2} a^2 \left(1 - \frac{m^2}{j_{m\mu}^{\prime 2}}\right) J_m(j_{m\mu}')^2 = \operatorname{const.} \frac{\gamma_0}{\rho_0} \frac{k^2}{a^2 \gamma_0} a^2 = \operatorname{const.} \frac{1}{\rho_0 c_0^2} = \operatorname{constant}$$

since $\rho_0 c_0^2$ is, apart from a factor, equal to the constant mean pressure.

8.5 Reflection at an isolated turning point

An important property of expression (8.55) for P_0 is that it becomes invalid when $\gamma_0 = 0$. So when the medium and diameter vary in such a way that at some point $X = X_0$ wave number γ_0 vanishes, the present method breaks down [206, 172, 173, 175, 232]. In a small interval around X_0 the mode does *not* vary slowly and locally a different approximation is necessary.

When γ_0^2 changes sign, and γ_0 changes from real into imaginary, the mode is split up into a cut-on reflected part and a cut-off transmitted part. If X_0 is isolated, such that there are no interfering neighbouring points of vanishing γ_0 , it is clear that no power is transmitted beyond X_0 ($\operatorname{Re}(\gamma_0) = 0$ in (8.56)), and the wave has to reflect at X_0 . Therefore, a point where wave number γ_0 vanishes is called a “turning point”.

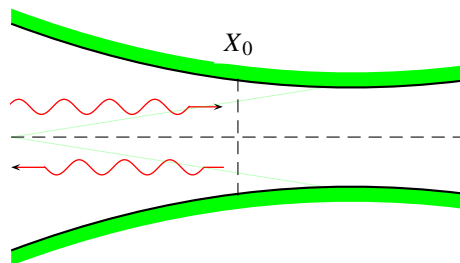


Figure 8.4 Turning point X_0 , where a mode changes from cut-on to cut-off.

Asymptotically, a turning point region is a boundary layer and the appropriate analysis is that of matched asymptotic analysis (section 8.8), in the context of the WKB method (see [15, 83]). However,

since the physics of the subject is most relevant in this section on slowly varying ducts, we will present the pertaining results here².

Assume at $X = X_0$ a transition from cut-on to cut-off, so $\frac{\partial}{\partial X} \gamma_0^2 < 0$ or

$$\frac{c'_0(X_0)}{c_0(X_0)} - \frac{a'(X_0)}{a(X_0)} > 0, \quad \text{or} \quad \alpha'(X_0) - k'(X_0) > 0.$$

Consider an incident, reflected and transmitted wave of the type found above (equations 8.50,8.54,8.55). So in $X < X_0$, where γ_0 is real positive, we have the incident and reflected waves

$$p(x, r, \theta) = \frac{k(X)\alpha(X)}{\sqrt{\gamma_0(X)}} J_m(\alpha(X)r) e^{-im\theta} \left[e^{-i\varepsilon^{-1} \int_{X_0}^X \gamma_0(X') dX'} + R e^{i\varepsilon^{-1} \int_{X_0}^X \gamma_0(X') dX'} \right] \quad (8.57)$$

with reflection coefficient R to be determined. In $X > X_0$, where γ_0 is imaginary negative, we have the transmitted wave

$$p(x, r, \theta) = T \frac{k(X)\alpha(X)}{\sqrt{\gamma_0(X)}} J_m(\alpha(X)r) e^{-im\theta} e^{-i\varepsilon^{-1} \int_{X_0}^X \gamma_0(X') dX'}. \quad (8.58)$$

with transmission coefficient T to be determined, while $\sqrt{\gamma_0} = e^{-\frac{1}{4}\pi i} \sqrt{|\gamma_0|}$ will be taken.

This set of approximate solutions of equation (8.46), valid outside the turning point region, constitute the outer solution. Inside the turning point region this approximation breaks down. The approximation is invalid here, because neglected terms of equation (8.46) are now dominant, and another approximate equation is to be used. This will give us the inner or boundary layer solution. To determine the unknown constants (here: R and T), inner and outer solution are asymptotically matched.

For the matching it is necessary to determine the asymptotic behaviour of the outer solution in the limit $X \rightarrow X_0$, and the boundary layer thickness (*i.e.* the appropriate local coordinate).

From the limiting behaviour of the outer solution in the turning point region (see below), we can estimate the order of magnitude of the solution. From a balance of terms in the differential equation (8.46) it transpires that the turning point boundary layer is of thickness $X - X_0 = O(\varepsilon^{2/3})$, leading to a boundary layer variable ξ given by

$$X = X_0 + \varepsilon^{2/3} \xi.$$

Since for $\varepsilon \rightarrow 0$

$$\gamma_0^2(X) = \gamma_0^2(X_0 + \varepsilon^{2/3} \xi) = -2\varepsilon^{2/3} k_0(\alpha'_0 - k'_0) \xi + O(\varepsilon^{4/3} \xi^2),$$

²As is explained in section 8.8, the steps in the process of determining the boundary layer thickness and equations, and finally the matching, are very much coupled, and usually too lengthy to present in detail. Therefore, to keep the present example concise, we will present the results with a limited amount of explanation.

where $k_0 = k(X_0)$, $k'_0 = k'(X_0)$, etc., we have

$$\frac{1}{\varepsilon} \int_{X_0}^X \gamma_0(X') dX' = \begin{cases} -\frac{2}{3} |\bar{\xi}|^{3/2} = -\zeta, & \text{if } \xi < 0 \\ -i \frac{2}{3} \bar{\xi}^{3/2} = -i\zeta, & \text{if } \xi > 0 \end{cases}$$

where we introduced

$$\bar{\xi} = \{2k_0(\alpha'_0 - k'_0)\}^{1/3} \xi \quad \text{and} \quad \zeta = \frac{2}{3} |\bar{\xi}|^{3/2}.$$

The limiting behaviour for $X \uparrow X_0$ is now given by

$$p \simeq \frac{k_0 \alpha_0}{\{2\varepsilon k_0(\alpha'_0 - k'_0)\}^{1/6} |\bar{\xi}|^{1/4}} J_m(\alpha_0 r) e^{-im\theta} \left(e^{i\zeta} + R e^{-i\zeta} \right), \quad (8.59)$$

while it is for $X \downarrow X_0$ given by

$$p \simeq T \frac{e^{\frac{1}{4}\pi i} k_0 \alpha_0}{\{2\varepsilon k_0(\alpha'_0 - k'_0)\}^{1/6} \bar{\xi}^{1/4}} J_m(\alpha_0 r) e^{-im\theta} e^{-\zeta}. \quad (8.60)$$

Since the boundary layer is relatively thin, also compared to the radial coordinate, the behaviour of the incident mode remains rather unaffected in radial direction, and we can assume in the turning point region

$$p(x, r, \theta) = J_m(\alpha(X)r) \psi(\xi) e^{-im\theta}.$$

From the properties of the Bessel equation (D.1), we have

$$\frac{\partial^2 p}{\partial r^2} + \frac{1}{r} \frac{\partial p}{\partial r} + \frac{1}{r^2} \frac{\partial^2 p}{\partial \theta^2} + k^2 p = \gamma_0^2 p = O(\varepsilon^{2/3}) p.$$

Hence, equation (8.46) yields

$$k^2 \nabla \cdot \left(\frac{1}{k^2} \nabla p \right) + k^2 p \simeq \varepsilon^{2/3} \frac{\partial^2 p}{\partial \xi^2} + \gamma_0^2 p = \varepsilon^{2/3} J_m(\alpha(X)r) e^{-im\theta} \left\{ \frac{\partial^2 \psi}{\partial \xi^2} - 2k_0(\alpha'_0 - k'_0) \xi \psi \right\} = 0$$

which is, written in variable $\bar{\xi}$, equivalent to Airy's equation (D.83)

$$\frac{\partial^2 \psi}{\partial \bar{\xi}^2} - \bar{\xi} \psi = 0.$$

This has the general solution (see figure 8.5)

$$\psi(\xi) = a Ai(\bar{\xi}) + b Bi(\bar{\xi}),$$

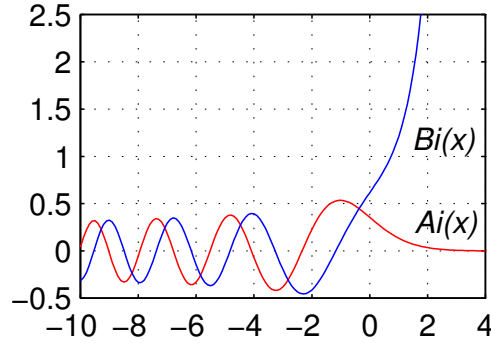


Figure 8.5 Airy functions

where a and b , parallel with R and T , are now determined from matching. Using the asymptotic expressions (D.84,D.85) for Airy functions, we find that for $\bar{\xi}$ large with $1 \ll \bar{\xi} \ll \varepsilon^{-2/3}$, equation (8.60) matches the inner solution if

$$\frac{a}{2\sqrt{\pi}\bar{\xi}^{1/4}} e^{-\zeta} + \frac{b}{\sqrt{\pi}\bar{\xi}^{1/4}} e^{\zeta} \sim T \frac{e^{\frac{1}{4}\pi i} k_0 \alpha_0}{\{2\varepsilon k_0(\alpha'_0 - k'_0)\}^{1/6} \bar{\xi}^{1/4}} e^{-\zeta}.$$

Since $e^{\zeta} \rightarrow \infty$, we can only have $b = 0$, and thus

$$a = \frac{2\sqrt{\pi} T k_0 \alpha_0 e^{\frac{1}{4}\pi i}}{\{2\varepsilon k_0(\alpha'_0 - k'_0)\}^{1/6}}.$$

If $-\bar{\xi}$ is large with $1 \ll -\bar{\xi} \ll \varepsilon^{-2/3}$ we use the asymptotic expression (D.84), and find that equation (8.59) matches the inner solution if

$$\frac{a}{\sqrt{\pi} |\bar{\xi}|^{1/4}} \cos(\zeta - \frac{1}{4}\pi) \sim \frac{k_0 \alpha_0}{\{2\varepsilon k_0(\alpha'_0 - k'_0)\}^{1/6} |\bar{\xi}|^{1/4}} (e^{i\zeta} + R e^{-i\zeta}),$$

or

$$T e^{\frac{1}{4}\pi i} (e^{i\zeta - \frac{1}{4}\pi i} + e^{-i\zeta + \frac{1}{4}\pi i}) = T e^{i\zeta} + T i e^{-i\zeta} \sim e^{i\zeta} + R e^{-i\zeta}.$$

So, finally, we have

$$T = 1, \quad R = i. \tag{8.61}$$

8.6 Ray acoustics in temperature gradient

When a sound wave propagates in free space through a medium that varies on a much larger scale than the typical wave length (typically: temperature gradients, or wind with shear), the same ideas of multiple scales may be applied. In contrast to the duct, where the wave is confined by the duct walls, the waves may now freely refract and follow curved paths. These paths are called rays. This means that rays are not localized “beams” of sound, but only the tangents of the intensity vectors of a sound field.

Consider an infinite 3D medium with varying temperature but otherwise with a constant mean pressure, so that we have again equation (8.46), but now c varying more generally as a function of \mathbf{x}

$$\nabla \cdot (c_0^2 \nabla p) + \omega^2 p = 0, \quad c_0 = c_0(\varepsilon \mathbf{x}) \quad (8.62)$$

for a time harmonic sound field $p \propto e^{i\omega t}$. The typical lengthscale L of sound speed variations, estimated from $L^{-1} \sim \|\nabla c_0\|/c_0$, is assumed much larger than the typical wave length $\lambda \sim c_0/\omega$. In order to quantify this, we write $c_0 = c_0(\varepsilon \mathbf{x})$ where the small parameter ε is given by $\varepsilon = \lambda/L$. In the following, we will see that this introduction of ε is a convenient way of keeping the large and small terms apart.³

Assuming the field to be locally plane we try an approximate solution having the form of a plane wave but with slowly varying (real) amplitude $A = A(\mathbf{X}; \varepsilon)$ and phase $\tau = \tau(\mathbf{X})$

$$p(\mathbf{x}) = A e^{-i\tau/\varepsilon} \quad (8.63)$$

where $\mathbf{X} = \varepsilon \mathbf{x}$ the slow variable. The surfaces $\tau(\mathbf{X}) = \varepsilon \omega t$ describe the propagating wave front. Note that the vector field $\nabla \tau$ is *normal* to the surfaces $\tau = \text{constant}$ (section A.3). Define the operator

$$\bar{\nabla} = \left(\frac{\partial}{\partial X}, \frac{\partial}{\partial Y}, \frac{\partial}{\partial Z} \right)$$

so that $\nabla = \varepsilon \bar{\nabla}$. Define the local wave vector

$$\mathbf{k} = \bar{\nabla} \tau, \quad (8.64)$$

inspired by the fact that if we approximate locally $\tau(\mathbf{X}) = \tau_0 + \bar{\nabla} \tau \cdot \mathbf{X} + \dots$ (with τ_0 an unimportant constant), the wave becomes a plane wave $\simeq A_0 e^{i\omega t - i\mathbf{k} \cdot \mathbf{x}}$ with frequency ω and wave vector \mathbf{k} . Substitute (8.63) in (8.62):

$$\nabla p = (\varepsilon \bar{\nabla} A - i A \mathbf{k}) e^{-i\tau/\varepsilon}, \quad (8.65a)$$

$$\nabla^2 p = (\varepsilon^2 \bar{\nabla}^2 A - 2i\varepsilon \bar{\nabla} A \cdot \mathbf{k} - i\varepsilon A \bar{\nabla} \cdot \mathbf{k} - A |\mathbf{k}|^2) e^{-i\tau/\varepsilon}, \quad (8.65b)$$

³It should be noted that our point of view here is to think of the problem as a wave in a slowly varying medium, *i.e.* to consider L “large”. Another, equally valid point of view is to think of a medium with a high frequency wave, *i.e.* to scale the problem on L and to consider the wave length “short” or the frequency “high”.

to obtain

$$(\omega^2 - c_0^2 |\mathbf{k}|^2)A - i\varepsilon A^{-1} \bar{\nabla} \cdot (c_0^2 A^2 \mathbf{k}) + \varepsilon^2 \bar{\nabla} \cdot (c_0^2 \bar{\nabla} A) = 0. \quad (8.66)$$

Expand

$$A(\mathbf{X}; \varepsilon) = A_0(\mathbf{X}) + \varepsilon A_1(\mathbf{X}) + O(\varepsilon^2)$$

and collect like powers in (8.66). We find to leading order

$$c_0^2 |\mathbf{k}|^2 - \omega^2 = 0 \quad (8.67)$$

$$\bar{\nabla} \cdot (c_0^2 A_0^2 \mathbf{k}) = 0. \quad (8.68)$$

Equation (8.67) is the *eikonal equation*, which determines the wave fronts and the ray paths. Equation (8.68) is called the *transport equation* and describes the *conservation of wave action*, which is here equivalent to *conservation of energy* [125, 260]. It relates the amplitude variation to diverging or converging rays.

The eikonal equation is a nonlinear first order partial differential equation, of hyperbolic type, which can always be reduced to an ordinary differential equation along characteristics [38]. This is summarized by the following theorem ([260, p.65]).

Theorem 8.1 (General solution of 1st order PDE)

The solution of the first-order partial differential equation

$$H(\mathbf{k}, \tau, \mathbf{x}) = 0, \quad \mathbf{k} = \nabla \tau,$$

with consistent boundary conditions on a surface S , is given by the system of ordinary differential equations⁴

$$\frac{d\boldsymbol{\chi}}{d\lambda} = \nabla_{\mathbf{k}} H, \quad \frac{d\tau}{d\lambda} = \mathbf{k} \cdot \nabla_{\mathbf{k}} H, \quad \frac{d\mathbf{k}}{d\lambda} = -\mathbf{k} \frac{\partial H}{\partial \tau} - \nabla_{\mathbf{x}} H,$$

where the curve $\mathbf{x} = \boldsymbol{\chi}(\lambda)$, with parameter λ , is called a characteristic.

A characteristic forms a path along which the information of the boundary values on S is transferred to the point of observation. In general the characteristic depends on the solution, and both characteristic and solution are to be determined together. If more than one point of a characteristic is part of S , the boundary conditions are not independent, and in general inconsistent. If more than one characteristic passes through a point, the solution is not unique.

By starting from other, equivalent, equations $H(\mathbf{k}, \tau, \mathbf{x}) = 0$, we obtain the same solution but with other parametrizations.

⁴ $\nabla_{\mathbf{k}} H$ denotes the gradient in \mathbf{k} : $(\frac{\partial H}{\partial k_i})$; similar for $\nabla_{\mathbf{x}} H$.

Sometimes a preferable parametrization is the so-called natural parametrization, with λ equal to the arclength and $\|\frac{d\mathbf{x}}{d\lambda}\| = 1$.

The characteristics are here identical to the rays. By rewriting equation (8.67) as $\frac{1}{2}\varepsilon(c_0^2|\mathbf{k}|^2 - \omega^2)/\omega = 0$ and using theorem (8.1) (p.238), the characteristic variable is just the time t (but *not* the arclength), and we have the expected

$$\tau(\mathbf{X}(t)) = \varepsilon\omega t \tag{8.69}$$

along a ray $\mathbf{X} = \mathbf{X}(t)$ given by

$$\frac{d\mathbf{X}}{dt} = \varepsilon c_0 \frac{\mathbf{k}}{|\mathbf{k}|}, \tag{8.70a}$$

$$\frac{d\mathbf{k}}{dt} = -\varepsilon|\mathbf{k}|\nabla c_0. \tag{8.70b}$$

where $|\mathbf{k}| = \omega/c_0$. Equations (8.70) form a first order system of ordinary differential equations, called: “ray-tracing equations”. Together with suitable initial value conditions in \mathbf{k} and \mathbf{X} , they constitute an initial value problem that can be solved numerically by standard integration routines like a Runge-Kutta method.

Once we know the rays, the transport equation (8.68) can be solved as follows. Consider a small area S_1 of the surface $\tau = C_1$, and connect the points of S_1 via the rays (following the vector field \mathbf{k}) with the corresponding area S_2 on the surface $\tau = C_2$. Then the volume of rays connecting S_1 and S_2 is called a ray-tube. Since \mathbf{k} is just parallel to the tube’s surface, except for S_1 and S_2 where it is just ω/c_0 and perpendicular to it, we have (with Gauss’ theorem)

$$\int_{tube} \nabla \cdot (c_0^2 A_0^2 \mathbf{k}) d\mathbf{X} = 0 = \int_{S_2} c_0 A_0^2 ds - \int_{S_1} c_0 A_0^2 ds.$$

If we associate to a ray $\mathbf{X}(t)$ a ray-tube with cross section $S = S(\mathbf{X})$, the amplitude varies according to the relation

$$A_0^2(\mathbf{X})c_0(\mathbf{X})S(\mathbf{X}) = \text{constant along a ray tube.} \tag{8.71}$$

From equation (8.70b) it can be inferred that a ray (with direction \mathbf{k}) bends away from regions with higher sound speed. This explains why sound is carried far along a cold surface like water or snow, and not at all along for example hot sand. When the surface is cold there is a positive soundspeed gradient which causes the sound waves to bend downwards to the surface (figure 8.6). In combination with reflection at the surface the sound is trapped and tunnels through the layer adjacent to the surface. When the surface is hot there is a negative soundspeed gradient which causes the sound to bend upwards and so to disappear into free space.

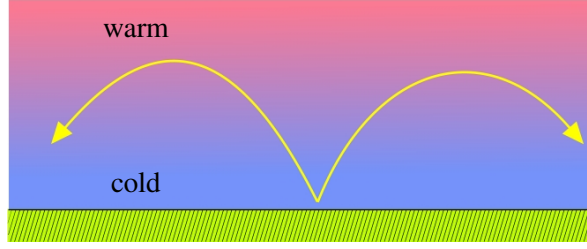


Figure 8.6 Refraction of sound rays in a temperature gradient.

We can make this more explicit for a sound speed that varies linearly in space. We have then the remarkable result of exact solutions of rays following plane circles. To show this in detail, it is necessary that we obtain a parametrization that corresponds with an arclength (in the slow coordinate \mathbf{X}). Therefore, we recast the eikonal equation in the form

$$H(\mathbf{X}, \tau, \mathbf{k}) = \frac{1}{2} \left(|\mathbf{k}| - \frac{\omega^2}{c_0^2 |\mathbf{k}|} \right) \quad (8.72)$$

and obtain from theorem (8.1)

$$\begin{aligned} \frac{d\mathbf{X}}{ds} &= \nabla_{\mathbf{k}} H = \frac{1}{2} \frac{\mathbf{k}}{|\mathbf{k}|} + \frac{1}{2} \frac{\omega^2}{c_0^2 |\mathbf{k}|^3} \mathbf{k} = \frac{\mathbf{k}}{|\mathbf{k}|} = \mathbf{t} \\ \frac{d\tau}{ds} &= \mathbf{k} \cdot \nabla_{\mathbf{k}} H = \frac{\mathbf{k} \cdot \mathbf{k}}{|\mathbf{k}|} = |\mathbf{k}| \\ \frac{d\mathbf{k}}{ds} &= -\mathbf{k} \frac{\partial H}{\partial \tau} - \nabla_{\mathbf{X}} H = 0 - \frac{\omega^2}{c_0^3 |\mathbf{k}|} \overline{\nabla} c_0 = -\frac{|\mathbf{k}|}{c_0} \overline{\nabla} c_0 \end{aligned}$$

The ray is given by the curve $\mathbf{X} = \mathbf{X}(s)$ and launched at $\mathbf{X}(0) = \varepsilon \mathbf{x}(0)$ in the direction $\mathbf{k}(0)$ with initial phase $\tau(0)$. Since we have applied the so-called natural parametrization, with s the arclength, $\frac{d}{ds} \mathbf{X} = \mathbf{t}$ is the unit tangent vector and $\frac{d^2}{ds^2} \mathbf{X}$ the curvature vector:

$$\boldsymbol{\kappa} = \frac{d^2 \mathbf{X}}{ds^2} = \frac{1}{\omega} \frac{d}{ds} (c_0 \mathbf{k}) = \frac{1}{\omega} \left[\frac{\mathbf{k}}{|\mathbf{k}|} (\overline{\nabla} c_0 \cdot \mathbf{k}) - |\mathbf{k}| \overline{\nabla} c_0 \right] \quad (8.73)$$

The curvature, or reciprocal radius, is then

$$|\boldsymbol{\kappa}| = \frac{1}{\omega} \left[|\mathbf{k}|^2 |\overline{\nabla} c_0|^2 - (\overline{\nabla} c_0 \cdot \mathbf{k})^2 \right]^{1/2} \quad (8.74)$$

Now we use the fact that c_0 varies linearly in (say) direction \mathbf{n} :

$$c_0 = q + \alpha (\mathbf{X} \cdot \mathbf{n}), \quad \overline{\nabla} c_0 = \alpha \mathbf{n}. \quad (8.75)$$

Decompose vector \mathbf{k} in a component in \mathbf{n} direction and one orthogonal to it

$$\mathbf{k} = k_0\mathbf{n} + k_1\mathbf{b}, \quad \text{with } \mathbf{n} \cdot \mathbf{b} = 0, \quad |\mathbf{b}| = 1. \quad (8.76)$$

Of course, $k_0 = (\mathbf{k} \cdot \mathbf{n})$ and $k_1 = (\mathbf{k} \cdot \mathbf{b})$. It follows from

$$\frac{d\mathbf{k}}{ds} = -\frac{|\mathbf{k}|}{c_0} \nabla c_0 = -\frac{|\mathbf{k}|}{c_0} \alpha \mathbf{n} \quad (8.77)$$

that \mathbf{k} only varies in \mathbf{n} -direction, while $k_1\mathbf{b}$ is constant, determined by the initial wave vector $\mathbf{k}(0)$. Since also \mathbf{n} is fixed, it is only $k_0 = k_0(s)$ that varies with s . So we go on with the curvature

$$\begin{aligned} \kappa &= \frac{1}{\omega|\mathbf{k}|} [\mathbf{k}(\nabla c_0 \cdot \mathbf{k}) - |\mathbf{k}|^2 \nabla c_0] = \frac{1}{\omega|\mathbf{k}|} [(k_0\mathbf{n} + k_1\mathbf{b})\alpha k_0 - (k_0^2 + k_1^2)\alpha \mathbf{n}] \\ &= \frac{1}{\omega|\mathbf{k}|} [\alpha k_0^2 \mathbf{n} + \alpha k_0 k_1 \mathbf{b} - \alpha k_0^2 \mathbf{n} - \alpha k_1^2 \mathbf{n}] = \frac{\alpha k_1}{\omega|\mathbf{k}|} (k_0 \mathbf{b} - k_1 \mathbf{n}) = \frac{\alpha k_1}{\omega} \mathbf{c} \end{aligned} \quad (8.78)$$

where vector

$$\mathbf{c} = \frac{k_0 \mathbf{b} - k_1 \mathbf{n}}{|\mathbf{k}|} \quad (8.79)$$

is the unit curvature vector (or principal normal unit vector) of curve $\mathbf{X}(s)$. Since \mathbf{n} and \mathbf{b} are constant, \mathbf{c} , and therefore \mathbf{X} , is in one plane. More precisely formulated: the normal vector of the plane of \mathbf{X} (the so-called osculating plane of \mathbf{X}) is

$$\mathbf{t} \times \mathbf{c} = \mathbf{n} \times \mathbf{b}$$

or the unit binormal vector of \mathbf{X} . Since \mathbf{n} and \mathbf{b} are constant, the torsion of \mathbf{X}

$$\frac{d}{ds}(\mathbf{t} \times \mathbf{c}) = 0$$

is zero, and \mathbf{X} is a plane curve. Furthermore, since the curvature

$$|\kappa| = \left| \frac{\alpha k_1}{\omega} \right|$$

is constant, the curve is a circle. The radius (in \mathbf{x} coordinates) is $R = |\omega/\alpha k_1 \varepsilon|$, and depends on the initial condition k_1 . The center of the circle is found at $\mathbf{x} = \mathbf{x}(0) + R\mathbf{c}$. See [127].

8.7 Refraction in shear flow

The propagation of sound waves in the atmosphere is greatly affected by wind. For example, the communication between two people, one downstream and one upstream, is not symmetric. The one upstream is easier to understand for the one downstream than the other way around. This is *not* because the wind “carries the waves faster”, but it is due to refraction by the wind gradient (the atmospheric boundary layer). This is seen as follows ([125]).

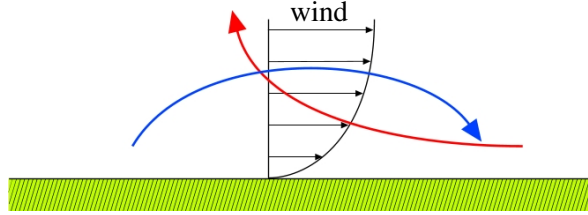


Figure 8.7 Refraction of sound rays in shear flow.

Consider the acoustic wave equations (2.51a-2.51d) for sound in an arbitrary mean flow. We assume the sound field to be time harmonic with a frequency high enough to adopt a ray approximation. The small parameter is now again $\varepsilon \sim c_0/\omega L$, with L a typical length scale for variations in the mean flow velocity \mathbf{v}_0 . Similar to the foregoing chapter we introduce the compressed variable $\mathbf{X} = \varepsilon \mathbf{x}$ and the ray approximations

$$p, \rho, \mathbf{v}, s = P(\mathbf{X}; \varepsilon), R(\mathbf{X}; \varepsilon), \mathbf{V}(\mathbf{X}; \varepsilon), S(\mathbf{X}; \varepsilon) \times e^{i\omega t - i\tau(\mathbf{X})/\varepsilon}$$

which are substituted in (2.51a-2.51d), with $\overline{\nabla} \tau = \mathbf{k}$, to obtain to leading order

$$\begin{aligned} \rho_0 \mathbf{V}(\omega - \mathbf{v}_0 \cdot \mathbf{k}) &= P \mathbf{k}, & R(\omega - \mathbf{v}_0 \cdot \mathbf{k}) &= \rho_0 \mathbf{V} \cdot \mathbf{k}, \\ S(\omega - \mathbf{v}_0 \cdot \mathbf{k}) &= 0, & P(\omega - \mathbf{v}_0 \cdot \mathbf{k}) &= c_0^2 R(\omega - \mathbf{v}_0 \cdot \mathbf{k}). \end{aligned}$$

This yields $S = 0$, $P = c_0^2 R$ and an eikonal equation

$$c_0^2 |\mathbf{k}|^2 = (\omega - \mathbf{v}_0 \cdot \mathbf{k})^2. \quad (8.80)$$

This equation is similar to (8.67). By rewriting eq. (8.80) as $\frac{1}{2} \varepsilon c_0^2 |\mathbf{k}|^2 / (\omega - \mathbf{v}_0 \cdot \mathbf{k}) - \frac{1}{2} \varepsilon (\omega - \mathbf{v}_0 \cdot \mathbf{k}) = 0$ and using theorem (8.1) (p.238), the characteristic variable is just the time t , and we have

$$\tau(\mathbf{X}) = \varepsilon \omega t$$

along the ray $\mathbf{X} = \mathbf{X}(t)$, given by⁵

$$\frac{d\mathbf{X}}{dt} = \varepsilon \left(c_0 \frac{\mathbf{k}}{|\mathbf{k}|} + \mathbf{v}_0 \right), \quad (8.81a)$$

$$\frac{d\mathbf{k}}{dt} = -\varepsilon (|\mathbf{k}| \overline{\nabla} c_0 + \overline{\nabla} \mathbf{v}_0 \cdot \mathbf{k}). \quad (8.81b)$$

⁵ $(\nabla \mathbf{v} \cdot \mathbf{k})_i = \sum_j \frac{\partial v_j}{\partial x_i} k_j$.

A popular, but unnecessary approximation is to write the above equations (8.81) in the same form as (8.70), by introducing an “effective sound speed” c_{eff} as follows.

$$\frac{d\mathbf{X}}{dt} \simeq \varepsilon c_{eff} \frac{\mathbf{k}}{|\mathbf{k}|}, \quad \frac{d\mathbf{k}}{dt} \simeq -\varepsilon |\mathbf{k}| \bar{\nabla} c_{eff}, \quad c_{eff} = c_0 + \frac{\mathbf{k}}{|\mathbf{k}|} \cdot \mathbf{v}_0.$$

This approximation is correct if $\mathbf{v}_0 - \frac{\mathbf{k}}{|\mathbf{k}|} (\frac{\mathbf{k}}{|\mathbf{k}|} \cdot \mathbf{v}_0)$ and $|\mathbf{k}| (\bar{\nabla} \frac{\mathbf{k}}{|\mathbf{k}|} \cdot \mathbf{v}_0)$ are negligible (for example when \mathbf{k} points mainly in the direction of \mathbf{v}_0 and varies little spatially). This depends, among other things, on the initial conditions and the trajectory traversed, and should always be checked afterwards. Moreover, the numerical solution is not simpler, so there seems to be no good reason to resort to this approximation.

For a simple parallel flow in x -direction, varying only in z , and a uniform sound speed

$$\mathbf{v}_0(\mathbf{X}) = (U_0(Z), 0, 0)$$

equation (8.81b) becomes

$$\frac{dk_x}{dt} = \frac{dk_y}{dt} = 0, \quad \frac{dk_z}{dt} = -\varepsilon U'_0(Z) k_x. \quad (8.82)$$

So, if we start with for example a vertical wave front $\mathbf{k} = k_x \mathbf{e}_x$, then a positive wind shear ($dU_0/dZ > 0$) will decrease the z -component k_z . In other words, the rays will bend towards the low wind-speed regions. Propagating with the wind, the waves bend down and remain near the ground; against the wind they bend up and disappear in the free space.

8.8 Matched asymptotic expansions

Introduction

Very often it happens that a simplifying limit applied to a more comprehensive model gives a correct approximation for the main part of the problem, but not everywhere: the limit is *non-uniform*. This non-uniformity may be in space, in time, or in any other variable. For the moment we think of non-uniformity in space. This non-uniformity may be a small region near a point, say $x = 0$, or it may be far away, *i.e.* for $x \rightarrow \infty$, but this is of course still a small region near the origin of $1/x$, so for the moment we think of a small region.

If this region of non-uniformity is crucial for the problem, for example because it contains a boundary condition, or a source, we may not be able to utilize the pursued limit and have to deal with the full problem (at least locally). This, however, is usually not true. The local nature of the non-uniformity itself gives often the possibility of another reduction. In such a case we call this a couple of limiting forms, “inner and outer problems”, and are evidence of the fact that we have apparently physically two connected but different problems as far as the dominating mechanism is concerned. (Depending

on the problem) we now have two simpler problems, serving as boundary conditions to each other via continuity or *matching* conditions.

Suppose we are interested in the solution of

$$\varepsilon \frac{dy}{dx} + y = \sin x, \quad y(0) = 1, \quad x \geq 0$$

for small positive ε , and suppose for the moment that we are not able to find an exact solution. It is natural to try to use the fact that ε is small. For example, from the structure of the problem, where both the source and the boundary value are $O(1)$, it is very likely to conclude that $y = O(1)$. If also the derivative y' is not very large (which is true for the most, but not, as we will see, everywhere), then a first approximation is clearly

$$y_0 \simeq \sin x.$$

We could substitute this into the original equation, and find a correction

$$y_1 \simeq \sin x - \varepsilon y_0' = \sin x - \varepsilon \cos x.$$

We can continue this indefinitely, and hope for a better and better approximation of the real solution. However, this can not be true: the approximate solution found this way is completely determined without integration constants, and we cannot apply anywhere the boundary condition $y(0) = 1$. In fact, the value at $x = 0$ that appears is something like $-\varepsilon \dots$, and quite far away from 1.

What's happening here? The cause of this all, is the fact that in the neighbourhood of $x = 0$, to be exact: for $x = O(\varepsilon)$, the solution changes its character over a very short distance (boundary layer), such that the derivative y' is now *not* $O(1)$, but very large: $O(\varepsilon^{-1})$. Since equation and solution are evidently closely related, also the equation becomes essentially different, and the above approximation of the equation is not valid anymore.

The remedy to this problem is that we have to stretch the variables such that the order of magnitude of the solution is reflected in the rescaling. In general this is far from obvious, and certainly part of the problem. In the present example it goes as follows. We write $x = \varepsilon \xi$ and $y(x) = Y(\xi)$, so that

$$\frac{dY}{d\xi} + Y = \sin(\varepsilon \xi), \quad Y(0) = 1,$$

Now we may construct another approximation, locally valid for $\xi = O(1)$

$$\frac{dY_0}{d\xi} + Y_0 \simeq 0, \quad Y_0(0) = 1,$$

with solution $Y_0(\xi) = e^{-\xi}$. We may continue to construct higher order corrections. Then we will see that for ξ large, respectively x small, this *inner* solution Y_0 smoothly changes into the above *outer* solution y_0 (matching), and together they form a uniform approximation.

General methodology

In the following we will describe some of the mathematical methodology in more detail ([163, 15, 57, 119, 45, 83, 115, 108]). We are interested in the limiting behaviour for $\varepsilon \downarrow 0$ of a sufficiently smooth function $\Phi(x; \varepsilon)$ with, say, $0 \leq x \leq 1$, $0 < \varepsilon \leq \varepsilon_0$. Φ has a **regular asymptotic approximation** on $[0, 1]$ if there exists a gauge-function $\mu_0(\varepsilon)$ and a shape-function $\Phi_0(x)$ such that

$$\lim_{\varepsilon \rightarrow 0} \left| \frac{\Phi(x; \varepsilon)}{\mu_0(\varepsilon)} - \Phi_0(x) \right| = 0 \quad \text{uniform in } x$$

or:

$$\Phi(x; \varepsilon) = \mu_0(\varepsilon)\Phi_0(x) + o(\mu_0) \quad (\varepsilon \rightarrow 0, \text{ uniform in } x).$$

A regular asymptotic series expansion, with gauge-functions $\mu_n(\varepsilon)$ and shape-functions $\Phi_n(x)$ is defined by induction, and we say

$$\Phi(x; \varepsilon) = \sum_{n=0}^N \mu_n(\varepsilon)\Phi_n(x) + o(\mu_N) \quad (\varepsilon \rightarrow 0, \text{ uniform in } x). \quad (8.83)$$

Note that neither gauge- nor shape-functions are unique. Furthermore, the series is only asymptotic in ε for *fixed* N . The limit $N \rightarrow \infty$ may be meaningless.

The functions that concern us here do *not* have a regular asymptotic expansion on the whole interval $[0, 1]$ but say, on any partial interval $[A, 1]$, $A > 0$, A fixed. We call this expansion the **outer-expansion**, valid in the “ $x = O(1)$ ”-outer region.

$$\Phi(x; \varepsilon) = \sum_{n=0}^N \mu_n(\varepsilon)\varphi_n(x) + o(\mu_N) \quad \varepsilon \rightarrow 0, x = O(1). \quad (8.84)$$

The functions do not have a regular expansion on the whole interval because the limit $\varepsilon \rightarrow 0$, $x \rightarrow 0$ is non-uniform and may not be exchanged. There is a gauge-function $\delta(\varepsilon)$, with $\lim_{\varepsilon \rightarrow 0} \delta(\varepsilon) = 0$, such that in the stretched coordinate

$$\xi = \frac{x}{\delta(\varepsilon)}$$

the function $\Psi(\xi; \varepsilon) = \Phi(\delta(\varepsilon)\xi; \varepsilon)$ has a non-trivial regular asymptotic series expansion on any partial interval $\xi \in [0, A]$, $A > 0$, A fixed. The adjective non-trivial is essential: the expansion must be “significant”, *i.e.* different from the outer-expansion in φ_n rewritten in ξ . For the *largest* $\delta(\varepsilon)$ with this property we call the expansion for Ψ the **inner-expansion** or boundary layer expansion, the region $\xi = O(1)$ or $x = O(\delta)$ being the boundary layer with thickness δ , and ξ the boundary layer variable. A boundary layer may be nested and may contain more boundary layers.

Suppose, $\Phi(x; \varepsilon)$ has an outer-expansion

$$\Phi(x; \varepsilon) = \sum_{k=0}^n \mu_k(\varepsilon) \varphi_k(x) + o(\mu_n) \quad (8.85)$$

and a boundary layer $x = O(\delta)$ with inner-expansion

$$\Psi(\xi; \varepsilon) = \sum_{k=0}^m \lambda_k(\varepsilon) \psi_k(\xi) + o(\lambda_m) \quad (8.86)$$

and suppose that both expansions are complementary, *i.e.* there is no other boundary layer in between $x = O(1)$ and $x = O(\delta)$, then the “overlap-hypothesis” says that both expansions represent the same function in an intermediate region of overlap. This overlap region may be described by a stretched variable $x = \eta(\varepsilon)\sigma$, asymptotically in between $O(1)$ and $O(\delta)$, so: $\delta \ll \eta \ll 1$. In the overlap region both expansions *match*, which means that asymptotically both expansions are equivalent and reduce to the same expressions. A widely used and relatively simple procedure is Van Dyke’s matchings rule [245]: the outer-expansion, rewritten in the inner-variable, has a regular series expansion, which is *equal* to the regular asymptotic expansion of the inner-expansion, rewritten in the outer-variable. Suppose that

$$\sum_{k=0}^n \mu_k(\varepsilon) \varphi_k(\delta\xi) = \sum_{k=0}^m \lambda_k(\varepsilon) \eta_k(\xi) + o(\lambda_m) \quad (8.87a)$$

$$\sum_{k=0}^m \lambda_k(\varepsilon) \psi_k(x/\delta) = \sum_{k=0}^n \mu_k(\varepsilon) \theta_k(x) + o(\mu_n) \quad (8.87b)$$

then the expansion of η_k back to x

$$\sum_{k=0}^n \lambda_k(\varepsilon) \eta_k(x/\delta) = \sum_{k=0}^n \mu_k(\varepsilon) \zeta_k(x) + o(\mu_n)$$

is such that $\zeta_k = \theta_k$ for $k = 0, \dots, n$.

The idea of matching is very important because it allows one to move smoothly from one regime into the other. The method of constructing local, but matching, expansions is therefore called “Matched Asymptotic Expansions” (MAE).

The most important application of this concept of inner- and outer-expansions is that approximate solutions of certain differential equations can be constructed for which the limit under a small parameter is apparently non-uniform. Typical examples in acoustics are small Helmholtz number problems where long waves are scattered by small objects or otherwise connected to a small geometrical size.

The main lines of argument for constructing a MAE solution to a differential equation + boundary conditions are as follows. Suppose Φ is given by the equation

$$D(\Phi', \Phi, x; \varepsilon) = 0 \quad + \text{ boundary conditions,} \tag{8.88}$$

where $\Phi' = d\Phi/dx$. Then we try to construct an outer solution by looking for “non-trivial degenerations” of D under $\varepsilon \rightarrow 0$, that is, find $\mu_0(\varepsilon)$ and $\nu_0(\varepsilon)$ such that

$$\lim_{\varepsilon \rightarrow 0} \nu_0^{-1}(\varepsilon) D(\mu_0 \varphi_0', \mu_0 \varphi_0, x; \varepsilon) = D_0(\varphi_0', \varphi_0, x) = 0 \tag{8.89}$$

has a non-trivial solution φ_0 . A series $\varphi = \mu_0 \varphi_0 + \mu_1 \varphi_1 + \dots$ is constructed by repeating the process for $D - \nu_0^{-1} D_0$, etc.

Suppose, the approximation is non-uniform (for example, not all boundary conditions can be satisfied), then we start looking for an inner-expansion if we have reasons to believe that the non-uniformity is of boundary-layer type. Presence, location and size of the boundary layer(s) are now found by the “correspondence principle”, that is the (heuristic) idea that if Φ behaves somehow differently in the boundary layer, the defining equation must also be essentially different. Therefore, we search for “significant degenerations” or “distinguished limits” of D . These are degenerations of D under $\varepsilon \rightarrow 0$, with scaled x and Φ , that contain the most information, and without being contained in other, richer, degenerations.

The next step is then to select from these distinguished limits the one(s) allowing a solution that matches with the outer solution and satisfies any applicable boundary condition.

Symbolically:

find

$$x_0, \delta(\varepsilon), \lambda(\varepsilon), \kappa(\varepsilon)$$

with

$$x = x_0 + \delta \xi, \quad \Phi(x; \varepsilon) = \lambda(\varepsilon) \Psi(\xi; \varepsilon)$$

such that

$$B_0(\psi_0', \psi_0, \xi) = \lim_{\varepsilon \rightarrow 0} \kappa^{-1} D(\delta^{-1} \lambda \Psi', \lambda \Psi, x_0 + \delta \xi; \varepsilon)$$

has the “richest” structure, and there exists a solution of

$$B_0(\psi_0', \psi_0, \xi) = 0$$

satisfying boundary and matching conditions. Again, an asymptotic expansion may be constructed inductively, by repeating the argument. It is of practical importance to note that the order estimate λ of Φ in the boundary layer is often determined a posteriori by boundary or matching conditions.

Simple example

A simple example to illustrate some of the main arguments is

$$D(\varphi', \varphi, x; \varepsilon) = \varepsilon \frac{d^2\varphi}{dx^2} + \frac{d\varphi}{dx} - 2x = 0, \quad \varphi(0) = \varphi(1) = 2. \quad (8.90)$$

The leading order outer-equation is evidently (with $\mu_0 = \nu_0 = 1$)

$$D_0 = \frac{d\varphi_0}{dx} - 2x = 0$$

with solution $\varphi_0 = x^2 + A$. The integration constant A can be determined by the boundary condition $\varphi_0(0) = 2$ at $x = 0$ or $\varphi_0(1) = 2$ at $x = 1$, but not both, so we expect a boundary layer at either end. By trial and error we find that no solution can be constructed if we assume a boundary layer at $x = 1$, so, inferring a boundary layer at $x = 0$, we have to use the boundary condition at $x = 1$ and find

$$\varphi_0 = x^2 + 1$$

The structure of the equation suggests a correction of $O(\varepsilon)$, so we try the expansion

$$\varphi = \varphi_0 + \varepsilon\varphi_1 + \varepsilon^2\varphi_2 + \dots$$

This results for φ_1 into the equation

$$\frac{d\varphi_1}{dx} + \frac{d^2\varphi_0}{dx^2} = 0, \quad \text{with } \varphi_1(1) = 0 \quad (\text{the } O(\varepsilon)\text{-term of the boundary condition),}$$

which has the solution

$$\varphi_1 = 2 - 2x.$$

Higher orders are straightforward:

$$\frac{d\varphi_n}{dx} = 0, \quad \text{with } \varphi_n(1) = 0$$

leading to solutions $\varphi_n \equiv 0$, and we find for the outer expansion

$$\varphi = x^2 + 1 + 2\varepsilon(1 - x) + O(\varepsilon^N). \quad (8.91)$$

We continue with the inner expansion, and find with $x_0 = 0$, $\varphi = \lambda\psi$, $x = \delta\xi$

$$\frac{\varepsilon\lambda}{\delta^2} \frac{d^2\psi}{d\xi^2} + \frac{\lambda}{\delta} \frac{d\psi}{d\xi} - 2\delta\xi = 0.$$

Both from the matching ($\varphi_{outer} \rightarrow 1$ for $x \downarrow 0$) and from the boundary condition ($\varphi(0) = 2$) we have to conclude that $\varphi_{inner} = O(1)$ and so $\lambda = 1$. Furthermore, the boundary layer has only a reason for existence if it comprises new effects, not described by the outer solution. From the correspondence principle we expect that new effects are only included if $(d^2\psi/d\xi^2)$ is included. So $\varepsilon\delta^{-2}$ must be at least as large as δ^{-1} , the largest of δ^{-1} and δ . From the principle that we look for the equation with the richest structure, it must be exactly as large, implying a boundary layer thickness $\delta = \varepsilon$. Thus we have $\kappa = \varepsilon^{-1}$, and the inner equation

$$\frac{d^2\psi}{d\xi^2} + \frac{d\psi}{d\xi} - 2\varepsilon^2\xi = 0.$$

From this equation it would *seem* that we have a series expansion without the $O(\varepsilon)$ -term, since the equation for this order would be the same as for the leading order. However, from matching with the outer solution:

$$\varphi_{outer} \rightarrow 1 + 2\varepsilon + \varepsilon^2(\xi^2 - 2\xi) + \dots \quad (x = \varepsilon\xi, \xi = O(1))$$

we see that an additional $O(\varepsilon)$ -term is to be included. So we substitute the series expansion:

$$\psi = \psi_0 + \varepsilon\psi_1 + \varepsilon^2\psi_2 + \dots \tag{8.92}$$

It is a simple matter to find

$$\begin{aligned} \frac{d^2\psi_0}{d\xi^2} + \frac{d\psi_0}{d\xi} &= 0, \quad \psi_0(0) = 2 \quad \rightarrow \quad \psi_0 = 2 + A_0(e^{-\xi} - 1) \\ \frac{d^2\psi_1}{d\xi^2} + \frac{d\psi_1}{d\xi} &= 0, \quad \psi_1(0) = 0 \quad \rightarrow \quad \psi_1 = A_1(e^{-\xi} - 1) \\ \frac{d^2\psi_2}{d\xi^2} + \frac{d\psi_2}{d\xi} &= 2\xi, \quad \psi_2(0) = 0 \quad \rightarrow \quad \psi_2 = \xi^2 - 2\xi + A_2(e^{-\xi} - 1) \end{aligned}$$

where constants A_0, A_1, A_2, \dots are to be determined from the matching condition that outer expansion (8.91) for $x \rightarrow 0$:

$$1 + x^2 + 2\varepsilon - 2\varepsilon x + \dots$$

must be functionally equal to inner expansion (8.92) for $\xi \rightarrow \infty$:

$$2 - A_0 - \varepsilon A_1 + x^2 - 2\varepsilon x - \varepsilon^2 A_2 + \dots$$

A full matching is obtained if we choose: $A_0 = 1, A_1 = -2, A_2 = 0$.

It is important to note that a matching is possible at all! Only a part of the terms can be matched by selection of the undetermined constants. For example, the coefficients of the x and x^2 terms are

already equal, without free constants. This is an important consistency check on the found solution, at least as long as no real proof is available. If no matching appears to be possible, almost certainly one of the assumptions made with the construction of the solution have to be reconsidered. Particularly notorious are logarithmic singularities of the outer field, not uncommon in 2D acoustical radiation problems ([119]). Even for such a simple (looking) problem as that of a plane wave scattered by a static compact sphere a careful approach is necessary to get the right results ([41]). On the other hand, only in rather rare cases, probably related to exceptional physical phenomena, no matching couple of inner and outer solutions is possible at all.

Summarizing: matching of inner- and outer expansion plays an important rôle in the following ways:

- i) it provides information about the sequence of order (gauge) functions $\{\mu_k\}$ and $\{\lambda_k\}$ of the expansions;
- ii) it allows us to determine unknown constants of integration;
- iii) it provides a check on the consistency of the solution, giving us confidence in the correctness.

8.9 Duct junction

A very simple problem that can be solved with matched asymptotic expansions is the reflection and transmission of low-frequency sound waves through a junction of two ducts with different diameter. The problem will appear to be so simple that the apparatus of MAE could justifiably be considered as a bit of an overkill. However, the method is completely analogous in many other duct problems, allows any extension to higher orders, and is therefore a good illustration.

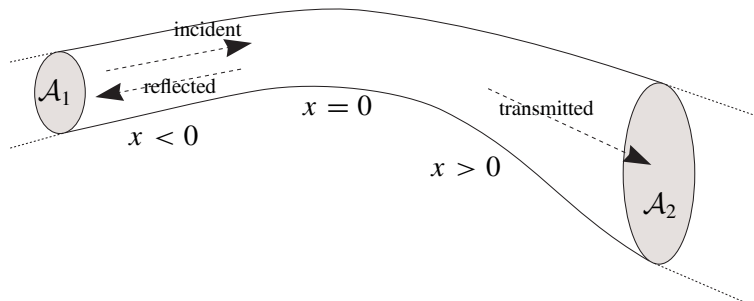


Figure 8.8 Duct junction.

Consider two straight hard walled ducts with cross section \mathcal{A}_1 (of size A_1) for $x < 0$, and cross section \mathcal{A}_2 (of size A_2) for $x > 0$, in some (here rather irrelevant) way joined together at $x = 0$ (figure 8.8). Apart from a region near this junction, the ducts have a constant cross section with a wall normal vector \mathbf{n}_{wall} independent of the axial position.

A sound wave with potential $\varphi_{in} = e^{i\omega t - ikx}$ is incident from $x = -\infty$. The wavelength is large compared to the duct diameter:

$$k\sqrt{A_1} = \varepsilon \ll 1. \quad (8.93)$$

To avoid uninteresting complications, we assume that in terms of ε the ratio A_1/A_2 is not close to 1 or 0: $A_1/A_2 = O(1)$, $A_1 \neq A_2$. Introduce dimensionless variables $X := kx$, $y := y/\sqrt{A_1}$, $z := z/\sqrt{A_1}$. Then for a uniform acoustic medium we have for a time harmonic scattered field φ

$$\varepsilon^2 \frac{\partial^2 \varphi}{\partial X^2} + \frac{\partial^2 \varphi}{\partial y^2} + \frac{\partial^2 \varphi}{\partial z^2} + \varepsilon^2 \varphi = 0 \quad (8.94)$$

$$\nabla \varphi \cdot \mathbf{n}_{wall} = 0 \quad \text{at the wall.}$$

In the outer region $\mathbf{x} = (X, y, z) = O(1)$ we expand in powers of ε (**not** ε^2 as will be clear later)

$$\varphi(\mathbf{x}; \varepsilon) = \varphi_0(\mathbf{x}) + \varepsilon \varphi_1(\mathbf{x}) + \varepsilon^2 \varphi_2(\mathbf{x}) + \dots \quad (8.95)$$

and substitute in (8.94) to find that all terms are function of the axial coordinate X only:

$$O(1) : \quad \left. \begin{array}{l} \frac{\partial^2 \varphi_0}{\partial y^2} + \frac{\partial^2 \varphi_0}{\partial z^2} = 0 \\ \nabla \varphi_0 \cdot \mathbf{n}_{wall} = 0 \end{array} \right\} \longrightarrow \varphi_0 = \varphi_0(X), \quad (8.96a)$$

$$O(\varepsilon) : \quad \left. \begin{array}{l} \frac{\partial^2 \varphi_1}{\partial y^2} + \frac{\partial^2 \varphi_1}{\partial z^2} = 0 \\ \nabla \varphi_1 \cdot \mathbf{n}_{wall} = 0 \end{array} \right\} \longrightarrow \varphi_1 = \varphi_1(X), \quad (8.96b)$$

$$O(\varepsilon^2) : \quad \left. \begin{array}{l} \frac{\partial^2 \varphi_2}{\partial y^2} + \frac{\partial^2 \varphi_2}{\partial z^2} + \frac{\partial^2 \varphi_0}{\partial X^2} + \varphi_0 = 0 \\ \nabla \varphi_2 \cdot \mathbf{n}_{wall} = 0 \end{array} \right\} \longrightarrow \begin{array}{l} \varphi_2 = \varphi_2(X), \\ \frac{\partial^2 \varphi_0}{\partial X^2} + \varphi_0 = 0. \end{array} \quad (8.96c)$$

This last result is obtained from integration over a cross section $\mathcal{A} \stackrel{\text{def}}{=} \{X = \text{constant}\}$ with size A , and applying Gauss' theorem

$$\int_{\mathcal{A}} \left(\frac{\partial^2 \varphi_2}{\partial y^2} + \frac{\partial^2 \varphi_2}{\partial z^2} + \frac{\partial^2 \varphi_0}{\partial X^2} + \varphi_0 \right) ds = \int_{\partial \mathcal{A}} (\nabla \varphi_2 \cdot \mathbf{n}_{wall}) d\ell + \left(\frac{\partial^2 \varphi_0}{\partial X^2} + \varphi_0 \right) A = 0.$$

Evidently, this process can be continued and we obtain

$$\varphi_0 = \begin{cases} e^{-iX} + R_0 e^{iX} & (X < 0) \\ T_0 e^{-iX} & (X > 0) \end{cases}$$

$$\varphi_n = \begin{cases} R_n e^{iX} & (X < 0) \\ T_n e^{-iX} & (X > 0) \end{cases}$$

or in other words

$$\varphi = \begin{cases} e^{-iX} + R e^{iX}, & R = R_0 + \varepsilon R_1 + \varepsilon^2 R_2 + \dots, & (X < 0) \\ T e^{-iX}, & T = T_0 + \varepsilon T_1 + \varepsilon^2 T_2 + \dots, & (X > 0) \end{cases} \quad (8.97)$$

The region $X = O(\varepsilon)$ appears to be a boundary layer, and we introduce

$$x = X/\varepsilon, \quad \Phi = \varphi(\varepsilon x, y, z; \varepsilon).$$

The equation for Φ becomes

$$\frac{\partial^2 \Phi}{\partial x^2} + \frac{\partial^2 \Phi}{\partial y^2} + \frac{\partial^2 \Phi}{\partial z^2} + \varepsilon^2 \Phi = 0 \quad (8.98)$$

$$\nabla \Phi \cdot \mathbf{n}_{wall} = 0 \quad \text{at the wall.}$$

but now with matching conditions for $x \rightarrow -\infty$ and $x \rightarrow +\infty$, *i.e.* $X \uparrow 0$ and $X \downarrow 0$ of the outer solution (8.97):

$$x \rightarrow -\infty : \Phi \simeq 1 + R_0 + \varepsilon(R_1 - ix + ixR_0) + \varepsilon^2(R_2 + ixR_1 - \frac{1}{2}x^2 - \frac{1}{2}x^2R_0) + \dots,$$

$$x \rightarrow +\infty : \Phi \simeq T_0 + \varepsilon(T_1 - ixT_0) + \varepsilon^2(T_2 - ixT_1 - \frac{1}{2}x^2T_0) + \dots.$$

Guided by the behaviour under matching we assume the expansion

$$\Phi = \Phi_0 + \varepsilon \Phi_1 + \varepsilon^2 \Phi_2 \dots,$$

then

$$\begin{aligned} O(1) : \quad \nabla^2 \Phi_0 &= 0, & \Phi_0 &= O(1) & (x \rightarrow \pm\infty) \\ O(\varepsilon) : \quad \nabla^2 \Phi_1 &= 0, & \Phi_1 &= O(x) & (x \rightarrow \pm\infty) \\ O(\varepsilon^2) : \quad \nabla^2 \Phi_2 &= -\Phi_0, & \Phi_2 &= O(x^2) & (x \rightarrow \pm\infty) \end{aligned} \quad (8.99)$$

In general, the solutions Φ_n are difficult to obtain. However, some progress can be made on global results of reflection and transmission by application of Gauss' Theorem. Consider a *large* volume \mathcal{V} , reaching from $x = x_1$ large negative, to $x = x_2$ large positive (large in variable x but small in variable

X , so that we can use the matching conditions). At $x = x_1$ the surface of \mathcal{V} consists of a cross section \mathcal{A}_1 , and at $x = x_2$ a cross section \mathcal{A}_2 . The size of \mathcal{V} is denoted by V , the sizes of \mathcal{A}_1 and \mathcal{A}_2 by A_1 and A_2 . Noting that $\nabla\Phi_0 \cdot \mathbf{n} = 0$ along the surface of \mathcal{V} , we obtain with Gauss' Theorem

$$\int_{\mathcal{V}} \Phi_0 \nabla^2 \Phi_0 \, d\mathbf{x} = \int_{\mathcal{V}} \nabla \cdot (\Phi_0 \nabla \Phi_0) - |\nabla \Phi_0|^2 \, d\mathbf{x} = - \int_{\mathcal{V}} |\nabla \Phi_0|^2 \, d\mathbf{x} = 0.$$

Since $|\nabla\Phi_0|^2$ is non-negative, the integral can only vanish if $\nabla\Phi_0 = 0$ and therefore $\Phi_0 = \text{a constant}$. From the matching condition it follows that $\Phi_0 = 1 + R_0 = T_0$. A second condition to determine R_0 and T_0 can be found by integrating

$$\int_{\mathcal{V}} \nabla^2 \Phi_1 \, d\mathbf{x} = - \int_{\mathcal{A}_1} \frac{\partial \Phi_1}{\partial x} \, ds + \int_{\mathcal{A}_2} \frac{\partial \Phi_1}{\partial x} \, ds = -(-i + iR_0)A_1 - iT_0A_2 = 0 \quad (8.100)$$

so that $(1 - R_0)A_1 = T_0A_2$, which yields

$$R_0 = \frac{A_1 - A_2}{A_1 + A_2}, \quad T_0 = \frac{2A_1}{A_1 + A_2}. \quad (8.101)$$

For the next order we need to know solution Φ_1 in some form. This depends on the actual shape of the duct. Inspired by [153], we consider the following example in 2D by using conformal mapping.

Example in 2D

We have a 2D duct of height b in $x < 0$ and height $a > b$ in $x > 0$. The top wall is everywhere at $y = a$. The bottom wall is at $y = a - b$ for $x < 0$ and $y = 0$ for $x > 0$. At $x = 0$ the duct height changes discontinuously. See figure 8.9.

We associate the duct with a region in the complex plane by $z = x + iy$. The inside of the duct is mapped to the upperhalf of the complex ζ -plane by the transformation⁶

$$z = \frac{a}{\pi} \log\left(\frac{1 + \tau}{1 - \tau}\right) - \frac{b}{\pi} \log\left(\frac{c + \tau}{c - \tau}\right), \quad \tau = \sqrt{\frac{\zeta - c^2}{\zeta - 1}}, \quad c = \frac{a}{b} > 1. \quad (8.102)$$

Just like above, we have for the 0-th order solution $\Phi_0 = \text{a constant}$, while

$$R_0 = -\frac{a - b}{a + b}, \quad T_0 = \frac{2b}{a + b}. \quad (8.103)$$

⁶The logarithms and square roots are defined by their principal value, meaning that the branch cuts are along the negative real axis, while $\log(1) = 0$ and $\sqrt{1} = 1$.

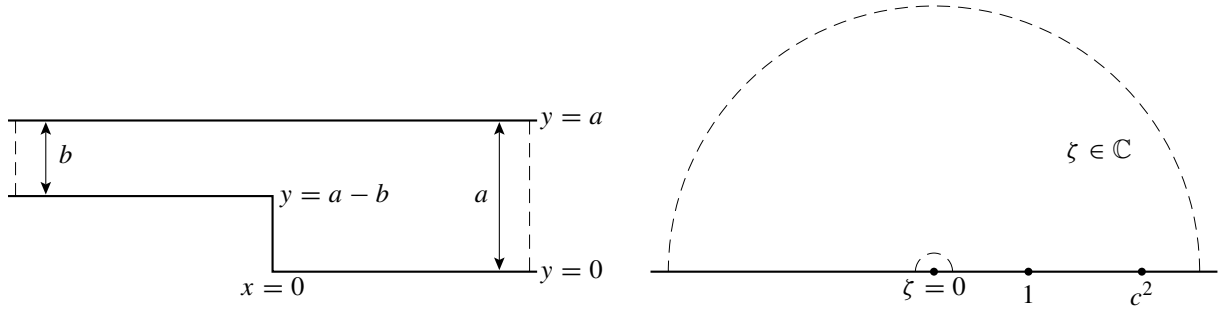


Figure 8.9 A duct of height b for $x < 0$ and height a for $x > 0$. Boundaries mapped to the real axis of the complex ζ -plane.

From the matchings conditions we conclude⁷ that the 1-st order solution Φ_1 corresponds to a flow from $x \sim -\infty$ to $x \sim \infty$ of flux $(1 - R_0)b = T_0a$. So we can write Φ_1 in transformed variable ζ as the real part of the complex potential of a simple source

$$F(\zeta) = Q \log(\zeta), \quad Q = (1 - R_0) \frac{b}{\pi} = T_0 \frac{a}{\pi}.$$

Noting that $\zeta \rightarrow 0$ corresponds with $x \rightarrow -\infty$ and $\zeta \rightarrow \infty$ with $x \rightarrow \infty$, the only thing we have to do to realise a matching, is to find the behaviour of F for $\zeta \rightarrow 0$ and $\zeta \rightarrow \infty$ in terms of z . We have

$$\begin{aligned} z &= i(a - b) + \frac{b}{\pi} \left[\frac{a}{b} \log\left(\frac{a+b}{a-b}\right) + \log\left(\frac{a^2 - b^2}{4a^2}\right) \right] + \frac{b}{\pi} \log \zeta + \dots \quad (\zeta \rightarrow 0) \\ z &= -\frac{a}{\pi} \left[\frac{b}{a} \log\left(\frac{a+b}{a-b}\right) + \log\left(\frac{a^2 - b^2}{4b^2}\right) \right] + \frac{a}{\pi} \log \zeta + \dots \quad (\zeta \rightarrow \infty) \end{aligned}$$

Recognising the term $\log \zeta \sim F$ in the expansions, we have thus for the real parts, when $x \rightarrow -\infty$,

$$\Phi_1 = \text{Re}(F) \simeq (1 - R_0)x - (1 - R_0) \frac{b}{\pi} \left[\frac{a}{b} \log\left(\frac{a+b}{a-b}\right) + \log\left(\frac{a^2 - b^2}{4a^2}\right) \right] \simeq (1 - R_0)x + iR_1,$$

and when $x \rightarrow \infty$

$$\Phi_1 = \text{Re}(F) \simeq T_0x + T_0 \frac{a}{\pi} \left[\frac{b}{a} \log\left(\frac{a+b}{a-b}\right) + \log\left(\frac{a^2 - b^2}{4b^2}\right) \right] \simeq T_0x + iT_1.$$

By identifying the corresponding terms in the matching conditions we have then

$$\begin{aligned} R_1 &= \frac{2iab}{\pi(a+b)} \left[\frac{a}{b} \log\left(\frac{a+b}{a-b}\right) + \log\left(\frac{a^2 - b^2}{4a^2}\right) \right], \\ T_1 &= \frac{-2iab}{\pi(a+b)} \left[\frac{b}{a} \log\left(\frac{a+b}{a-b}\right) + \log\left(\frac{a^2 - b^2}{4b^2}\right) \right]. \end{aligned} \tag{8.104}$$

Note that this result is the same for the configuration that results by adding to the duct its mirror in the line $y = a$, and using the above $\Phi_1(x, y)$ in $y < a$ and $\Phi_1(x, y) = \Phi_1(x, 2a - y)$ in $y > a$.

⁷We ignore the factor $-i$. The complex unit i comes from $e^{i\omega t}$. It has nothing to do with the complex unit in the ζ -plane.

8.10 Co-rotating line-vortices

In an inviscid infinite 2D medium a stationary line vortex produces a time-independent velocity and pressure field. Two of such vortices, however, move in each others velocity field. Two equally strong and equally orientated vortices rotate around a common centre, and produce a fluctuating velocity and pressure field (for a fixed observer).

If the velocities are relatively low, this field will be practically incompressible. A small fraction of the energy, however, will radiate away as sound [154, 40].

For a physically consistent problem (it is not possible in an inviscid medium to change the total amount of circulation) we position at the common centre a third vortex with a double but opposite vortex strength. By symmetry this vortex will not move but of course will contribute to the rotating motion of the other two.

Inviscid compressible irrotational flow depending on $x = r \cos \theta$, $y = r \sin \theta$ and t is described by

$$\frac{\partial \rho}{\partial t} + \nabla \varphi \cdot \nabla \rho + \rho \nabla^2 \varphi = 0, \quad (8.105a)$$

$$\rho \nabla \left(\frac{\partial \varphi}{\partial t} + \frac{1}{2} |\nabla \varphi|^2 \right) + \nabla p = 0, \quad (8.105b)$$

$$\frac{p}{p_0} = \left(\frac{\rho}{\rho_0} \right)^\gamma, \quad c^2 = \frac{dp}{d\rho} = \frac{\gamma p}{\rho}, \quad (8.105c)$$

with density ρ , pressure p , velocity potential φ , sound speed c and gas constant γ . Introduce the auxiliary quantity (c.f. (1.32b))

$$Q = \frac{\partial \varphi}{\partial t} + \frac{1}{2} |\nabla \varphi|^2 \quad (8.106)$$

then

$$(\gamma - 1)Q + c^2 = c_0^2 \quad (\text{constant}) \quad (8.107)$$

where under the assumption that $\varphi \rightarrow 0$ for $r \rightarrow \infty$ the constant c_0 is the far field sound speed. Hence

$$\frac{\partial Q}{\partial t} + \frac{c^2}{\rho} \frac{\partial \rho}{\partial t} = 0, \quad \nabla Q + \frac{c^2}{\rho} \nabla \rho = 0$$

and so

$$\left(c_0^2 - (\gamma - 1)Q \right) \nabla^2 \varphi = \frac{\partial Q}{\partial t} + \nabla \varphi \cdot \nabla Q. \quad (8.108)$$

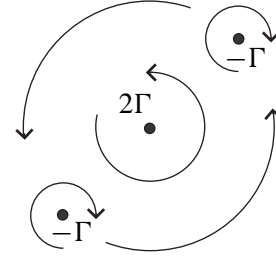


Figure 8.10 Three co-rotating vortices.

We will consider two vortices with vortex strength $-\Gamma$, positioned opposite to each other on the circle $r = a$, and a vortex of strength 2Γ at the origin $r = 0$. Their motion around each other will be incompressible as follows. Typical induced velocities are of the order of Γ/a , and we assume this to be small enough compared to the sound speed for locally incompressible flow:

$$\varepsilon = \frac{\Gamma}{ac_0} \ll 1. \quad (8.109)$$

Introduce dimensionless variables (where we keep for convenience the same notation):

$$t := t\Gamma/a^2, \quad x := x/a, \quad y := y/a, \quad \varphi := \varphi/\Gamma, \quad Q := Qa^2/\Gamma^2.$$

Equation (8.108) is then in dimensionless form

$$\left(1 - (\gamma - 1)\varepsilon^2 Q\right) \nabla^2 \varphi = \varepsilon^2 \left(\frac{\partial Q}{\partial t} + \nabla \varphi \cdot \nabla Q \right). \quad (8.110)$$

In the *inner region* $r = O(1)$, we have to leading order the Laplace equation for incompressible potential flow

$$\nabla^2 \varphi = 0 \quad (8.111)$$

with solution the sum⁸ of the contributions of the three co-rotating vortices

$$\varphi = \frac{1}{\pi} \arctan \frac{y}{x} - \frac{1}{2\pi} \arctan \frac{y - y_1(t)}{x - x_1(t)} - \frac{1}{2\pi} \arctan \frac{y - y_2(t)}{x - x_2(t)}. \quad (8.112)$$

The position vector $\mathbf{x}_1(t) = (x_1(t), y_1(t))$ (and similarly $\mathbf{x}_2(t)$) is determined by the observation that a vortex is just a property of the flow and therefore the velocity $\dot{\mathbf{x}}_1(t)$ must be equal to the induced velocity of the other vortices at $\mathbf{x} = \mathbf{x}_1$:

$$\frac{dx_1}{dt} = \frac{1}{2\pi} \frac{y_1 - y_2}{(x_1 - x_2)^2 + (y_1 - y_2)^2} - \frac{1}{\pi} \frac{y_1}{x_1^2 + y_1^2} \quad (8.113a)$$

$$\frac{dy_1}{dt} = -\frac{1}{2\pi} \frac{x_1 - x_2}{(x_1 - x_2)^2 + (y_1 - y_2)^2} + \frac{1}{\pi} \frac{x_1}{x_1^2 + y_1^2}. \quad (8.113b)$$

From symmetry $\mathbf{x}_2 = -\mathbf{x}_1$, and the solution along the circle $|\mathbf{x}| = 1$ is given by

$$x_1 = \cos\left(\frac{1}{2}\omega t\right), \quad y_1 = \sin\left(\frac{1}{2}\omega t\right), \quad \text{where } \omega = 3/2\pi, \quad (8.114)$$

and apart from an irrelevant phase shift. Solution (8.112) can now be written as

$$\varphi = \frac{1}{\pi} \theta - \frac{1}{2\pi} \arctan \left(\frac{r^2 \sin 2\theta - \sin \omega t}{r^2 \cos 2\theta - \cos \omega t} \right). \quad (8.115)$$

⁸Equation (8.111) is linear.

For matching with the outer field we need the behaviour of inner solution φ for $r \rightarrow \infty$:

$$\varphi \simeq \frac{\sin(\omega t - 2\theta)}{2\pi r^2} + \dots \quad (r \rightarrow \infty). \quad (8.116)$$

For the *outer region* we first observe that the time scale is dictated by the source, so this is the same everywhere. Then, if we scale $\tilde{r} = \delta(\varepsilon)r$, it follows from matching with equation (8.116) that $\varphi = O(\delta^2)$. A significant degeneration of (8.110) is obtained if $\delta = \varepsilon$, when $\nabla^2\varphi$ and $\partial^2\varphi/\partial t^2$ balance each other. Together we have:

$$r = \tilde{r}/\varepsilon, \quad \varphi = \varepsilon^2\tilde{\varphi} \quad (8.117a)$$

$$Q = \varepsilon^2\left(\frac{\partial\tilde{\varphi}}{\partial t} + \frac{1}{2}\varepsilon^4|\tilde{\nabla}\tilde{\varphi}|^2\right) = \varepsilon^2\tilde{Q} \quad (8.117b)$$

which gives

$$\left(1 - (\gamma - 1)\varepsilon^4\tilde{Q}\right)\tilde{\nabla}^2\tilde{\varphi} = \frac{\partial\tilde{Q}}{\partial t} + \varepsilon^4\tilde{\nabla}\tilde{\varphi} \cdot \tilde{\nabla}\tilde{Q} \quad (8.118)$$

To leading order, $\tilde{\varphi}$ satisfies the wave equation

$$\tilde{\nabla}^2\tilde{\varphi} - \frac{\partial^2\tilde{\varphi}}{\partial t^2} = 0 \quad (8.119)$$

with outward radiation conditions for $\tilde{r} \rightarrow \infty$ (no source at infinity), and a condition of matching with (8.116) for $\tilde{r} \downarrow 0$. This matching condition says that, on the scale of the outer solution, the inner solution behaves like a harmonic point source $\propto e^{2i\omega t}$ at $\tilde{r} = 0$, with properties to be determined.

Relevant point source solutions are

$$\tilde{\varphi} = \text{Re}\left\{AH_n^{(2)}(\omega\tilde{r})e^{i\omega t - in\theta}\right\} \quad (8.120)$$

with $H_n^{(2)}$ a Hankel function (Appendix D), and order n and amplitude A to be determined. For matching it is necessary that the behaviour for $\tilde{r} \downarrow 0$ coincides with (8.116):

$$\varepsilon^2 \text{Re}\left\{-A\frac{(n-1)!}{i\pi}\left(\frac{2}{\omega\tilde{r}}\right)^n e^{i\omega t - in\theta}\right\} \sim \frac{\sin(\omega t - 2\theta)}{2\pi r^2} \quad (8.121)$$

(if $n \geq 1$). Clearly, there is no other possibility than $n = 2$, and hence $A = -\frac{1}{8}\omega^2$. Note that this order 2 indicates an acoustic field equivalent to that of a rotating lateral quadrupole. In dimensional variables the acoustic far field is given by

$$\varphi \simeq \frac{\Gamma M^{3/2}}{2}\left(\frac{a}{\pi r}\right)^{1/2} \cos\left(\Omega(t - r/c_0) - 2\theta + \frac{1}{4}\pi\right). \quad (8.122)$$

where frequency Ω and vortex Mach number M are given by

$$\Omega = \frac{\omega\Gamma}{a^2} = \frac{3\Gamma}{2\pi a^2}, \quad M = \frac{\Omega a}{2c_0}.$$

We see that for fixed θ the waves radiate outwards ($r - c_0 t$ constant), for fixed r the waves rotate with positive orientation ($\theta - \frac{1}{2}\Omega t$ constant), and at a fixed time t the wave crests are localized along spirals ($r + 2\theta c_0/\Omega$ constant). This may be compared with a rotating lawn sprinkler.

The outward radiating time-averaged energy flux or intensity is found from equation (8.122) to be

$$I = \frac{8}{9}\pi\rho_0 c_0^3 M^7 \frac{a}{r}. \quad (8.123)$$

This functional dependence on U^7 in 2D is to be compared with the U^8 -law of Lighthill for turbulence noise (equation 6.69), and forms a confirmation of the estimates for turbulence in the Lighthill analogy.

We have now obtained the solution to leading order. Higher orders may be constructed in a similar fashion, but we will limit ourselves to the present one. For higher orders more and more equivalent far fields of higher order multipoles will appear.

We finally note that from a simple calculation the outward radiated 2D power is equal to $\frac{16}{9}\pi^2\rho_0 c_0^3 a M^7$. Strictly speaking, this amount of energy per time leaks away from the total energy of the system of vortices (which scales on $\rho_0\Gamma^2$), and we could try to include a small decay in time of the vortex strength Γ . This is, however, impossible in the present model.

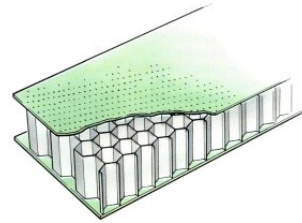
Exercises

- Determine (using Webster's horn equation) the right-running wave $p(x)$, with $p(0) = \hat{p}_0$, in an exponential horn with radius $a e^{mx}$.
- In a hot desert, a man is giving a speech to an audience. The mouth of the man and the ears of the audience are at a height of $y = h = 1.5$ m above the flat ground, given by $y = 0$. The ground is so hot compared to the air that a vertically stratified uniform temperature profile is established in the air. We assume for the region relevant here that this profile corresponds to a sound speed which is linear in y . The sound speed profile is given by: $c_0(y) = q(1 - \varepsilon y)$, where $q = 360$ m/s and $\varepsilon = \frac{1}{250}$ m⁻¹. Since the sound speed gradient is negative the sound waves are refracted upwards and will disappear into the air. Under the assumptions that the man speaks loud enough, that a typical wave length is small enough for ray acoustics to be applicable, and that we only consider rays that skim along the ground, what is the largest distance over which the man can be heard?
- Determine the suitable modelling assumptions and derive from the wave equations (F.29) and (F.34) the following generalized Webster equations

$$A^{-1} \frac{d}{dx} \left(\iint_{\mathcal{A}} c^2 d\sigma \frac{dp}{dx} \right) + \omega^2 p = 0, \quad (8.124)$$

$$(\rho_0 A)^{-1} \frac{d}{dx} \left(A \rho_0 \frac{d\phi}{dx} \right) - \left(i\omega + U \frac{d}{dx} \right) \left[c^{-2} \left(i\omega + U \frac{d}{dx} \right) \phi \right] = 0. \quad (8.125)$$

- d) A large array of acoustically compact equal Helmholtz resonators (all openings in upward direction) is covered by a top plate of negligible thickness. The plate is solid except for holes positioned exactly at the openings of the resonator, such that the plate has a uniform porosity $\sigma \in (0, 1)$ (= the open fraction). A time harmonic acoustic field $(p, \mathbf{v}) e^{i\omega t}$ is scattered by plate and Helmholtz resonators. Find an expression for the impedance of the plate surface. You may assume the model given by equation (5.41), without the nonlinear terms to start with. **Hint:** you may assume that the neck velocity $u'_n = -\sigma^{-1}(\mathbf{v} \cdot \mathbf{n})$; use (8.35).



- e) Derive the results of section 8.4 for a 2D duct given by $|y| < h(\epsilon x)$.

9 Effects of flow and motion

Being a fluid mechanical phenomenon itself, an acoustic wave may be greatly affected by mean flow effects like convection, refraction in shear, coupling with vorticity, scattering by turbulence, and many others. We will briefly consider here some of these effects.

9.1 Uniform mean flow, plane waves and edge diffraction

Consider a uniform mean flow in x direction with small irrotational perturbations¹. We have then for potential ϕ , pressure p , density ρ and velocity \mathbf{v} the problem given by

$$\begin{aligned} \frac{\partial^2 \phi}{\partial x^2} + \frac{\partial^2 \phi}{\partial y^2} + \frac{\partial^2 \phi}{\partial z^2} - \frac{1}{c_0^2} \left(\frac{\partial}{\partial t} + U_0 \frac{\partial}{\partial x} \right)^2 \phi &= 0, \\ p = -\rho_0 \left(\frac{\partial}{\partial t} + U_0 \frac{\partial}{\partial x} \right) \phi, \quad p = c_0^2 \rho, \quad \mathbf{v} = \nabla \phi \end{aligned} \quad (9.1)$$

where U_0 , ρ_0 and c_0 denote the mean flow velocity, density and sound speed, respectively. We assume in the following that $|U_0| < c_0$. The equation for ϕ is known as the convected wave equation.

9.1.1 Lorentz or Prandtl-Glauert transformation

By the following transformation (in aerodynamic context named after Prandtl and Glauert, but form originally due to Lorentz)

$$X = \frac{x}{\beta}, \quad T = \beta t + \frac{M}{\beta c_0} x, \quad M = \frac{U_0}{c_0}, \quad \beta = \sqrt{1 - M^2}, \quad (9.2)$$

the convected wave equation may be associated to a stationary problem with solution $\phi(x, y, z, t) = \psi(X, y, z, T)$ satisfying

$$\frac{\partial^2 \psi}{\partial X^2} + \frac{\partial^2 \psi}{\partial y^2} + \frac{\partial^2 \psi}{\partial z^2} - \frac{1}{c_0^2} \frac{\partial^2 \psi}{\partial T^2} = 0, \quad p = -\frac{\rho_0}{\beta} \left(\frac{\partial}{\partial T} + U_0 \frac{\partial}{\partial X} \right) \psi. \quad (9.3)$$

¹The assumption of irrotationality may depend on the type of source (1.25b), presence of singularities like edges, *etc.*

For a time harmonic field $e^{i\omega t} \phi(x, y, z) = e^{i\Omega T} \Phi(X, y, z)$, and so² $\phi(x, y, z) = e^{iKMx} \Phi(X, y, z)$, where $\Omega = \omega/\beta$, $k = \omega/c_0$ and $K = \Omega/c_0 = k/\beta$, we have

$$\frac{\partial^2 \Phi}{\partial X^2} + \frac{\partial^2 \Phi}{\partial y^2} + \frac{\partial^2 \Phi}{\partial z^2} + K^2 \Phi = 0, \quad p = -\frac{\rho_0}{\beta} \left(i\Omega + U_0 \frac{\partial}{\partial X} \right) \Phi \quad (9.4)$$

The pressure may be obtained from Φ , but since p satisfies the convected wave equation too, we may also associate the pressure field directly by the same transformation with a corresponding stationary pressure field. The results are **not** equivalent, however, and especially when the field contains singularities some care is in order. The pressure obtained directly is *no more singular* than the pressure of the stationary problem, but the pressure obtained via the potential is *one order more singular* due to the convected derivative, and may be linked to vortex shedding and Kutta condition. See below.

9.1.2 Plane waves

A plane wave (in x, y -plane) may be given by

$$p_i = a \exp\left(-ik \frac{x \cos \theta_n + y \sin \theta_n}{1 + M \cos \theta_n}\right) = a \exp\left(-ikr \frac{\cos(\theta - \theta_n)}{1 + M \cos \theta_n}\right) \quad (9.5)$$

where θ_n is the direction of the normal to the phase plane and $x = r \cos \theta$, $y = r \sin \theta$. This is physically not the most natural form, however, because θ_n is due to the mean flow not the direction of propagation. By comparison with a point source field far away, or from the intensity vector (*c.f.* (F.41,F.42))

$$\begin{aligned} \langle \mathbf{I} \rangle &= \langle (\rho_0 \mathbf{v} + \rho \mathbf{v}_0)(p/\rho_0 + \mathbf{v}_0 \cdot \mathbf{v}) \rangle = \frac{1}{2} \rho_0 \omega [(\beta^2 \text{Im}(\phi \phi_x^*) + kM|\phi|^2) \mathbf{e}_x + \text{Im}(\phi \phi_y^*) \mathbf{e}_y] \\ &= \frac{\frac{1}{2} \rho_0 \omega k |\phi|^2}{1 + M \cos \theta_n} [(\cos \theta_n + M) \mathbf{e}_x + \sin \theta_n \mathbf{e}_y] \end{aligned}$$

we can learn that θ_s , the direction of propagation (the direction of any shadows, fig. 9.1), is given by

$$\cos \theta_s = \frac{M + \cos \theta_n}{\sqrt{1 + 2M \cos \theta_n + M^2}}, \quad \sin \theta_s = \frac{\sin \theta_n}{\sqrt{1 + 2M \cos \theta_n + M^2}}. \quad (9.6)$$

By introducing the transformed angle Θ_s

$$\cos \Theta_s = \frac{\cos \theta_s}{\sqrt{1 - M^2 \sin^2 \theta_s}} = \frac{M + \cos \theta_n}{1 + M \cos \theta_n}, \quad (9.7)$$

$$\sin \Theta_s = \frac{\beta \sin \theta_s}{\sqrt{1 - M^2 \sin^2 \theta_s}} = \frac{\beta \sin \theta_n}{1 + M \cos \theta_n} \quad (9.8)$$

and the transformed polar coordinates $X = R \cos \Theta$, $y = R \sin \Theta$, we obtain the plane wave

$$p_i = a \exp(iKMx - iKR \cos(\Theta - \Theta_s)). \quad (9.9)$$

²Note, that ψ and Φ are not the same!

9.1.3 Half-plane diffraction problem

By using the foregoing transformation, we obtain from the classical Sommerfeld solution for the half-plane diffraction problem (see Jones [100]) of a plane wave (9.9), incident on a solid half plane along $y = 0, x < 0$ (fig. 9.1), the following solution (see Rienstra [197]) in terms of *potential*

$$\phi(x, y) = \frac{ia\beta^2}{\omega(1 - M \cos \Theta_s)} \exp(iKMX - iKR)(F(\Gamma_s) + F(\bar{\Gamma}_s)) \tag{9.10}$$

where

$$F(z) = \frac{e^{i\pi/4}}{\sqrt{\pi}} e^{iz^2} \int_z^\infty e^{-it^2} dt \quad \text{and} \quad \Gamma_s, \bar{\Gamma}_s = (2KR)^{1/2} \sin \frac{1}{2}(\Theta \mp \Theta_s). \tag{9.11}$$

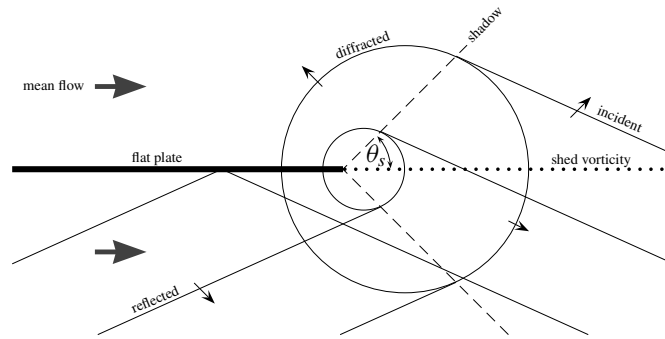


Figure 9.1 Sketch of scattered plane wave with mean flow

An interesting feature of this solution is the following. When we derive the corresponding pressure

$$p(x, y) = a \exp(iKMX - iKR)(F(\Gamma_s) + F(\bar{\Gamma}_s)) + a \frac{e^{-i\pi/4}}{\sqrt{\pi}} \frac{M \cos \frac{1}{2}\Theta_s}{1 - M \cos \Theta_s} \exp(iKMX - iKR) \sin \frac{1}{2}\Theta \left(\frac{2}{KR}\right)^{1/2}, \tag{9.12}$$

we see immediately that the first part is a solution by itself: it is a multiple of the solution of the potential. So the second part has to be a solution too. Furthermore, the first part is *regular* like ϕ , while this second part is *singular* at the scattering edge. As the second part decays for any $R \rightarrow \infty$, it does not describe the incident plane wave, and it may be dropped if we do not accept the singularity in p at the edge. So the found solution (9.12) is not unique by the existence of an eigensolution p_v

$$p_v(x, y) = \exp(iKMX - iKR) \frac{\sin \frac{1}{2}\Theta}{\sqrt{KR}}, \tag{9.13}$$

Without p_v , the solution is regular, otherwise it is singular. If we study p_v a bit deeper, it transpires that it has no continuous potential that decays to zero for large $|y|$. In fact, p_v corresponds to the field

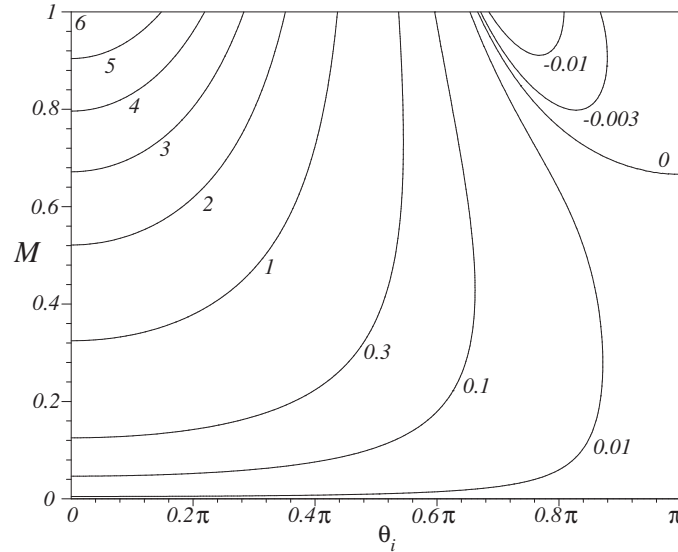


Figure 9.2 $(\rho_0\omega/|a|^2)\mathcal{P}$ as function of (M, θ_n) .

of vorticity (in the form of a vortex sheet) that is being shed from the edge. This may be more clear if we construct the corresponding potential ϕ_v for large x , to be compared with (3.66), which is

$$\phi_v \sim \text{sign}(y) \exp\left(-i\frac{\omega}{U_0}x - \frac{\omega}{U_0}|y|\right), \quad p_v \sim 0. \quad (9.14)$$

In conclusion: we obtain the singular solution by transforming the no-flow solution in potential form, and the regular solution from the no-flow solution in pressure form. Their difference is the field of the shed vortex sheet.

This shedding of vorticity costs acoustic energy, so on the one hand it is a sink of acoustic energy. On the other hand, the shed vortices moving near the solid plate produce also sound, and so the shedding of vorticity is also a source of sound (with the mean flow as the unlimited source of energy). The net sum of both can be negative or positive, depending on M and θ_n . Remarkably, the present model problem allows an exact relation (9.15) of the power absorbed by vortex shedding³. See figure 9.2.

$$\mathcal{P} = (|a|^2/\rho_0\omega)M \cos^2 \frac{1}{2}\theta_n (1 + M \cos \theta_n)(2 + 2M \cos \theta_n - M) \quad (9.15)$$

The assumption that just as much vorticity is shed that the pressure field is not singular anymore, is known as the unsteady Kutta condition. Physically, the amount of vortex shedding is controlled by

³This is *not* only the energy lost into the vortex sheet, but all *acoustic* energy lost by vortex shedding. For example, it includes the irrotational hydrodynamic energy (3.67) associated to the vortex sheet. The energy just lost into the vortex sheet would be $\mathcal{P} = (|a|^2/\rho_0\omega)M \cos^2 \frac{1}{2}\theta_n (1 + M \cos \theta_n)(1 + 2M \cos \theta_n - M)$. See Howe [88].

the viscous boundary layer thickness compared to the acoustic wave length and the amplitude (and the Mach number for high speed flow). These effects are not included in the present acoustic model, therefore they have to be included by an additional edge condition, for example the Kutta condition. As vorticity can only be shed from a trailing edge, a regular solution is only possible if $M > 0$. If $M < 0$ the edge is a leading edge and we have to leave the singular behaviour as it is.

9.2 Moving point source and Doppler shift

Consider a point (volume) source of strength $Q(t)$ (the volume flux), moving subsonically along the path $\mathbf{x} = \mathbf{x}_s(t)$ in a uniform acoustic medium. The generated sound field is described by

$$\frac{1}{c_0^2} \frac{\partial^2 p}{\partial t^2} - \nabla^2 p = \rho_0 \frac{\partial}{\partial t} \left\{ Q(t) \delta(\mathbf{R}(\mathbf{x}, t)) \right\}, \quad \mathbf{R}(\mathbf{x}, t) = \mathbf{x} - \mathbf{x}_s(t). \quad (9.16)$$

Using the free field Green's function (equation (6.37) or Appendix E)

$$G(\mathbf{x}, t | \mathbf{y}, \tau) = \frac{1}{4\pi |\mathbf{x} - \mathbf{y}|} \delta\left(t - \tau - \frac{|\mathbf{x} - \mathbf{y}|}{c_0}\right),$$

the solution for potential φ , with $p = -\rho_0 \frac{\partial}{\partial t} \varphi$, is given by

$$\begin{aligned} 4\pi \varphi(\mathbf{x}, t) &= - \int_{-\infty}^{\infty} \iiint_{\mathbb{R}^3} \frac{1}{|\mathbf{x} - \mathbf{y}|} \delta\left(t - \tau - \frac{|\mathbf{x} - \mathbf{y}|}{c_0}\right) Q(\tau) \delta(\mathbf{y} - \mathbf{x}_s(\tau)) \, \mathrm{d}\mathbf{y} \, \mathrm{d}\tau \\ &= - \int_{-\infty}^{\infty} \frac{Q(\tau)}{R(\mathbf{x}, \tau)} \delta\left(t - \tau - \frac{R(\mathbf{x}, \tau)}{c_0}\right) \, \mathrm{d}\tau, \quad R = |\mathbf{R}|. \end{aligned} \quad (9.17)$$

Using the δ -function integral (C.28)

$$\int_{-\infty}^{\infty} \delta(h(\tau)) g(\tau) \, \mathrm{d}\tau = \sum_i \frac{g(\tau_i)}{|h'(\tau_i)|}, \quad h(\tau_i) = 0 \quad (C.28)$$

this representation is very elegantly⁴ [55] reduced to the Liénard-Wiechert potential ([102, p.127])

$$4\pi \varphi(\mathbf{x}, t) = - \frac{Q_e}{R_e (1 - M_e \cos \vartheta_e)}, \quad (9.18)$$

where the subscript e denotes evaluation at time $t_e = t_e(\mathbf{x}, t)$, given by the equation

$$c_0(t - t_e) - R(\mathbf{x}, t_e) = 0. \quad (9.19)$$

⁴To appreciate the elegance the reader might compare it with the more traditional derivation as found in [153, p.721] for the less general problem of a point source moving with constant speed along a straight line.

Absolute values are suppressed because we assumed $|M_e| < 1$. Restriction (9.19) is entirely natural and to be expected. If we trace the observed acoustic perturbation back to its origin, we will find⁵ it to be created at time t_e by the source at position $\mathbf{x}_s(t_e)$ and strength $Q(t_e)$. Therefore, t_e is usually called *emission time*, or *retarded time*. It is important to note that by its implicit definition (9.19), t_e is a function of both t and \mathbf{x} .

Other convenient notations used here and below are

$$\mathbf{M} = \mathbf{x}'_s/c_0, \quad M = |\mathbf{M}|, \quad RM \cos \vartheta = \mathbf{R} \cdot \mathbf{M},$$

where M and \mathbf{M} are, respectively, the scalar and vectorial Mach number of the source, while ϑ is the angle between the source velocity vector and the observer's position, seen from the source. The combination $M \cos \vartheta$ is often also denoted by M_r .

By applying the chain rule to equation (9.19) we obtain the identities

$$\frac{\partial t_e}{\partial t} = \frac{1}{1 - M_e \cos \vartheta_e}, \quad \frac{\partial R_e}{\partial t} = -\frac{c_0 M_e \cos \vartheta_e}{1 - M_e \cos \vartheta_e},$$

$$\frac{\partial}{\partial t}(R_e M_e \cos \vartheta_e) = \frac{\mathbf{R}_e \cdot \mathbf{M}'_e - c_0 M_e^2}{1 - M_e \cos \vartheta_e}.$$

After differentiation of equation (9.18) with respect to time, we finally have

$$4\pi p(\mathbf{x}, t) = \frac{\rho_0 Q'_e}{R_e(1 - M_e \cos \vartheta_e)^2} + \rho_0 Q_e \frac{\mathbf{R}_e \cdot \mathbf{M}'_e + c_0 M_e (\cos \vartheta_e - M_e)}{R_e^2(1 - M_e \cos \vartheta_e)^3}. \quad (9.20)$$

The $O(R_e^{-1})$ -part dominates the far field, while the $O(R_e^{-2})$ -part dominates the near field [129]. A typical effect of motion is that both the pressure and the potential fields are increased by the ‘‘Doppler factor’’ $(1 - M_e \cos \vartheta_e)^{-1}$, but not with the same power. Furthermore, more Doppler factors appear for higher order multipole sources. (See Crighton [41].)

The name ‘‘Doppler factor’’ is due to its appearance in the well-known frequency shift of moving harmonic sources. Assume

$$Q(t) = Q_0 e^{i\omega_0 t}$$

with frequency ω_0 so high that we can *define* an instantaneous frequency ω for an observer of (9.20) at position \mathbf{x} :

$$\omega(t) = \frac{d}{dt}(\omega_0 t_e) = \frac{\omega_0}{1 - M_e \cos \vartheta_e}. \quad (9.21)$$

⁵A generalization to supersonic motion of the source involves in general a summation, according to (C.28), over more than one solution of equation (9.19). See [128] for an application with the Concorde aircraft.

This describes the *Doppler shift* of frequency ω_0 due to motion. Expression (9.20) is quite general. The more common forms are for a straight source path with constant velocity $\mathbf{x}_s(t) = (Vt, 0, 0)$ in which case M_e is constant and $\mathbf{x}_s'' = 0$.

Analogous to the above point volume source, or monopole, we can deduce the field of a moving point force, or dipole. For this we return to the original linearized gas dynamics equations in ρ , \mathbf{v} , and p with external force $\mathbf{F}(t)\delta(\mathbf{x} - \mathbf{x}_s(t))$, and eliminate ρ and \mathbf{v} to obtain:

$$\frac{1}{c_0^2} \frac{\partial^2 p}{\partial t^2} - \nabla^2 p = -\nabla \cdot \left\{ \mathbf{F}(t) \delta(\mathbf{R}(\mathbf{x}, t)) \right\}. \quad (9.22)$$

Following the same lines as in the monopole problem we have the solution

$$4\pi p(\mathbf{x}, t) = -\nabla \cdot \left(\frac{\mathbf{F}_e}{R_e(1 - M_e \cos \vartheta_e)} \right) \quad (9.23)$$

Here we see that a rotating force is not the same as a rotating $\nabla \cdot \mathbf{F}$ -field, since $t_e = t_e(\mathbf{x}, t)$. By application of the chain rule to equation (9.19) we derive:

$$\begin{aligned} \nabla R_e &= -c_0 \nabla t_e = \frac{\mathbf{R}_e}{R_e(1 - M_e \cos \vartheta_e)}, \\ \nabla(R_e M_e \cos \vartheta_e) &= \mathbf{M}_e - \frac{\mathbf{R}_e}{R_e(1 - M_e \cos \vartheta_e)} \left(\frac{\mathbf{R}_e \cdot \mathbf{M}'_e}{c_0} - M_e^2 \right), \end{aligned}$$

so that we have the general expression for a moving point force:

$$4\pi p(\mathbf{x}, t) = \frac{\mathbf{R}_e \cdot \mathbf{F}'_e - c_0 \mathbf{M}_e \cdot \mathbf{F}_e}{c_0 R_e^2 (1 - M_e \cos \vartheta_e)^2} + (\mathbf{R}_e \cdot \mathbf{F}_e) \frac{\mathbf{R}_e \cdot \mathbf{M}'_e + c_0 (1 - M_e^2)}{c_0 R_e^3 (1 - M_e \cos \vartheta_e)^3}. \quad (9.24)$$

The $O(R_e^{-1})$ -part dominates the far field, while the $O(R_e^{-2})$ -part dominates the near field [129].

It should be noted that the above distinction between a point source Q and a point force \mathbf{F} is rather idealized. In any real situation Q and \mathbf{F} are coupled, since in general a real mass source also produces a momentum change (see [55]).

9.3 Rotating monopole and dipole with moving observer

An application of the previous section is a model for (subsonic) propeller noise, due to Succi and Farassat [64, 237].

Two main sources of sound may be associated to a moving propeller blade: the displacement of fluid by the moving body leading to thickness noise, and the moving lift force distribution leading to loading noise. See the next section 9.4, equation (9.28). A description of the loading noise is obtained by

representing the propeller blade force by an equivalent distribution of point forces F_j , followed by a summation over j of the respective sound fields given by equation (9.24).

The thickness noise is a bit more involved. It can be shown (equation 9.32) that a compact moving body of fixed volume V generates a sound field, due to its displacement of fluid, given by the *time derivative* of equation (9.16) while $Q = V$, with solution the *time derivative* of equation (9.20).

$$4\pi p_{th}(\mathbf{x}, t) = \rho_0 V \frac{\partial^2}{\partial t^2} \frac{1}{R_e(1 - M_e \cos \vartheta_e)}.$$

(Equivalent forms in terms of spatial derivatives are also possible; see for example [27, 64].) By discretising the propeller blade volume by an equivalent collection of volumes V_j , the thickness noise is found by a summation over j of the respective sound fields.

The method is attractive in its relative simplicity, and easy programming. The formulas are laborious, however. Therefore, to illustrate the method, we will work out here the related problems of the far field of a subsonically rotating and translating monopole $Q = q_0$ and dipole f_0 . The position of the

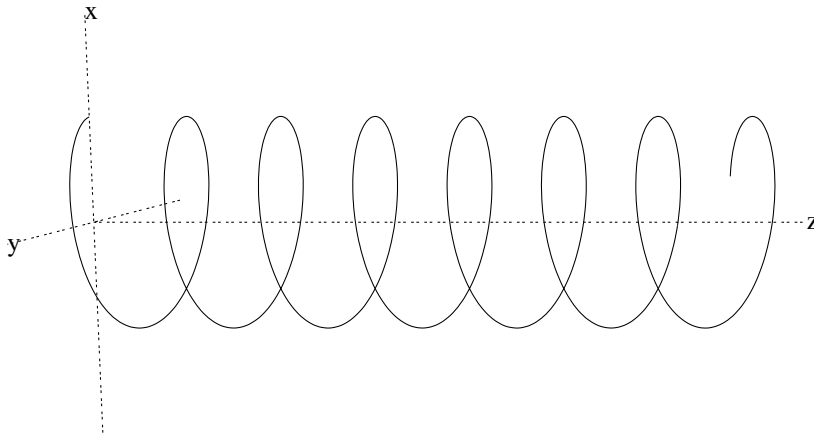


Figure 9.3 Trajectory of point, moving along helical path $\mathbf{x}_s(t)$.

point source, rotating in the x, y -plane along a circle of radius a with frequency ω , and translating along the z -axis with constant velocity U (figure 9.3), is given by

$$\mathbf{x}_s(t) = (a \cos \omega t, a \sin \omega t, Ut).$$

It is practically of most interest to consider an observer moving with the source, with forward speed U . Therefore, we start with the field of the source, given in the stationary medium by equation (9.20), and substitute for position vector \mathbf{x} the position of a co-moving observer $\mathbf{x}_o = (x_o, y_o, z_o)$, given in spherical coordinates by

$$\mathbf{x}_o(t) = (r \cos \phi \sin \vartheta, r \sin \phi \sin \vartheta, r \cos \vartheta + Ut).$$

With $\mathbf{R}_e^{(o)} = \mathbf{x}_o(t) - \mathbf{x}_s(t_e)$ we obtain the relations

$$\begin{aligned}\mathbf{R}_e^{(o)} \cdot \mathbf{M}_e &= M_R r \sin \vartheta \sin(\phi - \omega t_e) + M_F r \sin \vartheta + M_F^2 R_e^{(o)}, \\ \mathbf{R}_e^{(o)} \cdot \mathbf{M}'_e &= c_0 M_R^2 \left(1 - \frac{r}{a} \sin \vartheta \cos(\phi - \omega t_e)\right), \\ M_e^2 &= M_R^2 + M_F^2, \quad \text{where } M_R = \omega a / c_0, \quad M_F = U / c_0.\end{aligned}$$

The ‘‘far field’’ denotes the asymptotic behaviour for $(a/r) \rightarrow 0$. Since

$$c_0^2(t - t_e)^2 = (R_e^{(o)})^2 = r^2 - 2ar \sin \vartheta \cos(\phi - \omega t_e) + a^2 + 2Ur(t - t_e) \cos \vartheta + U^2(t - t_e)^2$$

and noting that asymptotically $t - t_e = O(r/c_0)$, we have for $a/r \rightarrow 0$

$$t_e = t - \frac{\tilde{r}}{c_0} + \frac{\tilde{a}}{c_0} \sin \vartheta \cos(\phi - \omega t + k\tilde{r}) + \dots$$

where $k = \omega/c_0$ and

$$\tilde{r} = r \frac{M_F \cos \vartheta + \sqrt{1 - M_F^2 \sin^2 \vartheta}}{1 - M_F^2}, \quad \tilde{a} = a \frac{1}{\sqrt{1 - M_F^2 \sin^2 \vartheta}}.$$

With this we find:

$$\begin{aligned}R_e^{(o)} &\simeq \tilde{r} - \tilde{a} \sin \vartheta \cos(\phi - \omega t + k\tilde{r}) \\ M_e \cos \vartheta_e &\simeq \frac{(1 - M_F^2) M_R \sin \vartheta \sin(\phi - \omega t + k\tilde{r}) + M_F \cos \vartheta + M_F^2 \sqrt{1 - M_F^2 \sin^2 \vartheta}}{M_F \cos \vartheta + \sqrt{1 - M_F^2 \sin^2 \vartheta}}\end{aligned}$$

Altogether in equation (9.20):

$$\begin{aligned}4\pi p(\mathbf{x}, t) &= \frac{\rho_0 c_0 q_0}{R_e^2 (1 - M_e \cos \vartheta_e)^3} \left(\frac{(\mathbf{R}_e^{(o)} \cdot \mathbf{M}'_e)}{c_0} + M_e \cos \vartheta_e - M_e^2 \right) \\ &\simeq - \frac{\rho_0 c_0 q_0}{ar} \frac{(1 - M_F^2)^2 M_R^2 \sin \vartheta \cos(\phi - \omega t + k\tilde{r})}{\left(M_F \cos \vartheta + \sqrt{1 - M_F^2 \sin^2 \vartheta} \right)^2 (1 - M_e \cos \vartheta_e)^3}\end{aligned} \quad (9.25)$$

We do have a $O(1/r)$ decay, and in spite of the $dQ(t)/dt = 0$, a nearly harmonic signal. Note the 2-lobe radiation pattern, *i.e.* 2 maxima perpendicular to the axis of rotation where $\sin \vartheta = 1$, and minima in the direction of the axis where $\sin \vartheta = 0$.

The rotating point force will portray a very simple propeller model. We assume the propeller to be concentrated in one point (this is a plausible approximation for the lowest harmonics) by a point force

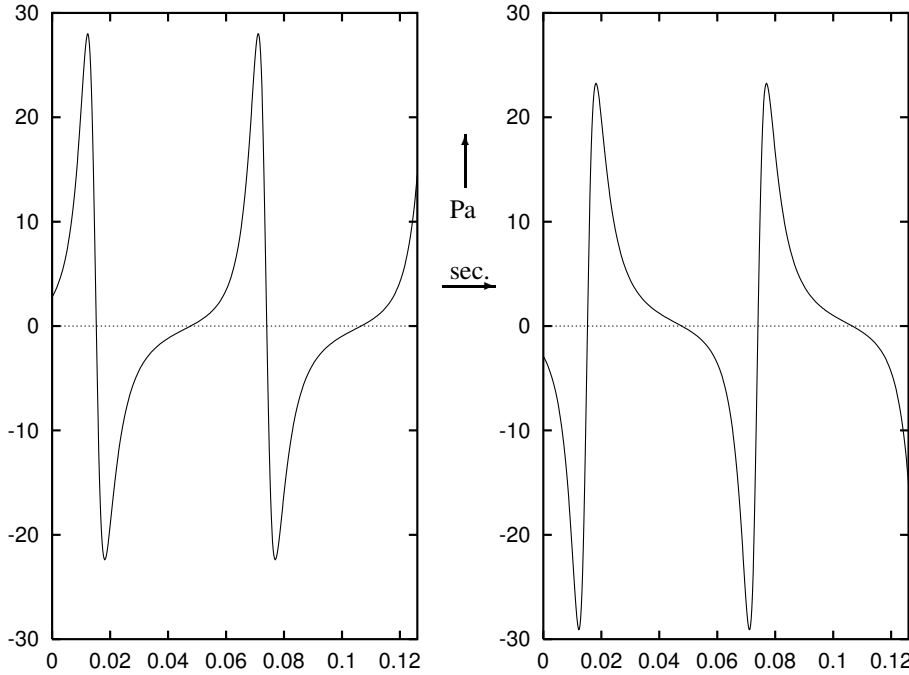


Figure 9.4 Time history of sound pressure generated by spiralling point source (left) and point force (right).

equal to the blade thrust force (the pressure jump across the blade integrated over the blade), in a direction perpendicular to the blade. Furthermore, the blade surface will practically coincide with the screw plane described by the velocity of a point on the blade $\mathbf{V} = U\mathbf{e}_z + \omega a\mathbf{e}_\theta$.

So normal to this plane we have the lift force

$$\mathbf{F}(t) = \frac{f_0}{\sqrt{U^2 + (\omega a)^2}}(U \sin \omega t, -U \cos \omega t, \omega a) \tag{9.26}$$

In figure 9.4 plots are made of the time history of the sound pressure generated by the above point source and point force, for the following parameters: $U = 145$ m/s, $c_0 = 316$ m/s, $a = 1.28$ m, $\omega = 2\pi \cdot 17$ /s, $f_0 = 700$ N, $\rho_0 = 1.2$ kg/m³, $q_0 = 1.8$ m³/s, for an observer moving with and in the plane of the source at a distance $x_0 = 2.5$ m. No far-field approximation has been made.

9.4 Ffowcs Williams & Hawkings equation for moving bodies

Curle (6.85) showed that the effect of a rigid body can be incorporated in the aero-acoustical analogy of Lighthill as additional source and force terms Q_m and \mathbf{F} . This approach has been generalized

by Ffowcs Williams and Hawkings who derived [68] a very general formulation valid for any moving body, enclosed by a surface $\mathcal{S}(t)$. Their derivation by means of generalized functions (surface distributions, section C.2.8) is an example of elegance and efficiency. Although originally meant to include the effect of moving closed surfaces into Lighthill's theory for aerodynamic sound, it is now a widely used starting point for theories of noise generation by moving bodies like propellers, even when turbulence noise is of little or no importance.

There is no unique relation between a source and its sound field, because a given field can be created by infinitely many equivalent but different sources (section 2.6.1). Therefore, there is no unique way to describe the effect of a surface $\mathcal{S}(t)$ in terms of an acoustic source distribution, and a simple and transparent choice is preferable. The choice put forward by Ffowcs Williams and Hawkings was both simple and transparent: just force any flow variable to vanish inside the enclosed volume. The resulting equations are automatically valid everywhere, and use can be made of the free field Green's function.

Consider a finite volume $\mathcal{V} = \mathcal{V}(t)$ with sufficiently smooth surface $\mathcal{S} = \mathcal{S}(t)$, moving continuously in space. Introduce a (smooth) function $f(\mathbf{x}, t)$ such that

$$f(\mathbf{x}, t) \begin{cases} < 0 & \text{if } \mathbf{x} \in \mathcal{V}(t), \\ = 0 & \text{if } \mathbf{x} \in \mathcal{S}(t), \\ > 0 & \text{if } \mathbf{x} \notin \mathcal{V}(t), \end{cases}$$

but otherwise arbitrary. If we multiply any physical quantity by the Heaviside function $H(f)$ – such as $\rho' H(f)$ – we obtain a new variable which vanishes identically within \mathcal{V} because $H(f) = 1$ in the fluid, and $H(f) = 0$ inside \mathcal{V} . Since $\nabla f|_{f=0}$ is directed normal outwards from \mathcal{V} , the outward normal \mathbf{n} of \mathcal{S} is given by (section A.3).

$$\mathbf{n}(\mathbf{x}, t) = \frac{\nabla f}{|\nabla f|} \Big|_{f=0}.$$

Let the surface $\mathcal{S}(t)$ be parametrized in time and space, by coordinates⁶ $(t; \lambda, \mu)$. A surface point $x_S(t) \in \mathcal{S}$ (consider λ and μ fixed), moving with velocity $\mathbf{U} = \dot{\mathbf{x}}_S$, remains at the surface for all time, so $f(\mathbf{x}_S(t), t) = 0$ for all t , and therefore

$$\frac{\partial f}{\partial t} = -\dot{\mathbf{x}}_S \cdot \nabla f = -(\mathbf{U} \cdot \mathbf{n}) |\nabla f|.$$

It is important to note that the normal velocity $(\mathbf{U} \cdot \mathbf{n})$ is a property of the surface, and is independent of the choice of f or parametrization. We now start the derivation by multiplying the exact equations

⁶When $\mathcal{S}(t)$ is the surface of a solid and undeformable body, it is natural to assume a spatial parametrization which is materially attached to the surface. This is, however, not necessary. Like the auxiliary function f , this parametrization is not unique, but that will appear to be of no importance.

(1.1,1.2) of motion for the fluid by $H(f)$:

$$\begin{aligned} H(f) \left[\frac{\partial \rho'}{\partial t} + \nabla \cdot (\rho \mathbf{v}) \right] &= 0, \\ H(f) \left[\frac{\partial}{\partial t} (\rho \mathbf{v}) + \nabla \cdot (\mathbf{P} + \rho \mathbf{v} \mathbf{v}) \right] &= 0, \end{aligned}$$

where $\rho' = \rho - \rho_0$ and ρ_0 is the mean level far away from the body. Although the original equations were only valid outside the body, the new equations are trivially satisfied inside \mathcal{V} , and so they are valid everywhere. By reordering the terms, and using the identity $\frac{\partial}{\partial t} H(f) = -\mathbf{U} \cdot \nabla H(f)$, the equations can be rewritten as equations for the new variables $\rho' H(f)$ and $\rho \mathbf{v} H(f)$ as follows.

$$\begin{aligned} \frac{\partial}{\partial t} [\rho' H(f)] + \nabla \cdot [\rho \mathbf{v} H(f)] &= [\rho_0 \mathbf{U} + \rho (\mathbf{v} - \mathbf{U})] \cdot \nabla H(f), \\ \frac{\partial}{\partial t} [\rho \mathbf{v} H(f)] + \nabla \cdot [(\rho \mathbf{v} \mathbf{v} + \mathbf{P}) H(f)] &= [\rho \mathbf{v} (\mathbf{v} - \mathbf{U}) + \mathbf{P}] \cdot \nabla H(f). \end{aligned}$$

Using the same procedure (subtracting the time-derivative of the mass equation from the divergence of the momentum equation) as for Lighthill's analogy (2.65), we find the Ffowcs Williams-Hawkings equations [68]:

$$\begin{aligned} \frac{\partial^2}{\partial t^2} \rho' H(f) - c_0^2 \nabla^2 \rho' H(f) &= \nabla \cdot \left[\nabla \cdot \left[(\rho \mathbf{v} \mathbf{v} - \boldsymbol{\tau} + (p' - c_0^2 \rho') \mathbf{I}) H(f) \right] \right] \\ &+ \frac{\partial}{\partial t} \left[(\rho (\mathbf{v} - \mathbf{U}) + \rho_0 \mathbf{U}) \cdot \nabla H(f) \right] - \nabla \cdot \left[(\rho \mathbf{v} (\mathbf{v} - \mathbf{U}) + p' \mathbf{I} - \boldsymbol{\tau}) \cdot \nabla H(f) \right]. \end{aligned} \quad (9.27)$$

The sources at the right hand side consist of the double divergence of the common quadrupole-type Lighthill stress tensor, and a time derivative and divergence of sources only present at the surface $f = 0$. Of course, the right hand side contains all the unknowns, and in principle this equation (9.27) is not simpler to solve than the original Navier-Stokes equations. However, as with Lighthill's analogy, the source terms are of aerodynamic nature, and can be solved separately, without including the very small acoustic back-reaction.

Very often, Lighthill's stress tensor $\rho \mathbf{v} \mathbf{v} - \boldsymbol{\tau} + (p' - c_0^2 \rho') \mathbf{I}$ and the shear stresses at the surface are negligible. Moreover, if the surface \mathcal{S} is solid such that $\mathbf{v} \cdot \mathbf{n} = \mathbf{U} \cdot \mathbf{n}$, and we change from density to pressure as our field variable, and define $\bar{p}' = p' H(f)$, we have a reduced form of the Ffowcs Williams-Hawkings equation, which is widely used for subsonic propeller and fan noise (no shocks) [64]

$$\frac{1}{c_0^2} \frac{\partial^2}{\partial t^2} \bar{p}' - \nabla^2 \bar{p}' = \frac{\partial}{\partial t} \left[\rho_0 \mathbf{U} \cdot \mathbf{n} |\nabla f| \delta(f) \right] - \nabla \cdot \left[p' \mathbf{n} |\nabla f| \delta(f) \right]. \quad (9.28)$$

The first source term is of purely geometrical nature, and describes the noise generated by the fluid displaced by the moving body. The associated field is called thickness noise. The second part depends

on the normal surface stresses due to the pressure distribution, and describes the noise generated by the moving force distribution. The associated field is called loading or lift noise.

If we know the pressure distribution along the surface, we can in principle solve this equation, in a way similar to the problem of the moving point source of section 9.2. Let us consider first the following prototype problem

$$\frac{1}{c_0^2} \frac{\partial^2}{\partial t^2} \varphi - \nabla^2 \varphi = Q(\mathbf{x}, t) |\nabla f| \delta(f). \quad (9.29)$$

By using the free field Green's function we can write

$$4\pi \varphi(\mathbf{x}, t) = \int \iiint \frac{Q(\mathbf{y}, \tau)}{R} \delta(t - \tau - R/c_0) |\nabla f| \delta(f) \, d\mathbf{y} \, d\tau,$$

where $R = |\mathbf{x} - \mathbf{y}(\tau)|$, the distance between observer's and source's position. Noting that $|\nabla f| \delta(f)$ is just equivalent to the surface distribution of $\mathcal{S}(t)$ (equation C.38), we can integrate $\delta(f)$ (equation C.37 or C.39) and write

$$4\pi \varphi(\mathbf{x}, t) = \int \iint_{\mathcal{S}(t)} \frac{Q(\mathbf{y}, \tau)}{R} \delta(t - \tau - R/c_0) \, d\sigma \, d\tau.$$

The integral over τ can be evaluated by noting that any contributions come from the solution $\tau = t_e$ of the emission-time equation (the zero of the argument of the remaining δ -function), given by

$$c_0(t - \tau) - R = 0,$$

which describes (for given \mathbf{x}, t) a surface in (\mathbf{y}, τ) -space, symbolically denoted by $\mathcal{S}(t_e)$. Analogous to the point source field (9.18) we have then

$$4\pi \varphi(\mathbf{x}, t) = \iint_{\mathcal{S}(t_e)} \frac{Q_e}{R_e(1 - M_e \cos \vartheta_e)} \, d\sigma. \quad (9.30)$$

As before, subscript e denotes evaluation at emission time t_e , and $M \cos \vartheta$ is the component of the vectorial Mach number of the source in the direction of the observer (in some literature also denoted by M_r). From this auxiliary solution we can now formulate a solution for \bar{p}' as follows

$$4\pi \bar{p}'(\mathbf{x}, t) = \frac{\partial}{\partial t} \iint_{\mathcal{S}(t_e)} \frac{\rho_0 \mathbf{U}_e \cdot \mathbf{n}_e}{R_e(1 - M_e \cos \vartheta_e)} \, d\sigma - \nabla \cdot \iint_{\mathcal{S}(t_e)} \frac{p_e \mathbf{n}_e}{R_e(1 - M_e \cos \vartheta_e)} \, d\sigma. \quad (9.31)$$

Extreme care should be taken in interpreting this equation, because for any \mathbf{x} and t the emission time t_e varies over the source region, while at the same time the source varies its position! Other forms

of the solution are available which might be easier to handle in certain applications; see *e.g.* Farassat [63, 64].

It is therefore interesting to consider the compact limit, in which case the typical wave length is much longer than the body size. The emission time does not vary significantly over the source region, and R_e and $M_e \cos \vartheta_e$ refer only to a single typical source coordinate \mathbf{x}_s , for example the centre of gravity. The source becomes equivalent to a point source (section 9.2,9.3).

A particularly interesting form (Farassat [64]) for the thickness noise component is found by writing the surface integral as a volume integral. Using

$$\rho_0 \mathbf{U} \cdot \mathbf{n} |\nabla f| \delta(f) = \frac{\partial}{\partial t} \rho_0 (1 - H(f)),$$

and noting that the function $1 - H(f)$ equals unity inside the body \mathcal{V} and zero elsewhere, we have for the thickness noise component of equation (9.31)

$$\frac{\partial}{\partial t} \iint_{S(t_e)} \frac{\rho_0 \mathbf{U}_e \cdot \mathbf{n}_e}{R_e (1 - M_e \cos \vartheta_e)} d\sigma = \frac{\partial^2}{\partial t^2} \iiint_{\mathcal{V}(t_e)} \frac{\rho_0}{R_e (1 - M_e \cos \vartheta_e)} d\mathbf{y}.$$

Since the volume integral of the constant 1 is just V , the volume of \mathcal{V} , and denoting the total force of the fluid on the body by

$$\mathbf{F}(t) = \iint_{S(t)} p \cdot \mathbf{n} d\sigma,$$

we have the compact limit of equation (9.31) (see also section 9.3)

$$4\pi \bar{p}'(\mathbf{x}, t) \simeq \frac{\partial^2}{\partial t^2} \left(\frac{\rho_0 V}{R_e (1 - M_e \cos \vartheta_e)} \right) - \nabla \cdot \left(\frac{\mathbf{F}_e}{R_e (1 - M_e \cos \vartheta_e)} \right). \tag{9.32}$$

Exercises

- a) Evaluate the expressions for the acoustic field of the propeller of equation 9.26 without forward speed ($U = 0$) and find the approximation for the far field. What can you tell about the typical lobes in the radiation pattern?
- b) Evaluate the expressions for the acoustic field of a moving point volume source (9.20) and point force (9.24) for the windtunnel situation: a moving source $\mathbf{x}_s = Vt \mathbf{e}_x$ and a moving observe $\mathbf{x} = \mathbf{a} + Vt \mathbf{e}_x$.

A Integral laws and related results

A.1 Reynolds' transport theorem

For an arbitrary single-valued scalar function $F = F(\mathbf{x}, t)$ with continuous derivatives, and an arbitrary control volume $V^*(t)$ with surface $S^*(t)$, outward-pointing unit-normal \mathbf{n} , and \mathbf{b} the local velocity of S^* , the following integral relation holds:

$$\frac{d}{dt} \iiint_{V^*} F \, d\mathbf{x} = \iiint_{V^*} \frac{\partial F}{\partial t} \, d\mathbf{x} + \iint_{S^*} F (\mathbf{b} \cdot \mathbf{n}) \, d\sigma. \quad (\text{A.1})$$

This theorem, known as Reynolds' Transport Theorem (see equation C.40), is used to translate integral conservation laws into differential conservation laws. Conservation laws such as mass conservation are understood most easily when they are applied to a so-called material volume $\bar{V} = \bar{V}(t)$ (enclosed by the surface $\bar{S} = \bar{S}(t)$), which is a volume contained in the fluid and with no fluid entering or leaving it. The concept arises when considering a fluid particle which is large in number of molecules, but small compared to the macroscopic scales in the problem. For a certain –diffusion controlled– period of time the particle keeps its identity, and can be labelled. In such a case we have for the fluid velocity \mathbf{v} at surface \bar{S}

$$(\mathbf{b} \cdot \mathbf{n}) = (\mathbf{v} \cdot \mathbf{n}).$$

Hence, for any property of the fluid $F = F(\mathbf{x}, t)$ with continuous derivatives, Reynold's theorem becomes:

$$\frac{d}{dt} \iiint_{\bar{V}} F \, d\mathbf{x} = \iiint_{\bar{V}} \frac{\partial F}{\partial t} \, d\mathbf{x} + \iint_{\bar{S}} F (\mathbf{v} \cdot \mathbf{n}) \, d\sigma, \quad (\text{A.2})$$

A.2 Conservation laws

The conservation laws (mass, momentum, energy) in integral form are more general than in differential form because they can be applied to flows with discontinuous properties. We will give here a summary of the basic formulae. A detailed derivation may be found in [176] or [241]. Consider a material volume \bar{V} with surface \bar{S} .

Mass conservation ($F = \rho$):

$$\frac{d}{dt} \iiint_{\bar{V}} \rho \, d\mathbf{x} = 0. \tag{A.3}$$

Momentum conservation ($F = \rho v_i$):

$$\frac{d}{dt} \iiint_{\bar{V}} \rho v_i \, d\mathbf{x} = \iiint_{\bar{V}} f_i \, d\mathbf{x} - \iint_{\bar{S}} P_{ij} n_j \, d\sigma. \tag{A.4}$$

Energy conservation ($F = \rho(e + \frac{1}{2}v^2)$, $v^2 = v_i v_i$):

$$\frac{d}{dt} \iiint_{\bar{V}} \rho(e + \frac{1}{2}v^2) \, d\mathbf{x} = \iiint_{\bar{V}} f_i v_i \, d\mathbf{x} - \iint_{\bar{S}} P_{ij} v_j n_i \, d\sigma - \iint_{\bar{S}} q_i n_i \, d\sigma. \tag{A.5}$$

Consider now an arbitrary control volume $V^*(t)$ with surface $S^*(t)$ and \mathbf{b} the local velocity of S^* . By applying (A.3) and (A.1) with $F = \rho$ we find:

$$\frac{d}{dt} \iiint_{V^*} \rho \, d\mathbf{x} = \iiint_{V^*} \frac{\partial \rho}{\partial t} \, d\mathbf{x} + \iint_{S^*} \rho b_i n_i \, d\sigma \tag{A.6}$$

$$\iiint_{\bar{V}} \frac{\partial \rho}{\partial t} \, d\mathbf{x} = - \iint_{\bar{S}} \rho v_i n_i \, d\sigma. \tag{A.7}$$

At any given instant we may identify V^* with a given material volume \bar{V} . Hence (A.7) can be used to eliminate the first integral on the right-hand side of (A.6) to obtain:

$$\frac{d}{dt} \iiint_{V^*} \rho \, d\mathbf{x} = \iint_{S^*} \rho(b_i - v_i) n_i \, d\sigma. \tag{A.8}$$

This can be applied to any volume V^* and in particular to a fixed volume ($b_i = 0$). In a similar way we have for the momentum:

$$\frac{d}{dt} \iiint_{V^*} \rho v_i \, d\mathbf{x} + \iint_{S^*} \rho v_i (v_j - b_j) n_j \, d\sigma = \iiint_{V^*} f_i \, d\mathbf{x} - \iint_{S^*} P_{ij} n_j \, d\sigma \tag{A.9}$$

and for the energy:

$$\begin{aligned} \frac{d}{dt} \iiint_{V^*} \rho(e + \frac{1}{2}v^2) \, d\mathbf{x} + \iint_{S^*} \rho(e + \frac{1}{2}v^2)(v_i - b_i) n_i \, d\sigma \\ = \iiint_{V^*} f_i v_i \, d\mathbf{x} - \iint_{S^*} P_{ij} v_j n_i \, d\sigma - \iint_{S^*} q_i n_i \, d\sigma. \end{aligned} \tag{A.10}$$

For the entropy s we further find:

$$\frac{d}{dt} \iiint_{V^*} \rho s \, d\mathbf{x} + \iint_{S^*} \rho s (v_i - b_i) n_i \, d\sigma + \iint_{S^*} \frac{1}{T} q_i n_i \, d\sigma \geq 0 \quad (\text{A.11})$$

where the equality is valid when the processes in the flow are reversible.

A.3 Normal vectors of level surfaces

A convenient way to describe a smooth surface \mathcal{S} is by means of a suitable smooth function $S(\mathbf{x})$, where $\mathbf{x} = (x, y, z)$, chosen such that the level surface $S(\mathbf{x}) = 0$ coincides with \mathcal{S} . So $S(\mathbf{x}) = 0$ if and only if $\mathbf{x} \in \mathcal{S}$. Then ∇S at $S = 0$ is a normal of \mathcal{S} , provided $\nabla S \neq 0$. This is seen as follows.

Consider a point \mathbf{x}_0 and a neighbouring point $\mathbf{x}_0 + \mathbf{h}$, both on the surface \mathcal{S} . Expand $S(\mathbf{x}_0 + \mathbf{h})$ into a Taylor series in \mathbf{h} . We then obtain

$$S(\mathbf{x}_0 + \mathbf{h}) = S(\mathbf{x}_0) + \mathbf{h} \cdot \nabla S(\mathbf{x}_0) + O(\mathbf{h}^2) \simeq \mathbf{h} \cdot \nabla S(\mathbf{x}_0) = 0.$$

Since in the limit for $|\mathbf{h}| \rightarrow 0$ the vector $\nabla S(\mathbf{x}_0)$ is normal to the tangent vector \mathbf{h} , it is normal to the surface \mathcal{S} . Furthermore, the unit normal vector $\mathbf{n}_S = \frac{\nabla S}{|\nabla S|}$ (at $S = 0$) is directed from the $S < 0$ -side to the $S > 0$ -side. If we expand $S(\mathbf{x})$ near $\mathbf{x}_0 \in \mathcal{S}$ we have $S(\mathbf{x}) = (\mathbf{x} - \mathbf{x}_0) \cdot \nabla S(\mathbf{x}_0) + \dots$, so, near the surface, $S(\mathbf{x})$ varies, to leading order, only in the coordinate normal to the surface.

A.4 Vector identities and theorems

Let ψ, ϕ and $\mathbf{a}, \mathbf{b}, \mathbf{c}, \mathbf{d}, \mathbf{v}$ denote well-behaved scalar functions and vector fields.

$$\mathbf{a} \cdot (\mathbf{b} \times \mathbf{c}) = \mathbf{b} \cdot (\mathbf{c} \times \mathbf{a}) = \mathbf{c} \cdot (\mathbf{a} \times \mathbf{b}) \quad (\text{A.12a})$$

$$\mathbf{a} \cdot (\mathbf{a} \times \mathbf{b}) = 0 \quad (\text{A.12b})$$

$$\mathbf{a} \times (\mathbf{b} \times \mathbf{c}) = \mathbf{b}(\mathbf{a} \cdot \mathbf{c}) - \mathbf{c}(\mathbf{a} \cdot \mathbf{b}) \quad (\text{A.12c})$$

$$(\mathbf{a} \times \mathbf{b}) \cdot (\mathbf{c} \times \mathbf{d}) = (\mathbf{a} \cdot \mathbf{c})(\mathbf{b} \cdot \mathbf{d}) - (\mathbf{a} \cdot \mathbf{d})(\mathbf{b} \cdot \mathbf{c}) \quad (\text{A.12d})$$

$$\nabla(\mathbf{a} \cdot \mathbf{b}) = \mathbf{a} \cdot \nabla \mathbf{b} + \mathbf{b} \cdot \nabla \mathbf{a} + \mathbf{a} \times (\nabla \times \mathbf{b}) + \mathbf{b} \times (\nabla \times \mathbf{a}) \quad (\text{A.12e})$$

$$\mathbf{a} \cdot \nabla(\mathbf{b} \cdot \mathbf{c}) = \mathbf{b} \cdot (\mathbf{a} \cdot \nabla \mathbf{c}) + \mathbf{c} \cdot (\mathbf{a} \cdot \nabla \mathbf{b}) \quad (\text{A.12f})$$

$$\nabla \cdot (\mathbf{a} \times \mathbf{b}) = \mathbf{b} \cdot (\nabla \times \mathbf{a}) - \mathbf{a} \cdot (\nabla \times \mathbf{b}) \quad (\text{A.12g})$$

$$\nabla \times (\mathbf{a} \times \mathbf{b}) = \mathbf{a}(\nabla \cdot \mathbf{b}) - \mathbf{b}(\nabla \cdot \mathbf{a}) - \mathbf{a} \cdot \nabla \mathbf{b} + \mathbf{b} \cdot \nabla \mathbf{a} \quad (\text{A.12h})$$

$$\nabla \times (\phi \mathbf{a}) = (\nabla \phi) \times \mathbf{a} + \phi (\nabla \times \mathbf{a}) \quad (\text{A.12i})$$

$$\nabla \times (\psi \nabla \phi) = (\nabla \psi) \times (\nabla \phi) \quad (\text{A.12j})$$

$$(\mathbf{v} \cdot \nabla) \mathbf{v} = \nabla \left(\frac{1}{2} v^2 \right) + (\nabla \times \mathbf{v}) \times \mathbf{v} \quad (\text{A.12k})$$

$$\mathbf{v} \cdot [(\mathbf{v} \cdot \nabla) \mathbf{v}] = \mathbf{v} \cdot \nabla \left(\frac{1}{2} v^2 \right) \quad (\text{A.12l})$$

Note that $\nabla \cdot (\nabla \times \mathbf{v}) = 0$ and $\nabla \times (\nabla \phi) = 0$.

Let Ω denote a three-dimensional volume with volume element dV , and $\partial\Omega$ a closed two-dimensional surface bounding Ω with area element dS and associated unit outward vector \mathbf{n} . Then we have the following integral relations.

Gauss' divergence theorem:
$$\int_{\Omega} \nabla \cdot \mathbf{v} \, dV = \oint_{\partial\Omega} \mathbf{v} \cdot \mathbf{n} \, dS \quad (\text{A.13a})$$

$$\int_{\Omega} \nabla \phi \, dV = \oint_{\partial\Omega} \phi \mathbf{n} \, dS \quad (\text{A.13b})$$

$$\int_{\Omega} \nabla \times \mathbf{v} \, dV = \oint_{\partial\Omega} \mathbf{n} \times \mathbf{v} \, dS \quad (\text{A.13c})$$

Green's first identity:
$$\int_{\Omega} (\phi \nabla^2 \psi + \nabla \phi \cdot \nabla \psi) \, dV = \oint_{\partial\Omega} \phi \nabla \psi \cdot \mathbf{n} \, dS \quad (\text{A.13d})$$

Green's second identity:
$$\int_{\Omega} (\phi \nabla^2 \psi - \psi \nabla^2 \phi) \, dV = \oint_{\partial\Omega} (\phi \nabla \psi - \psi \nabla \phi) \cdot \mathbf{n} \, dS \quad (\text{A.13e})$$

Let S denote a smooth orientable surface, bounded by the positively oriented contour C with line element $d\ell$. The normal \mathbf{n} to S is defined according to the right-hand-screw rule applied to C . Then

Stokes' theorem:
$$\int_S (\nabla \times \mathbf{v}) \cdot \mathbf{n} \, dS = \oint_C \mathbf{v} \cdot d\ell \quad (\text{A.14a})$$

$$\int_S \mathbf{n} \times \nabla \phi \, dS = \oint_C \phi d\ell \quad (\text{A.14b})$$

B Orders of magnitude: O and o .

In many cases it is necessary to indicate in a compact way the behaviour of some function $f(x)$, of variable or parameter x , as x tends to some limit (finite or infinite). The usual way to do this is by comparing with a simpler function $g(x)$. For this we have the *order symbols* O and o . When f is comparable with or dominated by g , we have

Definition B.1 $f(x) = O(g(x))$ as $x \rightarrow a$
means, that there is a constant C and an interval $(a - h, a + h)$
such that for all $x \in (a - h, a + h)$: $|f(x)| \leq C|g(x)|$.

When $x \downarrow a$ the interval is one-sided: $(a, a + h)$; similarly for $x \uparrow a$. For the behaviour at infinity we have

Definition B.2 $f(x) = O(g(x))$ as $x \rightarrow \infty$
means, that there is a constant C and an interval (x_0, ∞)
such that for all $x \in (x_0, \infty)$: $|f(x)| \leq C|g(x)|$.

Similarly for $x \rightarrow -\infty$. When f is essentially smaller than g we have

Definition B.3 $f(x) = o(g(x))$ as $x \rightarrow a$
means, that for every positive δ there is an interval $(a - \eta, a + \eta)$
such that for all $x \in (a - \eta, a + \eta)$: $|f(x)| \leq \delta|g(x)|$.

with obvious generalizations to $x \downarrow a$, $x \rightarrow \infty$, etc.

Theorem B.1 If $\lim \frac{f(x)}{g(x)}$ exists, and is finite, then $f(x) = O(g(x))$.

Theorem B.2 If $\lim \frac{f(x)}{g(x)} = 0$, then $f(x) = o(g(x))$.

Note that $f = o(g)$ implies $f = O(g)$, in which case the estimate $O(g)$ is only an upper limit, and not as informative as the “sharp O ”, defined by

Definition B.4 $f(x) = O_s(g(x))$ means: $f(x) = O(g(x))$ but $f(x) \neq o(g(x))$.

C Fourier transforms and generalized functions

C.1 Fourier transforms

The linearity of sound waves allows us to build up the acoustic field as a sum of simpler solutions of the wave equation. The most important example is the reduction into time harmonic components, or Fourier analysis. This is attractive in several respects. Mathematically, because the equation simplifies greatly if the coefficients in the wave equation are time-independent, and physically, because the Fourier spectrum represents the harmonic perception of sound.

Consider a function $p(t)$ with the following (sufficient, not necessary) conditions [31, 101, 124, 178, 263].

- p is continuous, except for at most a finite number of discontinuities where $p(t) = \frac{1}{2}[p(t+0) + p(t-0)]$.
- $|p(t)|$ and $|p(t)|^2$ are integrable.

Then the **Fourier transform** $\hat{p}(\omega)$ of $p(t)$ is defined as the complex function

$$\hat{p}(\omega) = \mathcal{F}_p(\omega) \stackrel{\text{def}}{=} \frac{1}{2\pi} \int_{-\infty}^{\infty} p(t) e^{-i\omega t} dt, \quad (\text{C.1})$$

while according to Fourier's inversion theorem, $p(t)$ is equal to the inverse Fourier transform

$$p(t) = \mathcal{F}_{\hat{p}}^{-1}(t) \stackrel{\text{def}}{=} \int_{-\infty}^{\infty} \hat{p}(\omega) e^{i\omega t} d\omega. \quad (\text{C.2})$$

The Fourier transform and its inverse are closely related. Apart from a sign change and a factor 2π , it is the same operation: $\mathcal{F}_{\hat{p}}^{-1}(t) = 2\pi \mathcal{F}_{\hat{p}}(-t)$. It is important to note that slight differences with respect to the factor $1/2\pi$, frequency $\omega = 2\pi f$, and the sign of the phase $i\omega t$ are common in the literature. Especially the prevailing $e^{\pm i\omega t}$ -convention should *always* be checked when referring or comparing to other work.

Some examples of Fourier transforms are:

$$\frac{1}{2\pi} \int_{-\infty}^{\infty} H(t) e^{-\alpha t} e^{-i\omega t} dt = \frac{1}{2\pi(\alpha + i\omega)}, \tag{C.3a}$$

$$\frac{1}{2\pi} \int_{-\infty}^{\infty} \frac{H(t)}{\sqrt{t}} e^{-\alpha t} e^{-i\omega t} dt = \frac{1}{2\sqrt{\pi}\sqrt{\alpha + i\omega}}, \tag{C.3b}$$

$$\frac{1}{2\pi} \int_{-\infty}^{\infty} \frac{1}{1+t^2} e^{-i\omega t} dt = \frac{1}{2} e^{-|\omega|}, \tag{C.3c}$$

$$\frac{1}{2\pi} \int_{-\infty}^{\infty} e^{-\frac{1}{2}t^2} e^{-i\omega t} dt = \frac{1}{\sqrt{2\pi}} e^{-\frac{1}{2}\omega^2}, \tag{C.3d}$$

where $\alpha > 0$, the ordinary square root is taken, and $H(t)$ denotes Heaviside's unit step function (C.29), which is $H(t) = 1$ for $t > 0$ and $H(t) = 0$ for $t < 0$.

Although it may seem to be no serious restriction to assume that a physically relevant signal $p(t)$ vanishes at $t = \pm\infty$, we deal in practice with simplified models, yielding expressions for $p(t)$ which do *not* decay at infinity (e.g. a constant, $\sin(\omega_0 t)$). So we have on the one hand the “real” $p(t)$ which is Fourier-transformable, and on the other hand the approximate “model” $p(t)$, which is not always Fourier-transformable. Is there a way to approximate, or at least get an idea of, the real Fourier transform, using the approximate $p(t)$? One way is to assume p to vanish outside a certain large interval $[-N, N]$, as for example:

$$\begin{aligned} \frac{1}{2\pi} \int_{-N}^N e^{-i\omega t} dt &= \frac{N \sin \omega N}{\pi \omega N} \\ \frac{1}{2\pi} \int_{-N}^N \sin(\omega_0 t) e^{-i\omega t} dt &= \frac{N}{2\pi i} \left(\frac{\sin(\omega - \omega_0)N}{(\omega - \omega_0)N} - \frac{\sin(\omega + \omega_0)N}{(\omega + \omega_0)N} \right). \end{aligned}$$

We see a large maximum ($\sim N/\pi$) depending on N near the dominating frequencies, and for the other frequencies an oscillatory behaviour, also depending on N , that is difficult to interpret. This is too vague and too arbitrary for general use. Therefore, a mathematically more consistent and satisfying approach, not depending on the arbitrary choice of the interval size, will be introduced later in terms of generalized functions.

Derivative

Since a derivative to t corresponds to a multiplication by $i\omega$ as follows

$$\frac{d}{dt} p(t) = \int_{-\infty}^{\infty} i\omega \hat{p}(\omega) e^{i\omega t} d\omega, \tag{C.4}$$

the wave equation reduces to the Helmholtz equation

$$\nabla^2 \varphi - \frac{1}{c^2} \frac{\partial^2 \varphi}{\partial t^2} = 0 \quad \xrightarrow{\text{F.T.}} \quad \nabla^2 \hat{\varphi} + \frac{\omega^2}{c^2} \hat{\varphi} = 0. \tag{C.5}$$

Further reduction is possible by Fourier transformation in space variables.

More dimensions and Hankel transform

Fourier transforms in n space dimensions is usually denoted as

$$\hat{f}(\mathbf{k}) = \frac{1}{(2\pi)^n} \int_{\mathbb{R}^n} f(\mathbf{x}) e^{i\mathbf{k}\cdot\mathbf{x}} d\mathbf{x}, \quad f(\mathbf{x}) = \int_{\mathbb{R}^n} \hat{f}(\mathbf{k}) e^{-i\mathbf{k}\cdot\mathbf{x}} d\mathbf{k}. \quad (\text{C.6})$$

The Hankel transform $\mathcal{H}_m(\phi; \rho)$ of a function $\phi(r)$, given by

$$\mathcal{H}_m(\phi; \rho) = \frac{1}{2\pi} \int_0^\infty \phi(r) J_m(\rho r) r dr \quad (\text{C.7})$$

arises naturally when the 2D Fourier transform of a function $f(\mathbf{x})$ is re-written in polar coordinates.

$$\begin{aligned} \hat{f}(\mathbf{k}) &= \frac{1}{4\pi^2} \iint_{\mathbb{R}^2} f(\mathbf{x}) e^{i\mathbf{k}\cdot\mathbf{x}} d\mathbf{x} = \frac{1}{4\pi^2} \int_0^\infty \int_0^{2\pi} \sum_{m=-\infty}^\infty f_m(r) e^{-im\theta} e^{i\rho r \cos(\theta-\alpha)} r d\theta dr \\ &= \frac{1}{2\pi} \sum_{m=-\infty}^\infty \int_0^\infty i^m f_m(r) J_m(\rho r) e^{-im\alpha} r dr = \sum_{m=-\infty}^\infty i^m e^{-im\alpha} \mathcal{H}_m(f_m; \rho) \end{aligned} \quad (\text{C.8})$$

where $\mathbf{x} = (r \cos \vartheta, r \sin \vartheta)$, $\mathbf{k} = (\rho \cos \alpha, \rho \sin \alpha)$,

$$f(\mathbf{x}) = \sum_{m=-\infty}^\infty f_m(r) e^{-im\vartheta}$$

and use is made of equation (D.63).

Multiplication and convolution

Fourier transformation is basically a linear operation and little can be said about other than linear combinations of transformed functions. Only for multiplication with powers of ω we have

$$\int_{-\infty}^\infty (i\omega)^n \hat{p}(\omega) e^{i\omega t} d\omega = \frac{d^n}{dt^n} p(t). \quad (\text{C.9})$$

For multiplication with a general $\hat{q}(\omega)$ we find the convolution product of $p(t)$ and $q(t)$, also known as the Convolution Theorem

$$(p*q)(t) = \frac{1}{2\pi} \int_{-\infty}^\infty p(t') q(t-t') dt' = \int_{-\infty}^\infty \hat{p}(\omega) \hat{q}(\omega) e^{i\omega t} d\omega. \quad (\text{C.10})$$

Note that in terms of generalized functions, to be introduced below, result (C.9) for the product with ω^n is a special case of the convolution theorem. A particular case is Parseval's theorem, obtained by taking¹ $q(t') = p^*(-t')$ and $t = 0$:

$$\int_{-\infty}^{\infty} |\hat{p}(\omega)|^2 d\omega = \frac{1}{2\pi} \int_{-\infty}^{\infty} |p(t')|^2 dt' \quad (\text{C.11})$$

which is in a suitable context a measure of the total energy of a signal $p(t)$.

Poisson's summation formula

Intuitively, it is clear that the high frequencies relate to the short time behaviour, and the low frequencies to the long time behaviour. An elegant result due to Poisson is making this explicit.

$$\sum_{n=-\infty}^{\infty} p(\lambda n) = \frac{2\pi}{\lambda} \sum_{n=-\infty}^{\infty} \hat{p}\left(\frac{2\pi n}{\lambda}\right). \quad (\text{C.12})$$

Sampling with large steps (λ large) of p yields information about the low part of the spectrum and *vice versa*.

Reality condition

Although $\hat{p}(\omega)$ is complex, the corresponding $p(t)$ is in any physical context real. Therefore, not any $\hat{p}(\omega)$ can occur. A given $\hat{p}(\omega)$ corresponds to a real signal $p(t)$ if it satisfies the *reality condition*

$$\hat{p}(-\omega) = \hat{p}(\omega)^*. \quad (\text{C.13})$$

This is just the consequence of $p(t)$, given by equation (C.2), being identically equal to its complex conjugate.

C.1.1 Causality condition

The wave equation and the equation of motion do not impose a direction for the time, if dissipation effects are neglected. The fact that the sound should be produced before we observe it (causality) is not a property automatically implied by our equations, and it should be imposed to the solution. The problem is simple for an initial value problem, where it suffices to require a zero field before the switch-on time. However, when we consider a time-harmonic solution, or in general based on Fourier analysis, it is not obvious any more because we assume the solution to be built up from stationary

¹ $z^* = x - iy$ denotes the complex conjugate of $z = x + iy$.

oscillations. Stationary means that it exists forever and has always existed. In such a case causality, *i.e.* the difference between cause and effect, is not readily clear. It is therefore of interest to investigate conditions for the Fourier transform that guarantees a causal signal.

No physical process can exist for all time. A process $p(t)$ that starts by some cause at some finite time $t = t_0$, while it vanishes before t_0 , is called *causal*. The corresponding Fourier transform

$$\hat{p}(\omega) = \frac{1}{2\pi} \int_{t_0}^{\infty} p(t) e^{-i\omega t} dt \tag{C.14}$$

has the property that $\hat{p}(\omega)$ is analytic² in the lower complex half-space

$$\text{Im}(\omega) < 0. \tag{C.15}$$

So this is a necessary condition on \hat{p} for p to be causal. Examples are the exponentially decaying functions, switched on at $t = 0$, of equations (C.3a) and (C.3b). The Fourier transforms are non-analytic in the upper half-plane (singularities at $\omega = i\alpha$ and a branch cut from $i\alpha$ up to $i\infty$), but are indeed analytic in the half-plane $\text{Im}(\omega) < \alpha$.

A sufficient condition³ is the following *causality condition* [178].

Theorem C.1 (Causality Condition)

If: (i) $\hat{p}(\omega)$ is analytic in $\text{Im}(\omega) \leq 0$, (ii) $|\hat{p}(\omega)|^2$ is integrable along the real axis, and (iii) there is a real t_0 such that $e^{i\omega t_0} \hat{p}(\omega) \rightarrow 0$ uniformly with regard to $\arg(\omega)$ for $|\omega| \rightarrow \infty$ in the lower complex half plane, then: $p(t)$ is causal, and vanishes for $t < t_0$.

(Note that the *lower* complex half-space becomes the *upper* half-space if the opposite Fourier sign convention is taken.) Consider as a typical example the inverse transform of equation (C.3a). When $t > 0$ the exponential factor $e^{i\omega t} = e^{i\text{Re}(\omega)t} e^{-\text{Im}(\omega)t}$ decays in the upper half plane, so the contour can be closed via the upper half plane, resulting in $2\pi i$ times the residue⁴ of the pole in $i\alpha$. When $t < 0$ the contour can be closed via the lower half plane, with zero result because the integrand is analytic there: causal as it should be.

$$\int_{-\infty}^{\infty} \frac{e^{i\omega t}}{2\pi(\alpha + i\omega)} d\omega = \begin{cases} e^{-\alpha t} & \text{if } t > 0, \\ 0 & \text{if } t < 0. \end{cases}$$

²Infinitely often differentiable in the complex variable ω .

³Cauchy's theorem [109] for analytic functions says that if f is analytic in the inner-region of a closed contour C in the complex plane, the integral of f along C is equal to zero: $\int_C f(z)dz = 0$. Under the conditions stated in theorem (C.1) (p.283) the function $\hat{p}(\omega) \exp(i\omega t)$ is analytic in the lower-half complex ω -plane. So its integral along the closed contour consisting of the real interval $[-R, R]$ and the semi-circle $\omega = R e^{i\theta}$, $-\pi < \theta < 0$, is equal to zero.

Let $R \rightarrow \infty$ while $t < 0$ ($= t_0$; the case of a general t_0 is similar). The factor $e^{i\omega t} = e^{i\text{Re}(\omega)t} e^{-\text{Im}(\omega)t}$ decays exponentially fast to zero in the lower complex ω -plane because $-\text{Im}(\omega)t < 0$. Hence, the contribution from the large semi-circle becomes exponentially small and vanishes. So the part along the real axis is also zero. However, this is just $p(t)$, the inverse Fourier transform of \hat{p} .

⁴If $z = z_0$ is a simple pole of $f(z)$, then the residue of f at z_0 is: $\text{Res}_f(z_0) = \lim_{z \rightarrow z_0} (z - z_0)f(z)$.

It should be noted that in the limit of no damping ($\alpha \downarrow 0$) the singularity of (C.3a) and (C.3b) at $\omega = i\alpha$ moves to $\omega = 0$, which is on the real axis. This is a bit of a problem if we are interested in the inverse transform⁵, because the real ω -axis is just the contour of integration, and a pole there would make the result of the integral ambiguous. The integral is to be interpreted via a suitable deformation⁶ of the contour, but this is either over or under the singularity, and the results are not the same. So, without further information this would leave us with two possible but different answers!

We do know, however, that this singularity comes from the complex upper half, so we have to indent the contour *under* the pole. This is exactly in agreement with the argument of causality: a causal signal has a Fourier transform that is analytic in the lower complex half-plane, so it is safe to indent the contour into the lower half-plane. The singularity is to be considered to belong to the upper half-plane.

This example is typical of the more general case of a signal $p(t)$, described via the inverse transform of its Fourier transform. If it occurs that, due to inherent idealizations of the model, this Fourier transform has singularities along the real ω axis, the causality condition tells us how to deal with this problem. Consider the following example. The transformed harmonic-like signal

$$\hat{p}(\omega) = -\frac{\omega_0}{2\pi} \frac{1}{\omega^2 - \omega_0^2}$$

has to be analytic in the lower half plane, so that the integration contour can be closed with zero result if $t < 0$. Therefore, the contour must be indented in $\text{Im}(\omega) < 0$ around $\omega = \omega_0$ and $\omega = -\omega_0$ (figure C.1). The result is then

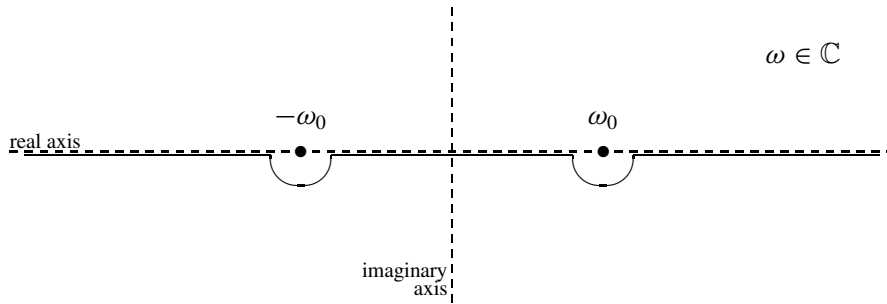


Figure C.1 Integration contour in complex ω -plane.

⁵We ignore for the moment the problem that for $\alpha = 0$ the original time signal is only Fourier transformable in the context of generalized functions.

⁶The integral of an analytic function does not change with deformation of the integration contour *within the region of analyticity*.

$$p(t) = H(t) \sin(\omega_0 t).$$

A more subtle example, dealing with complicated manipulations in two complex planes, is the following. Consider the field $p(x, t)$, described via a Fourier integral for both the x - and the t -dependence.

$$p(x, t) = \int_{-\infty}^{\infty} \int_{-\infty}^{\infty} \tilde{p}(k, \omega) e^{i\omega t - ikx} dk d\omega.$$

If $\tilde{p}(k, \omega)$, the time- and space-Fourier transformed $p(x, t)$, is given by:

$$\tilde{p}(k, \omega) = \frac{1}{4\pi^2 c_0^2} \frac{1}{k^2 - \omega^2/c_0^2}, \tag{C.16}$$

then the time-Fourier transformed $\hat{p}(x, \omega)$, given by

$$\hat{p}(x, \omega) = \frac{1}{4\pi^2 c_0^2} \int_{-\infty}^{\infty} \frac{e^{-ikx}}{k^2 - \omega^2/c_0^2} dk,$$

must be analytic in $\text{Im}(\omega) \leq 0$. This means that the contour in the complex k -plane (the real axis) must be indented up-around $k = \omega/c_0$ and down-around $k = -\omega/c_0$ (figure C.2). This is seen as

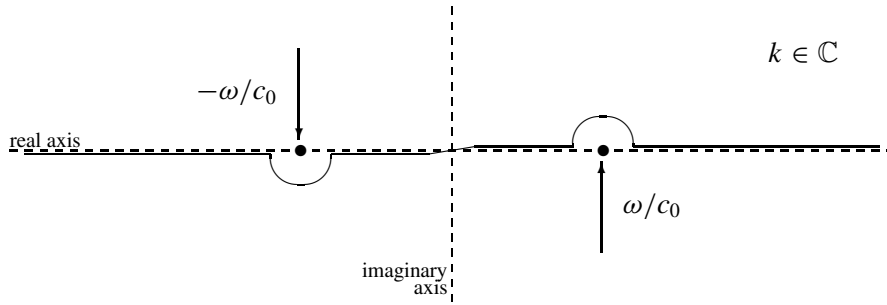


Figure C.2 Integration contour in complex k -plane. The arrows indicate the path of the poles $\pm\omega/c_0$ in the k -plane, when ω moves in its complex ω -plane from the negative imaginary half onto the real axis, as $\text{Im}(\omega) \uparrow 0$.

follows. For any value of $\pm\omega/c_0$ not on the k -contour, the integral exists and can be differentiated to ω any times, so $\hat{p}(x, \omega)$ is analytic in ω . However, when a pole $k = \omega/c_0$ or $k = -\omega/c_0$ crosses the contour, $\hat{p}(x, \omega)$ jumps discontinuously by an amount of the residue at that pole, and therefore $\hat{p}(x, \omega)$ is not analytic for any $\pm\omega/c_0$ on the contour. So, here, the value of the integral may be either the limit from above or from below. Since causality requires that $\hat{p}(x, \omega)$ is the analytic continuation from $\text{Im}(\omega) < 0$, we have to take the limit $\text{Im}(\omega) \uparrow 0$, *i.e.* from below for the pole $k = \omega/c_0$ and from above for the pole $k = -\omega/c_0$. Since a deformation of the integration contour for an analytic function

does not change the integral, these limits are most conveniently incorporated by a small deformation of the contour, in a direction opposite to the limit (Fig. C.2). The result is

$$\hat{p}(x, \omega) = \frac{e^{-i\omega|x|/c_0}}{4\pi i c_0 \omega}. \quad (\text{C.17})$$

As before, the pole $\omega = 0$ belongs to the upper ω -half plane, and we have (*c.f.* (4.84))

$$p(x, t) = \frac{1}{4\pi i c_0} \int_{-\infty}^{\infty} \frac{e^{i\omega(t-|x|/c_0)}}{\omega} d\omega = \frac{1}{2c_0} H(t - |x|/c_0). \quad (\text{C.18})$$

If we read $x - y$ for x and $t - \tau$ for t , this is just the one-dimensional Green's function. (See also below).

C.1.2 Phase and group velocity

The *phase velocity* of a wave in one spatial direction, and given by $e^{i\omega t - ikx}$ (ω and k real), is the velocity for which the phase $\omega t - kx = \text{constant}$. This is

$$v_{\text{phase}} = \frac{\omega}{k}. \quad (\text{C.19})$$

Since a harmonic wave is an idealization, any wave is really a packet of waves, with frequencies and wavenumbers related by a dispersion relation $\omega = \omega(k)$, and localized within a beginning and an end. This packet does not necessarily travel with the phase speed, but with the *group velocity*. This should also be the speed of the energy if an energy is defined.

To determine the group velocity for an *almost* harmonic wave ϕ , *i.e.* with a spatial Fourier representation concentrated near a single wave number k_0 , we may approximate

$$\begin{aligned} \phi(x, t) &= \int_{-\infty}^{\infty} \frac{f(k)}{2\varepsilon} e^{i\omega(k)t - ikx} dk \simeq \int_{k_0-\varepsilon}^{k_0+\varepsilon} \frac{f(k)}{2\varepsilon} e^{i\omega(k)t - ikx} dk \\ &\simeq \frac{f(k_0)}{2\varepsilon} e^{i\omega_0 t - ik_0 x} \int_{k_0-\varepsilon}^{k_0+\varepsilon} e^{i(k-k_0)\omega'_0 t - i(k-k_0)x} dk = f(k_0) \frac{\sin \varepsilon(x - \omega'_0 t)}{\varepsilon(x - \omega'_0 t)} e^{i\omega_0 t - ik_0 x} \end{aligned} \quad (\text{C.20})$$

with $\omega_0 = \omega(k_0)$, $\omega'_0 = \frac{d}{dk}\omega(k_0)$. This shows that ϕ is a wave packet centred around $x - \omega'_0 t = 0$, and therefore travelling with the velocity ω'_0 . In other words,

$$v_{\text{group}} = \left(\frac{d\omega}{dk} \right)_{k=k_0}. \quad (\text{C.21})$$

C.2 Generalized functions

C.2.1 Introduction

In reality dissipative effects will cause any discontinuity to be smooth and any signal to decay for $t \rightarrow \infty$, while any signal can be regarded to be absent for $t \rightarrow -\infty$. So the classical concept of (smooth) functions is more than adequate to describe any property of a real sound field. This is, however, not the case in most of our idealized models. For example, a point source of vanishing size but finite source strength cannot be described by any ordinary function: it would be something that is zero everywhere except in one point, where it is infinitely large. Another example is a non-decaying signal, even as common as $\sin(\omega t)$, which (classically) cannot be Fourier transformed: for some frequencies the Fourier integral is not defined and for others just infinitely large. Still, the spectrum of $\sin(\omega t)$, consisting of two isolated peaks at ω and $-\omega$, is almost a prototype!

Does that mean that our idealized models are wrong, or too restricted to be useful? No, not at all. Only our mathematical apparatus of functions is too restricted. It is therefore convenient, even vital for a lucid theory, to extend our meaning of function to the so-called generalized functions [124, 101, 263, 105, 65].

Technically speaking, *generalized functions* or tempered distributions are not functions with a point-wise definition. Their meaning is always defined in an integrated sense. There are many definitions and terminology⁷ of generalized function spaces, mathematically not equivalent, but all containing the elements most important in applications (delta function, Heaviside function, etc.). See for example [65].

C.2.2 Formal definition

In the present context we will follow the definition that is intuitively most appealing: the limit⁸ in a suitable function space \mathcal{G} , such that derivatives and Fourier transforms are always defined. This definition is analogous to the definition of real numbers by convergent sequences of rational numbers. We start with the space of the real, smooth, and very fast decaying *good functions*

$$\mathcal{G} \stackrel{\text{def}}{=} \left\{ f : \mathbb{R} \rightarrow \mathbb{R} \mid f^{(k)} \in C^\infty(\mathbb{R}) \text{ and } f^{(k)} = O(|x|^{-n}) (|x| \rightarrow \infty) \text{ for any } n, k \geq 0 \right\}. \quad (\text{C.22})$$

where $f^{(k)}(x) = \frac{d^k}{dx^k} f(x)$. A sequence $(f_n) \subset \mathcal{G}$ defines a generalized function if for every *testfunction* $g \in \mathcal{G}$ the sequence of real numbers

$$\lim_{n \rightarrow \infty} \int_{-\infty}^{\infty} f_n(x) g(x) dx \quad (\text{C.23})$$

⁷For example: generalized functions and tempered distributions when Fourier transformation is guaranteed, weak functions and distributions when derivatives are guaranteed.

⁸Technically termed: closure of...

exists as a real number (depending on g , of course).

Care is to be taken: although it is the limit of a sequence of ordinary functions, a generalized function is *not* an ordinary function. In particular, it is not a function with a pointwise and explicit meaning. It is only defined by the way its corresponding sequence (f_n) acts under integration. Furthermore, a generalized function may be defined by many equivalent regular sequences because it is only the limit that counts.

On the other hand, generalized functions really extend our definition of ordinary functions. It can be shown, that any reasonably behaving ordinary function is equivalent to a generalized function, and may be identified to it. Therefore, we retain the symbolism for integration, and write for a generalized function f defined by the sequence (f_n) and any $g \in \mathcal{G}$

$$\int_{-\infty}^{\infty} f(x)g(x) dx \stackrel{\text{def}}{=} \lim_{n \rightarrow \infty} \int_{-\infty}^{\infty} f_n(x)g(x) dx. \quad (\text{C.24})$$

C.2.3 The delta function and other examples

A very important generalized function is the delta function $\delta(x)$, defined (for example) by

$$\delta_n(x) = \left(\frac{n}{\pi}\right)^{1/2} e^{-nx^2}, \quad \text{or} \quad \delta_n(x) = \frac{\sin nx}{\pi x} e^{-x^2/n^2}. \quad (\text{C.25})$$

In the limit for $n \rightarrow \infty$ all contributions in the integral except from near $x = 0$ are suppressed, such that

$$\int_{-\infty}^{\infty} \delta(x)g(x) dx = g(0). \quad (\text{C.26})$$

The second expression of (C.25) illustrates that it is not necessary for a representation of $\delta(x)$ to vanish pointwise outside $x = 0$. Highly oscillatory behaviour outside the origin may be sufficient for the integral to vanish.

A useful identity is

$$\delta(ax) = \frac{1}{|a|} \delta(x), \quad (\text{C.27})$$

which at the same time shows that a delta function is not necessarily dimensionless, as it has the inverse dimension of its argument (or put in another way: $\delta(x)dx$ is dimensionless). A generalization of this identity yields, for a sufficiently smooth function h with $h' = \frac{dh}{dx} \neq 0$ at any zero of h , the following result:

$$\int_{-\infty}^{\infty} \delta(h(x))g(x) dx = \sum_i \frac{g(x_i)}{|h'(x_i)|}, \quad h(x_i) = 0 \quad (\text{C.28})$$

where the summation runs over all the zeros of h . This result may be derived from the fact that $\delta(h(x))$ is locally, near a zero x_i , equivalent to $\delta(h'(x_i)(x - x_i))$, so that $\delta(h(x)) = \sum \delta(x - x_i)/|h'(x_i)|$.

The sequence

$$H_n(x) = \left(\frac{1}{2} \tanh(nx) + \frac{1}{2}\right) e^{-x^2/n^2}$$

defines the Heaviside stepfunction $H(x)$. If the Heaviside generalized function is used as an ordinary function it has the pointwise definition

$$H(x) = \begin{cases} 0 & (x < 0) \\ \frac{1}{2} & (x = 0) \\ 1 & (x > 0) \end{cases} \tag{C.29}$$

Any C^∞ -function f , with algebraic behaviour for $|x| \rightarrow \infty$ (for example, polynomials), defines a generalized function (also called f) via the sequence $f_n(x) = f(x) \exp(-x^2/n^2)$, since for any good g

$$\lim_{n \rightarrow \infty} \int_{-\infty}^{\infty} f_n(x) g(x) dx = \int_{-\infty}^{\infty} f(x) g(x) dx.$$

Any C^∞ -function h with algebraic behaviour for $|x| \rightarrow \infty$ multiplied by a good function is a good function, so that the product of such a h with a generalized function f is well-defined. For example, the equation

$$xf(x) = 0$$

has a meaning in generalized sense, with the solution

$$f(x) = C\delta(x) \tag{C.30}$$

which is unique, up to the multiplicative constant C .

C.2.4 Derivatives

Every generalized function f defined by (f_n) has a derivative f' defined by (f'_n) , and also satisfying

$$\int_{-\infty}^{\infty} f'(x)g(x) dx = - \int_{-\infty}^{\infty} f(x)g'(x) dx. \tag{C.31}$$

Although generalized functions do not have a pointwise meaning, they are not arbitrarily *wild*. We have the general form given by the following theorem ([101, p.84]).

Theorem C.2 (General representation)

A necessary and sufficient condition for $f(x)$ to be a generalized function, is that there exist a continuous function $h(x)$ and positive numbers r and k such that $f(x)$ is a generalized r -th order derivative of $h(x)$

$$f(x) = \frac{d^r}{dx^r} h(x)$$

while $h(x)$ has the property that

$$\frac{h(x)}{(1+x^2)^{k/2}}$$

is bounded on \mathbb{R} .

For example:

$$\text{sign}(x) = 1 + 2H(x) = \frac{d}{dx}|x|, \quad \delta(x) = \frac{1}{2} \frac{d^2}{dx^2}|x|.$$

By differentiation of the equation $x\delta(x) = 0$ we obtain for the n -th derivative $\delta^{(n)}(x)$ the identity

$$x^n \delta^{(n)}(x) = (-1)^n n! \delta(x).$$

C.2.5 Fourier transforms

Every generalized function f defined by (f_n) has a Fourier transform \hat{f} defined by (\hat{f}_n) which is itself a generalized function. Indeed, since the Fourier transform \hat{g} of a good function g is a good function, we have using the convolution theorem a well-defined

$$\begin{aligned} \int_{-\infty}^{\infty} \hat{f}(\omega) \hat{g}(\omega) d\omega &= \lim_{n \rightarrow \infty} \int_{-\infty}^{\infty} \hat{f}_n(\omega) \hat{g}(\omega) d\omega = \frac{1}{2\pi} \lim_{n \rightarrow \infty} \int_{-\infty}^{\infty} f_n(x) g(-x) dx \\ &= \frac{1}{2\pi} \int_{-\infty}^{\infty} f(x) g(-x) dx. \end{aligned} \quad (\text{C.32})$$

Examples of Fourier transforms are

$$\begin{aligned} \frac{1}{2\pi} \int_{-\infty}^{\infty} \delta(x) e^{-i\omega x} dx &= \frac{1}{2\pi} \\ \frac{1}{2\pi} \int_{-\infty}^{\infty} e^{-i\omega x} dx &= \delta(\omega) \\ \frac{1}{2\pi} \int_{-\infty}^{\infty} \cos(\omega_0 x) e^{-i\omega x} dx &= \frac{1}{2} \delta(\omega - \omega_0) + \frac{1}{2} \delta(\omega + \omega_0), \\ \frac{1}{2\pi} \int_{-\infty}^{\infty} H(x) e^{-i\omega x} dx &= \text{P.V.} \left(\frac{1}{\pi i \omega} \right) + \frac{1}{2} \delta(\omega) = \frac{1}{2\pi i (\omega - i0)} \end{aligned} \quad (\text{C.33})$$

where P.V. denotes “principal value”, which means that under the integration sign the singularity is to be excluded in the following symmetric way: $P.V. \int_{-\infty}^{\infty} = \lim_{\varepsilon \downarrow 0} \int_{-\infty}^{-\varepsilon} + \int_{\varepsilon}^{\infty}$. The notation $\omega - i0$ means that the pole $\omega = 0$ is assumed to belong to the complex upper half plane, similar to (C.17).

If $-i \cotg(\omega)$ is a causal Fourier transform, the poles $\omega = n\pi$ belong to the complex upper half plane. In order to make sure that we approach the poles from the right side, we write

$$-i \cotg(\omega) = 1 + 2 \frac{e^{-2i\omega}}{1 - e^{-2i\omega}} = 1 + 2 \lim_{\varepsilon \downarrow 0} \sum_{n=1}^{\infty} e^{-2in\omega - 2\varepsilon n} = 1 + 2 \sum_{n=1}^{\infty} e^{-2in\omega},$$

and obtain for the back transform to time domain

$$\int_{-\infty}^{\infty} -i \cotg(\omega) e^{i\omega t} d\omega = 2\pi \delta(t) + 4\pi \sum_{n=1}^{\infty} \delta(t - 2n). \tag{C.34}$$

C.2.6 Products

Products of generalized functions are in general not defined. For example, depending on the defining sequences of $\delta(x)$ and $H(x)$, we may get $\delta(x)H(x) = C\delta(x)$ for any finite C . Therefore, integration along a semi-infinite or finite interval, which is to be interpreted as a multiplication of the integrand with suitable Heaviside functions, is not always defined.

Two generalized functions may be multiplied only when either of the two is locally equivalent to an ordinary function, or as a direct product when they depend on different variables. Some results are

$$\begin{aligned} \delta(x)H(x + 1) &= \delta(x), \\ \int_{-x_0}^{x_0} \delta(x) f(x) dx &= \int_{-\infty}^{\infty} \delta(x) f(x) dx \quad \text{if } x_0 > 0, \\ \int_{-\infty}^{\infty} \int_{-\infty}^{\infty} \delta(x)\delta(t) f(x, t) dt dx &= \int_{-\infty}^{\infty} \delta(x) \left[\int_{-\infty}^{\infty} \delta(t) f(x, t) dt \right] dx, \\ \int_{-\infty}^{\infty} \delta(t - \tau)\delta(\tau) d\tau &= \delta(t). \end{aligned}$$

C.2.7 Higher dimensions and Green’s functions

A generalization to several dimensions is possible [217], and many results are fairly straightforward after an obvious introduction of multi-dimensional good functions. For example, we may define a new generalized function $f(x)g(y)$ in \mathbb{R}^2 by the direct product of $f(x)$ and $g(y)$. For the delta function in \mathbb{R}^3 this leads to

$$\delta(\mathbf{x}) = \delta(x)\delta(y)\delta(z)$$

Care is required near the singular points of a coordinate transformation. For example, provided $\delta'(r)$ is considered to be an odd function in r , the 2-D delta function $\delta(\mathbf{x} - \mathbf{x}_0)$ may be written in polar coordinates ([101, p.306]) as

$$\delta(\mathbf{x} - \mathbf{x}_0) = \begin{cases} \frac{\delta(r - r_0)}{r_0} \sum_{n=-\infty}^{\infty} \delta(\vartheta - \vartheta_0 - 2\pi n) & \text{if } r_0 \neq 0, \\ -\frac{\delta'(r)}{\pi} & (r \geq 0) \quad \text{if } r_0 = 0. \end{cases} \quad (\text{C.35})$$

Relevant in the theory of 2-D incompressible potential flow are the following identities. The line source is a delta function source term in the mass equation:

$$\mathbf{v} = \frac{1}{r}(\cos \theta, \sin \theta, 0) \quad \text{satisfies} \quad \nabla \cdot \mathbf{v} = 2\pi \delta(x, y). \quad (\text{C.36a})$$

The line vortex is a delta function type vorticity field:

$$\mathbf{v} = \frac{1}{r}(-\sin \theta, \cos \theta, 0) \quad \text{satisfies} \quad \nabla \times \mathbf{v} = 2\pi \delta(x, y) \mathbf{e}_z. \quad (\text{C.36b})$$

A most important application of (more-dimensional) delta functions in the present context is that they allow a very direct definition of Green's functions. Classically, the Green's function G is defined in a rather complicated way, but in the context of generalized functions it appears to be just the field resulting from a delta function source. Consider for example the one dimensional wave equation (*c.f.* (4.81))

$$\frac{\partial^2 G}{\partial t^2} - c_0^2 \frac{\partial^2 G}{\partial x^2} = \delta(x - y) \delta(t - \tau).$$

After Fourier transformation to t and x we obtain

$$-\omega^2 \tilde{G} + c_0^2 k^2 \tilde{G} = \frac{1}{4\pi^2} e^{-i\omega\tau} e^{iky}$$

which yields equation (C.16) (apart from the amplitude) and then, after the described transformation back into space and time domain, the Green's function given by expression (C.18).

See Appendix E for a table of free field Green's functions in 1-, 2-, and 3-D, for the Laplace, Helmholtz, wave, and heat equations.

C.2.8 Surface distributions

Of particular interest are the so-called surface distributions $\delta_\Sigma(\mathbf{x})$ defined by the surface integral

$$\int_{\mathbb{R}^3} \delta_\Sigma(\mathbf{x}) \phi(\mathbf{x}) d\mathbf{x} = \int_\Sigma \phi(\mathbf{x}) d\sigma \quad (\text{C.37})$$

where ϕ is an arbitrary test function, and Σ denotes a smooth surface in \mathbb{R}^3 with surface element $d\sigma$. In practice, a surface is often defined by an equation $S(\mathbf{x}) = 0$ (section A.3). Near a point \mathbf{x}_0 on the surface, $S(\mathbf{x})$ varies to leading order only in the direction of the surface normal $\mathbf{e}_\nu = \nabla S_0 / |\nabla S_0|$,

$$S(\mathbf{x}) = (\mathbf{x} - \mathbf{x}_0) \cdot \nabla S_0 + \dots \simeq |\nabla S_0| \nu,$$

where $\nu = (\mathbf{x} - \mathbf{x}_0) \cdot \mathbf{e}_\nu$ and S_0 indicates evaluation at x_0 . Since δ_Σ is locally, after a suitable rotation and transformation of coordinates, equivalent to a one-dimensional delta function in ν , the coordinate normal to the surface, we have

$$\delta_\Sigma(\mathbf{x}) = \delta(\nu) = |\nabla S_0| \delta(|\nabla S_0| \nu) = |\nabla S_0| \delta(S). \tag{C.38}$$

Note that this result is in fact a generalization of formula (C.28). For sufficiently smooth h we have

$$\int_{\mathbb{R}^3} \delta(h(\mathbf{x})) g(\mathbf{x}) d\mathbf{x} = \sum_i \int_{\mathcal{S}_i} \frac{g(\mathbf{x})}{|\nabla h(\mathbf{x})|} d\sigma \tag{C.39}$$

where the summation runs over all the surfaces \mathcal{S}_i defined by the equation $h(\mathbf{x}) = 0$.

This concept of surface distributions has numerous important applications. For example, integral theorems like that of Gauss or Green [105], and Reynolds' Transport Theorem (section A.1) may be derived very elegantly and efficiently. We show it for Reynolds' Theorem and leave Gauss' theorem as an exercise.

Consider a finite volume $\mathcal{V} = \mathcal{V}(t)$ with sufficiently smooth surface $\mathcal{S} = \mathcal{S}(t)$, moving continuously in space. Introduce a (smooth) function $f(\mathbf{x}, t)$ such that

$$f(\mathbf{x}, t) \begin{cases} > 0 & \text{if } \mathbf{x} \in \mathcal{V}(t), \\ = 0 & \text{if } \mathbf{x} \in \mathcal{S}(t), \\ < 0 & \text{if } \mathbf{x} \notin \mathcal{V}(t), \end{cases}$$

but otherwise arbitrary. Since $\nabla f|_{f=0}$ is directed normal inwards into \mathcal{V} , the outward normal $\mathbf{n}_\mathcal{S}$ of \mathcal{S} is given by (section A.3)

$$\mathbf{n}_\mathcal{S}(\mathbf{x}, t) = - \left. \frac{\nabla f}{|\nabla f|} \right|_{f=0}.$$

Let the surface $\mathcal{S}(t)$ be parametrized in time and space, by coordinates $(t; \lambda, \mu)$. Like the auxiliary function f , this parametrization is not unique, but that will appear to be of no importance. A surface point $\mathbf{x}_\mathcal{S}(t) \in \mathcal{S}$ (consider λ and μ fixed), moving with velocity $\mathbf{b} = \dot{\mathbf{x}}_\mathcal{S}$, remains at the surface for all time, so $f(\mathbf{x}_\mathcal{S}(t), t) = 0$ for all t , and therefore also its time-derivative, and so

$$\frac{\partial f}{\partial t} = - \dot{\mathbf{x}}_\mathcal{S} \cdot \nabla f = |\nabla f| \mathbf{b} \cdot \mathbf{n}_\mathcal{S}.$$

The variation of a quality $F(\mathbf{x}, t)$, integrated over \mathcal{V} , is now given by

$$\begin{aligned} \frac{d}{dt} \int_{\mathcal{V}} F(\mathbf{x}, t) \, d\mathbf{x} &= \frac{d}{dt} \int_{\mathbb{R}^3} H(f) F(\mathbf{x}, t) \, d\mathbf{x} \\ &= \int_{\mathbb{R}^3} \left[H(f) \frac{\partial}{\partial t} F(\mathbf{x}, t) + \delta(f) \frac{\partial f}{\partial t} F(\mathbf{x}, t) \right] \, d\mathbf{x} \\ &= \int_{\mathcal{V}} \frac{\partial}{\partial t} F(\mathbf{x}, t) \, d\mathbf{x} + \int_{\mathcal{S}} (\mathbf{b} \cdot \mathbf{n}_S) F(\mathbf{x}, t) \, d\sigma. \end{aligned} \quad (\text{C.40})$$

where H denotes the Heaviside function, and use is made of equation (C.38). Note that, although in general \mathbf{b} is not unique, its normal component $\mathbf{b} \cdot \mathbf{n}_S$ is unique, in particular it is independent of the selected function f and parametrization.

C.3 Fourier series

A Fourier series (in complex form) is the following function $f(x)$, defined by the infinite sequence $\{c_n\}_{n=-\infty}^{\infty}$,

$$f(x) = \sum_{n=-\infty}^{\infty} c_n e^{2\pi i n x / L}. \quad (\text{C.41})$$

If the series converges, f is periodic with period L . For sufficiently well-behaved functions f the coefficients are given by

$$c_n = \frac{1}{L} \int_0^L f(x) e^{-2\pi i n x / L} \, dx. \quad (\text{C.42})$$

Classically, the Fourier series precedes both the Fourier transform and generalized functions. The classic theory is, however, rather complicated. On the other hand, Fourier series appear to have a much simpler structure when they are embedded in the generalized functions, in the following sense.

Fourier series are equivalent to the Fourier transform of periodic generalized functions.

A generalized function f is said to be periodic, with period L , if a coordinate shift

$$f(x) = f(x + L)$$

yields the same generalized function. We have the following couple of theorems ([124, 263]), telling us when a Fourier series is a generalized function, and *vice versa*.

Theorem C.3 (From Fourier series to generalized function)

A Fourier series (C.41) converges⁹ to a generalized function if and only if the coefficients c_n are of slow growth. This means, that there is a constant N such that $c_n = O(|n|^N)$ for $|n| \rightarrow \infty$. The generalized function it defines is periodic and unique.

Theorem C.4 (From generalized function to Fourier series)

The most general periodic generalized function is just the Fourier series: any periodic generalized function can be written as a Fourier series with Fourier coefficients c_n , while the Fourier transform is a periodic array of delta functions:

$$f(x) = \sum_{n=-\infty}^{\infty} c_n e^{2\pi i n x / L}, \quad (\text{C.43a})$$

$$\hat{f}(\omega) = \sum_{n=-\infty}^{\infty} c_n \delta\left(\omega - \frac{2\pi n}{L}\right), \quad c_n = \frac{1}{L} \int_{-\infty}^{\infty} f(x) U\left(\frac{x}{L}\right) e^{-2\pi i n x / L} dx. \quad (\text{C.43b})$$

Any Fourier series can be differentiated and integrated term by term.

$U \in C^\infty$ is an auxiliary smoothing function with the following properties:

$$U(x) = 0 \text{ for } |x| \geq 1, \quad U(x) + U(x-1) = 1 \text{ for } 0 \leq x \leq 1,$$

but otherwise arbitrary. U is necessary because a generalized function may not be integrable along a finite interval (for example, when singularities coincide with the end points).

If we are dealing with a generalized function defined by a *periodic absolutely-integrable ordinary function*, then U is not necessary, and the expression for c_n simplifies to the classical form (C.42). Although in such a case the Fourier series may converge in ordinary sense, this is not guaranteed, and the Fourier series is still to be interpreted in a generalized sense.

Examples are the “row of delta’s”

$$\sum_{n=-\infty}^{\infty} \delta(x-n) = \sum_{n=-\infty}^{\infty} e^{2\pi i n x} = 1 + 2 \sum_{n=1}^{\infty} \cos(2\pi n x), \quad (\text{C.44a})$$

with its Fourier transform

$$\frac{1}{2\pi} \sum_{n=-\infty}^{\infty} e^{-i\omega n} = \sum_{n=-\infty}^{\infty} \delta(\omega - 2\pi n), \quad (\text{C.44b})$$

and its N -th derivative

$$\sum_{n=-\infty}^{\infty} \delta^{(N)}(x-n) = \sum_{n=-\infty}^{\infty} (2\pi i n)^N e^{2\pi i n x}. \quad (\text{C.44c})$$

⁹As the generalized limit of, for example, $f_m(x) = \exp(-x^2/m^2) \sum_{n=-m}^m c_n e^{2\pi i n x / L}$.

Furthermore, the sawtooth or N-wave with simple discontinuities at $x = m$ ($m \in \mathbb{Z}$)

$$\left[\frac{1}{2} - x\right]_1 = \sum'_{n=-\infty}^{\infty} \frac{e^{2\pi i n x}}{2\pi i n} = \sum_{n=1}^{\infty} \frac{\sin(2\pi n x)}{\pi n}, \quad (\text{C.44d})$$

and a sequence of parabola's, continuous at $x = m$ ($m \in \mathbb{Z}$)

$$\frac{1}{2}\left[x - x^2 - \frac{1}{6}\right]_1 = \sum'_{n=-\infty}^{\infty} \frac{e^{2\pi i n x}}{(2\pi i n)^2} = -\sum_{n=1}^{\infty} \frac{\cos(2\pi n x)}{2\pi^2 n^2}. \quad (\text{C.44e})$$

\sum' denotes a sum excluding $n = 0$, $[\cdot]_L$ denotes the L -periodic continuation of a function $f(x)$ defined on the interval $[0, L]$:

$$\left[f(x)\right]_L = \sum_{n=-\infty}^{\infty} B\left(\frac{x}{L} - n\right) f(x - nL),$$

and B denotes the unit block function

$$B(x) = H(x) - H(x - 1) \equiv \begin{cases} 1 & \text{if } 0 \leq x \leq 1, \\ 0 & \text{otherwise.} \end{cases}$$

Apart from an additional x and $\frac{1}{2}x^2$, (C.44d) is the first integral and (C.44e) is the second integral of the row of delta's of (C.44a). In general it is true that any generalized Fourier series, with coefficients $c_n = O(|n|^N)$ ($|n| \rightarrow \infty$), is the $(N + 2)$ -th derivative of a continuous function. This shows that there is a limit to the seriousness of the singularities that these functions can have [124].

Related examples of some interest are:

$$-\log |2 \sin \pi x| = \sum_{n=1}^{\infty} \frac{\cos(2\pi n x)}{n}, \quad (\text{C.45a})$$

$$\frac{1}{2} \cotg(\pi x) = \sum_{n=1}^{\infty} \sin(2\pi n x), \quad (\text{C.45b})$$

$$-\frac{1}{2} \tan(\pi x) = \sum_{n=1}^{\infty} (-1)^n \sin(2\pi n x), \quad (\text{C.45c})$$

$$|\sin x| = \frac{2}{\pi} - \frac{1}{\pi} \sum_{n=1}^{\infty} \frac{\cos(2n x)}{n^2 - \frac{1}{4}}. \quad (\text{C.45d})$$

$$\sin x |\sin x| = -\frac{1}{\pi} \sum_{n=0}^{\infty} \frac{\sin(2n + 1)x}{(n^2 - \frac{1}{4})(n + \frac{3}{2})} \quad (\text{C.45e})$$

Until now we have considered only generalized Fourier series because of their more transparent properties. We have to be very cautious, however, when dealing in practice with divergent series. No attempt must be made to sum such a series numerically term by term! Numerical evaluation is only possible for classically convergent Fourier series. Some important results are the following.

For a given function f we have the following

Theorem C.5 (Existence of ordinary Fourier series)

If a function f is piecewise smooth¹⁰ on the interval $[0, L]$, such that $f(x) = \frac{1}{2}[f(x+) + f(x-)]$, then the Fourier series of f converges for every x to the L -periodic continuation of f .

For a given Fourier series we have the following

Theorem C.6 (Continuity of ordinary Fourier series)

If a Fourier series is absolutely convergent, i.e. $\sum |c_n| < \infty$, then it converges absolutely and uniformly to a continuous periodic function f , such that c_n are just f 's Fourier coefficients.

An example of the first theorem is (C.44d). Note that the similar looking (C.45a) just falls outside this category. Examples of the second are (C.44e) and (C.45d).

C.3.1 The Fast Fourier Transform

The standard numerical implementation of the calculation of a Fourier transform or Fourier coefficient is the *Fast Fourier Transform* algorithm [36]. This algorithm calculates for a given complex array $\{y_j\}$, $j = 0, \dots, N-1$ very efficiently (especially if N is a power of 2) the Discrete Fourier Transform

$$Y_k = \sum_{j=0}^{N-1} y_j \exp(-2\pi i j k / N), \quad k = 0, \dots, N-1. \quad (\text{C.46})$$

A Fourier coefficient (C.42) is calculated by discretizing the integral

$$c_n = \frac{1}{T} \int_0^T f(t) e^{-i\omega_n t} dt \simeq \frac{1}{T} \sum_{j=0}^{N-1} f(t_j) e^{-i\omega_n t_j} \frac{T}{N}, \quad \omega_n = \frac{2\pi n}{T}, \quad t_j = \frac{jT}{N}$$

and identifying $y_j = f(t_j)$ and $Y_n = Nc_n$.

¹⁰ f is piecewise continuous on $[0, L]$ if there are a finite number of open subintervals $0 < x < x_1, \dots, x_{N-1} < x < L$ on which f is continuous, while the limits $f(0+)$, $f(x_1\pm)$, \dots , $f(L-)$ exist. f is piecewise smooth if both f and f' are piecewise continuous.

A Fourier transform (C.1) is determined as follows. Restrict the infinite integral to a large enough finite interval $[-\frac{1}{2}T, \frac{1}{2}T]$, and consider only the values $\omega = \omega_k = 2\pi k/T$, for $k = -\frac{1}{2}N, \dots, \frac{1}{2}N - 1$, such that $e^{-i\omega_k T} = 1$ for all k . Then we have

$$\begin{aligned} F(\omega) &= \frac{1}{2\pi} \int_{-\infty}^{\infty} f(t) e^{-i\omega t} dt \simeq \frac{1}{2\pi} \int_{-\frac{1}{2}T}^{\frac{1}{2}T} f(t) e^{-i\omega t} dt \\ &= \frac{1}{2\pi} \int_0^{\frac{1}{2}T} f(t) e^{-i\omega t} dt + \frac{1}{2\pi} \int_{\frac{1}{2}T}^T f(t-T) e^{-i\omega t} dt. \end{aligned}$$

If we finally discretize the integrals

$$F(\omega_k) \simeq \frac{T}{2\pi N} \sum_{j=0}^{\frac{1}{2}N-1} f(t_j) e^{-i\omega_k t_j} + \frac{T}{2\pi N} \sum_{j=\frac{1}{2}N}^{N-1} f(t_j - T) e^{-i\omega_k t_j}.$$

we obtain the required result by identifying¹¹

$$y_j = \begin{cases} f(t_j) & \text{if } 0 \leq j \leq \frac{1}{2}N - 1, \\ f(t_j - T) & \text{if } \frac{1}{2}N \leq j \leq N - 1, \end{cases}$$

$$F(\omega_k) = \frac{T}{2\pi N} \begin{cases} Y_{k+N} & \text{if } -\frac{1}{2}N \leq k \leq -1, \\ Y_k & \text{if } 0 \leq k \leq \frac{1}{2}N - 1. \end{cases}$$

¹¹With parameters T and N and function f given, the above procedure can be written as the following MATLAB script

```
t = [-N/2 : N/2 - 1] * T/N;
w = [-N/2 : N/2 - 1] * 2 * pi/T;
F = (T/2/pi/N) * circshift(fft(circshift(f(t), N/2)), N/2);
```

D Bessel functions

The Bessel equation for integer m

$$y'' + \frac{1}{x}y' + \left(1 - \frac{m^2}{x^2}\right)y = 0 \quad (\text{D.1})$$

has two independent solutions [254, 1, 60, 74, 130]. Standardized forms are

$$J_m(x), \text{ } m\text{-th order ordinary Bessel function of the 1st kind,} \quad (\text{D.2a})$$

$$Y_m(x), \text{ } m\text{-th order ordinary Bessel function of the 2nd kind.} \quad (\text{D.2b})$$

J_m is regular in $x = 0$; Y_m is singular in $x = 0$ with branch cut along $x < 0$; for $m \geq 0$ is:

$$J_m(x) = \sum_{k=0}^{\infty} \frac{(-1)^k \left(\frac{1}{2}x\right)^{m+2k}}{k!(m+k)!} \quad (\text{D.3})$$

$$Y_m(x) = -\frac{1}{\pi} \sum_{k=0}^{m-1} \frac{(m-k-1)!}{k!} \left(\frac{1}{2}x\right)^{-m+2k} + \frac{2}{\pi} \log\left(\frac{1}{2}x\right) J_m(x) - \frac{1}{\pi} \sum_{k=0}^{\infty} \left\{ \psi(k+1) + \psi(m+k+1) \right\} \frac{(-1)^k \left(\frac{1}{2}x\right)^{m+2k}}{k!(m+k)!}$$

$$\text{with } \psi(1) = -\gamma, \quad \psi(n) = -\gamma + \sum_{k=1}^{n-1} \frac{1}{k}, \quad \gamma = 0.577215664901532$$

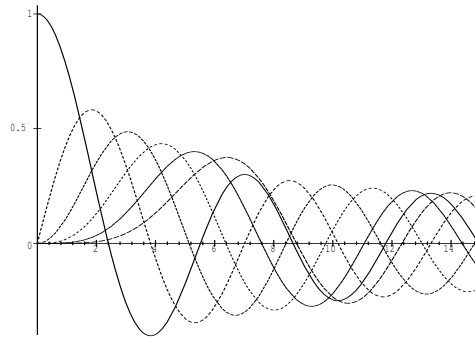


Figure D.1 Bessel function $J_n(x)$ as function of order and argument.

$$J_m(-x) = (-1)^m J_m(x), \quad (\text{D.4})$$

$$Y_m(-x) = \begin{cases} (-1)^m (Y_m(x) - 2i J_m(x)), & 0 < \arg(x) \leq \pi, \\ (-1)^m (Y_m(x) + 2i J_m(x)), & -\pi < \arg(x) \leq 0. \end{cases} \quad (\text{D.5})$$

$$J_{-m}(x) = (-1)^m J_m(x), \quad (\text{D.6})$$

$$Y_{-m}(x) = (-1)^m Y_m(x). \quad (\text{D.7})$$

Other common independent sets of solutions are the Hankel functions

$$H_m^{(1)}(x) = J_m(x) + iY_m(x), \quad (\text{D.8a})$$

$$H_m^{(2)}(x) = J_m(x) - iY_m(x). \quad (\text{D.8b})$$

Related are the modified Bessel functions of the 1st and 2nd kind

$$I_m(x) = (-i)^m J_m(ix) = i^m J_m(-ix) \quad (\text{D.9a})$$

$$K_m(x) = \begin{cases} \frac{1}{2}\pi i^{m+1} H_m^{(1)}(ix) & , \quad -\pi < \arg(x) \leq \frac{1}{2}\pi, \\ \frac{1}{2}\pi i^{m+1} H_m^{(1)}(ix) - 2\pi i^{m+1} J_m(ix) & , \quad \frac{1}{2}\pi < \arg(x) \leq \pi, \end{cases} \quad (\text{D.9b})$$

$$= \begin{cases} \frac{1}{2}\pi (-i)^{m+1} H_m^{(2)}(-ix) & , \quad -\frac{1}{2}\pi < \arg(x) \leq \pi, \\ \frac{1}{2}\pi (-i)^{m+1} H_m^{(2)}(-ix) - 2\pi (-i)^{m+1} J_m(-ix), & -\pi < \arg(x) \leq -\frac{1}{2}\pi, \end{cases} \quad (\text{D.9c})$$

satisfying

$$y'' + \frac{1}{x}y' - \left(1 + \frac{m^2}{x^2}\right)y = 0 \quad (\text{D.10})$$

I_m is regular in $x = 0$, K_m is singular in $x = 0$ with branch cut along $x < 0$.

$$I_m(-x) = (-1)^m I_m(x) \quad (\text{D.11})$$

$$K_m(-x) = \begin{cases} (-1)^m K_m(x) + \pi i I_m(x), & 0 < \arg(x) \leq \pi, \\ (-1)^m K_m(x) - \pi i I_m(x), & -\pi < \arg(x) \leq 0, \end{cases} \quad (\text{D.12})$$

$$I_{-m}(x) = I_m(x), \quad (\text{D.13})$$

$$K_{-m}(x) = K_m(x). \quad (\text{D.14})$$

Wronskians (with prime ' denoting derivative):

$$J_m(x)Y'_m(x) - Y_m(x)J'_m(x) = 2/\pi x \quad (\text{D.15})$$

$$H_m^{(1)}(x)H_m^{(2)'}(x) - H_m^{(2)}(x)H_m^{(1)'}(x) = -4i/\pi x \quad (\text{D.16})$$

$$I_m(x)K'_m(x) - K_m(x)I'_m(x) = -1/x \quad (\text{D.17})$$

$$J_m(x)Y_{m+1}(x) - Y_m(x)J_{m+1}(x) = -2/\pi x \quad (\text{D.18})$$

$$I_m(x)K_{m+1}(x) + K_m(x)I_{m+1}(x) = 1/x \quad (\text{D.19})$$

$J_m(x)$ and $J'_m(x)$ have an infinite number of real zeros, all of which are simple with the possible exception of $x = 0$. The μ -th positive ($\neq 0$) zeros are denoted by $j_{m\mu}$ and $j'_{m\mu}$ respectively, except that $x = 0$ is counted as the first zero of J'_0 : $j'_{01} = 0$. It follows that $j'_{0,\mu} = j_{1,\mu-1}$.

Asymptotically the zeros behave like

$$j_{m\mu} \simeq (\mu + \frac{1}{2}m - \frac{1}{4})\pi + O(\mu^{-1}) \quad (\mu \rightarrow \infty) \quad (\text{D.20a})$$

$$j'_{m\mu} \simeq (\mu + \frac{1}{2}m - \frac{3}{4})\pi + O(\mu^{-1}) \quad (\mu \rightarrow \infty) \quad (\text{D.20b})$$

$$j'_{m1} \simeq m + 0.8086 m^{1/3} + O(m^{-1/3}) \quad (m \rightarrow \infty). \quad (\text{D.20c})$$

Not only asymptotically but in general it is true that $j'_{m1} \geq m$.

Asymptotic behaviour for $x \rightarrow 0$:

$$J_m(x) \simeq (\frac{1}{2}x)^m/m!, \quad (\text{D.21})$$

$$Y_0(x) \simeq 2 \log(x)/\pi, \quad (\text{D.22})$$

$$Y_m(x) \simeq -(m-1)! (\frac{1}{2}x)^{-m}/\pi, \quad (\text{D.23})$$

$$H_0^{(1,2)}(x) \simeq \pm 2i \log(x)/\pi, \quad (\text{D.24})$$

$$H_m^{(1,2)}(x) \simeq \mp i(m-1)! (\frac{1}{2}x)^{-m}/\pi, \quad (\text{D.25})$$

$$I_m(x) \simeq (\frac{1}{2}x)^m/m!, \quad (\text{D.26})$$

$$K_0(x) \simeq -\log(x), \quad (\text{D.27})$$

$$K_m(x) \simeq \frac{1}{2}(m-1)! (\frac{1}{2}x)^{-m}, \quad (\text{D.28})$$

Asymptotic behaviour for $|x| \rightarrow \infty$ and m fixed:

$$J_m(x) \simeq (\frac{1}{2}\pi x)^{-\frac{1}{2}} \cos(x - \frac{1}{2}m\pi - \frac{1}{4}\pi), \quad (\text{D.29})$$

$$Y_m(x) \simeq (\frac{1}{2}\pi x)^{-\frac{1}{2}} \sin(x - \frac{1}{2}m\pi - \frac{1}{4}\pi), \quad (\text{D.30})$$

$$H_m^{(1,2)}(x) \simeq (\frac{1}{2}\pi x)^{-\frac{1}{2}} \exp[\pm i(x - \frac{1}{2}m\pi - \frac{1}{4}\pi)], \quad (\text{D.31})$$

$$I_m(x) \simeq (2\pi x)^{-\frac{1}{2}} e^x, \quad (|\arg(x)| < \frac{1}{2}\pi), \quad (\text{D.32})$$

$$K_m(x) \simeq (2x/\pi)^{-\frac{1}{2}} e^{-x}, \quad (|\arg(x)| < \frac{3}{2}\pi). \quad (\text{D.33})$$

Asymptotic behaviour for $|x| \rightarrow \infty$ and m^2/x fixed:

$$J_m(x) \simeq (\frac{1}{2}\pi x)^{-\frac{1}{2}} \cos(x - \frac{1}{2}\pi m - \frac{1}{4}\pi + \frac{1}{2}(m^2 - \frac{1}{4})x^{-1}), \quad (\text{D.34})$$

$$Y_m(x) \simeq (\frac{1}{2}\pi x)^{-\frac{1}{2}} \sin(x - \frac{1}{2}\pi m - \frac{1}{4}\pi + \frac{1}{2}(m^2 - \frac{1}{4})x^{-1}), \quad (\text{D.35})$$

$$H_m^{(1,2)}(x) \simeq (\frac{1}{2}\pi x)^{-\frac{1}{2}} \exp[\pm i(x - \frac{1}{2}\pi m - \frac{1}{4}\pi + \frac{1}{2}(m^2 - \frac{1}{4})x^{-1})], \quad (\text{D.36})$$

with absolute accuracy of $<1\%$ along $x > 2 + 2m + \frac{1}{13}m^{1.5}$ for any $0 \leq m \leq 100$. The corresponding approximating zero's of J_m and J'_m (and similarly for Y_m) are easily found to be

$$j_{m\mu} \simeq \frac{1}{2}(\mu + \frac{1}{2}m - \frac{1}{4})\pi + \frac{1}{2}\sqrt{(\mu + \frac{1}{2}m - \frac{1}{4})^2\pi^2 - 2m^2 + \frac{1}{2}}, \quad (\text{D.37})$$

$$j'_{m\mu} \simeq \frac{1}{2}(\mu + \frac{1}{2}m - \frac{3}{4})\pi + \frac{1}{2}\sqrt{(\mu + \frac{1}{2}m - \frac{3}{4})^2\pi^2 - 2m^2 + \frac{1}{2}}. \quad (\text{D.38})$$

Asymptotic behaviour for $m \rightarrow \infty$:

$$J_m(x) \simeq (2\pi m)^{-\frac{1}{2}} (ex/2m)^m, \quad (\text{D.39})$$

$$J_m(m) \simeq 2^{\frac{1}{3}} / (3^{\frac{2}{3}} \Gamma(\frac{2}{3}) m^{\frac{1}{3}}), \quad (\text{D.40})$$

$$J_m(mx) \simeq \begin{cases} (\frac{1}{2}\pi m \zeta_+)^{-\frac{1}{2}} \cos(m\zeta_+ - m \arctan \zeta_+ - \frac{1}{4}\pi), \\ (2\pi m \zeta_-)^{-\frac{1}{2}} \exp(m\zeta_- - m \operatorname{artanh} \zeta_-), \end{cases} \quad (\text{D.41})$$

$$Y_m(x) \simeq -(\frac{1}{2}\pi m)^{-\frac{1}{2}} (ex/2m)^{-m}, \quad (\text{D.42})$$

$$Y_m(m) \simeq -2^{\frac{1}{3}} / (3^{\frac{1}{6}} \Gamma(\frac{2}{3}) m^{\frac{1}{3}}), \quad (\text{D.43})$$

$$Y_m(mx) \simeq \begin{cases} (\frac{1}{2}\pi m \zeta_+)^{-\frac{1}{2}} \sin(m\zeta_+ - m \arctan \zeta_+ - \frac{1}{4}\pi), \\ -(\frac{1}{2}\pi m \zeta_-)^{-\frac{1}{2}} \exp(-m\zeta_- + m \operatorname{artanh} \zeta_-), \end{cases} \quad (\text{D.44})$$

where $\zeta_+ = \sqrt{x^2 - 1}$, valid for $x > 1$, and $\zeta_- = \sqrt{1 - x^2}$, valid for $0 < x < 1$.

For any continuous f , such that the integral exists, and $\alpha > 0$, we have

$$\lim_{m \rightarrow \infty} \int_0^\infty m J_m(m\alpha x) f(x) dx = \alpha^{-1} f(\alpha^{-1}). \quad (\text{D.45})$$

Important recurrence relations are

$$J_{m-1}(x) + J_{m+1}(x) = 2 \frac{m}{x} J_m(x), \quad (\text{D.46})$$

$$J_{m-1}(x) - J_{m+1}(x) = 2 J'_m(x), \quad (\text{D.47})$$

$$Y_{m-1}(x) + Y_{m+1}(x) = 2 \frac{m}{x} Y_m(x), \quad (\text{D.48})$$

$$Y_{m-1}(x) - Y_{m+1}(x) = 2 Y'_m(x), \quad (\text{D.49})$$

$$I_{m-1}(x) + I_{m+1}(x) = 2 I'_m(x), \quad (\text{D.50})$$

$$I_{m-1}(x) - I_{m+1}(x) = 2 \frac{m}{x} I_m(x), \quad (\text{D.51})$$

$$K_{m-1}(x) + K_{m+1}(x) = -2 K'_m(x), \quad (\text{D.52})$$

$$K_{m-1}(x) - K_{m+1}(x) = -2 \frac{m}{x} K_m(x). \quad (\text{D.53})$$

In particular:

$$\begin{aligned} J'_0(x) &= -J_1(x), & Y'_0(x) &= -Y_1(x), \\ I'_0(x) &= I_1(x), & K'_0(x) &= -K_1(x), \\ (x^{n+1} J_{n+1}(x))' &= x^{n+1} J_n(x), & (x^{n+1} I_{n+1}(x))' &= x^{n+1} I_n(x), \\ (x^{n+1} Y_{n+1}(x))' &= x^{n+1} Y_n(x), & (x^{n+1} K_{n+1}(x))' &= -x^{n+1} K_n(x). \end{aligned} \quad (\text{D.54})$$

Some useful relations involving series are

$$e^{ix \cos \vartheta} = \sum_{m=-\infty}^{\infty} i^m J_m(x) e^{im\vartheta}, \quad (\text{D.55})$$

$$J_0(kR) = \sum_{m=-\infty}^{\infty} e^{im(\vartheta-\varphi)} J_m(kr) J_m(k\varrho), \quad (\text{D.56})$$

$$\text{where: } R^2 = r^2 + \varrho^2 - 2r\varrho \cos(\vartheta - \varphi),$$

$$\frac{1}{r_0} \delta(r - r_0) = \begin{cases} \sum_{\mu=1}^{\infty} \frac{J_m(j'_{m\mu} r_0) J_m(j'_{m\mu} r)}{\frac{1}{2}(1 - m^2/j'^2_{m\mu}) J_m(j'_{m\mu})^2} & (0 < r, r_0 < 1), \\ \sum_{\mu=1}^{\infty} \frac{J_m(j_{m\mu} r_0) J_m(j_{m\mu} r)}{\frac{1}{2} J_m(j_{m\mu})^2} & (0 < r, r_0 < 1). \end{cases} \quad (\text{D.57})$$

Relations involving integrals:

$$\int x C_m(\alpha x) \tilde{C}_m(\beta x) dx = \frac{x}{\alpha^2 - \beta^2} \left\{ \beta C_m(\alpha x) \tilde{C}'_m(\beta x) - \alpha C'_m(\alpha x) \tilde{C}_m(\beta x) \right\}, \quad (\text{D.58})$$

$$\int x C_m(\alpha x) \tilde{C}_m(\alpha x) dx = \frac{1}{2} \left(x^2 - \frac{m^2}{\alpha^2} \right) C_m(\alpha x) \tilde{C}_m(\alpha x) + \frac{1}{2} x^2 C'_m(\alpha x) \tilde{C}'_m(\alpha x), \quad (\text{D.59})$$

where C_m , \tilde{C}_m is any linear combination of J_m , Y_m , $H_m^{(1)}$ and $H_m^{(2)}$,

$$\int x \mathcal{D}_m(\alpha x) \tilde{\mathcal{D}}_m(\beta x) dx = \frac{-x}{\alpha^2 - \beta^2} \left\{ \beta \mathcal{D}_m(\alpha x) \tilde{\mathcal{D}}'_m(\beta x) - \alpha \mathcal{D}'_m(\alpha x) \tilde{\mathcal{D}}_m(\beta x) \right\}, \quad (\text{D.60})$$

$$\int x \mathcal{D}_m(\alpha x) \tilde{\mathcal{D}}_m(\alpha x) dx = \frac{1}{2} \left(x^2 + \frac{m^2}{\alpha^2} \right) \mathcal{D}_m(\alpha x) \tilde{\mathcal{D}}_m(\alpha x) - \frac{1}{2} x^2 \mathcal{D}'_m(\alpha x) \tilde{\mathcal{D}}'_m(\alpha x), \quad (\text{D.61})$$

where \mathcal{D}_m , $\tilde{\mathcal{D}}_m$ is any linear combination of I_m and K_m ,

$$\int_0^\pi e^{ix \cos \vartheta} \cos(m\vartheta) d\vartheta = \frac{1}{2} \int_{-\pi}^\pi e^{ix \cos \vartheta + im\vartheta} d\vartheta = \pi i^m J_m(x), \quad (\text{D.62})$$

$$\frac{1}{2\pi} \int_{-\pi}^\pi e^{-im\vartheta + ix \sin \vartheta} d\vartheta = J_m(x), \quad (\text{D.63})$$

$$\int_0^\infty \frac{\alpha}{\gamma} e^{-i\gamma|z|} J_0(\varrho\alpha) d\alpha = \frac{e^{-ikr}}{-ir}, \quad \begin{cases} \gamma = \sqrt{k^2 - \alpha^2}, \text{Im}(\gamma) \leq 0, \\ r = \sqrt{\varrho^2 + z^2}, \quad k > 0, \end{cases} \quad (\text{D.64})$$

$$\int_{-\infty}^\infty e^{\pm ix \cosh y} dy = \pm \pi i H_0^{(1,2)}(x), \quad (\text{D.65})$$

$$\int_{-\infty}^\infty \frac{1}{\gamma} e^{-i\alpha x - i\gamma|y|} d\alpha = \pi H_0^{(2)}(kr), \quad \begin{cases} \gamma = \sqrt{k^2 - \alpha^2}, \text{Im}(\gamma) \leq 0, \\ r = \sqrt{x^2 + y^2}, \quad k > 0, \end{cases} \quad (\text{D.66})$$

$$\iint_{-\infty}^\infty \frac{1}{\gamma} e^{-i\alpha x - i\beta y - i\gamma|z|} d\alpha d\beta = 2\pi \frac{e^{-ikr}}{-ir}, \quad \begin{cases} \gamma = \sqrt{k^2 - \alpha^2 - \beta^2}, \\ \text{Im}(\gamma) \leq 0, \quad k > 0, \\ r = \sqrt{x^2 + y^2 + z^2}, \end{cases} \quad (\text{D.67})$$

$$\int_{-\infty-i0}^{\infty-i0} H_0^{(2)}(\omega r) e^{i\omega t} d\omega = 4i \frac{H(t-r)}{\sqrt{t^2 - r^2}}, \quad (\text{D.68})$$

$$\int_0^\infty \frac{x J_0(xr)}{x^2 - k^2} dx = \begin{cases} \frac{1}{2} \pi i H_0^{(1)}(kr) & (\text{Im}(k) > 0), \\ -\frac{1}{2} \pi i H_0^{(2)}(kr) & (\text{Im}(k) < 0), \end{cases} \quad (\text{D.69})$$

$$\int_0^{\infty} x^n J_n(x) e^{-ax} dx = \frac{1 \cdot 3 \cdot 5 \cdots (2n-1)}{(1+a^2)^{n+\frac{1}{2}}}, \quad (a > 0) \quad (\text{D.70})$$

$$\int_0^{\infty} x^n J_{n-1}(x) e^{-ax} dx = \frac{1 \cdot 3 \cdot 5 \cdots (2n-1)}{(1+a^2)^{n+\frac{1}{2}}} a,$$

$$\int_0^{\infty} x J_m(\alpha x) J_m(\beta x) dx = \frac{\delta(\alpha - \beta)}{\sqrt{\alpha\beta}} \quad (\alpha, \beta > 0), \quad (\text{D.71})$$

$$\int_0^{\infty} x Y_m(\alpha x) J_m(\beta x) dx = \frac{2}{\pi} \frac{1}{\alpha^2 - \beta^2} \left(\frac{\beta}{\alpha}\right)^m \quad (\text{Princ. Val.}), \quad (\text{D.72})$$

$$\int_0^{\infty} J_0(\alpha x) \sin(\beta x) dx = \frac{H(\beta - \alpha)}{\sqrt{\beta^2 - \alpha^2}}, \quad (\alpha, \beta > 0) \quad (\text{D.73})$$

$$\int_0^{\infty} J_0(\alpha x) \cos(\beta x) dx = \frac{H(\alpha - \beta)}{\sqrt{\alpha^2 - \beta^2}}, \quad (\alpha, \beta > 0) \quad (\text{D.74})$$

$$\int_0^{\infty} J_n(\alpha x) \sin(\beta x) dx = \begin{cases} \frac{\sin(n \arcsin(\frac{\beta}{\alpha}))}{\sqrt{\alpha^2 - \beta^2}} & (0 < \beta < \alpha), \\ \frac{\alpha^n \cos(\frac{1}{2}n\pi)}{\sqrt{\beta^2 - \alpha^2}(\beta + \sqrt{\beta^2 - \alpha^2})^n} & (0 < \alpha < \beta), \end{cases} \quad (\text{D.75})$$

$$\int_0^{\infty} J_n(\alpha x) \cos(\beta x) dx = \begin{cases} \frac{\cos(n \arcsin(\frac{\beta}{\alpha}))}{\sqrt{\alpha^2 - \beta^2}} & (0 < \beta < \alpha), \\ \frac{-\alpha^n \sin(\frac{1}{2}n\pi)}{\sqrt{\beta^2 - \alpha^2}(\beta + \sqrt{\beta^2 - \alpha^2})^n} & (0 < \alpha < \beta), \end{cases} \quad (\text{D.76})$$

$$\int_0^{\infty} Y_0(\alpha x) \sin(\beta x) dx = \begin{cases} \frac{2}{\pi} \frac{1}{\sqrt{\alpha^2 - \beta^2}} \arcsin(\frac{\beta}{\alpha}) & (0 < \beta < \alpha), \\ \frac{-1}{\pi \sqrt{\beta^2 - \alpha^2}} \operatorname{arcosh}(\frac{\beta}{\alpha}) & (0 < \alpha < \beta), \end{cases} \quad (\text{D.77})$$

$$\int_0^{\infty} Y_0(\alpha x) \cos(\beta x) dx = -\frac{H(\beta - \alpha)}{\sqrt{\beta^2 - \alpha^2}}, \quad (\alpha, \beta > 0) \quad (\text{D.78})$$

$$\int_0^{\infty} K_0(\alpha x) \sin(\beta x) dx = \frac{1}{\sqrt{\alpha^2 + \beta^2}} \operatorname{arsinh}(\frac{\beta}{\alpha}), \quad (\alpha, \beta > 0) \quad (\text{D.79})$$

$$\int_0^{\infty} K_0(\alpha x) \cos(\beta x) dx = \frac{\frac{1}{2}\pi}{\sqrt{\alpha^2 + \beta^2}} \quad (\alpha, \beta > 0) \quad (\text{D.80})$$

Related to Bessel functions of order $\frac{1}{3}$ are the Airy functions Ai and Bi [1], given by

$$Ai(x) = \frac{1}{\pi} \int_0^{\infty} \cos\left(\frac{1}{3}t^3 + xt\right) dt \quad (\text{D.81})$$

$$Bi(x) = \frac{1}{\pi} \int_0^{\infty} \left[\exp\left(-\frac{1}{3}t^3 + xt\right) + \sin\left(\frac{1}{3}t^3 + xt\right) \right] dt \quad (\text{D.82})$$

They are solutions of

$$y'' - xy = 0, \quad (\text{D.83})$$

with the following asymptotic behaviour (introduce $\zeta = \frac{2}{3}|x|^{3/2}$)

$$Ai(x) \simeq \begin{cases} \frac{\cos\left(\zeta - \frac{1}{4}\pi\right)}{\sqrt{\pi}|x|^{1/4} e^{-\zeta}} & (x \rightarrow -\infty), \\ \frac{1}{2\sqrt{\pi}x^{1/4}} & (x \rightarrow \infty), \end{cases} \quad (\text{D.84})$$

$$Bi(x) \simeq \begin{cases} \frac{\cos\left(\zeta + \frac{1}{4}\pi\right)}{\sqrt{\pi}|x|^{1/4} e^{\zeta}} & (x \rightarrow -\infty), \\ \frac{1}{\sqrt{\pi}x^{1/4}} & (x \rightarrow \infty). \end{cases} \quad (\text{D.85})$$

E Free field Green's functions

Some relevant Green's functions for the Laplace equation, the reduced wave equation (Helmholtz equation), the wave equation, and the diffusion equation (heat equation) are summarized in the table below for 1-, 2-, and 3-dimensional infinite space. The boundary conditions applied are (depending on the equation): symmetry, the function or its derivative vanishing at infinity, outward radiating (assuming a $e^{i\omega t}$ convention) and causality (vanishing before $t = 0$).

Equation	1-D	2-D	3-D
$\nabla^2 G = \delta(\mathbf{x})$	$\frac{1}{2} x $	$\frac{1}{2\pi} \log R$	$-\frac{1}{4\pi r}$
$\nabla^2 G + k^2 G = \delta(\mathbf{x})$	$\frac{i}{2k} e^{-ik x }$	$\frac{i}{4} H_0^{(2)}(kR)$	$-\frac{e^{-ikr}}{4\pi r}$
$\frac{\partial^2 G}{\partial t^2} - c^2 \nabla^2 G = \delta(\mathbf{x})\delta(t)$	$\frac{1}{2c} H(t - x /c)$	$\frac{1}{2\pi c^2} \frac{H(t - R/c)}{\sqrt{t^2 - R^2/c^2}}$	$\frac{\delta(t - r/c)}{4\pi c^2 r}$
$\frac{\partial G}{\partial t} - \alpha \nabla^2 G = \delta(\mathbf{x})\delta(t)$	$\frac{H(t) e^{-x^2/4\alpha t}}{(4\pi \alpha t)^{1/2}}$	$\frac{H(t) e^{-R^2/4\alpha t}}{4\pi \alpha t}$	$\frac{H(t) e^{-r^2/4\alpha t}}{(4\pi \alpha t)^{3/2}}$

Notation: $R = \sqrt{x^2 + y^2}$, $r = \sqrt{x^2 + y^2 + z^2}$.

F Summary of equations for fluid motion

For general reference we will describe here a large number of possible acoustic models, systematically derived from the compressible Navier-Stokes equations, under the assumptions of absence of friction and thermal conduction, and the fluid being a perfect gas. The flow is described by a steady mean flow and unsteady perturbations, upon which linearization and Fourier time-analysis is possible. Further simplifications are considered based on axi-symmetric geometry and mean flow.

F.1 Conservation laws and constitutive equations

The original laws of mass, momentum and energy conservation, written in terms of pressure p , density ρ , velocity vector \mathbf{v} , scalar velocity $v = |\mathbf{v}|$, viscous stress tensor $\boldsymbol{\tau}$, internal energy e , heat flux vector \mathbf{q} , and (for completeness) mass source \mathcal{Q} , momentum source \mathcal{F} and energy source \mathcal{E} are given by

$$\text{mass: } \frac{\partial}{\partial t} \rho + \nabla \cdot (\rho \mathbf{v}) = \mathcal{Q} \quad (\text{F.1})$$

$$\text{momentum: } \frac{\partial}{\partial t} (\rho \mathbf{v}) + \nabla \cdot (\rho \mathbf{v} \mathbf{v}) = -\nabla p + \nabla \cdot \boldsymbol{\tau} + \mathcal{F} \quad (\text{F.2})$$

$$\text{energy: } \frac{\partial}{\partial t} (\rho E) + \nabla \cdot (\rho E \mathbf{v}) = -\nabla \cdot \mathbf{q} - \nabla \cdot (p \mathbf{v}) + \nabla \cdot (\boldsymbol{\tau} \mathbf{v}) + \mathcal{E} \quad (\text{F.3})$$

while

$$E = e + \frac{1}{2} v^2. \quad (\text{F.4})$$

It is often convenient to introduce enthalpy or heat function

$$i = e + \frac{p}{\rho}, \quad (\text{F.5})$$

or entropy s and temperature T via the fundamental law of thermodynamics for a reversible process

$$T ds = de + p d\rho^{-1} = di - \rho^{-1} dp. \quad (\text{F.6})$$

With $\frac{d}{dt} = \frac{\partial}{\partial t} + \mathbf{v} \cdot \nabla$ for the convective derivative, the above conservation laws may be reduced to

$$\text{mass: } \frac{d}{dt} \rho = -\rho \nabla \cdot \mathbf{v} + \mathcal{Q} \quad (\text{F.7})$$

$$\text{momentum: } \rho \frac{d}{dt} \mathbf{v} = -\nabla p + \nabla \cdot \boldsymbol{\tau} + \mathcal{F} - \mathcal{Q} \mathbf{v} \quad (\text{F.8})$$

$$\text{energy: } \rho \frac{d}{dt} e = -\nabla \cdot \mathbf{q} - p \nabla \cdot \mathbf{v} + \boldsymbol{\tau} : \nabla \mathbf{v} + \mathcal{E} - \mathcal{Q} (e - \frac{1}{2} v^2) - \mathbf{v} \cdot \mathcal{F} \quad (\text{F.9a})$$

$$\rho \frac{d}{dt} i = \frac{d}{dt} p - \nabla \cdot \mathbf{q} + \boldsymbol{\tau} : \nabla \mathbf{v} + \mathcal{E} - \mathcal{Q} (i - \frac{1}{2} v^2) - \mathbf{v} \cdot \mathcal{F} \quad (\text{F.9b})$$

$$\rho T \frac{d}{dt} s = -\nabla \cdot \mathbf{q} + \boldsymbol{\tau} : \nabla \mathbf{v} + \mathcal{E} - \mathcal{Q} (i - \frac{1}{2} v^2) - \mathbf{v} \cdot \mathcal{F}. \quad (\text{F.9c})$$

Of the energy equations, the entropy form (F.9c) is the most convenient one for acoustic applications. (Further on in this section we will ignore the extra sources.)

For an *ideal* gas we have the following relations

$$p = \rho RT, \quad de = C_V dT, \quad di = C_P dT \quad (\text{F.10a,b,c})$$

where C_V is the heat capacity or specific heat at constant volume, C_P is the heat capacity or specific heat at constant pressure [116]. $C_V = C_V(T)$ and $C_P = C_P(T)$ are in general functions of temperature. R is the specific gas constant and γ the specific-heat ratio, which are practically constant and given by (the figures refer to air)

$$R = C_P - C_V = 286.73 \text{ J/kg K}, \quad \gamma = \frac{C_P}{C_V} = 1.402 \quad (\text{F.11a,b})$$

From equation (F.6) it then follows for an ideal gas that

$$ds = C_V \frac{dp}{p} - C_P \frac{d\rho}{\rho} \quad (\text{F.12})$$

while isentropic perturbations ($ds = 0$), like sound, propagate with the sound speed c given by

$$c^2 = \left(\frac{\partial p}{\partial \rho} \right)_s = \frac{\gamma p}{\rho} = \gamma RT. \quad (\text{F.13})$$

For a *perfect* gas, the specific heats are constant (*independent of T*), and we can integrate

$$e = C_V T + e_{\text{init}}, \quad i = C_P T + i_{\text{init}}, \quad s = C_V \log p - C_P \log \rho + s_{\text{init}}. \quad (\text{F.14a,b,c})$$

The integration “constants” e_{init} , i_{init} and s_{init} refer to the initial situation of each particle. So this result is only useful if we start with a fluid of uniform thermodynamical properties, or if we are able to trace back the pathlines (or streamlines for a steady flow).

F.2 Acoustic approximation

F.2.1 Inviscid and isentropic

In the acoustic realm we will consider, the viscous or turbulent stress terms will be assumed to play a role only in an aerodynamic source region, while any perturbation is too fast to be affected by thermal conduction. Therefore, for the applications of acoustic propagation we will ignore viscous shear stress ($\boldsymbol{\tau}$) and thermal conduction (\boldsymbol{q}). In particular, this is obtained as follows. We make dimensionless by scaling

310 **F** Summary of equations for fluid motion

$$\begin{aligned} \mathbf{x} &:= L\mathbf{x}, & \mathbf{v} &:= v_0\mathbf{v}, & t &:= \frac{L}{v_0}t, & \rho &:= \rho_0\rho, \\ dp &:= \rho_0v_0^2dp, & \boldsymbol{\tau} &:= \frac{\mu v_0}{L}\boldsymbol{\tau}, & \mathbf{q} &:= \frac{\kappa \Delta T}{L}\mathbf{q}, \\ T &:= T_0T, & dT &:= \Delta TdT, & ds &:= \frac{C_P \Delta T}{T_0}ds \end{aligned}$$

to get

$$\frac{d}{dt}\rho = -\rho\nabla\cdot\mathbf{v} \tag{F.15}$$

$$\rho\frac{d}{dt}\mathbf{v} = -\nabla p + \frac{1}{Re}\nabla\cdot\boldsymbol{\tau} \tag{F.16}$$

$$\rho T\frac{d}{dt}s = -\frac{1}{Pe}\nabla\cdot\mathbf{q} + \frac{Ec}{Re}\boldsymbol{\tau}:\nabla\mathbf{v}, \tag{F.17}$$

where $Re = \rho_0v_0L/\mu$ denotes the Reynolds number, $Pe = \rho_0C_Pv_0L/\kappa$ the Peclet number, and $Ec = v_0^2/C_P\Delta T$ the Eckert number. If the Reynolds number tends to infinity, usually also the Peclet number does, because $Pe = PrRe$ and the Prandtl number Pr is for most fluids and gases of order 1. Then, provided the Eckert number is not large, we obtain

$$\frac{d}{dt}\rho = -\rho\nabla\cdot\mathbf{v} \tag{F.18}$$

$$\rho\frac{d}{dt}\mathbf{v} = -\nabla p \tag{F.19}$$

$$\frac{d}{dt}s = 0 \tag{F.20}$$

which means that entropy remains constant, and thus $dh = \rho^{-1}dp$, along streamlines. Furthermore, we will assume the gas to be perfect, with the following thermodynamical closure relations

$$ds = C_V\frac{dp}{p} - C_P\frac{d\rho}{\rho}, \quad c^2 = \frac{\gamma p}{\rho}. \tag{F.21a}$$

By substituting equation (F.21a) into equation (F.20) we obtain

$$\frac{d}{dt}p = c^2\frac{d}{dt}\rho. \tag{F.21b}$$

If the flow is initially homentropic (s_{init} is uniformly constant) then

$$p \propto \rho^\gamma e^{s/C_V} \tag{F.21c}$$

If the flow is homentropic (s is uniformly constant) then

$$p \propto \rho^\gamma \tag{F.21d}$$

F.2.2 Perturbations of an inviscid non-heat conducting mean flow

When we have a steady mean flow with unsteady perturbations, given by

$$\mathbf{v} = \mathbf{v}_0 + \mathbf{v}', \quad p = p_0 + p', \quad \rho = \rho_0 + \rho', \quad s = s_0 + s' \quad (\text{F.22})$$

and linearize for small amplitude, we obtain for the mean flow

$$\nabla \cdot (\rho_0 \mathbf{v}_0) = 0 \quad (\text{F.23a})$$

$$\rho_0 (\mathbf{v}_0 \cdot \nabla) \mathbf{v}_0 = -\nabla p_0 \quad (\text{F.23b})$$

$$(\mathbf{v}_0 \cdot \nabla) s_0 = 0 \quad (\text{F.23c})$$

while

$$ds_0 = C_V \frac{dp_0}{p_0} - C_P \frac{d\rho_0}{\rho_0}, \quad c_0^2 = \frac{\gamma p_0}{\rho_0} \quad (\text{F.23d})$$

and the perturbations

$$\frac{\partial}{\partial t} \rho' + \nabla \cdot (\mathbf{v}_0 \rho' + \mathbf{v}' \rho_0) = 0 \quad (\text{F.24a})$$

$$\rho_0 \left(\frac{\partial}{\partial t} + \mathbf{v}_0 \cdot \nabla \right) \mathbf{v}' + \rho_0 (\mathbf{v}' \cdot \nabla) \mathbf{v}_0 + \rho' (\mathbf{v}_0 \cdot \nabla) \mathbf{v}_0 = -\nabla p' \quad (\text{F.24b})$$

$$\left(\frac{\partial}{\partial t} + \mathbf{v}_0 \cdot \nabla \right) s' + \mathbf{v}' \cdot \nabla s_0 = 0 \quad (\text{F.24c})$$

while, assuming $s'_{\text{init}} = 0$,

$$s' = \frac{C_V}{p_0} p' - \frac{C_P}{\rho_0} \rho' = \frac{C_V}{p_0} (p' - c_0^2 \rho'), \quad c' = \frac{1}{2} c_0 \left(\frac{p'}{p_0} - \frac{\rho'}{\rho_0} \right). \quad (\text{F.24d})$$

The expression for c' usually serves no purpose.

From equation (F.21b) we get for the mean flow $\mathbf{v}_0 \cdot \nabla p_0 = c_0^2 \mathbf{v}_0 \cdot \nabla \rho_0$, and for the perturbations an equation, equivalent to (F.24c) and (F.24d),

$$\frac{\partial}{\partial t} p' + \mathbf{v}_0 \cdot \nabla p' + \mathbf{v}' \cdot \nabla p_0 = c_0^2 \left(\frac{\partial}{\partial t} \rho' + \mathbf{v}_0 \cdot \nabla \rho' + \mathbf{v}' \cdot \nabla \rho_0 \right) + c_0^2 (\mathbf{v}_0 \cdot \nabla \rho_0) \left(\frac{p'}{p_0} - \frac{\rho'}{\rho_0} \right). \quad (\text{F.25})$$

If the mean flow is homentropic ($s_0 = \text{constant}$), we have $\nabla p_0 = c_0^2 \nabla \rho_0$ while the perturbations are isentropic along streamlines.

If the perturbations are entirely isentropic ($s' \equiv 0$), for example when $\mathbf{v}_0 = 0$ and $s_0 = \text{constant}$ or when the flow is homentropic (satisfying equation F.21d), the pressure and density perturbations are related by the usual

$$p' = c_0^2 \rho'. \quad (\text{F.26})$$

F.2.3 Myers' Energy Corollary

Myers' definition of energy [160, 161, 162] for unsteady disturbances propagating in moving fluid media is both consistent with the general conservation law of fluid energy and with the order of approximation in the linear model adopted to describe the disturbances. When the mass and momentum equations (F.1,F.2) and the general energy conservation law (F.3) for fluid motion is expanded to quadratic order, this 2nd order energy term may be reduced to the following conservation law for perturbation energy density E , energy flux \mathbf{I} , and dissipation \mathcal{D}

$$\frac{\partial}{\partial t}E + \nabla \cdot \mathbf{I} = -\mathcal{D} \quad (\text{F.27})$$

where (for simplicity we neglect viscous stress and heat conduction)

$$E = \frac{p'^2}{2\rho_0 c_0^2} + \frac{1}{2}\rho_0 v'^2 + \rho' \mathbf{v}_0 \cdot \mathbf{v}' + \frac{\rho_0 T_0 s'^2}{2C_p}, \quad (\text{F.28a})$$

$$\mathbf{I} = (\rho_0 \mathbf{v}' + \rho' \mathbf{v}_0) \left(\frac{p'}{\rho_0} + \mathbf{v}_0 \cdot \mathbf{v}' \right) + \rho_0 \mathbf{v}_0 T' s', \quad (\text{F.28b})$$

$$\mathcal{D} = -\rho_0 \mathbf{v}_0 \cdot (\boldsymbol{\omega}' \times \mathbf{v}') - \rho' \mathbf{v}' \cdot (\boldsymbol{\omega}_0 \times \mathbf{v}_0) + s' (\rho_0 \mathbf{v}' + \rho' \mathbf{v}_0) \cdot \nabla T_0 - s' \rho_0 \mathbf{v}_0 \cdot \nabla T'. \quad (\text{F.28c})$$

while the vorticity vector is denoted by $\nabla \times \mathbf{v} = \boldsymbol{\omega} = \boldsymbol{\omega}_0 + \boldsymbol{\omega}'$. Without mean flow this definition reduces to the traditional one. Note that, according to this definition, acoustic energy is entirely conserved in homentropic, irrotational flow. In vortical flow, the interaction with the mean flow may constitute a source or a sink of acoustic energy.

F.2.4 Zero mean flow

Without mean flow, such that $\mathbf{v}_0 = \nabla p_0 = 0$, the linearized equations for an inviscid non-heat conducting fluid may be reduced to

$$\frac{\partial^2}{\partial t^2} p' - \nabla \cdot (c_0^2 \nabla p') = 0. \quad (\text{F.29})$$

F.2.5 Time harmonic

When the perturbations are time-harmonic, given by

$$\mathbf{v}' = \text{Re}(\hat{\mathbf{v}} e^{i\omega t}), \quad p' = \text{Re}(\hat{p} e^{i\omega t}), \quad \rho' = \text{Re}(\hat{\rho} e^{i\omega t}), \quad s' = \text{Re}(\hat{s} e^{i\omega t}), \quad (\text{F.30})$$

we have in the usual complex notation

$$i\omega \hat{\rho} + \nabla \cdot (\mathbf{v}_0 \hat{\rho} + \hat{\mathbf{v}} \rho_0) = 0 \quad (\text{F.31a})$$

$$\rho_0(i\omega + \mathbf{v}_0 \cdot \nabla) \hat{\mathbf{v}} + \rho_0(\hat{\mathbf{v}} \cdot \nabla) \mathbf{v}_0 + \hat{\rho}(\mathbf{v}_0 \cdot \nabla) \mathbf{v}_0 = -\nabla \hat{p} \quad (\text{F.31b})$$

$$(i\omega + \mathbf{v}_0 \cdot \nabla) \hat{s} + \hat{\mathbf{v}} \cdot \nabla s_0 = 0 \quad (\text{F.31c})$$

$$\hat{s} = \frac{C_v}{\rho_0} (\hat{p} - c_0^2 \hat{\rho}). \quad (\text{F.31d})$$

F.2.6 Irrotational isentropic flow

When the flow is irrotational and isentropic everywhere (homotropic), we can introduce a potential for the velocity, where $\mathbf{v} = \nabla \phi$, and express p as a function of ρ only, such that we can integrate the momentum equation, and obtain the important simplification

$$\frac{\partial}{\partial t} \phi + \frac{1}{2} v^2 + \frac{c^2}{\gamma - 1} = \text{constant}, \quad \frac{p}{\rho^\gamma} = \text{constant}. \quad (\text{F.32})$$

For mean flow with harmonic perturbation, where $\phi = \phi_0 + \text{Re}(\hat{\phi} e^{i\omega t})$, we have then for the mean flow

$$\begin{aligned} \frac{1}{2} v_0^2 + \frac{c_0^2}{\gamma - 1} &= \text{constant}, \\ \nabla \cdot (\rho_0 \mathbf{v}_0) &= 0, \quad \frac{p_0}{\rho_0^\gamma} = \text{constant} \end{aligned} \quad (\text{F.33a})$$

and for the acoustic perturbations

$$\begin{aligned} (i\omega + \mathbf{v}_0 \cdot \nabla) \hat{\rho} + \hat{\rho} \nabla \cdot \mathbf{v}_0 + \nabla \cdot (\rho_0 \nabla \hat{\phi}) &= 0, \\ \rho_0(i\omega + \mathbf{v}_0 \cdot \nabla) \hat{\phi} + \hat{p} &= 0, \quad \hat{p} = c_0^2 \hat{\rho}. \end{aligned} \quad (\text{F.33b})$$

These last equations are further simplified (eliminate \hat{p} and $\hat{\rho}$ and use the fact that $\nabla \cdot (\rho_0 \mathbf{v}_0) = 0$) to the rather general convected wave equation

$$\rho_0^{-1} \nabla \cdot (\rho_0 \nabla \hat{\phi}) - (i\omega + \mathbf{v}_0 \cdot \nabla) \left[c_0^{-2} (i\omega + \mathbf{v}_0 \cdot \nabla) \hat{\phi} \right] = 0. \quad (\text{F.34})$$

F.2.7 Uniform mean flow

The simplest, but therefore probably most important configuration with mean flow, is the one with a uniform mean flow.

Axial mean velocity u_0 , mean pressure p_0 , density ρ_0 and sound speed c_0 are constants, so we have

$$(i\omega + u_0 \frac{\partial}{\partial x}) \hat{\rho} + \rho_0 \nabla \cdot \hat{\mathbf{v}} = 0, \quad (\text{F.35a})$$

$$\rho_0(i\omega + u_0 \frac{\partial}{\partial x})\hat{v} + \nabla \hat{p} = 0, \quad (\text{F.35b})$$

$$(i\omega + u_0 \frac{\partial}{\partial x})(\hat{p} - c_0^2 \hat{\rho}) = 0. \quad (\text{F.35c})$$

Equation (F.35c) shows that entropy perturbations are just convected by the mean flow. Without sources of entropy, the field is isentropic if we start with zero entropy.

We may split the perturbation velocity into a vortical part and an irrotational part (see equation 1.22) by introducing the vector potential (stream function) $\hat{\psi}$ and scalar potential $\hat{\phi}$ as follows

$$\hat{v} = \nabla \times \hat{\psi} + \nabla \hat{\phi}, \quad (\text{F.36})$$

If desired, the arbitrariness in $\hat{\psi}$ (we may add any ∇f , since $\nabla \times \nabla f \equiv 0$) may be removed by adding the gauge condition $\nabla \cdot \hat{\psi} = 0$, such that the vorticity is given by

$$\hat{\omega} = \nabla \times \hat{v} = \nabla(\nabla \cdot \hat{\psi}) - \nabla^2 \hat{\psi} = -\nabla^2 \hat{\psi}. \quad (\text{F.37})$$

By taking the curl of equation (F.35b) we can eliminate p and ϕ to produce an equation for the vorticity:

$$-(i\omega + u_0 \frac{\partial}{\partial x})\nabla^2 \hat{\psi} = (i\omega + u_0 \frac{\partial}{\partial x})\hat{\omega} = 0. \quad (\text{F.38})$$

This shows that vorticity perturbations are just convected by the mean flow. Without sources of vorticity, the field is irrotational if we start without vorticity.

Indeed, vorticity and pressure/density perturbations are decoupled. Since the divergence of a curl is zero, $\nabla \cdot \hat{v} = \nabla \cdot (\nabla \times \hat{\psi} + \nabla \hat{\phi}) = \nabla^2 \hat{\phi}$, equation (F.35a) becomes

$$(i\omega + u_0 \frac{\partial}{\partial x})\hat{\rho} + \rho_0 \nabla^2 \hat{\phi} = 0 \quad (\text{F.39})$$

By taking the divergence of equation (F.35b), and using equations (F.35a, F.35c), not assuming isentropy or irrotationality, we can eliminate ϕ and ρ to obtain the convected reduced wave equation for the pressure

$$c_0^2 \nabla^2 \hat{p} - (i\omega + u_0 \frac{\partial}{\partial x})^2 \hat{p} = 0. \quad (\text{F.40})$$

Plane wave solutions are given by

$$\hat{p} = A e^{-ik \cdot x}, \quad \hat{v} = \frac{\mathbf{k}}{\rho_0 \Omega} A e^{-ik \cdot x}, \quad \Omega = \omega - u_0 k_x, \quad c_0^2 |\mathbf{k}|^2 = \Omega^2, \quad (\text{F.41})$$

not propagating in \mathbf{k} -direction but in the direction of the intensity vector

$$\langle \mathbf{I} \rangle = \frac{\omega |A|^2}{2\rho_0 \Omega^2} (\mathbf{k} + M_0 |\mathbf{k}| \mathbf{e}_x), \quad M_0 = u_0/c_0. \quad (\text{F.42})$$

With some care, especially taking due notice of any singular edge behaviour, equation (F.40) may be transformed to the ordinary reduced wave equation

$$c_0^2 \nabla^2 \tilde{p} + \Omega^2 \tilde{p} = 0 \quad (\text{F.43})$$

by introducing

$$\begin{aligned} \hat{p}(x, r, \theta; \omega) &= \tilde{p}(X, r, \theta; \Omega) \exp(i \frac{\Omega M}{c_0} X), \\ \text{where } x &= \beta X, \omega = \beta \Omega, M = \frac{u_0}{c_0}, \beta = \sqrt{1 - M^2}. \end{aligned} \quad (\text{F.44})$$

F.2.8 Parallel mean flow

Assume a mean flow field parallel in x -direction with uniform mean pressure, *i.e.* $\mathbf{v}_0 = (u_0, 0, 0)$, $u_0 = u_0(y, z)$, $\rho_0 = \rho_0(y, z)$, $c_0 = c_0(y, z)$ and $p_0 = \text{constant}$. Then by taking the convective time derivative of the divergence of the momentum equation, eliminating the velocity, and using the fact that p_0 is constant, we obtain from (F.24) the equation

$$\left(\frac{\partial}{\partial t} + u_0 \frac{\partial}{\partial x}\right)^3 p + 2c_0^2 \frac{\partial}{\partial x} (\nabla_{\perp} u_0 \cdot \nabla_{\perp} p) - \left(\frac{\partial}{\partial t} + u_0 \frac{\partial}{\partial x}\right) \nabla \cdot (c_0^2 \nabla p) = 0, \quad (\text{F.45})$$

where ∇_{\perp} denotes (∂_y, ∂_z) . If we look for solutions of the form $p(x, y, z, t) = P(y, z) e^{i\omega t - ikx}$ and denote

$$\Omega = \frac{\omega - ku_0}{c_0},$$

we obtain a pre-form of the Pridmore-Brown equation [187, 211]

$$-i\Omega^3 c_0^3 P - 2ikc_0^2 (\nabla_{\perp} u_0 \cdot \nabla_{\perp} P) - i\Omega c_0 (-k^2 c_0^2 P + \nabla_{\perp} \cdot (c_0^2 \nabla_{\perp} P)) = 0.$$

By noting that $-k\nabla_{\perp} u_0 = \nabla_{\perp}(\Omega c_0)$, this equation can be further simplified into

$$\Omega^2 \nabla_{\perp} \cdot \left(\frac{1}{\Omega^2} \nabla_{\perp} P\right) + (\Omega^2 - k^2) P = 0. \quad (\text{F.46})$$

G Answers to exercises.

Chapter 1

- d) Only if thermodynamic equilibrium prevails.
e) The pressure on the piston p_1 can be related to the atmospheric pressure p_2 in the free jet by using the unsteady Bernoulli equation (1.32b) applied to an incompressible fluid ($\rho = \rho_0$):

$$\frac{\partial \Delta\phi}{\partial t} + \frac{1}{2}(v_2^2 - v_1^2) + \frac{p_2 - p_1}{\rho_0} = 0.$$

By neglecting the non-uniformity of the flow we have

$$\Delta\phi = \int_1^2 \mathbf{v} \cdot d\mathbf{l} \simeq v_1 \ell_1 + v_2 \ell_2.$$

Using the mass conservation law (1.19) for an incompressible fluid we find by continuity of the volume flux

$$A_1 v_1 = A_2 v_2.$$

Hence, the equation of Bernoulli becomes, with $v_1 = at$,

$$\frac{p_1 - p_2}{\rho_0} = a \left(\ell_1 + \frac{A_1}{A_2} \ell_2 \right) + \frac{1}{2} \left(\left(\frac{A_1}{A_2} \right)^2 - 1 \right) (at)^2.$$

At $t = 0$ we have a ratio of the pressure drop, determined by the ratio of the potential difference, of

$$\frac{v_1 \ell_1}{v_2 \ell_2} = \frac{A_1 \ell_1}{A_2 \ell_2}.$$

Chapter 2

- a) A depth of 100 m corresponds to a pressure of 10 bar, hence an air density ρ_g which is ten times higher than at 1 bar. Following (2.45) we have a speed of sound of 75 m/s. Note that $\rho_g c_g^2 = \gamma p$ so that c depends only on γ and not on other gas properties.
c) Mathematically, any sound speed can be used, but the simple physical meaning only appears when we choose the value that prevails at the listener's position.
d) Not necessarily. In an isentropic flow is $\frac{Ds}{Dt} = 0$, but $\nabla \cdot (\mathbf{v} \rho_0)$ vanishes only for an homentropic flow.
e) No, p' is more appropriate.
f) Certainly not.
g) Yes.
h) No. The fluid should be stagnant and uniform (quiescent).
i) No. $\rho c^2 = \gamma p$ so that ρc depends also on the temperature because $c = \sqrt{\gamma RT}$.
j) From the wave equation it follows that $\mathbf{k} = \omega \mathbf{n} / c_0$ for some real unit vector \mathbf{n} . So the surface is given by $c_0 t - \mathbf{n} \cdot \mathbf{x} = \text{constant}$, with real coefficients, and so defines a plane.

Chapter 3

- a) Every point of the line source has a different distance, and therefore different travel time, to the observer. Note the tail of the 2-D wave-equation Green's function (Appendix E) $(2\pi c^2)^{-1} H(t - R/c)/\sqrt{t^2 - R^2/c^2}$.
- b) The field P of one point source is given by (see Appendix E)
 $P_{tt} - c^2 \nabla^2 P = \delta(t - \tau)\delta(x - x_0)\delta(y - y_0)\delta(z)$ with solution
 $P = \delta(t - \tau - r_0/c)/4\pi c^2 r_0$ where $r_0 = \{(x - x_0)^2 + (y - y_0)^2 + z^2\}^{1/2}$.
 Integrate over all x_0, y_0 , introduce $x_0 = x + \{r_0^2 - z^2\}^{1/2} \cos \theta_0$ and
 $y_0 = y + \{r_0^2 - z^2\}^{1/2} \sin \theta_0$, and obtain the total field
 $p = \iint P dx_0 dy_0 = \frac{2\pi}{4\pi c^2} \int_{|z|}^{\infty} \delta(t - \tau - r_0/c) dr_0 = (2c)^{-1} H(t - \tau - |z|/c)$.
 This could have been anticipated from the fact that the problem is really one dimensional.

- c) From Appendix E we find the total field

$$p(x, y, z) = \frac{1}{4}i \sum_{n=-\infty}^{\infty} H_0^{(2)}(kR_n) \simeq \frac{1}{4}i \sum_{n=-\infty}^{\infty} (\frac{1}{2}\pi kR_n)^{-\frac{1}{2}} \exp(\frac{1}{4}\pi i - ikR_n)$$

where $R_n = ((x - nd)^2 + y^2)^{\frac{1}{2}} = (r^2 - 2rnd \cos \theta + n^2 d^2)^{\frac{1}{2}}$.

Consider the sources satisfying $-r \ll nd \ll r$, such that

$$R_n \simeq r - nd \cos \theta \quad (r \rightarrow \infty).$$

This part of the series looks like

$$\dots \simeq \frac{1}{4}i \sum (\frac{1}{2}\pi kr)^{-\frac{1}{2}} \exp(\frac{1}{4}\pi i - ikr + iknd \cos \theta)$$

and grows linearly with the number of terms if $\exp(iknd \cos \theta) = 1$, or $kd \cos \theta = 2\pi m$.

- d) The condition is now $\exp(-i\pi n + iknd \cos \theta) = 1$, or $kd \cos \theta = (2m + 1)\pi$.
- e) If x is made dimensionless by length L , we have $\delta(x) = \delta(\frac{x}{L}) = \frac{1}{L}\delta(\frac{x}{L})$. So the dimension of $\delta(x)$ is $(\text{length})^{-1}$.
- f) Multiply by a test function $\phi(x, y)$ and integrate

$$\dots = - \iint \frac{1}{r} \phi_r dx dy = - \int_0^{2\pi} \int_0^{\infty} \phi_r dr d\theta = 2\pi \phi(0, 0).$$

- g) Let S be given by an equation $f(x) = 0$, such that $f(x) > 0$ if and only if $x \in V$. The outward normal \mathbf{n} is then given by $\mathbf{n} = -(\nabla f/|\nabla f|)_{f=0}$. Since $H(f)\mathbf{v}$ vanishes outside V , we have

$$0 = \int \nabla \cdot [H(f)\mathbf{v}] dx = \int [H(f)\nabla \cdot \mathbf{v} + \delta(f)\mathbf{v} \cdot \nabla f] dx = \int_V \nabla \cdot \mathbf{v} dx - \int_S \mathbf{v} \cdot \mathbf{n} d\sigma.$$

- h) Only the terms contribute which satisfy $0 < 2nL \leq c_0 t$, so we obtain

$$(2 + R)g(t) = Rf(t) + 2 \sum_{n=1}^{\lfloor c_0 t/2L \rfloor} \left(f\left(t - \frac{2nL}{c_0}\right) - g\left(t - \frac{2nL}{c_0}\right) \right).$$

- i) $\hat{p}(x) = e^{-ikx} + R e^{ikx}$. If $\hat{p}(x_0) = 0$, we have $R = -e^{-2ikx_0}$.
 Since $\hat{p}(x_0) = 0$ and $\hat{v}(x_0) \neq 0$ we have simply $Z = 0$.
- j) $\hat{v}(x) = (\rho_0 c_0)^{-1} (e^{-ikx} - R e^{ikx})$. If $\hat{v}(x_0) = 0$, we have $R = e^{-2ikx_0}$.
 Since $\hat{v}(x_0) = 0$ and $\hat{p}(x_0) \neq 0$ we have simply $Z = \infty$.
- k) With $\hat{p}(x) = e^{-ikx} + R e^{ikx}$ and $\hat{v}(x) = (\rho_0 c_0)^{-1} (e^{-ikx} - R e^{ikx})$ we have $R = (Z_0 - \rho_0 c_0)/(Z_0 + \rho_0 c_0)$, so

$$Z_L = \rho_0 c_0 \frac{e^{ikL} + R e^{-ikL}}{e^{ikL} - R e^{-ikL}} = \rho_0 c_0 \frac{Z_0 + i\rho_0 c_0 \tan(kL)}{\rho_0 c_0 + iZ_0 \tan(kL)}.$$

- l) If $R > 0, m \geq 0, K \geq 0$, the zeros of $Z(\omega) = R + i\omega m - iK/\omega$ belong to the upper half plane. If $R = 0$ the zeros are real, and have to be counted to the upper half plane. The same for the real pole $\omega = 0$.

$$z(t) = 2\pi(R\delta(t) + m\delta'(t) + KH(t)), \quad y(t) = \frac{2\pi H(t)(\alpha e^{-\alpha t} - \beta e^{-\beta t})}{\sqrt{R^2 - 4mK}}, \quad \alpha, \beta = (R \pm \sqrt{R^2 - 4mK})/2m.$$

- m) From Ingard's boundary condition (3.43) we have $i\omega Z(\mathbf{v} \cdot \mathbf{e}_y) = i\Omega p$ which yields with $\Omega = \omega/(1 + M_0 \cos \vartheta)$ and $M_0 = u_0/c_0$ that $(1 + M_0 \cos \vartheta)Z \sin \vartheta / \rho_0 c_0 = (1 + R)/(1 - R)$, or

$$R = \frac{(1 + M_0 \cos \vartheta)Z \sin \vartheta - \rho_0 c_0}{(1 + M_0 \cos \vartheta)Z \sin \vartheta + \rho_0 c_0}, \quad \text{while } R = 0 \text{ if } Z = \frac{\rho_0 c_0}{\sin \vartheta (1 + M_0 \cos \vartheta)}.$$

- n) By using the filter property of the delta function, and the condition that $0 < \tau < t - |x|/c$, it is straightforward to find

$$p(\mathbf{x}, t) = \frac{1}{2c} \int_0^{t-|x|/c} f(\tau) d\tau, \quad = \frac{1}{2\pi} \int_0^{t-R/c} \frac{f(\tau)}{\sqrt{(t-\tau)^2 - \frac{R^2}{c^2}}} d\theta, \quad = \frac{1}{4\pi r} f\left(t - \frac{r}{c}\right),$$

respectively. Finally, we make for 2D the substitution $\tau = t - (R/c) \cosh \theta$.

The time harmonic solutions for large time are

$$\begin{aligned} 1D: \quad p(\mathbf{x}, t) &= \frac{i}{2k} (e^{i\omega t - ik|x|} - 1) \rightsquigarrow \frac{i}{2k} e^{i\omega t - ik|x|}, \\ 2D: \quad p(\mathbf{x}, t) &\simeq \frac{1}{2\pi} e^{i\omega t} \int_0^\infty e^{-ikR \cosh \theta} d\theta = \frac{i}{4} e^{i\omega t} H_0^{(2)}(kR), \\ 3D: \quad p(\mathbf{x}, t) &= -\frac{1}{4\pi r} e^{i\omega t - ikr}. \end{aligned}$$

Chapter 4

- a) For a wave $p' = \mathcal{G}(x + c_0 t)$ corresponding to a C^- characteristic propagating in a uniform region with (ρ_0, c_0) and $u_0 = 0$ the C^+ characteristics carry the message: $p' + \rho_0 c_0 u' = 0$ in the entire wave region. This implies that $p' = -\rho_0 c_0 u'$ along any C^- characteristic. Alternatively, we have from the momentum conservation law: $\rho_0 \frac{\partial}{\partial t} u' = -\frac{\partial}{\partial x} p' = -\frac{1}{c_0} \frac{\partial}{\partial t} p'$ because p' is a function of $(x + c_0 t)$ along a C^- characteristic. Integration with respect to time yields: $\rho_0 u' = -p'/c_0$.
- b) The piston induces the pressures $p'_I = \rho_{0,I} c_{0,I} u'$ and $p'_{II} = -\rho_{0,II} c_{0,II} u'$. The force amplitude is: $\hat{F} = S(\rho_I c_I + \rho_{II} c_{II}) \omega a = 9.15 \text{ N}$. As $p'_I - p'_{II} = 915 \text{ Pa} \ll \rho_0 c_0^2 \simeq 10^5 \text{ Pa}$ we can use a linear theory.
- c) The flow perturbation u' is such that the total flow velocity $u_0 + u' = 0$ at the closed valve. Hence we have $p_1 = -\rho_w c_w u' = \rho_w c_w u_0$ and $p_1 = -p_2$. For $u_0 = 0.01 \text{ m/s}$ we find $p_1 = -p_2 = 1.5 \times 10^4 \text{ Pa}$. For $u_0 = 1 \text{ m/s}$ we find $p_1 = 1.5 \times 10^6 \text{ Pa}$. The pressure p_2 can reach -15 bar if there is no cavitation. Otherwise it is limited to the vapour pressure of the water.
- d) $v_j = 2c_w(A/S)(1 - \sqrt{1 - (u_0/c_w)}) \simeq u_0 A/S$. $\Delta p \simeq \frac{1}{2} \rho_w (u_0 A/S)^2$.
- e) Energy conservation implies: $A_1 p'_1 u'_1 = A_2 p'_2 u'_2$, while mass conservation implies: $A_1 u'_1 = A_2 u'_2$. Substitution of the mass conservation law in the energy conservation law yields: $p'_1 = p'_2$.
- f) $R_{1,2} = T_{1,2} - 1 = (\rho_2 c_2 - \rho_1 c_1)/(\rho_2 c_2 + \rho_1 c_1)$.
 $R_{air,water} = 0.99945$, $T_{air,water} = 1.99945$. $R_{water,air} = -0.9989$, $T_{water,air} = 0.0011$.
- g) $T_1 - T_2 = 30 \text{ K}$, $\rho_1 c_1 / \rho_2 c_2 = \sqrt{T_2/T_1} = 1.05$. $R_{1,2} = -0.03$, $T_{1,2} = 0.97$.
- h) $(I_1^- / I_1^+) = R_{1,2}^2 = (\rho_1 c_1 - \rho_2 c_2)^2 / (\rho_1 c_1 + \rho_2 c_2)^2$,
 $(p_1^+ + p_1^-)(p_1^+ - p_1^-) / \rho_1 c_1 = I_1^+ - I_1^- = I_2^+$, $(I_2^+ / I_1^+) = 1 - (I_1^- / I_1^+)$.
- i) $R_{1,2} = 0.0256$, $p_1^+ = (\rho_1 c_1 \hat{u}_p) / (1 - R_{1,2} e^{-2ikL})$, $p_1^- = R_{1,2} p_1^+ e^{-2ikL}$, $p_2^+ = p_1^+ e^{-ikL} + p_1^- e^{ikL}$.
- j) $T_{1,2} = 2A_1 / (A_1 + A_2)$, $R_{1,2} = 1 - T_{1,2} = (A_1 - A_2) / (A_1 + A_2)$.
- k) $T_{1,2} = 2\rho_2 c_2 A_1 / (\rho_1 c_1 A_2 + \rho_2 c_2 A_2)$, $R_{1,2} = 1 - T_{1,2}$.
- l) $\lim_{A_2/A_1 \rightarrow 0} R_{1,2} = 1$, $\lim_{A_2/A_1 \rightarrow \infty} R_{1,2} = -1$.

m) For an orifice with wall thickness L and cross-sectional area A_d in a pipe of cross-sectional area A_p we have:

$$R = p_1^- / p_1^+ = ik(L + 2\delta)A_p / [2A_d + ik(L + 2\delta)A_p], \text{ where } k = \omega/c_0, \delta \simeq \frac{8}{3\pi} \sqrt{A_d/\pi}.$$

p) Without mean flow ($u_0 = 0$):

- At low amplitudes, when linear theory is valid, friction is negligible when $\delta_v^2 = 2\nu/\omega \ll A_d$.
- At large amplitudes, $u^2/\omega^2 A_d \geq 1$, flow separation will occur. Flow separation is induced by viscosity. If $\delta_v^2 \ll A_d$ then the exact value of the viscosity is not important to predict flow separation. We have reached a high Reynolds number limit.

With mean flow ($u_0 \neq 0$), we have the same answer as for large amplitudes.

o) Flow separation always occurs when the particle displacement is of the order of the diameter of the orifice: $u'_d \sim \omega d$.

In the pipe we have: $u'_D = u'_d(d/D)^2$. The critical level is given by $p' \sim \rho_0 c_0 \omega d (d/D)^2$.

At 10 Hz this corresponds to SPL = 110 dB.

At 100 Hz this corresponds to SPL = 130 dB.

At 1000 Hz this corresponds to SPL = 150 dB.

Within a hearing-aid device, sound is transferred from the amplifier (at the back of the ear) to the ear-drum by means of a pipe of $D = 1$ mm. An orifice of $d = 0.1$ mm placed in this pipe, will protect the ear by limiting sound level around 1 kHz to SPL = 130 dB. Such devices are indeed in everyday use.

p) In a stationary subsonic free jet induced by a mean flow we expect a uniform pressure. The first intuitive guess for a quasi-stationary theory is to assume that the inertial effects upstream of the orifice remain unchanged, while the inertial effects in the jet are negligible. This leads to the common assumption that the end correction of a thin orifice with a mean flow is at low frequencies half of the end correction in the absence of mean flow. Experiments by Ajello [3] indicate a much stronger reduction of the end-correction. In some circumstances negative end corrections are found (Ajello [3], Peters [181]). Indeed the theory for open pipe termination of Rienstra [198] indicates that we cannot predict end corrections intuitively.

q) $R = p_1^- / p_1^+ = [A_1 - (A_2 + A_3)] / [A_1 + (A_2 + A_3)].$

r) $R = p_1^- / p_1^+ = [(A_1 - A_3) \cos(kL) - iA_2 \sin(kL)] / [(A_1 - A_3) \cos(kL) + iA_2 \sin(kL)].$

$R = -1$ for $kL = \pi(n + 0.5)$, $R = 0$ for $A_2 = 0$ when $A_1 = A_3$ and $R = 1$ for $A_3 = 0$ when $kL = n\pi$ ($n = 0, 1, 2, 3, \dots$).

s) $\hat{p}_1^+ + \hat{p}_1^- = \hat{p}_b + \rho_w \omega^2 a_0 \hat{a}$. $\hat{p}_b / p_0 = -3\gamma \hat{a} / a_0$. $\hat{p}_1^- = R \hat{p}_1^+$.

$$A(\hat{p}_1^+ - \hat{p}_1^-) = A\hat{p}_2^+ - (\rho_w c_w) i \omega 4\pi a_0^2 \hat{a}$$

$$R = -[1 + iA(\omega^2 - \omega_0^2) / 2\pi \omega c_w a_0]^{-1} \text{ with } \omega_0^2 = 3\gamma p_0 / \rho_w a_0^2.$$

t) $\hat{p}_b / \hat{p}_{in} = [1 + (\frac{\omega}{\omega_0})^2 (\frac{2\pi i a_0}{Ak} - 1)]^{-1}$.

u) $\omega_0^2 a_0^2 / c_l^2 = 3\rho_l / \rho_w \ll 1$. At $p_0 = 1$ bar, $\rho_l / \rho_w = O(10^{-3})$.

v) $3\gamma l p_0 / \rho_w c_w^2 = O(10^{-4})$ hence $a_0 \omega / c_w < 10^{-2}$.

w) $\omega_0^2 \simeq 3\gamma l p_0 / 2\rho_w a_0^2$. $R = -[1 + A(\omega^2 - \omega_0^2) / 2\pi i \omega c_w a_0]^{-1}$.

x) When $a_0 = O(D)$ we do not have a radial flow around the bubble. The approximation used for small bubbles fails.

y) $[g] = s/m$.

z) $\omega^2 \hat{g} - c_0^2 \frac{d^2}{dx^2} \hat{g} = e^{-i\omega\tau} \delta(x - y) / 2\pi$.

Integration around $x = y$ yields: $-[\frac{d}{dx} \hat{g}]_{y^-}^{y^+} = e^{-i\omega\tau} / 2\pi c_0^2$.

$$[\frac{d}{dx} \hat{g}]_{\pm} = \mp i k \hat{g}^{\pm}. \text{ At } x = y \text{ we have } \hat{g}^{\pm} = e^{-i\omega\tau} / 4\pi i \omega c_0.$$

Hence $\hat{g}^{\pm} = \hat{g}_{x=y}^{\pm} e^{\mp i k(x-y)}$ with "+" for $x > y$ and "-" for $x < y$.

Therefore: $\hat{g} = e^{-i\omega\tau} e^{-ik|x-y|} / 4\pi i \omega c_0$.

A) Using the result of exercise z) we find:

$$\hat{g}^+(L|y) = \hat{g}_0(L|y) \quad \text{with} \quad \hat{g}_0(x|y) = e^{-i\omega\tau} e^{-ik|x-y|} / 4\pi i \omega c_0.$$

Furthermore:

$$\frac{Z_L}{\rho_0 c_0} = \frac{\hat{g}^+(L) + \hat{g}^-(L)}{\hat{g}^+(L) - \hat{g}^-(L)}, \quad R = \frac{Z_L - \rho_0 c_0}{Z_L + \rho_0 c_0} = \frac{\hat{g}^-(L)}{\hat{g}^+(L)}.$$

$$\text{Hence: } \hat{g}(x|y) = \hat{g}^+ + \hat{g}^- = \hat{g}_0(x|y) + R \hat{g}_0(x|2L - y).$$

This corresponds to the waves generated by the original source at y and an image source at $2L - y$.

B) The same answer as the previous exercise with (section 4.4.5):

$R = -1/[1 + A(\omega^2 - \omega_0^2)/(2\pi i \omega c_w a_0)]$ where A is the pipe cross-sectional area, a_0 the bubble radius and ω_0 the Minnaert frequency of the bubble.

C) For $|x_1 - y_1| \gg \sqrt{S}$ and $k_0^2 S \ll 1$ the Green's function is independent of the position (y_2, y_3) of the source in the cross section of the pipe. Hence we have: $g(x_1, t|y_1, \tau) = \int_{-\infty}^{\infty} \int_{-\infty}^{\infty} G(\mathbf{x}, t|\mathbf{y}, \tau) dy_2 dy_3 = SG(\mathbf{x}, t|\mathbf{y}, \tau)$.

D) Moving the source towards the observer by a distance Δy should induce the same change Δg in $g(x, t|y, \tau)$ as a displacement $\Delta x = -\Delta y$ of the observer in the direction of the source. The distance $|x - y|$ is in both cases reduced by the same amount.

$$\text{This implies that: } \Delta g = \frac{\partial g}{\partial y} \Delta y = -\frac{\partial g}{\partial x} \Delta x.$$

$$\text{E) } p' \simeq \rho' c_0^2 \sim M_0 \frac{1}{2} \rho_0 U_0^2 (d^2/S) = 2 \times 10^{-2} \text{ Pa.} \quad \text{SPL} = 60 \text{ dB.}$$

$$\text{F) SPL} = 63 \text{ dB.}$$

$$\text{G) } (S/a_0^2)(\rho_w c_w^2/3\gamma p_0)^{\frac{1}{2}} = 2.3 \times 10^4 \text{ or } 87 \text{ dB.} \quad \rho_w c_w^2/3\gamma p_0 = 5.4 \times 10^3 \text{ or } 75 \text{ dB.}$$

$$\text{H) } f \sim U_0/D = 0.1 \text{ kHz, } \omega_0/2\pi = 6.5 \text{ kHz.}$$

Chapter 5

$$\text{a) } Z(0) = \rho_0 c_0 \frac{(Z_L + \rho_0 c_0) + (Z_L - \rho_0 c_0) e^{-2ik_0 L}}{(Z_L + \rho_0 c_0) - (Z_L - \rho_0 c_0) e^{-2ik_0 L}}$$

For $Z_L = \infty$ we have $Z(0) = i\rho_0 c_0 \cotg(k_0 L)$. As $\text{Re } Z(0) = 0$ for $Z_L = \infty$ the piston does in general not generate any acoustical power unless there is resonance, *i.e.* $k_0 L = (n + \frac{1}{2})\pi$.

The acoustical field in the pipe is given by: $\hat{p} = \hat{p}^+ e^{-ik_0 x} + \hat{p}^- e^{ik_0 x}$.

The amplitudes \hat{p}^+ and \hat{p}^- are calculated from the piston velocity \hat{u}_p by using: $\rho_0 c_0 \hat{u}_p = \hat{p}^+ - \hat{p}^-$, $Z(0)\hat{u}_p = \hat{p}^+ + \hat{p}^-$.

$$\text{Hence: } \hat{p}^+ = \frac{1}{2}(Z(0) + \rho_0 c_0)\hat{u}_p, \quad \hat{p}^- = \frac{1}{2}(Z(0) - \rho_0 c_0)\hat{u}_p.$$

$$\text{b) } Z_L \simeq Z'_L + i\rho_0 \omega \delta.$$

$$\text{c) For } x < 0 \text{ we have } \hat{p}^+ = 0 \text{ while: } \hat{p}^- = \frac{1}{2}\rho_0 c_0 (S_p/S)\hat{u}_p (1 + e^{-ik_0 L}).$$

The condition that there is no radiation, $\hat{p}^- = 0$, is obtained for: $k_0 L = (2n + 1)\pi$, where $n = 0, 1, 2, \dots$

$$\text{d) } \hat{p} = \hat{p}^+ e^{ik_0 L} + \hat{p}^- e^{-ik_0 L},$$

$$\text{with: } \hat{p}^+ = \frac{\rho_0 c_0 \hat{u}_p (S + 2S_p)}{(S + 2S_p) - (S - 2S_p) e^{-2ik_0 L}}, \quad \text{and } \hat{p}^- = \frac{S - 2S_p}{S + 2S_p} \hat{p}^+.$$

Flow separation becomes dominant at the junction when:

$(\hat{p}^+ - \hat{p}^-)/\rho c_0^2 = O(k_0 \sqrt{S_1})$. The amplitude of the second harmonic \hat{p}_1 , generated by non-linearities, can be estimated from:

$$(\hat{p}_1/\hat{p}^+) \sim k_0 L (\hat{p}^+/\rho_0 c_0^2).$$

$$\text{e) Configuration a): } Z_p = \rho_0 c_0 \frac{(Z_1 + \rho_0 c_0) + (Z_1 - \rho_0 c_0) e^{-2ik_0 L}}{(Z_1 + \rho_0 c_0) - (Z_1 - \rho_0 c_0) e^{-2ik_0 L}},$$

where: $Z_1 = S_1 Z_2 Z_3 / (S_2 Z_3 + S_3 Z_2)$, $Z_2 = \rho_0 c_0$, $Z_3 = i \rho_0 c_0 \tan(k_0 L)$.

The system is not a closed resonator because the condition of zero pressure at the junction is never satisfied.

$$\text{Configuration b): } Z_p = \rho_0 c_0 \frac{(Z_1 + \rho_0 c_0) + (Z_1 - \rho_0 c_0) e^{-2ik_0 L}}{(Z_1 + \rho_0 c_0) - (Z_1 - \rho_0 c_0) e^{-2ik_0 L}},$$

where: $Z_1 = S_1 Z_2 Z_3(0) / (S_2 Z_3(0) + S_3 Z_2)$, $Z_2 = \rho_0 c_0$,

$$Z_3(0) = \rho_0 c_0 \frac{(Z_3(2L) + \rho_0 c_0) + (Z_3(2L) - \rho_0 c_0) e^{-2ik_0 L}}{(Z_3(2L) + \rho_0 c_0) - (Z_3(2L) - \rho_0 c_0) e^{-2ik_0 L}},$$

$Z_3(2L) = S_3 Z_4 Z_5 / (S_4 Z_5 + S_5 Z_4)$, $Z_4 = i \rho_0 c_0 \cotg(k_0 L)$, $Z_5 = \rho_0 c_0$.

The system is in resonance for $k_0 L = (n + \frac{1}{2})\pi$.

Configuration c): $Z_p = \frac{1}{2} \rho_0 c_0 i \tan(k_0 L)$.

The system is resonant for $k_0 L = (n + \frac{1}{2})\pi$.

f) At the mouthpiece we have: $\rho_0 c_0 \hat{u}_p = \hat{p}^+ - \hat{p}^-$.

If we assume friction losses to be dominant we have: $\hat{p}^- = \hat{p}^+ e^{-2\alpha L}$

$$\text{where: } \alpha = \frac{1}{D} \sqrt{\frac{\pi v}{c_0 L}} \left(1 + \frac{\gamma - 1}{\sqrt{v/a}}\right) \simeq 0.027 \text{ m}^{-1}.$$

Hence we find: $\hat{p}^+ \simeq 7.6 \times 10^3 \text{ Pa}$, and $\hat{p} = \hat{p}^+ + \hat{p}^- \simeq 2\hat{p}^+$.

The corresponding fluid particle oscillation amplitude Δ at the open pipe termination is: $\Delta \simeq \hat{p} / (\rho_0 c_0 \omega) \simeq 7 \times 10^{-2} \text{ m}$.

If we assume non-linear losses at the open pipe termination to be dominant we have (equation 5.24) $\hat{u} = \sqrt{(\frac{3}{2} \pi \hat{u}_p c_0)}$

and $\hat{p} \simeq \rho_0 c_0 \hat{u} \simeq 1.6 \times 10^4 \text{ Pa}$. Friction losses and flow separation losses are comparable and the acoustical fluid particle displacement is of the order of the pipe diameter.

g) $\hat{p}_1^+ - \hat{p}_1^- = \rho_0 c_0 \hat{u}_p$, $\hat{p}_1^+ e^{-ik_0 L_1} + \hat{p}_1^- e^{ik_0 L_1} = \hat{p}_2^+ + \hat{p}_2^-$,

$$(\hat{p}_1^+ e^{-ik_0 L_1} - \hat{p}_1^- e^{ik_0 L_1}) S_1 = (\hat{p}_2^+ - \hat{p}_2^-) S_2,$$

$$\hat{p}_2^+ e^{-ik_0 L_2} + \hat{p}_2^- e^{ik_0 L_2} = \hat{p}_3^+ + \hat{p}_3^-,$$

$$(\hat{p}_2^+ e^{-ik_0 L_2} - \hat{p}_2^- e^{ik_0 L_2}) S_2 = (\hat{p}_3^+ - \hat{p}_3^-) S_3,$$

$$\hat{p}_3^+ e^{-ik_0 L_3} + \hat{p}_3^- e^{ik_0 L_3} = 0, \quad \rho_0 c_0 \hat{u}_{ex} = \hat{p}_3^+ e^{-ik_0 L_3} - \hat{p}_3^- e^{ik_0 L_3}.$$

h) $\hat{p} = A \cos(kx)$ for $x < L$, while $\hat{p} = B e^{-ikx}$ for $x > L$. Suitable dimensionless groups are $z = kL$, $\alpha = c_M L / c_0 a$, $\lambda = \rho_0 L / \sigma$, where the propagation speed of transversal waves in the membrane $c_M = \sqrt{T/\sigma}$ is introduced. The resonance equation is then

$$(z - 8\alpha^2 z^{-1}) \sin z = \lambda e^{iz}.$$

$\lambda \rightarrow 0$ when the air density becomes negligible or when the membrane becomes very heavy. In that case we have the membrane-in-vacuum vibration $z \simeq \alpha \sqrt{8} + \dots$ and the closed pipe modes $z \simeq n\pi + \frac{\lambda}{n\pi - 8\alpha^2/n\pi} + \dots$ ($n = 1, 2, 3, \dots$).

So when $\lambda = 0$ (no energy is radiated) there are indeed undamped solutions with $\text{Im}(z) = \text{Im}(\omega) = 0$.

i) $m = \rho_0 S_n (\ell + 2\delta)$, $K = \rho_0 c_0^2 S_n^2 / V$.

$$\text{j) } \hat{p}_{in} = \frac{i \omega \rho_0 (\ell + 2\delta) \hat{Q}}{S_n \left(1 - \frac{\omega^2}{\omega_0^2}\right)}.$$

$$\text{k) } \frac{\hat{p}_{transmitted}}{\rho_0 c_0 \hat{u}_p} = \frac{2(1 - \omega^2/\omega_0^2) - (i\omega V/c_0 S)}{[2(1 - \omega^2/\omega_0^2) - (i\omega V/c_0 S)] e^{ik_0 L} - (i\omega V/c_0 S) e^{-ik_0 L}}.$$

There is no transmission when both $\omega = \omega_0$ and $k_0 L = (n + \frac{1}{2})\pi$.

l) Transmission and reflection coefficient:

$$T = \frac{\hat{p}_2^+}{\hat{p}_1^+} = \frac{1}{(1 + ik_0 \ell S_p / S_d)[1 - (\omega^2 / \omega_0^2) + (ik_0 V / 2S_p)]},$$

$$R = \frac{\hat{p}_1^-}{\hat{p}_1^+} = T + \frac{(ik_0 \ell S_p / S_n) - 1}{(ik_0 \ell S_p / S_n) + 1},$$

where: $\omega_0^2 = c_0^2 2S_d / (\ell V)$, and: $\ell \simeq 1.6 \sqrt{S_d / \pi} \simeq \sqrt{S_d}$.

$$\text{m) } T = 2 \left(2 - \frac{i\omega\rho_w c_w}{S_p(\gamma p_0 / V)(1 - \omega^2 / \omega_0^2)} \right)^{-1}, \quad R = T - 1, \quad \omega_0^2 = \left(\frac{\gamma p_0}{V} \right) \left(\frac{S}{\rho_w \ell} \right).$$

n) An energy balance yields: $\frac{1}{2} \hat{p}_{in} \hat{Q} = \frac{2}{3\pi} \rho_0 \hat{u}^3 S_n$, where we assumed that \hat{p}_{in} and \hat{Q} are in phase and that vortex shedding at the neck can be described by means of a quasi-stationary model. The internal pressure \hat{p}_{in} is related to the acoustical velocity \hat{u} through the neck by the momentum conservation law: $\hat{p}_{in} = \rho_0 i \omega \ell \hat{u}$. This yields: $\hat{u} = \sqrt{(3\pi \omega \ell \hat{Q} / 4S_n)}$ which is a factor $\sqrt{(2S_n k_0 \ell / S_p)}$ smaller than for a $\frac{1}{4}\lambda$ open pipe resonator.

$$\text{o) } \frac{\hat{p}_{in}}{\hat{p}_{ex}} = 1 + \frac{\omega_0 u_0 - c_0}{\omega_1 u_0} + i \left(1 + \frac{\omega_0^2}{\omega_1^2} \right), \quad \text{with } \omega_0^2 = c_0^2 S_n / (\ell V) \text{ and } \omega_1 = c_0 / \ell.$$

p) As there are no sources $q = 0$, we have:

$$\rho'(x, t) = -c_0^2 \int_{-\infty}^t \left[\rho'(y, \tau) \frac{\partial g_a}{\partial y_i} - g_a(x, t|y, \tau) \frac{\rho'(y, \tau)}{\partial y_i} \right]_{y=0} n_i d\tau, \quad g_a(x, t|y, \tau) = \iint_S G(x, t|y, \tau) dS(y).$$

Other contributions from the surface integral vanish if we assume that G has the same boundary conditions as the acoustic field on these surfaces. At $y = 0$, $(\partial g_a / \partial y_i) n_i = 0$. Furthermore we have: $\rho_0 \frac{\partial}{\partial \tau} u' = -c_0^2 \frac{\partial}{\partial y} \rho'$, and $n_1 = -1$ at $y = 0$, which yields: $p' = c_0^2 \rho' = \rho_0 c_0^2 \int_{-\infty}^t g_a(x, t|y, \tau) \frac{\partial}{\partial \tau} u' d\tau$. The final result is obtained by partial integration.

- q) $f \simeq c_0 / (2L)$, $\hat{u} / (\omega w) \simeq 1$ m/s. $\hat{p} \simeq \rho_0 c_0 \hat{u} \simeq 4 \times 10^2$ Pa. The ratio of acoustical particle displacement to pipe diameter is $w/D = 2 \times 10^{-2}$. We expect vortex shedding at the pipe ends to be a minor effect in a Rijke tube.
- r) Using an energy balance between sound production and dissipation by vortex shedding we have: $0.05 \frac{1}{2} \rho_0 u_0^2 \hat{u} B \times w \simeq \rho_0 \hat{u}^3 B \times w$, or: $|\hat{u}| \simeq 0.22 u_0$. The hydrodynamic resonance condition $f w / u_0 \simeq 0.4$ combined with the acoustic resonance condition $2\pi f = c_0 \sqrt{(wB / \ell V)}$ and the order of magnitude estimate $\ell \sim 2 \sqrt{(Bw / \pi)} = 0.44$ m yields: $f \simeq 18.5$ Hz and $u_0 \simeq 14$ m/s = 50 km/h, $|\hat{p}| = \rho_0 \omega \ell |\hat{u}| \simeq 43$ Pa. For a slit-like orifice we have $\ell \sim w$.
- s) The blowing pressure p_0 is a fair estimate. When \hat{p} reaches p_0 the flow velocity through the reed vanishes at high pressures, which provides a non-linear amplitude saturation mechanism.

Chapter 6

- a) The fluid pushed ahead of the sphere in the direction of the translation can be considered as generated by a source. The fluid sucked by the rear of the sphere corresponds to the sink.
- b) Qualitatively we find that the streamlines as observed in the reference frame moving with the vortex ring are very similar to those generated by a dipole or a translating sphere. Quantitatively the circulation $\Gamma = \oint \mathbf{v} \cdot d\mathbf{l}$ of the vortex corresponds to a discontinuity $\Delta\phi$ of the flow potential across a surface sustained by the vortex ring. Such a discontinuity can be generated by a dipole layer on this surface which replaces the vortex ring [reference Prandtl]. Assuming the dipole layer to consist out of a layer of sources at the front separated by a distance δ from a layer of sources at the rear, the potential difference is given by $\Delta\phi = u\delta$. The velocity u is the flow velocity between the two surfaces forming the dipole layer. Taking the projection S of the surface on a plane normal to the direction of propagation of the vortex ring, we can represent in first approximation the dipole layer by a single dipole of strength $uS\delta$ placed at the center of the ring and directed in the direction of propagation of the vortex ring.

- c) Electromagnetic waves are transversal to the direction of propagation like shear-waves. Acoustical waves are compression waves and hence longitudinal.
- d) $R = (\rho_{air}c_{air} - \rho_{water}c_{water})/(\rho_{air}c_{air} + \rho_{water}c_{water})$, $\rho_{air}c_{air} = 4 \times 10^2 \text{ kg/m}^2 \text{ s}$,
 $\rho_{water}c_{water} = 1.5 \times 10^6 \text{ kg/m}^2 \text{ s}$, $1 + R = 10^{-4}$.
- e) A dipole placed normal to a hard wall will radiate as a quadrupole because the image dipole is opposite to the original dipole. A dipole placed parallel to a hard wall will radiate as a dipole of double strength because the image has the same sign as the original.
- f) The radiated power increases by a factor two because the intensity is four times the original intensity but the radiation is limited to a half space.
- g) The first transverse mode of the duct has a pressure node in the middle of the duct. Hence a volume source placed on the axis of the duct experiences a zero impedance for this first mode. It cannot transfer energy to this mode.
- h) The vanishing acoustic pressure at the water surface $p' = 0$ precludes any plane wave propagation. The first propagating mode has a cut-on frequency $f_c = \frac{1}{4}c_0/h$ corresponding to a quarter wave length resonance.
- i) A dipole placed normal to the duct axis will not radiate at frequencies below the cut-off frequency of the first transverse mode in a duct with hard walls. This is explained by the destructive interference of the images of the dipole in the direction of the axis. On the other hand, however, when placed along the axis the dipole will very efficiently radiate plane waves at low frequencies. The amplitude of these waves are: $|\hat{p}| = \omega\rho_0\hat{Q}\delta/S$.
- j) Assume that the quadrupole is approximated by two dipoles (1 and 2), one very close to the surface of the cylinder ($r_1 \simeq R$) and one far away ($r_2 \gg R$). If the dipoles are directed radially, the dipole at the surface forms a quadrupole with its image ($r'_1 = R^2/r_1 \simeq R$), while the image of the other dipole is very close ($r'_2 = R^2/r_2 \ll R$) to the axis of the cylinder and very weak. The distance between the source and sink forming the second dipole is reduced by a factor (R^2/r_2^2) while the strength of each image is equal to that of the original source. As a result the dipole far away from the cylinder radiates independently of the dipole close to the cylinder.
 A very similar behaviour is found when the dipoles forming the quadrupole are normal to the radius of the cylinder (in tangential direction). Then the radiation of the dipole close to the surface is enhanced by a factor two, while that of the other dipole is not affected.
- k) Equal thrust implies: $\rho_1 u_1^2 D_1^2 = \rho_2 u_2^2 D_2^2$. If $\rho_1 = \rho_2$ we have $u_1 D_1 = u_2 D_2$. Assuming subsonic free cold jets we have: $I \sim u^8 D^2 = (uD)^8 / D^6$. Hence: $I_1/I_2 = D_2^6/D_1^6 = 2^6$ or a difference of 36 dB.
 In practice a low sound production does also correspond to a lower power $\frac{1}{2}\rho u^3 D^2 \sim (uD)^3/D$. The introduction of high bypass jet engines was aimed to reduce the propulsion costs, but it appeared to be also a very efficient noise reduction method.
- l) As the compressibility of an ideal gas is determined by the mean pressure there appears to be no monopole sound production upon mixing of a hot jet with a cold gas environment with equal specific-heat ratio γ . The sound is produced [149, 169] by the difference in acceleration between neighbouring particles experiencing the same pressure gradient but having different densities. This corresponds to a force in terms of the analogy of Lighthill and a dipole source of sound. Therefore the radiation scales in a subsonic case at $I \sim M^6$.
- m) The large contrast in compressibility \mathcal{K} between the bubbly liquid and the surrounding water results into a monopole type source (fluctuating volume). This corresponds to a scaling rule $I \sim M^4$.
- n) This effect is not significant in subsonic free jets.
- o) The characteristic frequency for turbulence in a free jet with circular cross section is u_0/D which implies that: $D/\lambda = Df/c \sim u_0/c_0$. Hence a subsonic free jet is a compact flow region with respect to sound production by turbulence.
 Note: for a free jet with a rectangular cross section $w \times h$ and $w \gg h$ the characteristic frequency of the turbulence is $0.03u_0/h$.

p) Using Curle's formula:

$$\rho' = \frac{x_i x_j}{4\pi |\mathbf{x}|^3 c_0^4} \frac{\partial^2}{\partial t^2} \iiint_V T_{ij}(\mathbf{y}, t - \frac{|\mathbf{x}|}{c_0}) d\mathbf{y} + \frac{x_j}{4\pi |\mathbf{x}|^2 c_0^3} \frac{\partial}{\partial t} F_j(t - \frac{|\mathbf{x}|}{c_0})$$

and $\frac{\partial}{\partial t} \sim u_0/D$, $T_{ij} \sim \rho_0 u_0^2$, $F_j \sim \rho_0 u_0^2 dD$, and $V \sim D^3$, we obtain:

$$\rho' \sim \frac{\rho_0 u_0^3 D}{4\pi |\mathbf{x}| c_0^3} \left(\frac{u_0}{c_0} + \frac{d}{D} \right).$$

The cylinder induces an enhancement of turbulence sound production by a factor $(1 + dc_0/Du_0)$. Blowing on a finger we indeed observe a significantly larger sound production than blowing without finger.

q) Sound production due to volume fluctuations V' of the bubble is given by:

$\rho' = (4\pi |\mathbf{x}| c_{water}^2)^{-1} (\partial^2/t^2) V'$, where, assuming isentropic oscillations of the bubble of initial volume $V_0 = 4\pi a_0^3/3$ at p_0 , we have: $V'/V_0 = -p'/\gamma_{air} p_0$. The typical pressure fluctuations in a free jet are of the order $p' \sim \rho_w u_0^2$. Assuming $\partial/\partial t \sim u_0/D$ we find

$$\frac{\rho'}{\rho_{water}} \sim \frac{D}{4\pi |\mathbf{x}|} \frac{u_0^4}{c_{water}^4} \frac{a_0^3}{D^3} \frac{\rho_{water} c_{water}^2}{p_0}.$$

The enhancement in sound production, when compared to no bubbles, is by a factor $(1 + (a_0/D)^3 (\rho_{water} c_{water}^2/p_0))$. Since $\rho_{water} c_{water}^2/p_0 = O(10^4)$, even a small bubble will already enhance the sound production considerably.

r) With a single blade the sound production as a result of the tangential component of the lift force (in the plane of the rotor) scales as: $\rho'/\rho_0 \sim C_L D(k_0 R)^3/8\pi |\mathbf{x}|$. The sound produced by the axial component is a factor u_0/c_0 weaker.

With two opposite blades, the lift forces in tangential direction form a quadrupole which result into a factor $k_0 R$ weaker sound radiation than in the case of the single blade. The sound production in a ventilator is actually dominated by non-ideal behaviour such as the non-uniformity of the incoming flow.

s) In a hard walled duct an ideal low speed axial ventilator will not produce any sound. The effect of the tangential forces is compensated by images in the walls while the pressure difference Δp induced by the axial force is constant. Non-uniformity of the incoming flow will induce fluctuations in the pressure difference Δp which are very efficiently radiated away. Especially the supports of the ventilators are to be placed downstream of the fan. Further sources of flow non-uniformity are the air intake or bends.

t) The sound production will be dominated by the interaction of the rotor blades with the thin wake of the wing. The resulting abrupt changes in lift force on the blades of the rotor induce both radial and axial sound radiation. The thinner the waker the higher the generated frequencies. As the ear is quite sensitive to relatively high frequencies an increase of the wake thickness can result into a significant reduction of noise (dBA).

u) The tip Mach number $\omega R/c_0 = k_0 R$ is of order unity. The rotor is therefore not compact at the rotation frequency, and certainly not at the higher harmonics.

v) The dominant contribution is from the unsteady force, given by $C_D \frac{1}{2} \rho_0 u_0^2$, on the body. This results into a sound production scaling as $(u_0/c_0)^3$ (see Curle's formula).

$$w) Z_L = \rho_0 c_0 \frac{1}{4} (k_0 a)^2, \quad Z_p = \rho_0 c_0 \frac{(Z_L + \rho_0 c_0) + (Z_L - \rho_0 c_0) e^{-2ik_0 L}}{(Z_L + \rho_0 c_0) - (Z_L - \rho_0 c_0) e^{-2ik_0 L}}.$$

$$x) \langle I \rangle = \frac{1}{4} [\hat{p}^* \hat{u} + \hat{p} \hat{u}^*] = \frac{1}{2} \text{Re}(Z_p) |\hat{u}|^2, \quad \text{and} \quad \langle W \rangle = \pi a^2 \langle I \rangle.$$

At resonance $k_0 L = (n + \frac{1}{2})\pi$ we find: $Z_p = \rho_0 c_0 (\rho_0 c_0 / Z_L)$ (see previous exercise). This corresponds to an enhancement $Z_p/Z_L = [4/(k_0 a)^2]^2$ of the radiated power.

$$y) \hat{p}r = A^+ e^{-ik_0 r} + A^- e^{ik_0 L}, \quad i\omega \rho_0 \hat{u}r = \hat{p} + ik_0 [A^+ e^{-ik_0 r} - A^- e^{ik_0 L}].$$

$(r_1/r_2)^2 = S_1/S_2$ and $r_1 = r_2 - L$, so $r_2 = L/(1 - \sqrt{S_1/S_2})$.

$$A^+ = \rho_0 c_0 \hat{u}_p r_1 / \left\{ [1 - i/(k_0 r_1)] e^{-ik_0 r_1} - R [1 + i/(k_0 r_1)] e^{ik_0 r_1} \right\}$$

$$R = \frac{A^-}{A^+} = - \frac{1 - \frac{1}{4}(k_0 a_2)^2 [1 - i/(k_0 r_2)]}{1 - \frac{1}{4}(k_0 a_2)^2 [1 + i/(k_0 r_2)]} e^{-2ik_0 r_2}$$

z) Except for the highest frequencies, there is no radiation into free-space. Hence the size of the loudspeaker compared to the acoustical wave-length is not relevant for the sound transfer from loudspeaker to eardrum. The Walkman loudspeaker acts almost directly onto the eardrum.

A) Friction losses are given by: $(1 - |\hat{p}^-/\hat{p}^+|)_f = 1 - e^{-2\alpha L} \simeq 2\alpha L$, where α can be calculated by using the formula of Kirchhoff. The friction is proportional to $\sqrt{\omega}$.

Radiation losses are given by: $(1 - |\hat{p}^-/\hat{p}^+|)_r = \frac{1}{2}(k_0 a)^2$, and are proportional to ω^2 . Using the results of exercise (5.f) we find

$$\text{for } f_0 : (1 - |\hat{p}^-/\hat{p}^+|)_f = 5 \cdot 10^{-2}, (1 - |\hat{p}^-/\hat{p}^+|)_r = 1.2 \cdot 10^{-4};$$

$$\text{for } f_1 = 3f_0 : (1 - |\hat{p}^-/\hat{p}^+|)_f = 9 \cdot 10^{-2}, (1 - |\hat{p}^-/\hat{p}^+|)_r = 1 \cdot 10^{-3};$$

$$\text{for } f_2 = 5f_0 : (1 - |\hat{p}^-/\hat{p}^+|)_f = 1.2 \cdot 10^{-1}, (1 - |\hat{p}^-/\hat{p}^+|)_r = 3 \cdot 10^{-3}.$$

In a flute of the same size as a clarinet the radiation losses are increased by a factor eight (two radiation holes and twice the fundamental frequency). The friction losses increase by a factor $\sqrt{2}$ due to the higher frequency.

B) Assuming a perfectly reflecting ground surface, the energy is distributed over a semi-sphere: $I = W_r/(2\pi r^2)$. As $I_{min} = 10^{-12} \text{ W/m}^2$, we find for $W_r = 5 \times 10^{-5} \text{ W}$ that $r \simeq 4 \text{ km}$.

C) In free space the bubble experiences the impedance of a compact sphere:

$$\text{Re}(Z) = \rho_{water} c_{water} (k_0 a_0)^2. \text{ In a pipe we have: } \text{Re}(Z) = \rho_{water} c_{water} 8\pi a_0^2/S.$$

D) As the twin pipes oscillate in opposite phase the radiation has a dipole character and is a factor $(k_0 2a)^2$ weaker than for an individual pipe. Such systems are therefore acoustically almost closed. In a duct a wall placed along the duct axis can form such a system of twin pipes if it is longer than the duct width. In such a case the oscillation of the system is called a Parker mode and does not radiate because the oscillation frequency is below the cut-off frequency for the first transverse mode. In fact the twin pipes forms with its images an infinite row of pipes. In a similar way such modes can occur in rotors or stators of turbines. This kind of oscillations have been reported by Spruyt [234] for grids placed in front of ventilators.

Chapter 7

a) (i) $k_c a = 2\pi f_c a / c_0 = j'_{11} = 1.84118$, so $f_c = 996.3 \text{ Hz}$.

(ii) $k_{11} = -15.93 i$, so $20 \log_{10} |e^{-ik_{11} D}| = -20|k_{11}|D \log_{10} e = -138.3D = -20$, and $D = 14.5 \text{ cm}$.

(iii) $k_{11} = -18.4 i$, so $D = 12.5 \text{ cm}$.

b) Since $\sigma_{m\mu} a \rightarrow \infty$, $I_m/I'_m \rightarrow 1$ and $\alpha_{m\mu} = i\sigma_{m\mu} \simeq -ik\rho_0 c_0/X$.

For $r \simeq a$

$$\frac{J_m(\alpha_{m\mu} r)}{J_m(\alpha_{m\mu} a)} e^{-ik_{m\mu} x} \simeq \left(\frac{a}{r}\right)^{1/2} e^{-\sigma_{m\mu}(a-r)} e^{-i\sqrt{k^2 + \alpha_{m\mu}^2} x}.$$

c) A simple point mass source $Q\delta(\mathbf{x} - \mathbf{x}_0) e^{i\omega t}$, where we take $x_0 = 0$, $\vartheta_0 = 0$, gives rise to the equation

$$\nabla^2 p + k^2 p = -i\omega Q \delta(x) \frac{1}{r_0} \delta(r - r_0) \sum_{m=-\infty}^{\infty} \delta(\vartheta - 2\pi m)$$

with solution

$$p(x, t, \vartheta) = \frac{\omega Q}{4\pi} \sum_{m=-\infty}^{\infty} \sum_{\mu=1}^{\infty} \frac{J_m(\alpha_{m\mu} r_0) J_m(\alpha_{m\mu} r) e^{-ik_{m\mu} |x| - im\vartheta}}{\frac{1}{2}(a^2 - m^2/\alpha_{m\mu}^2) J_m(\alpha_{m\mu} a)^2 k_{m\mu}}.$$

- d) $F(\alpha, Z) = i\omega\rho_0 J_m(\alpha R) + \alpha Z J'_m(\alpha R) = 0$, from which it immediately follows that Z , and hence Z_{opt} , is of the form $\rho_0\omega R K_m$ with $K_m = J_m(\alpha R)/i\alpha R J'_m(\alpha R)$. From $\frac{\partial}{\partial \alpha} F(\alpha, Z) = 0$ it follows that $\alpha R =: z$ is a (non-zero) solution of $z J'_m(z) + i(z^2 - m^2)^{\frac{1}{2}} J_m(z) = 0$, while $K_m = (z^2 - m^2)^{-\frac{1}{2}}$. Take the sign of the square root that yields $\text{Re}(Z) > 0$. A numerical zero-search reveals that $K_0 = 0.28330 - 0.12163i$, $K_1 = 0.20487 - 0.07049i$, $K_2 = 0.16628 - 0.05133i$.

Chapter 8

- a) Since $A(x) = \pi a^2 e^{2mx}$, we have $p(x) = \hat{p}_0 e^{-i\sqrt{k^2 - m^2}x - mx}$.
 b) Since $k_1 = |k|(R - h)/R$ and $\alpha = -q$ we have

$$R = \left| \frac{\omega}{\alpha k_1 \varepsilon} \right| = \frac{\omega R}{q|k|(R - h)\varepsilon} = \frac{R(1 - \varepsilon h)}{(R - h)\varepsilon}.$$

It follows that $R = \varepsilon^{-1} = 250$ m, and so the largest distance is $2\sqrt{2Rh - h^2} = 54.7$ m.

- d) Replace $\cos(\Omega\tau)$ and $\sin(\Omega\tau)$ by $e^{i\Omega\tau}$ and $-i e^{i\Omega\tau}$, express u'_n in y . Then it follows that

$$Z = \frac{1}{\sigma} \left[R + i\rho_0 \ell \omega - i\rho_0 c_0^2 \frac{S_n}{V\omega} \right].$$

Chapter 9

- a) With the propeller in vane position (no angle of attack) the lift force as defined in (9.26) is directed in z -direction only, and $M_e = M_R$. Using the results of section 9.3 we find

$$p(x, t) \simeq -\frac{f_0 M_R^2 \sin \theta \cos \theta \cos(\phi - \omega t + kr)}{4\pi a r (1 - M_R \sin \theta \cos(\phi - \omega t + kr))^3}.$$

The radiation pattern has zeros in the directions $\theta = 0^\circ, 90^\circ$, and 180° , while it has its main directions of radiation in (near) the conical surfaces $\theta = 45^\circ$ and 135° .

- b) $\mathbf{R} = \mathbf{a}$, $R = a$, so $t_e = t - a/c_0$, and $\mathbf{R} \cdot \mathbf{M} = Ma \cos \alpha$, and

$$4\pi p(x, t) = \frac{\rho_0 Q'_e}{a(1 - M \cos \alpha)^2} + \rho_0 Q_e V \frac{\cos \alpha - M}{a^2(1 - M \cos \alpha)^3} = \frac{1}{a^2(1 - M \cos \alpha^2)} \left(\frac{\mathbf{a} \cdot \mathbf{F}'_e}{c_0} - \mathbf{M} \cdot \mathbf{F}_e \right) + \frac{(1 - M^2)(\mathbf{a} \cdot \mathbf{F}_e)}{a^3(1 - M \cos \alpha)^3}.$$

Bibliography

- [1] M. Abramowitz and I.A. Stegun, editors. *Handbook of Mathematical Functions*, New York, 1964. National Bureau of Standards, Dover Publications, Inc.
- [2] J.D. Achenbach. *Wave Propagation in Elastic Solids*. Elsevier Science Publishers B.V., Amsterdam, 1975.
- [3] G. Ajello. *Mesures acoustique dans les guides d'ondes en présence d'écoulement*. PhD thesis, Université du Maine, Le Mans, France, 1997.
- [4] R. Akhavan, R.D. Kamm, and A.H. Shapiro. An investigation of transition to turbulence in bounded oscillatory Stokes flows. Part 1, Experiments. *Journal of Fluid Mechanics*, 225:395–422, 1991.
- [5] D.G. Albert. Observations of acoustic surface waves in outdoor sound propagation. *Journal of the Acoustical Society of America*, 113(5):2495–2500, 2003.
- [6] J. B. Alblas. On the diffraction of sound waves in a viscous medium. *Applied Scientific Research, Section A: Mechanics, Heat, Chemical Engineering, Mathematical Methods*, 66(4):237–262, 1957.
- [7] R. Althaus. Subharmonic acoustic resonances. In *Proceedings 16th Int. Symp. Shock Tubes And Waves (1987)*, D. Weinheim, editor, Aachen, 1988. VCH Verlagsgesellschaft.
- [8] A.B.C. Anderson. Structure and velocity of the periodic vortex-ring flow pattern of a primary Pfeifenton (pipe tone) jet. *Journal of the Acoustical Society of America*, 27:1048–1053, 1955.
- [9] K. Attenborough. Acoustical impedance models for outdoor ground surfaces. *Journal of Sound and Vibration*, 99:521–544, 1985.
- [10] Y. Aurégan and M. Leroux. Experimental evidence of an instability over an impedance wall in a duct flow. *Journal of Sound and Vibration*, 317:432–439, 2008.
- [11] B.J. Bayly. Onset and equilibration of oscillations in general Rijke devices. *Journal of the Acoustical Society of America*, 79:846–851, 1986.
- [12] D.W. Bechert. Sound absorption caused by vorticity shedding, demonstrated with a jet flow. *Journal of Sound and Vibration*, 70:389–405, 1980.
- [13] D.W. Bechert. Excitation of instability waves in free shear layers. *Journal of Fluid Mechanics*, 186:47–62, 1988.
- [14] A.H. Benade and E.V. Jansson. On plane and spherical waves in horns with nonuniform flare. I. Theory of radiation, resonance frequencies, and mode conversion. *Acustica*, 31(2):79–98, 1974.
- [15] C.M. Bender and S.A. Orszag. *Advanced Mathematical Methods for Scientists and Engineers*. McGraw-Hill Book Company, Inc., New York, 1978.
- [16] R.B. Bird, W.E. Stewart, and E.N. Lightfoot. *Transport Phenomena*. John Wiley & Sons, Inc., New York, 1960.
- [17] L. Bjørnø and P.N. Larsen. Noise of air jets from rectangular slits. *Acustica*, 54:247–256, 1984.
- [18] W.K. Blake. *Mechanics of Flow-induced Sound and Vibration, Volume I*. Academic Press, Orlando, 1986.
- [19] W.K. Blake and A. Powell. The development of contemporary views of flow-tone generation. In *Recent Advances in Aeroacoustics*, New York, 1983. Springer-Verlag.
- [20] R.D. Blevins. *Flow-induced Vibration*. Van Nostrand Reinhold, New York, 2nd edition, 1990.

- [21] G.J. Bloxsidge, A.P. Dowling, N. Hooper, and P.J. Langhorne. Active control of reheat buzz. *AIAA Journal*, 26:783–790, 1988.
- [22] C.J. Bouwkamp. A note on singularities occurring at sharp edges in electromagnetic diffraction theory. *Physica*, 12(7), 1946.
- [23] E.J. Brambley. Fundamental problems with the model of uniform flow over acoustic linings. *Journal of Sound and Vibration*, 322:1026–1073, 2009.
- [24] E.J. Brambley. A well-posed modified Myers boundary condition. In *16th AIAA/CEAS Aeroacoustics Conference*, Stockholm, Sweden, June 7–9 2010. AIAA-2010-3942.
- [25] E.J. Brambley and N. Peake. Surface-waves, stability, and scattering for a lined duct with flow. In *12th AIAA/CEAS Aeroacoustics Conference*, Cambridge, MA, May 8–10 2006. AIAA-2006-2688.
- [26] L.M. Brekhovskikh. Surface waves in acoustics. *Sov. Phys. Acoust.*, 5(1):3–12, 1959.
- [27] H.H. Brouwer. On the use of the method of matched asymptotic expansions in propeller aerodynamics and acoustics. *Journal of Fluid Mechanics*, 242:117–143, 1992.
- [28] J.C. Bruggeman, A. Hirschberg, M.E.H. van Dongen, A.P.J. Wijnands, and J. Gorter. Self-sustained aero-acoustic pulsations in gas transport systems: experimental study of the influence of closed side branches. *Journal of Sound and Vibration*, 150:371–393, 1991.
- [29] J.C. Bruggeman, J.C. Vellekoop, F.G.P. v.d. Knaap, and P.J. Keuning. Flow excited resonance in a cavity covered by a grid: theory and experiments. *Flow Noise Modeling, Measurement and Control ASME*, NCA Volume 11/FED Volume 130:135–144, 1991.
- [30] S.M. Candel and T.J. Poinsot. Interactions between acoustics and combustion. *Proceedings of the Institute of Acoustics*, 10(2):103–153, 1988.
- [31] D.C. Champeney. *A Handbook of Fourier Theorems*. Cambridge University Press, Cambridge, 1987.
- [32] C.J. Chapman. Sound radiation from a cylindrical duct. Part I. Ray structure of the duct modes and of the external field. *Journal of Fluid Mechanics*, 281:293–311, 1994.
- [33] W. Chester. Resonant oscillations in closed tubes. *Journal of Fluid Mechanics*, 18:44, 1964.
- [34] J.-F. Chevaugéon, N. Rémacle and X. Gallez. Discontinuous Galerkin implementation of the Extended Helmholtz resonator impedance model in time domain. In *12th AIAA/CEAS Aeroacoustics Conference*, Cambridge, MA, May 8–10 2006. AIAA-2006-2569.
- [35] J.W. Coltman. Jet drive mechanism in edge tones and organ pipes. *Journal of the Acoustical Society of America*, 60:725–733, 1976.
- [36] J.W. Cooley and J.W. Tukey. An algorithm for the machine calculation of complex Fourier Series. *Math. Comput.*, 19:297–301, 1965.
- [37] A.J. Cooper and N. Peake. Propagation of unsteady disturbances in a slowly varying duct with mean swirling flow. *Journal of Fluid Mechanics*, 445:207–234, 2001.
- [38] R. Courant and D. Hilbert. *Methods of Mathematical Physics, Volume II*. Interscience Publishers (John Wiley & Sons), 1962.
- [39] L. Cremer and M. Heckl. *Structure-Borne Sound*. Springer-Verlag, Berlin, 2nd edition, 1988. Translated and revised by E.E. Ungar.
- [40] D.G. Crighton. Basic principles of aerodynamic noise generation. *Progress in Aerospace Sciences*, 16(1):31–96, 1975.
- [41] D.G. Crighton. Scattering and diffraction of sound by moving bodies. *Journal of Fluid Mechanics*, 72:209–227, 1975.

- [42] D.G. Crighton. The Kutta condition in unsteady flow. *Annual Review of Fluid Mechanics*, 17:411–445, 1985.
- [43] D.G. Crighton. The jet edge-tone feedback cycle; linear theory for the operating stages. *Journal of Fluid Mechanics*, 234:361–391, 1992.
- [44] D.G. Crighton. Asymptotics – an indispensable complement to thought, computation and experiment in applied mathematical modelling. In *Proceedings of the Seventh European Conference on Mathematics in Industry, March 2-6, 1993, Montecatini*, A. Fasano and M. Primicerio, editors, volume ECMI 9, pages 3–19, Stuttgart, 1994. European Consortium for Mathematics in Industry, B.G.Teubner.
- [45] D.G. Crighton, A.P. Dowling, J.E. Ffowcs Williams, M. Heckl, and F.G. Leppington. *Modern Methods in Analytical Acoustics*. Lecture Notes. Springer-Verlag, London, 1992.
- [46] D.G. Crighton and J.E. Ffowcs Williams. Sound generation by turbulent two-phase flow. *Journal of Fluid Mechanics*, 36:585–603, 1969.
- [47] A. Cummings. Acoustic nonlinearities and power losses at orifices. *AIAA Journal*, 22:786–792, 1984.
- [48] A. Cummings. The effects of grazing turbulent pipe-flow on the impedance of an orifice. *Acustica*, 61:233–242, 1986.
- [49] A. Cummings. The response of a resonator under a turbulent boundary layer to a high amplitude non-harmonic sound field. *Journal of Sound and Vibration*, 115:321–328, 1987.
- [50] G.A. Daigle, M.R. Stinson, and D.I. Havelock. Experiments on surface waves over a model impedance plane using acoustical pulses. *Journal of the Acoustical Society of America*, 99:1993–2005, 1996.
- [51] J.P. Den Hartog. *Mechanical Vibrations*. McGraw-Hill Book Company, Inc., New York, 1956.
- [52] J.H.M. Disselhorst and L. van Wijngaarden. Flow in the exit of open pipes during acoustic resonance. *Journal of Fluid Mechanics*, 99:293–319, 1980.
- [53] P.E. Doak. Fluctuating total enthalpy as a generalized field. *Acoust. Phys.*, 44:677–685, 1995.
- [54] R.J. Donato. Model experiments on surface waves. *Journal of the Acoustical Society of America*, 63:700–703, 1978.
- [55] A.P. Dowling and J.E. Ffowcs Williams. *Sound and Sources of Sound*. Ellis Horwood Publishers, Chichester, 1983.
- [56] P.A. Durbin. Resonance in flows with vortex sheets and edges. *Journal of Fluid Mechanics*, 145:275–285, 1984.
- [57] W. Eckhaus. *Asymptotic Analysis of Singular Perturbations*. NorthHolland, Amsterdam, 1979.
- [58] D.M. Eckmann and J.B. Grotberg. Experiments on transition to turbulence in oscillatory pipe flow. *Journal of Fluid Mechanics*, 222:329–350, 1991.
- [59] E. Eisner. Complete solutions of the Webster horn equation. *Journal of the Acoustical Society of America*, 41:1126, 1967.
- [60] A. Erdelyi, W. Magnus, F. Oberhettinger, and F.G. Tricomi. *Higher Transcendental Functions, 3 Volumes*. McGraw-Hill Book Company, Inc., New York, 1953.
- [61] W. Eversman. The boundary condition at an impedance wall in a non-uniform duct with potential mean flow. *Journal of Sound and Vibration*, 246(1):63–69, 2001.
- [62] B. Fabre, A. Hirschberg, and A.P.J. Wijnands. Vortex shedding in steady oscillation of a flue organ pipe. *Acustica-Acta Acustica*, 82:863–877, 1996.
- [63] F. Farassat. Discontinuities in aerodynamics and aeroacoustics: the concept and application of generalized derivatives. *Journal of Sound and Vibration*, 55:165–193, 1977.
- [64] F. Farassat. Linear acoustic formulas for calculation of rotating blade noise. *AIAA Journal*, 19(9):1122–1130, 1981.
- [65] F. Farassat. Introduction to generalized functions with applications in aerodynamics and aeroacoustics. Technical Paper 3428, NASA, Langley Research Center – Hampton, Virginia, May 1994. Corrected Copy (April 1996).

- [66] J.E. Ffowcs Williams. Hydrodynamic noise. *Annual Review of Fluid Mechanics*, 1:197–222, 1969.
- [67] J.E. Ffowcs Williams. Sound sources in aerodynamics – fact and fiction. *AIAA Journal*, 20(3):307–315, 1982.
- [68] J.E. Ffowcs Williams and D.L. Hawkings. Sound generated by turbulence and surfaces in arbitrary motion. *Philosophical Transactions of the Royal Society of London*, A264:321–342, 1969.
- [69] M.J. Fisher and C.L. Morfey. *Jet noise*, chapter 14, pages 307–335. Ellis Horwood, Chichester, 1982.
- [70] N.H. Fletcher and T.D. Rossing. *The Physics of Musical Instruments*. Springer-Verlag, New York, 1991.
- [71] B. Gazengel, J. Gilbert, and N. Amir. Time domain simulation of single reed wind instrument. From the measured input impedance to the synthesis signal. Where are the traps? *Acta Acustica*, 3:445–472, 1995.
- [72] J. Gilbert, J. Kergomard, and E. Ngoya. Calculation of the steady state oscillations of a clarinet using the harmonic balance technique. *Journal of the Acoustical Society of America*, 86:35–41, 1989.
- [73] M.E. Goldstein. *Aeroacoustics*. McGraw-Hill Book Company, Inc., New York, 1976.
- [74] I.S. Gradshteyn and I.M. Ryzhik. *Table of Integrals, Series and Products*. Academic Press, London, 5th edition, 1994. Alan Jeffrey, editor.
- [75] Y.P. Guo. Sound diffraction and dissipation at a sharp trailing edge in a supersonic flow. *Journal of Sound and Vibration*, 145(2):179–193, 1991.
- [76] J.C. Hardin and D.S. Pope. Sound generation by flow over a two-dimensional cavity. *AIAA Journal*, 33:407–412, 1995.
- [77] M.A. Heckl. Active control of the noise from a Rijke tube. *Journal of Sound and Vibration*, 124:117–133, 1988.
- [78] H.H. Heller and S.E. Widnall. Sound radiation from rigid flow spoilers correlated with fluctuating forces. *Journal of the Acoustical Society of America*, 47:924–936, 1970.
- [79] A. Hirschberg. Aero-acoustics of wind instruments. In *Mechanics of Musical Instruments*, A. Hirschberg, J. Kergomard, and G. Weinreich, editors, pages 291–369, Wien New York, 1995. International Centre for Mechanical Sciences, Udine, It., Springer-Verlag.
- [80] A. Hirschberg, J. Gilbert, R. Msallam, and A.P.J. Wijnands. Shock waves in trombones. *Journal of the Acoustical Society of America*, 99(3):1754–1758, 1996.
- [81] A. Hirschberg, G. Thielens, and C. Luijten. Aero-acoustic sources. *Nederlands Akoestisch Genootschap NAG Journaal*, 129:3–13, 1995.
- [82] D.K. Holger, T.A. Wilson, and G.S. Beavers. Fluid mechanics of the edge tone. *Journal of the Acoustical Society of America*, 62:1116–1128, 1977.
- [83] M.H. Holmes. *Introduction to Perturbation Methods*. Springer-Verlag, New York, 1995.
- [84] M.S. Howe. Contributions to the theory of aerodynamic sound, with application to excess jet noise and the theory of the flute. *Journal of Fluid Mechanics*, 71:625–673, 1975.
- [85] M.S. Howe. The dissipation of sound at an edge. *Journal of Sound and Vibration*, 70:407–411, 1980.
- [86] M.S. Howe. The influence of mean shear on unsteady aperture flow, with application to acoustical diffraction and self-sustained cavity oscillations. *Journal of Fluid Mechanics*, 109:125–146, 1981.
- [87] M.S. Howe. On the theory of unsteady shearing flow over a slot. *Philosophical Transactions of the Royal Society of London Series A-Mathematical and Physical Sciences*, 303(1475):151–180, 1981.
- [88] M.S. Howe. On the absorption of sound by turbulence and other hydrodynamic flows. *I.M.A. Journal of Applied Mathematics*, 32:187–203, 1984.
- [89] M.S. Howe. Emendation of the Brown & Michel equation, with application to sound generation by vortex motion near a half-plane. *Journal of Fluid Mechanics*, 329:89–101, 1996.

- [90] H.H. Hubbard, editor. *Aeroacoustics of Flight Vehicles: Theory and Practice. Volume 1 Noise Sources; Volume 2 Noise Control (Nasa Reference Publication 1258)*. Acoustical Society of America, 1995.
- [91] P. Huerre and P.A. Monkewitch. Local and global instabilities in spatially developing flows. *Annual Review of Fluid Mechanics*, 22:473–537, 1990.
- [92] I.J. Hughes and A.P. Dowling. The absorption of sound by perforated linings. *Journal of Fluid Mechanics*, 218:299–335, 1990.
- [93] A. Iafrati and G. Riccardi. A numerical evaluation of viscous effects on vortex induced noise. *Journal of Sound and Vibration*, 196:129–146, 1996.
- [94] K.U. Ingard. On the theory and design of acoustic resonators. *Journal of the Acoustical Society of America*, 25:1073, 1953.
- [95] K.U. Ingard. Influence of fluid motion past a plane boundary on sound reflection, absorption, and transmission. *Journal of the Acoustical Society of America*, 31(7):1035–1036, 1959.
- [96] K.U. Ingard. *Fundamentals of Waves and Oscillations*. Cambridge University Press, Cambridge, 1988.
- [97] K.U. Ingard and S. Labate. Acoustic circulation effects and the non-linear impedance of orifices. *Journal of the Acoustical Society of America*, 22:211–218, 1950.
- [98] U. Ingard and H. Ising. Acoustic non-linearity of an orifice. *J. of the Acoustical Society of America*, 42:6–17, 1967.
- [99] P.L. Jenvey. The sound power from turbulence: a theory of the exchange of energy between the acoustic and non-acoustic fields. *Journal of Sound and Vibration*, 131:37–66, 1989.
- [100] D.S. Jones. *The Theory of Electromagnetism*. Pergamon Press, Oxford, 1964.
- [101] D.S. Jones. *The Theory of Generalised Functions*. Cambridge University Press, Cambridge, 2nd edition, 1982.
- [102] D.S. Jones. *Acoustic and Electromagnetic Waves*. Oxford Science Publications. Clarendon Press, Oxford, 1986.
- [103] M.C. Junger and D. Feit. *Sound, Structures and their Interaction*. MIT Press, Cambridge, Massachusetts, 2nd edition, 1986.
- [104] W.M. Jungowski. Some self induced supersonic flow oscillations. *Progress in Aerospace Science*, 18:151–175, 1978.
- [105] R.P. Kanwal. *Generalized Functions: Theory and Technique*. Birkhäuser, Boston, 2nd edition, 1998.
- [106] J.J. Keller, W. Egli, and J. Hellat. Thermally induced low-frequency oscillations. *Zeitschrift für angewandte Mathematik und Mechanik*, 36:250–274, 1985.
- [107] J. Kergomard. Comments on: Wall effects on sound propagation in tubes. *Journal of Sound and Vibration*, 98:149–155, 1985.
- [108] J. Kevorkian and J.D. Cole. *Perturbation Methods in Applied Mathematics*. Springer-Verlag, New York, 1981.
- [109] K. Knopp. *Theory of Functions*. Dover Publications, New York, 1945.
- [110] P.A. Kolkman. *Flow-induced Gate Vibrations*. PhD thesis, Delft University of Technology, 1976. also: Publ. no. 164 of Delft Hydr. Lab.
- [111] P.C. Kriesels, M.C.A.M. Peters, A. Hirschberg, A.P.J. Wijnands, A. Iafrati, G. Riccardi, R. Piva, and J.C. Bruggeman. High amplitude vortex-induced pulsations in a gas transport system. *Journal of Sound and Vibration*, 184:343–368, 1995.
- [112] A.H.W.M. Kuijpers, S.W. Rienstra, G. Verbeek, and J.W. Verheij. The acoustic radiation of baffled finite baffled ducts with vibrating walls. *Journal of Sound and Vibration*, 216(3):461–493, 1998.
- [113] P.K. Kundu and I.M. Cohen. *Fluid Mechanics*. Academic Press, New York, 2nd edition, 2002.

- [114] Y.P. Kwon and B.H. Lee. Stability of the Rijke thermoacoustic oscillation. *Journal of the Acoustical Society of America*, 78:1414–1420, 1985.
- [115] P.A. Lagerstrom. *Matched Asymptotic Expansions: Ideas and Techniques*. Springer-Verlag, New York, 1988.
- [116] L.D. Landau and E.M. Lifshitz. *Fluid Mechanics*. Pergamon Press, Oxford, 2nd edition, 1987.
- [117] S.W. Lee, W.R. Jones, and J.J. Campbell. Convergence of numerical solutions of iris-type discontinuity problems. *IEEE Transactions on Microwave Theory and Techniques*, MIT-19(6):528–536, 1971.
- [118] T.G. Leighton. *The Acoustic Bubble*. Academic Press, London, 1994.
- [119] M.B. Lesser and D.G. Crighton. Physical acoustics and the method of matched asymptotic expansions. In *Physical Acoustics Volume XI*, W.P. Mason and R.N. Thurston, editors. Academic Press, New York, 1975.
- [120] H. Levine. Output of acoustical sources. *Journal of the Acoustical Society of America*, 67(6):1935–1946, 1980.
- [121] H. Levine and J. Schwinger. On the radiation of sound from an unflanged circular pipe. *Physical Review*, 73:383–406, 1948.
- [122] M.J. Lighthill. On sound generated aerodynamically I. *Proceedings of the Royal Society of London*, Series A211:564–587, 1952.
- [123] M.J. Lighthill. On sound generated aerodynamically II. *Proceedings of the Royal Society of London*, Series A222:1–32, 1954.
- [124] M.J. Lighthill. *Introduction to Fourier Analysis and Generalised Functions*. Cambridge University Press, Cambridge, 1958.
- [125] M.J. Lighthill. The Fourth Annual Fairey Lecture: The propagation of sound through moving fluids. *Journal of Sound and Vibration*, 24(4):471–492, 1972.
- [126] M.J. Lighthill. *Waves in Fluids*. Cambridge University Press, Cambridge, 1978.
- [127] M.M. Lipschutz. *Schaum's Outline of Theory and Problems of Differential Geometry*. McGraw-Hill Book Company, Inc., 1969.
- [128] L. Liszka. Long-distance focusing of Concorde sonic boom. *Journal of the Acoustical Society of America*, 64(2):631–635, 1978.
- [129] M.V. Lowson. The sound field for singularities in motion. *Proceedings of the Royal Society of London Series A-Mathematical and Physical Sciences*, 286:559–572, 1965.
- [130] Y.L. Luke. *The Special Functions and their Approximations Vol.1 and Vol.2*, volume 53 of *Mathematics in Science and Engineering*. Academic Press, New York, London, 1969.
- [131] P.H. Masterman and P.J.B. Clarricoats. Computer field-matching solution of waveguide transverse discontinuities. *Proc. IEE*, 118(1):51–63, 1971.
- [132] P.H. Masterman, P.J.B. Clarricoats, and C.D. Hannaford. Computer method of solving waveguide-iris problems. *Electronics Letters*, 5(2):23–25, 1969.
- [133] R.M.M Mattheij, S.W. Rienstra, and J.H.M. ten Thije Boonkamp. *Partial Differential Equations: Modeling, Analysis, Computation*. SIAM (Society for Industrial and Applied Mathematics), Philadelphia, 2005. xxxiv + 665 pages / Softcover / ISBN 0-89871-594-6.
- [134] A.C. McIntosh. The effect of upstream acoustic forcing and feedback on the stability and resonance behaviour of anchored flames. *Combustion Science and Technology*, 49:143–167, 1986.
- [135] M.E. McIntyre, R.T. Schumacher, and Woodhouse J. On the oscillations of musical instruments. *Journal of the Acoustical Society of America*, 74:1325–1345, 1983.
- [136] W.C. Meecham. Surface and volume sound from boundary layers. *Journal of the Acoustical Society of America*, 37:516–522, 1965.

- [137] M. Meissner. Self-sustained deep cavity oscillations induced by grazing flow. *Acustica*, 62:220–228, 1987.
- [138] T.H. Melling. The acoustic impedance of perforates at medium and high sound pressure levels. *Journal of Sound and Vibration*, 29:1–65, 1973.
- [139] H.J. Merk. Analysis of heat-driven oscillations of gas flows. *Applied Scientific Research*, A6:402–420, 1956–57.
- [140] P. Merkli and H. Thomann. Transition to turbulence in oscillating pipe flow. *Journal of Fluid Mechanics*, 68:567–575, 1975.
- [141] A. Michalke. On the propagation of sound generated in a pipe of circular cross-section with uniform mean flow. *Journal of Sound and Vibration*, 134:203–234, 1989.
- [142] L.M. Milne-Thomson. *Theoretical Hydrodynamics*. Macmillan Educ. Ltd, Houndmills, UK, 5th edition, 1968.
- [143] R. Mittra, T. Itoh, and T.-S. Li. Analytical and numerical studies of the relative convergence phenomenon arising in the solution of an integral equation by the moment method.
- [144] R. Mittra and S.W. Lee. *Analytical Techniques in the Theory of Guided Waves*. The Macmillan Company, New York, 1971.
- [145] W. Möhring. Energy conservation, time-reversal invariance and reciprocity in ducts with flow. *Journal of Fluid Mechanics*, 431:223–237, 2001.
- [146] A. Monorchio, R. Mittra, and G. Manara. Generalized scattering matrix technique. In *Encyclopedia of RF and Microwave Engineering*, pages 1767–1777. John Wiley & Sons, Inc, 2005.
- [147] F. Monteghetti, D. Matignon, E. Piot, and L. Pascal. Design of broadband time-domain impedance boundary conditions using the oscillatory-diffusive representation of acoustical models. *Journal of the Acoustical Society of America*, 140:1663–1674, 2016.
- [148] C.L. Morfey. Sound transmission and generation in ducts with flow. *Jrnl. of Sound and Vibration*, 14:37–55, 1971.
- [149] C.L. Morfey. Amplification of aerodynamic noise by convected flow inhomogeneities. *Journal of Sound and Vibration*, 31:391–397, 1973.
- [150] C.L. Morfey. Sound radiation due to unsteady dissipation in turbulent flows. *Journal of Sound and Vibration*, 48:95–111, 1984.
- [151] P.M. Morse. *Vibration and Sound*. McGraw-Hill, New York, 2nd edition, 1948.
- [152] P.M. Morse and H. Feshbach. *Methods of Theoretical Physics Volume I*. McGraw-Hill Book Company, Inc., New York, 1953.
- [153] P.M. Morse and K.U. Ingard. *Theoretical Acoustics*. McGraw-Hill Book Company, Inc., New York, 1968.
- [154] E.-A. Müller and F. Obermeier. The spinning vortices as a source of sound. *AGARD CP22, Paper 22*, 1967.
- [155] U.A. Müller and N. Rott. Thermally driven acoustic oscillations: Part VI. Excitation and power. *Zeitschrift für angewandte Mathematik und Mechanik*, 34:607–626, 1983.
- [156] R.M. Munt. The interaction of sound with a subsonic jet issuing from a semi-infinite cylindrical pipe. *Journal of Fluid Mechanics*, 83(4):609–640, 1977.
- [157] R.M. Munt. Acoustic radiation properties of a jet pipe with subsonic jet flow: I. the cold jet reflection coefficient. *Journal of Sound and Vibration*, 142(3):413–436, 1990.
- [158] R.E. Musafir. A discussion on the structure of aeroacoustic wave equations. In *Proceedings of the 4th Congress on Acoustics, Marseille, France*, pages 923–926, Toulouse, Fr., April 1997. Teknea edition.
- [159] M.K. Myers. On the acoustic boundary condition in the presence of flow. *Journal of Sound and Vibration*, 71(3):429–434, 1980.
- [160] M.K. Myers. An exact energy corollary for homentropic flow. *Journal of Sound and Vibration*, 109:277–284, 1986.

334 Bibliography

- [161] M.K. Myers. Generalization and extension of the law of acoustic energy conservation in a nonuniform flow. In *24th Aerospace Sciences Meeting*, Reno, Nevada, January 6–9 1986. AIAA. AIAA 86–0471.
- [162] M.K. Myers. Transport of energy by disturbances in arbitrary flows. *Jrnl. of Fluid Mechanics*, 226:383–400, 1991.
- [163] A.H. Nayfeh. *Perturbation Methods*. John Wiley & Sons, Inc., 1973.
- [164] A.H. Nayfeh and D.P. Telonis. Acoustic propagation in ducts with varying cross section. *Journal of the Acoustical Society of America*, 54(6):1654–1661, 1973.
- [165] P.A. Nelson, N.A. Halliwell, and P.E. Doak. Fluid dynamics of a flow excited resonance, Part I: the experiment. *Journal of Sound and Vibration*, 78:15–38, 1981.
- [166] P.A. Nelson, N.A. Halliwell, and P.E. Doak. Fluid dynamics of a flow excited resonance, Part II: flow acoustic interaction. *Journal of Sound and Vibration*, 91(3):375–402, 1983.
- [167] J. Nicolas, J.-L. Berry, and G.A. Daigle. Propagation of sound above a finite layer of snow. *Journal of the Acoustical Society of America*, 77:67–73, 1985.
- [168] M.P. Norton. *Fundamentals of Noise and Vibration Analysis for Engineers*. Cambridge University Press, Cambridge, 1989.
- [169] F. Obermeier. Sound generation by heated subsonic jets. *Journal of Sound and Vibration*, 41:463–472, 1975.
- [170] F. Obermeier. Aerodynamic sound generation caused by viscous processes. *Journal of Sound and Vibration*, 99:111–120, 1985.
- [171] H. Ockendon, J.R. Ockendon, M.R. Peake, and W. Chester. Geometrical effects in resonant gas oscillations. *Journal of Fluid Mechanics*, 257:201–217, 1993.
- [172] N.C. Ovenden. Near cut-on/cut-off transitions in lined ducts with flow. In *8th AIAA/CEAS Aeroacoustics Conference*, Breckenridge, CO, June 17–19 2002. AIAA 2002–2445.
- [173] N.C. Ovenden, W. Eversman, and S.W. Rienstra. Cut-on cut-off transition in flow ducts: Comparing multiple-scales and finite-element solutions. In *10th AIAA/CEAS Aeroacoustics Conference*, Manchester, UK, May 10–12 2004. AIAA 2004–2945.
- [174] N.C. Ovenden and S.W. Rienstra. Mode-matching strategies in slowly varying engine ducts. *AIAA Journal*, 42(9):1832–1840, 2004.
- [175] N.O. Ovenden. A uniformly valid multiple scales solution for cut-on cut-off transition of sound in flow ducts. *Journal of Sound and Vibration*, 286:403–416, 2005.
- [176] J.A. Owczarek. *Fundamentals of Gasdynamics*. International Textbook Company, Scranton, Pennsylvania, 1964.
- [177] P.H.M.W. in 't Panhuis, S.W. Rienstra, J. Molenaar, and J.J.M. J.J.M. Slot. Weakly nonlinear thermoacoustics for stacks with slowly varying pore cross-sections. *Journal of Fluid Mechanics*, 618:41–70, 2009.
- [178] A. Papoulis. *The Fourier Integral and its Applications*. McGraw-Hill Book Company, Inc., New York, 1962.
- [179] A.R. Paterson. *A First Course in Fluid Dynamics*. Cambridge University Press, Cambridge, 1983.
- [180] M.C.A.M. Peters and A. Hirschberg. Acoustically induced periodic vortex shedding at sharp edged open channel ends: simple vortex models. *Journal of Sound and Vibration*, 161:281–299, 1993.
- [181] M.C.A.M. Peters, A. Hirschberg, A.J. Reijnen, and A.P.J. Wijnands. Damping and reflection coefficient measurements for an open pipe at low Mach and low Helmholtz numbers. *Journal of Fluid Mechanics*, 256:499–534, 1993.
- [182] J.L. Peube and Y. Gervais. Thermoacoustique des cavités. *Revue d'Acoustique*, 82:68–71, 1987.
- [183] A.D. Pierce. *Acoustics: an Introduction to its Physical Principles and Applications*. McGraw-Hill Book Company, Inc., New York, 1981. Also available from the Acoustical Society of America.

- [184] L.J. Poldervaart, A.P.J. Wijnands, L.H.A.M. van Moll, and E.J. van Voorthuisen. Modes of Vibration. Audio-Visueel Centrum, 1974. film.
- [185] A. Powell. Mechanism of aerodynamic sound production. Technical Report 466, AGARD, 1963.
- [186] A. Powell. Some aspects of aeroacoustics: From Rayleigh until today. *Journal of Vibration and Acoustics*, 112:145–159, 1990.
- [187] D.C. Pridmore-Brown. Sound propagation in a fluid flowing through an attenuating duct. *Journal of Fluid Mechanics*, 4:393–406, 1958.
- [188] A. Prosperetti. The thermal behaviour of oscillating gas bubbles. *Journal of Fluid Mechanics*, 222:587–616, 1991.
- [189] A. Prosperetti and H.N. Ögüz. The impact of drops on liquid surfaces and underwater noise of rain. *Annual Review of Fluid Mechanics*, 25:577–602, 1993.
- [190] A.A. Putnam, F.E. Belles, and J.A.C. Kentfield. Pulse combustion. *Progress in Energy and Combustion Science*, 12:43–79, 1986.
- [191] R. Radebaugh and S. Herrmann. Refrigeration efficiency of pulse-tube refrigerators. In *Proceedings of 4th Int. Cryocooler Conference*, pages 119–134, 1988.
- [192] R. Raspet and G.E. Baird. The acoustic surface wave above a complex impedance ground surface. *Journal of the Acoustical Society of America*, 85:638–640, 1989.
- [193] R.L. Raun, M.W. Beckstead, J.C. Finlinson, and K.P. Brooks. A review of Rijke tubes, Rijke burners and related devices. *Progress in Energy and Combustion Science*, 19:313–364, 1993.
- [194] J.W.S. Rayleigh. *The Theory of Sound, Volume I and II*. Dover edition, New York, 1945.
- [195] G. Reethof. Turbulence-generated noise in pipe flow. *Annual Review of Fluid Mechanics*, 10:333–67, 1978.
- [196] H.S. Ribner. Effects of jet flow on jet noise via an extension to Lighthill model. *Journal of Fluid Mechanics*, 321:1–24, 1996.
- [197] S.W. Rienstra. Sound diffraction at a trailing edge. *Journal of Fluid Mechanics*, 108:443–460, 1981.
- [198] S.W. Rienstra. A small Strouhal number analysis for acoustic wave–jet flow–pipe interaction. *Journal of Sound and Vibration*, 86(4):539–556, 1983.
- [199] S.W. Rienstra. Acoustic radiation from a semi-infinite annular duct in a uniform subsonic mean flow. *Journal of Sound and Vibration*, 94(2):267–288, 1984.
- [200] S.W. Rienstra. Hydrodynamic instabilities and surface waves in a flow over an impedance wall. In *Proceedings IUTAM Symposium 'Aero- and Hydro-Acoustics' 1985 Lyon*, G. Comte-Bellot and J.E. Ffowcs Williams, editors, pages 483–490, Heidelberg, 1986. Springer-Verlag.
- [201] S.W. Rienstra. 1-D reflection at an impedance wall. *Journal of Sound and Vibration*, 125:43–51, 1988.
- [202] S.W. Rienstra. Sound transmission in a slowly varying lined flow duct. *Nieuw Archief voor Wiskunde*, 4de Serie, Deel 6(1–2):157–167, 1988.
- [203] S.W. Rienstra. Acoustical detection of obstructions in a pipe with a temperature gradient. In *Topics in Engineering Mathematics*, A. van der Burgh and J. Simonis, editors, pages 151–179. Kluwer Acad. Publishers, Dordrecht, 1992.
- [204] S.W. Rienstra. A note on the Kutta condition in Glauert's solution of the thin aerofoil problem. *Journal of Engineering Mathematics*, 26:61–69, 1992.
- [205] S.W. Rienstra. Sound transmission in slowly varying circular and annular ducts with flow. *Journal of Fluid Mechanics*, 380:279–296, 1999.
- [206] S.W. Rienstra. Cut-on cut-off transition of sound in slowly varying flow ducts. *Aerotechnica - Missili e Spazio*, 79(3–4):93–97, 2000. Special issue in memory of David Crighton.

- [207] S.W. Rienstra. A classification of duct modes based on surface waves. *Wave Motion*, 37(2):119–135, 2003.
- [208] S.W. Rienstra. Sound propagation in slowly varying lined flow ducts of arbitrary cross section. *Journal of Fluid Mechanics*, 495:157–173, 2003.
- [209] S.W. Rienstra. Webster’s horn equation revisited. *SIAM Journal on Applied Mathematics*, 65(6):1981–2004, 2005.
- [210] S.W. Rienstra. Impedance models in time domain, including the Extended Helmholtz resonator model. In *12th AIAA/CEAS Aeroacoustics Conference*, Cambridge, MA, May 8–10 2006. AIAA -2006-2686.
- [211] S.W. Rienstra. Numerical and asymptotic solutions of the Pridmore-Brown equation. *AIAA Journal*, 58(7):3001–3018, 2020.
- [212] S.W. Rienstra and M. Darau. Boundary layer thickness effects of the hydrodynamic instability along an impedance wall. *Journal of Fluid Mechanics*, 671:559–573, 2011.
- [213] S.W. Rienstra and W. Eversman. A numerical comparison between multiple-scales and finite-element solution for sound propagation in lined flow ducts. *Journal of Fluid Mechanics*, 437:366–383, 2001.
- [214] P.L. Rijke. Notiz über eine neue Art, die Luft in einer an beiden Enden offenen Röhre in Schwingungen zu versetzen. *Annalen der Physik*, 107:339–343, 1859.
- [215] D. Rockwell. Oscillations of impinging shear layers. *AIAA Journal*, 21:645–664, 1983.
- [216] D. Rockwell and E. Naudascher. Self sustaining oscillations of flow past cavities. *Journal of Fluid Engineering, Trans. ASME*, 100:152–165, 1978.
- [217] D. Rockwell and E. Naudascher. Self-sustained oscillations of impinging free shear layers. *Annual Review of Fluid Mechanics*, 11:67–94, 1979.
- [218] D. Ronneberger. The acoustical impedance of holes in the wall of flow ducts. *Journal of Sound and Vibration*, 24:133–150, 1972.
- [219] D. Ronneberger and C. Ahrens. Wall shear stress caused by small amplitude perturbations of turbulent boundary-layer flow: an experimental investigation. *Journal of Fluid Mechanics*, 83:433–464, 1977.
- [220] N. Rott. Damped and thermally driven acoustic oscillations in wide and narrow tubes. *Zeitschrift für angewandte Mathematik und Mechanik*, 20:230–243, 1969.
- [221] N. Rott. Thermally driven acoustic oscillations: Part II. Stability limit for helium. *Zeitschrift für angewandte Mathematik und Mechanik*, 24:54–72, 1973.
- [222] N. Rott. Thermally driven acoustic oscillations: Part III. Second-order heat flux. *Zeitschrift für angewandte Mathematik und Mechanik*, 26:43–49, 1975.
- [223] N. Rott. Thermally driven acoustic oscillations: Part IV. Tubes with variable cross-section. *Zeitschrift für angewandte Mathematik und Mechanik*, 27:197–224, 1976.
- [224] V. Salmon. Generalized plane wave horn theory. *Journal of the Acoustical Society of America*, 17:199–218, 1946.
- [225] V. Salmon. A new family of horns. *Journal of the Acoustical Society of America*, 17:212–218, 1946.
- [226] H. Sato. The stability and transition of a two-dimensional jet. *Journal of Fluid Mechanics*, 7:53–80, 1960.
- [227] H. Schlichting. *Boundary-layer Theory*. McGraw-Hill Book Company, Inc., New York, 6th edition, 1968.
- [228] J.B.H.M. Schulten. *Sound Generation by Ducted Fans and Propellers as a Lifting Surface Problem*. PhD thesis, University of Twente, Enschede, The Netherlands, 1993. ISBN 90-9005714-5.
- [229] C.H. Shadle. *The Acoustics of Fricative Consonants*. PhD thesis, Dept. of Electrical Engineering and Computer-Science, MIT, Cambridge, Massachusetts, 1985. Report R.L.E. No. 506.
- [230] A.H. Shapiro. *The dynamics and thermodynamics of compressible flow*, volume I. Ronald Press Comp., NY, 1953.

- [231] D.K. Sing and S.W. Rienstra. Nonlinear asymptotic impedance model for a Helmholtz resonator liner. *Journal of Sound and Vibration*, 333(15):3536–3549, 2014.
- [232] A.F. Smith, N.O. Ovenden, and R.I. Bowles. Flow and geometry induced scattering of high frequency acoustic duct modes. *Wave Motion*, 49:109–124, 2012.
- [233] M.J.T. Smith. *Aircraft Noise*. Cambridge University Press, Cambridge, 1989.
- [234] A.G. Spruyt. Stromings-geïnduceerde akoestische resonanties in de industrie. *Nederlands Akoestisch Genootschap NAG Journaal*, 22:1–12, 1972.
- [235] A.O. St. Hilaire, T.A. Wilson, and G.S. Beavers. Aerodynamic excitation of the harmonium reed. *Journal of Fluid Mechanics*, 49:803–816, 1971.
- [236] M.R. Stinson and G.A. Daigle. Surface wave formation at an impedance discontinuity. *Journal of the Acoustical Society of America*, 102(6):3269–3275, 1997.
- [237] G.P. Succi. Design of quiet propellers. *SAE Paper*, 790584, 1979.
- [238] G.W. Swift. Thermo-acoustic engines and refrigerators. *Physics Today*, pages 22–28, July 1995.
- [239] G.W. Swift, R.A. Martin, R. Radebaugh, and K.M. McDermott. First measurements with a thermoacoustic driver for an orifice-pulse-tube refrigerator. *Journal of the Acoustical Society of America, Sup. 1*, 88:595, 1990. 120th ASA meeting, San Diego, CA.
- [240] H Tennekes and J.L. Lumley. *A First Course of Turbulence*. MIT Press, 1972.
- [241] P.A. Thompson. *Compressible-Fluid Dynamics*. McGraw-Hill Book Company, Inc., New York, 1972.
- [242] H. Tijdeman. On the propagation of sound waves in cylindrical tubes. *Jrnl. of Sound and Vibration*, 39:1–33, 1975.
- [243] H. Tijdeman. *Investigations of the transonic flow around oscillating airfoils*. PhD thesis, Delft University of Technology, Delft, NL, 1977.
- [244] J.M. Tyler and T.G. Sofrin. Axial flow compressor noise studies. *Transactions of the Society of Automotive Engineers*, 70:309–332, 1962.
- [245] M. Van Dyke. *Perturbation Methods in Fluid Mechanics*. Parabolic Press, Stanford, CA, 1975. Annotated edition from original 1964, Academic Press.
- [246] M.P. Verge, R. Caussé, B. Fabre, A. Hirschberg, A.P.J. Wijnands, and A. van Steenberg. Jet oscillations and jet drive in recorder-like instruments. *Acta Acustica*, 2:403–419, 1994.
- [247] M.P. Verge, B. Fabre, A. Hirschberg, and A.P.J. Wijnands. Sound production in recorderlike instruments, I: Dimensionless amplitude of the internal acoustic field. *Journal of the Acoustical Society of America*, 101:2914–2924, 1997.
- [248] M.P. Verge, B. Fabre, W.E.A. Mahu, A. Hirschberg, R.R. van Hassel, A.P.J. Wijnands, J.J. de Vries, and C.J. Hogendoorn. Jet formation and jet velocity fluctuations in a flue organ pipe. *Journal of the Acoustical Society of America*, 95:1119–1132, 1994.
- [249] M.P. Verge, A. Hirschberg, and R.R. Caussé. Sound production in recorderlike instruments, II: A simulation model. *Journal of the Acoustical Society of America*, 101:2925–2939, 1997.
- [250] R. Verzicco and G. Vittori. Direct simulation of transition in Stokes boundary layer. *Physics of Fluid A*, 8:1341–1343, 1996.
- [251] W.G. Vincenti and C.H. Kruger Jr. *Introduction to Physical Gas Dynamics*. R.E. Krieger Pub. Co., Malabar, Florida, 1986. Reprint of the 1967 edition, Wiley & Sons, NY.
- [252] F. Vuillot. Vortex-shedding phenomena in solid rocket motors. *Journal of Propulsion and Power*, 11:626–639, 1995.
- [253] Q. Wang and K.M. Li. Surface waves over a convex impedance surface. *Journal of the Acoustical Society of America*, 106(5):2345–2357, 1999.

338 Bibliography

- [254] G.N. Watson. *A Treatise on the Theory of Bessel Functions*. Cambridge Univ. Press, London, 2nd edition, 1944.
- [255] D.S. Weavers. Flow-induced vibrations in valves operating at small openings. In *Practical experiences with flow induced vibrations*, E. Naudascher and D. Rockwell, editors. Springer-Verlag, Berlin, 1980.
- [256] A.G. Webster. Acoustical impedance, and the theory of horns and of the phonograph. *Proc. Natl. Acad. Sci. (U.S.)*, 5:275–282, 1919.
- [257] L.A. Weinstein. *The Theory of Diffraction and the Factorization Method*. Golem Press, Boulder, Colorado, 1974.
- [258] A.R. Wenzel. Propagation of waves along an impedance boundary. *Journal of the Acoustical Society of America*, 55(5):956–963, 1974.
- [259] J. Wheatley, T. Hofler, G.W. Swift, and A. Migliori. Understanding some simple phenomena in thermoacoustics with applications to acoustical heat engines. *American Journal of Physics*, 53:147–161, 1985.
- [260] G.B. Whitham. *Linear and Nonlinear Waves*. John Wiley & Sons, Inc., 1974.
- [261] T.A. Wilson, G.S. Beavers, M.A. De Coster, D.K. Holger, and D. Regenfuss. Experiments on the fluid mechanics of whistling. *Journal of the Acoustical Society of America*, 50:366–372, 1971.
- [262] C.P. Wu. Variational and iterative methods for waveguides and arrays. In *Computer Techniques for Electromagnetics (chapter 5)*, R. Mittra, editor, pages 266–304. Pergamon Press, Oxford, 1973.
- [263] A.H. Zemanian. *Distribution Theory and Transform Analysis*. McGraw-Hill Book Company, Inc., New York, 1965.
- [264] S. Ziada and E.T. Bühlmann. Self-excited resonances of two side-branches in close proximity. *Journal of Fluids and Structures*, 6:583–601, 1992.
- [265] G. Zouloulas and N. Rott. Thermally driven acoustic oscillations: Part V. Gas-liquid oscillations. *Zeitschrift für angewandte Mathematik und Mechanik*, 27:325–334, 1976.

Index

- acoustic intensity, 10, 31, 36, 60, 92, 153, 162, 181, 186, 236, 257
- Avogadro number, 11, 17
- barotropic, 3
- Bessel function, 179, 186, 230, 234, 298
 - Airy function, 234
 - Hankel function, 256, 299
 - Hankel transform, 280
- Biot-Savart law, 111
- blade passing frequency, 195, 196
- Boltzmann constant, 17
- branch cut, 48, 50, 54, 179, 282
- bubble, 10, 19, 20, 63, 84–88, 100, 101, 151–153, 165
- causality, 15, 16, 38, 39, 44–46, 281–284, 290, 306
- causality condition, 282
- characteristics, 65, 66, 68, 69, 71, 96, 115, 135, 237, 238
- clarinet, 13, 24, 128–131
- compact, 16, 29, 31, 35, 42, 55, 63, 73, 74, 76, 79, 83, 112, 121, 147, 149–152, 160, 162–165, 169, 170, 249, 266, 272
- constitutive equations, 1–3, 13, 21, 64, 65, 122, 124, 148
- convolution, 38, 45, 63, 131, 202, 280, 281, 289
- Cremer's optimum, 187, 215
- Crocco, 7, 28, 29, 33, 35
- Curle, 164, 166, 169, 268
- cut-off, 62, 95, 181, 182, 194, 195, 197, 214, 220, 232, 233
- cut-on, 181, 182, 197, 232, 233
- delta function, 287, 290, 291, 294
- diffraction
 - duct exit, 211
 - half-plane, 261
- Doppler, 163, 263, 264
- duct acoustics, 62, 114, 176
 - cylindrical, 178
 - Green's function, 197
 - junction, 249
 - mean flow, 188
 - modal amplitude, 194
 - open end, 211
 - rectangular, 182
 - slowly varying, 229
 - vibrating wall, 202
 - Webster's horn, 217
- edge condition, 203, 209
- end correction, 80, 122, 123, 170, 212
- energy, 2, 5, 7, 20, 29, 31, 33–35, 37, 60, 62, 63, 81, 87, 89, 90, 148, 170, 180, 182, 203, 220, 237, 257, 273, 274, 311
 - density, 31, 32
 - flux, 10, 31, 43, 92, 149
 - internal, 18
 - vortex shedding, 141, 262
- enthalpy, 6, 7, 33, 83
- entropy, 3, 5, 26, 29, 32, 71, 132, 161, 164, 275
 - homentropic, 6, 28, 30, 33, 34, 64, 70, 74, 79, 97, 162, 163
 - isentropic, 12, 18, 21, 26, 33, 65, 74, 93, 152
 - non-isentropic, 26, 27
 - spot, 76, 102, 132
- evanescent waves, 54, 181, 194
- Ffowcs Williams-Hawkings equation, 268
- Fourier
 - analysis, 69, 177, 281
 - FFT, 296
 - law, 2
 - number, 12
 - series, 126, 194, 195, 202, 226, 293–296
 - transform, 41, 44, 45, 60, 100, 126, 132, 153, 201, 202, 278–280, 282–286, 289, 291, 294
- Gauss' divergence theorem, 276
- generalized function, 286
 - surface distribution, 269, 291
- Green's function, 38–40, 42, 95, 97, 98, 100, 102, 125–127, 147, 153, 166, 168, 197, 285, 290, 291, 306
- Green's identities, 276
- group velocity, 182, 189, 285
- Heaviside function, 117, 269, 279, 288, 293
- Helmholtz
 - equation, 42, 54, 218, 229, 279, 291, 306

- number, 17, 211, 245
- resonator, 46, 121, 123, 124, 138, 142, 224
- ill-posed, 52, 56
- images, 96, 117, 125, 147, 158, 160, 165
- impedance, 41, 42, 63, 120, 126, 129, 131, 150–152, 169–171
 - admittance, 41
 - causality, 44, 45
 - characteristic, 10, 76
 - energy, 43
 - radiation, 160
 - reactance, 41
 - reflection, 43, 44
 - resistance, 41
 - specific, 41, 42
 - surface wave, 47
 - wall, 46, 49, 92, 183, 184, 186, 203
- Ingard-Myers condition, 48, 52
- instability, 52
- iris, 207
- Kármán, 60, 111
- Kirchhoff, 29, 30, 33, 36, 94
- Kutta condition, 109, 262
- Liénard-Wiechert potential, 263
- Lighthill, 24–26, 29, 35, 37, 97, 101, 107, 147, 158, 161–164, 167, 257, 268, 270
- matched asymptotic expansions, 232, 233, 249
- mean flow, 22
 - irrotational homentropic, 312
 - parallel, 314
 - uniform, 22, 312
- meromorphic, 199, 201
- Minnaert frequency, 86, 152
- modes
 - bi-orthogonality, 178
 - cylindrical duct, 178
 - duct mode, 177
 - mean flow, 188
 - rectangular duct, 182
- multiple scales, 220, 223, 224, 236
- multipole expansion, 155
- orifice, 42, 79–84, 99, 118, 123
- Parseval’s theorem, 281
- phase velocity, 182, 189, 285
- piecewise smooth, 296
- plane waves, 260
- Poisson’s summation formula, 281
- Prandtl-Glauert transformation, 259
- Pridmore-Brown equation, 314
- rain, 87
- ray acoustics, 236, 241
- reflection, 43, 56, 69, 76, 83, 84, 88, 90, 96, 101, 131, 132, 160, 187, 203, 206, 238, 249, 251
 - coefficient, 78, 82, 85, 86, 89, 211, 212, 233
 - turning point, 232
- refraction, 18, 214
 - shear layer, 163
 - temperature gradient, 238
 - wind shear, 241
- resonance, 19, 24, 63, 72, 86, 87, 97, 100, 101, 113, 114, 118, 120, 121, 123, 127, 131, 139, 151, 152, 182, 212, 214, 221–223
- Reynolds
 - number, 12, 94, 97, 108, 111, 162, 166
 - stress, 26, 162, 164
 - transport theorem, 292
- Riemann invariant, 65
- Rijke tube, 127, 133–135, 137, 138
- rotor-stator interaction, 195, 197
- Snell’s law, 56, 57
- Sommerfeld’s condition, 16, 153
- specific-heat ratio, 18
- Stokes’ theorem, 276
- Strouhal number, 60, 82, 119, 123
 - acoustical, 11
- surface distributions, 271
- surface wave, 47, 48, 50–52, 184, 186, 192, 215
- transmission, 42, 56, 57, 62, 203, 206, 249, 251
 - coefficient, 78, 206, 233
- trombone, 72
- uniqueness, 22
- vortex, 29, 82, 113, 114, 140, 141
 - line, 111, 254, 255, 257, 291
 - shedding, 11, 59, 80, 82, 83, 118, 119, 140, 141, 166, 167, 262
 - sheet, 49, 59, 60
 - sound, 27, 28, 35, 36, 119
 - street, 60, 111
 - vorticity, 111
- Walkman, 55